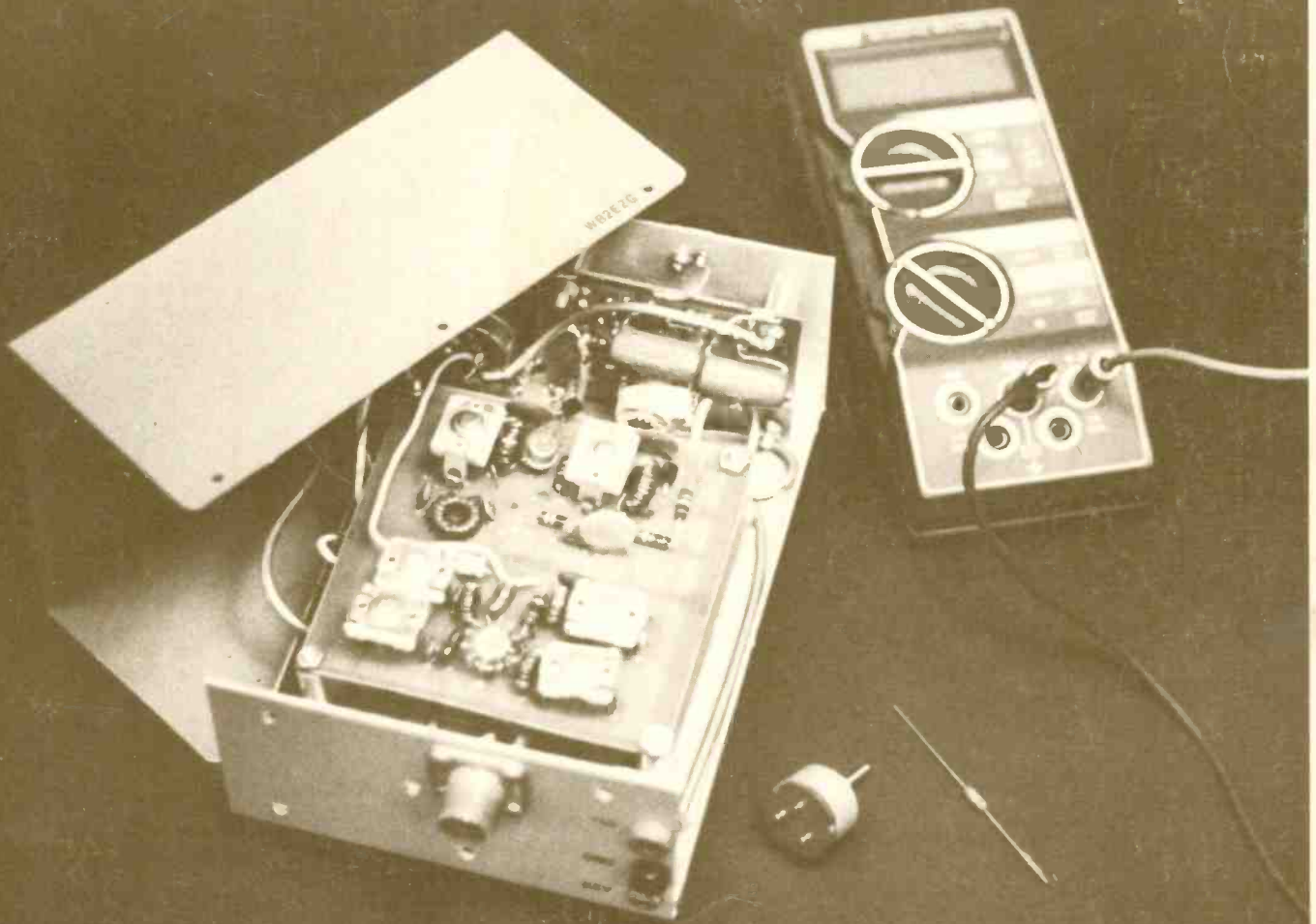


A McGraw-Hill Publication

# Electronics Designer's Casebook Number 4





9  
103-15927  
12  
120

# Designer's Casebook

---

PREPARED BY  
THE EDITORS OF  
**Electronics**

Fourth in a continuing series of selected Designer's Casebook sections of Electronics Magazine. This edition includes Electronics issues from January 18, 1979 through June 5, 1980. Also included are feature articles and items from Engineer's Notebook of particular interest to the circuit designer.

---

Price: \$5.00 North America  
\$12.00 outside North America  
Printed in U.S.A.



All material copyrighted by

## **Electronics**

McGraw-Hill, Inc.  
1221 Avenue of the Americas  
New York, New York 10020



# TABLE OF CONTENTS

## AUDIO AND ANALOG

---

|   |     |
|---|-----|
| Acoustic protector damps telephone-line transients .....          | 5   |
| Peak detector recovers narrow pulses accurately .....             | 15  |
| Optoisolator initializes signal-averaging circuit .....           | 16  |
| Charge pump cuts compandor's attack time .....                    | 23  |
| Bidirectional optoisolator puts two LEDs nose to nose .....       | 27  |
| Wideband peak detector recovers short pulses .....                | 29  |
| Compact industrial ammeter measures 10-ampere peaks .....         | 89  |
| Dual light-emitting diode synthesizes polychromatic light .....   | 92  |
| Low-cost fiber-optic link handles 20 megabit/s data rates .....   | 104 |
| Switching converter improves a-d converter sensitivity .....      | 110 |
| Peak-reading millivoltmeter responds instantaneously .....        | 113 |
| Talking meter voices dc voltage readings .....                    | 114 |
| Magnetic levitator suspends small objects .....                   | 121 |
| Semiconductor thermometer is accurate over wide range .....       | 135 |
| Linear sense amplifier raises sensitivity of touch keyboard ..... | 136 |
| Level shifter builds high-voltage op-amp block .....              | 136 |
| Time-shared analog bus multiplexes audio signals .....            | 143 |
| Test-set characterizes FET's AGC response .....                   | 152 |
| Low-cost logarithmic amp works over one decade .....              | 154 |
| Reducing a PLL's phase jitter .....                               | 161 |
| Digital voltmeter has audible output .....                        | 163 |

## CONTROL

---

|  |     |
|--|-----|
| Standard ICs provide raster scan interface .....           | 1   |
| Coordinate converter aligns piezoelectric positioner ..... | 4   |
| Hybrid servo system minimizes hunting .....                | 14  |
| Controller halts playback when taped voice pauses .....    | 20  |
| Annunciator control uses only passive components .....     | 24  |
| LEDs track signal level in visual data monitor .....       | 25  |
| C-MOS triac trigger cuts parts count .....                 | 35  |
| Optoelectronic alarm circuit is time sensitive .....       | 41  |
| Gray-code counter steps torque motor .....                 | 46  |
| One-chip power amplifier controls dc motor's speed .....   | 112 |
| Remote controller sets universal motor's speed .....       | 124 |
| Frequency-marking controller indexes tape segments .....   | 128 |
| High-frequency operation with the AM9513 controller .....  | 129 |
| Removing residual voltage in dc generators .....           | 131 |
| Moving-dot indicator tracks bipolar signals .....          | 132 |
| Implementing interrupts for bit-slice processors .....     | 144 |

## DESIGN

---

|   |    |
|---|----|
| What to look for in logic timing analyzers .....                        | 49 |
| Analog ICs divide accurately to conquer computation problems .....      | 55 |
| Field-programmable arrays: powerful alternatives to random logic .....  | 63 |
| Sequencers and arrays transform truth tables into working systems ..... | 69 |
| Supersensitive measurement demands critical input design .....          | 77 |
| Transistors—A hot tip for accurate temperature sensing .....            | 82 |

## FILTERS

---

|  |     |
|--|-----|
| Notch filter and meter measure power-line harmonics .....      | 28  |
| Bridged-T selects filter's notch frequency and bandwidth ..... | 34  |
| One-chip gyrator simplifies active filter .....                | 36  |
| Tunable equalizers set amplitude and delay .....               | 98  |
| Tone detector sharpens digital filter's response .....         | 107 |
| Sampling filters simplify converter's offset measurement ..... | 156 |
| Dual-slope filters optimize speaker's crossover response ..... | 157 |

## LOGIC

---

|  |     |
|--|-----|
| Gates replace PROM in Intellec 8 bootstrap loader .....            | 2   |
| Time-shared counters simplify multiplexed display .....            | 6   |
| TTL and C-MOS interface unites microprocessor and calculator ..... | 7   |
| Synchronous counters provide programmable pulse delays .....       | 10  |
| Counter delivers data in signed or complemented form .....         | 11  |
| Epitaxial phototransistor with feedback has fast response .....    | 13  |
| Five-state LED display monitors paging system .....                | 17  |
| Cascaded C-MOS blocks form binary-to-BCD converters .....          | 26  |
| Digital peak detector finds 4-bit highs and lows .....             | 31  |
| Phase-locked loop aids in measuring capacitance .....              | 32  |
| LED dot/bar driver simplifies solid-state scope .....              | 33  |
| LSI counter simplifies display for am/fm radio .....               | 37  |
| Digital phase meter display angles in degrees or radians .....     | 42  |
| Single-step exerciser aids 8085 debugging .....                    | 43  |
| Software-based controller simplifies PROM programmer .....         | 47  |
| Counter banks stagger radar's pulse rate .....                     | 88  |
| Doubling the character rate handled by CRT controllers .....       | 102 |
| Electronic security lock has nonvolatile latch memory .....        | 106 |
| Delay circuit replicates pulses of variable width .....            | 116 |
| C-MOS counter sets divider's modulus .....                         | 122 |
| PLL's lock indicator detects latching simply .....                 | 139 |
| Three-clip logic analyzer maps four-input truth table .....        | 140 |
| 4-by-4 matrix chip encodes larger arrays .....                     | 142 |
| Low-cost autoranger scales DVM over four decades .....             | 148 |
| Improved burglar alarm discourages auto thieves .....              | 149 |
| LR oscillator indicates inductance directly .....                  | 150 |
| One-chip multiplexer simplifies eight-trace scope .....            | 151 |
| Hall sensors and flip-flop sustain pendulum's swing .....          | 154 |
| Low-cost alphanumeric decoder drives British-flag display .....    | 158 |
| Contact tester quantifies open-, short-circuit tendencies .....    | 160 |

## POWER SUPPLIES

---

|   |     |
|---|-----|
| Micropower regulator has low dropout voltage              | 21  |
| Switching converter raises linear regulator's efficiency  | 37  |
| Electronic sink simulates load for testing power supplies | 44  |
| Floating current source drives automatized test fixture   | 87  |
| Current source for I <sup>2</sup> L saves energy          | 90  |
| Solar-powered regulator charges batteries efficiently     | 97  |
| Switched load checks power supply response                | 99  |
| Reducing the dropout voltage of programmable regulators   | 101 |
| Dc-dc converter maintains high efficiency                 | 117 |
| Foldback limiter protects high-current regulators         | 123 |
| High-voltage regulator is immune to burnout               | 125 |

## SIGNAL CONVERSION

---

|   |     |
|---|-----|
| Missing-pulse detector handles variable frequencies         | 22  |
| Balanced modulator chip multiplies three signals            | 39  |
| Single a-d converter cuts cost of droopless sample and hold | 45  |
| Cupless anemometer has diode wind-sensor                    | 96  |
| Line-frequency converter transforms 50 Hz to 60 Hz          | 105 |
| Frequency discriminator has ultra-sharp response            | 117 |
| Hall-probe adapter converts DMM into gaussmeter             | 119 |
| PSK modulator resolves phase shifts to 22.5°                | 141 |
| FM decoder improves SCA subcarrier detection                | 153 |

## SIGNAL SOURCES

---

|  |     |
|--|-----|
| Circuit phase-locks function generators over 360°        | 3   |
| C-MOS oscillator has 50% duty cycle                      | 12  |
| Rate multiplier controls noninteger frequency divider    | 18  |
| Standby crystal time base backs up line-powered clock    | 18  |
| Serrodyne amplifier generates wideband linear ramp       | 30  |
| Wide-range pulse generator displays timing parameters    | 34  |
| Hyperbolic clock inverts time                            | 40  |
| High-speed generator pulses ECL loads                    | 91  |
| Maximum-length shift register generates white noise      | 93  |
| 12-hour clock tells time out loud                        | 94  |
| Pseudorandom generator has programmable sequence length  | 100 |
| LC network adapts PLL for crystal-overtone operation     | 107 |
| D-a converter simplifies hyperbolic clock                | 109 |
| Ramp generator has separate slope and frequency controls | 111 |
| Autocorrecting driver rights pulse polarity              | 120 |
| Bipolar current mirror scales, inverts signals           | 126 |
| Digital pulse shifter covers 0° to 360° range            | 127 |
| Low-level modulator sweeps generator over narrow range   | 133 |





# Standard ICs provide raster scan interface

by Serge Poplavsky  
University of New South Wales, Kensington, Australia

One master oscillator and a few counters, flip-flops, and gates make a baud-rate clock with a sync generator that produces horizontal and vertical pulses for noninterlaced raster scanning of a cathode-ray tube. In it, standard integrated circuits are used to generate rates up to 38.4 kilbauds (the upper limit of most generators is only 9,600 bauds) and sync pulses for producing 312 lines at a 50-hertz refreshing rate (or 260 lines for a 60-Hz rate). Thus the circuit is a low-cost solution to building an important part of any data terminal.

All clock rates are derived from one crystal-controlled oscillator, A<sub>1</sub>, which uses the 7209 and a crystal cut for 7.9872 megahertz. The master clock frequency is then divided by 13 by A<sub>2</sub>, the 74LS161 presetable counter. A<sub>2</sub> generates a frequency 16 times 38.4 kilbauds, suit-

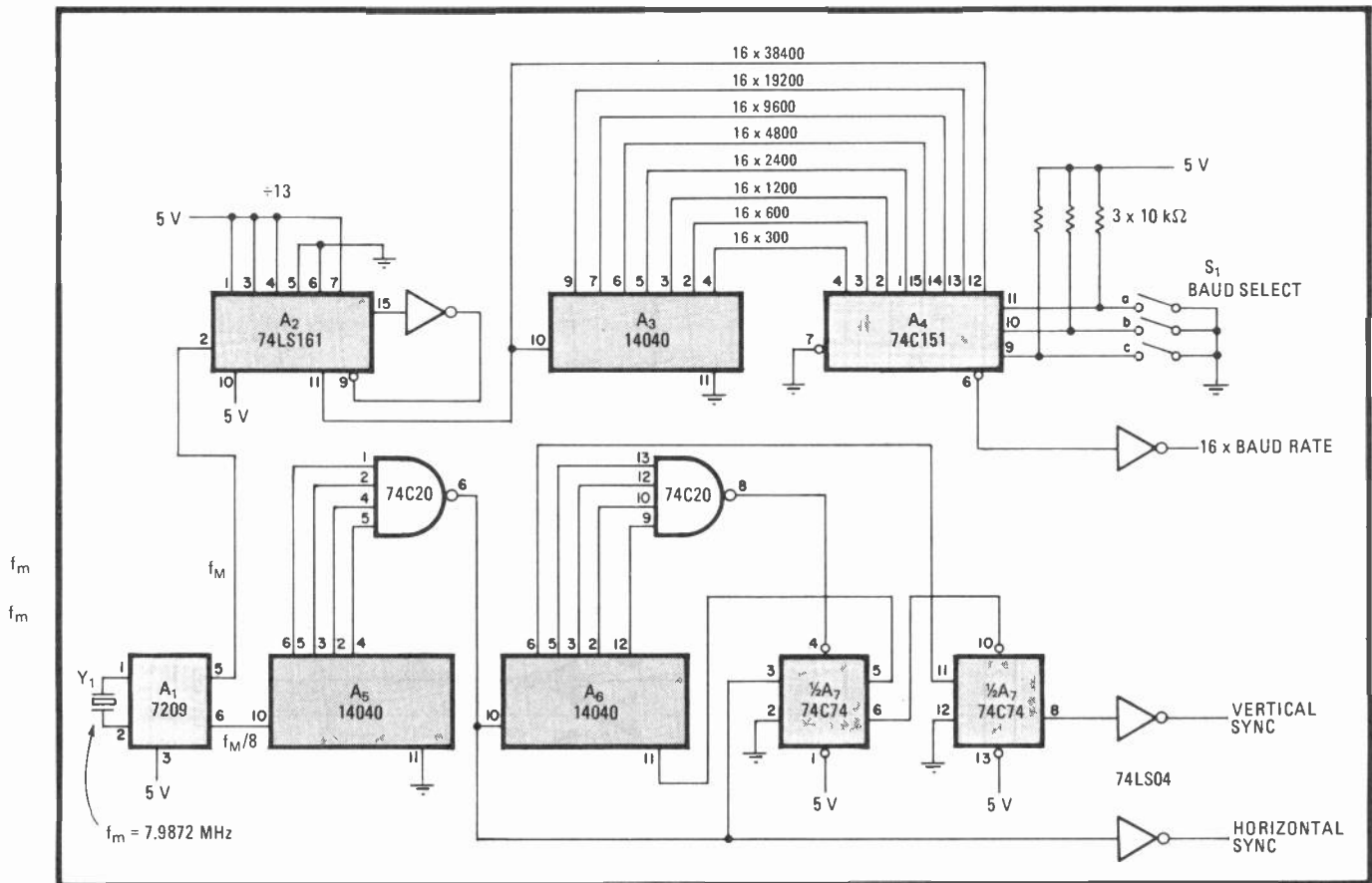
able for interfacing with universal asynchronous receiver-transmitters or similar modems.

This frequency is further divided by A<sub>3</sub>, the 14040 binary counter. Thus, rates extending from 16×300 bauds to 16×19.2 kilbauds will appear at its output.

S<sub>1</sub>, which is used in A<sub>4</sub>, the 74C151 one-of-eight-line multiplexer, selects the baud rate desired. When all switches are open, a rate of 300 bauds is selected. Closing switch a, the least significant bit (i.e., binary number 1), selects a baud rate of 600, and so on.

The horizontal sync pulses for the cathode-ray tube are derived from A<sub>5</sub> and a four-input NAND gate, which generates a frequency of 15,600 Hz, each pulse lasting 4 microseconds. The vertical sync frequency, either 50 or 60 Hz, is obtained from A<sub>6</sub>-A<sub>7</sub> and a four-input NAND gate.

Dividing the horizontal sync pulses by 312 or 260 (for 50 or 60 Hz, respectively), the binary counter, A<sub>6</sub>, which in this case is wired as a divide-by-312 device, drives two flip-flops (A<sub>7</sub>). A<sub>7</sub> resets the counter and generates vertical sync pulses, each 256 μs long. □



**Versatile.** Using standard integrated circuits, combination baud-rate generator and sync generator for CRT works up to 38.4 kilbauds and can be wired to generate sync pulses suitable for a 50- or 60-Hz refreshing rate. All frequencies are derived from one oscillator.

# Gates replace PROM in Intellec-8 bootstrap loader

by Simon Gagné and Bernard Boulé  
*Université Laval, Department of Electrical Engineering, Quebec, Canada*

In what may be the most cost-effective solution yet for implementing a bootstrap loader for Intel's popular Intellec-8 development system, logic gates are used to replace the jump-to-monitor routine stored in a programmable read-only memory (PROM).<sup>1</sup> This simple method of automatically accessing the system's monitor, or executive-control routines, is possible because the set of 8-bit logic signals required at the data bus to access the monitor on power-up can be easily generated.

In the Intellec-8, the monitor is located at address 3800 (hexadecimal). Therefore, a jump instruction is used to advance the program counter from location 0 to 3800H. To avoid the manual programming required

after each power-up, the previous solution was to use a PROM programmed with the instruction (C3 00 38).

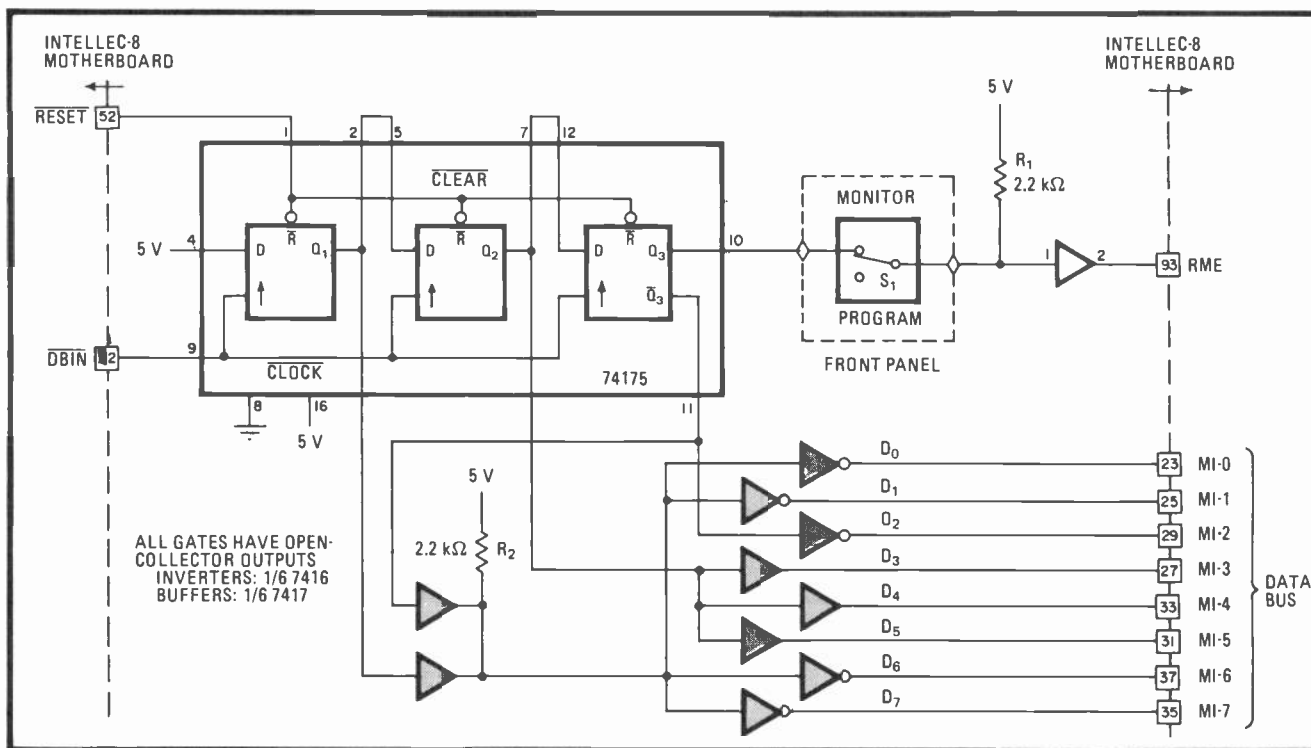
The logic signals required on data bus lines D<sub>0</sub>-D<sub>7</sub> for achieving the three-byte jump instruction are shown in Fig. 1a. The output of each flip-flop in the three-stage 74175 shift register, previously used to enable the PROM, together with simple logic, can synthesize this sequence.

When the outputs of the shift register (Q<sub>1</sub>, Q<sub>2</sub>, and Q<sub>3</sub>) alone are stepped with system clock  $\overline{DBIN}$ , they generate the signal pattern shown in Fig. 1b. Comparison of Fig. 1a and 1b reveals that the identical patterns of lines D<sub>0</sub>-D<sub>1</sub> and D<sub>6</sub>-D<sub>7</sub> can be generated by forming the logic function  $\overline{Q_1} + Q_3$ . It is also seen that bits D<sub>3</sub>, D<sub>4</sub>, and D<sub>5</sub> are identical to the Q<sub>2</sub> output of the shift register and the D<sub>2</sub> bit is identical to the Q<sub>3</sub> output, so that the Q<sub>2</sub> and Q<sub>3</sub> signals can simply be connected to these corresponding data lines through noninverting buffers. To make the final circuit, which appears in Fig. 2, operational, switch S<sub>1</sub> need only be placed in the monitor position for automatic loading on power-up. □

**References**  
 1. "PROM adds bootstrap loader to Intellec-8 development system," *Electronics*, April 27, 1978, p. 126.

| Instruction | Op code | D <sub>7</sub> | D <sub>6</sub> | D <sub>5</sub> | D <sub>4</sub> | D <sub>3</sub> | D <sub>2</sub> | D <sub>1</sub> | D <sub>0</sub> | Condition                      | Q <sub>1</sub> | Q <sub>2</sub> | Q <sub>3</sub> |
|-------------|---------|----------------|----------------|----------------|----------------|----------------|----------------|----------------|----------------|--------------------------------|----------------|----------------|----------------|
| JMP 3800H   | C3      | 1              | 1              | 0              | 0              | 0              | 0              | 1              | 1              | RESET                          | 0              | 0              | 0              |
|             | 00      | 0              | 0              | 0              | 0              | 0              | 0              | 0              | 0              | AFTER FIRST $\overline{DBIN}$  | 1              | 0              | 0              |
|             | 38      | 0              | 0              | 1              | 1              | 1              | 0              | 0              | 0              | AFTER SECOND $\overline{DBIN}$ | 1              | 1              | 0              |
| (AFTER JMP) | FF      | 1              | 1              | 1              | 1              | 1              | 1              | 1              | 1              | AFTER THIRD $\overline{DBIN}$  | 1              | 1              | 1              |

**1. Synthesis.** Table outlines logic sequence required on data bus for achieving jump operation in order to enter Intellec-8's executive program (a). Outputs of clocked three-stage shift register of basic circuit generate signals (b), which can be used to synthesize D<sub>0</sub>-D<sub>1</sub> and D<sub>6</sub>-D<sub>7</sub> signals if function  $\overline{Q_1} + Q_3$  is formed with logic gates. Q<sub>2</sub> output is by itself identical to D<sub>3</sub>, D<sub>4</sub>, and D<sub>5</sub>. Q<sub>3</sub> output is identical to D<sub>2</sub>.



**2. Implementation.** Circuit for accessing system's monitor uses open-collector logic gates, which replace programmable read-only memory in original configuration. Circuit is armed by placing front-panel switch S<sub>1</sub> in monitor position before each power-up of system.

# Circuit phase-locks function generators over 360°

by Lawrence W. Shacklette  
Seton Hall University, South Orange, N. J.

This circuit locks a low-cost function generator without a voltage-controlled-oscillator (VCO) input to a second inexpensive generator having such a phase-reference feature. A J-K flip-flop, two one-shots, two comparators, and an operational amplifier are linked in a feedback arrangement that includes the programmable generator as the VCO in a phase-locked loop (PLL). The resultant circuit provides a selectable phase shift between generator outputs over the range of 0° to 360°.

In operation, the output of the low-cost generator,  $v_1$ , passes through a high-pass filter to a zero-crossing detector that employs a 311 comparator ( $M_1$ ), as shown. A dual monostable multivibrator and J-K flip-flop follow. Although these two devices can be eliminated, they enable the phase-locked loop to be operated at the center of its locking range for any phase shift. This arrangement ensures that two often desired phase angles, 0° and 180°, fall within the capture range of the PLL, so that if locking is lost, it will be automatically regained.

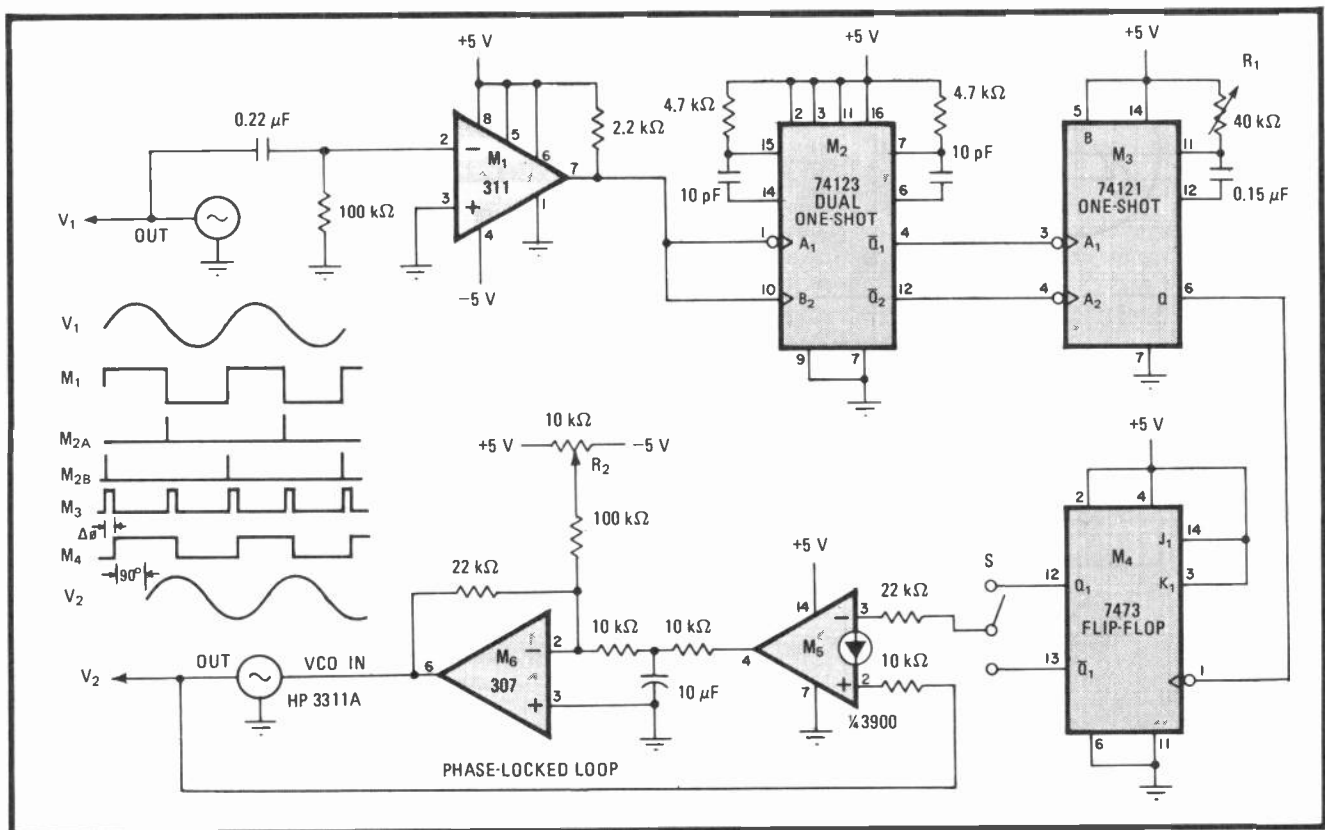
The outputs of the dual one-shot,  $M_2$ , wired so that each fires on opposite edges of the signal applied to its

inputs (see timing diagram), are fed to the OR input of  $M_3$ , whose on time is selected by potentiometer  $R_1$ . Thus  $R_1$  controls the amount of phase shift.

$M_3$  produces two pulses for each cycle of  $v_1$  and triggers the J-K flip-flop,  $M_4$ , on each negative edge. The flip-flop thus produces a square wave with a frequency equal to  $v_1$ , but shifted in phase by up to 180°. An additional shift of 180° can be obtained by using switch  $S$  to connect the Q output of  $M_4$  to the inverting input of the 3900 Norton amplifier.

The adjustable-phase square wave serves as a reference signal for the phase-locked loop, which is composed of the 3900, a low-pass filter, a buffer (307), and a VCO (the second function generator, a Hewlett-Packard 3311A). The input signal to the VCO is a negative dc voltage that is the inverted sum of the filtered output of the 3900 and the voltage selected by the offset control,  $R_2$ . By turning the generator's front-panel control or  $R_2$ , the free-running frequency of the loop can be adjusted.

Because the reference signal is a square wave, the PLL will lock onto either the fundamental of  $v_1$  or its odd harmonics. Selection of a particular harmonic is made by adjusting the free-running frequency to the approximate value of the harmonic desired. Half-multiple harmonics ( $1/2f_1$ ,  $3/2f_1$ ,  $5/2f_1$ , etc.) can be produced at  $v_2$  by breaking the  $\bar{Q}_1$ - $A_1$  connection between  $M_2$  and  $M_3$  and tying  $A_1$  to +5 volts. Even harmonics can be obtained by using the remaining flip-flop in the 7473 as a divide-by-2 counter, and placing it between the output of the VCO and the 3900's noninverting input. □



**Phase-locked.** Comparators, one-shots, and flip-flop combine to provide stable locking of generators without phase-reference feature to those having a VCO input.  $R_1$  and  $S$  are used to select phase of  $v_2$  with respect to  $v_1$ ; phase can be adjusted from 0° to 360°.  $M_2$  and  $M_4$  ensure that locking is regained if it is lost, and  $R_2$  controls lock frequency, which may be set to integer or half-integer harmonics of  $v_1$ .

# Coordinate converter aligns piezoelectric positioner

by Lawrence E. Schmutz  
Adaptive Optics Associates, Cambridge, Mass.

Piezoelectric tilt elements of the kind used to position laser beams and optical scanners can be aligned with the help of this circuit, which converts the transducer's high input driving voltages, normally resolved in X-Y coordinates, into corresponding coordinates (a, b, c) in a nonorthogonal three-axis system. Only one quad operational amplifier and two resistor-array packages are used for the transformation.

The geometry of many popular piezoelectric positioning elements (a), as for example the Burleigh Instruments' PZ-80, is such that:

$$x = c - a \quad y = b - \frac{1}{2}(a + c) \quad 0 = a + b + c$$

Solving these equations simultaneously for a, b, and c

yields:

$$a = \frac{1}{2}x - \frac{1}{2}y \quad b = \frac{2}{3}y \quad c = -\frac{1}{2}x - \frac{1}{3}y$$

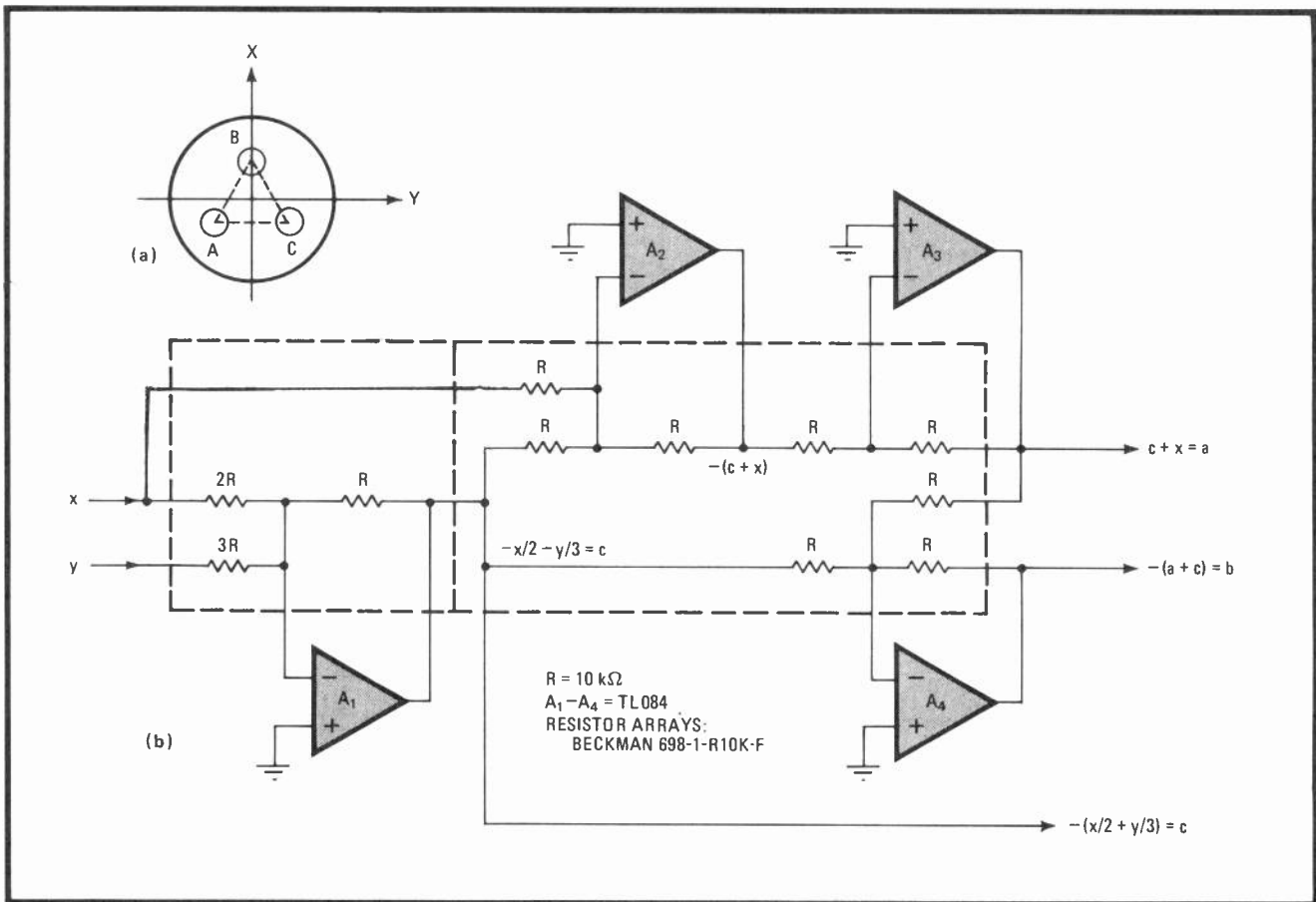
Simplifying further:

$$a = c + x \quad b = -(a + c) \quad c = -(x/2 + y/3)$$

The last set of equations is easily implemented by using precision resistors to set the gain of several op amps (b).

Resistor arrays in dual in-line packages will perform the transformation accurately, for their elements have a tolerance of  $\pm 0.5\%$ . The overall circuit uncertainty becomes  $\pm 1\%$  when two arrays are configured as shown. To ensure that the circuit occupies no more space than that taken by three dual in-line packages, the resistors are grouped in their respective arrays as shown by the dotted lines.

The TL084 op amp is more than adequate for the circuit accuracy desired, since in most applications the piezoelectric devices operate in the lower audio-frequency range.  $\square$



**Beaming true.** Input information for positioning laser beam, normally presented in X-Y coordinates, must be converted into three-axis coordinates for many piezoelectric transducers (a). One op amp and two precision resistor arrays perform the transformation (b).

# Acoustic protector damps telephone-line transients

by Gil Marosi  
Intech Function Modules Inc., Santa Clara, Calif.

By limiting the transients on telephone lines, this acoustic shock protector prevents those sudden high sound levels that can damage the ear badly enough to cause loss of hearing. It holds the maximum peak-to-peak voltage at the receiver of a telephone headset to 50 millivolts.

A four-terminal device, the shock protector is inserted between the receiver side of the telephone hybrid and the receiver proper. A block diagram of the circuit, which operates from a single 5-volt supply, is shown in (a). Input signals are amplified by a factor of 5 and applied to a voltage-controlled, variable-gain stage. Because this stage also attenuates the signal to the degree indicated by the actual level of a feedback signal, further amplification may be needed, and is available, to retain the loop's gain margin. A voltage doubler then converts the

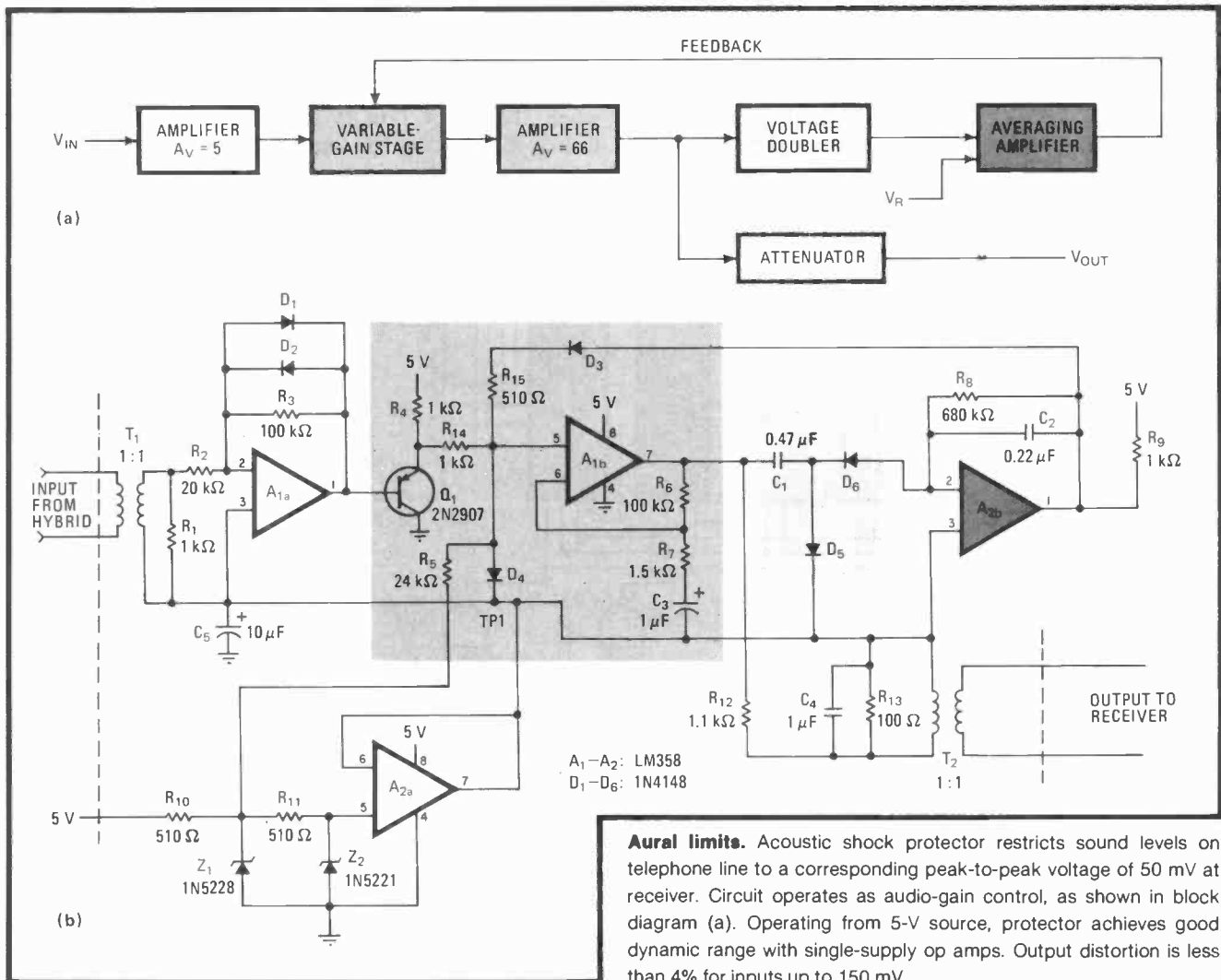
amplifier signal to a dc voltage. This voltage is compared with a preset reference at the inputs of an averaging amplifier.

The output of the averager, which is essentially an integrating network, is connected to the variable-gain stage. As the input voltage from the hybrid becomes greater, so does the feedback voltage, and thus still more attenuation is provided for the variable-gain stage.

As for the actual circuit (b), transformers  $T_1$  and  $T_2$  isolate the protector from the floating telephone line, so that the circuit operates from a 5-v supply referred to ground.  $A_{1a}$ , one half of an LM358 operational amplifier, provides the required amplification of the input signal.  $D_1$  and  $D_2$  clamp  $A_{1a}$ 's output to 0.7 v and introduce the signal to buffer  $Q_1$ . This transistor, along with  $R_4$ - $R_7$ ,  $R_{14}$ ,  $D_4$ ,  $A_{1b}$ , and  $C_3$ , make up the variable-gain stage.

Zeners  $Z_1$  and  $Z_2$  and op amp  $A_{2a}$  bias  $A_{1a}$  and  $A_{1b}$  so that input signals to those stages swing about a quiescent point of 2 v. The circuit thus provides maximum dynamic range. Note that most op amps require a 12-v supply to achieve a comparable range.

$Q_1$ 's output is converted to a current with the aid of  $R_{14}$ . Current flows through  $D_4$ , which operates as a current-controlled variable resistor.  $D_4$  is biased through



**Aural limits.** Acoustic shock protector restricts sound levels on telephone line to a corresponding peak-to-peak voltage of 50 mV at receiver. Circuit operates as audio-gain control, as shown in block diagram (a). Operating from 5-V source, protector achieves good dynamic range with single-supply op amps. Output distortion is less than 4% for inputs up to 150 mV.

$R_5$  such that its nominal resistance is 500 ohms.

The voltage at the noninverting input of  $A_{1b}$  is amplified and applied to the voltage doubler ( $C_1$ ,  $D_5$ , and  $D_6$ ).  $A_{2b}$  and its associated circuit perform the averaging function that provides a feedback current to the variable-gain stage. The gain from input to output is unity until the amplifier's input threshold—set at 50 mV—is exceeded. The acoustic shock protector then operates as an automatic gain control for inputs up to 150 mV. The

output distortion up to that point does not exceed 4%. Beyond 150 mV, however, the protector simply clamps the output to 50 mV p-p without regard to distortion.

Because the phone receiver is an inductive device, its impedance increases with frequency.  $C_4$  is placed across  $R_{14}$  to compensate for this rise in impedance. The overall gain of the acoustic shock protector is thus held flat to within 1 decibel from 300 hertz to 3 kilohertz so long as the output of  $A_{1b}$  is below 600 mV or so. □

## Time-shared counters simplify multiplexed display

by Darryl Morris  
Northeast Electronics, Concord, N. H.

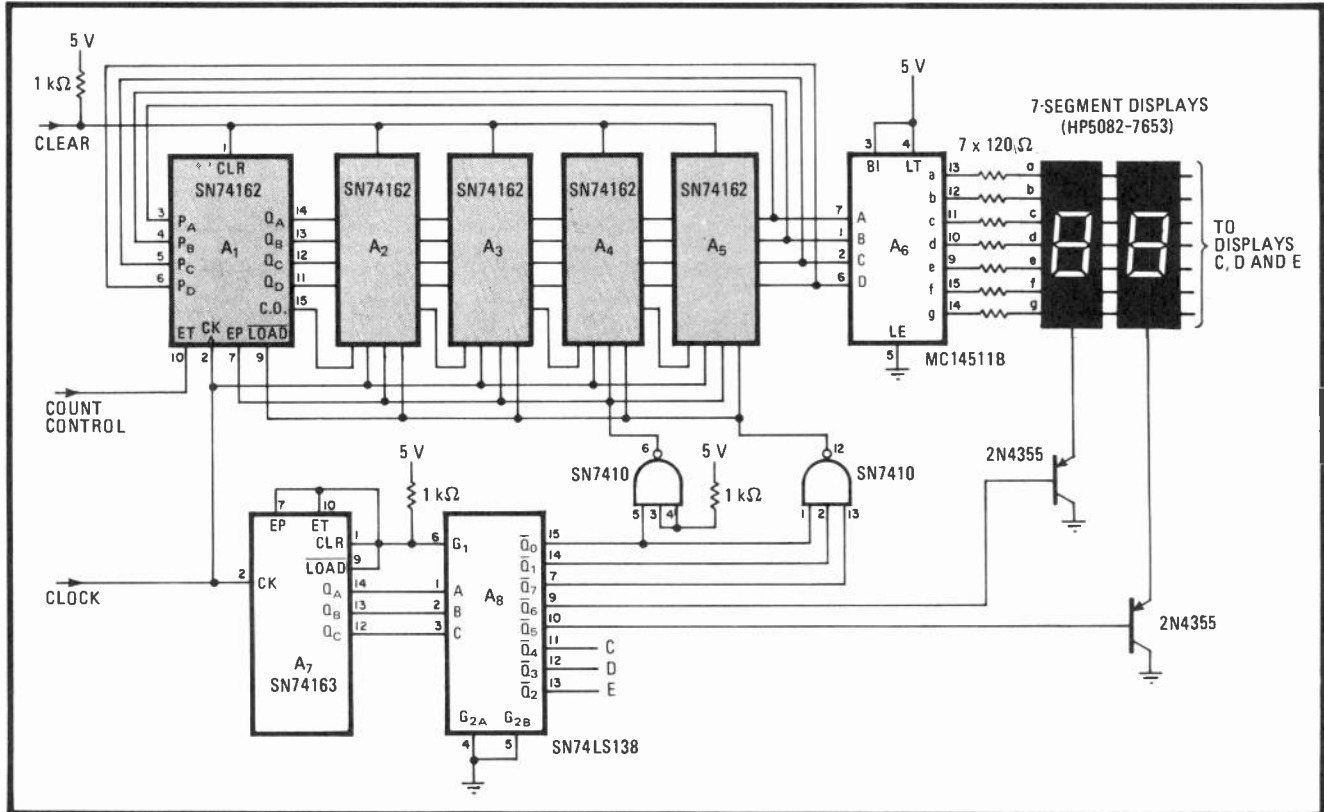
Although multiplexed display circuits reduce the number of components otherwise required for decoding on a per-digit basis, additional hardware is then needed to select and multiplex various lines to the display. But if a display is driven by a frequency counter, as is often the case, the counter itself can be made to perform the multiplexing with only minimal extra circuitry.

Multiplexing is done by using a master clock having several times the frequency of the normal clock, depending on the number of digits to be multiplexed, and by

time-sharing the counters between the count and display mode. In the count mode, the  $\overline{LOAD}$  and enable-P (EP) inputs of the counters shown are high and  $A_1$ – $A_5$  function as a conventional cascaded counter circuit under control of the enable-T (ET) input of  $A_1$ . The counter circuit advances one count for each clock period during which the count control line is high.

During the display mode, the control line and  $\overline{LOAD}$  input of  $A_1$ – $A_5$  move low. The counters now accept data at their preload inputs,  $P_A$ – $P_D$ . Because the preload inputs are connected to each preceding set of a counter's outputs,  $A_1$ – $A_5$  operates as a 4-bit-wide recirculating shift register when clocked. Thus, the contents of each counter is rotated past the seven-segment decoder ( $A_6$ ) during its display interval, and the appropriate digit in the display is strobed by the mode controller,  $A_7$  and  $A_8$ .

This technique offers the best saving in chip count when the count rate is slow or numbers are to be displayed only after the counted event has terminated. □



**Time-shared.** Counter circuit switches between count and display modes without selector devices. Counter operates as 4-bit-wide recirculating shift register. Master clock frequency is assumed to be several times that used for the counting circuits.

# TTL and C-MOS interface unites microprocessor with calculator

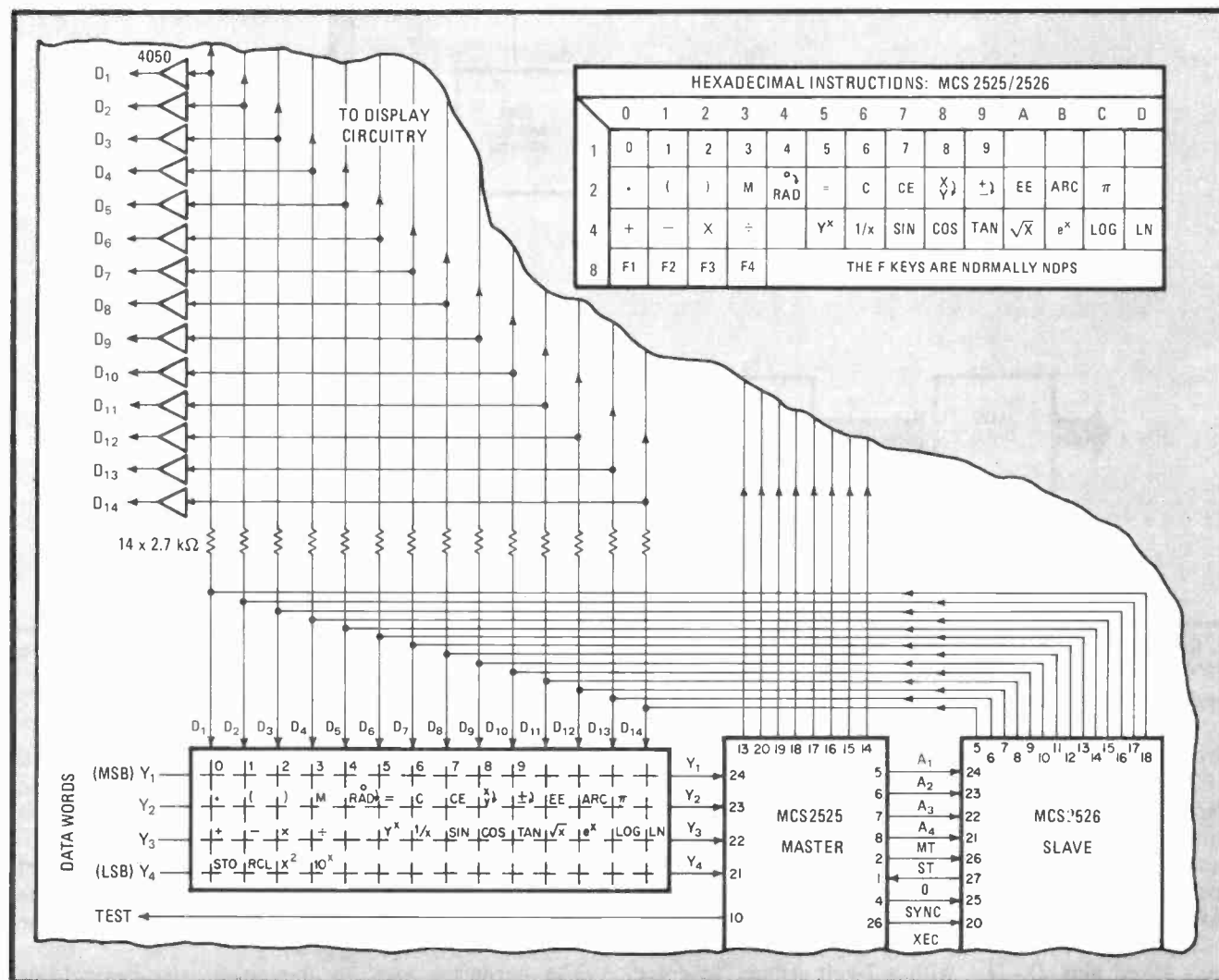
by Bert K. Erickson  
Fayetteville, N. Y.

This interface combines a general-purpose scientific calculator, which performs rapid arithmetic operations, with the extensive memory of 8-bit microprocessor-based systems into a system that has the advantages of both. Here, the calculator can program or be programmed exclusively by the microprocessor; ultimately, of course, it is programmed by software residing in system memory. Alternatively, the calculator can be used for its

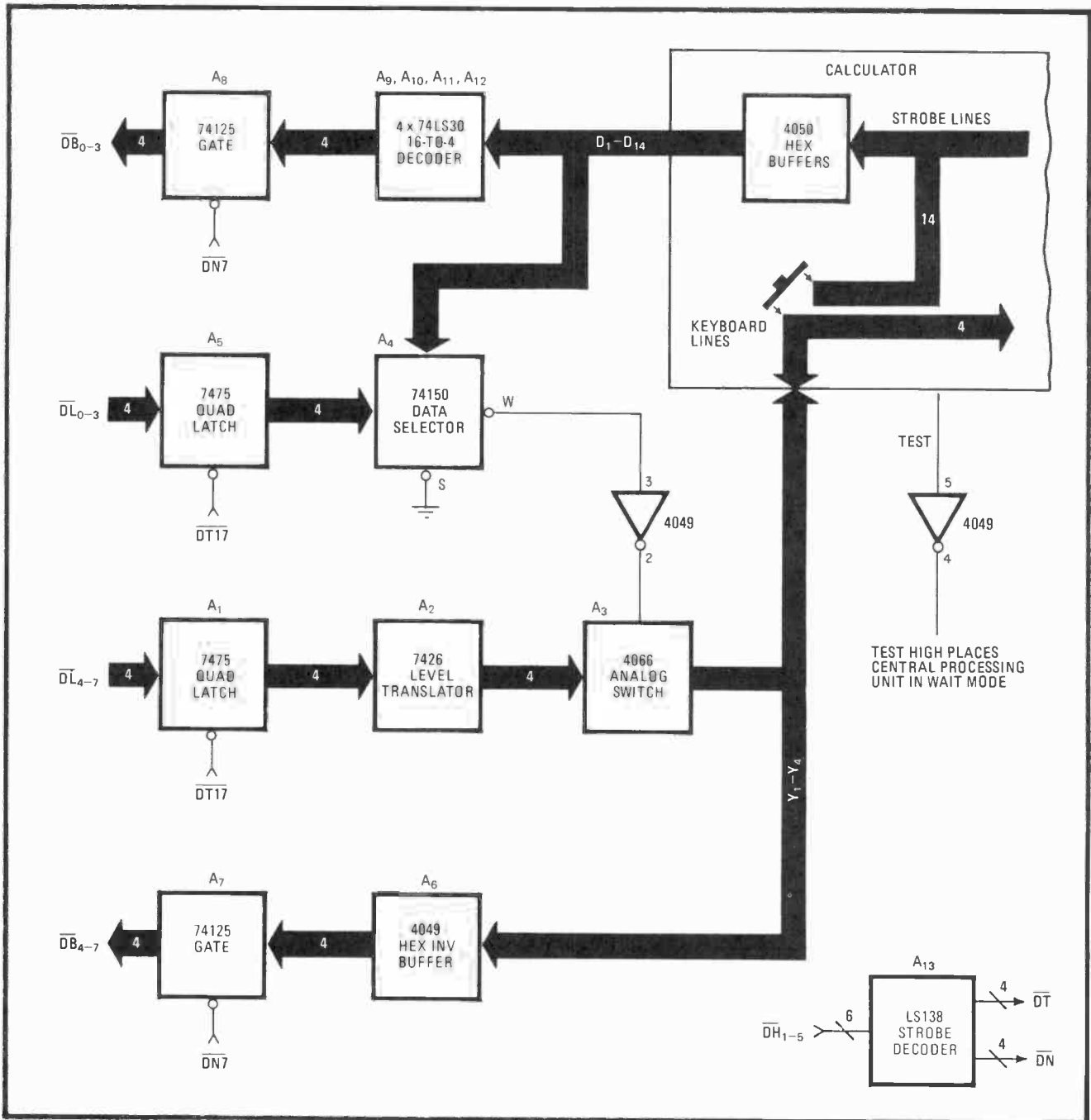
normal purpose. Using transistor-transistor-logic and complementary-metal-oxide-semiconductor devices, the interface costs less than \$20 dollars.

Virtually any microprocessor can be united with any calculator, assuming the calculator's keyboard can be accessed. In general, the keyboard scanning lines will be connected to the calculator's corresponding display driver pins and to the microprocessor system through appropriate circuitry. A two-key roll-over feature that inhibits data entry when two keys are depressed simultaneously should be included. Several lines from the microprocessor will be connected to the keyboard so that microprocessor instructions can be entered into the calculator.

Figure 1 shows how a typical calculator (MOS Technology's two-chip MCS2525/2526) was initially modified to interface with a microprocessor. A set of buffers (4050) serves as the link between the strobe lines and the



1. Lines of command. MCS2525/2526 calculator chip pair sends instructions to 8000 microprocessor through appropriate 4050 buffers when corresponding key is depressed. Alternatively, microprocessor can program calculator when half of data word is introduced at Y<sub>1</sub>-Y<sub>4</sub>; other half of data word and calculator's strobe circuits generate D<sub>1</sub>-D<sub>14</sub> signals at keypad, so that key closures are simulated.



**2. Control.** Interface transmits keypad instructions to 8000 processor and also aids in simulating key closure for calculator programming by 8000. Accompanying sample program for displaying digits sequentially has built-in delay instructions to slow input-data rate, so that a keyboard scan can be completed for each word entered at the calculator. Two-key roll-over protection is also provided.

input to the microprocessor for programming by the MCS2525/2526. The 2.7-kilohm resistors are used to decouple the calculator from the buffer input in order to minimize loading of the MCS2525/2526. Decoupling resistors should also be placed in series with the calculator's input lines,  $Y_1$ - $Y_4$ , where microprocessor instructions (data words) to the 2525/2526 are entered.

The MCS2525/2526 automatically scans the calculator's keyed pins,  $D_1$ - $D_{14}$ , with a 7-volt strobe. To enter an instruction from the microprocessor, a keypad closure is simulated from the data entered at lines  $Y_1$ - $Y_4$  and on lines  $D_1$ - $D_{14}$ . By applying the first 4 bits of the 8-bit data

word at the Y lines and by introducing the last four bits at the D lines, key closure is simulated. For example, to enter digit 5, line  $Y_1$  must be brought high while  $D_6$  is being strobed (an instruction corresponding to hexadecimal number 15, as shown in the particular instruction set for this microprocessor-calculator). Alternatively, the microprocessor can be programmed by depressing the appropriate key on the keypad.

The hardware used to implement the keypad-line coding is shown in Fig. 2. For generating calculator instructions, the upper 4 bits of the data word, which are eventually applied to  $Y_1$ - $Y_4$ , is latched into  $A_1$ . The



output of A<sub>1</sub> is shifted in level by open-collector gate A<sub>2</sub>, and the 7-v strobe is applied to the keyboard lines by analog switch A<sub>3</sub>.

A<sub>3</sub> is switched on by selector A<sub>4</sub> through the 4050 buffers, and A<sub>4</sub> is scanned in the same sequence as the columns of the keypad. The input line selected for enabling A<sub>3</sub> at the proper time is determined by the lower 4 bits of the data word stored in A<sub>5</sub>. Information stored in the microprocessor can now be processed by the calculator, providing the instructions are applied to Y<sub>1</sub>-Y<sub>4</sub> at a slow rate (the time it takes to depress a key manually). Time delays are therefore required, since the microprocessor can generate instructions much faster than the calculator can scan the keypad. The delays are provided by the program itself.

If the microprocessor is to be controlled by the calculator, its keypad rows are interrogated by A<sub>6</sub> and applied to the input port of A<sub>7</sub>. The keyboard columns are scanned and applied to the input port of A<sub>8</sub>.

As for the actual programming of the calculator by the microprocessor (in this case an 8000), a sample program is shown in the table. This program generates the digits 1 through 9 on the calculator's display in succession. When all digits are displayed, they blink three times. The sequence then repeats. Though this subroutine has little practical value, it demonstrates several characteristics of the software required for programming.

The program, stored in random-access memory, is switched to the starting address on page 0, and the restart address is entered on the keypad. The program is then initiated with an interrupt request to the microprocessor, which may be entered from the keypad if one of the unused function keys is wired appropriately for the interrupt code required.

The RST 6 branch instruction provides the calculator with ample time to complete a keypad scan between program steps. To absolutely prevent instructions from arriving at the calculator's input while an instruction is being executed, the test pin of the MCS2525/2526 can be connected to the microprocessor's wait input. Instructions A8, 35 simulate the two-key roll-over feature mentioned earlier. □

| MICROPROCESSOR / CALCULATOR TEST PROGRAM:<br>SEQUENTIAL DIGIT DISPLAY |             |             |   |          |                     |
|---|-------------|-------------|---|----------|---------------------|
| Label   | DH register | DL register | Op code   | Mnemonic | Comments            |
| RST 6   | 01          | 30          | 5F  | OUT 17   | Keyboard scan delay |
|   |             | 31          | 10  | INR C    |                     |
|   |             | 32          | 48  | JNZ      |                     |
|   |             | 33          | 31  | 31       |                     |
|   |             | 34          | 01  | 01       |                     |
|   |             | 35          | 07  | RET      |                     |
|   |             | ·           | ·   | ·        |                     |
| RST 7   | 01          | 38          | 0E  | MVI B    | Set first digit     |
|   |             | 39          | 11  | 11       | Set digit count     |
|   |             | 3A          | 26  | MVI E    |                     |
|   |             | 3B          | 1D  | 1D       |                     |
|   |             | 3C          | C1  | MOV AB   | Set display time    |
|   |             | 3D          | 1E  | MVI D    |                     |
|   |             | 3E          | E0  | E0       |                     |
|   |             | 3F          | 35  | RST 6    | Display sequence    |
|   |             | 40          | 18  | INR D    |                     |
|   |             | 41          | 48  | JNZ      |                     |
|   |             | 42          | 3F  | 3F       |                     |
|   |             | 43          | 01  | 01       | Release digit       |
|   |             | 44          | A8  | XRA A    |                     |
|   |             | 45          | 35  | RST 6    |                     |
| 46  | 08          | INR B       | Enter and display next digit if zero is not set |          |                     |
| 47  | C1          | MOV AB      |   |          |                     |
| 48  | BC          | CMP E       |   |          |                     |
| 49  | 48          | JNZ         |   |          |                     |
| 4A  | 3D          | 3D          | Enter clear                                     |          |                     |
| 4B  | 01          | 01          |   |          |                     |
| 4C  | 06          | MVI A       | Release clear                                   |          |                     |
| 4D  | 26          | 26          |   |          |                     |
| 4E  | 35          | RST 6       | Repeat subroutine                               |          |                     |
| 4F  | A8          | XRA A       |   |          |                     |
| 50  | 35          | RST 6       |   |          |                     |
| 51  | 3D          | RST 7       |   |          |                     |

# Synchronous counters provide programmable pulse delays

by R. E. S. Abdel-Aal  
Sunderland Polytechnic, Sunderland, England

In this circuit, cascade counters are digitally programmed to provide pulse delays of 50 nanoseconds to 3.25 milliseconds, accurate to within 50 ns. Selected by a 15-bit binary number, N, the delays can be ordered in 100-ns steps.

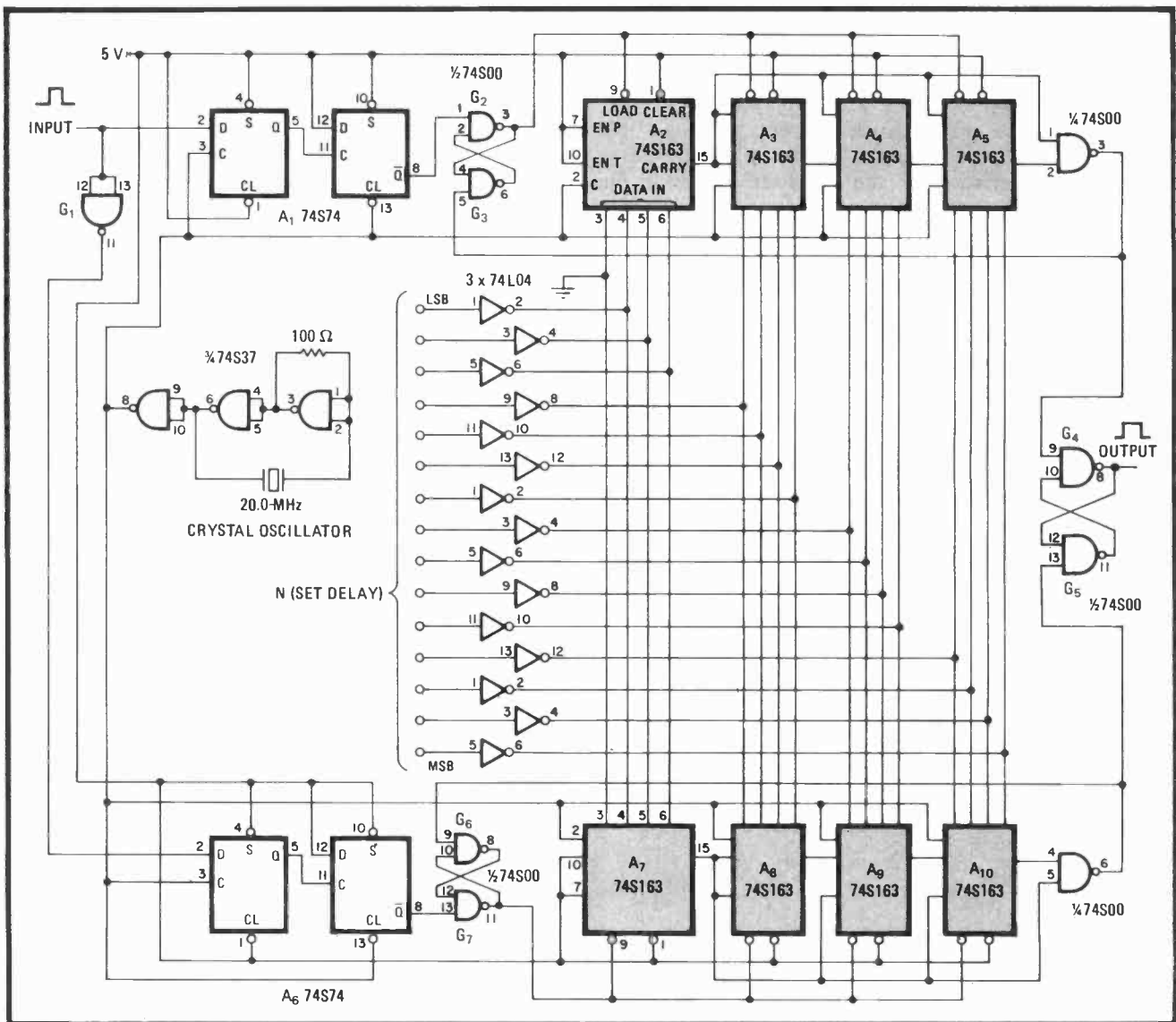
Two chains of synchronous counters, driven by a 20-megahertz clock, delay the input pulse's leading and trailing edge separately. Input pulses, which are asynchronous, are first applied to a dual D flip-flop, A<sub>1</sub>, as shown. A<sub>1</sub> generates a single negative-going clock pulse

when triggered by the 20-MHz clock. The pulse is used to set the bistable latch, G<sub>2</sub>-G<sub>3</sub>, thus enabling counters A<sub>2</sub>-A<sub>5</sub> to delay its leading edge.

A<sub>2</sub>-A<sub>5</sub> are wired to perform a fast look-ahead operation for the high-speed multistage counting required. To eliminate glitches that might upset the counter, the carry outputs of both A<sub>1</sub> and A<sub>5</sub> are brought to a NAND gate and then to G<sub>2</sub>-G<sub>3</sub>. This ensures the latch will be reset and the desired N value loaded into the counter only after the previous delay period is ended, despite the differential delays that exist in the signal path.

The input pulse is inverted by G<sub>1</sub> and applied to flip-flop A<sub>6</sub> for the counters that provide delay on the trailing edge of the pulse, A<sub>7</sub>-A<sub>10</sub>. G<sub>6</sub>-G<sub>7</sub> and A<sub>7</sub>-A<sub>10</sub> perform the function identical to G<sub>2</sub>-G<sub>3</sub> and A<sub>2</sub>-A<sub>5</sub>.

In actual operation, both counter chains are programmed by the set-delay lines, which are connected to their data-in ports. The delay time is given by  $T = 50(1 + 2N)$  ns. At the end of the delay period, N is



**Two-edge retardation.** Counter chains, of which one starts counting on arrival of the positive edge of an input pulse, the other on its negative edge, use a 20-MHz clock to provide repeatable delays of 50 ns to 3.25 ms on both edges of signal. Delays produced are accurate to within 50 ns. Amount of delay is selected with 15-bit word (M). Width of input signal to be processed must be at least 60 ns.

loaded into both counter chains. Note that the circuit is wired such that the N inputs must be active high, ensuring that maximum delay will correspond to a value of N that, when read as a number in standard binary form, is maximum.

Upon the arrival of the leading edge of the input pulse,  $A_2$ – $A_5$  count up, starting from the number loaded. Simi-

larly,  $A_7$ – $A_{10}$  count up on the trailing edge of the pulse. The carry pulse generated by  $A_5$  signifies the end of the delay period. This signal is united with the carry pulse generated by the trailing-edge counter  $A_{10}$ , at flip-flop  $G_4$ – $G_5$ . The signal at the output of  $G_4$ – $G_5$  thus has the same width as the input pulse, but is delayed by a period of time proportional to the number N. □

## Counter delivers data in signed or complemented form

by N. Bhaskara Rao  
U.V.C.E., Department of Electrical Engineering, Bangalore, India

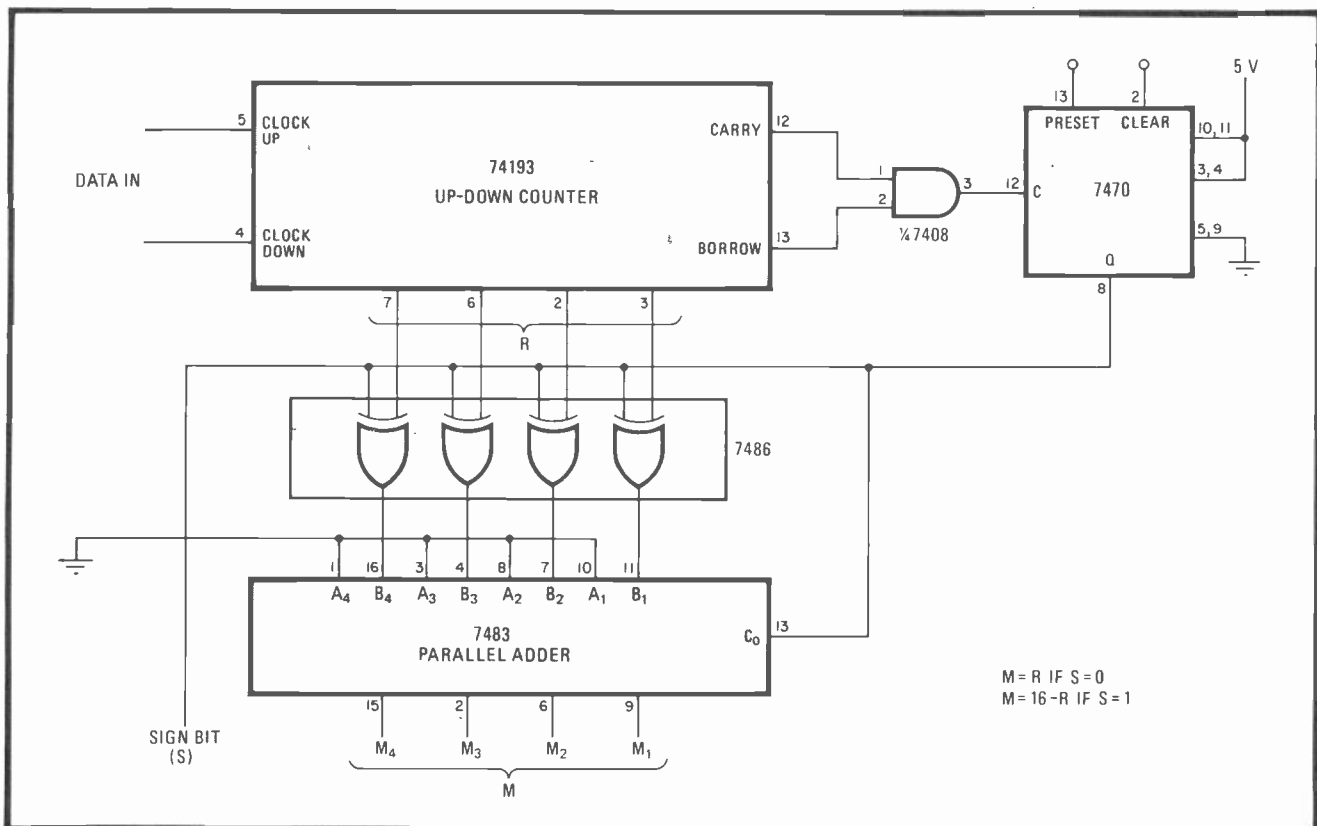
Adding one chip to the basic digital-averaging circuit proposed by Frazier [*Electronics*, Nov. 9, 1978, p. 114] forms a data counter whose outputs express a negative number not only by its magnitude and sign, but by its 2's complement as well. Expressing numbers in the latter form enhances the circuit's usefulness by allowing direct interfacing with computer circuits.

The circuit shown works differently from Frazier's, which generates a sign bit and reverses the direction of the count when the counter is about to move down

through zero. Instead, the 74193 is allowed to go below zero, where its R output becomes 15 and the state of its borrow output changes, thereby clocking the 7470 flip-flop. The 7470's Q output, which is the sign bit, S, then moves high.

The sign bit and the R bits are applied to the 7483 4-bit full adder (not part of the original circuit) through the 7486 exclusive-OR gates. The 7483 and 7486 together form an add-or-subtract unit. As a result, the output of the adder, M, will be equal to R if the 74193 indicates it holds a positive count ( $S = 0$ ), and will be equal to  $16 - R$  if the 74193 has gone negative ( $S = 1$ ).

If  $S = 0$ , the R bits, as seen at the output of the 74193, will represent the binary equivalent of the number. Any negative number will be represented by its 2's complement value and an enabled borrow bit. □



**Number forms.** Availability of any number in both binary equivalent or magnitude-sign forms enhance circuit's interfacing capability. Data generated by 74193, expressed as binary number (R bits), is converted into magnitude-sign form by add-or-subtract unit 7483–7486. R represents the 2's complement of any negative number when counter steps down through zero.

# C-MOS oscillator has 50% duty cycle

by Bill Olschewski  
Burr-Brown Research Corp. Tucson, Ariz.

Astable multivibrators built with complementary-metal-oxide-semiconductor gates suffer one major drawback—their duty cycle may vary from 25% to 75% because of the variations of each gate's switching-threshold voltage ( $V_{TH}$ ). Variations in the  $V_{TH}$  can be canceled and the desired square-wave output therefore attained by adding a C-MOS inverter and three resistors to the basic circuit. The gate-resistor combination uses negative feedback to perform the compensation.

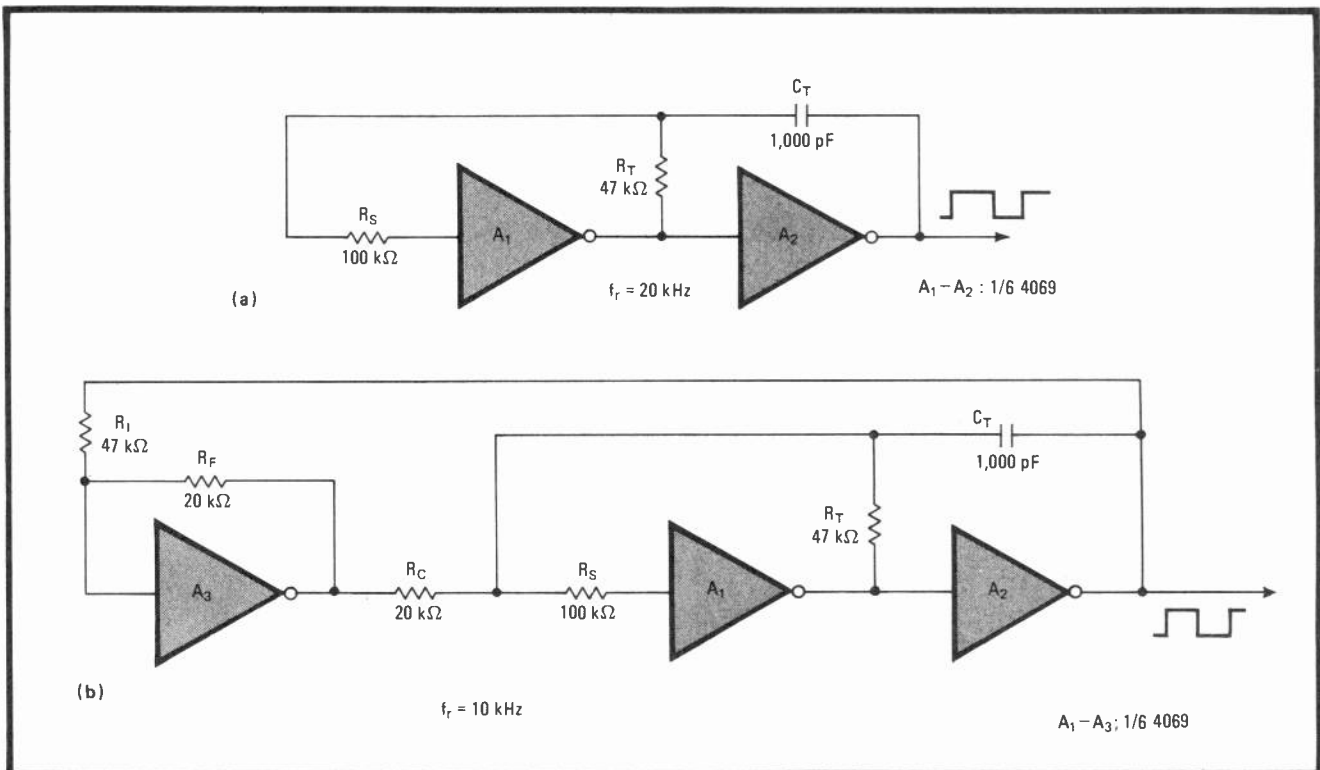
The standard astable multivibrator is shown in (a) of the figure. Running at a frequency ( $f = 1/2R_T C_T$ ) that is almost independent of the individual gate used, the circuit nevertheless has an unpredictable duty cycle because of a  $V_{TH}$  that can vary by up to 40% on either side of  $V_{DD}/2$ , where  $V_{DD}$  is the supply voltage. If a 50% duty cycle is required, either this circuit must be followed by an edge-triggered flip-flop, or each circuit must be individually adjusted using two trim pots and a

diode (see RCA application note ICAN-6267).

The circuit in (b) eliminates these drawbacks. Inverter  $A_3$  creates a second negative-feedback path around  $A_1$  (the signal flow through  $R_T$  constitutes the prime path).  $A_3$  is operated at a low closed-loop gain, much like an operational amplifier working in the linear portion of its characteristic. As a result,  $A_3$ 's inverted threshold voltage can be combined with the negative feedback voltage and injected into  $A_1$ . If the ratio  $R_F/R_1$  equals the ratio  $R_C/R_T$ , complete cancellation of threshold errors between  $A_1$  and  $A_3$  can be obtained. It is assumed that  $A_1$  and  $A_3$  are contained in the same package along with  $A_2$  and that their  $V_{TH}$ s are essentially equal.

Since  $A_3$ 's gain must be set so that its output will not saturate with a  $\pm 40\%$  variation of  $V_{TH}$ , resistor values must be selected so that  $R_1/R_F = 2.33$ . At the same time, the correct gain for  $A_3$  is set when  $R_C R_1 = R_F R_T$ . In these circumstances, and ignoring stray and input capacitances, the multivibrator's operating frequency will be  $f = 1/R_T C_T$  and the duty cycle will be 50%.

Note that the operating frequency, in this case 20 kHz, is twice that of the standard astable circuit using the same values of  $C_T$ ,  $R_T$ , and  $R_S$  because of the second feedback path. □



**Right on.** Standard astable multivibrator using C-MOS gates (a) has unpredictable duty cycle because of variable switching-threshold voltages. Adding inverter and three resistors (b) creates second negative feedback path around  $A_1$ , forcing  $A_1$  and  $A_2$ 's switching point to half the supply voltage, so that 50% duty cycle is attained and square waves are produced.

# Epitaxial phototransistor with feedback has fast response

by Vernon P. O'Neil  
 Motorola Inc., Discrete Semiconductor Division, Phoenix, Ariz.

A high-gain negative-feedback loop will reduce the response time of an epitaxial phototransistor to 100 nanoseconds—a significant improvement over several schemes previously suggested.<sup>1,2,3</sup> Because of its construction, the epitaxial device all but eliminates the diffusion of carriers into its depletion region from the bulk collector region, which slows a conventional non-epitaxial phototransistor's operating speed. And added feedback reduces the input-signal swing across the collector-base junction to 1% of what it is normally, further reducing the input-capacitance charge and discharge times.

The MRD 300 phototransistor shown in the circuit has a typical rise time of 2.5 microseconds and a fall

time of 4  $\mu$ s if operated in the conventional emitter-follower configuration. In this modified circuit  $Q_2$  serves as the feedback amplifier that keeps the base of the phototransistor at an almost constant voltage for changes in input-signal level. Thus the effective input capacitance that must be charged and discharged is reduced.  $Q_3$  serves as a buffer. Note that using feedback that is negative enables the switching times to be maximally reduced without fear of creating instability (that is, oscillations can be generated with circuits using positive feedback).

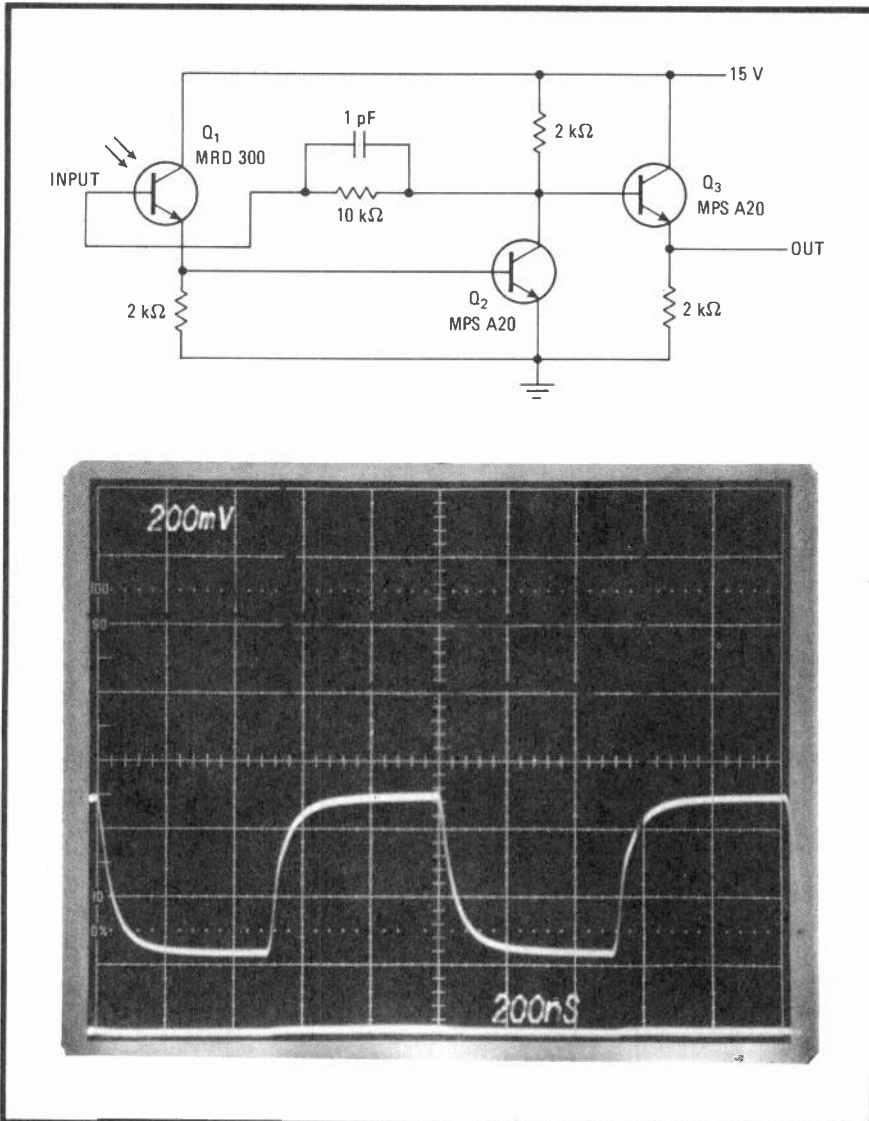
With this circuit, both the rise time and the fall time of the phototransistor are reduced to 100 ns. The output voltage is equal to the product of feedback resistance (10 kilohms) and the collector-base photocurrent. The photograph shows a typical output waveform.

As for the phototransistor itself, it can be hard to determine from data sheets if one is epitaxial or not. The best way to find out is to consult the manufacturer. □

#### References

1. "Why not a cascode optocoupler?", Electronics, March 2, 1978, p. 132.
2. "Why not a cascode optocoupler? Here's why not", Electronics, April 27, 1978, p. 154.
3. "Bootstrapping a phototransistor improves its pulse response", Electronics, Aug. 17, 1978, p. 105.

**Speedy.** Collector-to-base capacitance of phototransistor  $Q_1$  is reduced by employing epitaxial device (MRD 300) and high-gain negative feedback ( $Q_2$ ), so that operating speed can be increased. Emitter-follower  $Q_3$  provides low-impedance output. Photograph shows typical output response.



# Hybrid servo system minimizes hunting

by C. V. Rajaraman  
ISRO, Trivandrum, India

Although the shunt comparator circuit of Vojnovic<sup>1</sup> is simple and tends to reduce the overshoot and hunting problems inherent in a high-speed digital servo system, difficulties may arise when the servomechanism is continually called upon to follow small changes in position. Digital subtraction circuits, on the other hand, will increase system stability but are more expensive and very complex. But the two most popular techniques for synthesizing the control circuit—the no-shunt comparator method and the aforementioned subtractor method—can be combined to form a hybrid system that is more accurate than the first and less complex and costly than the second.

As shown in the figure,  $A_1$  and  $A_2$  compare lines 5–12 (the coarse bits) of a 12-bit command input with their feedback-data counterparts, which are derived from the motor position by a shaft encoder. Comparing the coarse

bits in this manner enables the system to converge quickly on the desired position.

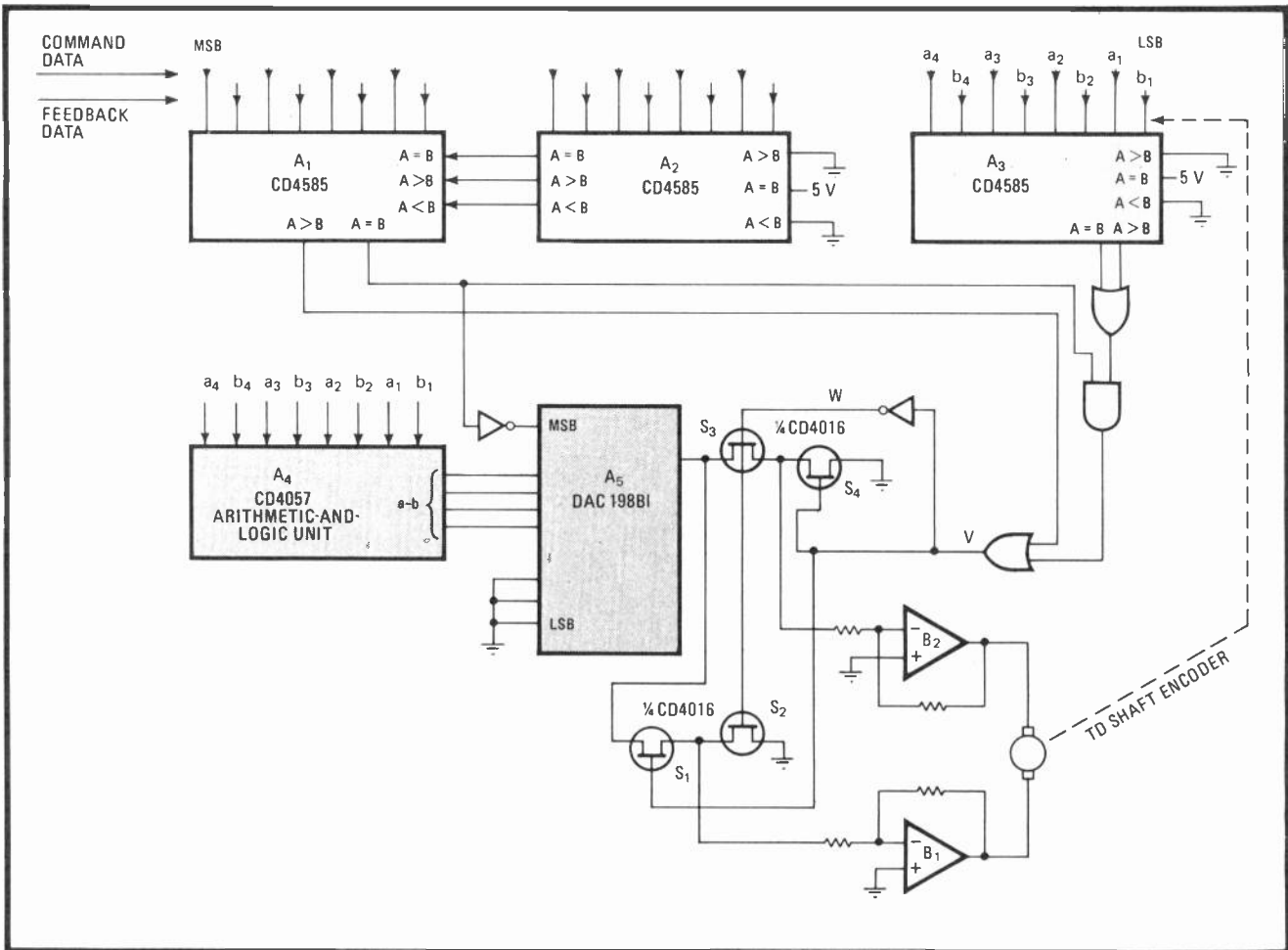
At the same time, the low-order (fine) bits of the command word are compared by  $A_3$ , and  $A_4$  is programmed to find  $a \sim b$ , the difference between the two 4-bit binary words. The  $a \sim b$  result is then transformed into an equivalent analog signal by the digital-to-analog converter,  $A_5$ . Using the d-a converter allows a precise voltage to be applied to the motor, instead of the constant-magnitude (logic 1) signal that a comparator-type circuit would generate whenever there was an  $a \sim b$  offset of any value. Thus the motor has little tendency to overshoot its intended mark.

As for transferring the voltage from the converter to the motor,  $V$  moves high either when the coarse-bit comparison yields  $A = B$  and the state between the fine bits are such that  $A = B$  or  $A > B$ , or when just the coarse-bit comparison yields  $A > B$ .

Under these conditions,  $S_1$  and  $S_4$  turn on, and operational amplifier  $B_1$  moves high to drive the motor. Under any other bit-comparison condition,  $W$  moves high and turns on  $S_2$ ,  $S_3$ , and  $B_2$ , to drive the motor in the other direction. □

### References

1. B. Vojnovic, "Shunt comparator stabilizes high-speed digital servo," *Electronics*, March 16, 1978, p. 149.



**End of search.** Comparators and subtractor in servo position motor without oscillations. Comparison of high-order bits enables motor to converge on desired location. Fine-bit comparison with a d-a converter resolves precise feedback voltages to minimize overshooting.

# Peak detector recovers narrow pulses accurately

by Jerome Leiner  
Loral Electronic Systems, Yonkers, N. Y.

This peak detector can accurately process input data pulses as narrow as 50 nanoseconds and as high as 3 volts. The recovered voltage is always within 1% of the input signal's true value.

In the circuit shown, emitter-coupled logic generates a -0.2- to -3-volt signal for input into amplifier A<sub>1</sub>. Assuming a pulse with a 50-nanosecond width and a rise and fall time of 5 ns, that leaves storage capacitor C<sub>4</sub> only 45 ns in which to charge. The LH0024 op amp used for A<sub>1</sub> has wide bandwidth and a high slew rate to accommodate the fast charging required.

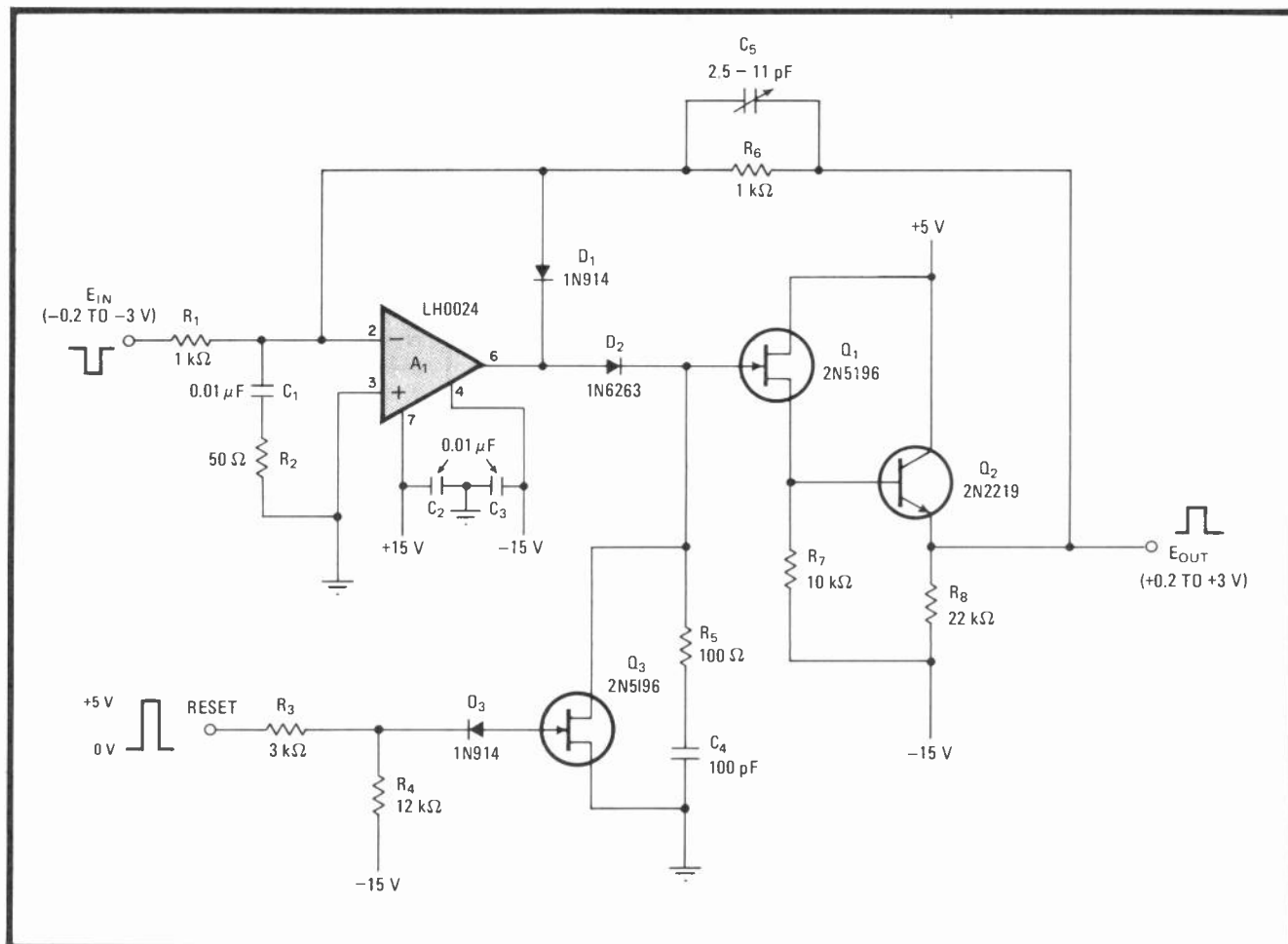
Q<sub>1</sub> acts as a buffer to prevent C<sub>4</sub> from discharging through R<sub>7</sub> between system reset pulses. The voltage at Q<sub>1</sub> appears at Q<sub>2</sub> and is fed back to A<sub>1</sub>, to be compared with E<sub>in</sub>. When E<sub>out</sub> reaches E<sub>in</sub>, D<sub>2</sub> becomes back-biased and the stored charge is held until C<sub>4</sub> is intentionally discharged by the reset signal. D<sub>2</sub> remains back-biased during discharge.

A<sub>1</sub> is normally used as an amplifier, and so it will be driven into negative saturation whenever the input signal drops below the output level. D<sub>1</sub> prevents this by clamping the amplifier output.

C<sub>1</sub> and R<sub>2</sub> provide A<sub>1</sub> with input- and feedback-signal stabilization. C<sub>3</sub> compensates for A<sub>1</sub>'s input capacitance. Note that if C<sub>1</sub>R<sub>2</sub> were placed at the output of A<sub>1</sub>, a larger charging current would be required for a given input signal. Because this current is usually limited, A<sub>1</sub>'s effective slew rate would be reduced.

The peak detector is optimized by shorting D<sub>2</sub> and then adjusting C<sub>1</sub>, R<sub>2</sub>, and C<sub>3</sub> for minimum overshoot and ringing on a series of fast data pulses. □

**Fast and precise.** Using one op amp, one transistor, and two field-effect transistors, peak detector recovers data pulses having amplitudes of up to 3 volts and widths as narrow as 50 nanoseconds. Output voltage is within 1% of the input data's true value under all signal conditions.



# Optoisolator initializes signal-averaging circuit

by J. Ross Macdonald, Department of Physics and Astronomy, University of North Carolina, Chapel Hill

Long-term averaging circuits require an initializing voltage on their capacitive storage element in order to become almost immediately operational on power up. Here, an optoisolator is used to quickly charge the capacitor with a voltage derived either from the input signal itself or from any dc voltage, the two sources most widely used. The optoisolator circuit is superior to an initializer that uses a relay, which, besides having the disadvantage of being electromechanical, also draws power continuously.

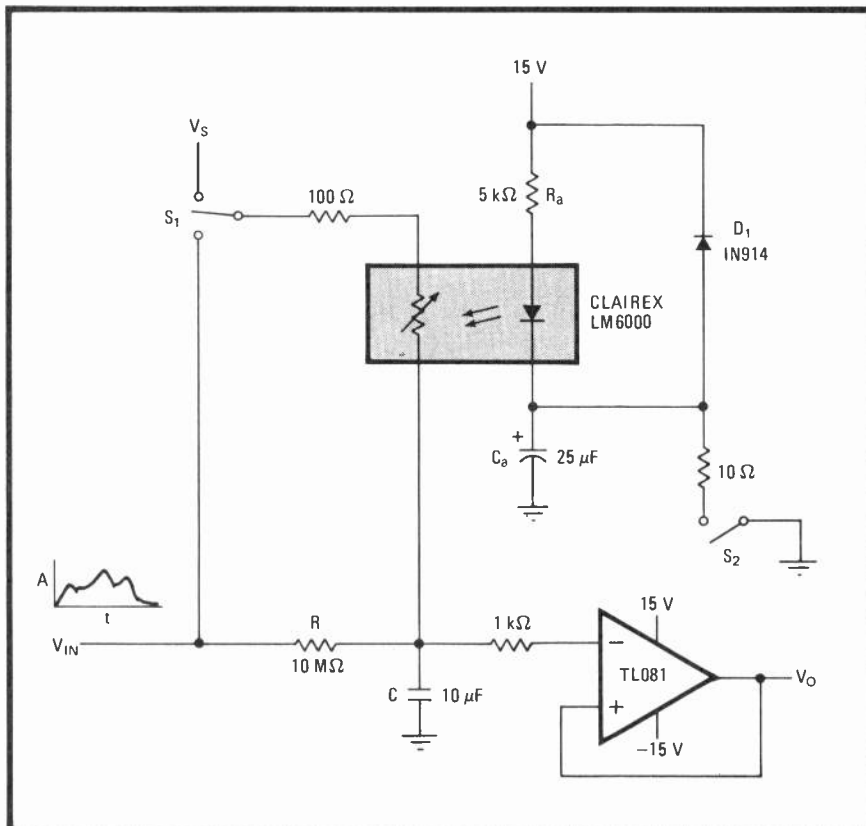
In a circuit that averages a signal over a long period (see figure), the resistor-capacitor (RC) time constant may be on the order of a minute or more. Thus, the output of the averager ( $V_o$ ) during the time  $t = 0-1$  minute is considered to be the circuit's transient response to the input signal, where  $t$  is measured from the time that power is applied to the circuit. In most cases, especially when the circuit is part of a more complex system, it is not feasible to wait that long before the RC

network starts generating a true average value.

The difficulty may be circumvented by using an optoisolator and a switch,  $S_1$ , to charge  $C$  on power up. Assume it is desired to charge  $C$  from a dc voltage,  $V_s$ . When power is applied,  $C_a$ , which may be 25 microfarads or more, is charged through  $R_a$ . Consequently, as current flows through the photodiode, the value of the photoresistance element in the LM 6000 optoisolator is reduced from more than  $10^9$  ohms to about 1 kilohm. Thus, in a few tens of milliseconds,  $C$  charges to  $V_s$  through the element, if  $S_1$  is placed in the  $V_s$  position. As  $C_a$  becomes fully charged, the resistance of the element quickly increases to at least  $10^9$  ohms, and the circuit is ready to operate in its intended averaging mode.

When power is removed,  $C_a$  discharges through  $D_1$ , so that the on-off power cycle can be repeated fairly rapidly.  $C$  also discharges slowly through  $R$ . This action is of little consequence in circuit operation on a subsequent power up. Note that  $S_2$ , a momentary-contact switch, allows the resetting process to be repeated at any time, even while the circuit is active.

To initialize  $C$  from the input signal, it is only necessary to connect  $S_1$  to  $V_{in}$  prior to power up (or at any time if  $S_2$  is utilized). Otherwise the initializing operation is the same as before. □



**Speedy average.** Optoisolator enables long-term averager to operate almost immediately after power up by presenting an initializing voltage to circuit's sampling capacitor,  $C$ . Charge is introduced through isolator's low-resistance photoelement. Either a dc voltage or the input signal can be used as the initializing source.



## Five-state LED display monitors paging system

by D. F. Fleshren  
Springfield, Va.

This paging station circuit uses a single red- or green-light-emitting diode to alert the user to any of five distinct paging conditions. It is a simple, extremely easy-to-build monitor designed to be part of a large paging system. Two relays and a 555 timer send a signal to the LED (a Monsanto MV5491 or Xciton XC5491) to produce the following signals:

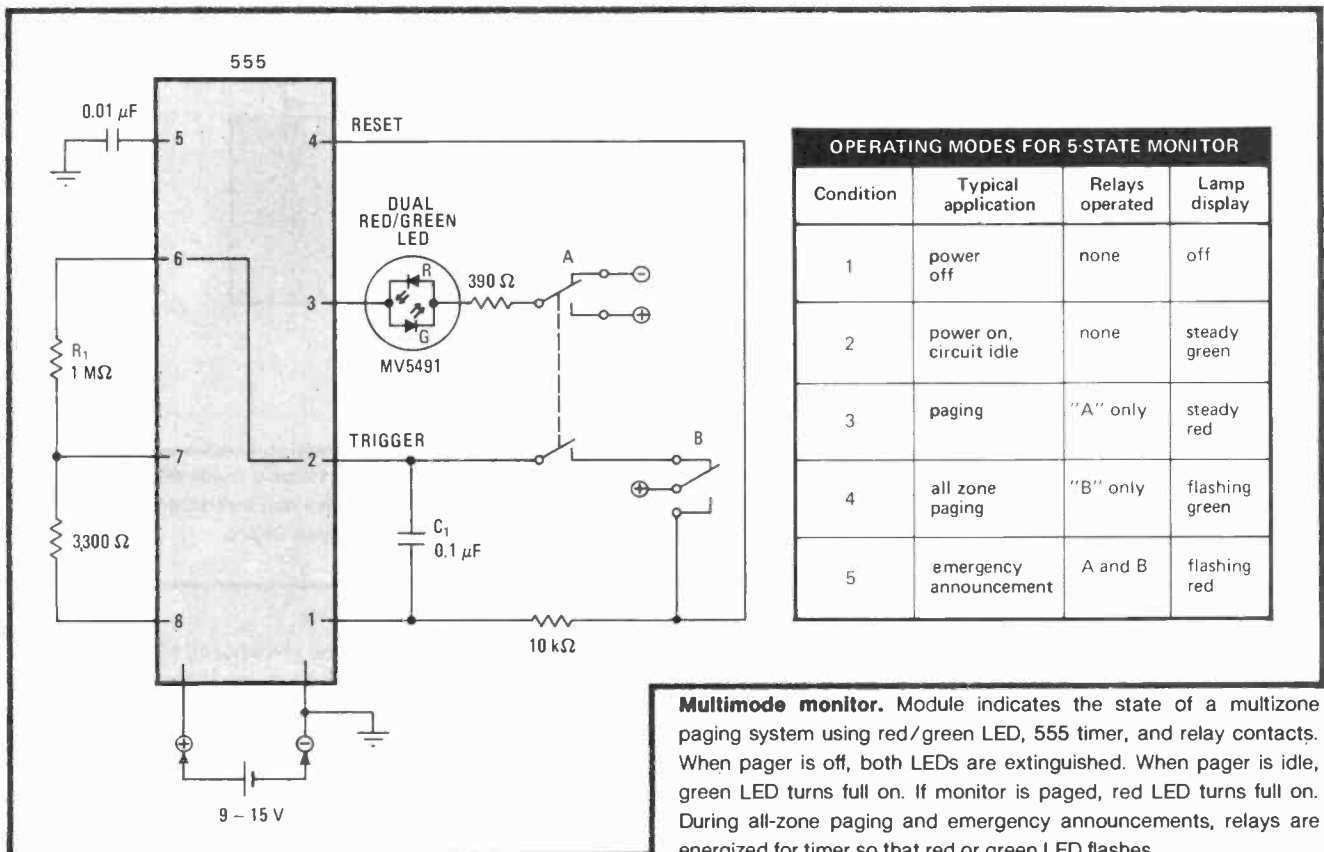
- Off (no power) indicates that paging has been cut off to that station or the region in which it is located.
- Steady green signifies that the station is operational, but is not being paged.
- Steady red is the individual station's paging signal.

- Flashing green tells the user that all stations in the system are being alerted.
- Flashing red signals an emergency situation to all monitoring stations.

An external signal triggering relay A controls the color of the LED, changing it from its green (idle) condition to red. Relay B is excited when all stations are to be called. This second relay puts the 555 timer in the astable mode, changing the LED's usual dc state to an on-off oscillation of about 7.5 hertz at a duty cycle of 50%. The frequency of oscillation can be adjusted by suitably selecting  $R_1$  and  $C_1$ . In the emergency red flashing mode, both relays must be tripped by external signals.

This circuit can readily be adapted to signal a single panel-mounted lamp. To derive the five operating modes, the relay contacts must be replaced by the contacts on a suitably wired rotary switch.

Supply voltage for the 555 may vary from 9 to 15 volts; with a 12-v supply, current drain is about 40 milliamperes. □



## Rate multiplier controls noninteger frequency divider

by Michael F. Black  
Texas Instruments Inc., Dallas, Texas

Frequency dividers capable of dividing by integer and noninteger values can be built inexpensively from very few parts now that synchronous binary rate multipliers are available on single chips. To increase the resolution of the noninteger value, the rate multipliers are simply cascaded.

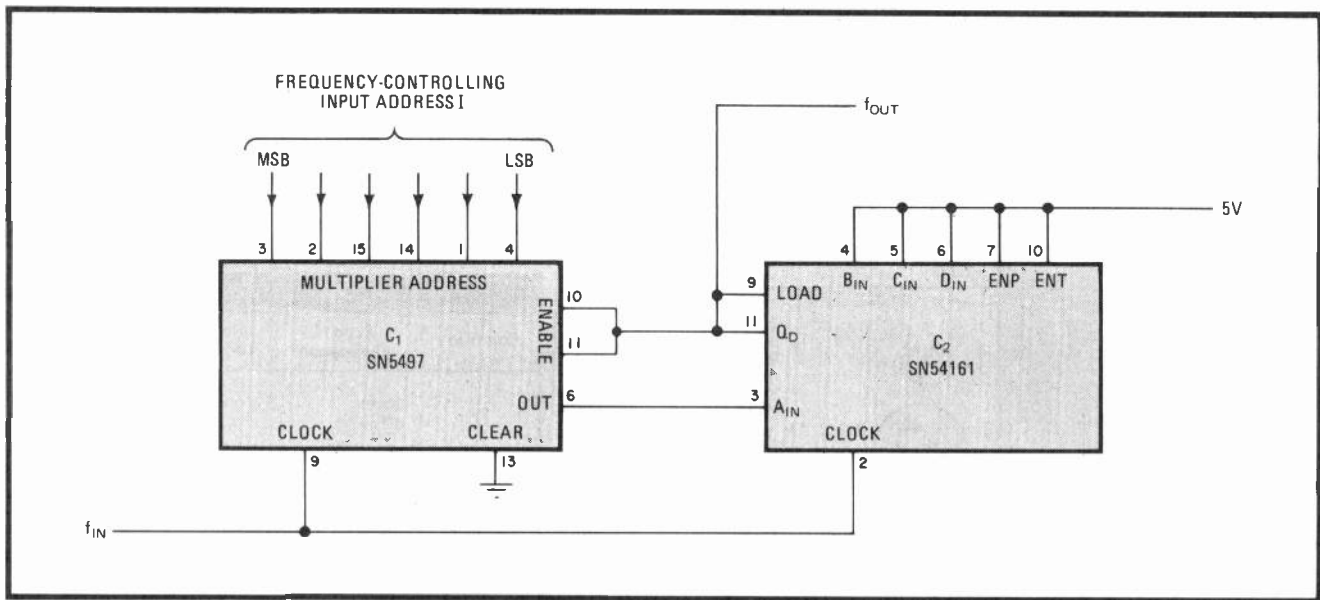
The ratio at which division is performed is set in an indirect manner by the 5497 rate multiplier. This number lies between two values preset in the 54161 synchronous counter,  $n$  and  $n - 1$ . The circuit divides the input frequency by a ratio directly proportional to the time the counter spends in the  $n$  mode versus the time it spends in the  $n - 1$  mode.

The number of input pulses rate multiplier  $C_1$  passes to synchronous counter  $C_2$  is proportional to input address  $I$ . In this instance the counter is preloaded at either 14 or 15 by inputs  $A_{in}$  through  $D_{in}$ .  $C_1$ 's output (pin 6) is connected to the counter's input  $A_{in}$ . Address  $I$  consequently controls the percentage of time the counter spends at divide values  $n = 2$  and  $n = 3$ .

The rate multiplier's pulse-train output frequency is  $f = f_{in}(I/M)$ , where  $M$  is the size of the rate multiplier (in this case  $2^6 = 64$ ). This particular circuit configuration results in  $f_{out} = M(f_{in})/(nM - I)$ . The actual divide ratio is  $n' = n - (I/M)$ .

The value of  $M$  determines the size of the available frequency step. The circuit as shown has been used to set  $f_{out}$  from 4 to 6 megahertz in steps of about 30 kilohertz; adding one more six-line rate multiplier would bring the step size down to about 400 hertz. Frequency steps in hundredths of a hertz can be easily obtained by cascading more multipliers.

This divider circuit will generate the exact number of clock pulses per second desired, but there will be some phase jitter, with  $\Delta\phi = 360/n$ .  $\square$



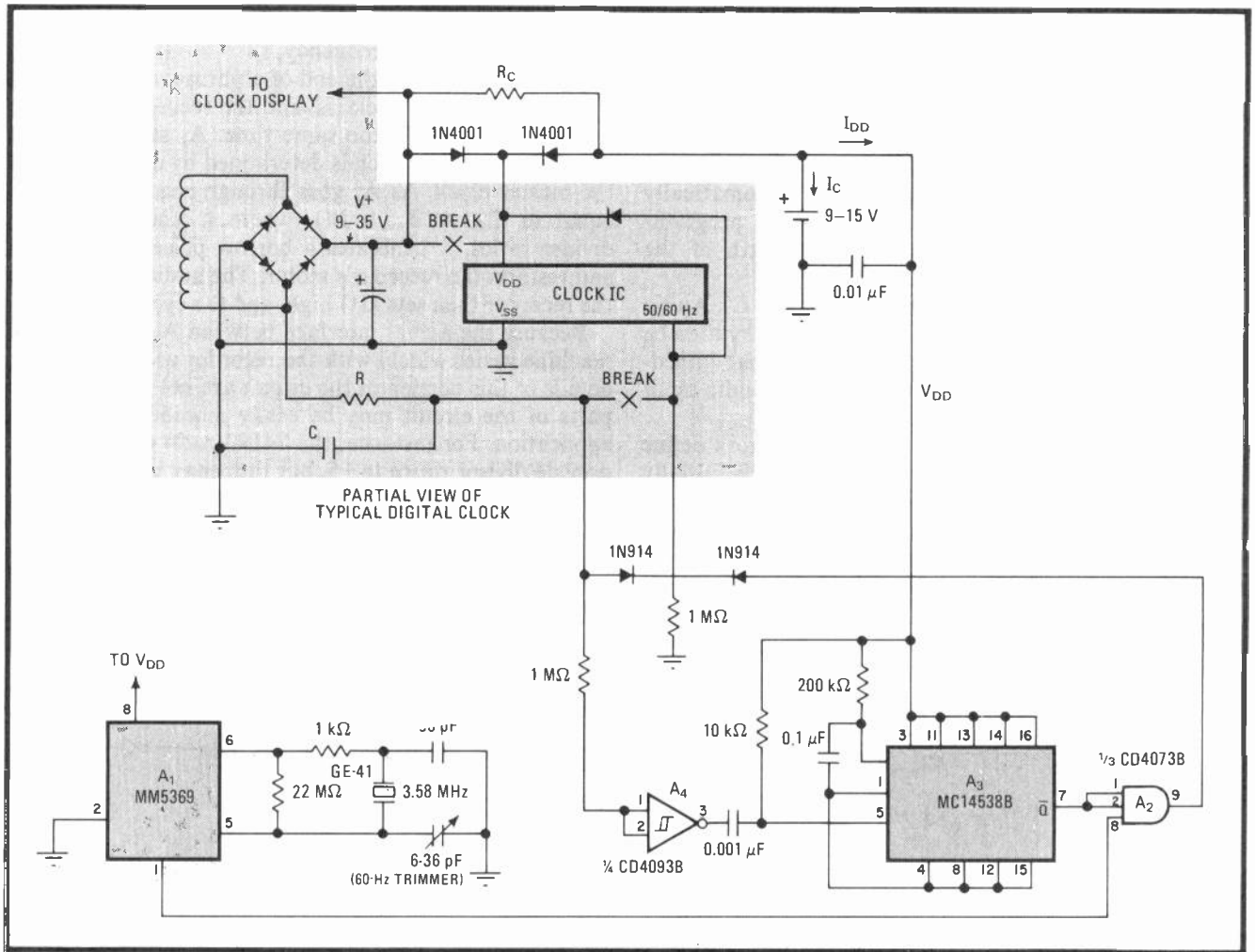
**Continuous division.** Synchronous frequency counter uses rate multiplier in two-chip circuit to program circuit's divide ratio at any value. Output frequency is proportional to the time spent between two preset divide values,  $n$  and  $n - 1$ . Multipliers can be cascaded for step-size resolution all the way down to hundredths of a hertz. The amount of phase jitter at the output, in degrees, equals  $360/n$ .

## Standby crystal time base backs up line-powered clock

by William D. Kraengel, Jr.  
Valley Stream, N.Y.

This battery-powered, crystal-controlled time base provides accurate and glitch-free performance when it takes over as the 60-hertz frequency standard that drives a digital clock during a power outage. The cost of the unit is about \$7.

More long-interval timing circuits would probably use the ac power line as a time base because of its long-term average-frequency accuracy (1 part in  $10^7$ ), were it not



**Standby standard.** Battery-powered, crystal-controlled time base, having sufficient accuracy for most short-term applications, takes over clock-driving duties of digital chronometer in event of ac power loss. Unit uses 3.58-MHz oscillator, which is divided down to 60 hertz.

for the transients and blackouts that occur frequently. This back-up time base takes over smoothly in such instances and has sufficient accuracy over a period of several hours to satisfy all but the most demanding applications.

The standby time base uses a low-cost crystal oscillating at 3.58 megahertz, which is generally the frequency required for the color-burst circuits in standard television receivers. The frequency produced by the crystal's programmable oscillator-divider chip, A<sub>1</sub>, is 60 hertz. This signal is fed to one input of an AND gate, A<sub>2</sub>, which is activated if line power is lost.

During normal operation, the battery is trickle-charged (I<sub>c</sub>) by the clock's supply through R<sub>c</sub>, at a rate of 0.01 C, where C is the capacity of the battery in ampere-hours. R<sub>c</sub> is equal to  $(V^+ - V_{bat}) / (I_c + I_{DD})$ , where I<sub>DD</sub> = 2.5 milliamperes. The digital clock must be modified slightly, as shown, in order to lengthen the charge life of the battery. Thus the digital clock's display will be blanked while the battery is the power source.

Meanwhile, one-shot A<sub>3</sub>, configured as a missing-pulse detector, is triggered by Schmitt trigger A<sub>4</sub> at the beginning of each cycle of the ac input.

The one-shot's pulse width is 20 milliseconds, slightly longer than the period of the 60-Hz line input. Thus, A<sub>3</sub> is continually retriggered, and so A<sub>2</sub> is disabled.

With a loss of line power, the battery takes over the supply chores. A<sub>3</sub> times out, and then A<sub>2</sub> is enabled, so that the 60-Hz signal derived by the crystal circuit drives the digital clock's timing chip. The maximum length of time between the power outage and the first clock pulse from the standby unit is 8.3 milliseconds.

Almost the reverse action occurs when the ac line power is restored. When the filter capacitor in the clock's power supply recharges enough for the line pulses to rise above the set threshold of the Schmitt trigger, the one-shot is triggered, and the AND gate is disabled. As the voltage across the filter capacitor rises further, the power source duties revert back to the digital clock's power supply. □

# Controller halts playback when taped voice pauses

by N. Bhaskara Rao  
U.V.C.E., Department of Electrical Engineering, Bangalore, India

Few typists can transcribe a dictated message or speech without stopping the tape recorder from time to time. The illustrated circuit stops the recorder automatically at the end of a sentence or other pause. Its programmable halt time is proportional to the length of the preceding playback segment.

The circuit is preset on power up by  $R_1$  and  $C_1$ . Audio signals from the output of the tape recorder may then be fed into a buffer amplifier having a low output impedance, so that a dc voltage proportional to the audio input is produced by the full-wave rectifier,  $D_1$  and  $D_2$ .

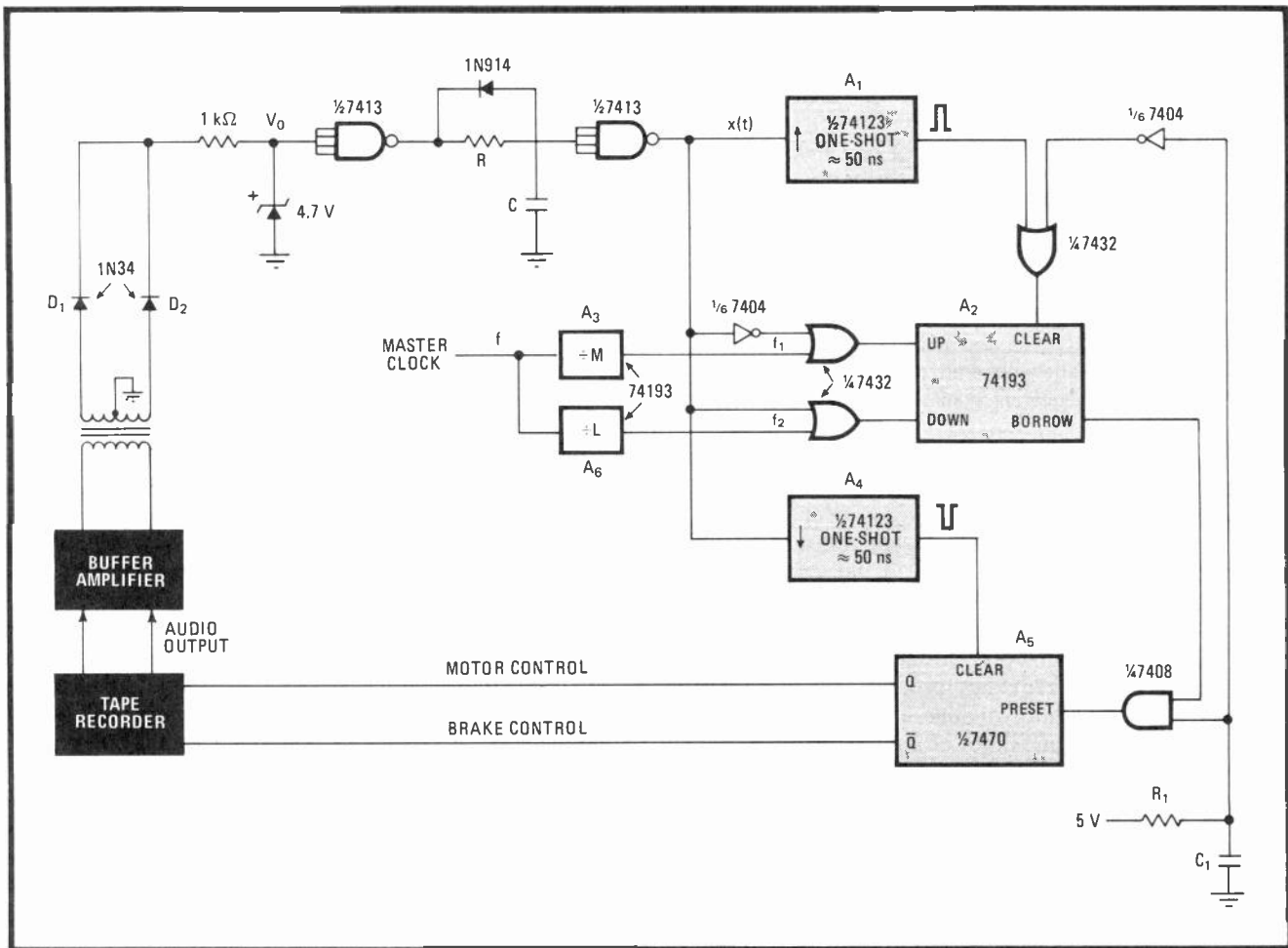
The 7413 Schmitt triggers and an RC network define the time delay,  $T$ . The voltage at  $x(t)$ , which is initially set high by the audio signal, goes low when  $V_0$  is low for a period greater than  $T$ , so that any pause in the audio signal triggers the recorder-halting circuit. The delay time selected may be varied for the particular applica-

tion by adjusting one or both elements of the RC network.

As one-shot  $A_1$  is triggered by  $x(t)$ ,  $A_2$  is cleared and starts to count up. If the time during which  $x(t)$  is high is  $T_{on}$ , then the output of  $A_2$  at the end of that period is given by  $N = f_1 T_{on}$ , where  $f_1$  is derived from divider  $A_3$  and the master clock frequency,  $f$ .

As  $x(t)$  goes low at the end of a phrase, one-shot  $A_4$  is triggered, flip-flop  $A_5$  clears, and the recorder's motor is braked to a halt. At the same time,  $A_2$  starts to count down at a rate,  $f_2$ , which is determined by divider  $A_6$  and the master clock. As  $A_2$  goes through zero after a time equal to  $T_{off} = T_{on}(L/M)$ , where  $L$  and  $M$  are the divider ratios, it generates a borrow pulse that sets  $A_5$  and restarts the recorder's motor. The audio output from the recorder then sets  $x(t)$  high, and the cycle repeats.

Because the actual interface between  $A_5$  and the tape machine varies widely with the recorder used, the wiring details of this portion of the circuit are not shown. Other parts of the circuit may be easily modified to suit the application. For instance, the 74193 ratio counters each provide divisor ratios to 15, but they may be replaced by dividers that provide any value of  $L$  and  $M$ . □



**Pausing for write time.** Unit brakes tape recorder's drive after each sentence of taped message to provide transcription secretary with time to write information. Circuit uses up-down counter to derive a halt time proportional to the length of the preceding playback period.

## Micropower regulator has low dropout voltage

by Kelvin Shih  
General Motors Proving Ground, Milford, Mich.

Designed specifically to regulate the output of lithium batteries, which have a low terminal voltage at low temperatures, this circuit provides a stable 5.0 volts at 10 milliamperes for an input voltage as low as 5.2 v.

The low dropout voltage of the regulator ( $5.2 - 5.0 = 0.2$  v) is attained in part by operating the circuit's output transistor in the common-emitter mode. As a result, its collector-to-emitter voltage drop is much lower than the base-to-emitter drop of transistors operated as emitter followers in standard regulators. And, because it uses a low-power operational amplifier operating from a single supply, and a low-current, low-voltage zener diode for

the voltage reference, the regulator's idle current is only 250 microamperes.

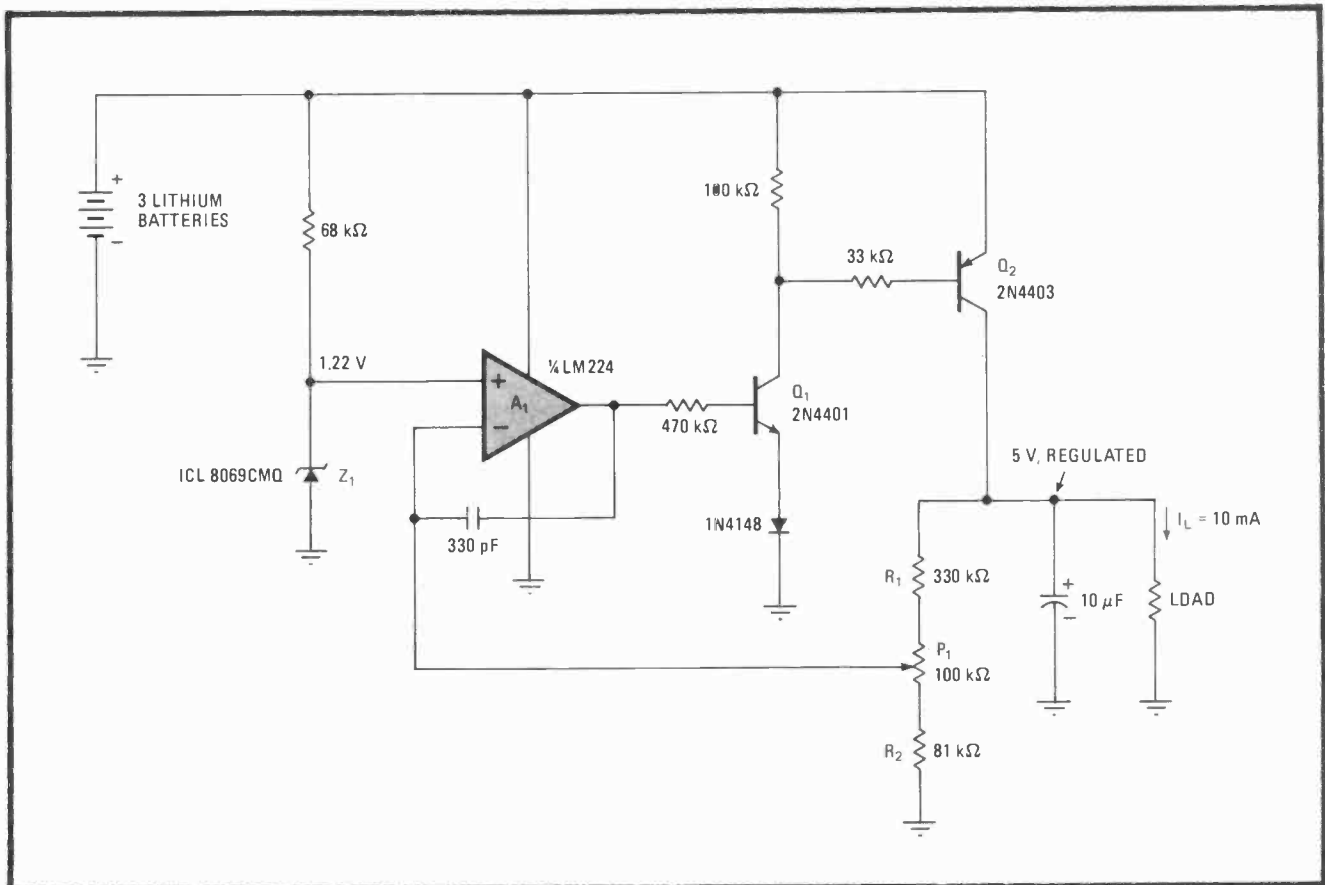
Three lithium batteries drive the regulator shown in the figure. Their terminal voltage is usually 3 v per cell at room temperature, but it will drop to 2 v at  $-40^{\circ}\text{C}$ .

$Z_1$  provides a low-voltage reference (1.22 v) to the noninverting input of the LM224 op amp,  $A_1$ . The Intersil ICL 8069CMQ zener has been selected because it requires only  $50\ \mu\text{A}$  of bias current and has a temperature coefficient of better than 50 parts per million/ $^{\circ}\text{C}$ .

The 1.22-v reference is compared to the output voltage from a divider network ( $R_1, R_2, P_1$ ), which is used to trim the output voltage to the desired value. Any voltage difference appearing at the output of  $A_1$  drives transistor  $Q_1$ , and thus determines the drive current to  $Q_2$ . As a result,  $Q_2$  conducts more heavily if the output voltage is low, or limits the application of battery voltage to the load if the output voltage is high.

There will be no observable change of output voltage for an input voltage variation between 5.2 and 10 v, over the temperature range of  $-40^{\circ}\text{C}$  to  $+70^{\circ}\text{C}$ . □

**Dropout minimum.** Voltage regulator for lithium batteries maintains 5-volt output for a minimum input voltage of 5.2 v. Output voltage is constant over the temperature range  $-40^{\circ}\text{C}$  to  $+70^{\circ}\text{C}$ . Using a low-power op amp operating from a single-ended supply, and a low-current zener, the circuit holds the idle current to  $250\ \mu\text{A}$ , well below the 2 to 10 mA required by standard regulators.



# Missing-pulse detector handles variable frequencies

by Joe Lyle and Jerry Titsworth  
*Bendix Corp., Aircraft Brake and Strut Division, South Bend, Ind.*

Virtually all missing-pulse detectors require an input signal of fixed frequency in order to operate satisfactorily. They malfunction when the input frequency varies because their circuits employ detection networks that have a fixed time constant. Through the implementation of inexpensive voltage-to-frequency and frequency-to-voltage converters to derive an average, or reference, frequency that tracks the input signal, this circuit can pinpoint missing pulses without being affected by input frequency variations.

As shown in the figure,  $A_1$  and  $A_2$  establish the reference frequency,  $f_{ref}$ , using input frequency  $f_{in}$ . Miss-

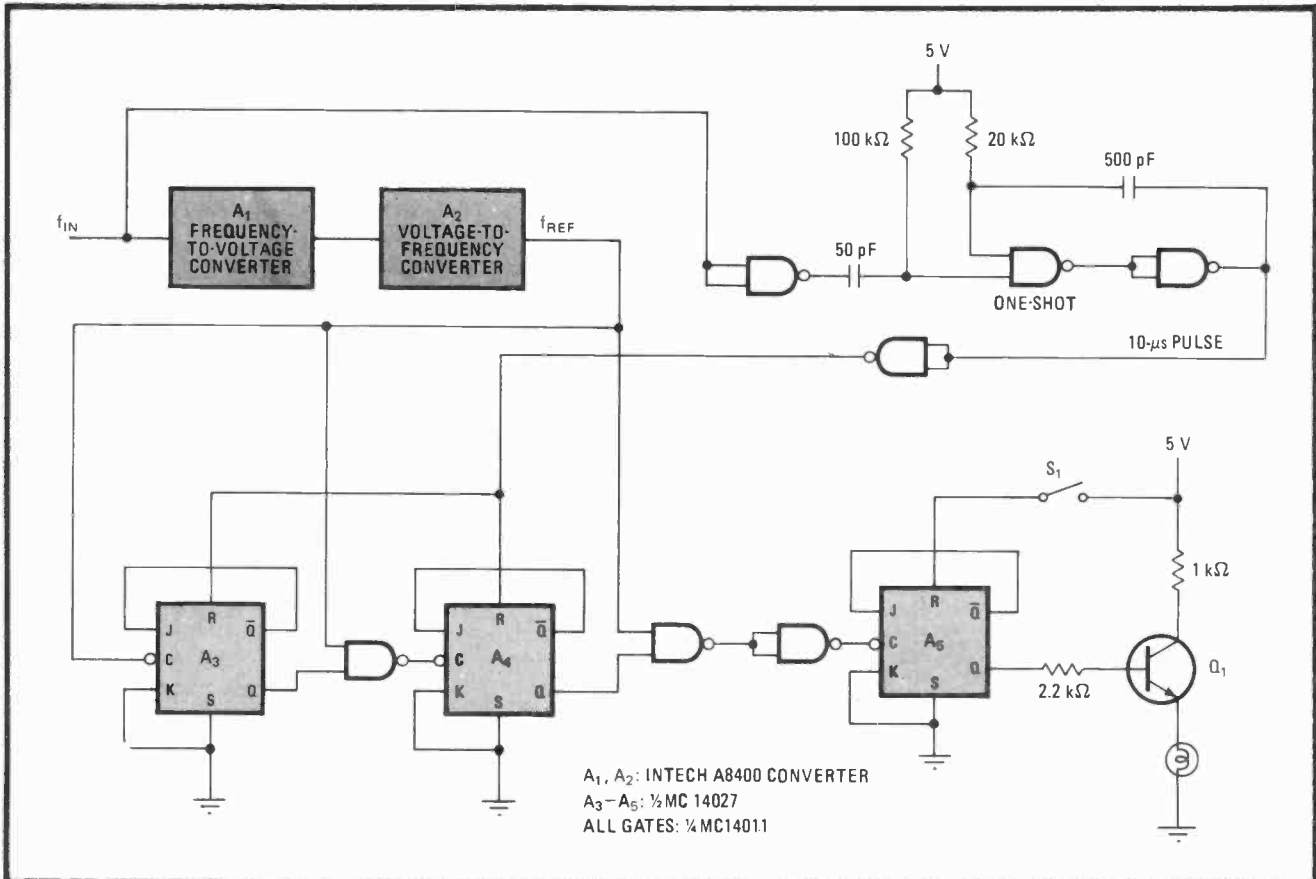
ing pulses do not change the reference because of the integrating capacitors within the converters. Meanwhile, the three NAND gates comprising the one-shot produce pulses of 10 microseconds in duration, with a frequency determined by the input signal.

The chip labeled  $A_4$  is clocked by  $f_{ref}$  and  $A_3$  through a NAND gate. As long as the input train is continuous, the Q output of  $A_4$  is low. If a missing pulse is detected, however, the one-shot will not generate a pulse to the reset pin of  $A_3$ , and the Q output of  $A_3$  (which is also clocked by  $f_{ref}$ ) will go high to clock  $A_4$ .  $A_4$  and  $f_{ref}$  will then switch  $A_5$ 's Q output to high.

This turns on transistor  $Q_1$  and the pilot lamp glows. Switch  $S_1$  is used to reset the circuit after a missing pulse has been detected. Note that circuit operation remains independent of the input frequency, since the arrival of  $f_{ref}$  and the 10- $\mu$ s pulse at  $A_3$  is synchronized to  $f_{in}$ .

The circuit should be calibrated by setting  $A_1$  for an output voltage of 10 when a 10-kilohertz input signal is applied. Similarly,  $A_2$  should be set to generate a 10-kHz signal for a 10-v input. □

**Synchronous.** The circuit detects the missing pulse independently of the pulse train frequency. Voltage-to-frequency and frequency-to-voltage converters derive a reference frequency whose average remains the same for small anomalies occurring in the pulse train: converters' integrating capacitors hold  $f_{ref}$  steady despite missing pulses. The reference in this way serves as a synchronous clock.



# Charge pump cuts compandor's attack time

by Devlin M. Gualtieri  
*Allied Chemical Corp., Morristown, N. J.*

Integrated-circuit compandors such as the Signetics NE570 could be more effective in high-fidelity noise-reduction schemes if it were not for one built-in shortcoming: their slow attack time permits large input signals to overdrive the device's compressor and thereby create distortion. But by adding a quad operational amplifier, a diode, and a few resistors, the compandor's attack-to-decay ratio (which is internally set at 1:5) can be dynamically controlled. Specifically, the attack time can be decreased for a given decay period. This concept can be extended to any charge-storage circuit, such as a sample-and-hold module, to speed voltage-level acquisition for a given set of circuit parameters.

The NE570 contains a full-wave rectifier, a variable-gain stage, and other peripheral circuits. The rectifier converts an audio-input signal into a pulsating direct current, which is averaged by an external filter capacitor, C, connected to the compandor's C<sub>RECT</sub> terminal. The average value of the signal determines the gain of the variable-gain stage.

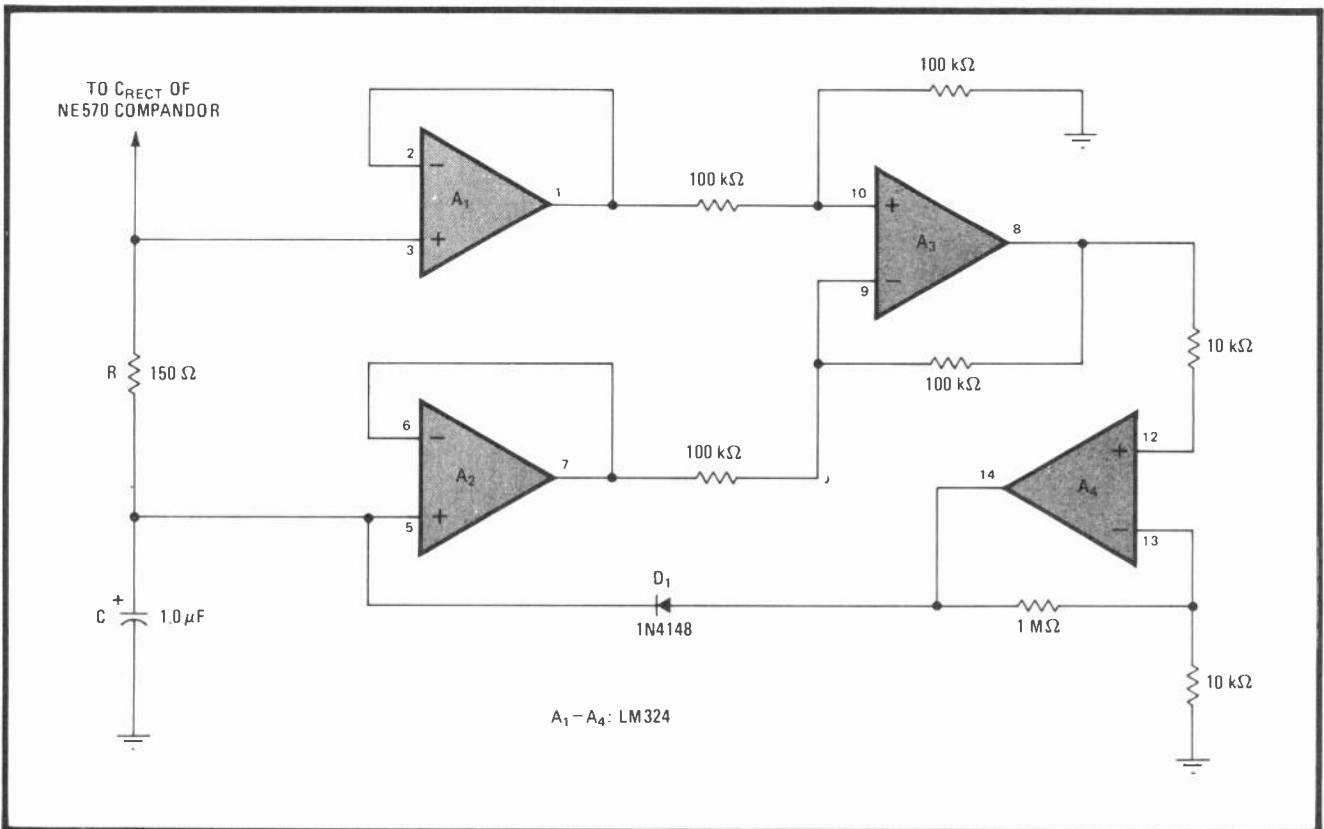
The compandor's attack and decay times are inversely

proportional to the value of the filter capacitor. Thus attack time could be reduced simply by substituting a smaller capacitor for C. But the circuit's purpose is to reduce attack time without using a smaller C, because the third-order harmonic distortion generated when the compandor processes low- and medium-amplitude signals increases as the value of C decreases. The effective capacitance of C during charging is reduced by using this circuit as a pump to charge C more quickly for large input signals, thereby shortening attack time without appreciably reducing the average capacitance of C.

The averaging capacitor is connected to the compandor's rectifier through a 150-ohm resistor, R. At low signal levels, the LM324 quad op amp is not active, so that R contributes only 0.2% additional distortion to what would normally be expected with C alone.

When the rectifier processes a large signal, the relatively large voltage drop across R activates the circuit. Differential amplifier A<sub>1</sub>-A<sub>3</sub> generates a large voltage at the input to A<sub>4</sub>. This causes A<sub>4</sub> to charge C through D<sub>1</sub> at its short-circuit value of 40 milliamperes. C is effectively charged at 40 volts per millisecond, which corresponds to an attack time of less than 0.1 ms.

The threshold of the enhanced attack rate, which is set by the quiescent 1.3-v drop across C and the 0.7-v drop across D<sub>1</sub>, is approximately 0.1 v root mean square (-20 dBm) with respect to the rectifier input. □



**Dynamic.** Circuit for decreasing NE570's attack time for large signals uses a quad operational amplifier for quick charging of compandor's averaging capacitor, C, in this way reducing its effective value. The fundamental waveform distortion from the compandor output is substantially reduced as a result, but third-harmonic distortion for low- and medium-amplitude signals is not substantially increased.

# Annunciator control uses only passive components

by John A. Haase  
Fort Collins, Colo.

Combining relays with other passive components, this circuit provides time delays of anywhere from milliseconds to minutes without the need for the polarizing potentials normally required by monostable multivibrators. Such an electromechanical arrangement is ideally suited to the implementation of a practical call controller, or annunciator.

Delays are produced by first generating a staircase voltage. Pushing button PB<sub>1</sub> momentarily latches relay K<sub>1</sub> and energizes its bell circuit. The bridge circuit used with each relay permits the use of an inexpensive dc relay.

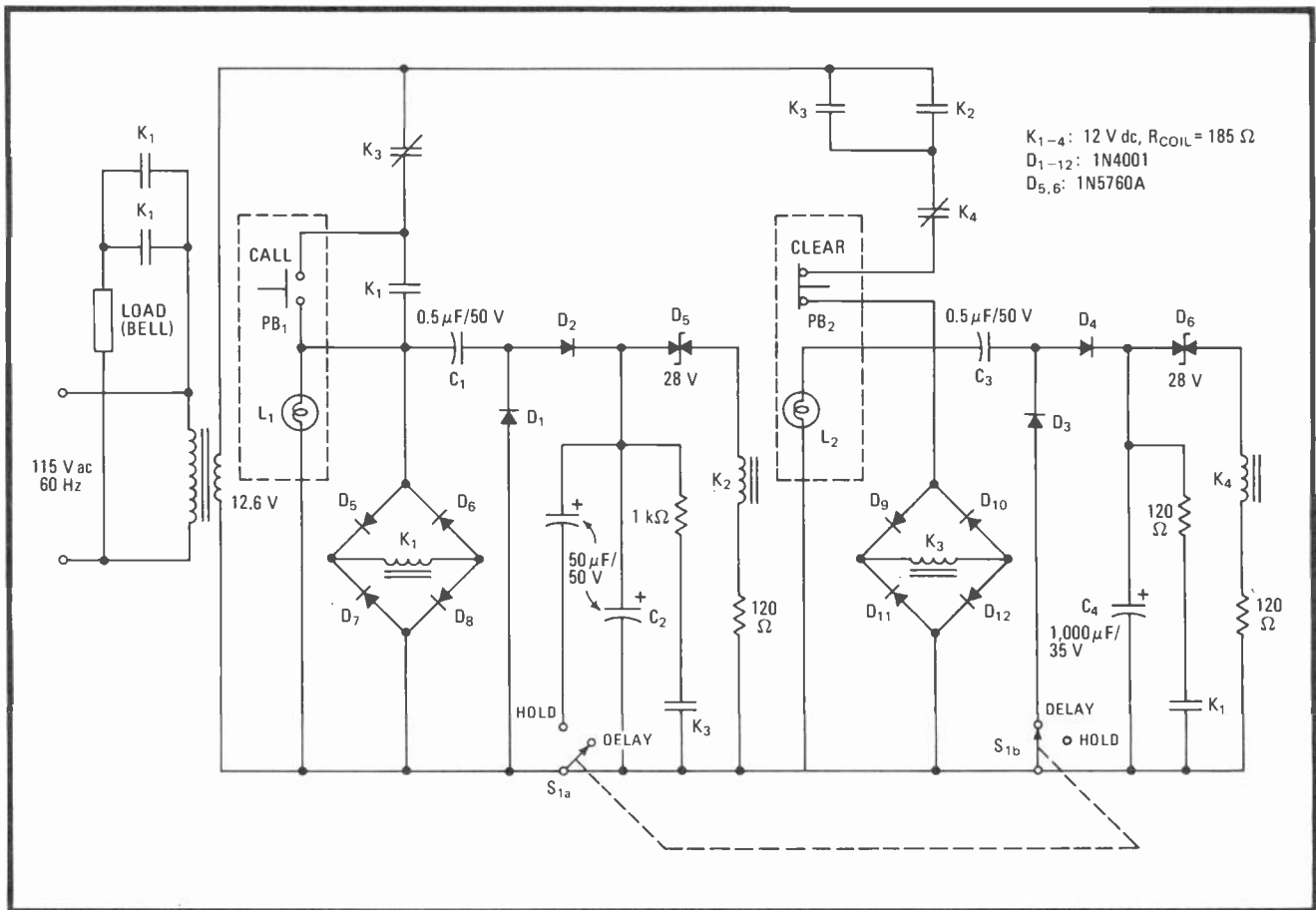
Call-indicator lamp L<sub>1</sub> then lights, and supply voltage is applied to C<sub>1</sub>, C<sub>2</sub>, D<sub>1</sub>, and D<sub>2</sub>, which make up the staircase generator. The step interval of the rising output voltage, V, at the junction of D<sub>2</sub> and C<sub>2</sub> becomes  $\Delta V_o = C_1 E(10^3)/C_2$  millivolts per cycle, where E = 12.6(1.414) = 18 volts. Note that the diodes are consid-

ered passive elements in this application, as their characteristic curve, per se, is not utilized in the generation of the staircase waveform.

Circuit constants are selected so that D<sub>5</sub>, which serves as a comparator, breaks down after 155 cycles (2 seconds), when output voltage V reaches 28 v. Relay K<sub>2</sub> is then energized, enabling K<sub>3</sub> to close and lamp L<sub>2</sub> to light, because the alternating voltage is applied to a second delay circuit through one of the normally open contacts of K<sub>2</sub>. At the same time, voltage to relay K<sub>1</sub> is removed, since the normally closed relay contact of K<sub>3</sub> (in K<sub>1</sub>'s energizing path) opens. Simultaneously, C<sub>2</sub> is discharged by K<sub>3</sub>'s closed relay contact (in series with the 1-kilohm resistor).

Relay K<sub>3</sub> remains closed for 80 seconds to prevent repeated (and most times annoying) calls. At that time, the output voltage across C<sub>4</sub>, generated by the second staircase waveform, steps to 28, whereupon D<sub>6</sub> breaks down and relay K<sub>4</sub> is energized. Relay K<sub>3</sub> then opens and the path of relay K<sub>1</sub> is reactivated to accommodate call requests, while C<sub>4</sub> discharges.

Call requests may be extended to 4 seconds by placing switch S<sub>1</sub> in the hold position. In this mode, relay K<sub>4</sub> does not come into play, so the user must wait an infinite inhibiting time before initiating a second call request. Under this condition, push button PB<sub>2</sub> must be depressed to clear the circuit so that it can respond to calls. □



**Charged delay.** Electromechanical relays and other passive components form charge pump that generates a time-dependent staircase voltage, V, for call controller. By suitably selecting diodes D<sub>5</sub> and D<sub>6</sub> so that their breakdown voltages conform to some preset value of V, the circuit provides delay. Depressing PB<sub>1</sub> rings bell for 2 seconds. inhibits circuit for 80 seconds to prevent quick second requests.



# LEDs track signal level in visual data monitor

by Michael O. Paiva  
Teledyne Semiconductor, Mountain View, Calif.

In this circuit, a matrix of light-emitting diodes is combined with an analog-to-digital converter and multiplexing logic to form a dual-setpoint meter. The LEDs are used to track changes in the input data and display the setpoints. The unit may be considered a variation of the analog panel meter; it will find many uses in industrial control applications where it is necessary to observe quick changes while determining whether data is within a preset range. By adding a dual comparator to the circuit, an alarm can be sounded when the input level goes outside the range.

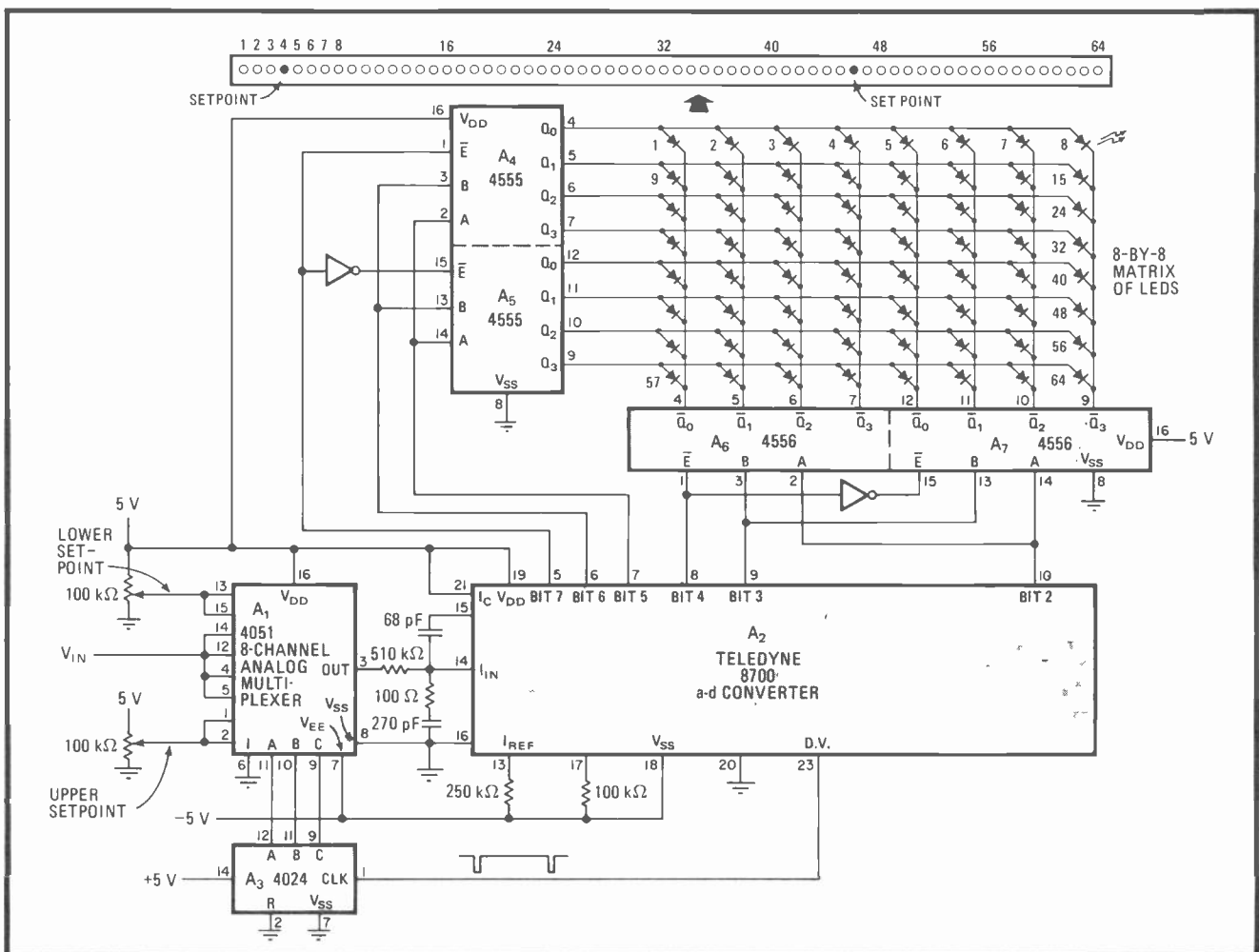
The signal to be tracked,  $V_{in}$ , and the upper and lower setpoint voltages are applied to an eight-channel multiplexer,  $A_1$ . The a-d converter,  $A_2$ , samples channel 1 first. After the conversion, pin 23 of  $A_2$  goes high and

advances the binary counter,  $A_3$ .  $A_3$  then addresses the second channel of the multiplexer, and so on, until each channel is scanned in sequence.

Bits 2 through 8 of the a-d converter, representing the binary equivalent of the voltage sampled, drive  $A_4$ – $A_7$ , which are wired as two one-of-eight decoders. Thus each voltage is converted into a control signal that drives one diode in the eight-by-eight-diode matrix.

The setpoint voltages are sampled twice during each scan cycle (each is connected to two input channels), while the input signal,  $V_{in}$ , is connected to four channels and so is scanned four times per cycle. Thus the brightness of the LED corresponding to  $V_{in}$  is twice that of the setpoint LEDs, making it easy to differentiate between the three signals.

The circuit's worst-case response time is two scan cycles.  $A_2$  has a conversion time of 1 millisecond, so that the display will require 2 ms to follow a change in  $V_{in}$  and 4 ms to follow any change in the setpoint potentials. Because of this high refresh rate, no flicker will be observed on the LED display. □



**Visualizing voltage.** Eight-by-eight-LED matrix and C-MOS logic form analog dual-setpoint meter. Setpoint potentials and data voltage  $V_{in}$  are each introduced into multiplexer and scanned in sequence, then converted into control signals that light the appropriate LEDs in the matrix. Setpoint LEDs are half the brightness of the LED representing  $V_{in}$  because they are sampled at half the rate.

# Cascaded C-MOS blocks form binary-to-BCD converters

by Haim Bitner

Seforad-Applied Radiation Ltd., Emek Hayarden, Israel

Low-power complementary-metal-oxide-semiconductor adders and comparators are easily combined to form this 4-bit binary-to-BCD converter. When the basic adder-comparator blocks are cascaded, the converter can be expanded to turn  $n$  binary input bits into a binary-coded-decimal output. The circuit is simpler than one using counters, and read-only memories are eliminated.

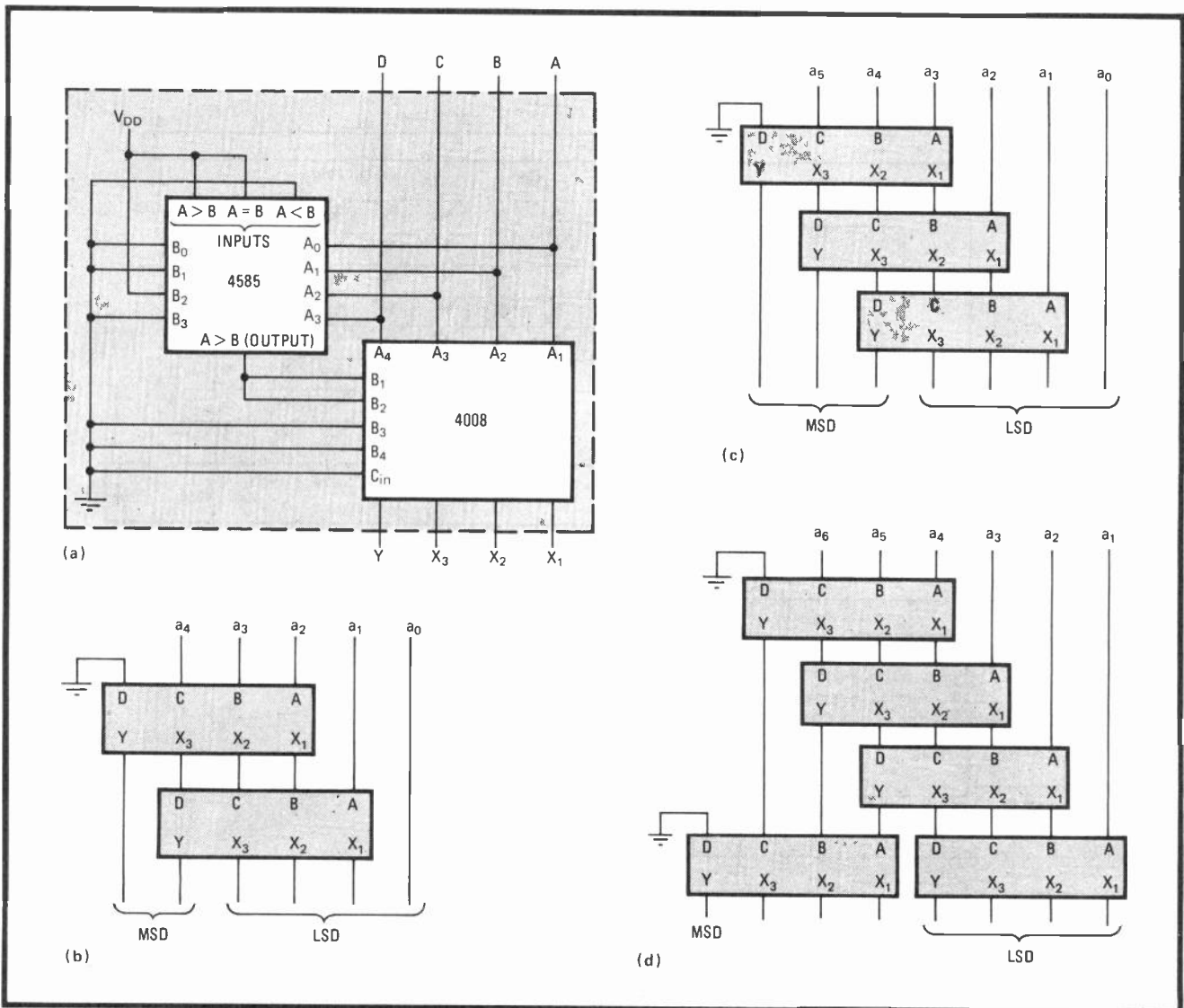
Comprising the basic 4-bit converter block (a) are the 4008 full adder and the 4585 comparator. The binary inputs are introduced at A-C, with A being the next to least significant bit, and D grounded. The BCD output appears at  $X_1$ - $X_3$  and Y of the 4008. The LSB input

bypasses the unit and becomes the LSB output.

The 4585 compares the input bits to a binary number (0100) which is hard-wired to pins  $B_0$ - $B_3$ . Thus the output of the 4585 is low if the number at A-D is less or equal to 4. The  $X_1$ - $X_3$  outputs of the 4008 are then identical to the input bits.

If the input number becomes greater than 4 (that is, greater than 0100), the 4585's output moves high, and so binary number 0011 is placed on the  $B_1$  and  $B_2$  inputs of the 4008 adder. Thus, 3 is added to the input number and the Y output of the 4008 goes high, indicating the most significant digit is active.

By cascading units, 5-bit (b), 6-bit (c) and 7-bit (d) converters can be built. The method can be used to extend indefinitely the number of bits processed. Note that the value of the least significant input bit ( $a_0$ ) is numerically equal to its BCD-equivalent and so passes straight from input to output in all cases. □



**Add infinitum.** Low-power binary-to-BCD converter (a) requires only C-MOS adder and comparator for processing 4 bits. Unit is so configured that basic building blocks can be easily combined to form 5-bit (b), 6-bit (c), and 7-bit (d) converters.

# Bidirectional optoisolator puts two LEDs nose to nose

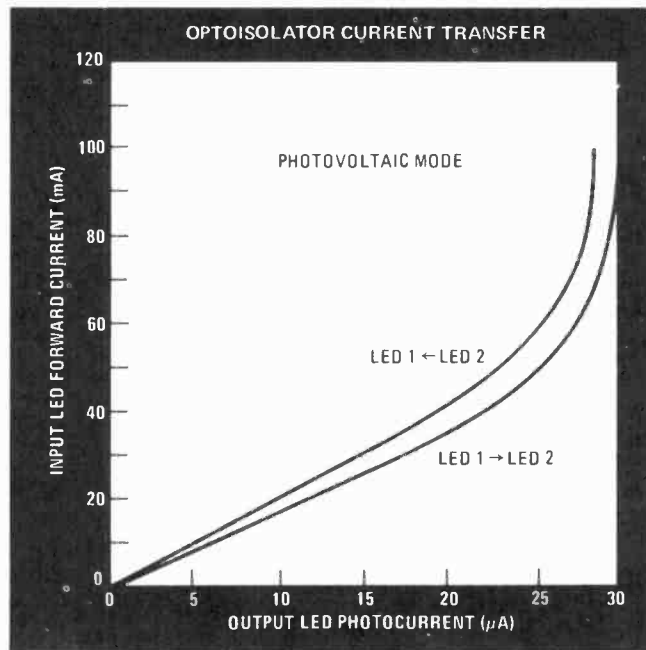
by Forrest M. Mims III  
San Marcos, Texas

As conventional optoisolators employ a separate source and sensor, they can transfer current in only one direction. A few photodetectors and electroluminescent diodes can double as both a source and sensor, however, and when they are suitably connected they offer users a convenient way to build a low-cost bidirectional optoisolator, as shown here.

Two OP-195 LEDs, which have gallium-arsenide-silicon infrared emitters, can be made to transfer signals in either direction if they are placed nose to nose in a short length of heat-shrinkable tubing and secured in place by heating the tubing. Alternatively, the LEDs may be quite far apart if they are coupled by a plastic or glass-fiber waveguide.

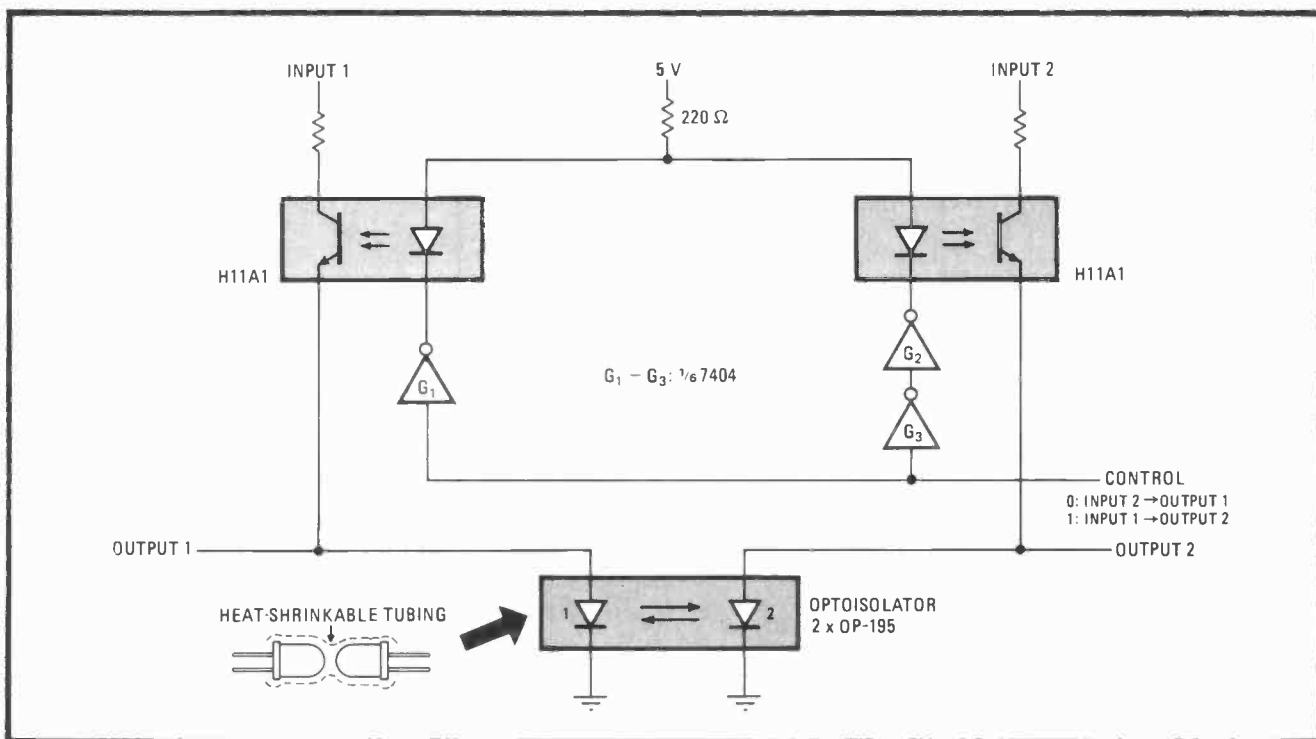
In either case, the current transfer ratio ( $I_o/I_{in}$ ) for the pair, with proper biasing, will be 0.06% for an input current of 20 milliamperes. This ratio is far too low for many applications but is good enough for some specialized roles where a bidirectional path is required. In any case, the output signal can be amplified or buffered, as necessary.

A logic-control voltage and two H11A1 optoisolators serve as the input/output port selector. Whichever of the OP-195 devices is designated the output diode may be



connected in the reverse-biased photo-conductive mode or the unbiased photovoltaic mode. In the latter case, the output device is not biased. The response of the optocoupler operating in this mode for a given signal-input current is shown in the plot. Note the device linearity is completely adequate for duplex voice communication.

The photovoltaic current transfer ratio is virtually identical to that for photoconductive operation up to an input current of 20 milliamperes. The ratios begin to depart considerably above 40 mA. □



**Either way.** Standard light-emitting diodes encased in heat-shrink tubing can be made to function as a bidirectional transmission link. Alternatively, LEDs may be coupled through optical fibers. Control circuit for selecting input/output port arrangement is simple, using two optoisolators and three inverters. Circuit's current-transfer ratio suffices for many small-signal applications.

# Notch filter and meter measure power-line harmonics

by Henno Normet  
 Diversified Electronics Inc., Leesburg, Fla.

Valid measurements of core loss in power-line transformers and various other magnetic devices require total harmonic distortion (THD) levels under specified limits—usually 3%. This inexpensive circuit determines the THD present in a 60-hertz waveform, over the range of 0 to 10%. Here, a notch filter is used to eliminate the voltage source's 60-Hz fundamental component, allowing an ac voltmeter to measure the remaining harmonic components.

The adjustable-Q Wien-bridge notch filter discussed in a previous article<sup>1</sup> proved to be best adapted for this application. Resistors  $R_{11}$  and  $R_{12}$  of the bridge (see shaded portion of figure) are selected to give the notch filter a Q of 10. The resulting null is sharp enough to pass a 180-Hz signal without attenuation, the lowest harmonic to appear as a component of distortion.

Component selection for the rest of the filter is also important to the achievement of good notch depth.  $C_1$  and  $C_2$  should be matched within 1%, and high-accuracy resistors used where indicated by asterisks. Metal-film

resistors and polycarbonate capacitors help keep frequency drift and aging to a minimum.

For initial balancing of the bridge, a low-distortion 2-v signal at 60 Hz is applied at point A. With  $SW_1$  in the test position,  $R_8$  and  $R_{10}$  are adjusted for a zero reading on the meter, M. If an audio oscillator is not available as a signal source, full line voltage may be applied to the input terminals, in which case  $R_8$  and  $R_{10}$  are adjusted for a minimum reading on the meter.

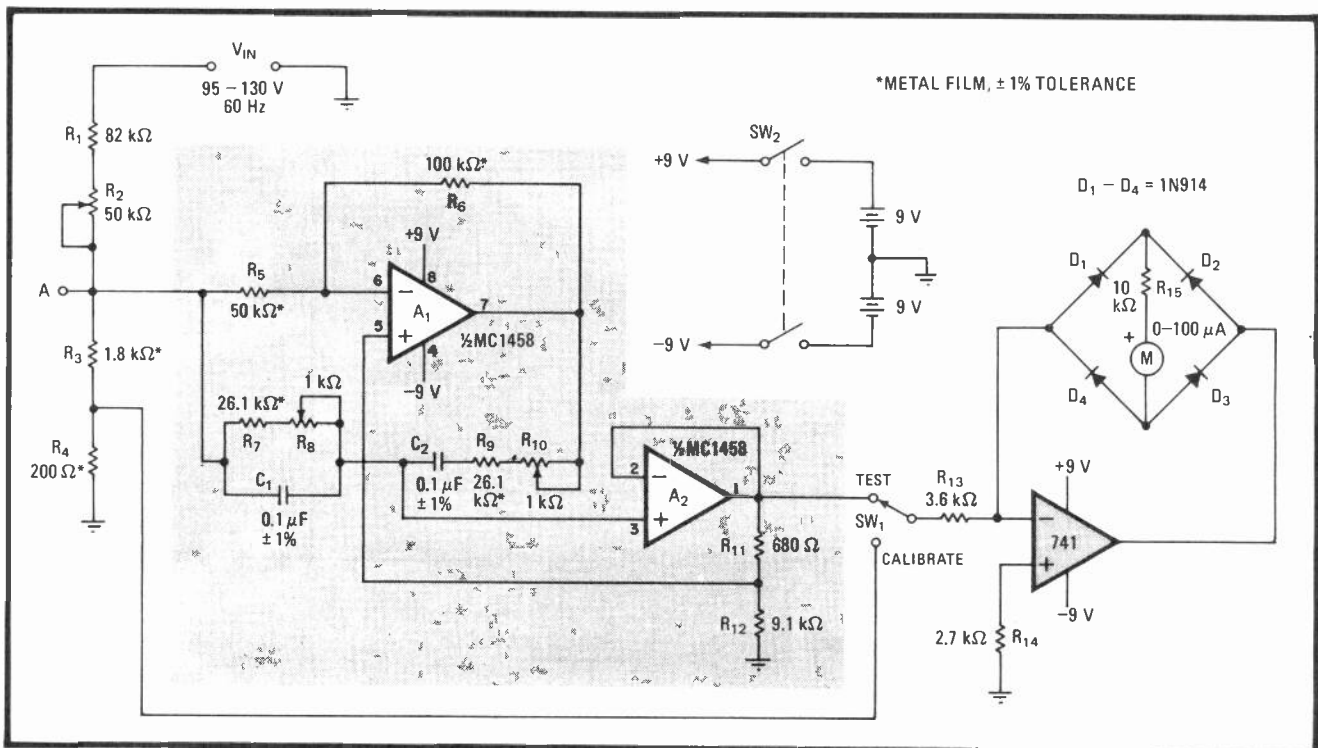
In operation,  $SW_1$  is first placed in the calibrate position and line voltage applied at the circuit input,  $V_{in}$ .  $R_2$  is then adjusted for a maximum (full-scale) reading.

The switch is then placed in the test position, whereupon the input signal passes through the notch filter. Percent of THD may then be read directly. Note that the accuracy of the reading depends upon the accuracy of the 10:1 voltage divider,  $R_3$  and  $R_4$ .

The definition of THD requires that both the calibration and measurement procedure be carried out with a root-mean-square-responding meter. However, in the 0-10% distortion range, a less costly average-responding meter will provide 10% accuracy, which is acceptable in most applications. □

### References

1. "Wien bridge and op amp select notch filter's bandwidth", *Electronics*, Dec. 7, 1978, p. 124.



**Handling harmonics.** Wien-bridge notch filter rejects 60-Hz power-line fundamental frequency so that total harmonic distortion present in signal can be measured. Meter measures THD over 0-to-10% range. An rms-responding meter should be used, but an average-responding meter is acceptable. Results are displayed in percent, with an accuracy directly proportional to the tolerance of resistors in divider  $R_3$ - $R_4$ .

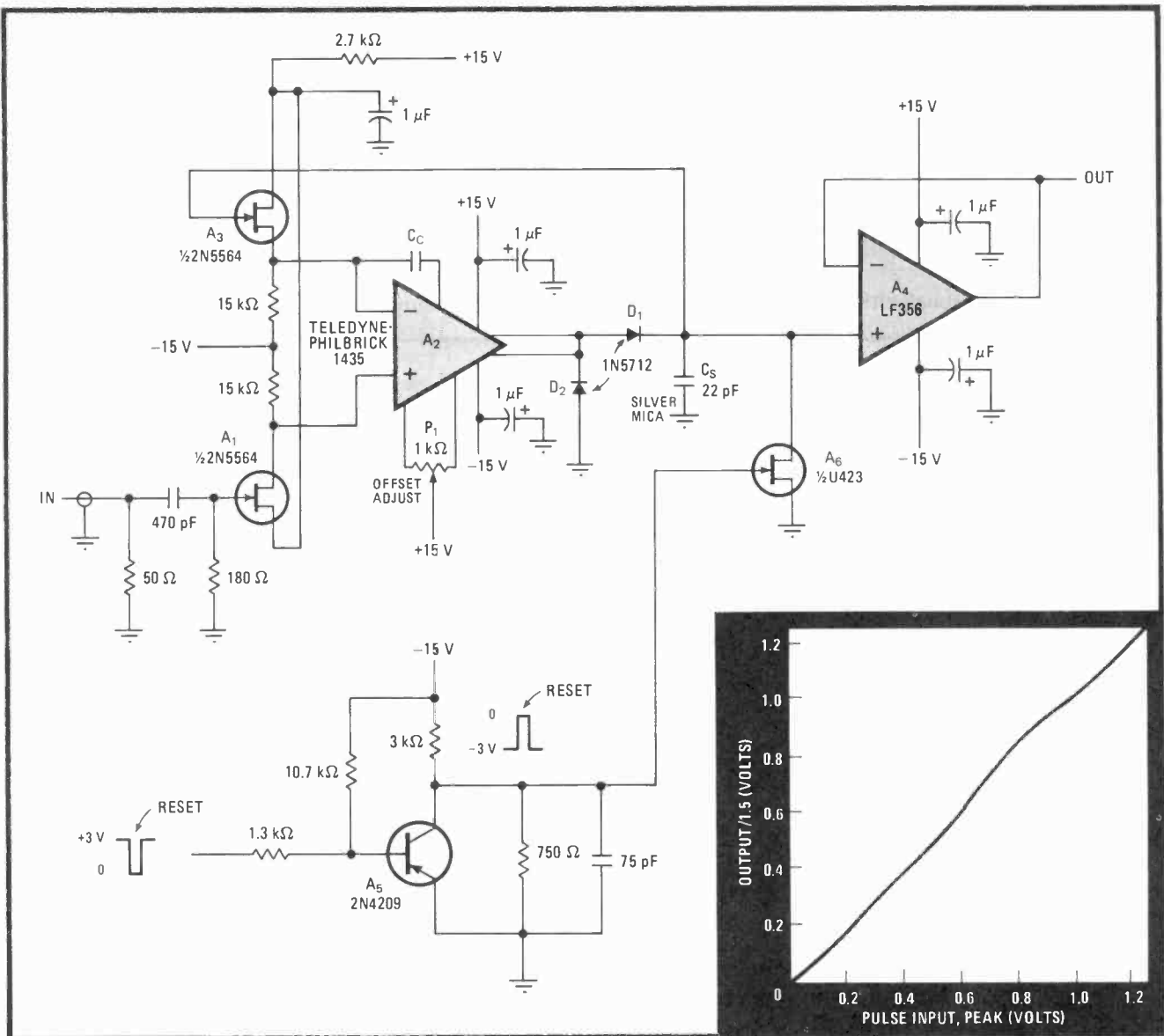
# Wideband peak detector recovers short pulses

by Saul Malkiel  
Advanced Technology Systems, Roselle, N. J.

Using a Schottky-barrier diode for detection and a wideband operational amplifier, this peak detector recovers data pulses as narrow as 10 nanoseconds in the range of 0.1 to 1.3 volts. The circuit's linearity as a percentage of the full scale output is 4%.

The input signal, whose rise time is assumed to be a minimum of 10 ns, is applied to one side of the differential source follower, A<sub>1</sub>-A<sub>3</sub>, via a 50-ohm coaxial cable. A blocking capacitor removes any baseline shifts. The output of this JFET follower is then applied to the wideband amplifier, A<sub>2</sub>. The amplifier has a gain-bandwidth product of 1 gigahertz.

The output of the amplifier switches on diode detector D<sub>1</sub> so that a charging current can be delivered to storage capacitor C<sub>s</sub>. When there is overshoot, source follower A<sub>3</sub> is turned on more heavily than A<sub>1</sub> so that A<sub>2</sub> may be driven negative. D<sub>2</sub> then comes into play, acting to limit the amplifier's negative excursion. The excursion, coupled through D<sub>1</sub>'s shunt capacitance, reduces the



**Narrow capture.** Wideband amplifier and fast diode detect pulses having widths as small as 10 ns. Output-to-input voltage linearity of circuit is 4%, and linearity is virtually independent of pulse width. Response is illustrated in curve at bottom right.

# Phase-locked loop aids in measuring capacitance

by Ronald E. Pyle  
Tracor Inc., Austin, Texas

In this circuit, a phase-locked loop (PLL) aids in measuring an unknown capacitance to within 1% of its true value, over the range of approximately 10 picofarads to 1 microfarad.

As the figure shows, the unknown capacitance,  $C_x$ , is part of low-pass filter  $R_T C_x$ . The filter's output serves as one input to the PLL's phase comparator, the other input being derived from the loop's voltage-controlled oscillator (VCO). Circuit operation is based on the principle that the phase lag at the filter's output is  $45^\circ$  at  $f_o$ , the filter's center frequency. The PLL thus acts to generate a frequency having a  $45^\circ$  lag on the other port of its phase comparator, locking the loop. The output frequency of the oscillator at locking represents an index of the capacitance measured.

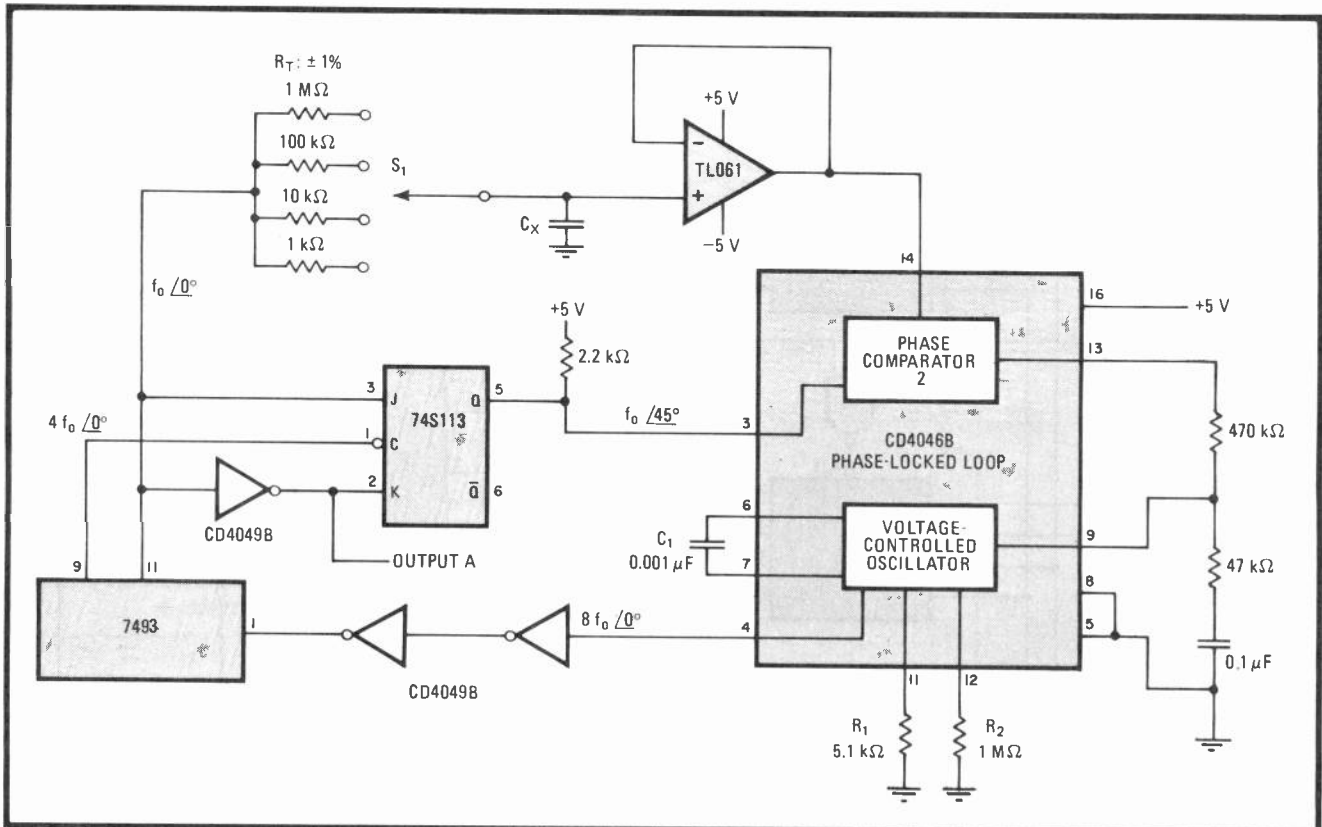
The output frequency of the VCO in the CD4046B PLL

passes through a buffer and is divided by 2 and 8 by the 7493 4-bit counter. These signals are next routed to the 74S113 J-K flip-flop, which generates a wave shifted  $45^\circ$  with respect to the input signal on the J port.

The flip-flop's output is then compared with the filter's output signal at phase comparator 2 of the 4046B. This comparator is an edge-controlled network that indicates  $0^\circ$  phase difference between the input test signal and the VCO-derived signal, when locking is achieved. The 4046's locking and capture range is approximately two decades, which is what makes it possible to measure the wide range of capacitances mentioned above. Suitable selection of  $R_1$  and  $C_1$  extends the measurement range still further.

A frequency counter measures the output of the circuit in the locked condition as  $f_o = 1/2\pi R_T C_x$ . From this the unknown capacitance can readily be determined. Look-up capacitance tables plotted as a function of  $f_o$  and  $R_T$  can be readily constructed for rapid checking. Alternatively, extra hardware may be added to convert the frequency into a capacitance value directly, thus forming a self-contained digital capacitance meter. □

Engineer's notebook is a regular feature in *Electronics*. We invite readers to submit original design shortcuts, calculation aids, measurement and test techniques, and other ideas for saving engineering time or cost. We'll pay \$50 for each item published.



**Filtering an answer.** A phase-locked loop finds the center frequency,  $f_o$ , of low-pass filter  $R_T C_x$ , thus enabling determination of test capacitance  $C_x$ , from  $f_o = \pi R_T C_x$ . The VCO derives an output whose phase lag matches that of the lag at the filter output at the PLL's comparator, so that locked state is achieved. The VCO output,  $f_o$ , thus represents an index of the capacitance measured.

# LED dot/bar driver simplifies solid-state scope

by Forrest M. Mims III  
San Marcos, Texas

The design of this solid-state scope is simplified by use of a one-chip driver to address the rows of the light-emitting-diode matrix comprising the scope's display. The circuit is a viable alternative to a scope that has previously been described.<sup>1</sup>

The unit will handle input signals in the audio-frequency range. Signals to be displayed are applied to pin 5 of the National LM3914 dot/bar driver and resolved to one of ten active-low output levels. Note that R<sub>3</sub> provides a programmable current control for all LEDs in the display. Thus, current-limiting resistors are not required at each output port of the driver. Pin 7 is connected to an internal 1.2-V reference so, as a result, current through R<sub>3</sub> is approximately equal to one tenth the LED current; thus, with R<sub>3</sub> = 1.2 kilohms, the LED

current becomes equal to 10 milliamperes.

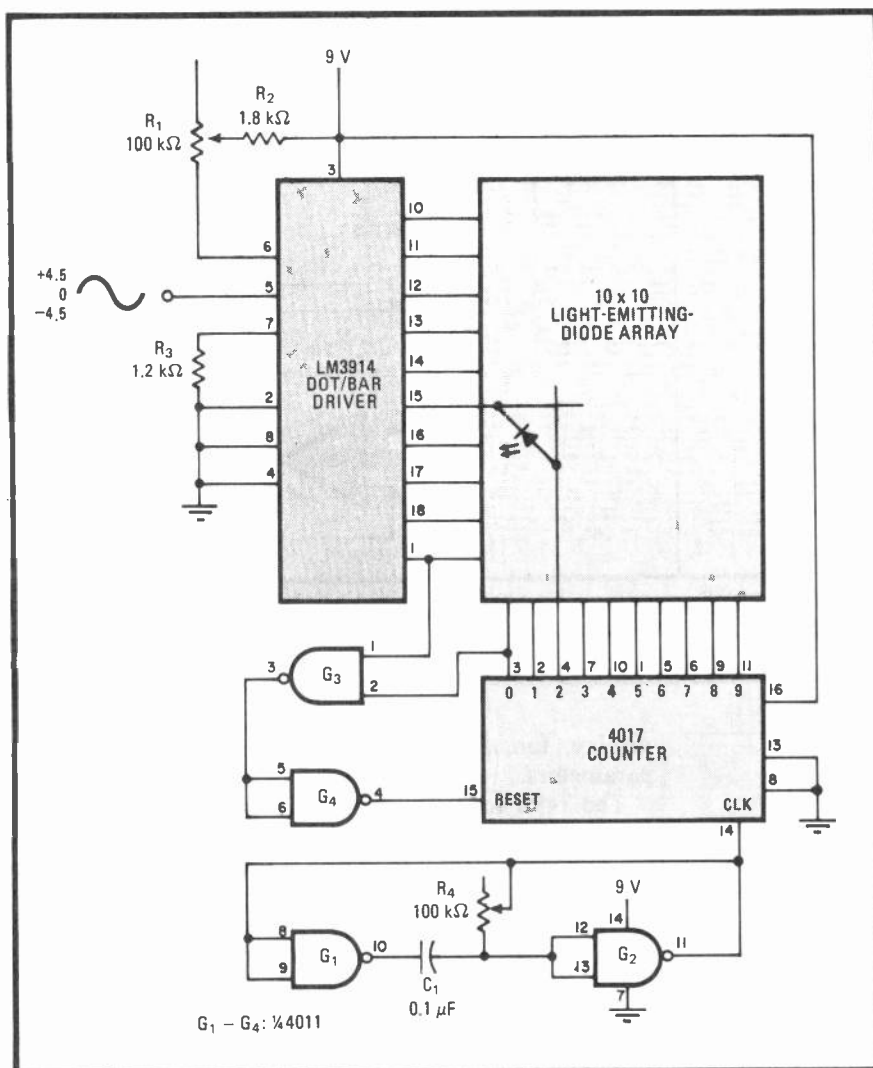
The 4017 Johnson counter and accompanying gates comprise the scope's horizontal-sweep circuit. The sweep oscillator driving the counter is made from half a 4011 quad-NAND gate, G<sub>1</sub> and G<sub>2</sub>, its frequency controlled by resistor-capacitor combination C<sub>1</sub>-R<sub>4</sub>. In this way, the instantaneous input voltage is resolved to 1 LED in 100. G<sub>3</sub> and G<sub>4</sub> provide automatic triggering of the sweep.

As for the LED display itself, bar arrays that contain 10 diodes each are easier to use and provide a more uniform display than discrete diodes, and are therefore recommended. Another option is to employ miniature matrix arrays of five by seven dots. At least one firm, IEE Inc. (7740 Lemona Ave., Van Nuys, Calif. 91405), offers such displays that can be mounted adjacent to each other without a gap in the LED columns.

Both the vertical and horizontal driving sections of the basic scope can be readily expanded. For instance, five cascaded counters and five cascaded dot/bar chips can drive a 50-by-50-diode matrix, forming a scope with a display resolution of 1 LED in 2,500. □

## References

1. Vernon Boyd, "LED bar-segment array forms low-cost scope display," *Electronics*, Nov. 24, 1977, p. 128.



**Drive center.** One-chip dot/bar driver reduces complexity of vertical scanning portion of scope having light-emitting diode display. Horizontal scanning portion uses G<sub>1</sub> and G<sub>2</sub> for clock, wired as astable multivibrator, and 4017 counter. Display resolution is 1 LED in 100.

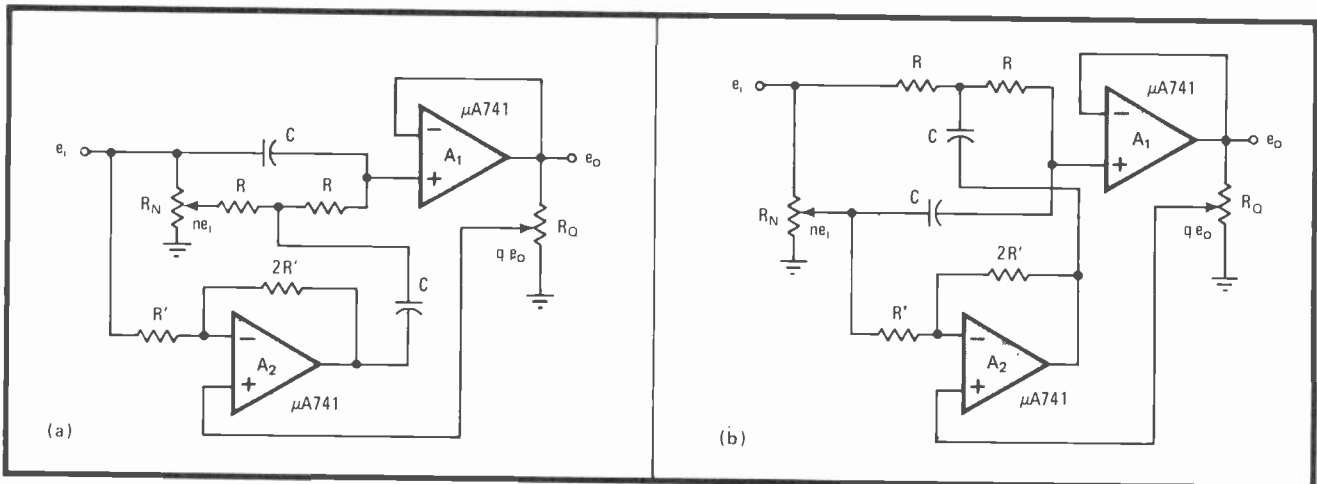
## Bridged-T selects filter's notch frequency and bandwidth

by P. V. Ananda Mohan  
Indian Telephone Industries Ltd., Bangalore, India

If a bridged-T network is used in place of the Wien bridge in the notch filter proposed by Fellot,<sup>1</sup> both the bandwidth and the frequency may be independently adjusted. The bridged-T approach has been explored previously<sup>2</sup> as an extension of some work carried out on parallel-T notch filters, and, as illustrated here, the technique offers an excellent way of building units that are simple and versatile.

$R_N$  and  $R_Q$  comprise the balancing arms of the bridged-T network (note  $A_1$  is a unity-gain buffer) as seen in (a). In this configuration, the circuit's transfer function is:

$$e_o/e_i = [ns^2 + \omega_o^2]/[s^2 + 3(1-q)s\omega_o + \omega_o^2]$$



**Changing tune.** Using bridged-T network in place of Wien-bridge arrangement in notch filter enables independent control of filter's bandwidth and frequency. Circuit can be configured for tuning filter above (a) or below (b) its natural radian frequency  $\omega_o = 1/RC$ .

where  $n$  and  $q$  are selected by  $R_N$  and  $R_Q$ , respectively, and  $\omega_o = 1/RC$ . Note that  $0 \leq n, q \leq 1$ , and that the frequency of the notch is

$$\omega_n = \omega_o/n^{1/2}$$

Therefore for this circuit  $\omega_n$  will always be equal to or greater than  $\omega_o$ .

The bandwidth is adjusted with  $R_Q$ , and  $Q_s$  greater than 1,000 will be realized when high-gain operational amplifiers are used. In general,  $Q_s$  will be higher than can be achieved with parallel-T networks. The notch depth is at least 50 decibels throughout the operating range.  $R_N$  and  $R_Q$  must only be at least 10 times smaller than  $R$  to achieve the stated filter characteristics.

By modifying the circuit slightly, as in (b), the transfer function becomes:

$$e_o/e_i = [s^2 + n\omega_o^2]/[s^2 + 3(1-q)s\omega_o + \omega_o^2]$$

and the notch frequency  $\omega_n$  is made tunable for frequencies below  $\omega_o$ , so that  $\omega_n = \omega_o n^{1/2}$ . □

### References

1. Dominique Fellot, "Wien bridge and op amp select notch filter's bandwidth," *Electronics*, Dec. 7, 1978, p. 124.
2. "An Active RC Bridged-T Notch Filter," *Proc. IEEE*, August 1977, p. 208.

## Wide-range pulse generator displays timing parameters

by C. L. Bhat and R. C. Yadav  
Bhabha Atomic Research Center, Srinagar, India

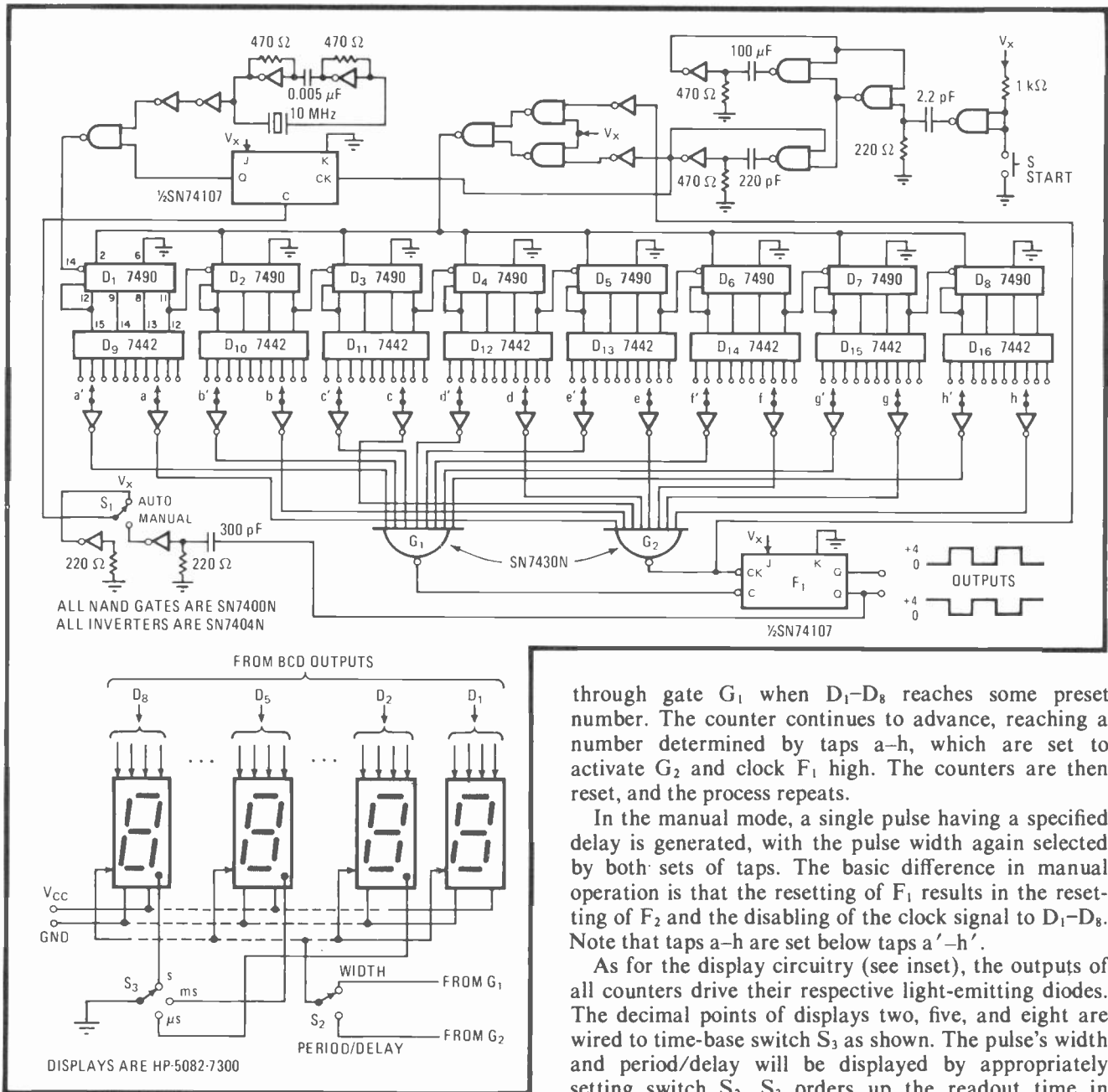
In this circuit, cascaded decade counters provide adjustable pulse width, period, and delay from 0.1 microsecond to 10 seconds. This generator contains an LED digit

display, too, for direct readout of the various pulse parameters.

The 7490 counters,  $D_1$ - $D_8$ , serve simultaneously as a frequency divider and preset counter unit. Depressing the momentary-contact switch  $S$  resets  $D_1$ - $D_8$  and gates the 10-megahertz clock through to the counters, whereupon they advance upward from zero.

When operated in the automatic mode (switch  $S_1$ ), the unit will generate pulses with repetition frequency and width controlled by the clock frequency and the position of two sets of taps at the output of the 7442 4-to-10-line decoders. Here taps a'-h' bring output flip-flop  $F_1$  low





through gate  $G_1$  when  $D_1$ - $D_8$  reaches some preset number. The counter continues to advance, reaching a number determined by taps a-h, which are set to activate  $G_2$  and clock  $F_1$  high. The counters are then reset, and the process repeats.

In the manual mode, a single pulse having a specified delay is generated, with the pulse width again selected by both sets of taps. The basic difference in manual operation is that the resetting of  $F_1$  results in the resetting of  $F_2$  and the disabling of the clock signal to  $D_1$ - $D_8$ . Note that taps a-h are set below taps a'-h'.

As for the display circuitry (see inset), the outputs of all counters drive their respective light-emitting diodes. The decimal points of displays two, five, and eight are wired to time-base switch  $S_3$  as shown. The pulse's width and period/delay will be displayed by appropriately setting switch  $S_2$ .  $S_3$  orders up the readout time in seconds, milliseconds, or microseconds. □

**Watching width.** Pulse generator provides adjustable width and period over a 0.1-microsecond-to-10-second range. A single pulse of specified delay may also be generated. LED-digit display gives direct readout. Wiring of display-switching circuitry (inset) is simple.

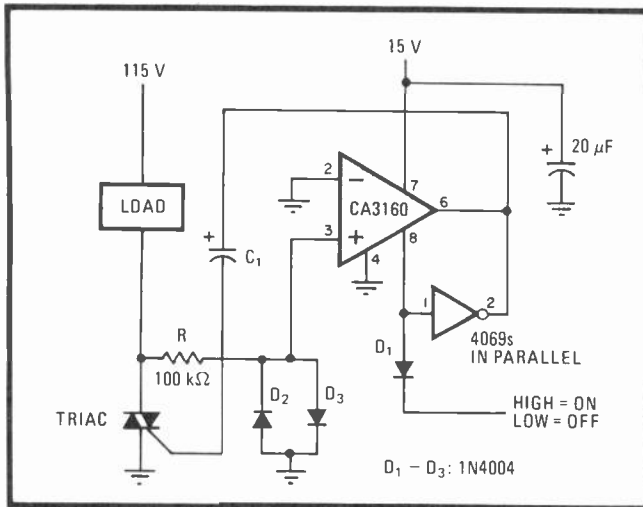
## C-MOS triac trigger cuts parts count

by Hul Tytus  
Tytus & Co., Cincinnati, Ohio

Integrated circuits made to trigger triacs often consume large amounts of power and require biasing schemes

substantially increasing the number of components in the circuit facing the ac load. But by using a C-MOS operational amplifier, the circuit shown can deliver a peak current of 100 milliamperes to the triac, draws an average current of only a few milliamperes and uses a minimum of parts.

Circuit operation is based on the fact that the output of a C-MOS device acts as a current source or sink. As the ac-input voltage rises up through zero, the CA3160 generates a positive-going current pulse of a preset magnitude and charges  $C_1$ , which determines the triac's



**Diminutive driver.** C-MOS operational amplifier, operated from a single supply, minimizes power drain and parts count in triac trigger that can source 100 milliamperes. C-MOS inverters may be placed in parallel with op amp for circuit to drive heavier loads.

pulsing time. As the ac line voltage completes a half cycle and drops through zero,  $C_1$  discharges through the op amp, which now serves as a current sink, so that the triac is again fired.

Note that several 4069 inverters can be placed in parallel with the op amp's strobe (pin 8) and normal outputs to drive heavier loads. Pin 8 and  $D_1$  may also serve as a control terminal, enabling operation with 4049s permanently wired into the circuit.

The maximum rated trigger current of the triac should equal the minimum current the 3160 and 4069s are capable of sourcing. The pulse time for the triac—typically measured in microseconds—should equal the time necessary for the ac supply to generate the necessary conduction voltage across the triac, plus  $t_T$  max, the maximum trigger time for the triac. The value of capacitance required for a given trigger current,  $I$ , triac pulse time,  $t$ , and maximum trigger voltage,  $V_T$ , is given by:

$$C_1 = I t / (0.75 V_{dd} - V_T)$$

where  $V_{dd}$  is the op amp's supply voltage. □

## One-chip gyrator simplifies active filter

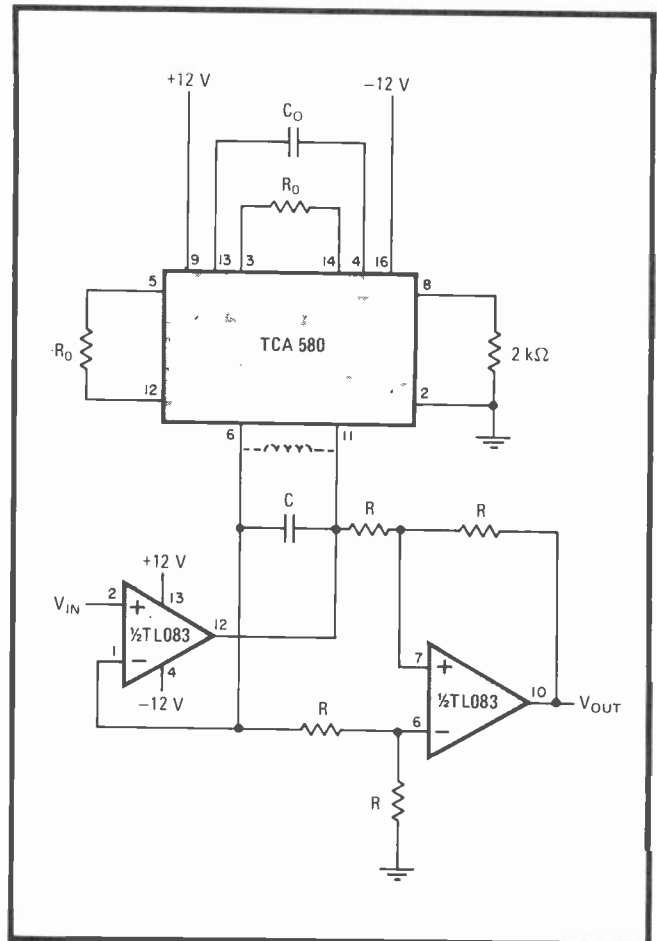
by Kamil Kraus  
Rokycany, Czechoslovakia

Now that gyrators, or impedance inverters, are available on a single integrated circuit, active filters with both high input impedance and few component-sensitivity problems can be easily built in a small area with a minimum of parts. This one uses only one other active component—a dual operational amplifier—to provide low-pass, high-pass, bandpass, or band-reject response at reasonable cost over the dc range to 10 kilohertz.

The low-cost TL-083 op amp has been selected for use in the circuit because of its virtually negligible input-offset voltage and input-bias current. These characteristics are required to achieve a high input impedance over the range of interest and to realize the optimum response of the filter.

The Signetics TCA 580 gyrator simulates the relatively large inductor needed for the required LC (passive) network. The inductance across pins 6 and 11, and thus in parallel with capacitor  $C$ , is  $L = C_0 R_0^2$ . The resonant (center) frequency of the LC combination, in turn, is  $f_0 = 1/2\pi (LC)^{1/2}$ , with its quality factor  $Q = R(C/L)^{1/2}$ . Thus the filter, which is shown configured on the band-pass mode, can be made to work at any frequency and  $Q$ , once its components are suitably selected.

The circuit can be transformed into a low-pass filter if its output is applied to an integrator whose time constant is  $RC$ . Similarly, it will function as a high-pass filter if its output is applied to a differentiator whose time constant is  $RC$ . For band-reject operation,  $C$  must be placed in series with the simulated inductor. □



**Optimal.** Gyrator and operational amplifier comprise a simple two-chip bandpass filter with high impedance and state-of-the-art stability. Filter configuration remains the same for high-pass and low-pass operation; only an external differentiator or the integrator, respectively, need be added. For the band-reject mode,  $C$  is placed in series with a simulated inductor.

## Switching converter raises linear regulator's efficiency

by Sadeddin Kulturel  
Istanbul, Turkey

The low ripple and fast recovery of a series-pass voltage regulator can be attained at the high efficiency of a switching regulator if both are combined. In this circuit, the performance is achieved by using the switching circuit as a preregulator for the linear element.

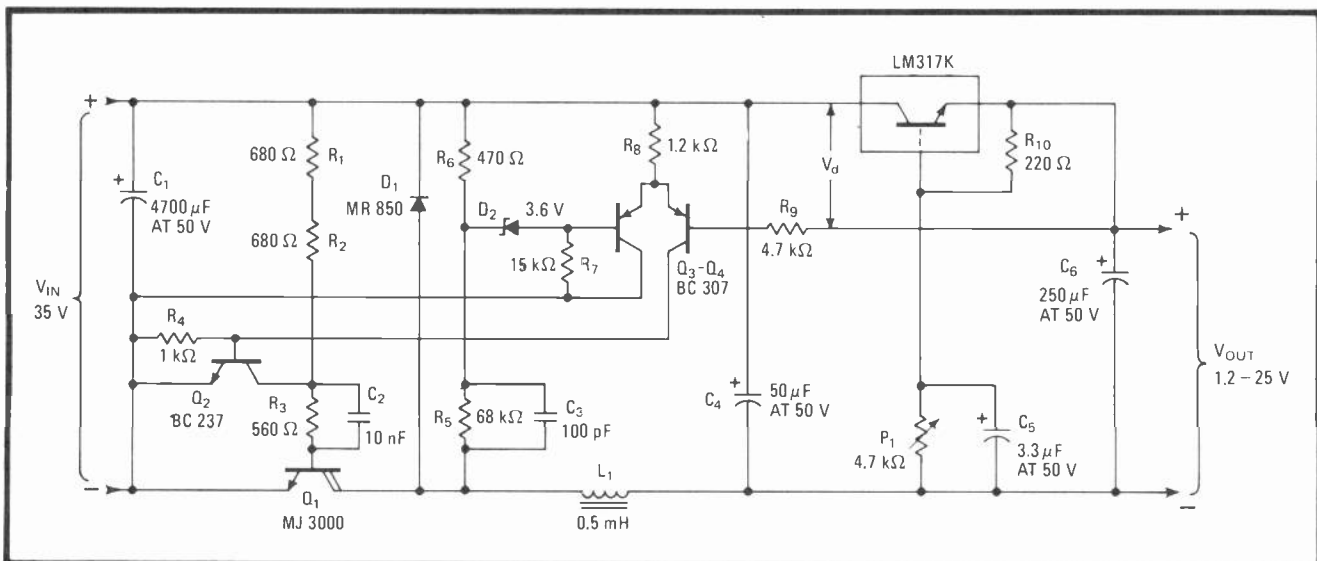
As shown in the illustration of the general circuit, which is designed to transform the 35-volt raw input into a well-regulated output, heat dissipation across the LM317K series element can be reduced if it is made to handle a switched, rather than a continuous, input. Here, the switching regulator is formed by transistors  $Q_1$ – $Q_4$ ,  $D_1$ , and  $L_1$ . During power up,  $Q_1$ , driven through  $R_1$ – $R_3$ ,

is brought into saturation.  $Q_2$  remains off and  $Q_3$  is turned on.

Switching occurs when  $V_d$  equals 3.6 volts, which is  $D_2$ 's zener voltage.  $Q_4$  then turns on, as does  $Q_2$ , and  $Q_3$  is turned off.

As  $Q_2$  turns on,  $Q_1$  switches off, and because of the positive voltage spike created by  $L_1$ , load current is momentarily forced through  $D_1$  as  $V_d$  decreases. When  $V_d$  reaches the lower hysteresis threshold of  $Q_3$  as established by  $R_5$  and  $R_6$ ,  $Q_2$  and  $Q_4$  turn off, and  $Q_1$  turns on, completing the switching cycle. With the supply's negative path restored,  $V_d$  rises until it reaches  $V_2$ , and the process is repeated.

The linear regulator can be of any type, including a three-terminal, nonadjustable device. Note that a switching current regulator can be formed if the regulator is replaced by a resistor. In that case, the switching current will be  $I_s = V_z/R$ . □



**Mixed mode.** Switched and linear regulators are combined to form a unit that has the advantages of both—low ripple, fast response, and high efficiency. Here a switched circuit serves as a preregulator for the linear series-pass element, the LM317K.

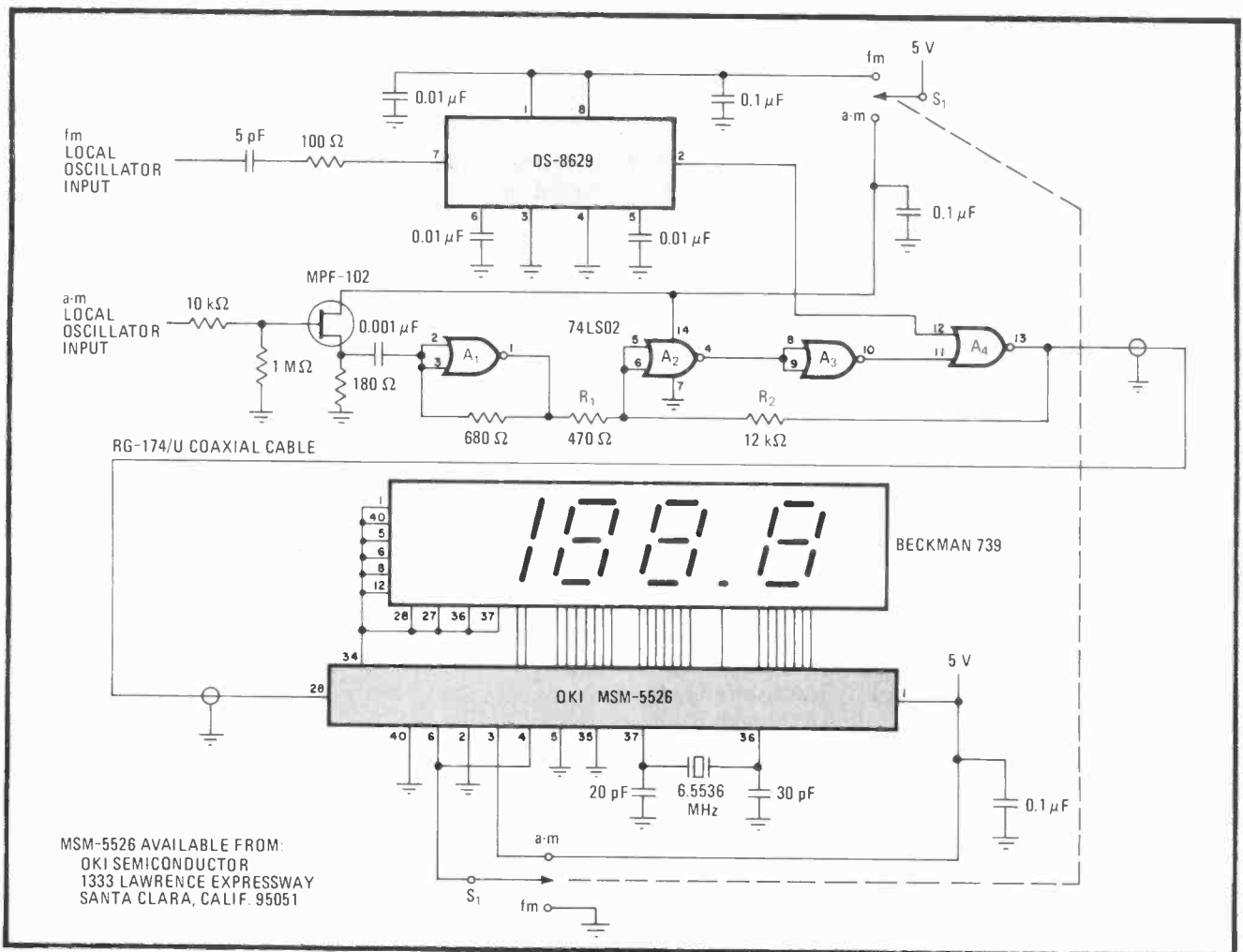
## LSI counter simplifies display for a-m/fm radio

by Gary McClellan  
Beckman Instruments Inc., Fullerton, Calif.

The design of a display providing a direct readout of any frequency tuned by an a-m/fm radio is made simple with

this circuit, which uses a large-scale integrated counter-driver to determine the frequency of the receiver's local oscillator. The counter is unique in that it contains circuitry that subtracts the receiver's intermediate frequency from the local oscillator frequency in order that the true channel frequency may be found. The combination of this counter, a one-chip prescaler, and a 3½-digit liquid-crystal display makes for a compact and relatively low-cost unit.

The circuit is housed in two separate modules, one containing the preamplifier, prescaler, and logic, and the



**i-f compensation.** MSI and LSI chips reduce cost and complexity of display for a-m/fm radio. MSM-5526 counter has circuitry for subtracting receiver's i-f frequency (see table) from radio's local oscillator input so that the true channel frequency may be displayed.

other the counter and LCD components. In this way, the first module can be mounted on the receiver's radio frequency assembly (keeping unwanted pickup to a minimum), and the other may be placed at any convenient spot for viewing.

In the a-m mode, signals are applied to the MPF-102 field-effect transistor. The input impedance of this stage is high, and consequently loading of the local oscillator is minimal. A<sub>1</sub> operates in its linear region and thus serves to amplify the local oscillator signal.

Schmitt trigger A<sub>2</sub>-A<sub>4</sub> squares up the signal to transistor-logic levels, then applies it to the MSM-5526 counter. R<sub>1</sub> and R<sub>2</sub> set the hysteresis of the trigger.

The MSM-5526 contains a read-only memory that may be programmed with any i-f value (see table). Also contained is the subtraction circuitry discussed previously, and the necessary decoders/drivers for presenting the 3½-digit Beckman LCD with the difference frequency in kilohertz. Generally, the local oscillator will always lie above the incoming frequency in the modern a-m receiver, as reflected in the table. The same condition holds true most of the time in fm receivers, but there is a provision for achieving a positive offset if one of the older receivers is being used. Note that if all programmable pins are set at logic 0, an i-f of 455 kHz for a-m

| MSM-5526 INTERMEDIATE-FREQUENCY OFFSET |                 |   |   |        |                                   |
|--|-----------------|---|---|--------|-----------------------------------|
| Display mode                           | Input-pin state |   |   |        | Offset<br>(a-m in kHz, fm in MHz) |
|  | 2               | 3 | 4 | 5      |                                   |
| a-m<br>(pin 6 high)                    | H               | H | H | X      | -452.5                            |
|  | L               | H | H | X      | -454.5                            |
|  | H               | L | H | X      | -456.5                            |
|  | L               | L | H | X      | -465.5                            |
|  | H               | H | L | X      | -467.5                            |
|  | L               | H | L | X      | -469.5                            |
| fm<br>(pin 6 low)                      | H               | H | H | H      | 10.68                             |
|  | L               | H | H | H      | 10.71                             |
|  | H               | L | H | H      | 10.75                             |
|  | L               | L | H | H      | 10.79                             |
|  | H               | H | L | H      | 10.82                             |
|  | L               | H | L | H      | -10.58                            |
|  | H               | L | L | H      | -10.60                            |
|  | L               | L | L | H      | -10.61                            |
|  | H               | H | H | L      | -10.62                            |
|  | L               | H | H | L      | -10.63                            |
|  | H               | L | H | L      | -10.65                            |
|  | L               | L | H | L      | -10.66                            |
|  | H               | H | L | L      | -10.69                            |
|  | L               | H | L | L      | -10.70                            |
| H                                      | L               | L | L | -10.72 |                                   |
| L                                      | L               | L | L | -10.73 |                                   |

and 10.7 MHz for fm will be subtracted.

In the fm mode, the receiver's local oscillator is applied to the DS-8629 prescaler. This prescaler has high sensitivity, and the local oscillator need only be capable of supplying a minimum of 12 mV at 100 MHz.

The DS-8629 divides the incoming frequency by 100. Then the signal is gated through to the counter via A<sub>4</sub>. In this configuration, an i-f equal to 1/100 the fm receiver's nominal value (10.7 MHz) is subtracted from the input frequency to the counter, and the result is displayed in megahertz.

A number of practical considerations must be taken into account when building this display. Specifically, the presence of the prescaler will introduce a typical shift of

500 Hz in the read-out frequency. The error may be eliminated entirely by simple adjustment of the 30-picofarad air-variable trimming capacitor, located at pin 36 of the counter.

The first module should be shielded from the receiver's tuner if noise in the fm mode is to be held to a minimum. Housing the module in an aluminum enclosure will suffice in most cases. And although the liquid-crystal display will tend to generate less noise than many light-emitting-diode displays now available, shielding it may also be necessary in extreme cases.

Both modules should be coupled via a coaxial cable. Otherwise a broadband hiss may be heard when the unit is placed in the a-m mode. □

## Balanced modulator chip multiplies three signals

by Henrique Sarmento Malvar

Department of Electrical Engineering, University of Brazilia, Brazil

Three signals can be multiplied by a one-chip double-balanced modulator, a device normally capable of mixing only two. In this case, the third input is introduced at the bias port of Fairchild's  $\mu$ A796, enabling the unit's transconductance to be varied at an audio rate, which effects modulation. Although the technique reduces the bandwidth and dynamic range over which the device can operate, the three-input mixer will still be useful in many applications, notably for generating discrete sidebands and synthesizing music.

The output voltage from the mixer,  $V_o$ , is the product of a carrier switching function,  $V_c$ , and a modulated signal,  $V_s$ . Because the bias signal,  $V_b$ , controls the conductivity of transistors that are effectively in series with the usual modulating signal, it is simply regarded as

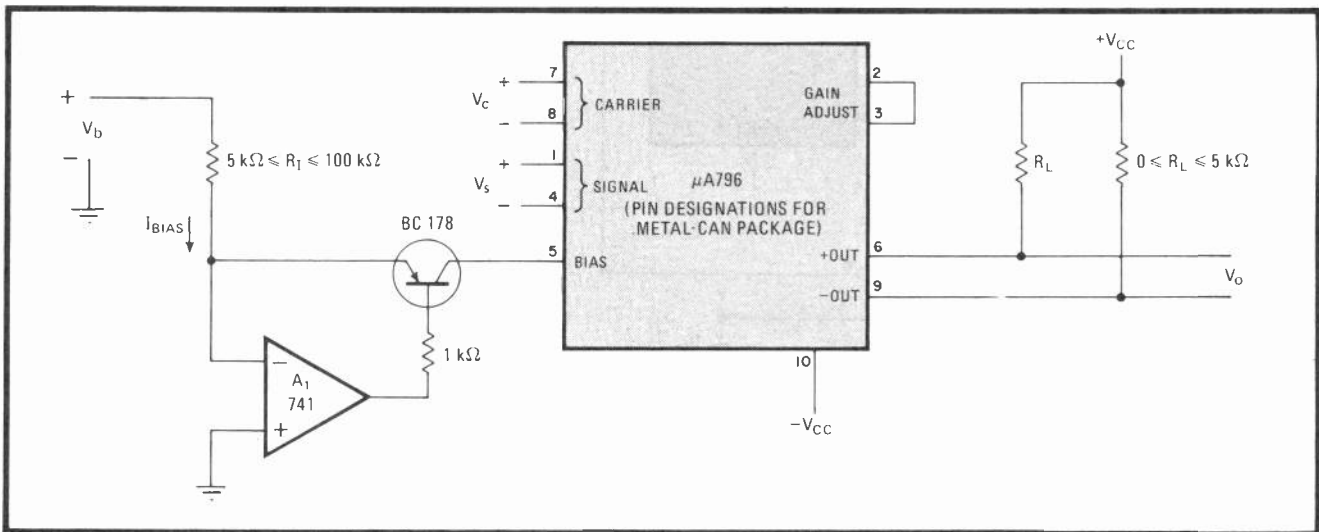
a second modulating signal such that  $V_o = kV_bV_cV_s$ , where  $k = 0.00064R_L/R_1$  over a small dynamic range and the voltages are in millivolts.

Note that  $V_c$  and  $V_s$  may be positive or negative but that  $V_b$  must always be positive to prevent the reverse-biasing of the internal transistors connected to pin 5. When  $V_b$  is negative, A<sub>1</sub> blocks the application of negative voltage by turning off the BC 178 transistor.

Note also that  $k$  will vary nonlinearly with the amplitude of  $V_c$  and  $V_s$ , and in order to keep  $k$  within 1% of its given value, both voltages must not exceed 8 millivolts root mean square.  $V_b$  will not affect  $k$  if  $I_{bias} \ll 1$  milliamperes. Unfortunately,  $k$  also is sensitive to temperature changes ( $-0.67\%/^{\circ}\text{C}$ ), and this factor can limit the circuit's effectiveness in high-accuracy applications.

The output frequencies generated by the mixing process will be  $|f_c \pm f_s|$ , and  $|f_c \pm f_s \pm f_b|$ , where the  $f$  subscripts correspond to their voltage counterparts. There will be no output if any of the driving signals are disconnected.

Signal inputs  $V_c$  and  $V_s$  may have an  $f_c$  or  $f_s$  of one megahertz at the maximum. The third input,  $V_b$ , will be band-limited to 20 kilohertz, however, because of the relatively poor frequency response of the 741. □



**Biased mixer.** A balanced modulator can be configured to multiply three signals by introducing the third signal to the bias port. The bias current, which normally sets the dc operating point of device, is varied at an audio rate to effect linear modulation over a small dynamic range.

# Hyperbolic clock inverts time

by Keith Baxter  
New Haven, Conn.

Instruments designed to measure speed must contain circuits for converting a time function,  $t$ , to units of  $1/t$  in order to calculate rate. This circuit aids in plotting the hyperbolic curve ( $1/t$ ) using relatively few parts and, notably, having no need for logarithmic dividers.

As shown in the figure, a start pulse triggers transmission gate  $S_1$ , initiating the measurement cycle. At that time,  $A_1$  and  $A_2$  are reset. Current  $I_1$  thereupon charges  $C_1$  linearly, and thus a ramp voltage is applied at the noninverting input of  $A_3$ .

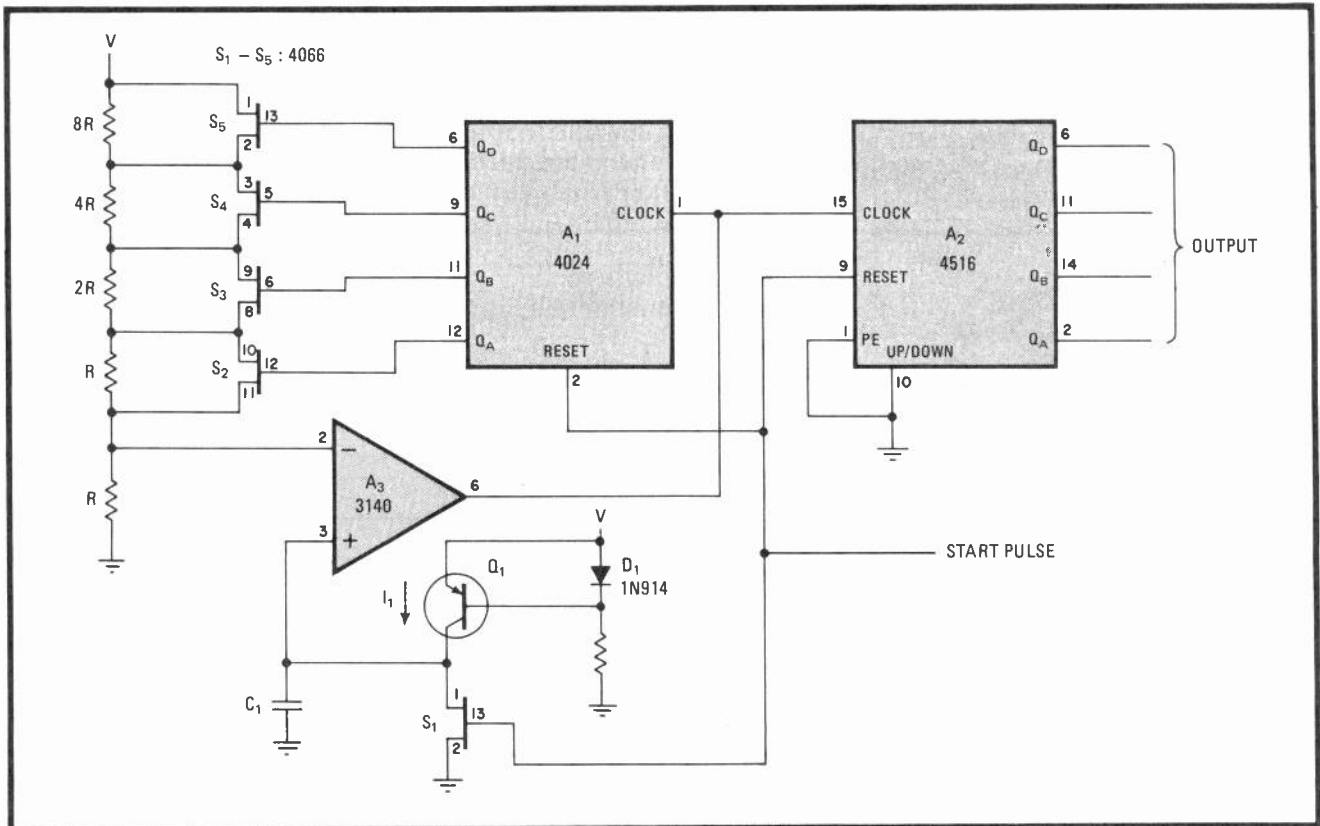
When the ramp voltage reaches  $1/16$  volt, the potential at the lowermost tap on the resistor voltage divider  $A_3$  moves high and advances counter  $A_1$ . At this instant, the total elapsed time is  $1/16 (C_1/I_1)$  V.

Switch  $S_2$  is then activated, so that the second resistor

in the ladder is shorted. Thus the voltage at the inverting port of  $A_3$  increases to  $1/15$  v. When the ramp voltage reaches this value,  $A_3$  again moves high and fires  $A_2$ . This action occurs at an elapsed time of  $1/15 (C_1/I_1)$  V. The process continues as  $A_1$  counts to 15 in a binary sequence and either all combinations of the resistor ladder are shorted or the measurement cycle ends (start pulse held at logic 1). It is assumed the data will be stored in a latch prior to the start pulse, because  $A_2$  will be reset. At that time,  $A_2$  will have counted down with each clock from  $A_3$  to provide an output corresponding to an elapsed time of  $1/t (C_1/I_1)$  V, where  $t$  may assume integer values from 1 to 15. Note that comparable circuit action cannot be realized easily with an astable multivibrator operating as a fixed-frequency source for stepping  $A_2$ ; that is, the circuit is not performing a time-to-frequency conversion.

The contents of  $A_2$  at the termination of the measurement cycle provide a direct indication of an object's speed. The factor  $(C_1/I_1)V$  may be adjusted to 1 by suitable choice of component values or set to a multiplicative constant as required. Also, to reduce the voltage divider increment, the resistor ladder may be expanded by cascading counters and their appropriate circuitry. □

**Time twist.** Circuit inverts time function,  $t$ , to  $1/t$  in order to measure speed. Note that unit does not perform a standard time-to-frequency conversion. Ramp voltage derived from current generator is compared with resistive-ladder voltage at  $A_3$ , and  $A_1$ - $A_2$  are clocked each time the ramp exceeds changing ladder potential. Output of down counter,  $A_2$ , yields rate.



# Optoelectronic alarm circuit is time-sensitive

by Forrest M. Mims III  
San Marcos, Texas

Using an optoelectronic slot switch and a 556 dual timer operating as both a pulse generator and missing-pulse detector, this circuit generates an alarm when an opaque object blocks the light input for longer than a preset time interval. It has many applications and is especially useful when united with a slotted disk to monitor motor speed stroboscopically, indicating when the steady-state rotation rate is too high or low. It can also be used on the production line for checking the width of materials.

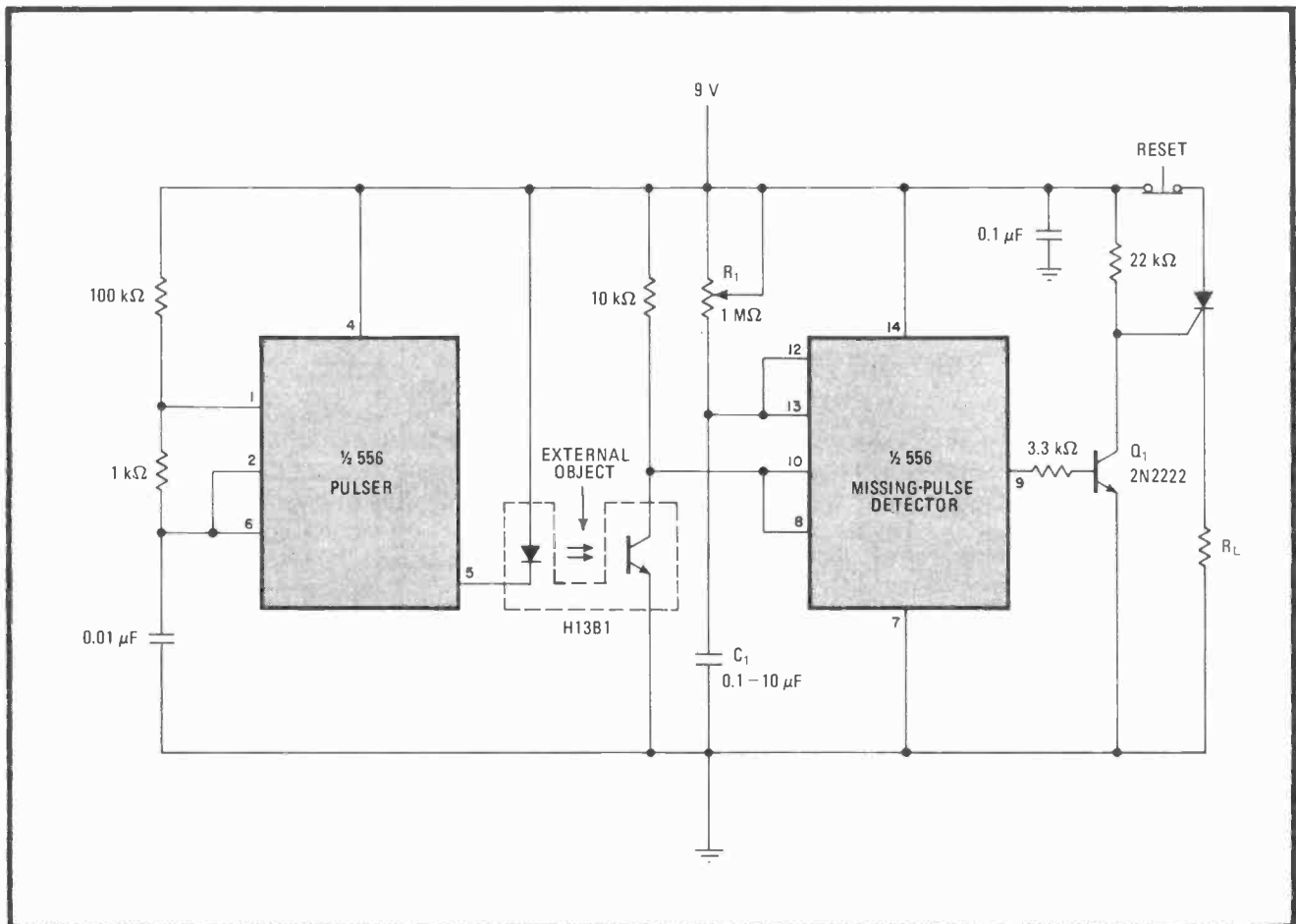
Generally, the output of the pulser periodically activates the light-emitting diode of the H13B1 switch. Other sensors may be used; Darlington photosensing

transistors, though, are the most sensitive. In this case, the pulser's operating frequency is set at 1.42 kilohertz, but it may be suitably selected by replacing the 100-kilohm resistor at pin 1 with a potentiometer.

As shown, the H13B1 is built with a slot of several millimeters separating its LED from the output photo-transistor so that objects can be placed in the air gap between them. When the slot is not blocked, the photo-transistor continuously resets the missing-pulse detector. Should the light path be blocked, pin 8 will remain high and the threshold voltage at pin 12 will fall at a rate determined by the adjustable  $R_1C_1$  time constant.

Depending on the value of this constant, which can be selected for delays from microseconds to seconds, the detector will generate a step voltage if it is not reset within that period. The signal is then inverted by  $Q_1$ , which in turn fires the silicon controlled rectifier to drive the load,  $R_L$ .

**Light block.** Pulser operating as astable multivibrator triggers LED in slot switch so that missing-pulse detector is periodically reset. Interruptions in light beam caused by external object cut off reset pulses, causing circuit to generate alarm if interval exceeds preset time.



# Digital phase meter displays angles in degrees or radians

by Tagore J. John  
Meerut, Uttar Pradesh, India

In this unit, the phase angle between two signals is measured and displayed digitally, and so the instrument is less costly than its counterparts that use precision linear circuits and expensive meter movements. The angle can be displayed in degrees, radians, or grads (400 grads = 360°). The accuracy of the instrument is  $\pm 1$  least significant count, independent of signal differences in amplitude or wave shape.

Generally, the reference and test signals are applied to channel A and channel B, respectively, as shown in the figure. Q<sub>1</sub> and Q<sub>2</sub> generate short pulses (i.e. less than 30 microseconds) to the counting logic as each signal passes upward through its zero-crossing point. To initiate the counting cycle, the logic circuit simply gates the output of an oscillator through to the 74192 counters on the

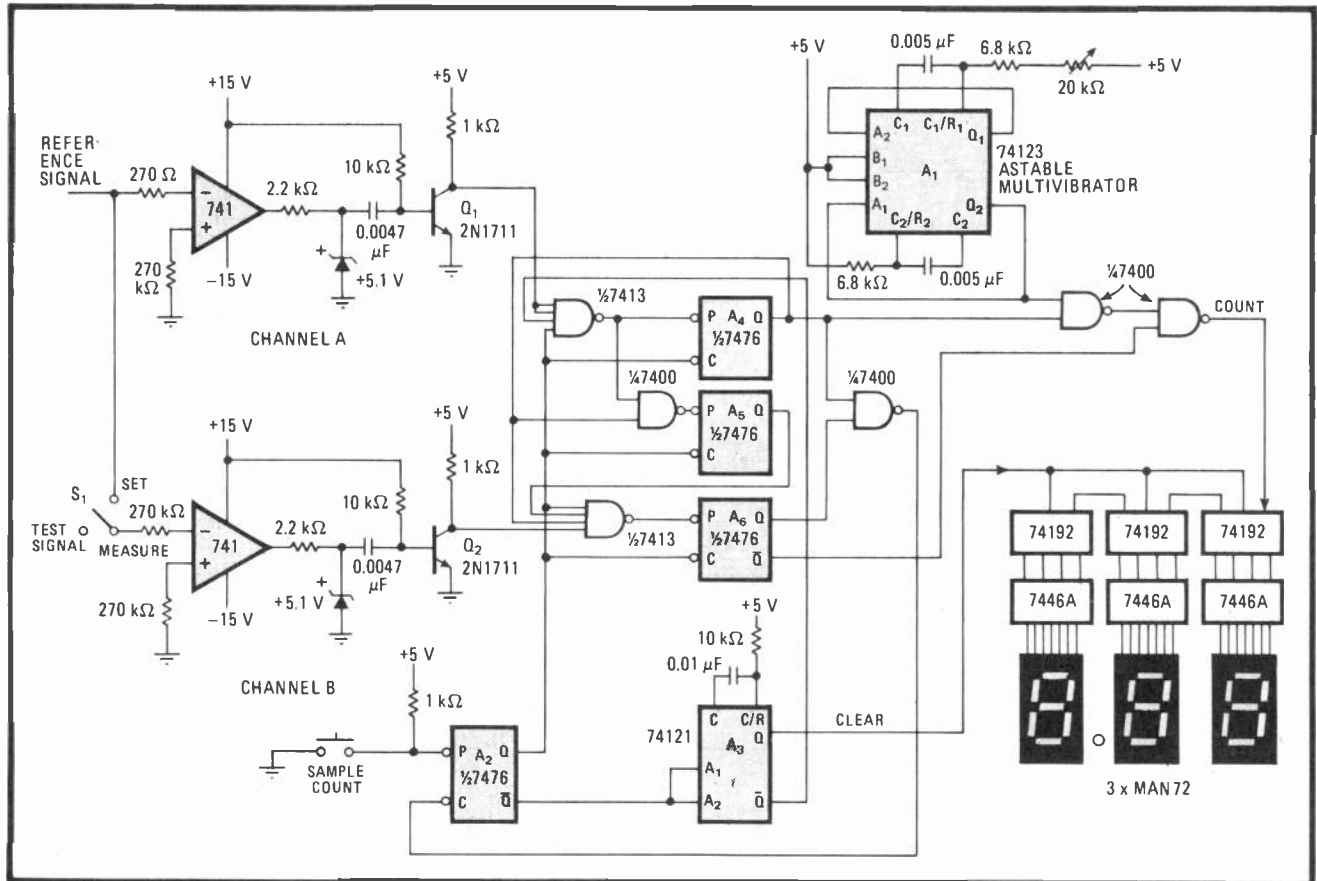
first zero-crossing pulse from Q<sub>1</sub>. The zero-crossing pulse from Q<sub>2</sub> terminates the count. The number displayed thus represents the phase difference expressed in the desired units, provided A<sub>1</sub>'s frequency is appropriately selected.

The instrument is calibrated by placing S<sub>1</sub> in the set position, introducing a reference signal, and depressing the sample-count push button as A<sub>1</sub> is adjusted for a display output of 360 (if output in degrees is desired), 400 (in grads), or 628 (in radians).

In normal operation, depressing the sample-count push button initiates the count cycle. Flip-flop A<sub>2</sub> is preset and fires one-shot A<sub>3</sub>, whereupon the display is cleared.

Q<sub>1</sub>'s first pulse sets flip-flops A<sub>4</sub> and A<sub>5</sub> and gates A<sub>1</sub>'s output through to the 74192 counters. With a pulse from Q<sub>2</sub>, flip-flop A<sub>6</sub> is set, and the output of the NAND gate driving the counters is disabled. Meanwhile, A<sub>2</sub> is cleared in order that the unit may then be readied for a new sample count.

The phase angles will be displayed directly. Provision should be made, however, for activating the decimal point to the right of the left-most digit when radians are displayed. □



**Digital differential.** Phase angle between two signals is determined to within  $\pm 1$  least significant count. Using standard chips, angle is digitally measured and can be displayed in degrees, radians, or grads, provided frequency of counting oscillator, A<sub>1</sub>, is appropriately selected.



# Single-step exerciser aids 8085 debugging

by Scott Nintzel  
Medtronic Inc., Minneapolis, Minn.

The ability to step through a microprocessor-based program is a virtual necessity during its debug and test phases. But certain processors, such as the 8085, require a minimum input frequency of 1 megahertz, so that stepping cannot be achieved merely by using a clock whose frequency corresponds to the rate at which the user wishes to move through the program. With two flip-flops, some logic, and a simple switch arrangement, however, single-stepping can be carried through without disturbing the basic operation of the processor.

Every 8085 instruction requires at least one machine cycle, each of which in turn consists of several parts known as T states. The first cycle of each instruction is referred to as the op code fetch cycle. Single-step operation can be attained by adding an integral number of waiting cycles or  $T_{wait}$  states to the op code fetch cycle with the single-step circuitry.

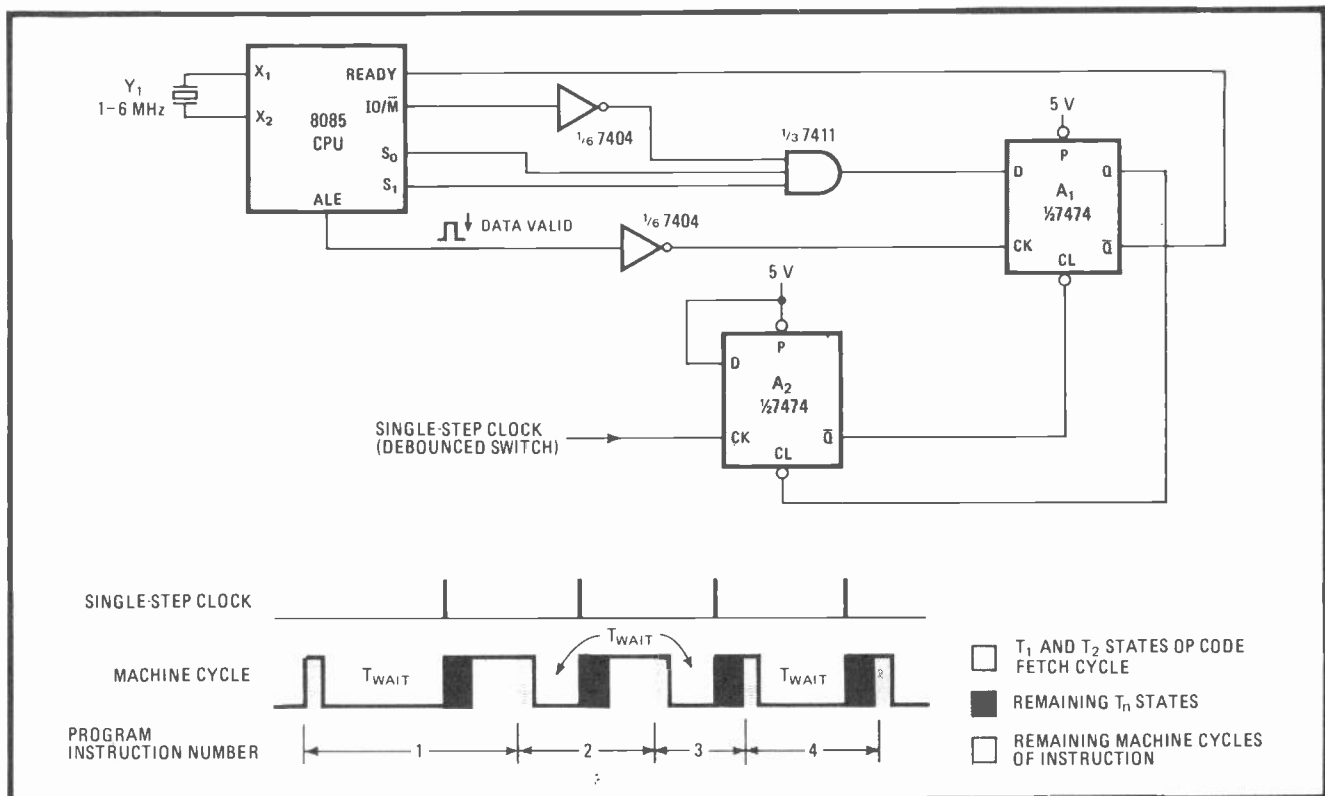
Operation is clarified in the figure and the timing

diagram. Immediately after a system reset, the central processing unit of the 8085 processes the first program instruction through state  $T_2$  of the op code fetch. The address-latch enable (ALE) line then moves low.

Lines  $IO/\overline{M}$ ,  $S_0$ , and  $S_1$  of the CPU are examined at this time. Because the 8085 is in the fetch portion of the cycle,  $IO/\overline{M}$  will be low and  $S_0$ - $S_1$  will be high, so flip-flop  $A_1$  will be set. Thus the CPU's ready line will be brought low, and the 8085 will enter the wait state. Therefore, in the initial case, instruction 1 of the program will not be completed until a single-step command is received.

Then,  $A_2$  clears  $A_1$ , the ready line is brought high, and the remaining  $T_n$  states and machine cycles are executed, as are the  $T_1$  and  $T_2$  states of the next instruction cycle. At this time, the machine reenters the  $T_{wait}$  state and remains there until cleared, as discussed previously.

A debounced switch or slow-running clock made from gates can be used to generate the single-step command, and total chip count for the unit should not exceed three ICs. Note that  $A_2$  is required to ensure that  $A_1$  clears quickly enough to allow capture of the subsequent fetch cycle. Without  $A_2$ , the pulse width of the single-step clock might be too long, and disturb the setting of  $A_1$ . □



**Walking through.** Simple single-step controller for debugging 8085 routines places CPU in wait state between program instructions. Processor is made to execute last part of one instruction and first part of next before halting, thereby advancing one location at a time.

# Electronic sink simulates load for testing power supplies

by Henry Santana  
Hewlett Packard Co., Loveland Instrument Division, Loveland, Colo.

The bank of bulky, high-power load resistors normally required to check the current-delivery capability of various power supplies can be eliminated by this programmable load. Able to simulate an equivalent resistance as low as a few milliohms and handle input powers up to 50 watts, this compact unit, which uses operational amplifiers and transistors to limit the amount of current it will sink, serves as a good general-purpose device for production-line testing. It can be built for \$40.

The idea behind the circuit is explained with the aid of (a). Neglecting the on-resistance of transistor  $Q_1$ , and considering that a virtual ground exists between the inverting and noninverting inputs of operational amplifier  $A_1$ :

$$V_1 = V_{in} = K\alpha V_2 \quad 0 < \alpha < 1 \quad (1)$$

where  $K$  represents the gain of  $A_2$ ,  $\alpha$  is selected by a

potentiometer, and  $V_2$  is a floating supply required to maintain the necessary bias on the control transistor. Also note that  $V_2 = I_{in}R_a$ . When this expression is substituted in Eq. 1, it is seen that:

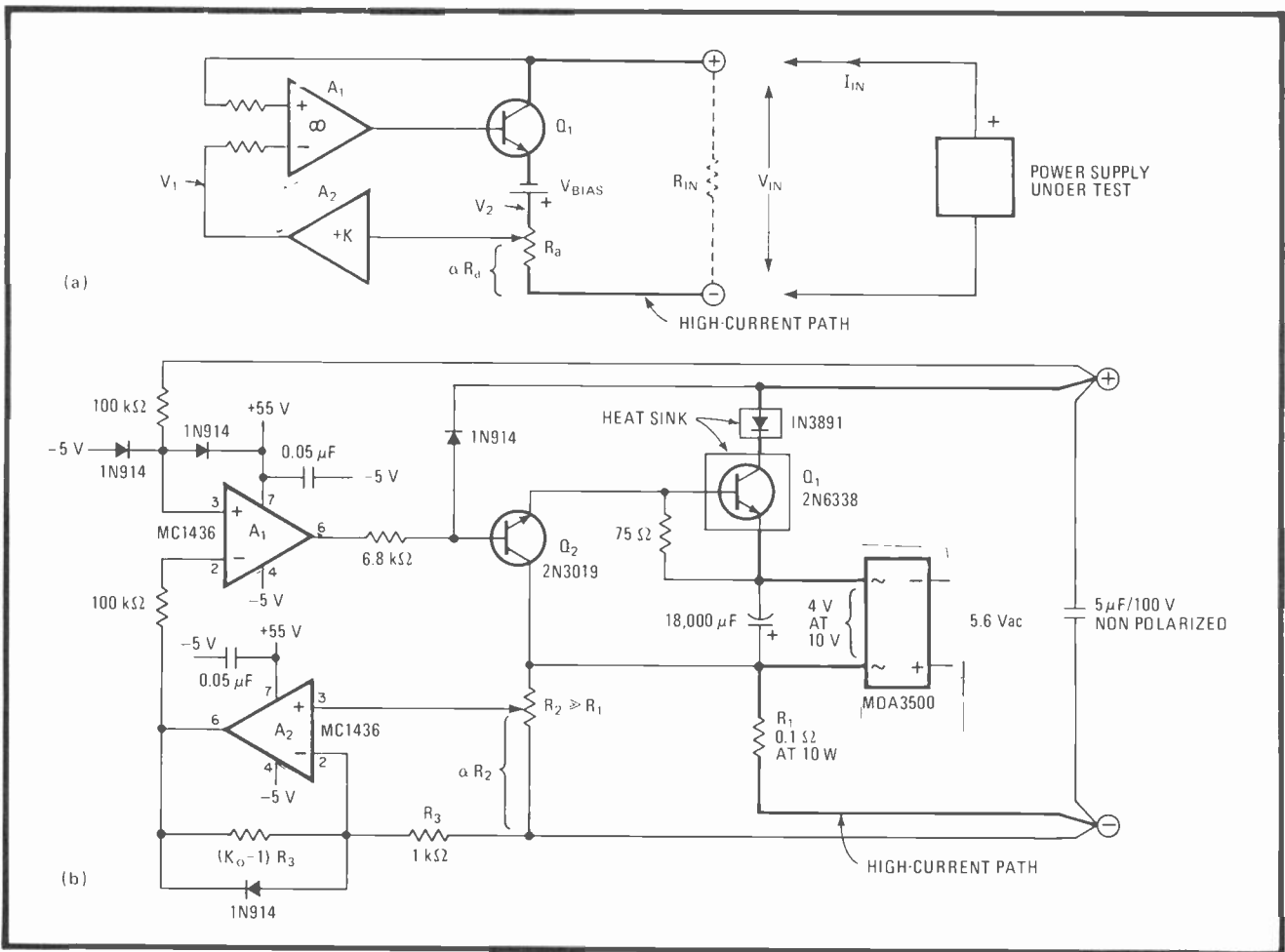
$$R_{in} = V_{in}/I_{in} = K\alpha R_a \quad (2)$$

and therefore the resistance seen by the power supply under test can be set by  $R_a$ .

The circuit required to implement the idealized configuration is shown in (b). High-voltage op amps are used for  $A_1$  and  $A_2$  to handle the large input potentials expected.  $Q_2$  has been added in order to supply adequate drive current to the output (control) transistor.  $R_a$  in (a) is represented by  $R_1$  and  $R_2$  in (b), where the value of  $R_1$  is made small in order to minimize the voltage ( $V_2$ ) needed to bias the control transistor.

If the gain of  $A_2$  is selected for  $K = 500$ ,  $R_{in}$  can be made to vary from approximately 0 to 50 ohms. If  $R_2$  can be selected digitally, any resistor value in this range can be automatically ordered up. The unit can withstand a maximum input voltage of 50 volts and input currents up to 10 amperes, though the maximum input power cannot exceed 50 watts, as mentioned previously.

The components in the path of high current should be mounted on suitable heat sinks, for the power dissipated is approximately  $P_d = (5 + V_{in})I_{in}$ . □



**Equivalent resistor.** Suitably configured op amp and power transistor combination (a) will function as a programmable electronic load. Practical implementation of idealized circuit is shown in (b). Unit handles a maximum power input of 50 watts.

# Single a-d converter cuts cost of droopless sample-and-hold

by Carl Andren  
Harris Corp., Electronics Systems Division, Melbourne, Fla.

Because leakage currents cause droop, sample-and-hold circuits with capacitors as storage elements cannot retain a sampled voltage indefinitely. This is the major reason designers, to improve sample-and-hold performance, have resorted to converters combining analog-to-digital and digital-to-analog converter functions. But a single a-d device can be made to perform both functions alternately, thus cutting the cost and complexity of the two-converter scheme. Only one operational amplifier and a solid-state switch are needed in addition.

The more popular forms of a-d converter use a successive-approximation register that—with the aid of a self-contained comparator and a d-a converter—generates a digital estimate of the sampled analog voltage. When the comparison has been approximated to the least significant bit, the measurement is ended and an end-of-conversion signal is generated. If the unit is then config-

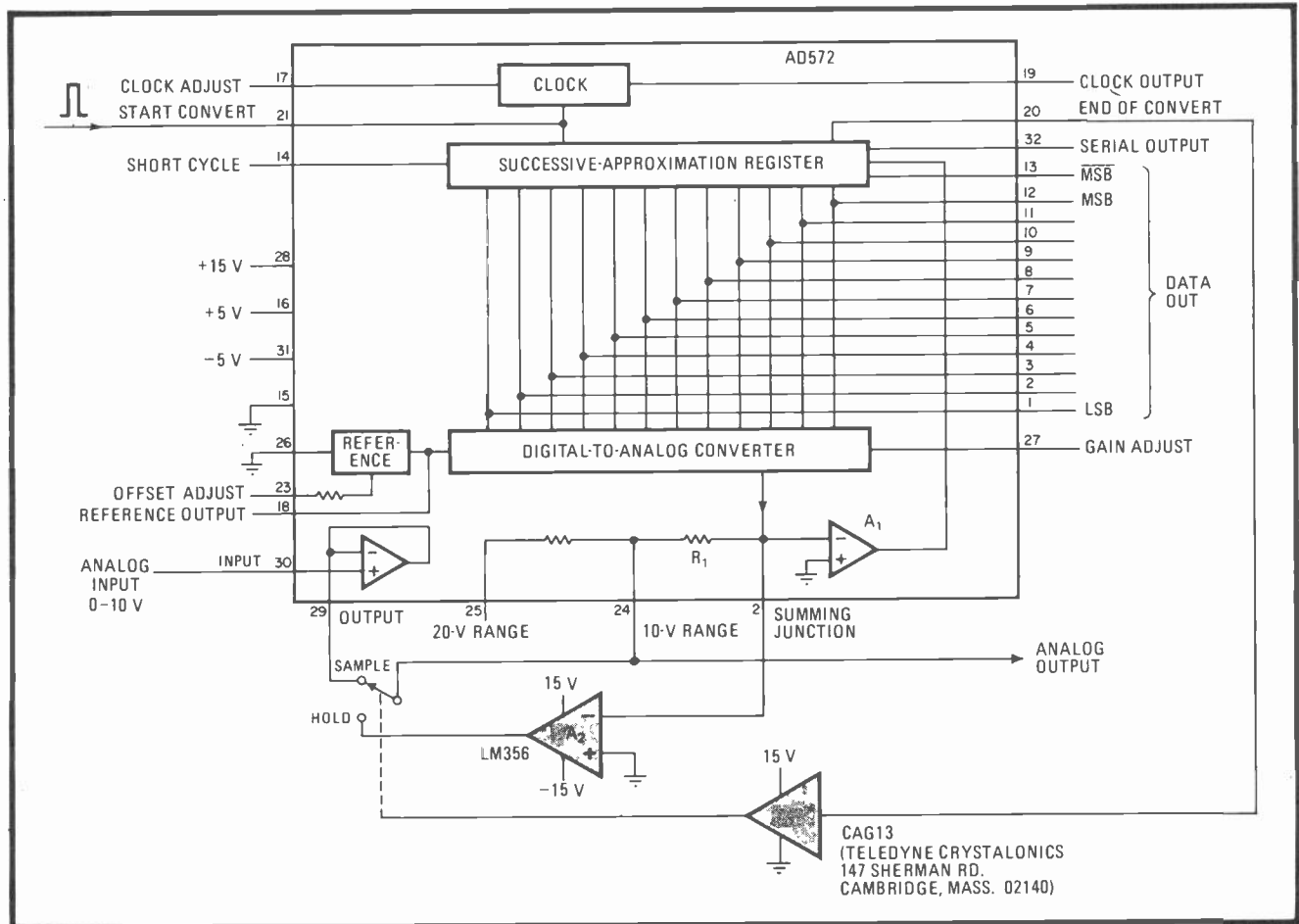
ured as a latched d-a converter, the sampled analog voltage may be recovered and held indefinitely (assuming that one input of the comparator is accessible).

As shown, in the normal a-d conversion mode of a representative device like the AD572, a start-convert pulse initiates the measurement. An analog voltage, applied across resistor  $R_1$  in the summing junction of comparator  $A_1$ , can then be sampled.

The successive-approximation register generates a 12-bit equivalent of the analog voltage and also drives the d-a converter that is connected to  $A_1$ 's summing junction. The d-a converter then attempts to null  $A_1$ 's output, whereupon the end-of-conversion signal (EOC) is generated. The sampling period takes a nominal time of 2.5 microseconds.

In this circuit, the EOC signal energizes a solid-state relay (CAG13) so that the converter can be switched to the holding mode.  $R_1$  is then placed at the output of an op amp,  $A_2$ .

$A_2$ 's output maintains  $A_1$ 's summing junction at a voltage null so that the output voltage becomes the potential across  $R_1$ —that is, the sampled voltage. Note that the switch resistance and  $A_2$ 's input-bias current are taken into consideration for both modes and therefore they are not, for all practical purposes, sources of error in the measurement. □



**Inverting the converting.** This analog-to-digital converter, when it is combined with an op amp and switch, can provide d-a function on the hold portion of sample-and-hold cycle, thereby reducing cost and complexity of the usual two-converter (a-d-d-a) scheme. No sampling-peak capacitor is required in the converter sampling technique, so that the sample-voltage droop is eliminated.

# Gray-code counter steps torque motor

by Thomas L. Clarke  
Miami, Fla.

The positional accuracy of a simple stepping-motor system is limited by the response of its mechanical drive. This drawback can be eliminated electronically by using a position sensor and a counter working in Gray code to control the motor. The mechanical-drive circuit can be simplified with digital logic to reduce system errors and nonlinearities. A four-state Gray-code counter enables the system to move smoothly from its starting point to the desired position.

In this circuit, the summed quadrature outputs of a photoelectric sensor and the counter (see inset) set the position of the system. With suitable clock signals, the counter is advanced one location, causing the motor's position to change and the output from the sensor to vary accordingly. Thus the system is rotated 90° for each clock signal.

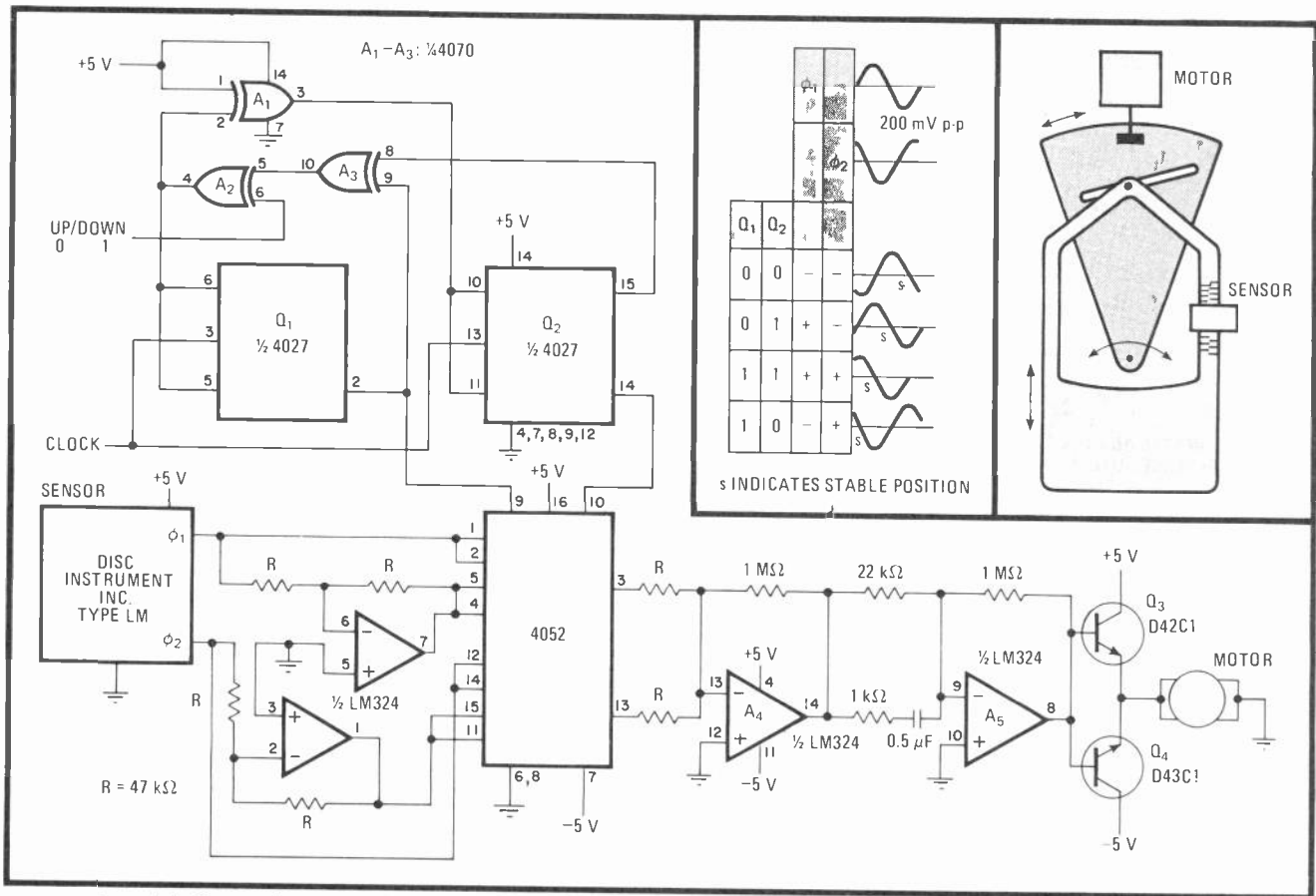
This circuit is intended for visual setting of a desired position through manual control of the clock and up/down inputs. For automatic tracking, the sensor's

output must be compared to the desired position with additional circuitry in order to generate those signals.

Flip-flops  $Q_1$  and  $Q_2$  and exclusive-OR gates  $A_1$ - $A_3$  comprise the up-down Gray-code counter. The direction of the counting is determined by the logic state at the up/down input.

The output of the counter changes on the positive transition of each clock pulse. Depending upon the state of the counter, either the normal or inverted sine-wave outputs of the sensor are summed at the output of the 4052 four-input multiplexer. As a consequence, the output from  $A_4$  forces the system to a new position, which is reflected at the sensor as its output steps a quarter cycle. The motor is driven through  $Q_3$  and  $Q_4$  by a positional signal that progressively advances or recedes (depending upon the state of the up/down counter) by a quarter cycle.

A minimum settling time of a few milliseconds is set for the system by the lead-compensation components between stages  $A_4$  and  $A_5$ . Lead compensation is required in this situation because the system response is that of a double integration network that acts to saturate  $Q_3$  and  $Q_4$ . The open loop would tend to be sluggish without the lead compensation, which reduces the effective system gain at low frequencies. □

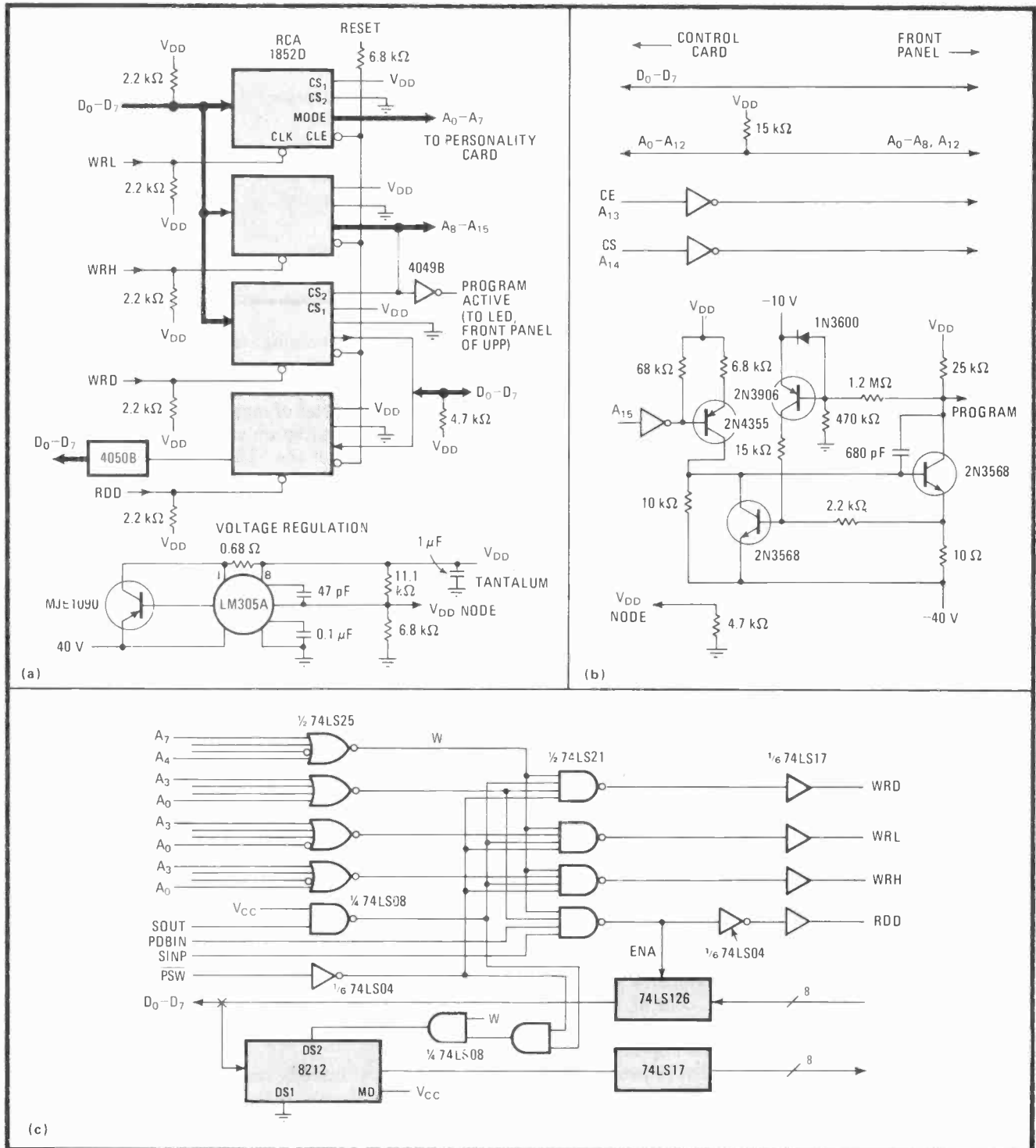


**Smooth.** Four-state Gray-code counter  $Q_1$ - $Q_2$  provides signal that, when summed with output of optical sensor by 4052 multiplexer and op amp  $A_4$ , generates quadrature output for smooth stepping of motor in quarter-cycle increments. Compensation network between  $A_4$  and  $A_5$  prevents saturation of  $Q_3$  and  $Q_4$ , eliminating sluggish system response by reducing effective gain at low frequencies.

# Software-based controller simplifies PROM programmer

by R. F. Hobson  
Simon Fraser University, Burnaby, British Columbia, Canada

While Intel's popular Universal PROM Programmer (UPP) works effectively in its intended capacity as a system development tool, it has two major drawbacks. First, the so-called personality cards that are required for manually programming each type of programmable read-only memory are expensive and much too complicated to build. Second, it is restricted to Intel PROMs, so that the newer complementary-MOS erasable-PROM



**Burning softly.** Complexity of control board (a) and personality cards (b) in universal PROM programmer are reduced if software-based controller leads system's host computer through various read/write burn-in phases. Personality card is shown for the IM6604 PROM. S-100 bus interface (c) units UPP to 8080 host processor. Small program (table) guides 8080 through write-and-verify sequence.

WRITE-AND-VERIFY SEQUENCE: IM6604 E-PROM

| Write/Verify Routine |                    | Pulse Routine   |                   |
|----------------------|--------------------|-----------------|-------------------|
| Statement            | Comment            | Statement       | Comment           |
| COUNT: DS 1          |                    | PROG EQU 80H    | CONTROL BIT.      |
| WRITE: PUSH B        |                    | PULSE: PUSH PSW |                   |
|                      |                    | PUSH B          |                   |
|                      |                    | MOV A,D         | ADDR/CTL BYTE.    |
|                      | LATCH DATA BYTE.   | ORI PROG        | SET PROGRAM BIT.  |
| XRA A                |                    | MVI B,0EH       | SET 14MS COUNT.   |
| STA COUNT            | INITIALIZE COUNT.  | CALL HOUT       | START PROG PULSE. |
| POP PSW              |                    | CALL MSDLAY     | HOLD IT.          |
| CALL ADDR            | LATCH ADDRESS.     | XRI PROG        | CLEAR PULSE BIT.  |
| CALL INFO0           | INITIALIZE CRT.    | CALL HOUT       | RESET PROG PULSE. |
| WLP: CALL PULSE      | SEND A PROG PULSE. | MVI B,07H       | 7MS COUNT.        |
|                      | VERIFY             | CALL MSDLAY     | WAIT (2/3 DC).    |
| MOV B,A              | SAVE DATA BYTE.    | POP B           |                   |
| LDA COUNT            |                    | POP PSW         |                   |
| INR A                | BUMP UP COUNT.     | RET             |                   |
| STA COUNT            |                    |                 |                   |
| CALL READ            | GET CELL CONTENTS. |                 |                   |
| CMP B                | COMPARE WITH DATA. |                 |                   |
| JZ BURN              | EXIT IF VERIFIED.  |                 |                   |
| CALL INFO1           | UPDATE CRT.        |                 |                   |
| LDA COUNT            |                    |                 |                   |
| CPI 030H             | PULSE LIMIT ...    |                 |                   |
| MOV A,B              |                    |                 |                   |
| JC WLP               | EXCEEDED?          |                 |                   |
| STC                  | IF SO EXIT.        |                 |                   |
| POP B                |                    |                 |                   |
| RET                  |                    |                 |                   |
| BURN: . . . . .      | LAST WRITE OK,     |                 |                   |
|                      | BURN AND EXIT.     |                 |                   |

information; the remaining output line is used for a data-output latch.

Of the 16 PROM-address lines available, 12 are used to address up to 4 kilobytes of memory. The remaining four lines can be used for program and chip control. Consider the personality card of the 512-by-8-bit IM6604 PROM, for example (b in figure). There, line A<sub>15</sub> is used for a program pulse enable, A<sub>14</sub> and A<sub>13</sub> are used for chip select and chip enable, respectively, while line A<sub>12</sub> is used for a strobe pulse. The popular 27XX E-PROM series would require only two control lines. Because the 27XX chips are powered by 5 volts, while C-MOS devices require 10 V for programming, the 27XX's personality card would interface to the host computer through open-collector devices.

chips cannot be programmed. The personality cards can be simplified and the UPP peripheral device made more versatile, however, if a software-based controller guides the system's host computer through the various read/write phases required to program and verify the contents of PROMs.

The basic UPP interface has eight data-input and eight data-output lines, along with read-data, read-acknowledge, and read-status ports. Also included is a write-data line, a write high-address and write low-address line, and an interrupt line. A pulsed control signal required for programming each PROM location is handled via a 4-bit 4040 microprocessor on a control card in the UPP.

The best way to simplify such a peripheral is to have the host computer provide the timing, control, and logic necessary for programming, reading, and verifying the contents of PROMs and E-PROMs. The complexity of the UPP's control card is then reduced to that shown in (a) of the figure, where the 4040-based setup is replaced by four C-MOS I/O chips (RCA 1852D).

The host computer consequently sees one input port and three output ports. The input port is used for returning the contents of a selected memory word. Two of the output ports are used for latching address and control

In general, then, a personality card will consist of a bidirectional data bus, the required number of address lines, and a pulser circuit. It is thus used mainly to route the bus lines to the proper front-panel pin positions on the UPP. The pulse circuit must be designed to be reset by the UPP's front-panel reset button. This can be accomplished by connecting the reset line to the 1852D's CLE inputs. For completeness, the program control line (on the control card) is also connected to the program LED on the front panel.

A typical S-100 bus interface for the modified UPP is shown in (c). I/O ports 32, 33, and 34 have been decoded for a data strobe (read), write low-address, and write high-address, respectively. Interface software must include a timing subroutine and program pulse and verification routines particular to the PROM that is programmed.

As for the programming required, the sequence in the table outlines the steps necessary for the write-and-verify operation in the IM6604. The program is written for the host 8080A microprocessor. □

# What to look for in logic timing analyzers

More channels, assorted speeds, display options, novel triggering schemes ensure there's an instrument for every digital timing problem

by Martin Marshall, *Marshall Enterprises, San Francisco, Calif.*

□ Logic timing analyzers have learned a lot of new tricks in the six short years of their existence. From the start their high-speed asynchronous clocking marked them as the instruments of choice for solving hardware-related problems like short-duration glitches, skewed signal arrival, and intermittent timing failures. Software troubles are usually taken on with logic state analyzers that synchronize their clocking with the clock of the system being tested and thus are 5 to 10 times slower. But sometimes problems that appear to be software-generated are in fact hardware-related and require the more detailed analysis possible with the faster asynchronous instrument.

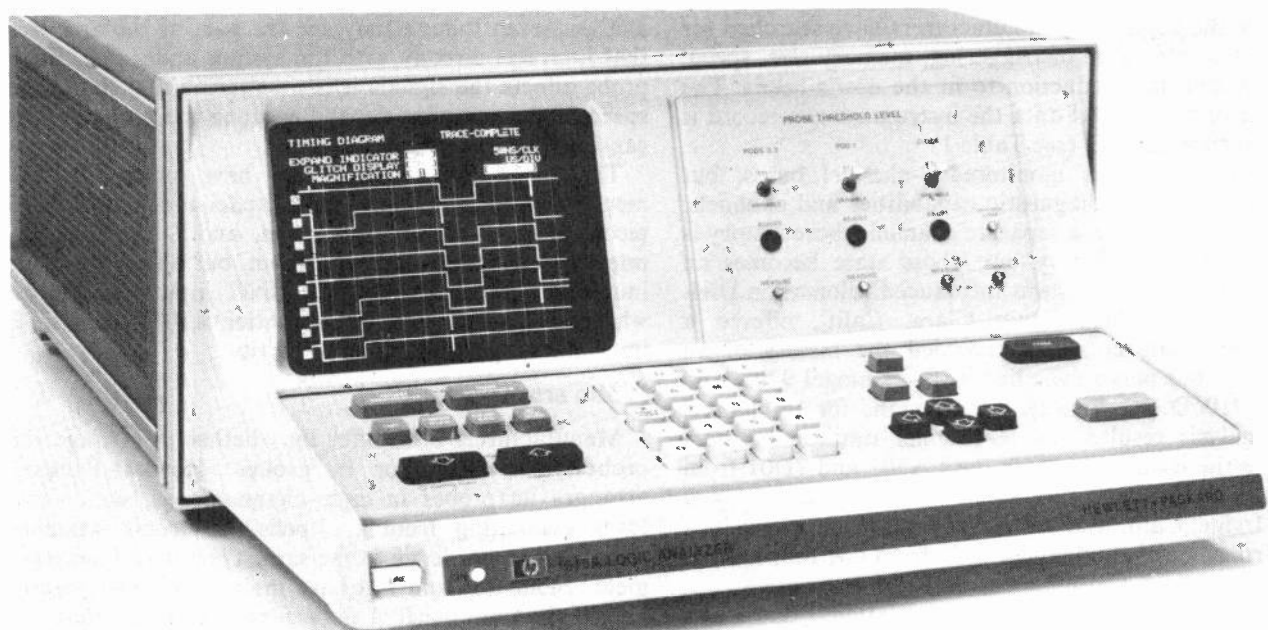
## Small time windows

Most currently available logic timing analyzers are capable of both synchronous and faster asynchronous operation. In either mode, the analyzer monitors digital signals on address, data, or control lines, confirming proper word construction on a bit-by-bit basis.

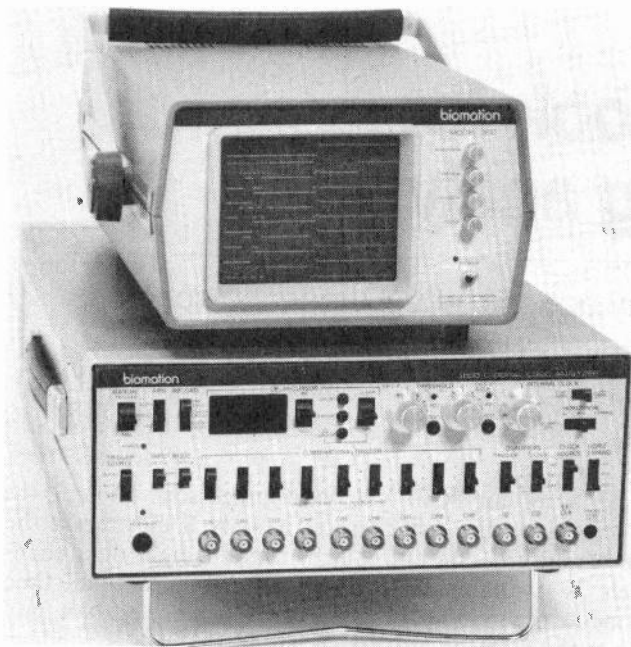
An example of the need for a timing analyzer's inherent speed advantage appears upon examining the status

activity of an 8080-type microprocessor. Though the microprocessor itself operates at only 2 megahertz the status information multiplexed onto its eight data channels is available only within a 50-nanosecond time window occurring between system clock cycles. Not only must the 8 status bits arrive within that 50-ns window, but two sync lines must change state as well. To examine the skew of these signals properly, the 50-ns interval should be broken down into five 10-ns samples. This is possible only if the analyzer is running at a 100-MHz sampling rate. A state analyzer running synchronously at 2 MHz cannot perform this kind of analysis, as the skew of the signals would not be magnified sufficiently.

Examining the timing relationships of a microprocessor to its peripheral chips, or of timing within non-microprocessor-based systems, brings up further examples. Even a slower microprocessor such as the 1-MHz 6800 chip features input/output data hold times in the 10-ns range. Faster, newer chips like Nippon Electric's high-speed version of the Advanced Micro Devices AMD 2900 can be added to the list of examples. Such a bipolar chip, with its 60-ns instruction cycle time,



**1. Grabbing the glitch.** In addition to data, the timing analyzer displays fast transients or glitches that can affect the system's operation. The glitch detection circuit stretches the duration to one sampling interval. Glitches can be seen above at the center and right side of the CRT.



**2. Separate CRT.** Logic analyzers often require an oscilloscope or a separate CRT for timing display. The 100-MHz Biomation 9100 D offers eight data channels, a sync channel, and choice of clock or trigger qualifier channels. It has a word depth of 1,024 words.

demands the high speed of the timing analyzer.

Another advantage timing analyzers have over most state analyzers is their ability to detect glitches. These infrequent transients are too short for detection at synchronous sampling times, but they affect system operation nonetheless. Special latching circuitry detects glitches as short as 5 ns in duration and stretches the transients to one sample interval for recording by the analyzer. Figure 1 shows several waveforms containing glitches captured and displayed using this circuitry.

### Evolution of the timing analyzer

Since the beginning, manufacturers have searched for the best combination of triggering, memory size, speed, display, and data reduction to fit the user's needs. The number of channels of data the instrument can record is also of prime concern (see Table 1).

The earliest units monitored 8-channel buses, but users needed more diagnostic capabilities and channels. The trigger qualifier, a separate channel whose history is not recorded in memory but whose state becomes an added trigger criterion, was introduced. Biomation Division of Gould Inc., Santa Clara, Calif., offered a 9-channel analyzer which recorded the history of an 8-channel bus plus a sync line, with its model 920D and model 9100D (see Fig. 2). User demand for 16-channel bus analysis resulted in 16-channel timing analyzers such as the Biomation 1650; the LA501 and 7D01 from Tektronix Inc., Beaverton, Ore.; model 740 from Moxon Inc., Irvine, Calif.; the 50D16 from BP Instruments Inc., Cupertino, Calif.; and model 1850 from E-H International Inc., Oakland, Calif.

The latest increase in channel population is due to the synthesis of timing and state analysis in the Biomation K100D and the 1615A from Hewlett-Packard Co.,

Colorado Springs (Colo.) division. The reason for the combination of instruments is that timing analysis need only be done on a single bus, whereas state analysis may usefully include more than one bus. The HP 1615A offers 8 channels for timing analysis and assigns 16 channels to state analysis; this allows monitoring of a 16-bit address bus plus an 8-bit data bus.

The K100D's 16 channels can perform timing and/or state analysis; with an optional adapter, the unit can be configured as a 32-channel data domain instrument. This permits the monitoring of a 16-bit address bus and a 16-bit data bus, or an address bus, an 8-bit data bus, and various control lines within the system.

### How fast is fast enough?

Manufacturers have differed on how fast a timing analyzer should be, with some even presenting the user with a choice of speeds in different products. The first timing analyzers operated at 10 MHz, but none manufactured since then are slower than 20 MHz. Today's units run at 20, 50, 100, or even 200 MHz—which is the proper selection? The answer, of course, depends upon the speed of the equipment that the user wishes to analyze. The user must determine the minimum time interval to be resolved in the system. Often skew factors in the hardware logic of the system, rather than the clock rate presented on the bus, determine this figure.

If that minimum interval is 50 ns, then a 20-MHz analyzer such as the HP 1615A, Biomation 920D, or Moxon 740 (Fig. 3) is the answer. If it is 20 ns, then one of the 50-MHz analyzers such as the Biomation 1650, E-H 1850, or E-H 1320 can be considered. At 10 ns there is the 100-MHz Biomation K100D and Biomation 9100D; and at 5 ns, or 200 MHz, the Biomation 8200. The Tektronix plug-in timing analyzer, model 7D01, is chameleon-like with respect to speed. It is configurable for 20 MHz on 16 channels, 50 MHz on 8 channels, or 100 MHz on 4 channels.

Probes are sometimes a forgotten component of logic analysis, even though they are the part of the analyzer that interacts directly with the system under test. Each probe affects the signals it is monitoring and limits the speed of the analyzer, depending upon the probe's input capacitance and impedance.

The faster timing analyzers have probes in the megohm impedance range and capacitances of 5 to 15 picofarads. Tektronix, Biomation, and E-H all specify impedances higher than 1 megohm, but E-H specifies its impedance at the analyzer's BNC input connectors, whereas Tektronix and the Biomation K100D have their impedances specified at the probe tip.

### Probe arrangement

Manufacturers also differ on whether to arrange the probes individually or in groups. Hewlett-Packard arranges its probes in eight-channel pods, with short leads emanating from the pods; Tektronix attaches somewhat longer leads to the same type of pod arrangement. Biomation and E-H have individual probes beginning at the front panel of the analyzer, claiming that this allows easier connection of physically divergent parts of the system at the same time. Tektronix and Biomation





**3. Analyzers evolve.** This Moxon 740 timing analyzer can monitor up to 16 channels of data at a 20-MHz sampling rate. The elimination of numerous front-panel switches and addition of a CRT were two evolutionary changes in logic analyzer design.

K100D analyzers reduce the degradation of high-speed signals by using hybrid circuits close to the point of probing. Tektronix places the hybrid circuitry in the probe pod; the K100D puts one in the tip of each individual probe (Fig. 4).

#### Triggering is the key

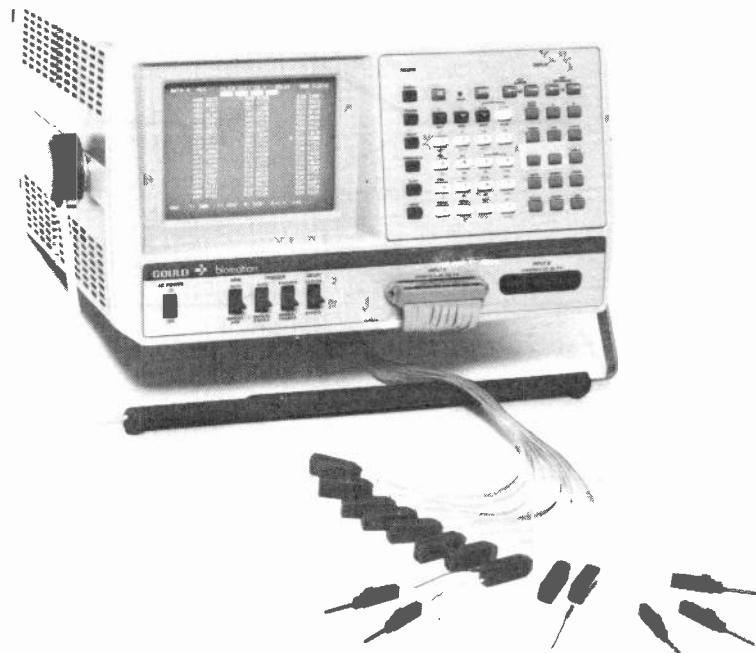
Although speed is a major factor in excluding some timing analyzers, final selection requires evaluating the analyzer's ability to trigger, its ease of use, and its ability to reduce the captured data into an intelligible display. The first of these criteria, triggering, has become an art form nearly as sophisticated as the programming techniques it unravels.

The earliest and simplest triggering criterion is the parallel word trigger. All of the analyzers have it. If the analyzer is connected to a 16-bit address bus and the selected trigger word comes along, the analyzer stops recording and its memory stores pretrigger information up to its capacity.

Clock delay was the next feature added. With it, the user can examine the program in blocks, using the same trigger word. Examining sequential blocks of program is made possible by increasing the clock delay on successive analyzer recordings (Fig. 5).

However, programs invariably contain subroutine loops and even nested loops, and potential trigger words occur many times on successive passes. To allow the analyzer to pick apart these loops, a pass counter was added to the triggering section. The pass counter delays recording into memory by counting trigger word occurrences, rather than clock cycles, to allow triggering on the *n*th pass through a subroutine. Nearly all the latest timing analyzers have this feature.

Only two, however, can make use of on-board sequential word triggering. These are the Biomation K100D and the HP 1615A. Sequential word triggering is a very useful technique for selecting a unique program path out of a seemingly ambiguous set of paths. The analyzer will



**4. Hybrid probes.** Each Biomation K100D probe has a hybrid circuit providing a high-impedance input for high-speed signal monitoring. The K100D performs state as well as timing analysis and features an extensive array of triggering and display capabilities.

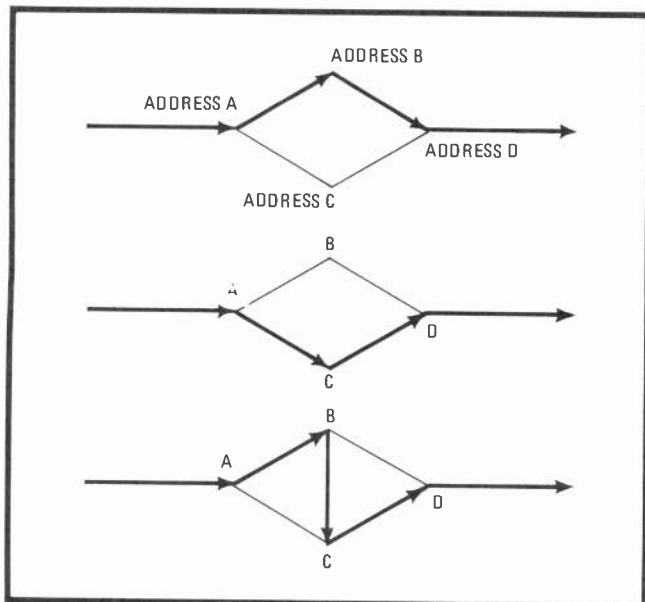


**5. Trigger tactics.** The BP Instruments model 50D16 16-channel timing analyzer's triggering capabilities include parallel word, clock delay, and events delay. The last two permit examination of a sequential program block or subroutines by increasing trigger delay.

trigger on word B, but only when it is preceded by word A. In hardware terms, word A arms the analyzer and word B (or the *n*th occurrence of word B) triggers it.

In software terms, one can picture a program path through a subroutine beginning with word A and ending with word D. Between A and D, there are three distinct paths by way of words B and C. These are ABD, ACD, and ABCD (Fig. 6). The three paths can be distinguished by triggering on sequences of words BD, AC, and BC, respectively.

In a typical application, words A, B, C, and D are



**6. Separating address flow paths.** Sequential triggering can be used to sort out program paths that are otherwise indistinguishable to the logic analyzer. In practice, sequential triggering can be used to define key I/O maneuvers such as a particular subroutine.

16-bit addresses in a microcomputer program. When triggered, the analyzer's memory will store a listing of the program's address flow. The K100D can take the extra step of qualifying the analyzer's trigger on sequential 18-bit words, allowing one to include control line signals in the trigger as well as a 16-bit address bus.

HP's model 1615A performs sequential triggering somewhat differently. Its 8-channel timing bus can arm its 16-channel state analysis bus, or vice versa. Triggering on successive 16-bit address words is not included on the model 1615A.

Intermittent failures are the most troublesome because they occur infrequently and do not show up during normal repetitive measurements. To combat intermittent logic problems, a number of analyzers

include a trigger-on-noncomparison mode.

The mode works like this. The unit captures a normal block of data from a suspected portion of the program, using trigger criteria X, Y, and Z, and transfers it into a second reference memory inside the analyzer. Next, using the noncomparison mode, the analyzer will first wait for data that meets criteria XYZ. When that data arrives, it will compare the captured data with the normal data in its reference memory. If the data is different, the instrument triggers. If not, it re-arms itself and waits for criteria XYZ to recur.

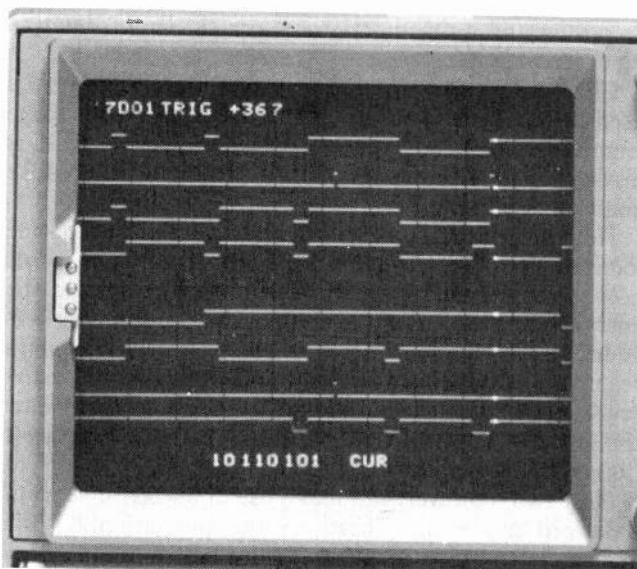
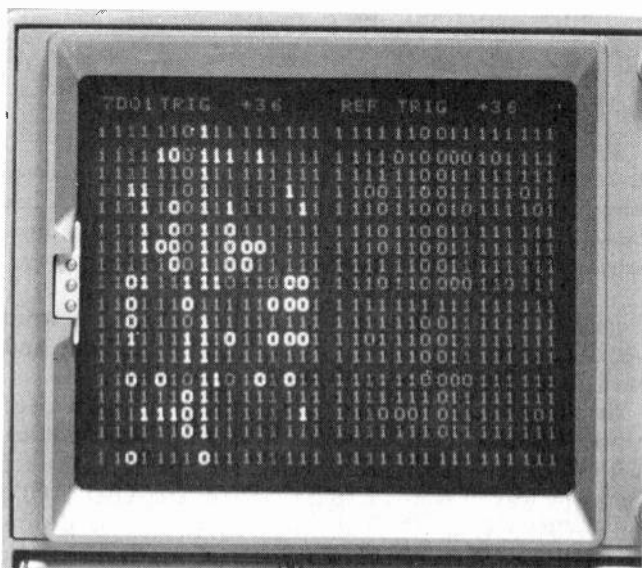
### Reducing the captured data

Biomation's K100D adds a useful twist to this process. It can define both the channel width and the word depth of the memory used for comparison. For example, suppose an unusual combination of data in subroutine A is suspected of causing a jump to an incorrect address. If the data in subroutine A is always changing, then it is possible to limit the comparison to just the 16 address channels, even though the analyzer is simultaneously recording the data bus.

Next, given that subroutine A is 103 addresses long, the comparison can be limited to just those 103 words in the reference memory. This is most useful in the likely case that subroutine A is accessed from any of a number of different places and exits into other subroutines. In other analyzers, the length of the comparison memory is fixed, but the number of channels compared can still be limited very simply by pulling the probes off the unwanted channels.

### Trigger on disappearance

Another convenient triggering feature shared by the E-H 1850 and Biomation K100D is the ability to trigger on either the appearance or disappearance of the trigger word. This is helpful in triggering on the end of a message using the system's message-valid signals. For example, it may be that three control lines must go high in order that a peripheral device receive a message on a



**7. Displaying the data.** Tektronix' 7D01 logic analyzer features data domain (left) and timing diagram (right) display formats. It offers a vertical line, or cursor—the bit makeup of the data word it intersects is displayed at bottom (right). Trigger word position reads out at top.

LOGIC TIMING ANALYZERS COMPARED

| Manufacturer and model | Maximum speed (MHz) |                   | Channels         | Memory depth (words) | Triggering                      |                  |             |               |                 |                      |                        |                  | Digital holdoff (samples/time) | Built-in CRT                  | Display format   |
|------------------------|---------------------|-------------------|------------------|----------------------|---------------------------------|------------------|-------------|---------------|-----------------|----------------------|------------------------|------------------|--------------------------------|-------------------------------|------------------|
|                        |                     |                   |                  |                      | 1st appearance or disappearance | Clock delay      | Event delay | Parallel word | Sequential word | No. clock qualifiers | No. trigger qualifiers | Reference memory |                                |                               |                  |
| Biomation K100D        | 100                 | 16 <sup>a,b</sup> | 1,024            | yes                  | yes                             | yes              | yes         | yes           | yes             | 2                    | 2                      | yes              | 14 samples                     | yes                           | T, A, B, O, H, S |
| 920                    | 20                  | 9                 | 256              | no                   | yes                             | yes              | yes         | no            | no              | 1                    | 1                      | no               | none                           | no                            | T                |
| 1650/116               | 50                  | 16                | 512              | yes                  | yes                             | no               | yes         | no            | no              | 1                    | 2                      | yes              | none                           | no                            | T, O, H, M       |
| 9100D                  | 100                 | 9                 | 1,024            | yes                  | yes                             | yes              | yes         | no            | no              | 1                    | 1                      | no               | none                           | no                            | T                |
| 8200                   | 200                 | 8                 | 2,048            | yes                  | no                              | no               | yes         | no            | no              | no                   | no                     | no               | none                           | yes                           | T                |
| B P Instruments 20D    | 20                  | 8                 | 256              | no                   | yes                             | no               | yes         | no            | no              | no                   | no                     | no               | none                           | no                            | T                |
| 50D16                  | 50                  | 16                | 510 <sup>c</sup> | yes                  | yes                             | yes              | yes         | no            | no              | no                   | 5                      | yes              | 3 samples                      | no                            | T, B, O, H, M    |
| E-H International 1850 | 50                  | 18                | 512              | yes                  | yes                             | yes              | yes         | no            | 1 <sup>g</sup>  | 3 <sup>g</sup>       | yes                    | 4 samples        | no                             | T, B, O, H, M                 |                  |
| Hewlett-Packard 1615A  | 20                  | 8 <sup>a</sup>    | 256              | yes                  | yes                             | yes              | yes         | yes           | 6               | no                   | no                     | 15 ns to 2 μs    | yes                            | <sup>f</sup> T, B, O, H       |                  |
| Moxon 740              | 20                  | 16                | 64               | no                   | yes                             | yes              | yes         | no            | 1               | no                   | no                     | none             | yes                            | T, B, O, H                    |                  |
| 745                    | 20                  | 16                | 1,024            | no                   | yes                             | yes              | yes         | no            | 1               | no                   | no                     | none             | yes                            | T, B, O, H                    |                  |
| Tektronix 7D01F/7704   | 100                 | 4                 | 1,016            | no                   | yes <sup>d</sup>                | yes <sup>d</sup> | yes         | no            | 1               | 2                    | yes                    | 10 ns to 300 ns  | yes                            | <sup>e</sup> T, B, O, H, S, M |                  |
|                        | 50                  | 8                 | 508              | no                   | yes <sup>d</sup>                | yes <sup>d</sup> | yes         | no            | 1               | 2                    | yes                    |                  | yes                            |                               |                  |
|                        | 20                  | 16                | 254              | no                   | yes <sup>d</sup>                | yes <sup>d</sup> | yes         | no            | 1               | 2                    | yes                    |                  | yes                            |                               |                  |

Notes: <sup>a</sup>16-state channels included  
<sup>b</sup>32-state channel option  
<sup>c</sup>2,046-word memory option  
<sup>d</sup>Delay feature option  
<sup>e</sup>ASCII character option  
<sup>f</sup>Glitch only included  
<sup>g</sup>With optional probe pod

T = timing  
 B = binary  
 O = octal  
 H = hexadecimal  
 M = mapping  
 S = search  
 A = ASCII

separate 8-bit data bus. To find the end of the message, the unit can be triggered when the three control lines go from 1-1-1 to any other state. The easiest way to do this is to set the analyzer to trigger on the first disappearance of the trigger word 1-1-1.

**Glitch filtering**

The timing analyzer's equivalent to the oscilloscope's trigger holdoff feature is called digital filtering, glitch filtering, or digital trigger holdoff. It simply requires that the trigger word remain valid for more than one sampling interval. It is especially useful when examining three-state buses or systems that are insensitive to very short glitches. In these cases one may be sampling at five times system clock speed and yet not want to generate a false trigger on a glitch that is only a fifth of a system clock interval in duration.

E-H's model 1850 will digitally filter a trigger word for up to 4 samples, whereas Biomation's model K100D will filter for up to 14 samples. HP's 1615A filters a trigger from 15 ns to as long as 2 microseconds; Tektronix'

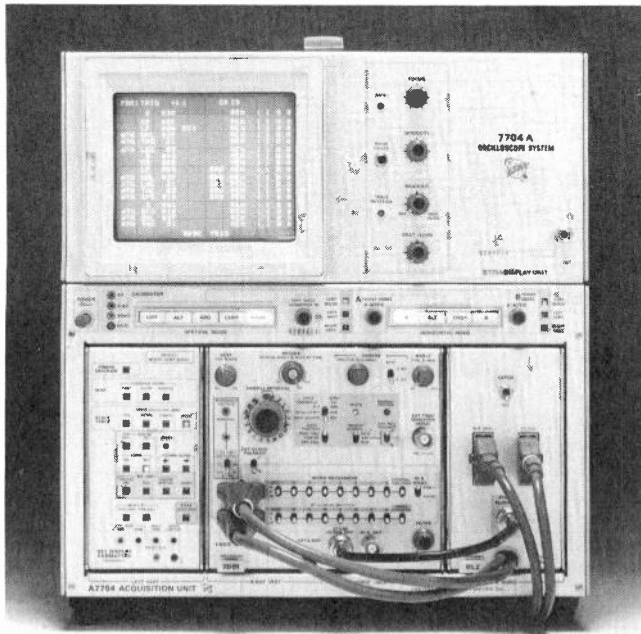
model 7D01 will filter from 10 to 300 ns.

Interpreting the analyzer's data often depends on the display method chosen. This means the captured data must be reduced into more convenient forms.

The first timing analyzers offered only a timing diagram display. However, manufacturers soon realized that their timing analyzers would also be used for state analysis, so they included data domain display formats such as binary, octal, and hexadecimal representations of the data (Fig. 7, left). Most timing analyzers currently available have these display modes, along with other auxiliary display features.

**Cursor calculations**

One of the most useful of these is the cursor. This is a vertical line superimposed on the CRT that not only helps align the raw data vertically, but is also helpful in calculations. For example, the position of the cursor in the analyzer's memory is read out digitally on the CRT (Fig. 7, right), as is the position of the trigger word. To find the time difference between two points, the cursor



**8. ASCII format.** The optional ASCII character display converts 7-bit ASCII information into letters, numbers, and symbols for direct interpretation of program statements. This feature is helpful in debugging software-generated problems.

position readings are subtracted after placing the cursor successively over the two points.

Biomation's model K100D has two cursors and reads out their difference in position and time directly. The two cursors are also used to define the word depth of the comparison memory for the trigger-on-noncomparison (or the comparison) mode.

Horizontal magnification in the timing diagram mode has become another standard feature. The magnification factor is displayed digitally on the CRT on the Tektronix and Hewlett-Packard models. It registers automatically on the time line transversing the middle of the Biomation K100D's CRT screen.

The time line is a row of dots showing sample intervals, with intensified dots every five markers and digital readout of the location of the first, last, and center sample displayed. Expansion factor readout is also given. Previous Biomation analyzers and the E-H model 1850, also have a horizontal expansion feature, but the magnification factor is not read out on the CRT.

### ASCII display mode

An optional feature worth considering is an ASCII character display offered by both the Tektronix 7D01 and Biomation's K100D. This mode displays 7-bit ASCII information directly as ASCII characters on the CRT. The Tektronix unit uses a separate plug-in ASCII module in place of the normal formatter (Fig. 8). The K100D houses ASCII circuitry inside its mainframe.

These two analyzers also provide a search mode for scanning the analyzer's memory for a user-specified word. This feature is useful when observing the number of passes through a given subroutine, for checking access to portions of a program, and for finding unnecessarily long loops. The word can be keyed in on the K100D; the

7D01 selects it from among those words in the analyzer's reference memory.

The number of occurrences of the searched-for word is read out digitally on the K100D's CRT, and an asterisk is placed next to each such word in a data domain listing of the data. Repeatedly pushing the 7D01's search button and counting the number of button pushes on one sweep through the memory gives the number of occurrences of the searched-for word.

Strictly speaking, a logic analyzer's usefulness lies in its data acquisition and data display features. But as the analyzer's sophistication increases, so does the possibility of error in control settings. To combat this, HP, Biomation, and Moxon have gone to keyboard control of the instruments' functions, with the result that the front panel of the logic analyzers look more like computer terminals than oscilloscopes or minicomputers.

Keyboard entry complements the use of a microprocessor inside the analyzer to perform self-checking as well as calculation and display functions. On older timing analyzers, the user's memory of trigger and control settings was mechanical, indicated by the position of the switches on the front panel. Keyboard-controlled models display the settings on the CRT either in menu format, as in the HP 1615A, or in a status display mode, as in the Biomation K100D.

The microprocessor inside both units performs the housekeeping chore of making sure the key connections are operating at each startup. The Biomation K100D's microprocessor performs the additional function of controlling an error light on the instrument's front panel. It goes on whenever the operator makes a mistake in entering control settings.

### Future timing analysis

From probes to display output, the logic timing analyzer has come a long way since 1973. Further improvements will probably be in the area of finding smarter ways to reduce the captured data. Perhaps data-reduction schemes such as Hewlett-Packard's signature analysis techniques [*Electronics*, March 1, 1977, p. 89] may be implemented.

Another possibility is the addition of an RS-232 interface capability so that the analyzer can be used for remote analysis. This could permit a centrally located diagnostic center to perform and interpret tests using a telephone modem. Such a center could take advantage of computer-aided diagnosis and a factory service team to locate problems remotely. The on-site technician would only be needed to position the probes.

Timing analyzers may also eventually use on-board programmable read-only memories to store previous trigger settings and comparison data tables. This would allow a measurement to be repeated by a single press of a button, avoiding the resetting of every function on a complex analyzer.

The complexity of logic timing analyzers must expand along with the complexity of the digital designs they are intended to debug. And since highly skilled personnel remain in short supply, future analyzers are bound to use microprocessors to do more and therefore ask less of their operators. □

# Analog ICs divide accurately to conquer computation problems

Housed in dual in-line packages, the hybrids can multiply, divide, or take the square root

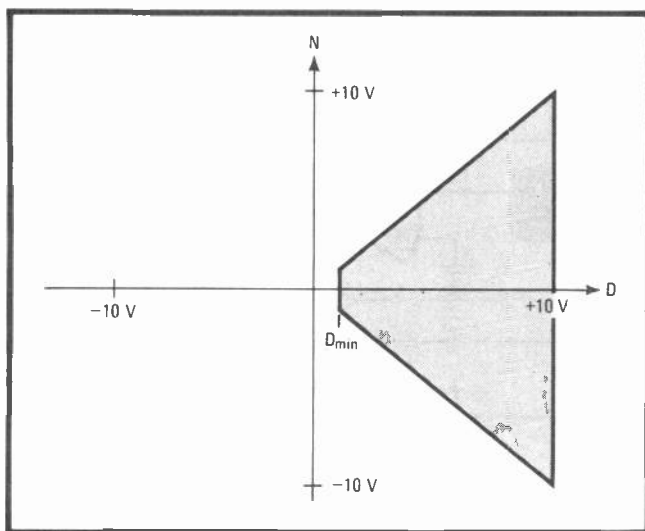
by Yu Jen Wong, *Burr-Brown Research Corp., Tucson, Ariz.*

□ Although analog dividers are basic building blocks in a wide variety of applications, until recently they remained bulky, very limited in operating range, and prohibitively expensive. Within the past two years, though, they have profited from the kinds of technological and design advances that have characterized the progress of integrated circuits in other areas.

Now, dedicated analog dividers are available in dual in-line packages, and their low price—typically less than \$20—has gone hand in hand with performance that has improved by orders of magnitude. Burr-Brown Research Corp., for instance, makes a hybrid precision divider, the 4291, with a guaranteed maximum error of less than 0.25% over a 100/1 denominator voltage. With optional external trims, the error may be held to 0.10% over a 1,000/1 range.

## What is an analog divider?

Analog dividers are widely used in such applications as ratiometric measurements, percentage computations, transducer and bridge linearization, automatic level- and gain-control systems, voltage-controlled amplifiers, and analog simulations. They may be thought of as black



**1. Operating region.** The shaded area represents the operating region of a two-quadrant divider. A one-quadrant divider will perform in either the top or bottom half of the shaded area. Below  $D_{min}$ , the denominator exhibits unacceptably large errors.

boxes having two inputs and one output and the transfer function given by the equation:

$$E_o = K(N/D)$$

where:

$E_o$  = output voltage

$K$  = a constant

$N$  = numerator input

$D$  = denominator input

For most commercial packaged dividers,  $K$  is internally set at 10. Since the divisor can never pass through zero,  $D$  is always unipolar. Because  $N$  can be bipolar, the divider will operate in two of the four quadrants, as shown in Fig. 1; it is therefore called a two-quadrant divider. Dividers that are designed for operation with  $N$  of one polarity are called one-quadrant dividers. At this point, no commercial four-quadrant divider exists, because it is impractical, though not impossible, to design one that would accept bipolar denominator voltages with a dead zone around zero.

There are two limiting conditions for every divider. First, the absolute value of  $N$  must be smaller than that of  $D$  to prevent the output from saturating beyond 10 volts. Second, a lower limit,  $D_{min}$ , is always specified for the denominator below which the divider will exhibit unacceptably large errors. These two conditions define the operating region of a divider (the shaded area in Fig. 1). For one-quadrant dividers, the operating region is either the top or the bottom half of the operating region of a two-quadrant divider.

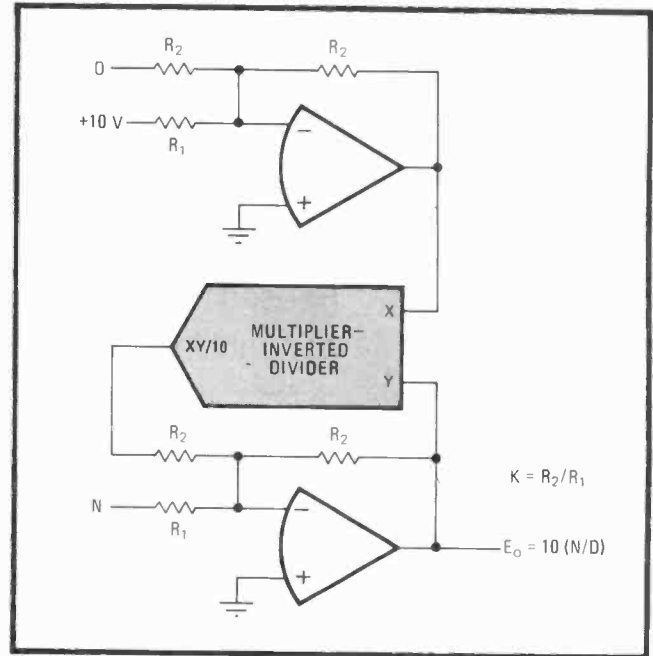
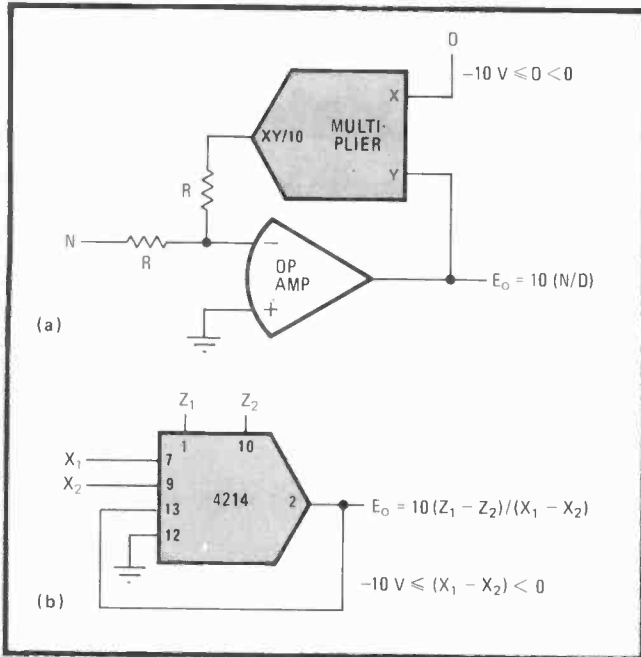
## Performing division with multipliers

The oldest and perhaps still the most common method of performing analog division is to connect a multiplier in a feedback loop of an operational amplifier (Fig. 2a). An extra op amp is not needed with commercial packaged multipliers, since their output op amps can be employed through external pin connections.

Figure 2b shows a 4214 transconductance multiplier connected as a differential divider. One limitation of the multiplier-inverted divider (MID) is its limited divisor range. The divider error that limits the ranges can be estimated by:

$$\epsilon_d \doteq 10(\epsilon_m/D)$$

where  $\epsilon_m$  is the multiplier error specified by the manufac-



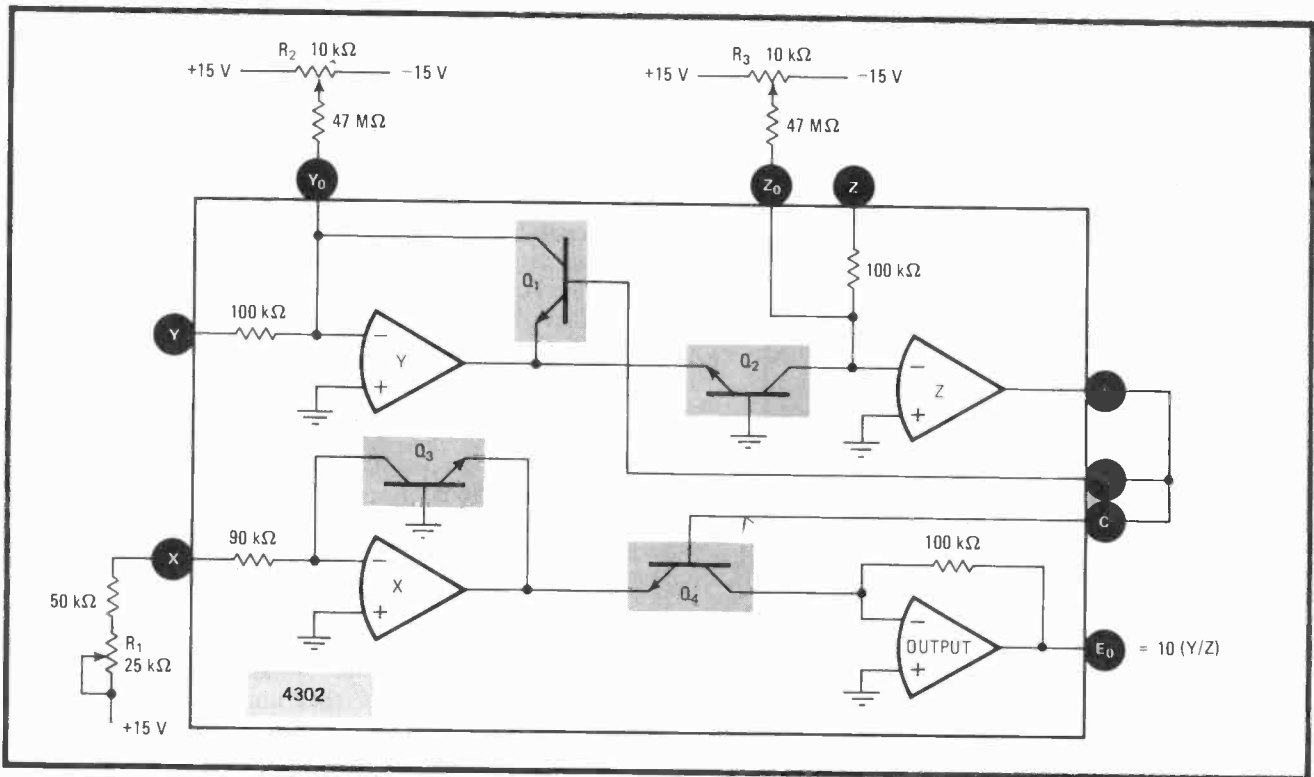
**2. Economizing space.** An analog divider can be constructed by connecting an analog multiplier in the feedback loop of an op amp (a). Packaged multipliers (b) do not require that extra op amp to be pin-programmed for performing division.

**3. More accurate.** The multiplier-inverted divider exhibits improved accuracy when connected in the manner shown. The error equation is given approximately by  $\epsilon_d \approx 10\epsilon_m / (KD)$ , where K is the ratio of  $R_2$  to  $R_1$  and can be used to optimize the divisor's range.

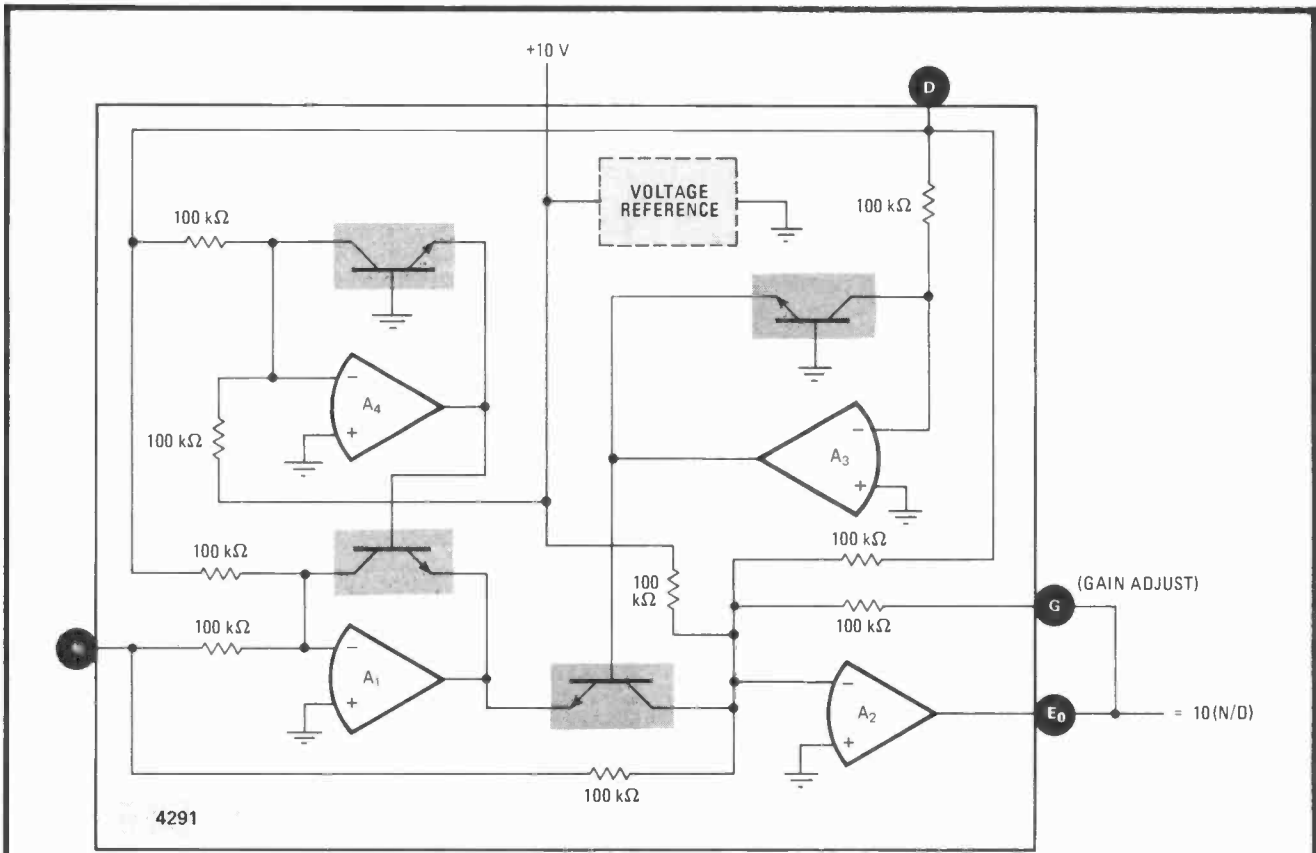
turer and D is the denominator voltage. With a 0.5% transconductance multiplier, the divider error will go as high as 5% when D goes down from 10 to 1 v. Hence, for practical purposes, these dividers are accurate only over a 10/1 denominator range.

of and preamplifying the divisor input and then shifting back at the output stage. In Fig. 3, with K defined by the ratio  $R_2/R_1$ , the divider error given by  $\epsilon_d \approx 10\epsilon_m/D$  will be reduced by a factor of K. However, the divisor input is thus limited to  $-20/K$  volts. When  $K = 2$ , the divisor will swing within the same range of 0 to  $-10$  v. In other

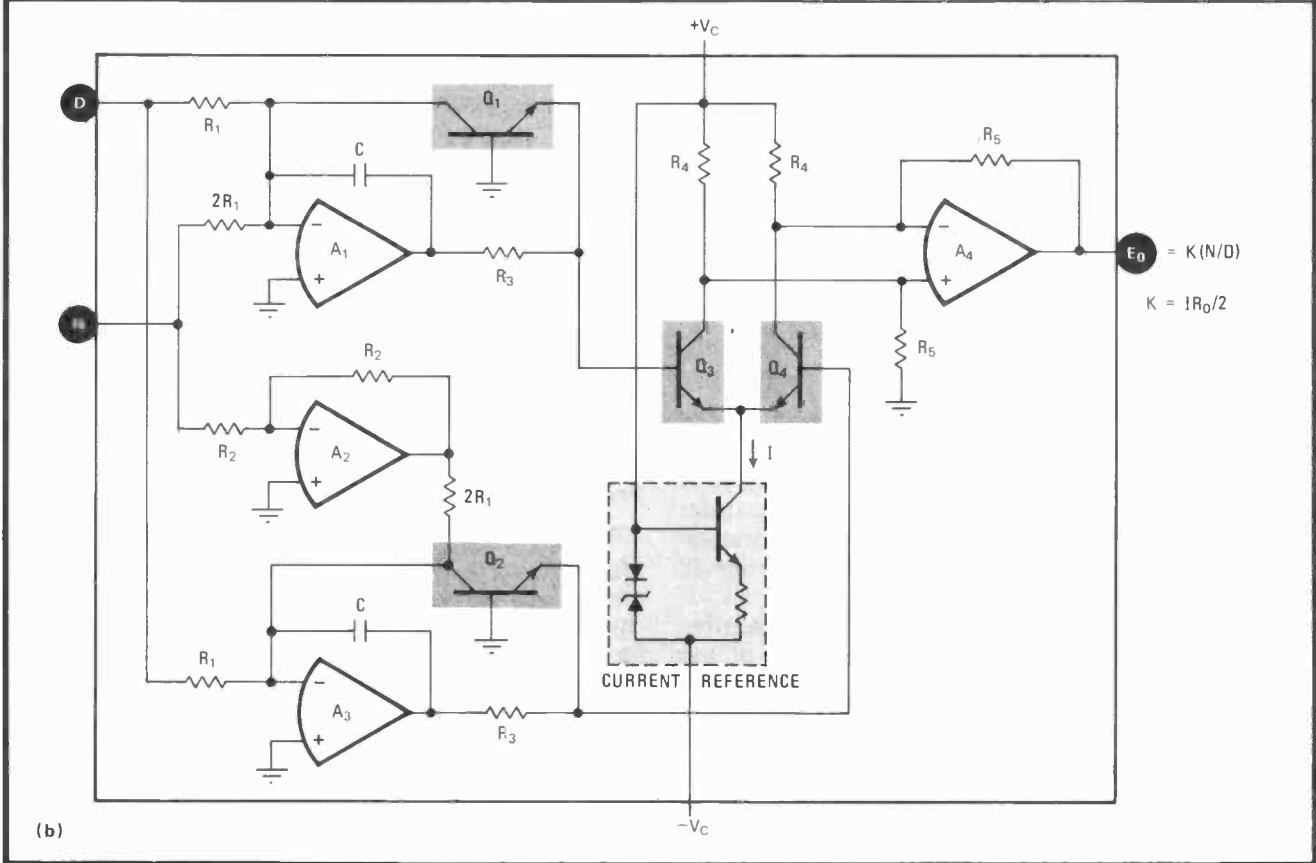
The divider error can be reduced by shifting the level



**4. Converted converter.** The multifunction converter may be used as a precision one-quadrant divider with a maximum error of 0.25% over a 100/1 denominator range. The maximum error can be reduced to 0.1% over a 1,000/1 range by using potentiometers  $R_2$  and  $R_3$ .

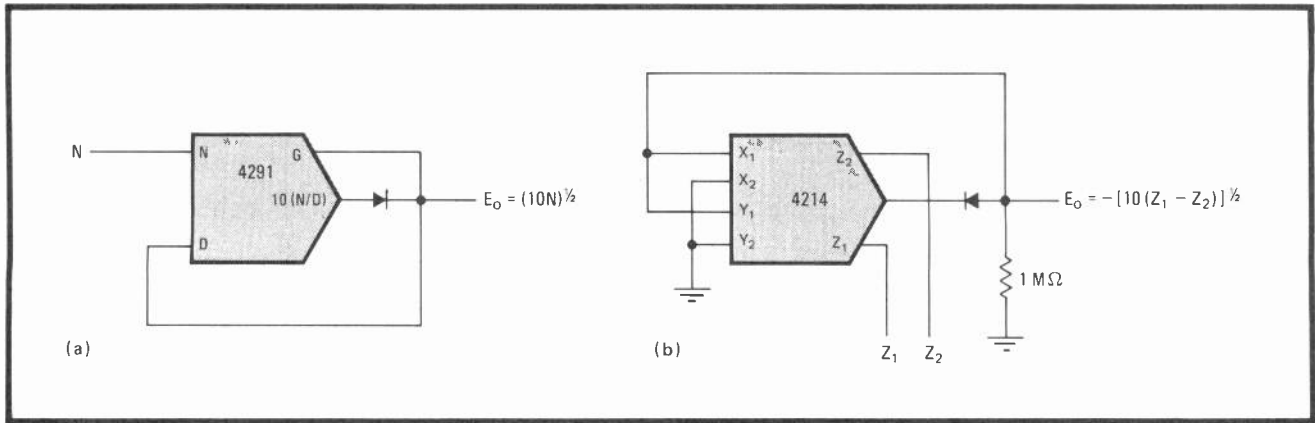


(a)



(b)

**5. Divider IC.** The four op amps and the four logging transistors shown in the functional diagram (a) are rearranged and the voltage reference is replaced by a current reference to form a log-antilog divider that maintains a constant-level bandwidth with decreasing divisor voltages (b).



words, the divider error can be cut in half without sacrificing the divisor's dynamic range. With  $K$  greater than 2, say,  $K = 10$ , the divisor is limited to the range of 0 to  $-2$  v.

### One-quadrant divider

The well-known multifunction converter (MFC), through different external connections, can be used as a precision divider whose accuracy and dynamic range greatly exceed that of a multiplier-inverted divider. It is, however, good for one-quadrant operation only, whereas the MID is a two-quadrant divider.

The functional diagram of this converter is shown in Fig. 4. Its transfer function is given by:

$$E_o = X(Y/Z)^m$$

where  $m$  is determined by two external resistors and can range from 0.2 to 5. The circuit can be analyzed by applying to each of the four transistors used to achieve the logarithmic relationship,  $Q_1$ - $Q_4$ , the Ebers-Moll equation:

$$V_{be} = (KT/q)\ln(I_c/I_s)$$

where:

$V_{be}$  = base-to-emitter voltage

$K$  = Boltzmann's constant ( $8.62 \times 10^{-5}$  electron-volt/K)

$T$  = absolute temperature

$q$  = charge of an electron (1 eV)

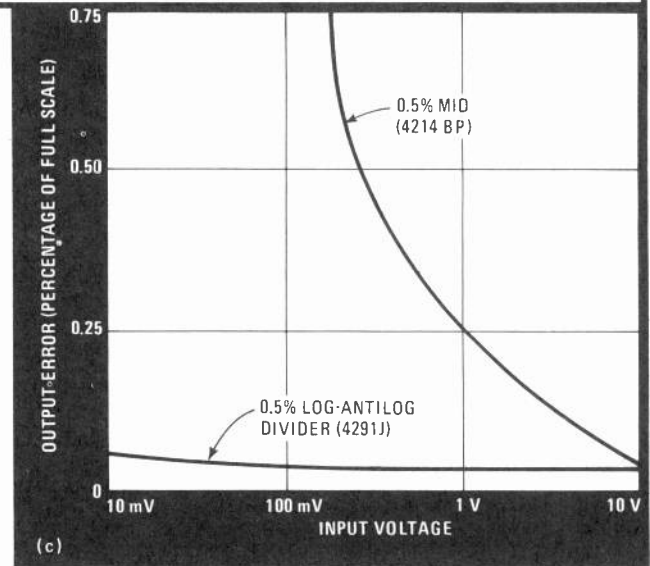
$I_c$  = collector current

$I_s$  = emitter saturation current

Solving the equation for each of the four transistors simultaneously yields the converter's simple transfer function. This procedure assumes that the four transistors are matched, so that  $I_s$  and  $T$  are the same for all four equations.

The multifunction converter is capable of operating over a 100/1 denominator range with an error of less than 0.25%. At low input-signal levels, the offset voltages and bias currents of the Y and Z op amps contribute most of the errors. By trimming them out with potentiometers  $R_2$  and  $R_3$ , the maximum error can be reduced to 0.1% over a 1,000/1 dynamic range.  $R_1$  is used to trim out gain errors.

The 4291 analog divider has been optimized as a log-antilog divider. It is specified to be the most accurate two-quadrant, self-contained divider available in IC



6. Taking the square root. Implementing either the multiplier-inverted divider (a) or the log-antilog divider (b) for finding the square root is a matter of the degree of accuracy wanted. Typical error curves for the two types are shown in the graph (c).

form. It operates in principle very similarly to a multifunction converter, but has several additional features. For one, it contains an internal level-shifting circuit for two-quadrant operation. For another, it is laser-trimmed to hold total error to less than 0.25% over a 100/1 dynamic range. In addition, both linearity compensation and an on-board temperature-compensated reference are provided.

### Precise for two quadrants

The divider's functional circuit diagram is given in Fig. 5a.  $Q_1$ - $Q_4$  are the four logging transistors, which are always laid out on a monolithic chip along a thermal equilibrium line. Their geometries are specially designed for maximum conformity to a logarithmic output. In fact, log-conformity error is less than 0.05% over four decades of collector current from 100 microamperes to 10 nanoamperes. Thus, the divider can maintain its accuracy over many decades of denominator voltages.

The error sources at low input levels are mainly due to the offset voltages and bias currents of the numerator and denominator input op amps, and not to the logging transistors. Optional trims are usually provided by manufacturers in order to eliminate the offsets and bias



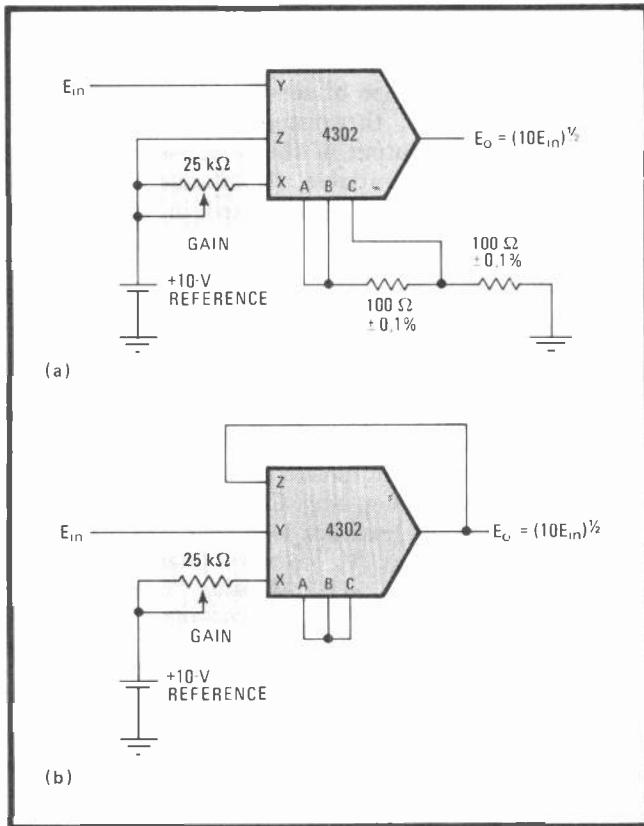
currents that are inherent in all op amps.

As with the multifunction converter and the multiplier-inverted divider, the bandwidth of the log-antilog divider decreases almost linearly with divisor voltage level; for example, a 400-kilohertz divider at a 10-v divisor voltage will become a 4-kHz divider at a 100-microvolt divisor voltage. By rearranging the four logging transistors and the four op amps and replacing the voltage reference by a current reference, a log-antilog divider whose bandwidth remains constant at high level even with decreasing divisor voltages can be realized (Fig. 5b).

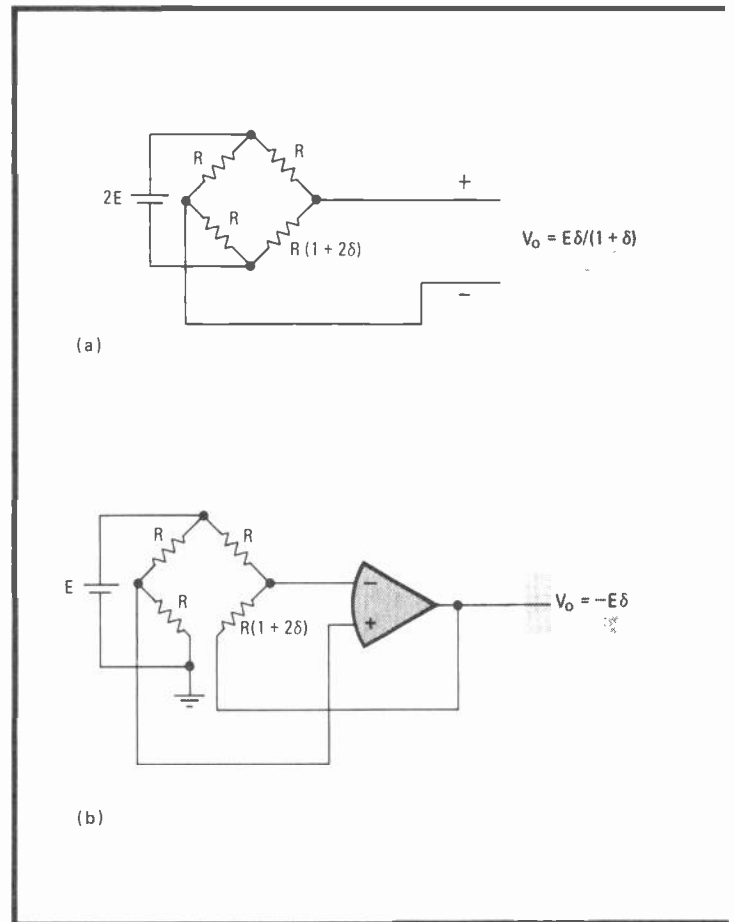
Notice that the current through the output stage ( $Q_3$ ,  $Q_4$ , and  $A_4$ ) is determined by the reference current,  $I$ , and remains constant. If  $I$  is set high, the divider's bandwidth will stay fairly flat from a 10-v divisor voltage down to 100 mV and then start to drop gradually, at a much slower rate than the circuit in Fig. 5a. Using 741-type op amps and setting  $I$  equal to  $200 \mu\text{A}$ , typical component values are:

- $R_1 = 50 \text{ kilohms}$
- $R_2 = 10 \text{ k}\Omega$
- $R_3 = 33 \text{ k}\Omega$
- $R_4 = 10 \text{ k}\Omega$
- $R_5 = 100 \text{ k}\Omega$
- $C = 33 \text{ picofarads}$

As mentioned before, the offset voltages and bias currents of the op amps should be nulled out for low-signal operations. Unfortunately, with a reference current in place of a reference voltage, this divider circuit cannot be readily used as a three-input multiplier-divider to perform  $E_o = XY/Z$ .



**7. Another approach.** The multifunction converter (here, the 4302) may also be used as a square-rooter. To implement the transfer function,  $E_o = X(YZ)^m$ ,  $m$  can be set equal to  $1/2$  (a) or to 1 (b), with the other connections appropriately made.



**8. Linearizing bridges.** The Wheatstone bridge has a nonlinear output dependent on the input variable (a). It may be linearized by using an op amp in a feedback loop (b), a multiplier-inverted divider (c), or an MID with an instrumentation amplifier (d).

One application of a precision divider is computing the square root of an input signal, often required in process-control systems. If the divisor's input is connected to its output terminal, the divider's transfer function, that is,  $E_o = 10N/D$ , becomes:

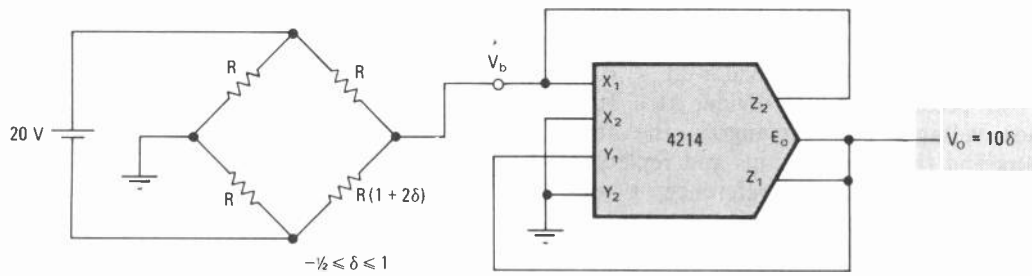
$$E_o = 10(N/E_o) = (10N)^{1/2}$$

The output is now proportional to the square root of the input,  $N$ .

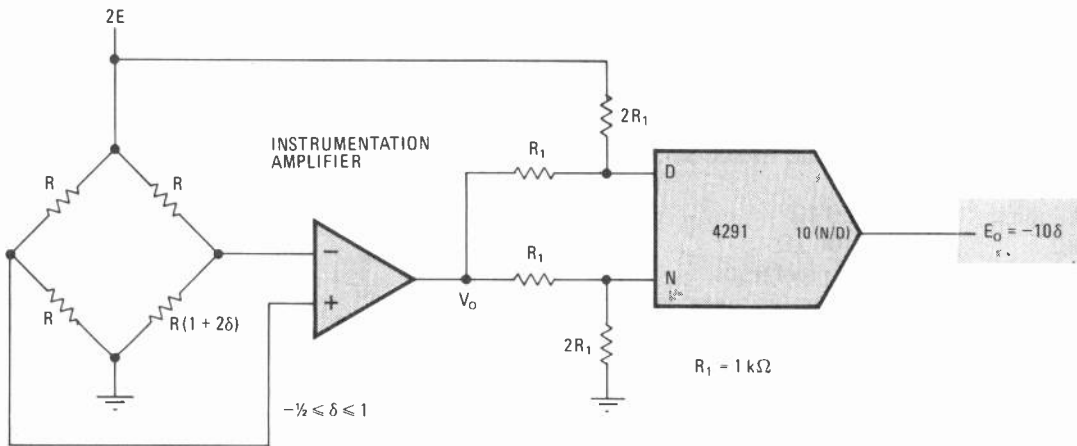
### Square-rooters

Square-rooters employing a multiplier-inverted divider and a log-antilog divider are shown in Fig. 6a and 6b, respectively. Since  $E_o$  is always unipolar, adding a diode at the output of the divider will help prevent the square-rooter from saturating to the opposite supply voltage, which is occasionally caused by power-supply transients. In Fig. 6b, a 1-megohm output load may be necessary to turn on the diode, because the input impedances of the divider are so high (about  $10 \text{ M}\Omega$ ) that, without the load, practically no current will flow through the diode.

The square-rooter's accuracy is strictly dependent upon the accuracy of the divider employed. With a multiplier-inverted divider, the accuracy is poor at low input voltages. The error-versus-signal voltage can be estimated from:



(c)



(d)

$$E_o = (10E_{in} + 10\epsilon_m)^{1/2}$$

where  $E_o$  and  $E_{in}$  are the square-rooter's output and input voltages, respectively, and  $\epsilon_m$  is the multiplier error specified by the manufacturer. For example, for a 0.5% multiplier,  $\epsilon_m = 50$  mV maximum, and therefore the square-rooter's error would be 25 mV maximum at  $E_{in} = 10$  v, but would be 109 mV maximum at  $E_{in} = 500$  mV.

Figure 6c compares the typical error curves of square-rooters built with a multiplier-inverted divider and those made with a log-antilog divider. Typical errors would normally be much lower than in the graph. As can be seen, if small-signal accuracy is critical, a precision divider like the log-antilog type should be used.

With an external voltage reference, a multifunction converter may also be used to build a square-rooter. There are two ways to implement this function. The straightforward method is to set  $m = 1/2$  with two matched resistors and connect X and Z to a 10-v reference (Fig. 7a). Then the output voltage becomes:

$$E_o = 10(Y/10)^{1/2} = (10Y)^{1/2}$$

Alternatively,  $m$  can be set to 1 as in Fig. 7b and the X input connected to a +10-v reference. By shorting Z to the output,  $E_o$ , the transfer function becomes:

$$E_o = 10(Y/E_o) = (10Y)^{1/2}$$

The accuracy of this square-rooter is about equal to that of a log-antilog divider.

The familiar Wheatstone bridge is widely used in

measuring the resistance of sensors like strain gauges, pressure transducers, thermistors, and servo motors. Unfortunately, the output of the bridge is a nonlinear function of the input variable, the change in the resistance being measured. As illustrated in Fig. 8a, the output voltage,  $V_o$ , is related to the input variable,  $\delta$ , by:

$$V_o = E\delta/(1 \pm \delta)$$

where  $2E$  is the bridge supply voltage.

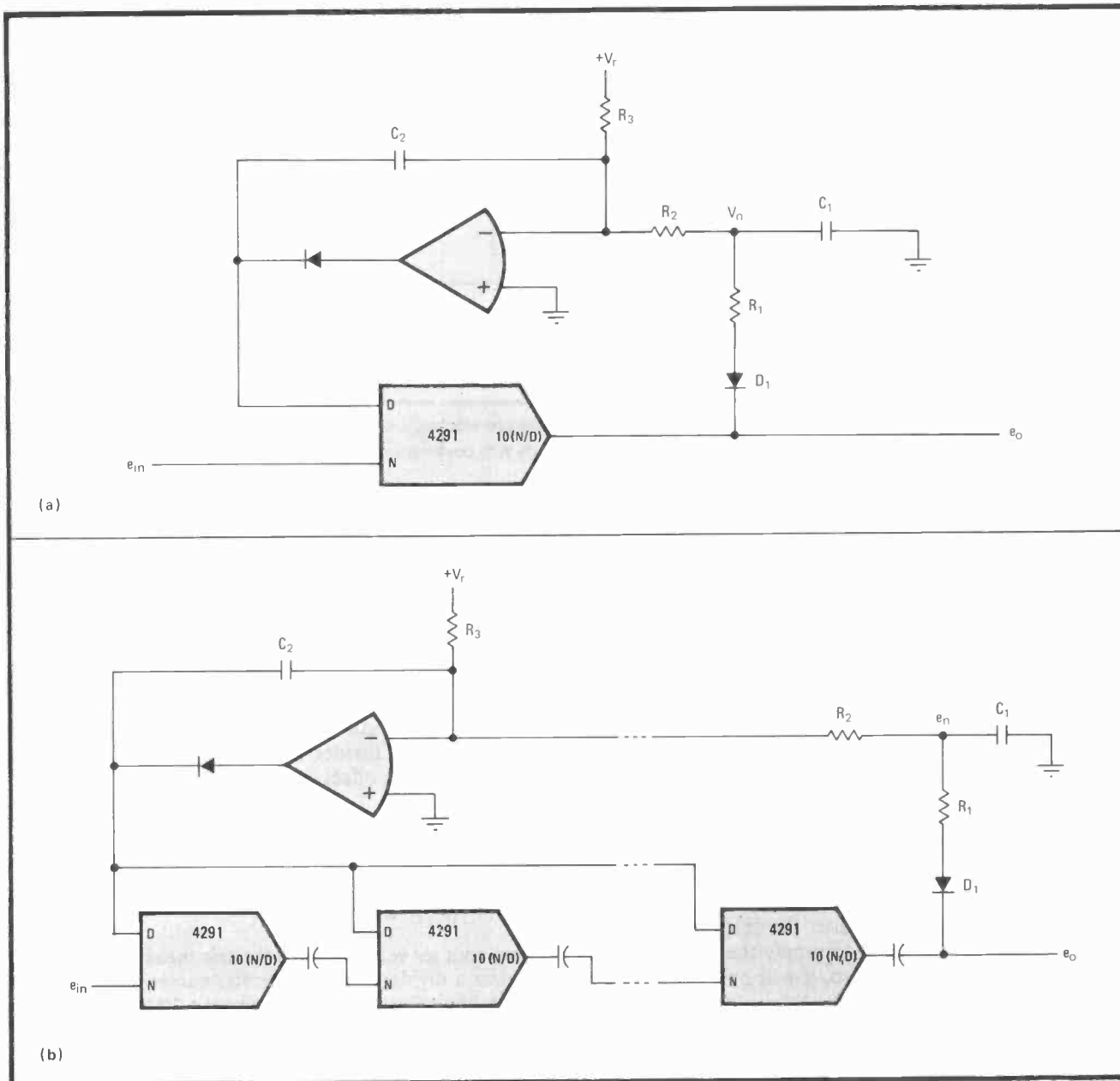
### Linearizing the bridge

Because direct measurement and manipulation of nonlinear data is often undesirable, a circuit is needed to first linearize the bridge function. The simplest method of linearization uses an op amp. Connecting the variable-resistance arm in the feedback loop (Fig. 8b) causes the output of the op amp,  $V_o$ , to vary linearly with the variable,  $\delta$ . Thus,  $V_o = -E\delta$ . However, some inexpensive bridges are packaged in four-terminal boxes and therefore will not work with this method, which requires five terminals.

A low-cost multiplier-inverted divider with differential Z inputs can, however, implement the inverse of the bridge function and linearize it. In Fig. 8c, the output voltage of the bridge,  $V_b$ , is given by:

$$V_b = 10\delta/(1 + \delta)$$

and the multiplier-inverted divider provides the transfer function,  $V_o = 10V_b/(10 - V_b)$ . The series connection of these two nonlinear circuits results in a linear function,



9. **Controlling gain.** The bandwidth of a 40-dB automatic-gain-control circuit using the 4291 (a), will be increased by  $n$  times, or its tracking range by  $n$  times, by cascading  $n$  dividers in the feedback loop shown in (b). The 400-kHz bandwidth, however, cannot be exceeded.

that is,  $V_o = 10\delta$ .

If the bridge supply voltage is single-ended, rather than floating as in Fig. 8c, an instrumentation amplifier is needed to convert the two output terminals of the bridge to a single output. The amplifier can be used effectively to compensate for bridge voltage variations. By inverting the signal such that  $V_o = -E\delta/(1+\delta)$  and using four resistors to sum the bridge voltage with, and divide it by,  $V_o$  (Fig. 8d), the divider's denominator and numerator voltage become:

$$D = \frac{2R_{iD}}{3R_{iD} + 2R_1} (E + V_o)$$

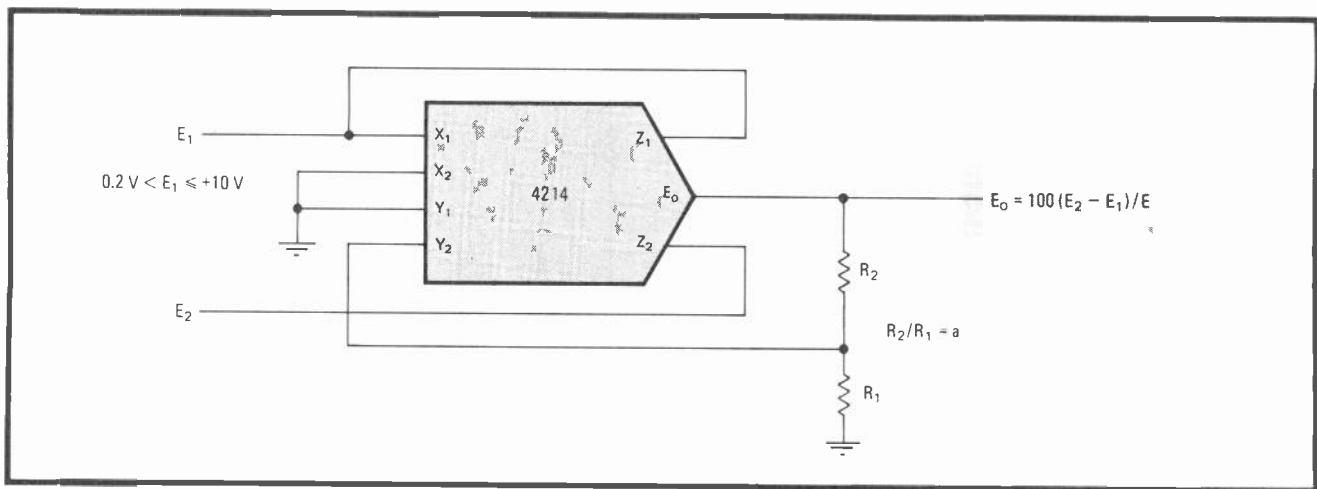
$$N = \frac{2R_{iN}}{3R_{iN} + 2R_1} V_o$$

respectively, where  $R_{iD}$  is the input impedance of the divider's denominator input and  $R_{iN}$  is that of the numerator input.

The cleverness of this circuit becomes clear when  $D$  and  $N$  are substituted into the divider's simple transfer function,  $E_o = 10N/D$ . The bridge voltage,  $2E$ , and the input impedance,  $R_i$  ( $= R_{iN} = R_{iD}$ ), cancel out, resulting in  $E_o = -10\delta$ . Therefore, the output is independent of the bridge supply voltage. When  $R_1$  is much smaller than  $R_i$ , the circuit is insensitive to the value of  $R_i$ .

### Controlling the gain automatically

To compensate for amplitude fluctuations of any given signal, nothing less than a well-designed automatic-gain-control circuit will do. A good AGC circuit is one that can keep the output constant over a wide dynamic range of



**10. A natural application.** Direct readouts in percentage of such parameters as efficiency, distortion, gain/loss, and error are easily obtained by connecting a 4214 in a configuration that provides an output of  $1\text{ V} = 1\%$  with deviations measured up to  $\pm 10\%$ .

input signal levels (tracking range). Analog dividers are excellent candidates for such applications.

The tracking range of an AGC is directly related to the denominator's operating range of the divider employed. For example, if a divider has a divisor operating range from 10 v down to 100 mV, the AGC circuit associated with it will track ac signals over a 40-decibel range.

Figure 9a shows an AGC circuit using a two-quadrant log-antilog divider. The divider serves as a voltage-controlled amplifier whose output increases with a decrease in divisor voltage. Diode  $D_1$  rectifies the output voltage,  $e_o$ . Low-pass filter  $R_1$ - $C_1$  produces a negative voltage,  $V_n$ , proportional to the negative peak of  $e_o$ . The integrator, comparing  $V_n$  with a positive reference voltage,  $V_r$ , determines the divisor voltage of the divider.

Automatic gain control is achieved thus: as the input signal,  $e_{in}$ , increases,  $e_o$  tends to increase, pushing  $V_n$  further negative. This increases the integrator's output voltage, which is connected to supply the divisor's input. As the divisor voltage goes up, it will pull  $e_o$  back down until it reaches an equilibrium.

Typical values for audio applications are:

$$R_1 = R_2/10 = R_3/10 = 1\text{ k}\Omega$$

$$C_1 = 10C_2 = 10\text{ }\mu\text{F}$$

$$V_r = 0.3\text{ v}$$

These values will provide a 2-v peak-to-peak output amplitude, which can be reset by adjusting either  $R_3$  or  $V_r$ . For subaudio frequencies, an increase in the values of both  $C_1$  and  $C_2$  is necessary.

The upper frequency limit is determined by the bandwidth of the divider, and the bandwidth of most dividers decreases with decreases in divisor voltage. This means that the bandwidth of the AGC will decrease with input signal voltages.

As an example, with a divider's 3-dB bandwidth specified for 400 kHz at a 10-v divisor voltage, the bandwidth will be, as a rule of thumb, 40 kHz at a 1-v divisor voltage and 4 kHz at a 100-mV divisor voltage. With these specifications, a 40-dB AGC circuit will operate over a 40-dB signal range only up to 4 kHz and over a 20-dB range up to 40 kHz. Although it can function up to 400 kHz, the circuit will have no practical tracking range at those frequencies.

The bandwidth of the AGC circuit can be expanded by cascading two or more dividers in the feedback loop (Fig. 9b). For the 40-dB example, each of the dividers operates actually over  $40/n$  dB, where  $n$  is the number of dividers cascaded. The bandwidth of the AGC circuit will thus be increased by  $n$  times, but will, of course, never exceed the divider's maximum bandwidth of 40 kHz. The cascading technique will also increase the tracking range of the AGC circuit by  $n$  times; that is, two 40-dB dividers will yield an 80-dB AGC circuit. Ac coupling at the output of each divider is recommended to eliminate unwanted divider offset voltages.

### Taking ratios

For ratiometric applications, a divider naturally comes to mind. Percentage measurement:

$$E_o = 100(E_2 - E_1)/E_1$$

is just another version of ratiometric measurement, but it requires a divider with differential numerator inputs and adjustable gain (from the nominal 10 to 100). With low-cost IC dividers, it is practical to provide direct readout in percentages of such parameters as efficiency, distortion, gain/loss, error, and so on.

Figure 10 shows a percentage measurement circuit employing a differential multiplier-inverted divider. The circuit, which provides  $1\text{ v} = 1\%$ , is capable of measuring  $\pm 10\%$  deviations. Wider deviations can be measured by decreasing the ratio of  $R_2/R_1$ , and narrower variations by increasing the ratio. If the dynamic range of  $E_1$  is too wide for a multiplier-inverted divider to handle, a log-antilog divider may be employed, but an extra operational amplifier will be needed to take the difference  $E_2 - E_1$ .

The percentage circuit can also be used to sort components by first converting the component's parameter into a voltage and comparing it with a reference. A comparator at the output of the percentage circuit may then be set to separate units beyond a specified limit.  $\square$

### References

1. Y. J. Wong and W. E. Ott, "Function Circuits: Design and Applications," McGraw-Hill, New York, 1976.
2. J. G. Graeme, "Designing with Operation Amplifiers: Applications Alternatives," McGraw-Hill, New York, 1977.



# Field-programmable arrays: powerful alternatives to random logic

---

Bridging design gap, TTL-compatible logic family  
is described in Part 1 of a two-part article

---

by Napoleone Cavlan and Stephen J. Durham, *Signetics Corp., Sunnyvale, Calif.*

□ With the steady growth of integrated circuit technologies, hardly a day goes by without the news that yet another chip has made scores of discrete TTL packages obsolete. Yet, though large-scale integration is packing entire system architectures onto a few chips, it is still impossible to complete a design without some discrete logic to hold the framework together.

The increase of LSI has thus created the need for efficient ways to bridge the gaps between large functional islands. Because of complexity, performance, or uniqueness, these bridges have evolved into nontrivial random-logic configurations that still rely on clusters of small- and medium-scale integrated circuits, whose fixed functions never quite fit the problem. Now Signetics

Corp. has attempted to meet the need with a field-programmable logic family.

The family spans three ranges of complexity: at the low end are the field-programmable gate arrays (FPGAs); covering the middle range are the more complex logic arrays (FPLAs); and finally there are the logic sequencers (FPLSSs). These last, most complex elements have built-in registers and enable the designer to proceed from state diagram directly to hardware. The family, summed up in the table on p. 110, is compatible with TTL and operates from a +5-volt supply.

The devices provide a powerful and compact alternative to random logic, replacing discrete gates, wires, and connectors, with significant savings in board space,

| FIELD-PROGRAMMABLE LOGIC FAMILY |   |                  |        |                        |                    |                       |             |              |                        |
|---------------------------------|---|------------------|--------|------------------------|--------------------|-----------------------|-------------|--------------|------------------------|
| Device                          | Organization  | Device           | Inputs | Outputs <sup>(1)</sup> | Chip enable (CE)   | I <sub>cc</sub> (max) | Delay (max) | Availability | Package <sup>(2)</sup> |
| FPGA                            | • AND/NAND  | 82S102<br>82S103 | 16     | 9 OC<br>9 TS           | yes                | 170<br>mA             | 35 ns       | now          | N                      |
| FPLA                            | • AND-OR/<br>NOR  | 82S100<br>82S101 |        | 8 TS<br>8 OC           |                    |                       | no          | 50 ns        | now                    |
|                                 | • AND-OR<br>• Self-enable<br>output                     | 82S106<br>82S107 |        | 8 OC<br>8 TS           | 70 ns              |                       |             | 4Q79         | N                      |
| FPLS                            | • AND-OR  | 82S104           |        | 8 OC                   | yes <sup>(3)</sup> |                       | 90 ns       | 4Q79         | N, F                   |
|                                 | • Complement<br>array                                   | 82S105           |        | 8 TS                   |                    |                       |             |              |                        |
|                                 | • 6-bit state<br>register<br>• 8-bit output<br>register |                  |        |                        |                    |                       |             |              |                        |

<sup>(1)</sup> OC = open collector    TS = three-state  
<sup>(2)</sup> N = plastic    F = Cerdip  
<sup>(3)</sup> CE input may be optionally programmed as preset.

power, and cost. Moreover, since all devices can be programmed and modified in the field (as programmable read-only memories can) using readily available programming equipment, the logic can be changed to meet new customer requirements or specifications, or to recover quickly from design errors—after delivery to the field—without expensive printed-circuit-board retooling.

### Programming options

Depending on their complexity, members of the programmable logic family have internal AND gates, OR gates, S-R flip-flops, true or complement buffers, and exclusive-OR (EXOR) gates. Those elements can be combined to perform single-level, double-level, and sequential logic functions—all by blowing fuse links.

There are other fuse options in output structures for the entire logic family, too, since either active-high or active-low functions can be generated without additional hardware or signal delay. Finally, the family is well suited to bus-organized environments such as microprocessor systems, since all its members offer, in addition to open-collector outputs, three-state outputs whose signals are in the high-impedance state until activated by a chip-enable input.

All the logic elements perform standard logic functions that can be represented by augmenting conventional logic symbols with a few new definitions so that they can represent multiple-input gates (see "How the FPLF defines logic," p. 65).

### The gate arrays

The simplest member in the family is the field-programmable gate array, which performs single-level logic functions. The equivalent logic diagram for the FPGA is shown in Fig. 1. The two gate arrays currently available are open-collector (82S102) and three-state output (82S103) versions of the same array, which comprise nine NAND gates fuse-selectively connected to 16 common inputs by true/complement buffers.

Fuses in the FPGAs allow individual outputs to be complemented to AND, so that by proper manipulation of the input polarities, and by using De Morgan's theorem, AND, OR, NAND, and NOR logic functions can be easily implemented. The parts thus serve as universal logic elements that can be tailored to applications requiring random logic, as in fault monitors, code detectors, and address decoders for microcomputer systems with memory-mapped I/O.

### The logic arrays

Devices performing two-level combinational logic functions are grouped into the field-programmable logic array (FPLA) category. These elements are a step up in complexity from gate arrays, capable of generating AND-OR, AND-NOR, and their De Morgan equivalents. There are at present two array types in the FPLA family, each with either open-collector or three-state outputs.

The equivalent logic diagram of the first array type, the open-collector output 82S101 (or three-state output 82S100), is shown in Fig. 2. The first level of logic in the device is made up of 48 AND gates fuse-connectable to any of 16 common inputs by true/complement buffers. The second logic level consists of eight OR gates—one per device output—each capable of being selectively coupled to any of the 48 gates. Finally, fusing options are included for generating true or complementary outputs.

The second logic array type, the 82S106/107, has nearly the same organization as the first. The exception is that an additional OR gate with fixed inputs has been added to generate an internal enable command for the output structure. That self-enable is generated whenever any of the AND gates become logically true, which occurs when the external input code matches the internal AND-gate program. In the absence of such a match, all device outputs are unconditionally disabled. The self-enable signal is available externally—the chip-enable input (CE) pin on the 82S100/101 becomes an open-collector output called FLAG. Because of this feature, the 82S106/107 can be viewed as a content-addressable programmable read-only memory, ideally suited to modifying data in large ROMs, as will be shown in the second part of this article.

### Shared gates

Both array types benefit from the second level of logic. The advantage here is that the AND gates can be shared—OR gates can couple with up to 48 AND gates. Also, a key advantage of this arrangement over single-level logic is that it allows editing—disconnecting invalid AND terms from the OR array and replacing them with spare AND gates (Fig. 3).

Open-collector versions of both gate-array and logic-array devices can form wired-AND outputs in order to expand the number of AND gates available on a single chip. This solves the problem that is posed by applications exceeding the resources of a single device. The only restriction is that the expanded outputs have to be programmed to be active-low.

By far the most powerful members of the family are the field-programmable logic sequencers (FPLS), which add on-chip registers to arrays of AND and OR gates. The

## How the FPLF defines logic

For the most part, schematic representation of logic in the field-programmable logic family follows conventional notation—the devices include AND, OR, and exclusive-OR (EXOR) gates, as well as set-reset (S-R) flip-flops and true or complement buffers. To simplify the representation of fuse-link programmability, however, the FPLF schematics use a matrix arrangement with cross-point coupling to represent intact fuse links.

For example, (a) in the figure shows a typical input and AND gate of a gate array. The square "solder dot" represents a fixed internal connection. Both the line from input A and the line from the output of the inverter intersect the vertical input line of the AND gate; in actuality, fuse links make both connections. An intact fuse link is represented by a round solder dot. Blowing either of the fuse links will determine whether the input to the AND gate is A, or its complement,  $\bar{A}$ . (Leaving both fuses intact holds the output of the AND low, whereas blowing both fuses results in a "don't care" situation, an output that is independent of either input.)

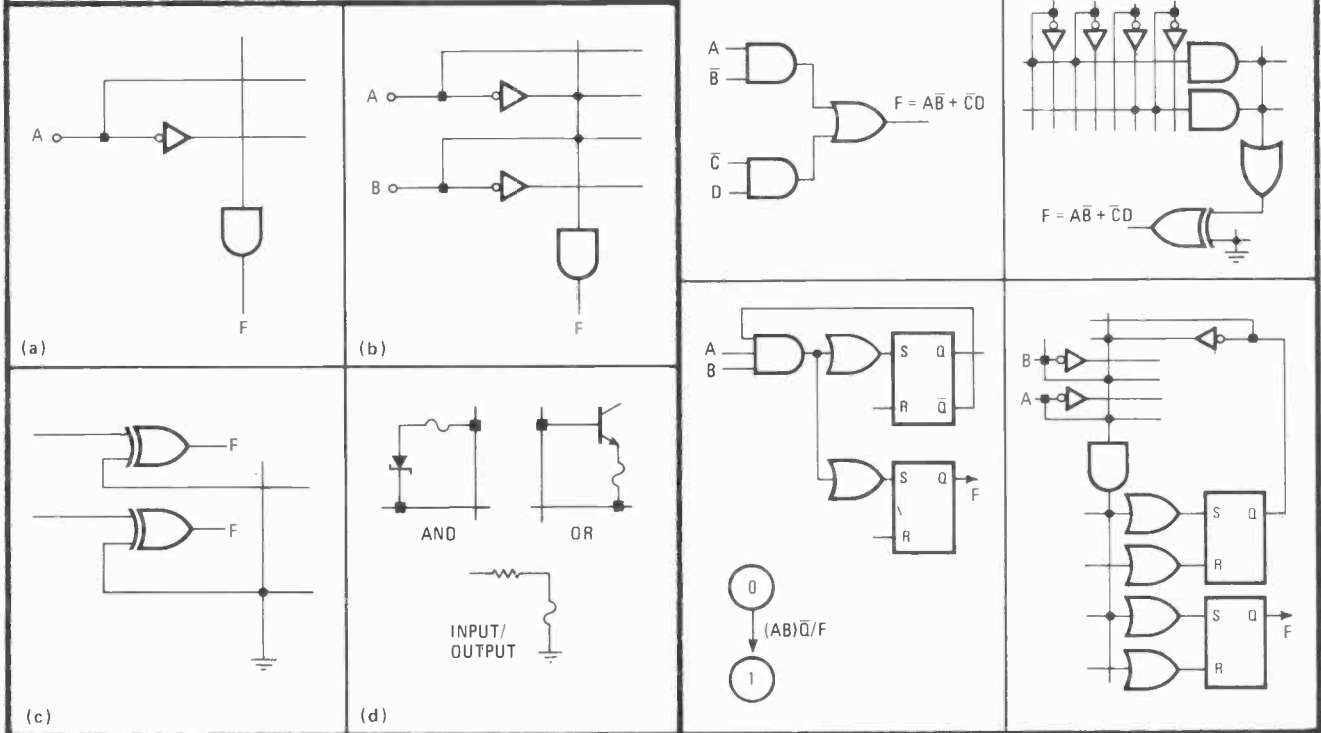
Extending the matrix and cross-point coupling approach a step further, (b) shows the configuration of a two-input AND gate. Since the input to the AND gate crosses the four lines of inputs A and B as well as their complements, the gate serves as a four-input AND while appearing to be a single-input gate. Since the members of the field-programmable logic family have 16 inputs intersecting each AND gate, the gates are actually 32-input devices; the number of inputs used is determined finally by the number of fuses left intact. Thus, in (b), solder dots (or

intact fuse links) create the logical equation  $F = \bar{A}\bar{B}$ .

The exclusive-OR gates on all outputs of the logic-family devices allow programming for either active-high or active-low output signals. As shown in (c), a fuse link grounding one of the two inputs of an EXOR gate results in an active-high output; blowing the fuse results in an output that is active-low.

The details of the fusing mechanisms are shown in (d). AND gates have a fuse in series with a Schottky diode, while OR gate fusing uses an npn transistor. The fuses for the true/complement input buffers and active-high/active-low outputs are in series with resistors.

The analogy between fixed and programmed logic is best shown by the examples in the table. The first example is typical of the single-level logic to which the gate array is applicable. The two-level logic of the second example is satisfied by the logic arrays. Finally, the registered state machine that executes the state transition of the third example is a candidate for the field-programmable logic sequencers.

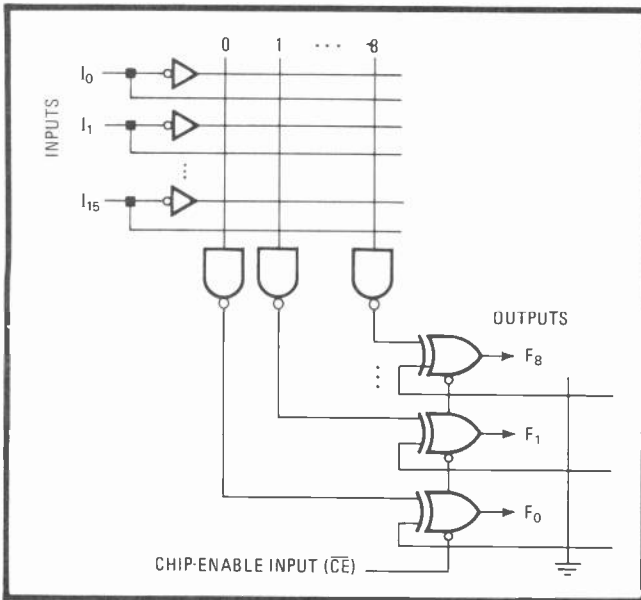


sequencers are actually self-contained state machines, since they can be programmed to perform any synchronously clocked logic sequence.

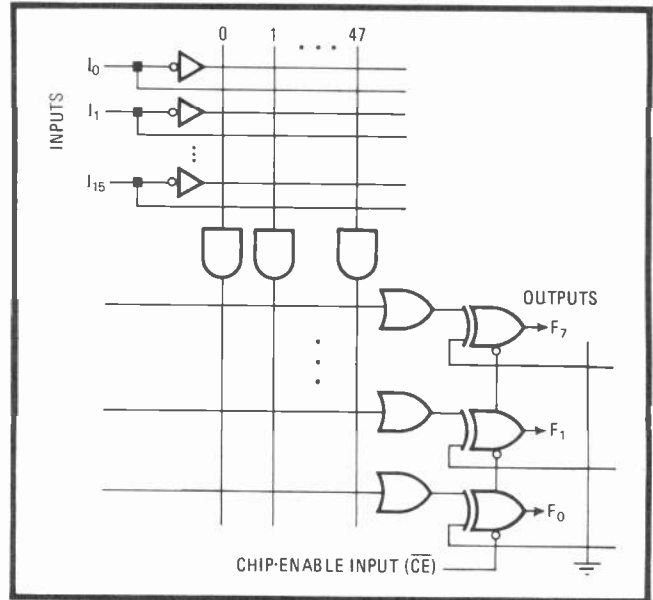
State machines, whose general structure is shown in Fig. 4a, usually take two forms: Moore machines, in

which the output is a function of the present state only; and Mealy machines, whose output is a function of both the present state and the present input.

Figure 4b shows the basic architecture of the open-collector output 82S104 (or three-state output 82S105),



**1. Gate array.** The simplest device in Signetics' field-programmable logic is the gate array, capable of single-level logic. Any of 16 inputs can connect to nine NAND gates by true/complement buffers. Since both outputs can be complemented to AND, manipulating De Morgan's theorem makes the device a universal logic element.

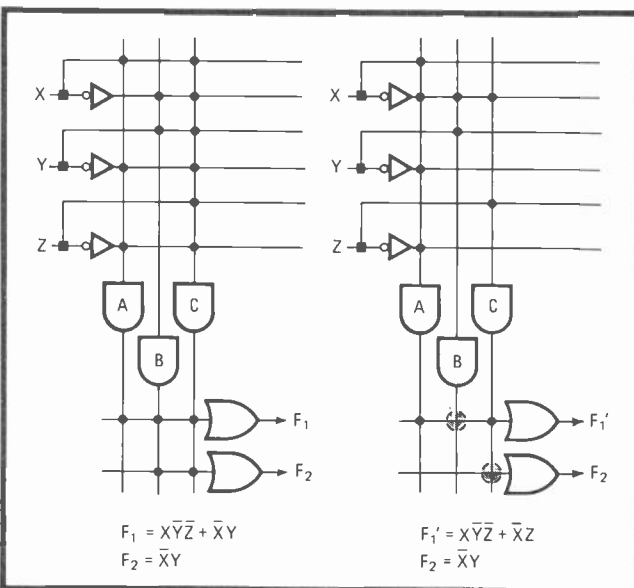


**2. Double deep.** The field-programmable logic array carries out two-level combinational logic. The 16 inputs couple to 48 AND gates, which in turn connect to any of nine OR gates. Either true or complement outputs are provided.

the first members of the FPLS family. With the FPLS, a user may program any logic sequence that can be expressed as a series of jumps between stable states triggered by a valid input condition  $I$  at clock time  $t$ . The number of states in the sequence depends on the length and complexity of the desired algorithm.

A typical state diagram is shown in Fig. 5. The state from which a jump originates is called the present state  $P$ , and that at which it terminates is the next state  $N$ . A jump always causes a change in state, but may or may not cause a change in the machine's output  $F$ .

All states are arbitrarily assigned and stored in the state register, where the clock and next-state information from the combinational logic are the inputs. State jumps can occur only when transition terms are true. A transition term is, by definition, the logical AND function of the clock, present state, and valid inputs; hence,  $T_n = t \cdot I \cdot P$ . However, since the clock is actually applied to the state register, it may be removed from the equation. When  $T_n$  is true, a control signal is generated that, at clock time  $t$ , forces the contents of the state register from  $P$  to  $N$  and, if necessary, changes the contents of the output register.



**3. Editing.** The logic array's programmable OR gates allow sharing of AND gates, as with gate B at left. The OR array also allows easy editing of logic statements when design changes are made; note how spare gate C at right was used to modify output  $F_1$  to  $F_1'$ .

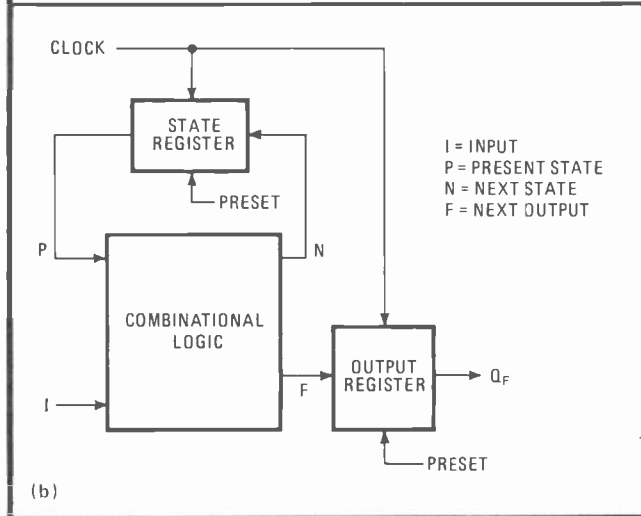
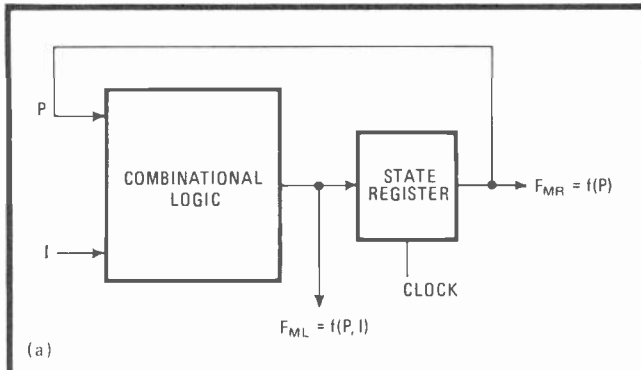
### FPLS organization

The architecture of the 82S104/105 is a natural extension of the static logic structure of the FPLA. It accepts 16 input variables and provides eight output functions. It has a 6-bit state register and an 8-bit output register; all the internal registers are automatically preset to logic 1 when power is applied. The FPLS provides for 48 transition terms, which can be selected to be either true or complementary.

A look at the equivalent logic diagram of the FPLS (Fig. 6) shows its extension of the static FPLA. The AND and OR gate arrays of the latter have been expanded to control the set and reset ( $S$  and  $R$ ) inputs of six flip-flops (the state register) and to monitor the register's contents over an internal feedback path. Also, an independent 8-bit output register has been added to store output commands generated during state transitions and to hold the output constant during state sequences involving no output changes.

The AND array comprises 48 positive AND gates, each with 44 input connections from a set of true/complement buffers. The AND gates are used to form logic products of 16 external inputs ( $I_0$  to  $I_{15}$ ) with six present-state ( $P$ ) inputs fed back from the state register. The gates are





**4. State machine.** A state machine (a) takes either a Mealy or Moore form. The architecture of the field-programmable logic sequencer (b) is that of a self-contained Mealy machine, where the output is a function of both the present state and the present input.

therefore called transition terms because, like the transition terms in state diagrams, they issue next-state commands.

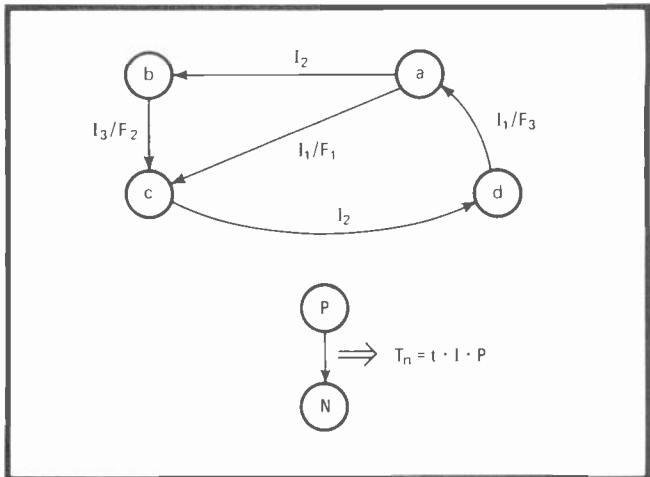
The OR array contains 28 positive OR gates, each with 48 input connections to all 48 AND gates. The outputs of the ORs drive the set and reset inputs of the 14 S-R flip-flops that are state and output registers.

The FPLS is made still more flexible by a complement array comprising a single 48-input OR gate that drives an inverter, which then feeds back into the AND array. The complement array forms a bridge between the AND and OR arrays for generating NAND functions of input-jump conditions; the user programs it in such a way as to suit each transition term.

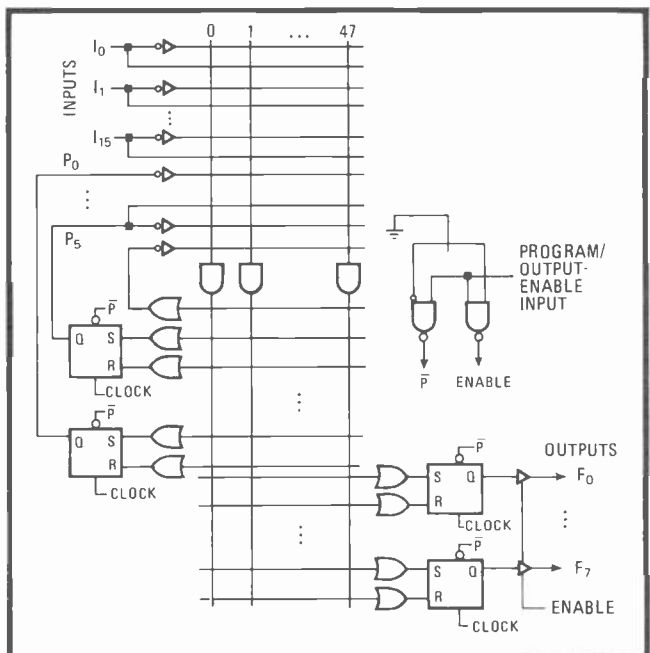
### De Morgan's theorem

De Morgan's theorem to reduce logic terms can be easily implemented with the complementary array so that the most use is made of the AND gates. For example, if the transition term is  $T = (Q)(\bar{X} + \bar{Y} + \bar{Z})$ , where Q is the output of the state register and  $\bar{X}$ ,  $\bar{Y}$ , and  $\bar{Z}$  are inputs, three AND gates in the FPLS are required. However, De Morgan's theorem changes the transition term to  $T = (Q) \bar{X}\bar{Y}\bar{Z}$ , which requires only two AND gates.

The complementary array is also an efficient means of aborting a clocked sequence in the absence of valid jump conditions. As Fig. 7 shows, considerable minimization



**5. State diagram.** Example of a state diagram (a) with four states—A, B, C, and D.  $I_1$ – $I_3$  are jump conditions, which trigger output changes  $F_1$ – $F_3$ . A state change (b) gives rise to transition term  $T_n$ , which is logical AND of clock t, input I, and present state P.

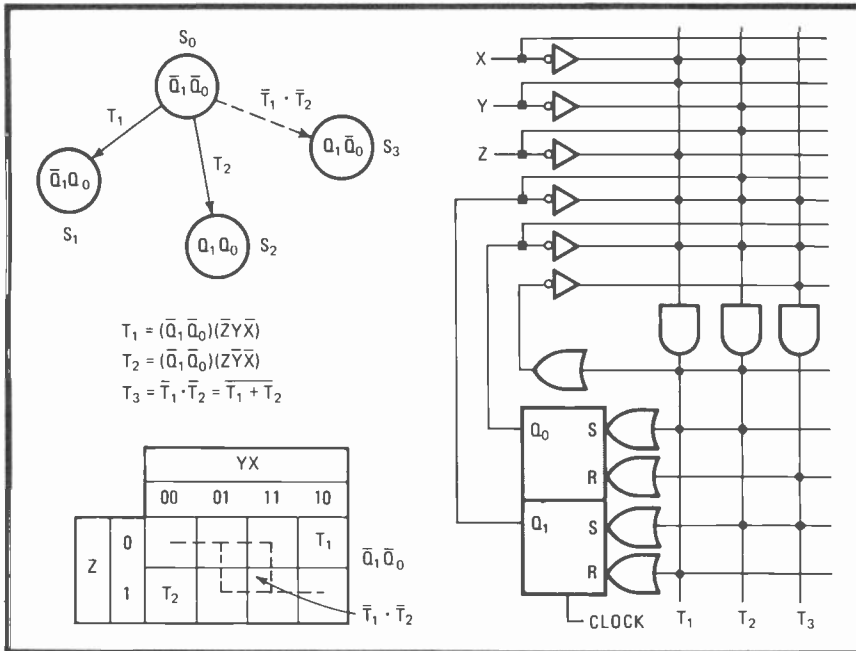


**6. Sequencer.** The field-programmable logic sequencer has 16 outputs, 48 AND gates, and 28 OR gates, plus 14 flip-flops that serve as state and output registers. Either an asynchronous preset input or an output-enable input is available as a programming option.

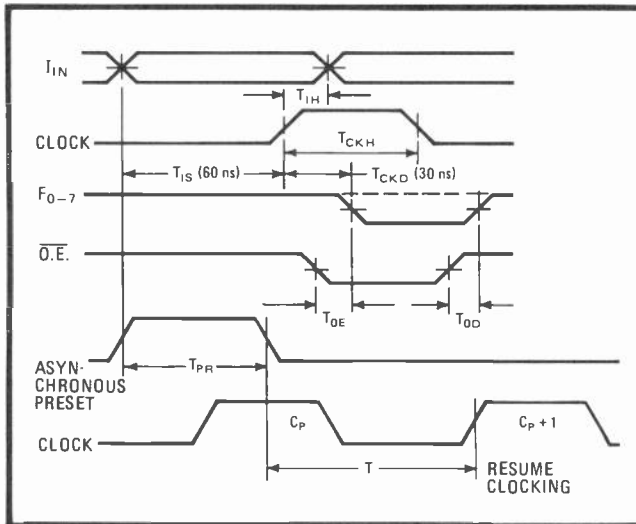
of AND gates is possible when the detection of valid jumps involves many complements of jump functions, especially as the number of variables increases.

All clocked S-R flip-flops that make up the state and output registers offer the option of asynchronous pre-setting to all 1s. The 64-state total that can be represented by the state register is adequate in most cases to chart algorithms involving fewer than 48 nonredundant transitions. The register accepts next-state commands (N) from the OR array and supplies present-state information (P) to the AND array.

The output register is similar to the state register, except it has eight states for servicing eight output functions. It accepts the next-output commands  $F_0$ – $F_7$



**7. Complementary.** Use of AND gates in the FPLS is greatly reduced by the complement array, a single 48-input OR gate driving an inverter that feeds back into the AND array. In this example, the default jump from state  $S_0$  to  $S_3$  is reduced from three AND gates to a single gate  $T_3$ .



**8. Timing.** Minimum clock duration for the FPLS is 20 nanoseconds. Minimum width of preset input, which overrides clock, is 40 ns. Normal clocking resumes with the first full clock pulse following a negative clock transition after the trailing edge of the present signal.

from the OR array and then reflects its contents to the device outputs through the buffered Q outputs of each of the flip-flops. Also, as an added feature to enhance fault isolation, driving input  $I_0$  to +10 volts will route the contents of the state register ( $P_0$ - $P_5$ ) directly to outputs  $F_0$ - $F_5$  without any alteration of the contents of the output register. However, the feature is not recommended for use in a normal mode of operation (as in a Moore machine). This is because it increases the device's maximum current by 5 to 10 milliamperes and thereby lowers the maximum ambient temperature rating of the package by approximately 5°C.

As a final programming option in the 82S104/105, a pin can function as either an active-high asynchronous preset (pr) or an active-low output enable ( $\overline{OE}$ ). The output-enable function forces all outputs to logic 1 (or to

high impedance in the 82S105) and is normally used when the device is sharing a bus. It does not inhibit clocking of the internal registers. The asynchronous preset option, on the other hand, is useful when the logic sequence requires an immediate state-independent return to initial conditions. The state register and output register can also be synchronously preset independently of one another by dedicating that function to one of the input variables in conjunction with a single transition term and a clock pulse.

### Timing constraints

The maximum clock rate of the 82S104/105 can be inferred from its timing diagram (Fig. 8), which shows worst-case delays and setup requirements during a typical I/O cycle. Using stable external inputs as a reference, the device can be clocked after a minimum setup time of 60 nanoseconds. The next output (as well as the next internal state) will be valid 30 ns after the positive edge of the clock, giving a total I/O delay of 90 ns. Since both output enable and disable delays are also 30 ns, when the  $\overline{OE}$  pin is used its signal's edge should occur prior to or coincidentally with the clock in order to avoid increasing I/O delays.

The asynchronous preset option includes a clock lockout feature that eliminates the potential hazard of spurious clocking. But, as the timing diagram shows, when using the lockout feature it is possible to miss one clock pulse, which may be prohibitive in some applications.

# Sequencers and arrays transform truth tables into working systems

by Napoleone Cavlan and Stephen J. Durham  
*Signetics Corp., Sunnyvale, Calif.*

□ Because of its power and flexibility, the Signetics field-programmable logic family is ideal for replacing the discrete logic normally used to interface large-scale integrated devices, as shown in Part 1 [July 5, 1979, p. 109]. The examples of applications that follow show how to exploit its special features.

In designing with these gate and logic arrays and logic sequencers, the user need concern himself only with generating truth tables associated with the state diagrams or sets of Boolean logic equations that define his function. The one restriction is that he must use logic symbols corresponding to the status of fuse links.

As indicated in Fig. 1, an extra set of symbols is needed to describe all the states of FPLF gates corresponding to all combinations of blown and unblown fuse links. Once ordered into truth tables, the user-defined functions are then directly mapped onto standard program tables furnished with FPLF elements, whose fuses are then blown by a logic-type programmer. As the user gains experience, he can manipulate logic variables intuitively and can eventually implement algorithms directly on the program tables with only the device schematics for reference. (The formal step of deriving state diagrams and logic equations will not be considered here.)

Because of their simple and uncommitted structure, FPLF elements are suited to a wide variety of applications, several of them already well documented. The following examples illustrate the typical use of each logic element and match devices with applications.

### Bus translator

Signetics' Instructor 50 microcomputer system is built around the 2650 microprocessor; but for compatibility with other systems and peripheral devices in the hobbyist market, it interfaces to the S100 bus, which is based mainly on 8080 microprocessor signals. Yet to carry out the seemingly unwieldy task of bus translation, only a single FPGA is needed. The gate array translates the logical combinations of timing, enable, and control signals supplied by the 2650 and its I/O hardware into control signals entirely compatible with the S100 bus definitions, as shown in Fig. 2.

The programmable feature of the FPGA is strategically

invaluable in this case since the S100 bus is not yet totally standardized. The FPGA permits easy adaptation of the interface to changes in specifications, which are subject to arbitrary manipulation by manufacturers in the hobby arena.

### Two-level logic

The logic arrays add a second level of combinational logic to the gate arrays, and thus another level of versatility. AND/OR combinations of the FPLAS are well suited to carrying out polynomial equations and the like, as shown in the next example.

In systems that transfer large blocks of data, a cyclic redundancy check (CRC) scheme can significantly improve data integrity. The technique appends a check word to a transmitted sequence of data, and the receiving end uses that word to check for errors. A cyclical division of the transmitted data by an industry-standard polynomial generates the CRC word; the remainder from the division forms the check word.

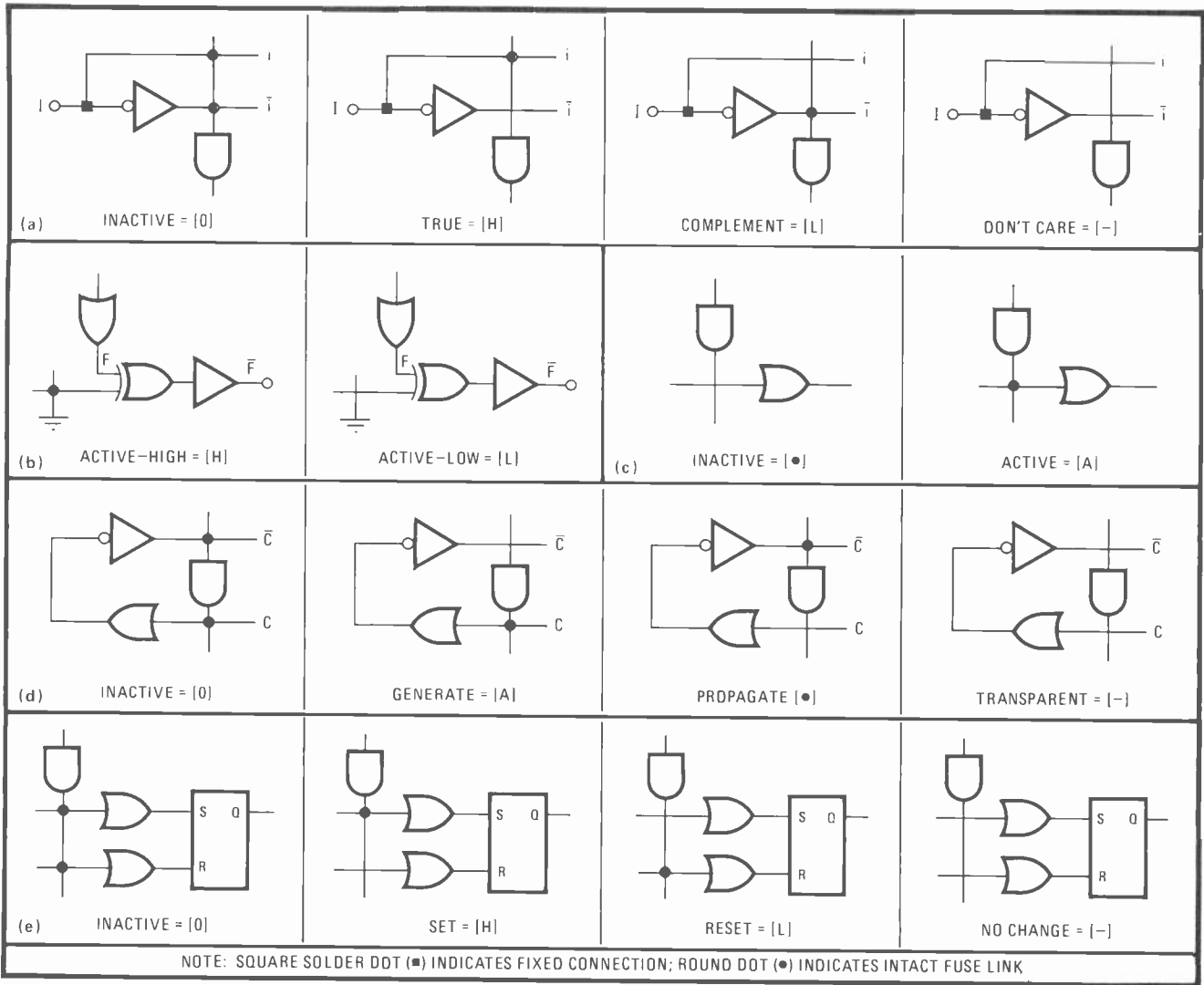
Polynomials lend themselves to serial manipulation, and serial CRC generation and checking are easy to implement. But in a multiple-line data system with parallel organization, a considerable amount of hardware may be needed for parallel-to-serial conversion. Moreover, the multiple-bit clocking for each word carries an inherent speed loss—a factor of 8 for a byte-oriented system. A parallel CRC generator-checker circuit is the answer, developed from the set of logic equations describing the function of the circuit in the form of a state machine.

The general design of the CRC circuit is shown in Fig. 3a, along with the logic equation set for the popular CRC polynomial  $P(x) = x^{16} + x^{15} + x + 1$ . Figure 3b shows that the entire byte-wide parallel CRC generator-checker circuit can be implemented with only five chips: two 8-bit latches, two FPLAS, and an FPGA. The FPLAS contain the set of logic equations controlling the flip-flop inputs, which are expanded from EXOR form to sum-of-products form. In Fig. 3a, variables  $N_0-N_{15}$  represent the next CRC word after clocking, based on the current word  $B_0-B_{15}$  and the present input byte  $D_0-D_7$ .

CRC generation begins by driving the RESET line low to initialize the latches to zero. Pulsing the clock line then transfers the first byte of the data block in at  $D_0-D_7$ . Subsequent bytes are clocked in the same way. The cyclic nature of this design places no limit on the size of the data block that can be processed. During data transmission, the 16-bit CRC word is available at outputs  $B_0-B_{15}$  after the last data byte has been clocked in; it is appended as two check bytes to the data in the block.

### Checking

The circuit is used in the check mode when receiving data containing CRC characters. The last 2 bytes in the data block received are CRC send characters. They too are clocked in and contribute to form a final receive pair of CRC characters, which, for error-free transmission, must both be zero. If an error has occurred,  $B_0-B_{15}$  will be nonzero. The FPGA will detect the nonzero condition and generate an error signal. This parallel CRC format can operate on data blocks at speeds in excess of 5.7



**1. New notation.** The many combinations of blown and unblown fuse links in the field-programmable logic family require new notation. The four possibilities for AND gates are shown in (a), while those for exclusive-OR outputs are in (b). The combinations for OR gates are in (c). The complement array in the logic sequencers is detailed in (d). Finally, OR gates controlling the flip-flops in sequencers are in (e).

megabytes per second.

An interesting use for the FPLA is in changing data at a few locations of a read-only memory (see "How to patch a read-only memory," p. 74).

The abilities of the field-programmable logic sequencer are well-demonstrated by its use as a controller for a cartridge-tape transport. In this example, one chip replaces many—a distinct advantage if the controller is to be packed on a single-board microcomputer. Although the chip's function is complex, it can be programmed methodically and worked directly from a flow chart.

### Controller routines

The controller executes fixed routines in response to status and input commands that may originate from an input/output bus or a monitoring station. Its outputs operate the velocity servo that drives the cartridge, form I/O status signals, and enable writing of data. The input and output signals of the one-chip controller are shown in detail in Fig. 4.

The controller carries out these eight routines:

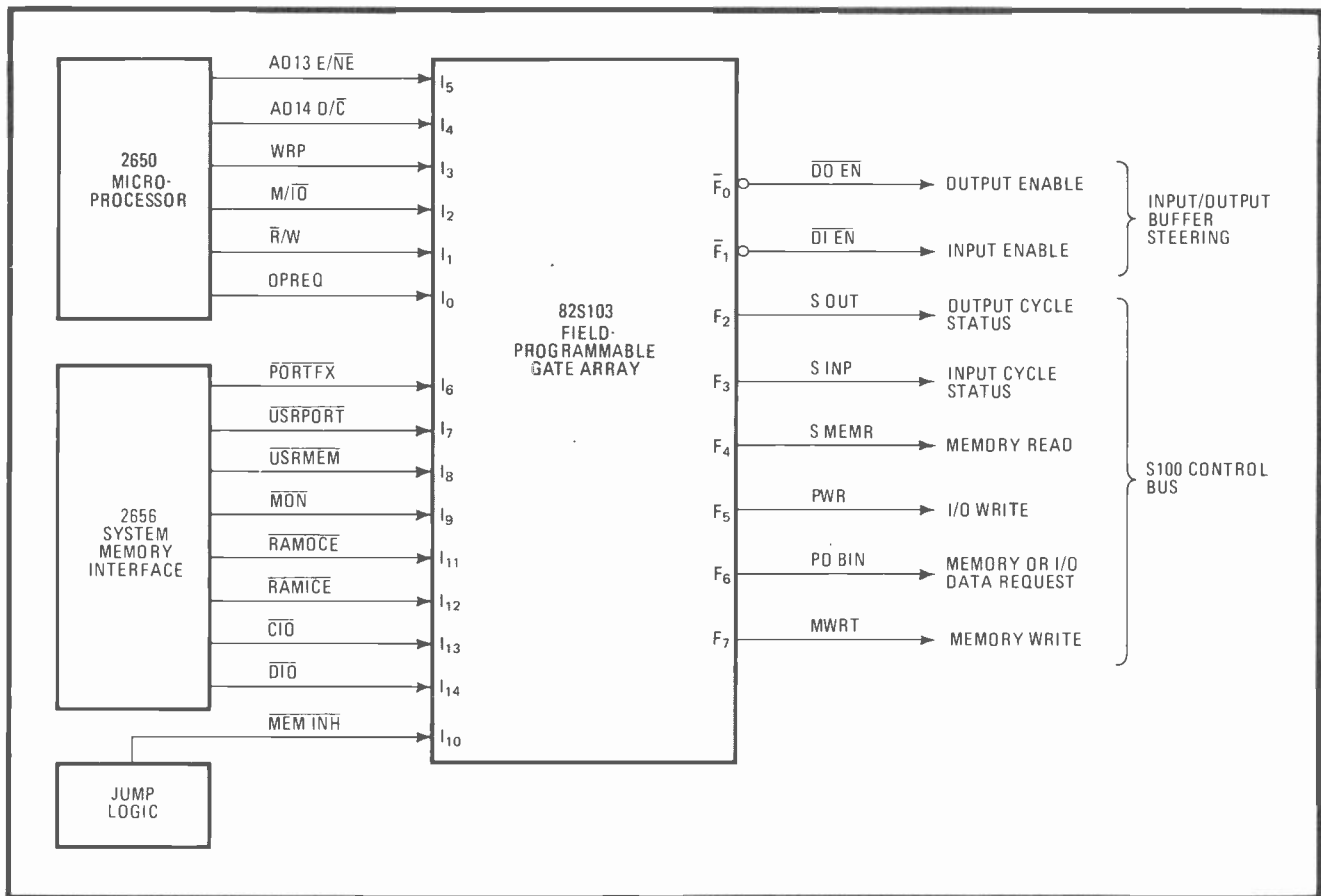
- Move tape fast-forward.

- Move tape slow-forward.
- Move tape fast-reverse.
- Move tape slow-reverse.
- Bring tape to load point when cartridge is inserted.
- Rewind tape to load point.
- Rewind tape to beginning and eject cartridge in response to unload command.
- Rewind tape to beginning and eject cartridge in response to auto-unload true condition.

The routines could be represented concisely in a conventional Mealy state diagram, but that often obscures the actual machine function. Flow charts are more easily understood, where input variables, machine states, and output functions are given variable names. Such a chart is shown in Fig. 5.

### Diagramming the flow

What would be transition terms in a Mealy state machine become true/false statements regarding the system inputs (taken one at a time) in the chart. The correlation is most obvious in the simple example in Fig. 6. The flow chart in (a) shows a conditional change from



**2. Translator.** Getting S100 bus signals, which are mostly 8080 microprocessor signals, out of a 2650 microprocessor calls for a field-programmable gate array. One 82S103 translates signals from the 2650 and its companion 2656 interfacing chip to the hobby bus.

state A to state B. The conditions in the flow chart's diamonds must be simultaneously satisfied for the state change to occur. The conditions take on variable names, and for this example, which arbitrarily assumes a 4-bit state register, three inputs, and two outputs, the corresponding state diagram is shown in Fig. 6b.

The transition from A to B denotes a jump from 10 ( $1010_2$ ) to 13 ( $1101_2$ ) and an output transition to 2 ( $10_2$ ) at the next clock pulse if the combination  $X_n = 4$  ( $100_2$ ) is true. The transition is synthesized by forming a transition term  $T = P_3\bar{P}_2P_1\bar{P}_0I_2\bar{I}_1\bar{I}_0$  and using term T at the next clock pulse to generate next-state and next-output commands for the state and output registers, respectively. For the state register, flip-flops  $N_0$  and  $N_2$  are set by connecting T to set lines  $S_0$  and  $S_2$ , and flip-flop  $N_1$  is reset by coupling T to the  $R_1$  reset line. Similarly, for the output register bit  $F_0$  is reset and bit  $F_1$  is set by connecting T to corresponding flip-flop reset ( $R_0$ ) and set ( $S_1$ ) lines.

### Controller conditions

Referring again to the controller flow chart, it can be seen that whenever the tape-drive power is turned on, or when an interlock is opened, the transport must be stopped. That is achieved by an input signal to the controller called  $\overline{\text{INTRDY}}$  that resets the state register with an unconditional jump to state 1 or STOP. When that occurs, all outputs on the FPLS chip become inactive, WRITE is inhibited, and speed and direction are

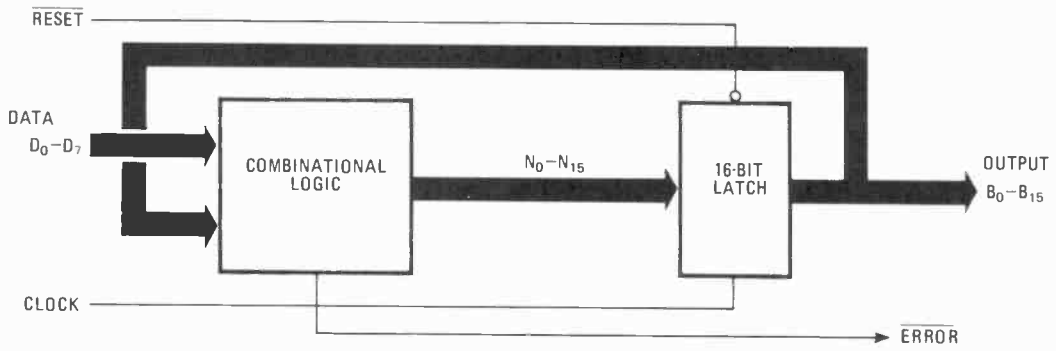
arbitrarily set to SLOW and REVERSE. From the STOP state, operation into any mode occurs by state and output jumps when all of the intervening conditions are simultaneously satisfied.

As an example, writing at normal speed will occur with a jump from state 1 to state 3, which requires that the following criteria be satisfied:

- The data cartridge is in place; therefore CIP is true.
- The drive has been addressed; SEL is true.
- The tape has been commanded to run; TR is true.
- The controller is not in state 6; state 6 is false.
- The tape should move slowly; therefore  $\overline{\text{FAST}}$  is true (an active-low signal).
- The tape should move forward;  $\overline{\text{FWD}}$  is true.

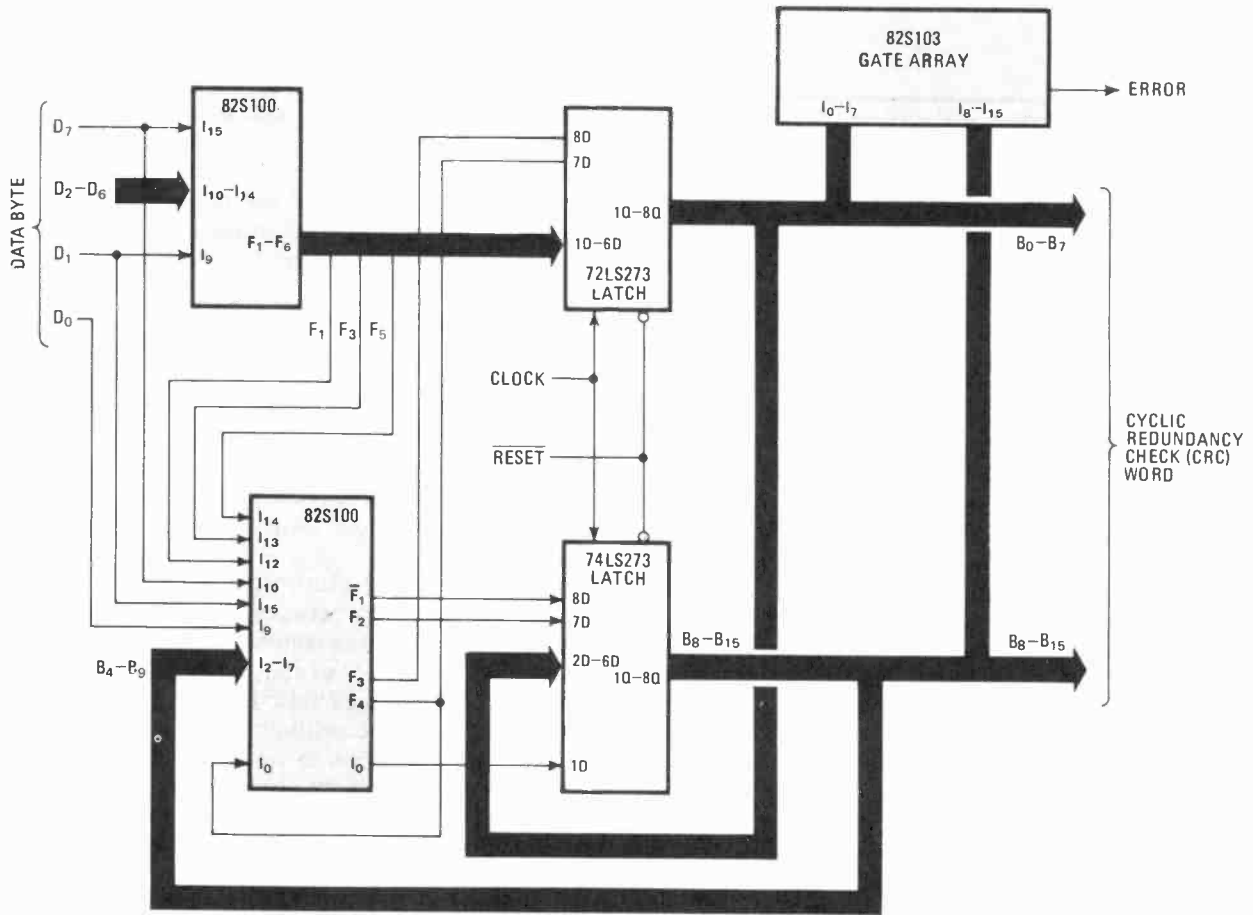
In tracing the jump between these states two things must be noted. First, the commands RWD, UNL, and TR are mutually exclusive, so that when either is true the others can be considered false or "don't care." Second, after  $\text{TR} = \text{true}$ , the condition (State = 6?) is inserted to indicate invalid jumps to states 2 and 3, which could originate from state 6 with an AUTO UNL false. Clearly, these should be avoided to inhibit honoring requests for read slow (or fast) forward while stopped at the end of the tape. So, the (State = 6?) condition is a reminder to avoid programming  $6 \rightarrow 2$  and  $6 \rightarrow 3$  state jumps in the FPLS. A similar argument holds for (State = 7?) and (State = 11?) conditions.

After data has been either written or read, the tape drive is commanded to stop by TR false, which causes a



$$\begin{aligned}
 N_0 &= D_0 \oplus D_1 \oplus D_2 \oplus D_3 \oplus D_4 \oplus D_5 \oplus D_6 \oplus D_7 \oplus B_8 \oplus B_9 \\
 &\quad \oplus B_{10} \oplus B_{11} \oplus B_{12} \oplus B_{13} \oplus B_{14} \oplus B_{15} \\
 N_1 &= D_0 \oplus D_1 \oplus D_2 \oplus D_3 \oplus D_4 \oplus D_5 \oplus D_6 \oplus B_9 \oplus B_{10} \oplus B_{11} \\
 &\quad \oplus B_{12} \oplus B_{13} \oplus B_{14} \oplus B_{15} \\
 N_2 &= D_6 \oplus D_7 \oplus B_8 \oplus B_9 \\
 N_3 &= D_5 \oplus D_6 \oplus B_9 \oplus B_{10} \\
 N_4 &= D_4 \oplus D_5 \oplus B_{10} \oplus B_{11} \\
 N_5 &= D_3 \oplus D_4 \oplus B_{11} \oplus B_{12} \\
 N_6 &= D_2 \oplus D_3 \oplus B_{12} \oplus B_{13} \\
 N_7 &= D_1 \oplus D_2 \oplus B_{13} \oplus B_{14} \\
 N_8 &= D_0 \oplus D_1 \oplus B_0 \oplus B_{14} \oplus B_{15} \\
 N_9 &= D_0 \oplus B_1 \oplus B_{15} \\
 N_{10} &= B_2 \\
 N_{11} &= B_3 \\
 N_{12} &= B_4 \\
 N_{13} &= B_5 \\
 N_{14} &= B_6 \\
 N_{15} &= D_0 \oplus D_1 \oplus D_2 \oplus D_3 \oplus D_4 \oplus D_5 \oplus D_6 \oplus D_7 \oplus B_7 \oplus B_8 \\
 &\quad \oplus B_9 \oplus B_{10} \oplus B_{11} \oplus B_{12} \oplus B_{13} \oplus B_{14} \oplus B_{15} \\
 \text{ERROR} &= \bar{B}_0 \cdot \bar{B}_1 \cdot \bar{B}_2 \cdot \bar{B}_3 \dots \bar{B}_{15}
 \end{aligned}$$

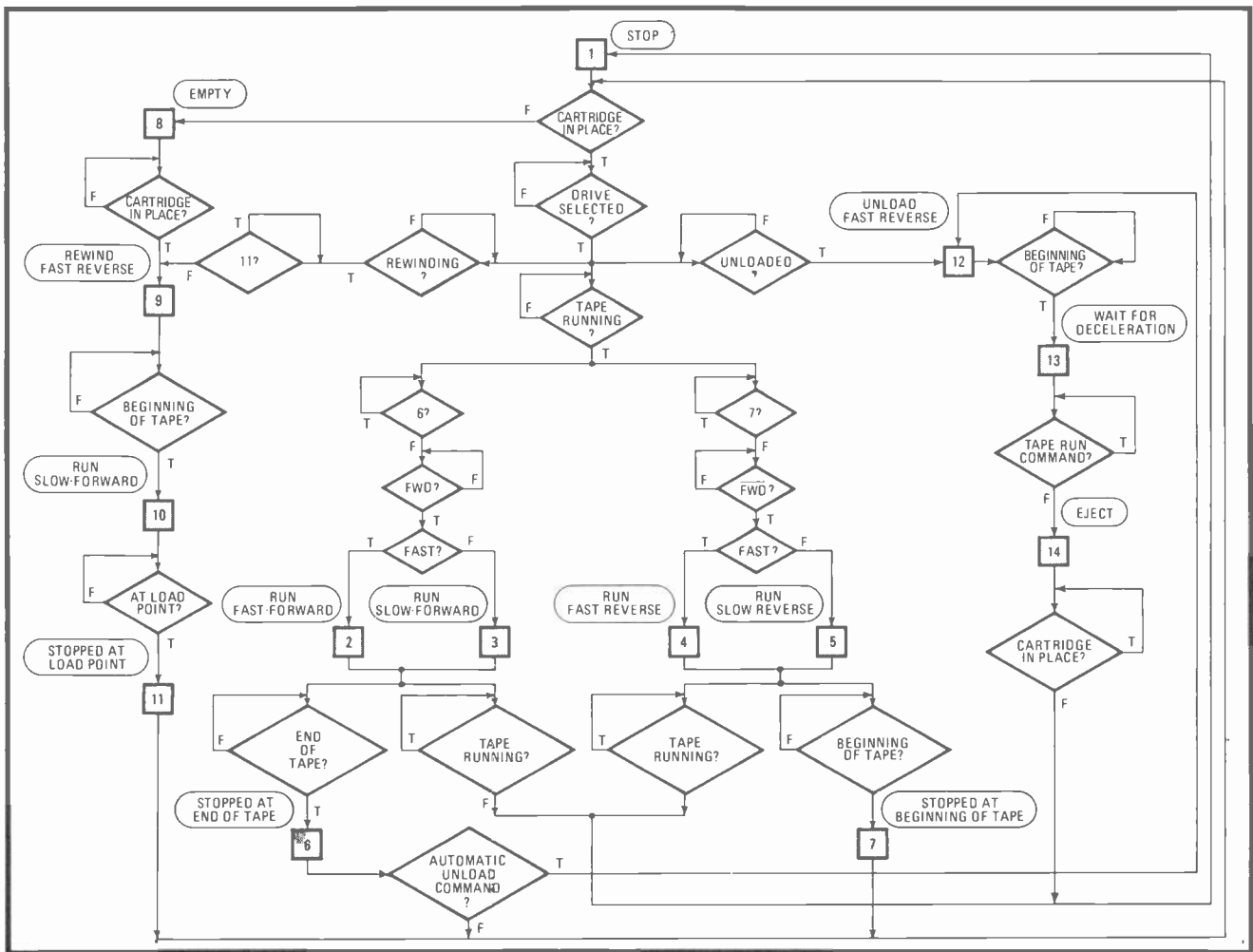
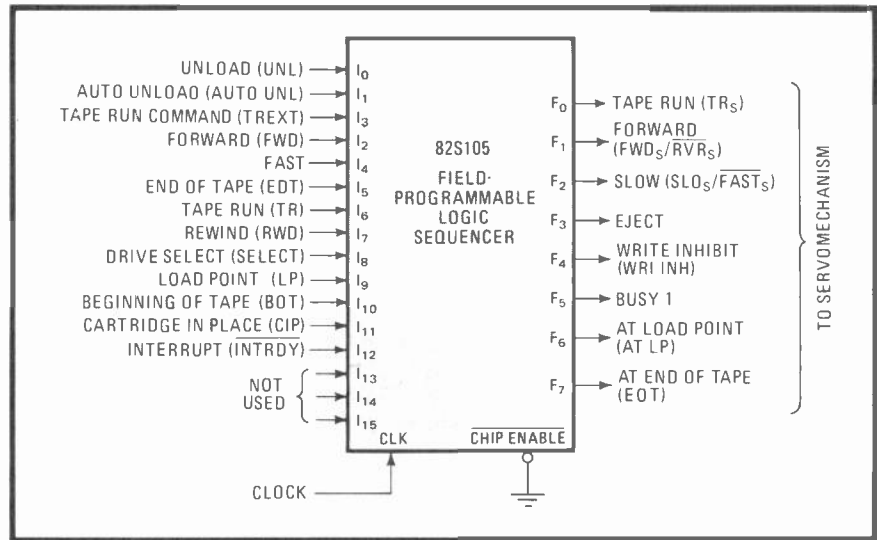
(a)



(b)

**3. Error-free.** The technique of using a cyclic redundancy check (CRC) word for error-free data transmission requires complex logic to generate the word (a). A pair of logic arrays, two latches, and a gate array (b) do the job, which usually requires a boardful of chips.

**4. Tape controller.** A field-programmable logic sequencer like this tape controller can perform extremely complex tasks. The 82S105 receives commands from an input/output bus or monitor, and provides all the necessary signals for driving the tape-transport servo-motor mechanism.



**5. Goes with the flow.** The first step in designing the controller is preparing a flow chart of the operation. The chart is much easier to understand than a state diagram or Mealy machine, yet provides all the information needed for programming the logic-sequencer chip.

jump from state 3 (RUN SLOW FORWARD) to state 1. By similar arguments, the tape drive can be run either fast or slow in either forward or reverse directions by jumping to states 2, 4, and 5.

When the end of tape is reached (EOT true), the tape drive is stopped. That is implemented by jumps 2 → 6 or

3 → 6. Once in state 6, the tape drive can no longer move in the forward direction because of the State 6 false condition preceding states 2 and 3. If AUTO UNL is true, the drive will automatically rewind (state 12), wait for tape to decelerate (state 13), eject the tape cartridge (state 14) and stop. If AUTO UNL is false, the drive must

## How to patch a read-only memory

It is a shame to throw away read-only memories. But often firmware-based systems must commit control programs to large mask-programmed ROMs, only to have a design revision requiring a new program—and a new ROM. If no pin-compatible, user-programmable ROM is available, the customer could end up waiting out the 5-to-10-week turn-around time for the new mask parts—and throwing away his inventory of old ROMs.

One way to save an obsolete ROM (or even PROMs—it hurts to throw them away, too) is by patching, which redirects certain addresses to an adjunct smaller memory. This can be done most efficiently with an 82S107 field-programmable logic array.

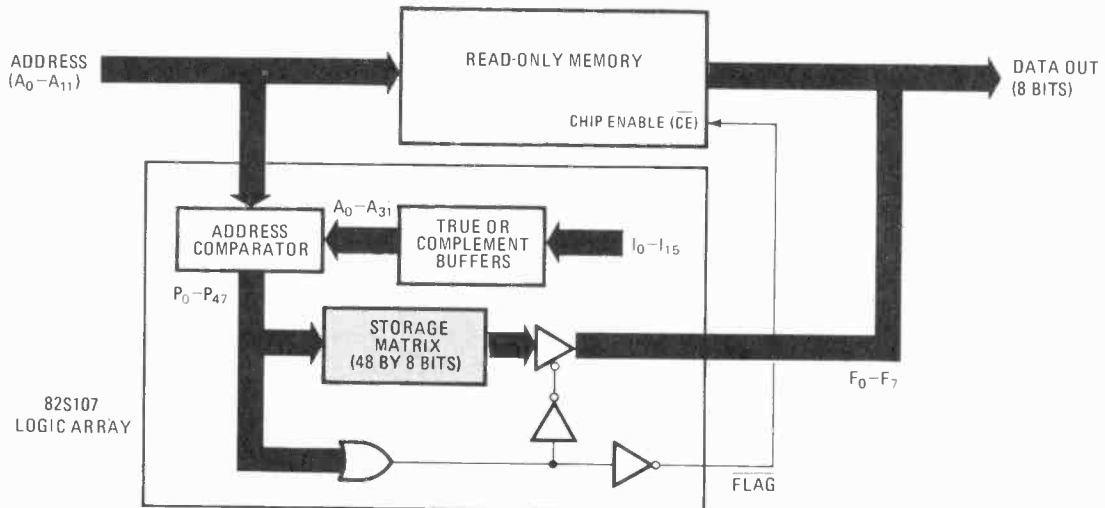
As a ROM patch (FPRP), the FPLA becomes a programmable, content-addressable PROM that continually monitors the address bus. As shown in the figure, when the FPRP encounters a match that signals a correction of data, its flag output ( $\overline{FL}$ ) disables the ROM, and new data from the FPRP is put on the output bus. If, for example, address 750 were to be given 7F, and addresses OA4-OA7 were all to be reassigned B4, the FPRP would be programmed as in the table. For a 12-bit address, only inputs  $I_0$ - $I_{11}$  are used, and the remaining four,  $I_{12}$ - $I_{15}$  then become "don't care." (Incidentally, inputs  $I_0$  and  $I_1$  in the

second product term are also "don't care" because they define an address block of four locations.)

The address comparator can patch up to 48 non-overlapping addresses anywhere within a memory field of 64 kilobytes. Block addressing is possible, too, using the FPRP's true or complement input buffers. Moreover, the number of addresses can be expanded by hooking several devices in parallel and wire-ANDing their flag outputs.

Since the outputs of the ROM patch primarily define a byte of memory data rather than a set of logic functions, output polarity is not controlled. Also, to maintain compatibility with the gate array, the FPRP generates its self-enable signal with a fixed multiple-input OR gate; the only disadvantage of that method is addresses (AND terms), once programmed, may no longer be deleted.

The ROM patch affords a recovery strategy effective in several design situations, including modifications of dedicated application programs, operating systems, assemblers, and monitor routines. It also permits on-site optimization of system parameters, in accordance with, say, environmental variables, and allows custom function options and product-line diversification. The customer need only allot board space next to the mask ROM for an FPRP; no parts are actually used until program changes are required after the product is in the field.



PROGRAM TABLE FOR ROM PATCH

| Input address | No. | Product term     |    |    |    |    |    |   |   |   |   |   |   | Active level    |   |   |   |   |   |   |   | Output data |   |   |   |    |
|---------------|-----|------------------|----|----|----|----|----|---|---|---|---|---|---|-----------------|---|---|---|---|---|---|---|-------------|---|---|---|----|
|               |     | Comparator input |    |    |    |    |    |   |   |   |   |   |   | Output function |   |   |   |   |   |   |   |             |   |   |   |    |
|               |     | 15               | 14 | 13 | 12 | 11 | 10 | 9 | 8 | 7 | 6 | 5 | 4 | 3               | 2 | 1 | 0 | 7 | 6 | 5 | 4 |             | 3 | 2 | 1 | 0  |
| 750           | 0   | -                | -  | -  | -  | L  | H  | H | H | L | H | L | H | L               | L | L | L | A | • | A | • | A           | • | • | A | A9 |
| 5FE           | 1   | -                | -  | -  | -  | L  | H  | L | H | H | H | H | H | H               | H | L | L | • | A | A | A | A           | A | A | A | 7F |
| OA4-OA7       | 2   | -                | -  | -  | -  | L  | L  | L | L | H | L | H | L | L               | H | - | - | A | • | A | A | •           | A | • | • | B4 |

| A<sub>11</sub> ————— A<sub>0</sub> | | D<sub>7</sub> ————— D<sub>0</sub> |

wait for either a rewind command (RWD), an unload command (UNL), or reverse command (FWD).

If the tape is moved in the reverse direction until the beginning (BOT), the drive is stopped. This is implemented by a jump from states 4 or 5 to state 7. Once in state 7, the tape drive can no longer move in the reverse

direction because of the state 7 false condition preceding states 4 and 5. The tape will remain stopped at the beginning until TWD, UNL, or FWD commands are given.

If no cartridge is in place (CIP false) when the tape drive is turned on, the controller will jump from state 1 to 8, and signal EMPTY. When a cartridge is installed,





TABLE 1: COMPARISON OF DESIGN ALTERNATIVES FOR TAPE CONTROLLER

| Parameter                     | Field-programmable logic sequencer | Discrete logic        | Monolithic Memories Inc.'s Programmable Array Logic |
|-------------------------------|------------------------------------|-----------------------|---|
| Chip count                    | 1 chip                             | 6 chips               | 14 chips  |
| Circuit-board area            | 0.84 in. <sup>2</sup>              | 2.13 in. <sup>2</sup> | 3.78 in. <sup>2</sup>                               |
| Power (typical)               | 0.60 W                             | 1.36 W                | 4.8 W   |
| Speed                         | 90 ns/state                        | 132 ns/state          | 105 ns/state  |
| Voltage                       | +5 V                               | +5 V                  | +5 V  |
| Cost (high-volume production) | \$12                               | \$14                  | \$48  |

TABLE 2: PROGRAMMING EQUIPMENT FOR THE FIELD-PROGRAMMABLE LOGIC FAMILY

| Type   | Manufacturer        | Model    | Field-programmable device |             |           |                 | Availability   |
|--------|---------------------|----------|---------------------------|-------------|-----------|-----------------|----------------|
|        |                     |          | Gate array                | Logic array | ROM patch | Logic sequencer |                |
| Logic  | Signetics           | FP-103   | •                         |             |           |                 | now            |
|        |                     | FP-104   |                           | •           | •         | •               |                |
|        | Curtis              | PR-100   |                           | •           |           |                 |                |
|        |                     | PR-100A  |                           | •           | •         |                 |                |
|        | Data I/O            | 10       |                           | •           | •         |                 |                |
| Memory | Data I/O            | 17,19    | •                         | •           | •         | •               | 3Q79           |
|        | Sunrise Electronics | SM100    |                           | •           | •         |                 | now            |
|        |                     |          | •                         |             |           | •               | in development |
| Hybrid | Stag                | PPX-Plus |                           | •           | •         |                 | now            |
|        |                     |          | •                         |             |           | •               | in development |

forward (FWD), and fast (FAST).

The flow chart of the controller routines is complete with 14 states and 36 state jumps (including synchronous reset). As such, four state-register flip-flops sufficiently represent all states. All state jumps can be directly programmed into the chip from the flow chart. All state jumps occur on the leading edge of the clock.

The advantage of a controller built with the FPLS is best shown by a comparison to discrete logic, which would comprise PROMs, latches, and gates, using the same state diagram as for the FPLS. Table 1 compares the FPLS controller with a discrete implementation as well as with Monolithic Memories Inc.'s Programmable Array Logic chips, in several aspects.

**Programming**

The key to design flexibility with programmable logic is the availability of programming equipment. The need for PROMs in this equipment has led to a large number of memory programmers being offered by several manufacturers. Generally, they operate with personality card sets that meet the requirements of various PROM technologies. Suppliers have already begun developing sets compatible with memory programmers for logic devices.

Hardware is expected to be available by the end of the third quarter of this year.

For the concept to work, the logic devices must be manipulated as memory chips are—by defining the desired fusing pattern in terms of an address-data relationship. Although this tends to obscure the logic function of the device, which is not visible on the program table, it is sure to provide low-cost programming equipment that can be manned by low-skilled labor.

Logic programming is another possibility, and low-cost equipment is already available from Signetics. Logic programmers allow direct entry of the logic function from the program table; no reference to the device logic diagram is necessary, and the user need not specify the status of each individual link in a device. Such programmers are more convenient for engineering use during the initial design phase, but with their high programming speed—about 10 seconds per device—can also be effective in production. Their only drawback is that they are dedicated machines and cannot program PROMs.

Some manufacturers offer a hybrid type of PROM programmer that can also be configured to do logic programming. Table 2 shows the various options available to prospective users now, or in the near future. □

# Supersensitive measurement demands critical input design

The more esoteric sources of current and leakage must be taken into account when counting electrons

by Robert Miles, *Keithley Instruments Inc., Cleveland, Ohio*

□ The success of the ongoing quest for electronic devices that do their jobs with less current at lower voltages brings with it an attendant problem: that of convenient measurement of these extremely low currents, voltages, and charges.

Recent improvements in MOS field-effect transistors and the development of complementary-MOS logic, bipolar FETs, and MOS FET operational amplifiers have reduced input and operational current requirements by decades. The widespread use of these and related devices with input currents in the picoampere range has increased the demand for ultralow-current and ultra-high-impedance measurements.

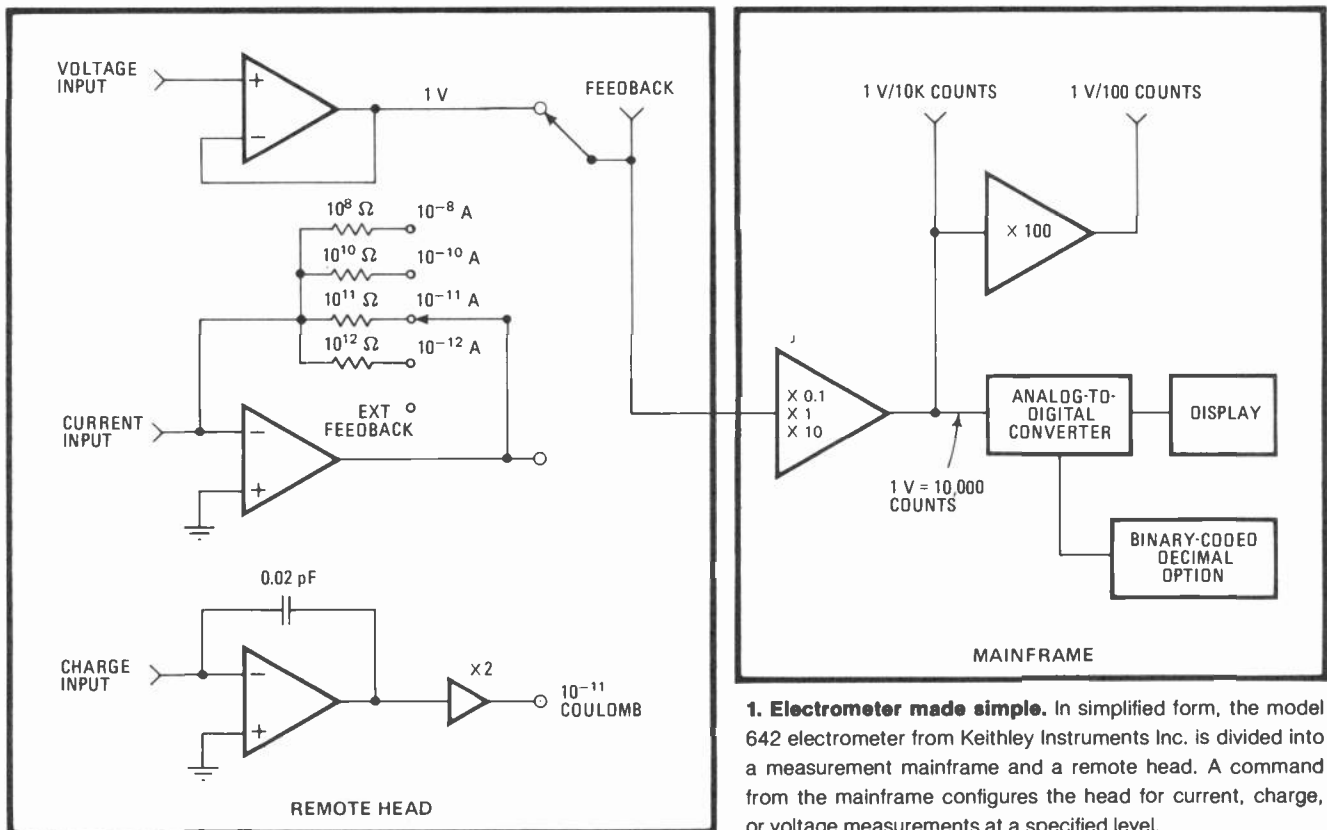
Many other situations exist that require convenient, low-current measurements, such as the examination of semiconductor current-voltage relationships, low-level photodetector response, and other phenomena in special-

ized applications of physics and chemistry. The design of a portable, solid-state instrument such as the Keithley model 642 electrometer [*Electronics*, Dec. 7, 1978, p.159] shown in Fig. 1 embodies the concepts and techniques necessary to make measurements at these levels and so bears close examination.

## Extremes

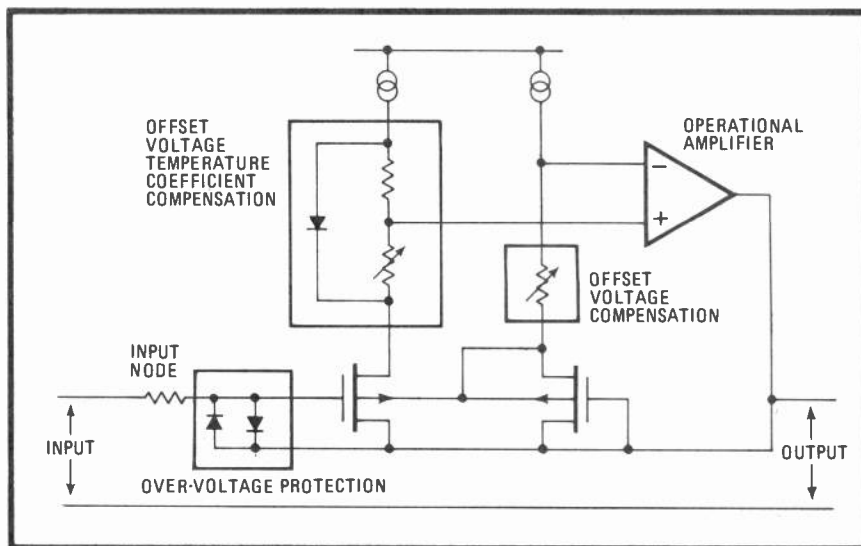
Basically, an electrometer is a refined direct-current multimeter. It can be used for virtually any task normally performed by a conventional multimeter. But its input characteristics permit it to perform voltage, current, resistance, and charge measurements far beyond the realm of the conventional multimeter.

An electrometer's input resistance is very high, typically above  $10^{14}$  ohms and sometimes as high as  $10^{16}$   $\Omega$ . Offset current at the input is typically  $5 \times 10^{-14}$  ampere



**1. Electrometer made simple.** In simplified form, the model 642 electrometer from Keithley Instruments Inc. is divided into a measurement mainframe and a remote head. A command from the mainframe configures the head for current, charge, or voltage measurements at a specified level.

**2. More for less.** In addition to providing less expensive circuitry, the use of MOS field-effect transistors in the electrometer's input circuit allows compensation for offset voltage and its temperature coefficient. Both compensation networks can be independently located in either source lead.



or lower. These characteristics allow voltage measurement that causes only an extremely small amount of circuit loading. Electrometers are capable of monitoring current levels down to the theoretical limits imposed by the level of the input offset current: the Keithley 642's most sensitive current scale reads 200 femtoamperes full-scale. Full-scale charge readings on the instrument's 4½-digit display go from  $10^{-10}$  to  $10^{-12}$  coulomb; currents below  $10^{-15}$  A are generally best measured using the charge function and a strip-chart recorder to monitor the analog output. In this way, resolutions of  $10^{-17}$  A can be achieved. Its high input resistance and low current offset also enable the electrometer to measure resistances from ordinary levels up to extremely high values.

At these levels of measurement, the user must always be sure that the interconnecting structure that carries the signal from the current or voltage source being measured to the input connector of the electrometer does not contribute to or otherwise degrade that signal.

### Detection

Central to any electrometer design is the active input device that detects the voltage imbalance at the input junction (or input node). A number of useful criteria exist for the selection and evaluation of such devices: the input gate current and resistance, the offset voltage stability with time and temperature, the voltage and current noise, and the complexity of any associated circuitry needed.

The electrometer input devices most widely used today are MOS FETs, but it is difficult to obtain them with input gate currents below  $10^{-14}$  A. For the model 642, a minimum input current requirement of  $5 \times 10^{-17}$  A was established (about 300 electrons per second).

Other instruments capable of measuring inputs at this level employ a vibrating capacitor, or reed, as the input device. These capacitors and their associated circuitry are relatively costly, and the circuitry presents additional performance problems. The forward gain block in a vibrating reed configuration consists of an alternating-current amplifier with multiple poles in its response when mapped in the complex frequency plane. The amplifier's stability is easily compromised if there is an

additional pole in any feedback network.

A solid-state input device, on the other hand, with an output response down to dc, permits the use of an integrated circuit operational amplifier with only a single, dominant pole in its response. Its performance stability with feedback is therefore much better than that of the vibrating reed circuitry. Its overall cost is lower, as well.

### Plugging the leaks

The MOS FET input gate current is lowered by dealing with two of its major leakage mechanisms: that of the header and the leads. Special die processing and packaging eliminates all unguarded leakage paths save that of the silicon dioxide gate insulation. The MOS FET die is mounted on an alumina substrate which in turn is affixed to a TO-8-package metal header. The use of the alumina substrate avoids committing the header to the MOS FET substrate, so each lead in this package passes through a glass feed-through insulator and is both shielded and guarded from all other leads by the header. Guarding is a construction technique wherein all potential leakage paths from the conductor being guarded are interrupted by another conductor that is driven (by a low-impedance source) to the potential of the guarded conductor.

Another advantage in using MOS FETs is that they allow compensation for offset voltage and its temperature coefficient. In the 642 electrometer, the input MOS FET is operated as a source follower, with another MOS FET providing a gate-to-source voltage reference; each MOS FET's source is driven by a constant current supply, as shown in Fig. 2. The operational amplifier gain block is then driven from the dual MOS FET source. The offset-voltage temperature coefficient is cancelled by a portion of the forward voltage of a silicon diode mounted in close proximity to the input MOS FET. A fixed-source resistance is used to cancel any residual MOS FET offset or diode forward voltage. With this configuration, a voltage-offset temperature coefficient of 30 microvolts/°C is obtained; vibrating-reed input devices typically have a temperature coefficient of about  $100 \mu\text{V}/^\circ\text{C}$ .

In the light of the sensitive input characteristics of any

## Three measurement demons

**Heat.** In a resistor, the kinetic energy of molecules produces motion of electrical charges. These charge movements result in noise called Johnson, thermal, or heat noise. In theory, the power available from this motion is constant and given by:

$$P = 4kT\Delta f$$

where  $k$  = Boltzmann's constant,  $T$  = temperature in kelvins, and  $\Delta f$  = the noise bandwidth in hertz over which the measurement is being made. Metallic conductors approach this theoretical noise level; other materials produce more noise than theory predicts. From the equation, Johnson voltage noise ( $E$ , in volts root mean square) developed in a resistor,  $R$ , can be found:

$$E = (4kT\Delta fR)^{1/2}$$

and Johnson current noise ( $I$ , in amperes rms) becomes:

$$I = (4kT\Delta f/R)^{1/2}$$

**Pressure.** Piezoelectric currents are generated when mechanical stress is applied to certain insulating materials, notably ceramics and other crystalline material. Teflon

and some other plastics used for insulated terminals and interconnecting hardware exhibit what is known as a space charge effect, wherein an applied force creates a change in capacitance and thus a charge redistribution. The behavior is the same as for piezoelectric materials: a physical force creates a current.

**Friction.** Triboelectrically generated currents result from the creation of charges at the interface between a conductor and an insulator due to frictional forces at the interface, as in the case of a cable that is moved. The mechanism involved is one of rubbing off electrons, creating a charge imbalance and thus a current flow. Low noise cables are available that have a conductive coating (usually graphite) at the metal-insulator boundary, reducing this effect significantly. Currents down to 1 picoampere can be measured using cables treated in this manner. Rigidly securing the cable from any movement will permit its use down to a few femptoamperes. Rigid airline coaxial cable such as GenRad GR874 series is suitable down to 0.1 fA. Below this current level, special connection schemes and the use of high quality insulators such as sapphire are required.

electrometer, input over-voltage protection is essential. Silicon diodes can be used to limit the input-to-guard potential during input overload, but an additional leakage source at the input is the price paid. Available devices reduce this leakage to  $10^{-14}$  or  $10^{-15}$  A.

To obtain better leakage characteristics, the junction characteristics of diodes made from other materials were examined. Experimentation showed that gallium phosphide (GaP) diodes had better leakage characteristics at low voltages, with both forward and reverse bias.

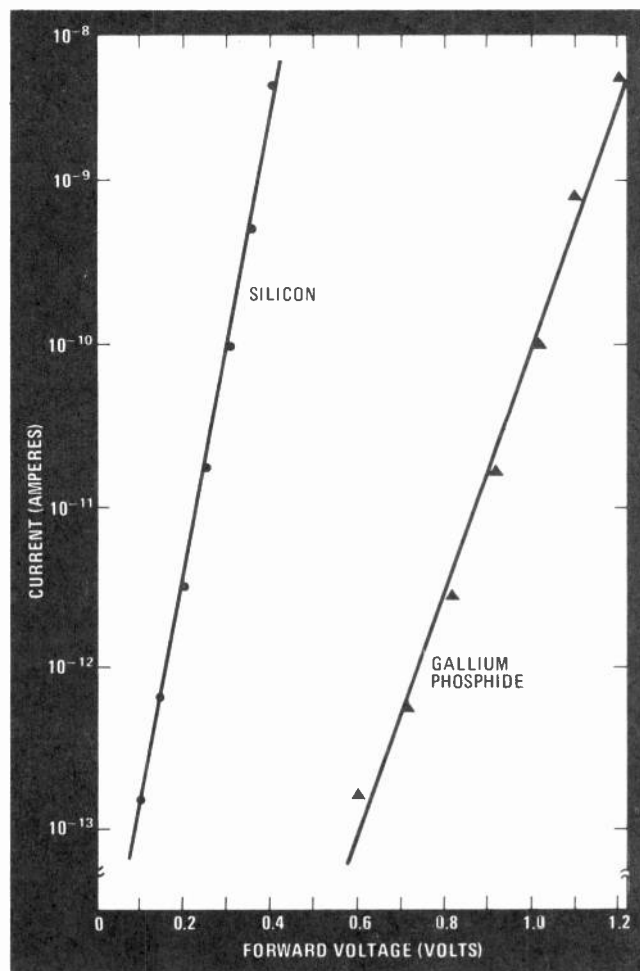
### Johnson noise

A more important concern is the impact of the input protection device on the instrument's input current noise. To minimize Johnson current noise (see "Three measurement demons") that could degrade input resolution, particularly in the charge function, the resistance across the amplifier input must be maximized. A number of sources contribute to input resistance, including structural insulators, the input MOS FET, and the input protection device. Of these, the resistance of the input protection device is the most significant.

Evaluation of available silicon and gallium phosphide diodes yielded the characteristic current-voltage plots shown in Fig. 3. By extrapolating these plots, an estimate of the junction resistance at zero forward bias for silicon ( $7.5 \times 10^{12} \Omega$ ) and gallium phosphide ( $3.9 \times 10^{16} \Omega$ ) was obtained.

Although these figures have not been rigorously verified for very small forward bias voltages, they serve to indicate the superiority of GaP, which is borne out in the actual performance of the 642. The GaP diodes are connected back-to-back in the instrument and mounted in a guarded package similar to that used for the input MOS FET. The resistance in series with the input (see Fig. 2) limits the input overload current.

The selection of an insulating material to mechanical-



**3. Si vs GaP.** The choice of gallium phosphide rather than silicon diodes for overvoltage protection is dictated by GaP's higher junction resistance. Estimates of both diode types' resistances near zero forward voltage are obtained from the slope of the plots shown.

TABLE 1: PROPERTIES OF INSULATING MATERIALS

| Material           | Volume resistivity (ohm-centimeters) | Resistance to water absorption | Minimal piezoelectric effects | Minimal triboelectric effects |
|--------------------|--------------------------------------|--------------------------------|-------------------------------|-------------------------------|
| Sapphire           | $10^{16} - 10^{18}$                  | ■                              | ■                             | □                             |
| Teflon             | $10^{17} - 10^{18}$                  | ■                              | ■                             | ■                             |
| Polyethylene       | $10^{14} - 10^{18}$                  | □                              | ■                             | □                             |
| Polystyrene        | $10^{12} - 10^{18}$                  | □                              | □                             | ■                             |
| Kel-F              | $10^{17} - 10^{18}$                  | ■                              | □                             | ■                             |
| Ceramic            | $10^{12} - 10^{14}$                  | ■                              | □                             | ■                             |
| Nylon              | $10^{12} - 10^{14}$                  | ■                              | □                             | ■                             |
| Glass epoxy        | $10^{10} - 10^{17}$                  | ■                              | □                             | ■                             |
| Polyvinyl chloride | $10^{10} - 10^{15}$                  | ■                              | □                             | □                             |
| Phenolic           | $10^5 - 10^{12}$                     | ■                              | ■                             | ■                             |

|     |   |   |
|-----|---|---|
| Key | ■ | Very good in regard to the property       |
|     | □ | Moderately good in regard to the property |
|     | ■ | Weak in regard to the property            |

TABLE 2: COMMON THERMOELECTRIC POTENTIALS

| Materials  | Potential (microvolts/°C) |
|------------|---------------------------|
| Cu - Cu    | 0.2                       |
| Cu - Ag    | 0.3                       |
| Cu - Au    | 0.3                       |
| Cu - Cd/Sn | 0.3                       |
| Cu - Pb/Sn | 1 - 3                     |
| Cu - CuO   | 1,000                     |

ly support and electrically isolate the input node is a key element in the performance of any electrometer or low-current instrument. Material properties that must be considered are volume resistivity, water absorption, and susceptibility to piezoelectric and triboelectric effects (see "Three measurement demons"). Table 1 compares these properties for many commonly available insulating materials. Not only is sapphire an excellent choice for its insulating properties, but it provides a rigid mounting surface for the input node. Its performance in the 642 was further enhanced through the use of guarding.

As important as the input device, input protection, and insulation are to the operation of the electrometer is their structural configuration. In the 642's remote head, the input node (Fig. 4) is a rod-like conductor that runs downward from the input connector to the MOS FET input device and its protecting GaP diodes. A guard tube

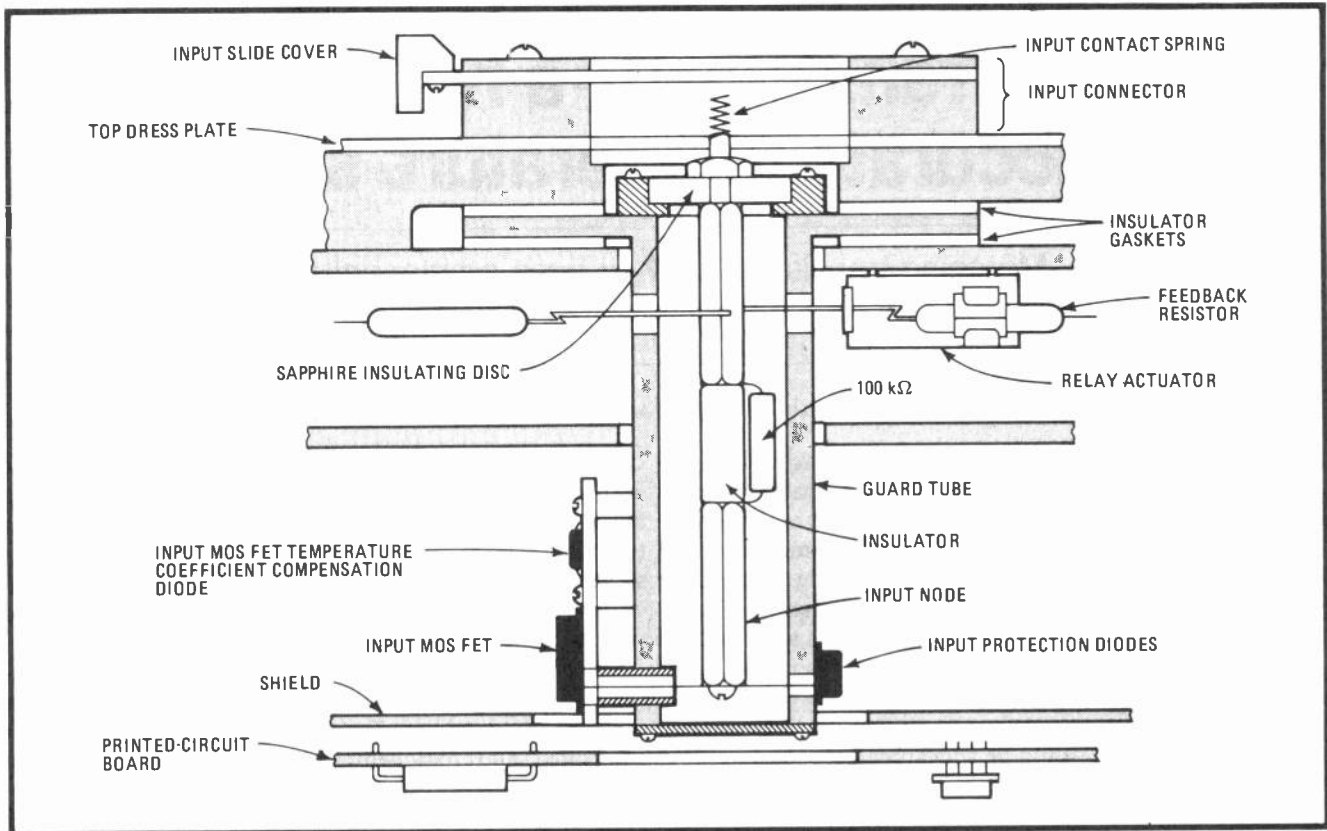
surrounds the conductor coaxially and a sapphire insulating disk supports the conductor at the connector end. The input devices at the opposite end are mounted on the guard tube. Minimizing the volume surrounding the input node reduces the ion-chamber effect caused by background radiation.

Feedback connections are made through holes along the length of the guard tube. Feedback elements are used to convert the input current or charge to a voltage that can in turn be transformed by an analog-to-digital converter into a numerical value for display. The high-value resistors used for current-to-voltage conversion are mechanically supported by their glass enclosure; a special relay mechanically manipulates a lead from the resistors so that it contacts the input node through a hole in the guard tube. Charge-to-voltage conversion is accomplished by connecting a specially constructed sapphire-insulated, air-dielectric capacitor to the node in much the same way as are the high-value resistors. The feedback elements and the relay actuators are mounted radially on two levels along the length of the guard tube and normal to it.

**Avoiding ionization**

The rest of the remote-head electronics are on a printed-circuit board at the bottom of the enclosure; this circuitry is shielded by a metal plate to prevent it from ionizing air in the region around the input node.

Within the realm of low-current measurement, ionizing radiation can be a significant source of error currents. As noted, the susceptible portion of the struc-



**4. Heading off trouble.** Careful design and solid construction of the 642's remote head prevent problems from a number of sources: piezoelectric and triboelectric potentials, electromagnetic coupling, alpha radiation, and vibration, among others.

ture is the air volume between the input node and the guard tube, which in effect forms an ion chamber.

The air ionization along the path of an alpha particle greatly exceeds that caused by any other constituent of background radiation. Since alpha particles will not pass through metals of any appreciable thickness, the only possible alpha sources that can affect measurements are the metals used to construct the node and guard—a fact that has been experimentally verified. Similar sources of low-level radiation have recently been credited with causing soft errors in charge-coupled devices and dynamic MOS memories.

The alpha-particle emissions of various materials have been measured; this data was consulted in designing the 642. Domestic lead produces many alpha particles, but there is no detectable activity above background for cadmium, so cadmium-plated, low-lead brass was used throughout the remote head. Cadmium solder was used in place of tin-lead solder for structural and electrical connections in the vicinity of the input node to further minimize alpha radiation. Other low-alpha materials are gold and silver.

Although thermoelectric potentials do not normally present problems in high-impedance circuits, they can be a factor when operating at high voltage sensitivities. They develop at the junctions of dissimilar metals, a fact that is made use of in thermocouples. The potentials are a function of the metals' properties, their impurities, and the temperature gradient across the junction. Table 2 lists some typical thermoelectric potentials.

With careful mechanical design, these error sources

can be reduced or eliminated. When dissimilar-metal junctions cannot be avoided, heat sinks can be arranged so as to reduce the temperature gradient across them.

By dividing an electrometer into a mainframe with the controls and display and a separate remote input head, the sensitive input circuitry can be located directly at the signal source, and the path over which low-level signals must travel can be minimized. This separation also removes the instrument's operator from the measurement environment, where he might inadvertently affect the sensitive circuitry.

#### Physical integrity

Rigid construction of all parts of the remote head serves to reduce or eliminate spurious input signals due to vibration or distortion. A sealed environment and an internal, replaceable or rechargeable dessicant help to maintain the integrity of the remote head's internal insulators and high-impedance circuitry. (The external insulators that support the input node must be kept clean since contamination or high humidity may degrade the insulator's surface resistivity or, in the case of contamination by ionic chemicals, weak "batteries" between two conductors may form. The guarded insulator minimizes the effect of shunt resistance in the former case, but has no effect in the latter.)

A contaminant not normally considered is light. At ultralow current levels, photoemission—predominantly from solid-state components—can become significant. For the 642, this problem is addressed by using opaque glass feed-through insulators for such devices' leads. □

# Transistors—a hot tip for accurate temperature sensing

Matching transistors by their base-emitter voltage  
and dc gain ensures consistent operation from unit to unit

by Pat O'Neil and Carl Derrington, *Motorola Semiconductor Products Inc., Phoenix*

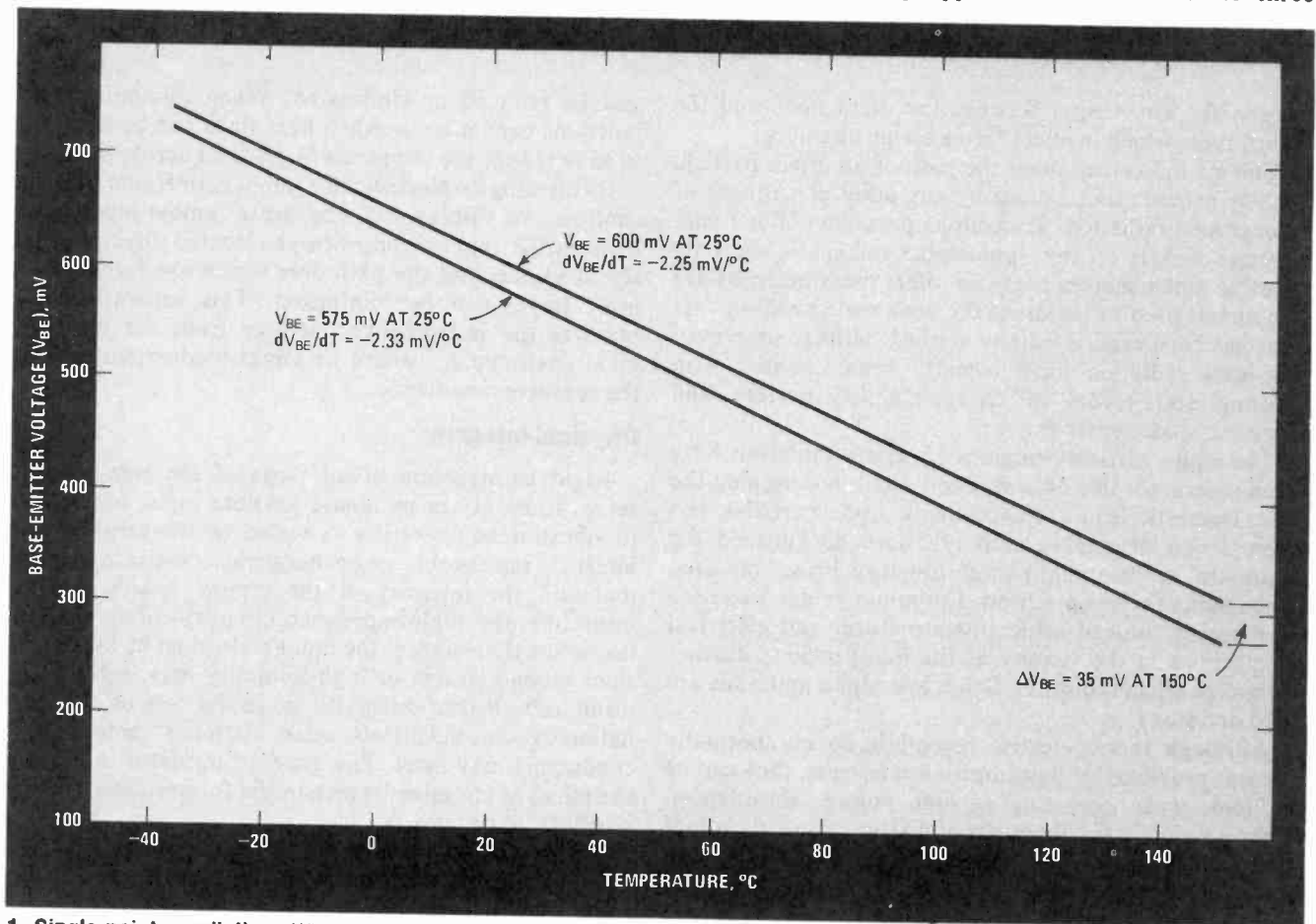
□ Transistors would seem to be ideal temperature sensors. Their low cost, their ability to operate consistently over long periods, and their sensitivity and linearity recommend them for this use. For some time, in fact, temperature measurements have been made using the base-emitter voltage of forward-biased transistors.

The big problem in using transistors in this application has been that of finding transistors with characteristics matched closely enough to allow them to be used interchangeably. If it were not for this difficulty, their use as temperature sensors would be widespread indeed.

The quest for interchangeable semiconductor sensors has led manufacturers to build monolithic integrated

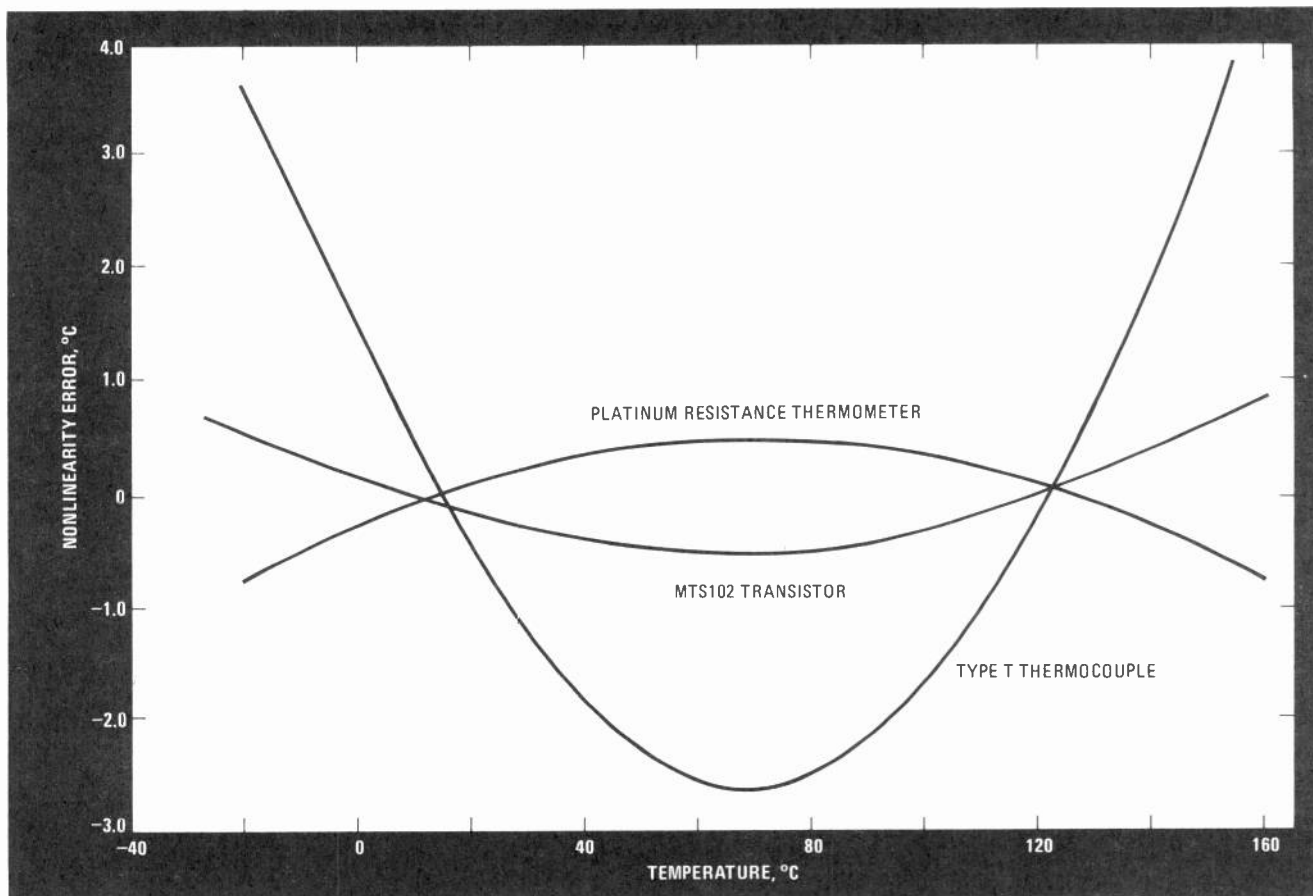
circuits whose output is the difference of two junctions with differing current densities or ones that employ laser trimming to equalize circuit parameters. Although these techniques do provide interchangeable devices, they do so at a cost that prohibits their use in throwaway applications—monitoring the curing temperature of concrete with imbedded sensors, for example.

But the improvements in production line capability that make large-scale integration possible also make it possible to produce discrete transistors with tightly controlled and matched geometries. Motorola's MTS family is a transistor series selected specifically for temperature sensing applications. It consists of three



**1. Single-point prediction.** When transistors have the same dc gain, their performance across a range of temperatures can be predicted by measuring their base-emitter voltage at a specific temperature. Variation in  $V_{BE}$  can result in large errors.





**2. In context.** Although they are inherently nonlinear, transistors perform quite admirably when compared to other devices. Between  $-40^{\circ}$  and  $+150^{\circ}\text{C}$ , the MTS102 rivals more expensive platinum resistance thermometers and easily outshines type T thermocouples.

transistor types: the 102, 103, and 105, which provide guaranteed accuracies to within  $\pm 2^{\circ}$ ,  $\pm 3^{\circ}$ , and  $\pm 5^{\circ}\text{C}$ , respectively, over the range from  $-40^{\circ}$  to  $+150^{\circ}\text{C}$ .

Transistors with these accuracies are obtained by screening transistors for matched direct-current gain and base-emitter voltage at room temperature, using a constant collector current of 100 microamperes. For any type within the family, the base-emitter voltage ( $V_{BE}$ ) must be within a specified tolerance; nominal  $V_{BE}$  may be any value from 580 to 620 millivolts. For example, the  $V_{BE}$  of an MTS102 is matched to a tolerance of  $\pm 3\text{ mV}$  and the nominal figure, say 600 mV, is printed on its package. Any MTS102 can be used to replace another with the same  $V_{BE}$  with the stated  $\pm 2^{\circ}\text{C}$  accuracy maintained. In matched lots of 10,000, the sensors are priced at 27 to 66 cents apiece, depending upon the temperature tolerance.

### Electrical consistency

For any given series of transistor temperature sensors, it is necessary to specify only the relevant and measurable electrical characteristics— $V_{BE}$  and the direct current gain at some temperature—to ensure consistent operation within a known tolerance from sensor to sensor. Furthermore, circuits can be built using such transistors that provide accuracies within  $\pm 0.01^{\circ}\text{C}$ . The design of these circuits requires an understanding of the temperature dependence of the transistors' measured parameters. The best route is an examination of the equations that

describe a transistor's operation.

The base-emitter junction of a transistor can be regarded as a simple pn junction diode. If a constant current,  $I_F$ , is forced through the junction in a forward direction, then its relation to the measurable junction voltage,  $V_J$ , is given by the Shockley equation:

$$I_F = I_{sat} e^{qV_J/kT-1} \quad (1)$$

where  $k$  is Boltzmann's constant,  $q$  is the net charge in coulombs,  $T$  is the temperature in kelvins, and  $I_{sat}$  is the saturation current.

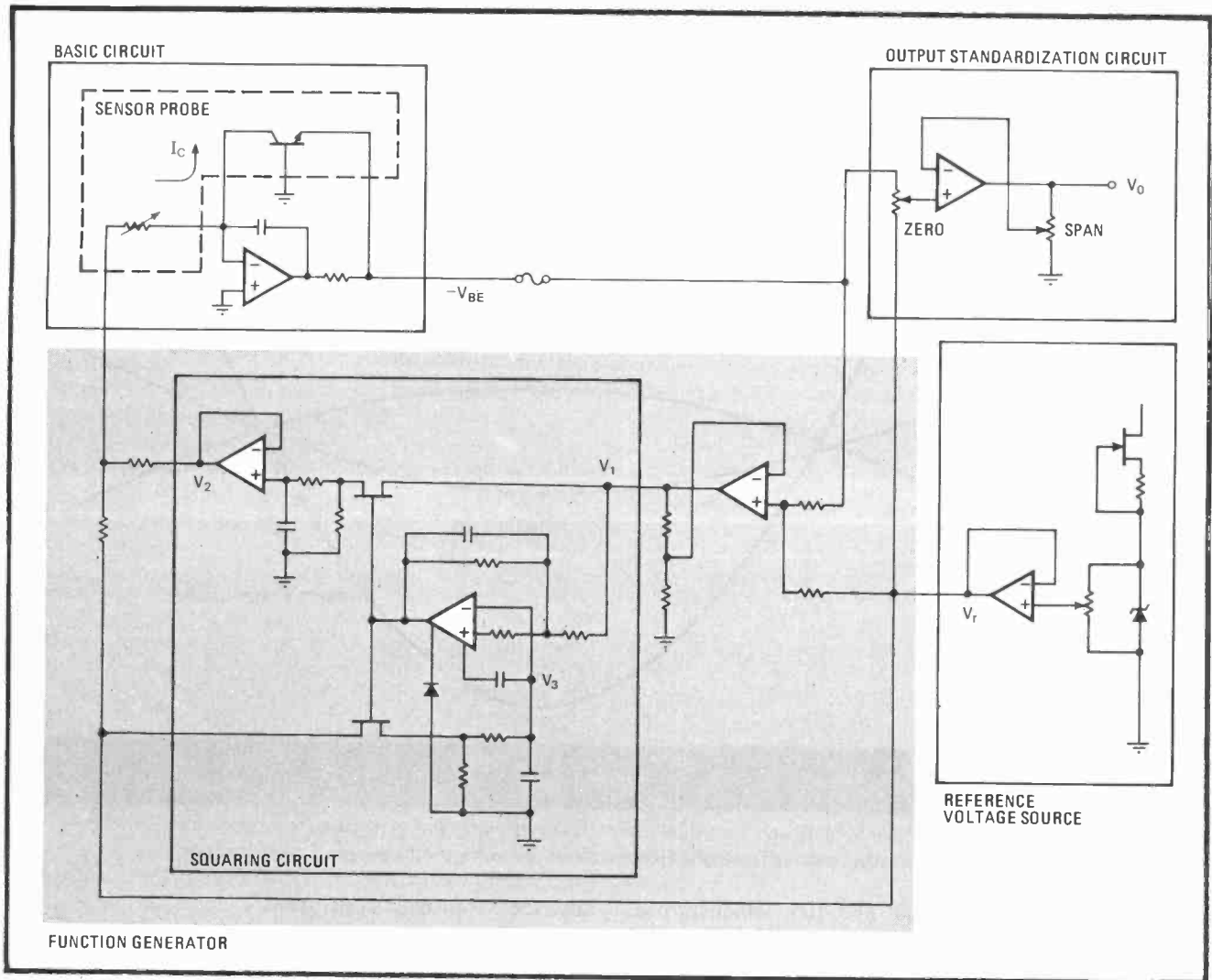
When the junction voltage is sufficiently large (that is, when the diode is sufficiently forward-biased), the  $-1$  term in the exponent can be ignored and the equation can be expressed in terms of  $V_J$ :

$$V_J \cong (kT/q) \ln(I_O/I_{sat}) \quad (2)$$

With  $I_F$  held constant, if all other terms in the equation were independent of temperature, the junction voltage would be directly proportional to the thermal voltage expression  $kT/q$  and thus to temperature  $T$ . Unfortunately, the saturation current is composed of two temperature-dependent currents: that due to the hole diffusion,  $I_p$ , and that for the electrons,  $I_n$ . The hole-diffusion current is given by:

$$I_p = qA(D_p/L_p)p_{no}$$

where  $A$  is the area of the device,  $D_p$  is the diffusion constant for the holes,  $L_p$  is the diffusion length for holes



**3. High accuracy.** To obtain high performance, the collector current of temperature-sensing transistors can be varied in accordance with temperature (reflected by base-emitter voltage) raised to some power. The squaring circuit shown performs this function.

in the n region, and  $p_{no}$  is the equilibrium hole concentration in the n region.

The last term,  $p_{no}$ , is temperature-dependent and is defined by:

$$p_{no} = n_i^2 / N_D$$

where  $N_D$  is the concentration of donor atoms imparted to the material by doping and  $n_i^2$ , the square of the intrinsic concentration, is given by:

$$n_i^2 = N_c N_v e^{-E_g / kT}$$

The terms  $N_c$  and  $N_v$  are the equivalent concentrations of conduction and valence states for the doped material;  $E_g$  is the potential of the energy gap between bands in electron volts.

### Defining saturation

The equation for  $I_n$  is similar to that for  $I_p$ , with appropriate substitution of n terms for p terms:  $D_n$  is the diffusion constant for electrons,  $L_n$  is the diffusion length for electrons, and  $N_A$  is the concentration of acceptor atoms.

Adding the equation for  $I_p$  to the equivalent equation

for  $I_n$  results in the following expression for the saturation current:

$$I_{sat} = I_p + I_n = qAN_c N_v e^{-E_g / kT} g \quad (3)$$

where  $g$  represents  $[D_p / (L_p N_D)] + [D_n / (L_n N_A)]$ . Substituting this expression into Eq. 2 gives:

$$V_j \cong E_g / q + (kT / q) \ln [I_F / (qAN_c N_v g)]$$

Again, this seems to result in a directly linear relationship of voltage to temperature. But the terms  $D_p$  and  $D_n$  are both related to temperature-dependent terms: the thermal velocities of holes and electrons. Furthermore, this dependence need not be identical. So while the quantity represented by  $g$  above can be obtained by a measurement of  $V_j$  at a specific temperature, finding that two  $V_j$ s are equal at that temperature in no way guarantees that they will be equal at another.

Fortunately, there is the familiar dc gain term for the transistor,  $h_{FE}$ . This term represents the relationship:

$$h_{FE} = I_n / I_p = [D_n / (L_n N_A)] / [D_p / (L_p N_D)]$$

If the dc gains of two transistors are equal, it means that  $I_n$  and  $I_p$  vary in the same way with respect to one

## Bounding the error

The curves in Fig. 1, which are used to set a tolerance for  $V_{BE}$  that limits the temperature measurement error, assume a linearity for transistors that does not exist, as experience proves. A demonstration that these linear curves form the boundaries of possible error is required for confidence in their use.

The assumption that the transistor's  $V_{BE}$  is linear leads to the following expression for the approximate value of  $V_{BE}$  ( $\tilde{V}_{BE}$ ):

$$\tilde{V}_{BE} = \tilde{V}_{BE1} + (dV_{BE}/dT)(T - T_1)$$

Since the measured curve is not linear, the error in the above expression can be minimized by using the following linear regression coefficients to adjust measured values:

$$\frac{d\tilde{V}_{BE}}{dT} = \frac{\{V_{BE} - \langle V_{BE} \rangle\}(T - \langle T \rangle)}{\{T - \langle T \rangle\}^2}$$

$$\tilde{V}_{BE1} = \langle V_{BE} \rangle - (dV_{BE}/dT)(\langle T \rangle - T_1)$$

where the symbols  $\langle \rangle$  indicate the average value of the enclosed quantity within the operating range.

If  $T_1$  is now chosen to be the average temperature in the

range from  $T_1 - \Delta T$  to  $T_1 + \Delta T$ , the above equation can be restated as:

$$\frac{d\tilde{V}_{BE}}{dT} = \frac{(r/3)(k/q) - (V_{g0} - V_{BE1})/T_1 - (r/2)(k/q)(T_1/\Delta T)^2[1 - f_1(1 + \Delta T/T_1)(1 - 2\Delta T/T_1) + f_2(1 - \Delta T/T_1)(1 + 2\Delta T/T_1)]}{\tilde{V}_{BE1} = V_{BE1} + (r/2)(k/q)T_1(1 - f_1 + f_2)}$$

where

$$f_1 = (1 + \Delta T/T_1)/[2(\Delta T/T_1)\ln(1 + \Delta T/T_1)]$$

$$f_2 = (1 - \Delta T/T_1)/[2(\Delta T/T_1)\ln(1 - \Delta T/T_1)]$$

An examination of these expressions indicates that a simple bounded estimate of the error resulting from the assumption of linearity is obtained by joining the extreme points of the  $V_{BE}$ -versus-temperature curves, as has been done in Fig. 1. At temperature  $T_1$ , the resulting error is:

$$\Delta\tilde{V}_{BE} = (r/2)(k/q)[(1 + \Delta T/T_1)\ln(1 + \Delta T/T_1) + (1 - \Delta T/T_1)\ln(1 - \Delta T/T_1)]$$

another. So if two transistors have equivalent  $h_{FE}$  and  $V_f$  (which, for a transistor rather than a diode, is the base-emitter voltage  $V_{BE}$ ), they will react in the same way with temperature variation. Thus they will be interchangeable for temperature-sensing applications.

### Inherent nonlinearity

While defining the base-emitter voltage and dc gain does ensure similar operation, the inherent nonlinearity of the transistor must be considered if devices are to operate within a desired tolerance. Starting with the linear equations above, it is possible to move into the world of real, nonlinear operation to see how these parameters dictate actual performance.

For a transistor,  $I_F$  in Eq. 1 is actually the collector current  $I_C$ . If the summation term is expressed as a function of temperature,  $T$ , raised to some power  $r$ , substituting Eq. 3 for  $I_{BE}$  in Eq. 1 yields:

$$I_C = A' T^r e^{-qV_{BE}/kT} e^{qV_{BE}/kT} \quad (4)$$

$A'$  represents the pre-exponential constants  $qAN_cN_v$ , and the band-gap potential of silicon at 0 K ( $V_{g0}$ ) multiplied by charge  $q$  has been substituted for the more general term  $E_G$ .

When the collector current is constant and  $V_{BE}$  is sufficiently large that the  $-1$  term in the exponent of Eq. 4 can be ignored, it is possible to express  $V_{BE}$  in terms of a specific base-emitter voltage,  $V_{BE1}$ , known at temperature  $T_1$ :

$$V_{BE} = V_{BE1}(T/T_1) + V_{g0}(1 - T/T_1) - r(kT/q)\ln(T/T_1)$$

This represents the basic relationship governing the operation of the transistor as a temperature sensor. Taking this equation's derivative with respect to temperature naturally gives the rate of change of  $V_{BE}$  with respect to temperature, usually referred to as the temperature coefficient:

$$dV_{BE}/dT = -rk/q - (V_{g0} - V_{BE})/T$$

For the MTS series of transistors, an empirical version of this equation has been determined using a  $V_{BE}$  of 600 millivolts at 25°C:

$$dV_{BE}/dT = -2.25 + 0.0033(V_{BE} - 600) \text{ mV}/^\circ\text{C}$$

Figure 1 plots this equation when the actual  $V_{BE}$  is 600 mV and when it is 575 mV. Comparison of the two curves shows that variation in  $V_{BE}$  can result in measurement errors of as much as 15°C. Fortunately, it can be shown (see "Bounding the error," above) that specifying the maximum change in  $V_{BE}$  at the extreme points of the curve limits the possible measurement error.

Measured nonlinearity for a typical MTS102 transistor is shown in Fig. 2, along with typical nonlinearity curves for a type T thermocouple and a platinum resistance thermometer. Calculating the regression coefficients for a least-squares fit to a straight line ( $R^2 = 1.00000$  for a perfectly linear device) yields a value of 0.99866 for a type T thermocouple and 0.99999 for the MTS102 and the platinum resistance thermometer. This indicates that the transistor is far superior to the thermocouple and equal in capability to the more expensive platinum thermometer for this range.

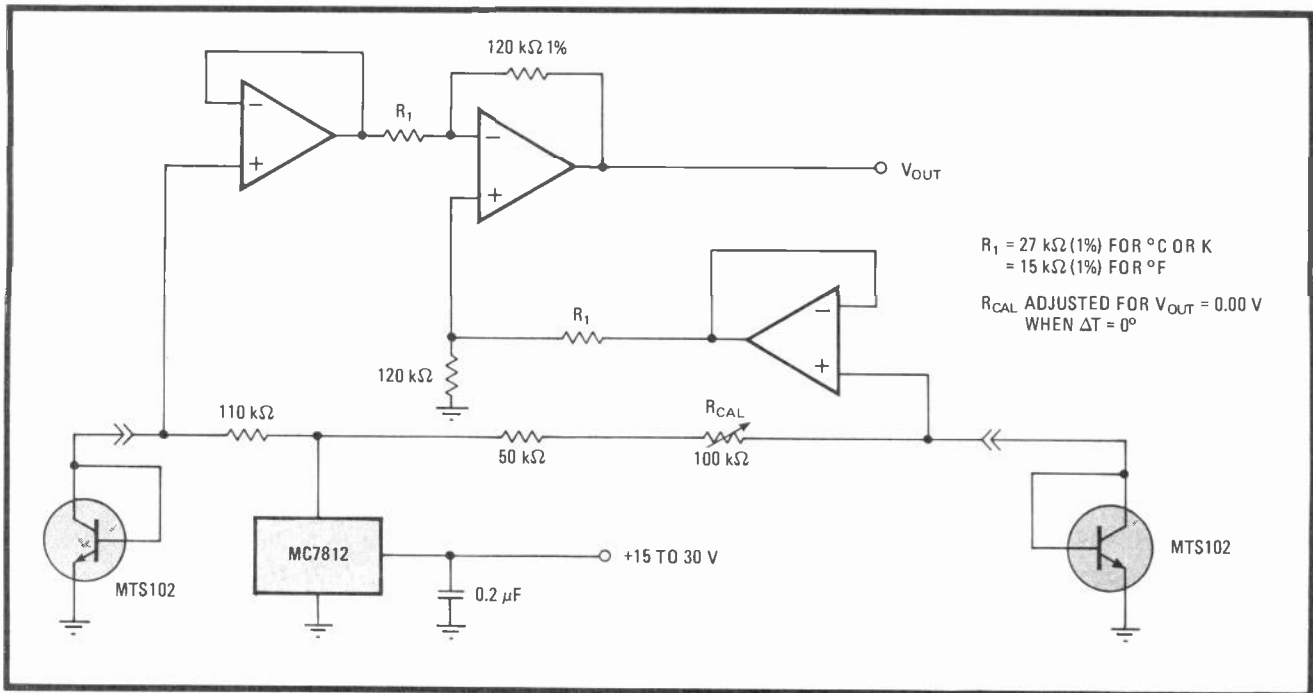
### Circuits improve accuracy

There are, of course, many applications in which the error due to the nonlinearity shown would be unacceptable. For such cases, it has been found that the operation of transistor temperature sensors can be improved if the collector current  $I_C$  is forced to react in accordance with this equation:

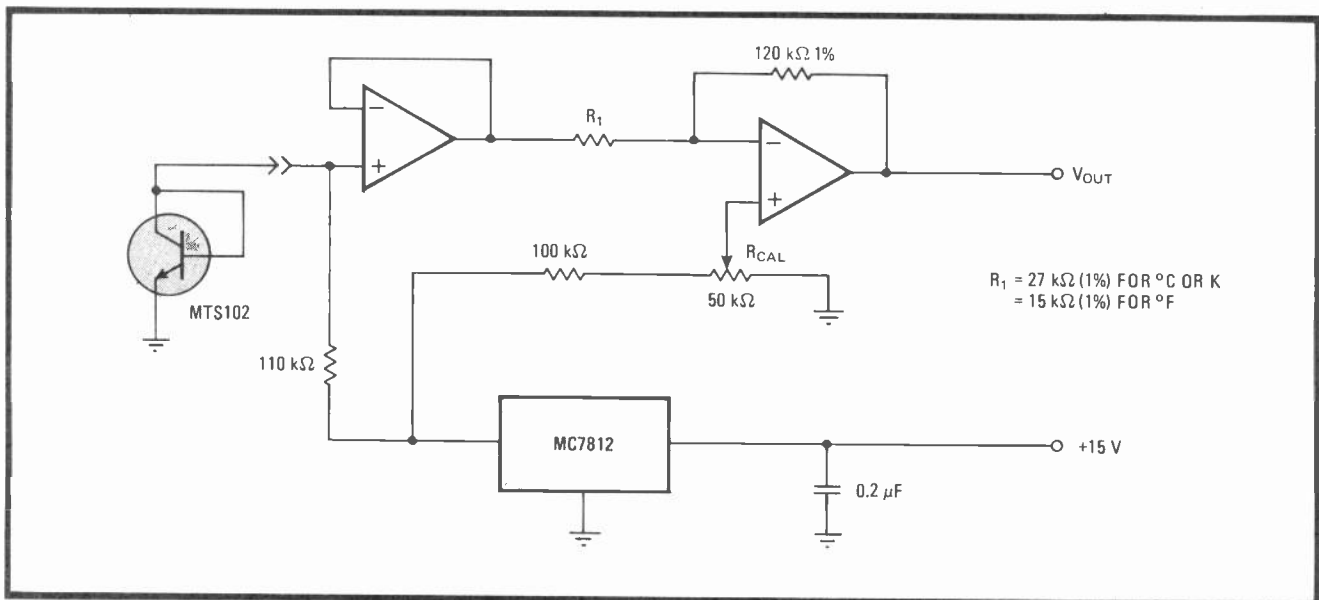
$$I_C = I_{C1}(T/T_1)^x$$

where  $I_{C1}$  is the collector current at  $T_1$ . The theoretical value of  $x$  at which nonlinearity ceases is  $r$ , the exponent of  $T$  in Eq. 4.

Using this concept, practical circuits have been built in which a standard transistor used as a sensor yielded accuracies within  $\pm 0.1^\circ\text{C}$  (see Fig. 3).<sup>1</sup> Using a more



**4. Simple difference.** Differential temperature readings, frequently needed in process controlling, can be inexpensively obtained using the configuration shown. The same circuit could also be used to set an alarm when temperature stability is critical.



**5. Even simpler.** A single transistor version of the circuit shown in Fig. 4 requires even fewer components. Since the transistor itself is inexpensive, it and others like it can be left in place and the remaining circuitry built into a portable meter.

complex and precise squaring circuit and three-point calibration,  $\pm 0.01^\circ\text{C}$  uncertainty can be achieved. It is also interesting to note that the worst-case error occurs when  $x$  is equal to zero (that is, when  $I_C$  is constant), as has been assumed throughout the preceding analysis.

Since it is possible to match transistors so that their responses track variations in temperature, there are many low-cost designs that are commercially viable. For example, Fig. 4 shows a design for a differential temperature sensing system that could easily be used for process monitoring. The output voltage of Fig. 5 can become the input to a digital multimeter that displays temperature in kelvins or degrees Centigrade or Fahrenheit.

Design engineers faced with the task of devising new systems for monitoring and controlling temperature would do well to bear in mind three important advantages of the transistor temperature sensor. First, it can be used interchangeably and is low enough in cost to be disposable. Second, the high sensitivity of this type of sensor provides a potential for increased accuracy, which can be realized by conditioning the collector current. Third, the transistors' relatively high output and span can often eliminate the need for amplifiers. □

**References**

1. Akira Ohte and Michiaki Yamagata, "A Precision Silicon Transistor Thermometer," *IEEE Transactions on Instrumentation and Measurement*, Vol. IM-26, Dec. 1977, p. 338.

# Floating current source drives automatized test fixture

by Richard M. Fisher  
ADT Security Systems, Clifton, N. J.

This generator provides a programmable current to drive any load, making the unit ideal for production-line testing. Because the constant-current source floats—that is, is not connected to ground—it can drive loads energized either by positive or by negative potentials of as much as 90 volts.

The output current is resolved to 50 microamperes by the 10-bit input to a digital-to-analog converter (a). The maximum current that can be delivered to the load is slightly more than 50 milliamperes.

As shown, the 10-bit command input is transferred to the d-a device through optocouplers, thus isolating the DAC-10Z from ground paths under virtually all conditions. Note the 5-, +15-, and -15-v potentials for the

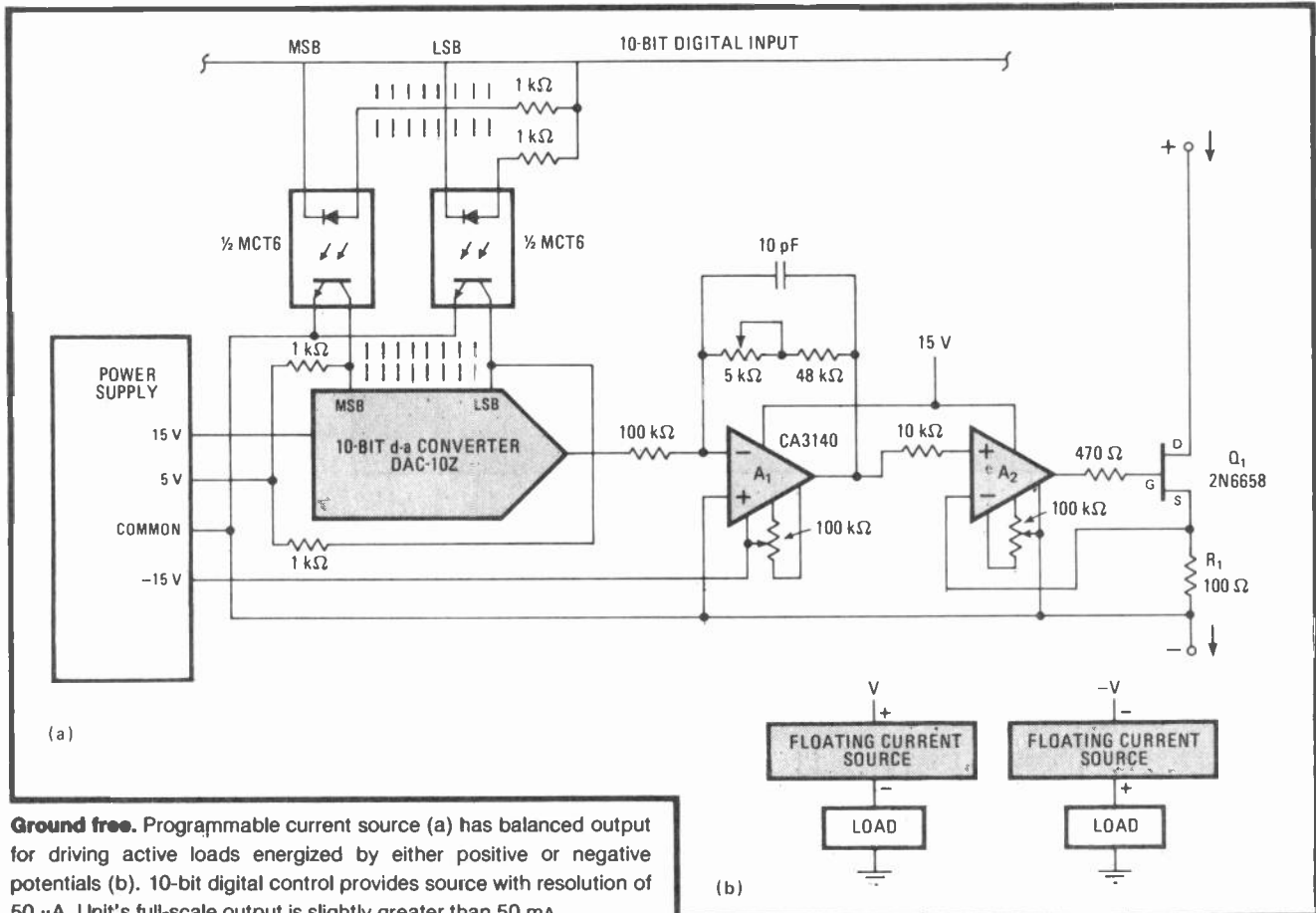
generator are obtained from circuitry associated with the isolated secondary winding of the transformer in the power supply.

Operational amplifier  $A_1$  inverts and scales the output of the d-a converter. The maximum output voltage from the converter is -9.99 volts and results in a full-scale output voltage of 5.115 V from  $A_1$ .  $A_2$ , in conjunction with  $R_1$  (= 100 ohms), thus provides a full-scale output current of 51.150 mA.

The V-groove MOS field-effect transistor,  $Q_1$ , serves as a voltage-to-current converter.  $Q_1$  performs the conversion at high accuracy, because the V-MOS device requires no gate current.

As for using the current source, implementation is easy with any energizing potential. If the device—the load—under test is driven by a positive voltage (b), it is necessary to connect the generator's positive output to the supply voltage. The negative port of the generator is brought to the load.

For negative potentials, the situation is similar, with source's positive terminal being connected to the load as shown. The negative port is connected to the supply voltage. □



**Ground free.** Programmable current source (a) has balanced output for driving active loads energized by either positive or negative potentials (b). 10-bit digital control provides source with resolution of 50  $\mu$ A. Unit's full-scale output is slightly greater than 50 mA.

# Counter banks stagger radar's pulse rate

by Prakash Dandekar  
Tata Electric Companies, Bombay, India

In many radar applications, the instantaneous pulse-repetition frequency must be varied in an orderly fashion to improve the read-out accuracy of the system's moving-target indicator. Considerable circuitry is usually required to achieve the so-called staggered operation, but as shown here, two sets of synchronous counters can be easily connected to control the prf over any range, while providing superior MTI performance.

Normally, designers resort to transmitting pulses at each of three selected periods only, in order to simplify circuitry. Specifically, a popular technique is to transmit a group of three 1-microsecond pulses spaced at 1, 1.1, and 1.2 milliseconds repeatedly. When this is done, however, the filtered output of the MTI is not uniform and so—aside from causing discontinuities in the curve of MTI filter output versus target velocity—this method creates blind velocity points, or ranges over which velocity cannot be determined accurately.

With this circuit, a perfectly smoothed response is achieved by increasing the number of staggered pulses per given time. Thus in this case, a group of 200 pulses,

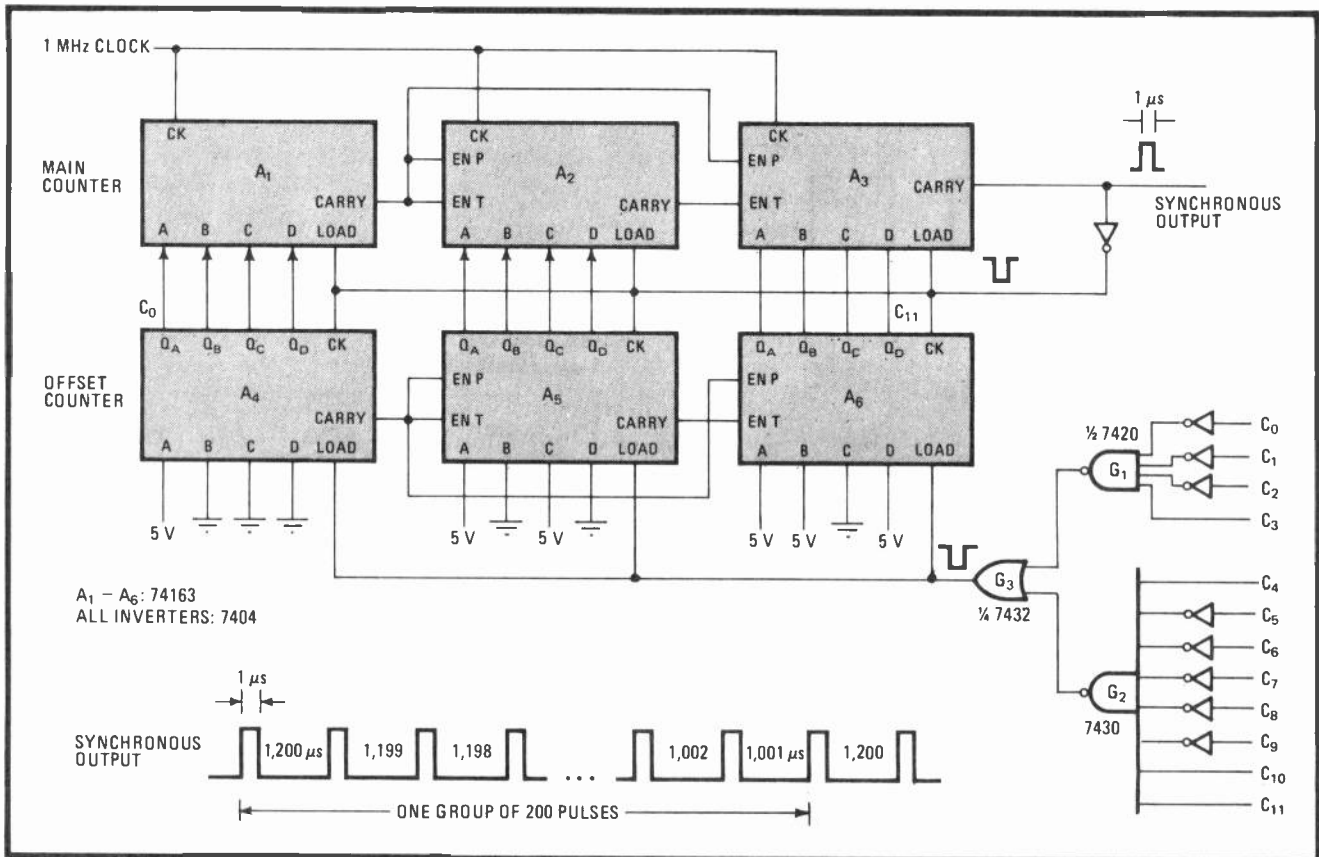
each having a time between pulses of  $(1,201 - M)$  micro-seconds, where  $M$  denotes the  $M$ th pulse of 200, are generated.

As shown, 12-bit counters  $A_1$ - $A_3$ , comprising the main counter chain, advance at a 1-megahertz rate. When the counter reaches its maximum, the carry output of  $A_3$ , serving as the synchronous output, is generated.

The same signal is used to preset the main counter to a 12-bit binary number,  $N$ , which is determined by the state of the offset counter  $A_4$ - $A_6$ . Because  $A_4$ - $A_6$  is also clocked, this unit is incremented with every sync pulse, so during each cycle the main counter is initialized at a higher value than it was previously. Thus the repetition time is reduced by  $1 \mu s$  on each pass.

Note that the offset counter is initialized at a minimum value of  $B51_{16}$  (see A-D inputs of  $A_4$ - $A_6$ ) and advances to a maximum of  $C18_{16}$  ( $= 2^{12}$ ) before it is reset by logic gates  $G_1$ - $G_3$ . Thus, the difference between the counter's maximum and minimum is 200 counts, meaning the instantaneous pulse-repetition rate will vary from 1,200 to 1,001 microseconds. The maximum and minimum values may be easily changed, however, so that any pulse-repetition frequency range can be set.

When the counter reaches 3,096, corresponding to a rate of  $1,001 \mu s$ ,  $A_4$ - $A_6$  is loaded with  $B51_{16}$ . The rate becomes  $1,200 \mu s$  once more, and the cycle is repeated. □



**Smooth staggering.** Two 12-bit counter chains generate a group of repeating  $N$  pulses spaced at  $(1,201 - M) \mu s$ , where  $M$  denotes the  $M$ th pulse of  $N$ , for incremental staggering of the radar-pulse rate. Master clock sets absolute value of maximum pulse-repetition frequency.

# Compact industrial ammeter measures 10-ampere peaks

by Paul Galluzzi  
Beverly, Mass.

A self-contained sample-and-hold amplifier and a digital panel meter make this device small, rugged, and suitable for measuring peak currents in industrial applications. Although not inexpensive (it can be built for about \$65 in small quantities), it is an easy to build, accurate, and reliable peak-reading ammeter.

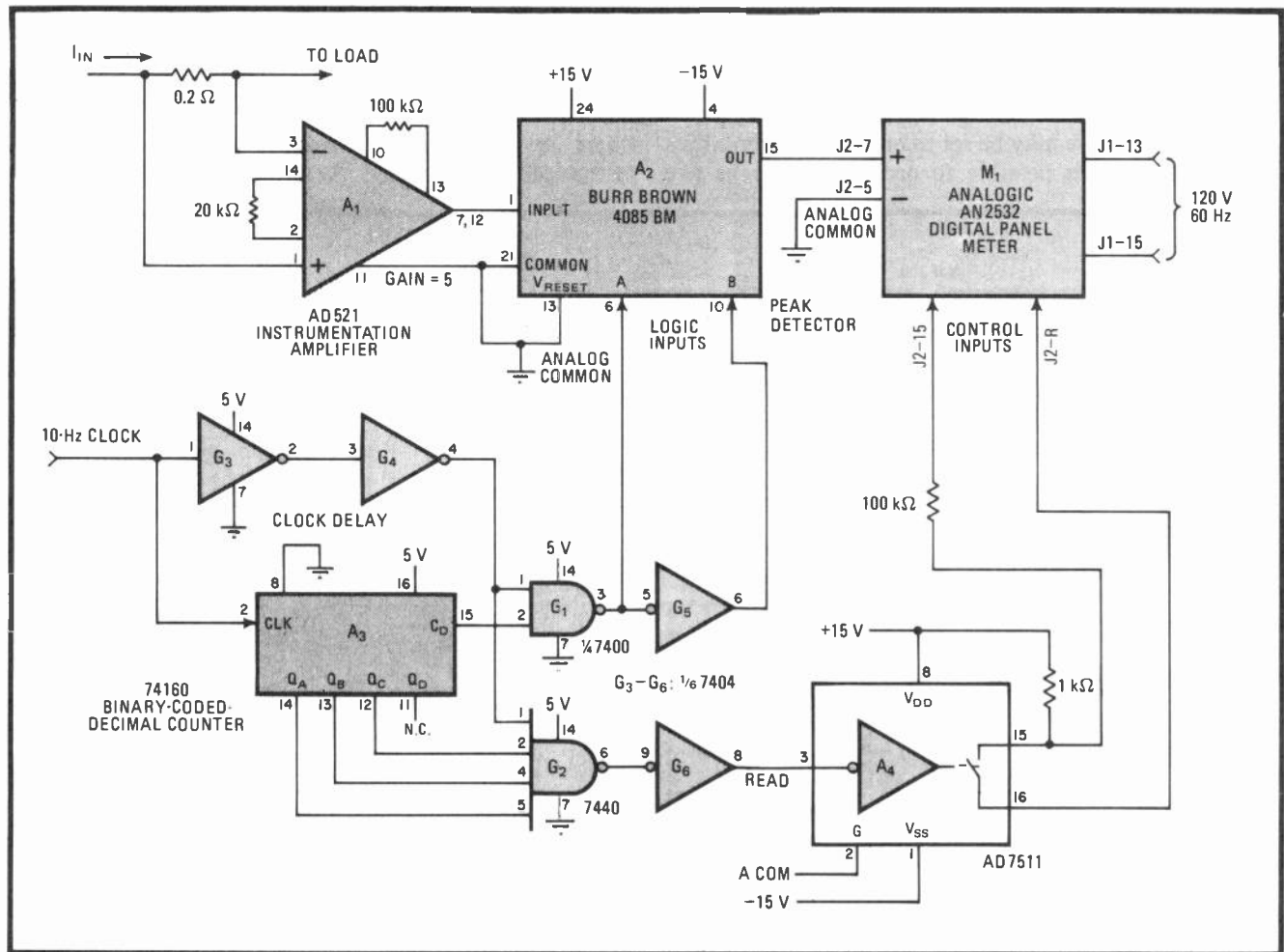
The 0-10-ampere pulses to be measured are converted to a voltage by instrumentation amplifier  $A_1$ , such that

the input to peak detector  $A_2$  swings 1 volt for each ampere at the circuit's input.  $A_2$ 's output voltage then drives digital voltmeter  $M_1$ .

The timing pulses for  $A_2$ 's sampling cycle are derived from a 10-Hz clock signal by gates  $G_1$ - $G_6$  and binary-coded-decimal counter  $A_3$ . The decoded clock pulse introduced at gate  $G_2$ , along with the delayed clock pulse from  $G_3$  and  $G_4$ , form the read pulse for sampling the output of the peak detector for a 50-millisecond interval, and holding that reading for the remainder of the one-second cycle.

During that time, clock inputs A and B reset  $A_2$  to zero. Flutter caused by the 50-ms sampling pulse cannot be detected visually. □

Designer's casebook is a regular feature in *Electronics*. We invite readers to submit original and unpublished circuit ideas and solutions to design problems. Explain briefly but thoroughly the circuit's operating principle and purpose. We'll pay \$50 for each item published.



**Rugged and reliable.** Ammeter using hybrid sample-and-hold amplifier, digital panel meter, and standard logic components is ideally suited for measuring pulses of peak current in hostile environments. Readout is in peak amperes, accurate to 0.1% over  $-25^{\circ}$  to  $85^{\circ}\text{C}$ .

# Current source for I<sup>2</sup>L saves energy

by Stephen H. Nussbaum  
Data/Ware Development Inc., San Diego, Calif.

To capitalize on the low-power advantages of integrated injection logic (I<sup>2</sup>L), a power source that also dissipates relatively small amounts of energy is required. This switched-mode supply provides programmable currents of up to 300 milliamperes at 2.3 volts to boards utilizing I<sup>2</sup>L loads, with an overhead of only a few milliamperes needed for running the circuit.

The voltage-current characteristics of I<sup>2</sup>L devices resemble those of the standard switching diode, whose operation is determined by the amount of driving current available. It is therefore necessary to drive these loads with a current source. Although a single high-value resistor in series with a voltage source would serve to deliver constant current, large amounts of power would be dissipated in the resistor. The difficulty is overcome with this circuit.

Q<sub>1</sub> and its associated components provide a reference current for the complementary-MOS quad analog switch, A<sub>1</sub>, in the reference-resistance subcircuit. The R<sub>2</sub>C<sub>3</sub> combination helps to stabilize the output against changes in input voltages.

A<sub>1</sub>'s switches are wired together such that its equivalent series resistance may be set to one of two values by a control signal. It is possible to order as many as five

current levels with this switch if additional programming inputs are introduced.

A<sub>1</sub>, with the aid of R<sub>3</sub>, serves partly as a current-to-voltage converter, so that low-power oscillator A<sub>2</sub> sees the reference current as a representative voltage at its inverting input. This potential will cause Q<sub>2</sub> to switch on periodically. R<sub>4</sub> provides positive feedback for hysteresis, thus controlling the rate at which A<sub>2</sub> and Q<sub>2</sub> are switched—16 kilohertz, in this case. The 10 to 30 millivolts of hysteresis also appears at the output, but this poses no problem with I<sup>2</sup>L loads.

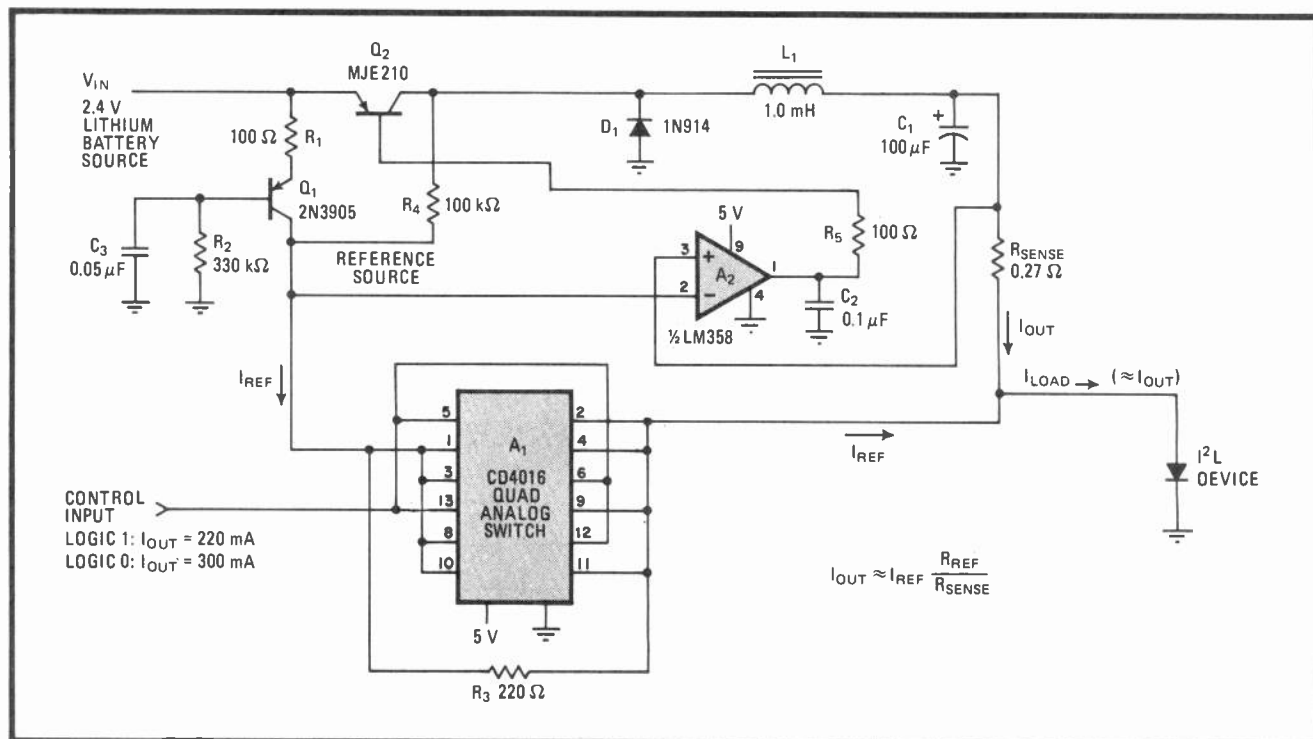
L<sub>1</sub> and C<sub>1</sub> comprise the switcher's required storage elements, acting to release energy to the load through R<sub>sense</sub> when Q<sub>2</sub> is off. R<sub>sense</sub> is part of a feedback network used to set I<sub>out</sub>.

Because the reference current and the output current at summed at the output node, A<sub>2</sub>'s input sees only the difference of these currents scaled to a voltage by their respective resistors, R<sub>sense</sub> and R<sub>ref</sub>. Thus the output current is set solely by the feedback loop. As a consequence of this arrangement,  $I_{out} \approx R_{ref} I_{ref} / R_{sense}$ . The efficiency of the supply is maximized by using a lower value of R<sub>sense</sub>, a faster op amp for A<sub>2</sub>, and a storage inductor (L<sub>1</sub>) with as little dc resistance as possible.

With R<sub>3</sub> = 220 ohms and with I<sub>ref</sub> = 0.60 mA, I<sub>out</sub> = 220 mA if a logic 1 is applied to the control input. I<sub>out</sub> = 300 mA for a logic 0. These values can be changed by suitable selection of I<sub>ref</sub>, of course, but R<sub>3</sub> may also be varied. Note that:

$$R_{ref} = [(r_{on}/n)R_3] / [(r_{on}/n) + R_3]$$

where n = number of switches and r<sub>on</sub> = on-state resistance of one switch in A<sub>1</sub>, typically 600 Ω. □



**Injecting current.** Switching source delivers constant current to members of low-power I<sup>2</sup>L logic family without wasting much power. Small reference current, C-MOS switches, and low-power oscillator contribute to circuit efficiency. Two-level current source, which generates up to 300 milliamperes at 2.3 volts, can provide one of five current values if additional programming inputs are introduced at switch A<sub>1</sub>.



# High-speed generator pulses ECL loads

by Andrew M. Hudor Jr.  
Department of Physics, University of Arizona, Tucson

Serving the needs of designers and technicians who work with high-speed digital circuits, this inexpensive two-chip pulse generator is invaluable in trouble-shooting emitter-coupled logic. Besides generating signals having frequency and duty cycles that are adjustable to its complementary outputs, the versatile generator also provides two ports at which pulses with a constant 50% duty cycle are available.

One section of a 10116 ECL line receiver,  $A_1$ , is used as an RC oscillator<sup>1</sup> whose period is determined by the potentiometer  $P_1$  and the capacitor selected by the frequency-range switch. With the values shown, the oscillator frequency can be varied from a few hundred hertz to more than 50 megahertz. The output of the oscillator is then buffered and squared up by a Schmitt trigger,  $A_2$ , which is the second section of the line receiver.

$A_2$ 's output toggles both sections of a 10131 dual-D flip-flop,  $A_3$  and  $A_4$ .  $A_3$  provides for a 50% duty cycle output, while  $A_4$  and the remaining section of the receiver,  $A_5$ , form an adjustable one-shot multivibrator. Here,  $A_5$  serves as a second Schmitt trigger.

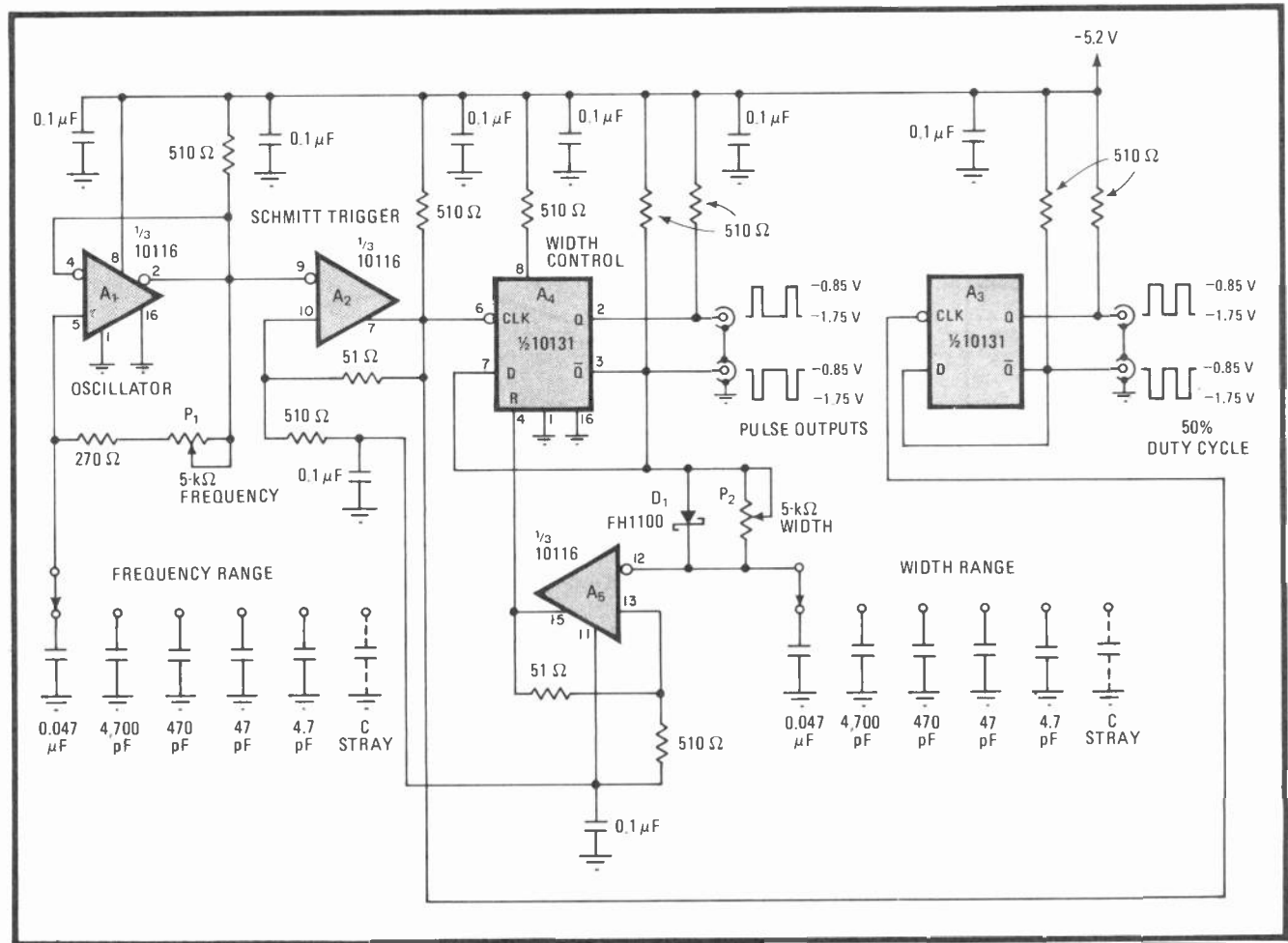
The Q output of  $A_4$  is fed to the input of the Schmitt trigger through an RC integrator formed by  $P_2$  and the capacitor selected by the width-range switch. When Q toggles low, the input to the  $A_5$  trigger slowly rises as the capacitor charges. When the trigger level is reached, the Schmitt trigger's output goes high, resetting  $A_3$  and  $A_4$ , and the process is repeated.

The time it takes for the integrator to reach the trigger level defines the pulse width. With the values shown, widths from 15 nanoseconds to 10 milliseconds can be selected. Upon resetting of the flip flops, Schottky diode  $D_1$  allows the capacitor to discharge rapidly. The width control allows adjustment of the duty cycle from nearly zero to 50%. For applications where a duty cycle greater than 50% is required, the complementary output should be used.

If desired, a buffer can be easily added at  $A_3$  and/or  $A_4$  in order to drive 50-ohm lines directly. □

### References

1. William A. Palm, "ECL IC oscillates from 10 to 50 MHz," *Electronics*, Circuit Designer's Casebook 14D, p. 109.



**Speedy.** Line receiver and dual flip-flop generate high-frequency pulse trains for emitter-coupled logic. Signals to 50 MHz having widths that are adjustable from 15 ns to 10 ms appear at generator's complementary outputs. Circuit also provides output at duty cycle of 50%.

# Dual light-emitting diode synthesizes polychromatic light

by Leonard M. Smithline  
Ithaca, N. Y.

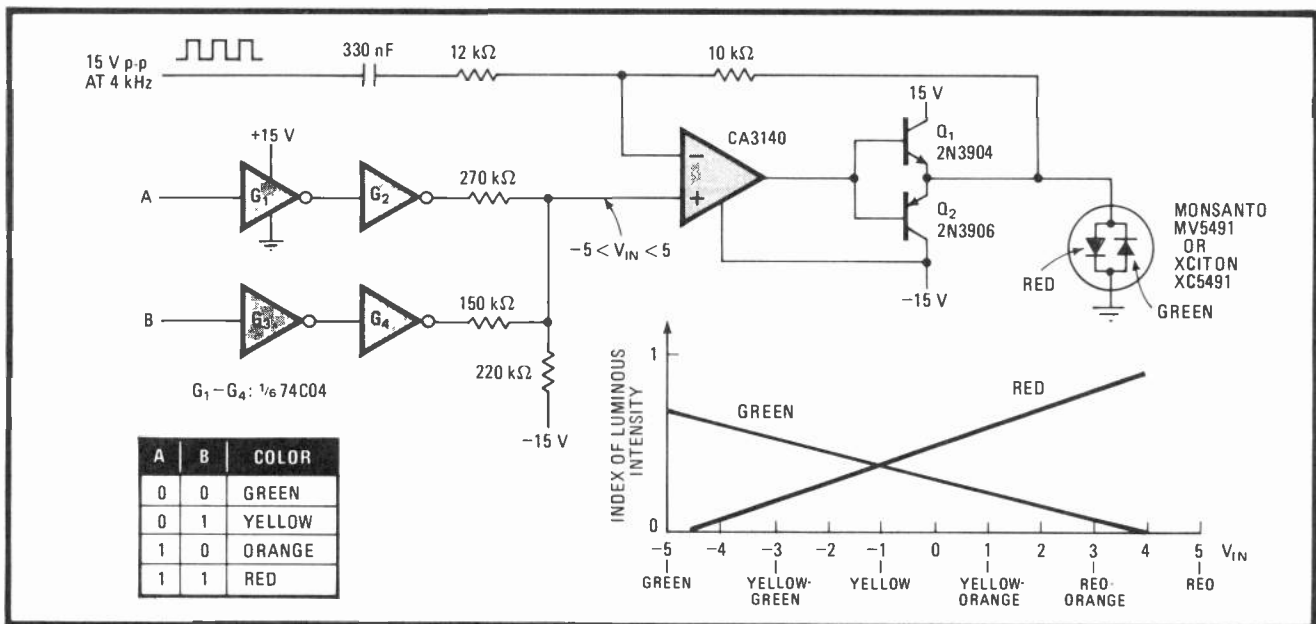
By controlling the drive to each element of a dual red or green light-emitting diode so as to mix the red and green lights in varying quantities, this digital circuit synthesizes four distinct hues from the two primary optical colors. With a slight modification, it can also make the diode vary gradually from green through yellow and orange to red in response to an analog input.

The LED used here may be either the Monsanto

MV5491 or the Xciton XC5491 (Fig. 1). The diodes inside either device are wired back to back and so cannot be driven simultaneously. They therefore need a multiplexer circuit to drive them at a fast enough rate for them to appear to be on simultaneously. Here a 4-kilohertz square wave provides the desired chopping action. The relative proportions of drive to the green or red LED are controlled by adding a dc bias to the square-wave drive at the noninverting input of the CA3140 operational amplifier, as shown.

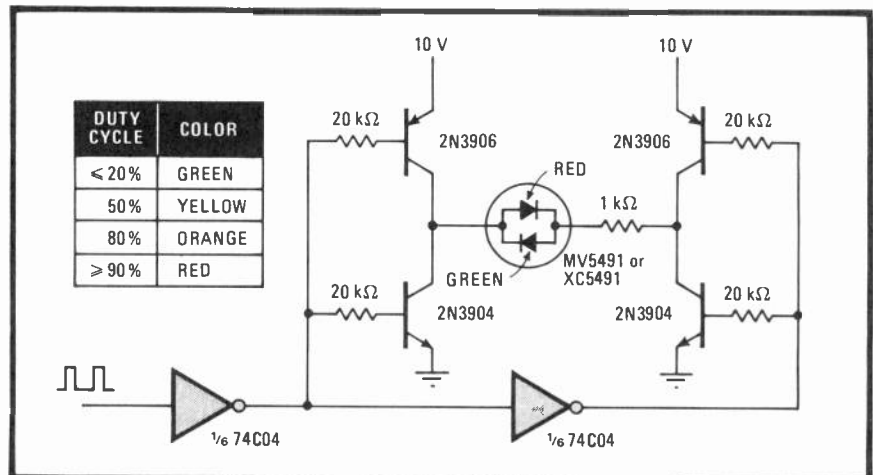
Thus, the states of A and B determine the color perceived by the mixing process, as seen in the table. Alternatively, an analog signal can be applied to the noninverting input of the op amp, whereupon the circuit response will be as shown in the graph.

For a thorough mixing of colors, the primary light sources should not only be viewed simultaneously (as



**1. Thoughts of hue.** Multiplexer's 4-kHz square wave, suitably offset with dc bias controlled by states of A and B, provides desired drive to each element of green/red photodiode for deriving perceived four-color output. Alternatively, analog signal may be applied to noninverting input of op amp for effecting gradual change in color, from green through red. Circuit response in either case is given in table and graph.

**2. Color cycle.** Generation of yellow and orange from red and green light may also be achieved through control of duty cycle of pulses driving light-emitting diodes. Pulse-width modulation requires only single supply.



# Maximum-length shift register generates white noise

by Henrique Sarmiento Malvar  
 Department of Electrical Engineering, University of Brasilia, Brazil

Using a circuit based on a maximum length sequence generator,<sup>1</sup> this simple unit inexpensively provides a source of white noise over a range of up to 200 kHz. It is far superior to generators that use a reverse-biased base-to-emitter transistor junction, which provides quasi-white noise over a very limited portion of the spectrum. Using two integrated circuits comprising a 25-stage shift register, it can be built for less than \$6.

A<sub>1</sub> and A<sub>2</sub> form the n-stage shift register driven by clock G<sub>1</sub>-G<sub>2</sub>, with A<sub>1</sub> an 18-stage device and A<sub>2</sub> being eight stages in length. A<sub>1</sub> and A<sub>2</sub> are driven simultaneously but out of phase with respect to each other.

The output from stage 7 of A<sub>2</sub> and the last stage of A<sub>1</sub> is applied to G<sub>3</sub> in the feedback loop G<sub>3</sub>-G<sub>4</sub>, so that a register sequence length of 2<sup>n-1</sup> clock periods is obtained.

Note that G<sub>4</sub> provides signal inversion, so that on power up (the all-zero output state of A<sub>1</sub> and A<sub>2</sub>), the noise generator will be self-starting.

It can be shown that the spectrum of the signal at the output of A<sub>2</sub> will contain several discrete frequencies, separated by  $f_c/(2^{n-1})$ , where  $f_c$  is the clock frequency, in this case 200 kHz. Because  $n$  is large, the separations between the discrete frequencies become so close (here, it will be 0.006 Hz with a sequence period of 150 seconds), that the spectrum may be considered continuous. So although the noise is pseudorandom because of the method used to produce it, the difference in the spectral properties of the noise as compared with the ideal is minimal.

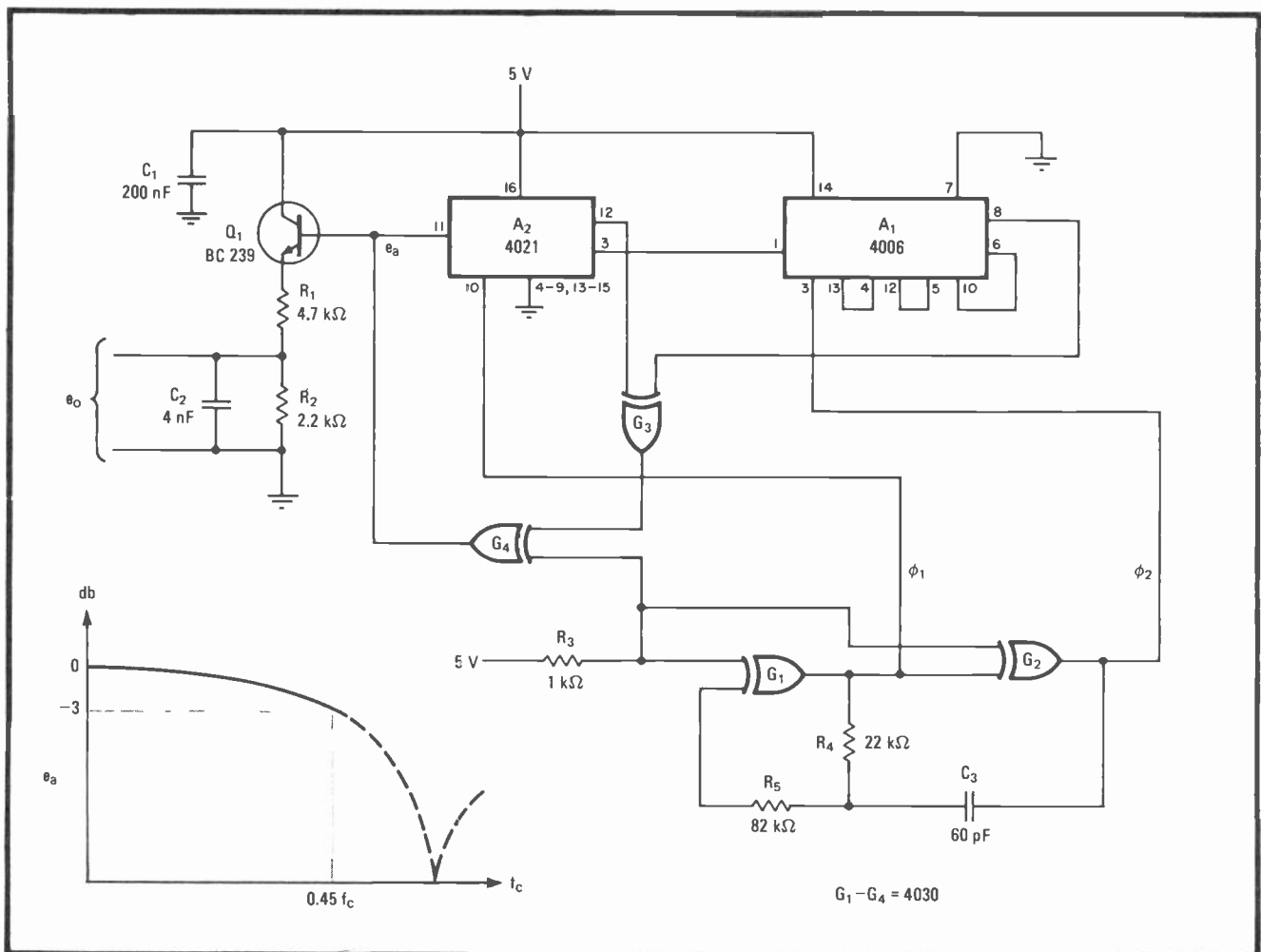
As for the amplitude of the output envelope, it will vary with frequency as  $(x^{-1} \sin x)^2$ , where  $x = f/f_c$ . Here, the -3-dB point will occur at  $f = 0.45 f_c$ , as shown in the curve at the lower left of the figure.

Q<sub>1</sub> serves as a buffer. The network R<sub>1</sub>R<sub>2</sub>C<sub>2</sub> is a low-pass filter that has been added for an application requiring noise to be confined (bandlimited) to the audio frequencies. Its -3 dB point occurs at 25 kHz. □

### References

1. I. H. Witten and P. H. C. Madams, "The Chatterbox-2," *Wireless World*, Jan. 1979, p. 77.

**Spectrum spread.** 25-stage shift register creates closely spaced signals of discrete frequency for generating pseudorandom white noise over wide range. Spectral response of source (bottom left) is flat from dc to 0.45  $f_c$ , where  $f_c$  is the clock frequency.



## 12-hour clock tells time out loud

by William S. Wagner  
Northern Kentucky University, Highland Heights, Kentucky

Combining a program written for the 6800 microprocessor and a four-chip interface, this system expresses clock time as an equivalent sequence of audio tones. Like the audio voltmeter previously described,<sup>1</sup> it allows determination of time when the clock face cannot be seen.

In this method, the exact time—expressed as *xxyy*, where *xx* denotes hours and *yy* denotes minutes—is converted to a series of tones of short duration (dits) to represent quantities extending from 1 to 9. The quantity 0 is represented by a single tone (dah) of a relatively long duration. A long pause separates hours from minutes. Thus, for example, a time of 02:41 would yield an audio output of dah, pause, dit-dit, long pause, dit-dit-dit, pause, dit.

Three frequency dividers ( $A_1$ – $A_3$ ), two gates ( $G_1$ – $G_2$ ), and a few passive components comprise the clock-to-microprocessor interface. The actual clock signal is derived from the highly accurate 60-Hz power line.

$A_1$  and  $A_2$ , each a divide-by-10 chip, and  $A_3$ , wired as a divide-by-12 device, produce a pulse with a 20-second period from the line input. This pulse serves as the

6800's hardware interrupt, which initiates the program and the generation of time markers exactly three times every minute. Other intervals can be selected by appropriate action of the divider ratio.

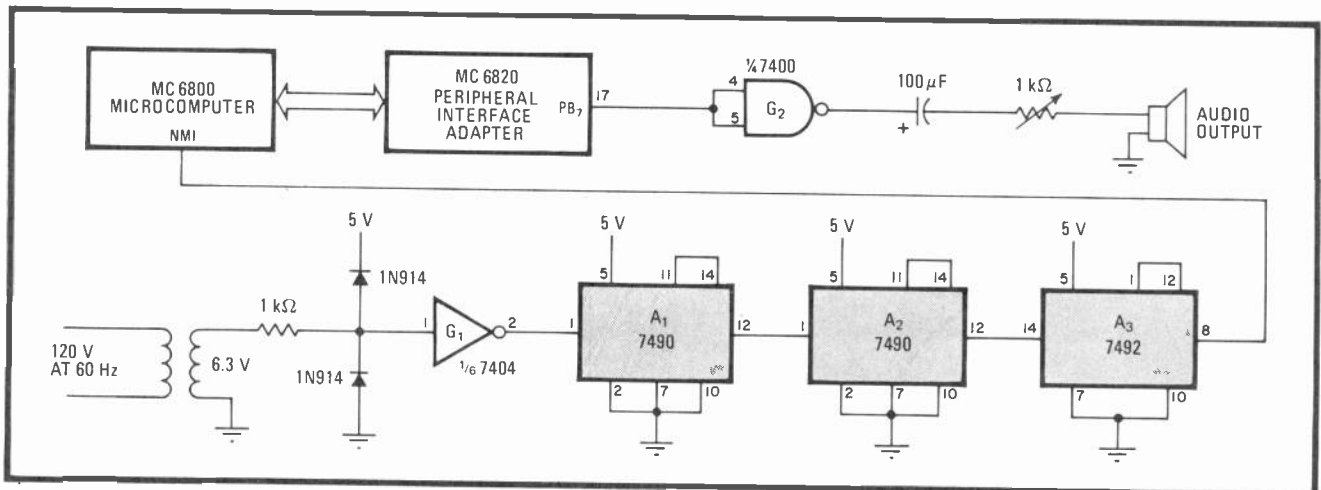
The clock is set to any desired starting time with software, where the initial hour is stored at program address 0002, minutes are stored in 0001, and seconds in 0000. Although seconds are not made audible, they are required in the program for updating the minutes unit once every three sampling periods.

When an interrupt is received, the initial time, expressed in hours and minutes, is converted to a set of four 4-bit binary-coded words in steps 0023–00A0 and is checked to determine if each word represents a 0 or an integer from 1 to 9. At this point the program determines whether short or long tones are to be transmitted. The instructions commencing at 0053 set the time interval between the processing of each individual word and between hours and minutes.

After the clock routine (01A0–01D6) increments the minutes and hours units as necessary, the dit and dah subroutines (at 0100 and 0120, respectively) are initiated. The program then halts and waits for a system interrupt, whereupon the process repeats. □

### References

1. William S. Wagner, "Digital voltmeter has audible output," *Electronics*, March 29, 1979, p. 120.



**Tick tones.** Microprocessor-based chronometer periodically derives audible time markers. System generates a pulse code, with numbers 1 to 9 represented by string of short tones and a zero represented by a long tone. Long pause between digits separates hours from minutes.

## 6800 PROGRAM FOR AUDIO CLOCK

| Address | Mnemonic  | Address | Mnemonic  | Address | Mnemonic  |
|---------|-----------|---------|-----------|---------|-----------|
| 0000    | (STORAGE) | 0073    | PULA      | 0134    | ASLA      |
| 0001    | "         | 0074    | ASLA      | 0135    | ASLA      |
| 0002    | "         | 0075    | PSHA      | 0136    | ASLA      |
| 0003    | LDX FF04  | 0076    | BCS 17    | 0137    | ASLA      |
| 0006    | STX 8802  | 0078    | BRA 1A    | 0138    | PSHA      |
| 0009    | WAI       | 007A    | LDA 08    | 0139    | JMP 0053  |
| 000A    | BRA FD    | 007C    | JSR 0100  | 0140    | LDX 03FF  |
| 0020    | STX 0015  | 007F    | BRA E8    | 0143    | ORAB 7F   |
| 0023    | LDS 00C0  | 0081    | LDA 04    | 0145    | STAB 8002 |
| 0026    | PSHA      | 0083    | JSR 0100  | 0148    | LDAA 25   |
| 0027    | ANDA 70   | 0086    | BRA E6    | 014A    | DECA      |
| 0029    | BGT 03    | 0088    | LDA 02    | 014B    | BNE FD    |
| 002B    | JMP 0120  | 008A    | JSR 0100  | 014D    | DEX       |
| 002E    | PULA      | 008D    | BRA E4    | 014E    | BEQ 03    |
| 002F    | ASLA      | 008F    | LDA 01    | 0150    | COMB      |
| 0030    | ASLA      | 0091    | JSR 0100  | 0151    | BRA F0    |
| 0031    | PSHA      | 0094    | LDAA 02   | 0153    | PULA      |
| 0032    | BCS 0C    | 0096    | LDX FFFF  | 0154    | ASLA      |
| 0034    | PULA      | 0099    | DEX       | 0155    | ASLA      |
| 0035    | ASLA      | 009A    | BNE FD    | 0156    | ASLA      |
| 0036    | PSHA      | 009C    | DECA      | 0157    | ASLA      |
| 0037    | BCS 0E    | 009D    | BNE F7    | 0158    | PSHA      |
| 0039    | PULA      | 009F    | PULA      | 0159    | JMP 0094  |
| 003A    | ASLA      | 00A0    | LDS 10    | 01A0    | LDX 0000  |
| 003B    | PSHA      | 00A2    | LDX 15    | 01A3    | LDAB 03   |
| 003C    | BCS 10    | 00A4    | RTS       | 01A5    | SEC       |
| 003E    | BRA 13    | 00A5    | JMP 0140  | 01A6    | BSR 0E    |
| 0040    | LDA 04    | 00FD    | JMP 01A0  | 01A8    | LDAB 60   |
| 0042    | JSR 0100  | 0100    | PSHA      | 01AA    | BSR 0A    |
| 0045    | BRA ED    | 0101    | LDX 00FF  | 01AC    | LDAB 13   |
| 0047    | LDA 02    | 0104    | ORAB 7F   | 01AE    | BSR 06    |
| 0049    | JSR 0100  | 0106    | STA 8002  | 01B0    | BSR 15    |
| 004C    | BRA EB    | 0109    | LDAA 25   | 01B2    | BSR 13    |
| 004E    | LDA 01    | 010B    | DECA      | 01B4    | DEX       |
| 0050    | JSR 0100  | 010C    | BNE FD    | 01B5    | RTI       |
| 0053    | LDAA 01   | 010E    | DEX       | 01B6    | LDAA 00,X |
| 0055    | LDX FFFF  | 010F    | BEQ 03    | 01B8    | ADCA 00   |
| 0058    | DEX       | 0111    | COMB      | 01BA    | DAA       |
| 0059    | BNE FD    | 0112    | BRA F0    | 01BB    | CBA       |
| 005B    | DECA      | 0114    | LDX 1FFF  | 01BC    | BCS 01    |
| 005C    | BNE F7    | 0117    | DEX       | 01BE    | CLRA      |
| 005E    | PULA      | 0118    | BNE FD    | 01BF    | STAA 00,X |
| 005F    | PSHA      | 011A    | PULA      | 01C1    | INX       |
| 0060    | ANDA F0   | 011B    | DECA      | 01C2    | TPA       |
| 0062    | BEQ 41    | 011C    | BNE E2    | 01C3    | EORA 01   |
| 0064    | PULA      | 011E    | RTS       | 01C5    | TAP       |
| 0065    | ASLA      | 0120    | LDX 03FF  | 01C6    | RTS       |
| 0066    | PSHA      | 0123    | ORAB 7F   | 01C7    | DEX       |
| 0067    | BCS 11    | 0125    | STAB 8002 | 01C8    | STS 10    |
| 0069    | PULA      | 0128    | LDAA 25   | 01CA    | LDAA 02   |
| 006A    | ASLA      | 012A    | DECA      | 01CC    | BEQ 05    |
| 006B    | PSHA      | 012B    | BNE FD    | 01CE    | LDAA 00,X |
| 006C    | BCS 13    | 012D    | DEX       | 01D0    | JMP 0020  |
| 006E    | PULA      | 012E    | BEQ 03    | 01D3    | INC 0002  |
| 006F    | ASLA      | 0130    | COMB      | 01D6    | BRA F6    |
| 0070    | PSHA      | 0131    | BRA F0    |         |           |
| 0071    | BCS 15    | 0133    | PULA      |         |           |

# Cupless anemometer has diode wind-sensor

by J. P. Scoseria  
Montevideo, Uruguay

Working well as a differential thermometer, this simple circuit can also be used to find wind speed by detecting the difference in junction voltage between two forward-biased diodes. Here, one junction is heated to a fixed temperature, and the other's temperature-dependent junction potential is made to vary with the cooling effect of the wind. Being totally solid-state, the unit eliminates all mechanical difficulties. The unit can also function as a psychrometer, or humidity indicator, if the heated junction is wetted down instead.

Diode  $D_1$  and a resistor are situated within the confines of a small one-of-a-kind aluminum enclosure built for this circuit.  $D_1$  is heated by the power dissipated by the resistor. The enclosure maintains a constant temperature throughout, independent of environmental changes, as in an oven. Although the absolute temperature reached by the diode junction is of little importance in this circuit, it will be a direct function of the power supplied to the block, the area of the block available for heat transfer, and its heat transfer coefficient.

The same general considerations exist for the stream-temperature sensor,  $D_2$ , which is placed in a similar

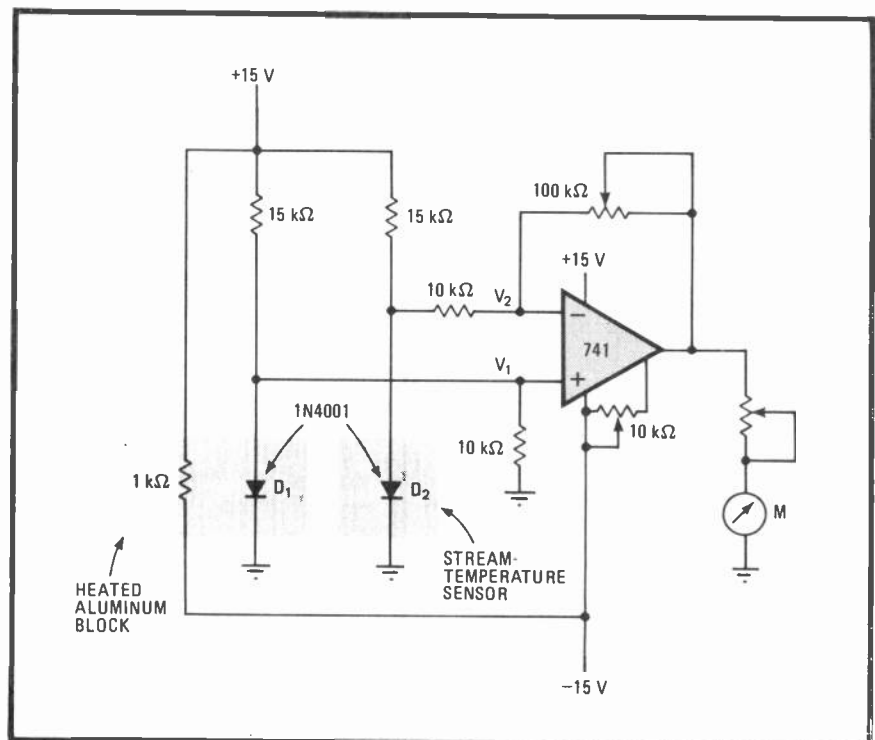
aluminum block to reduce temperature variations due to changes in wind speed (settling time  $\approx 2$  minutes). Here, however, the power supplied to the block is small, being about 1 milliwatt to activate  $D_2$ , and heat variations reach the junction from the outside.

Generally, the output from the 741 op amp is  $e_o = K(V_1 - V_2)$ , where  $K$  is a constant and  $V_1$  and  $V_2$  are functions of the temperature associated respectively with the heated block sensor and the wind speed. The voltages across both  $D_1$  and  $D_2$  drop by 2.5 millivolt for each degree Celsius rise, and so  $V_{d1} \approx 0.7 - 2.5(10^{-3})T_f$ , and  $V_{d2} \approx 0.7 - 2.5(10^{-3})T_w$ , where temperature  $T_f$  corresponds to  $V_1$  and  $T_w$  to  $V_2$ . As a result,  $e_o = K(-2.5)(10^{-3})(T_f - T_w)$ , and so the output of the op amp will be proportional to the temperature difference. The current that flows through ammeter  $M$  will thus vary linearly with temperature.

The relation between the wind's cooling factor and temperature is nonlinear, however, and because the initial zero-wind current in meter  $M$  is a function of the block temperature (and thus block size), and because the sensor temperature, and  $D_1$  and  $D_2$  are not driven from true constant-current sources, the calibration will not be uniform for any two units.

Although it would be ideal to have access to a wind tunnel for calibration, good results can be obtained with the aid of an automobile. Placing the sensor on the auto's antenna, with the meter set at maximum for zero wind speed, the unit can be calibrated satisfactorily on a windless day by noting  $M$ 's output as a function of the car's speed.  $\square$

**Ceaseless wind.** Temperature difference between heat oven surrounding diode junction  $D_1$  and stream sensor  $D_2$ , whose junction temperature varies with wind speed, is reflected as a change in current at  $M$ . Unit can be satisfactorily calibrated with auto's speedometer on a calm day.



# Solar-powered regulator charges batteries efficiently

by G. J. Millard  
*Volcanological Observatory, Rabaul, Papua New Guinea*

For use with solar panels, this simple and efficient regulator circuit provides an energy-saving solution to charging batteries of the lead-acid type commonly found in automobiles. Not considering the cost of the solar cells, assumed to be at hand for use in other projects, the regulator alone is under \$10.

Unlike many other shunt regulators that divert current into a resistor when the battery is fully charged, this circuit opens the charging path so that the resistors can be eliminated. This method is extremely advantageous when solar panels are used, for large resistors would otherwise be required to dissipate the high power levels typically encountered.

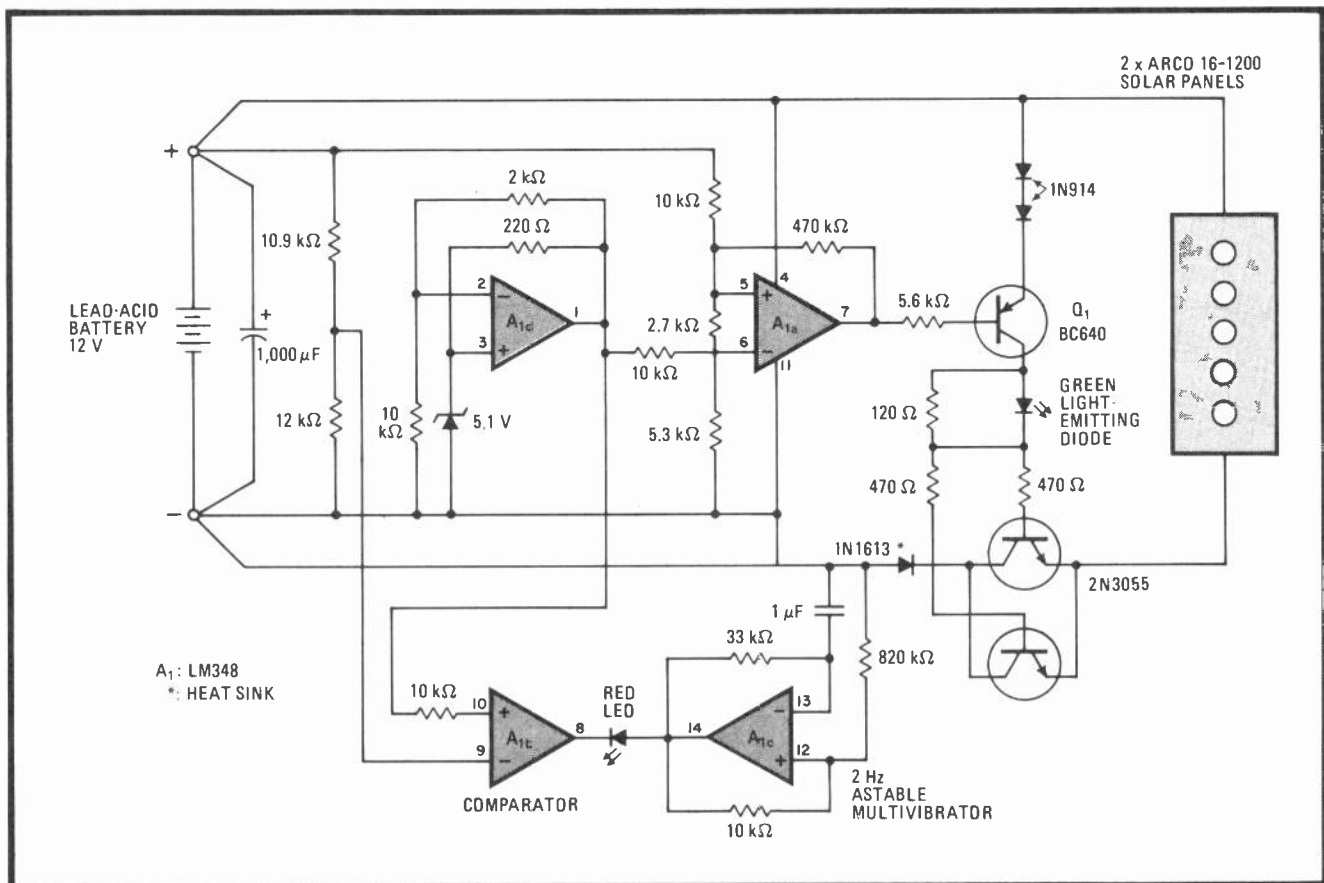
When the battery voltage,  $e_o$ , is below 13.5 volts

(normally the open-circuit potential of a 12-v battery), transistors  $Q_1$ ,  $Q_2$ , and  $Q_3$  turn on and charging current flows from the solar panels as required. The active green light-emitting diode indicates the battery is taking charge.

As  $e_o$  approaches the open-circuit voltage, op amp  $A_{1a}$  switches  $Q_1$ – $Q_3$  off. This condition is maintained until such time as the battery voltage drops to 13.2 v, whereupon the charge cycle repeats.

If the battery voltage should continue to fall from 13.2 to approximately 11.4 v, indicating a flat battery,  $A_{1b}$  switches low, causing a red LED to flash at a rate determined by the astable multivibrator  $A_{1c}$ , in this case oscillating at a frequency of 2 hertz.  $A_{1d}$  provides a reference of 6 v to maintain the switching points at the 11.4- and the 13.2-v levels.

The circuit will handle currents to 3 amperes. To draw larger currents, it is necessary to increase the base currents of  $Q_2$  and  $Q_3$  so that these transistors will remain in saturation during the charging periods. □



**Light charge.** Regulator for handling currents produced by solar panels charges lead-acid batteries without wasting excessive power. Circuit cuts off current to battery when its open-circuit voltage is greater than 13.5 v, eliminating need for dissipating power in resistors. Green LED indicates battery is charging. Flashing red LED indicates battery is flat (battery voltage below 11.4 v) and refuses to take charge.

# Tunable equalizers set amplitude and delay

by P. V. Ananda Mohan  
*Indian Telephone Industries Ltd., Bangalore, India*

Equalizing networks providing constant amplitude and/or delay over a wide range of frequencies are easily realized by utilizing the feed-forward and feed-back techniques of these tunable circuits. More specifically, a parallel-T arrangement of resistors and capacitors as shown in (a) makes it possible to select the equalizing delay with a single potentiometer. Equalization and selection of amplitude can be attained by adding a single operational amplifier stage of variable gain (b) to the basic circuit. If the parallel-T is made tunable (c), the equalizer's center frequency can be adjusted with very little difficulty.

The circuit that is illustrated in (a) is so configured that its transfer function is that of an all-pass network

having a roll-off dependent on circuit Q, or:

$$\frac{e_{out}}{e_{in}} = \frac{s^2 - s(\omega_o/Q) + \omega_o^2}{s^2 + s(\omega_o/Q) + \omega_o^2}$$

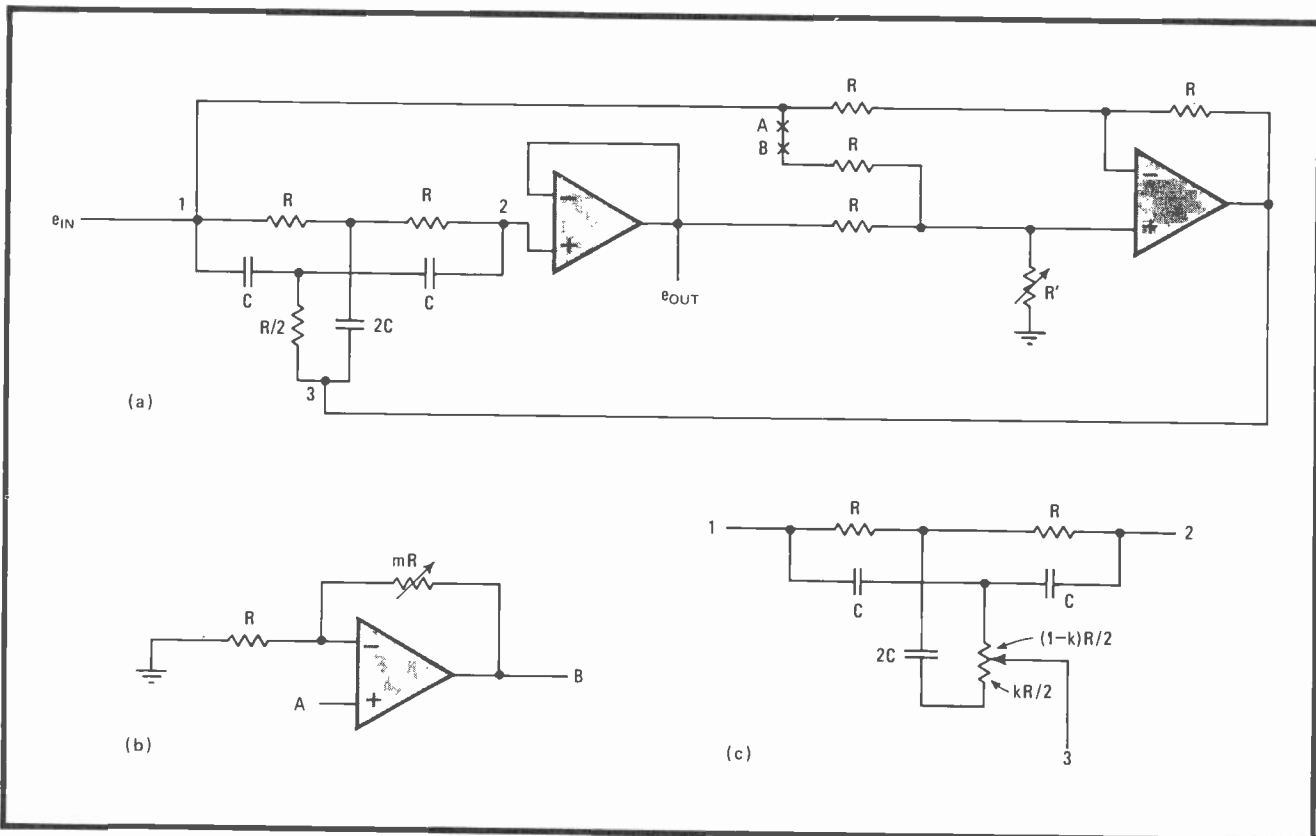
where  $\omega_o = 1/RC$  and  $Q = 1/4 + R'/2R$ . The amount of delay is selected with potentiometer  $R'$ , as the amount of phase shift introduced by the RC network is:

$$\theta = \pi - 2 \tan^{-1} [\omega \omega_o / Q(\omega_o^2 - \omega^2)]$$

where  $\theta$  will vary little about  $\omega_o$ , provided  $\omega$  is sufficiently removed from  $\omega_o$ .

If the op amp circuit (b) is placed between ports A and B in (a), the equalizer's gain at mid-frequency  $\omega_o$  becomes  $G = (2R'm)/R - 1$ , and so the gain may be set by varying  $R'$  and/or  $m$ . Note that the delay is still a function of  $R'$  and that  $G$  will not vary significantly over a wide range of frequencies.

The center frequency of the equalizer may be adjusted if the parallel-T network shown in (c) replaces the network in (a) enclosed between points 1 and 3. In this case,  $\omega_o = \omega_o/(1 - K^2)^{1/2}$  and  $Q = (1/4 + R/2R)/(1 - K^2)^{1/2}$ , where  $K$  is the fraction of the total resistance of  $P_2$ , as measured from its lower end. □



**Selection.** Parallel-T RC network simplifies design of tunable two-stage equalizer network. Delay is set with only a single control element,  $R'$  (a). Amplitude equalization or adjustment in network's center frequency is attained by adding op amp (b) and tunable RC (c), respectively.



# Switched load checks power supply response

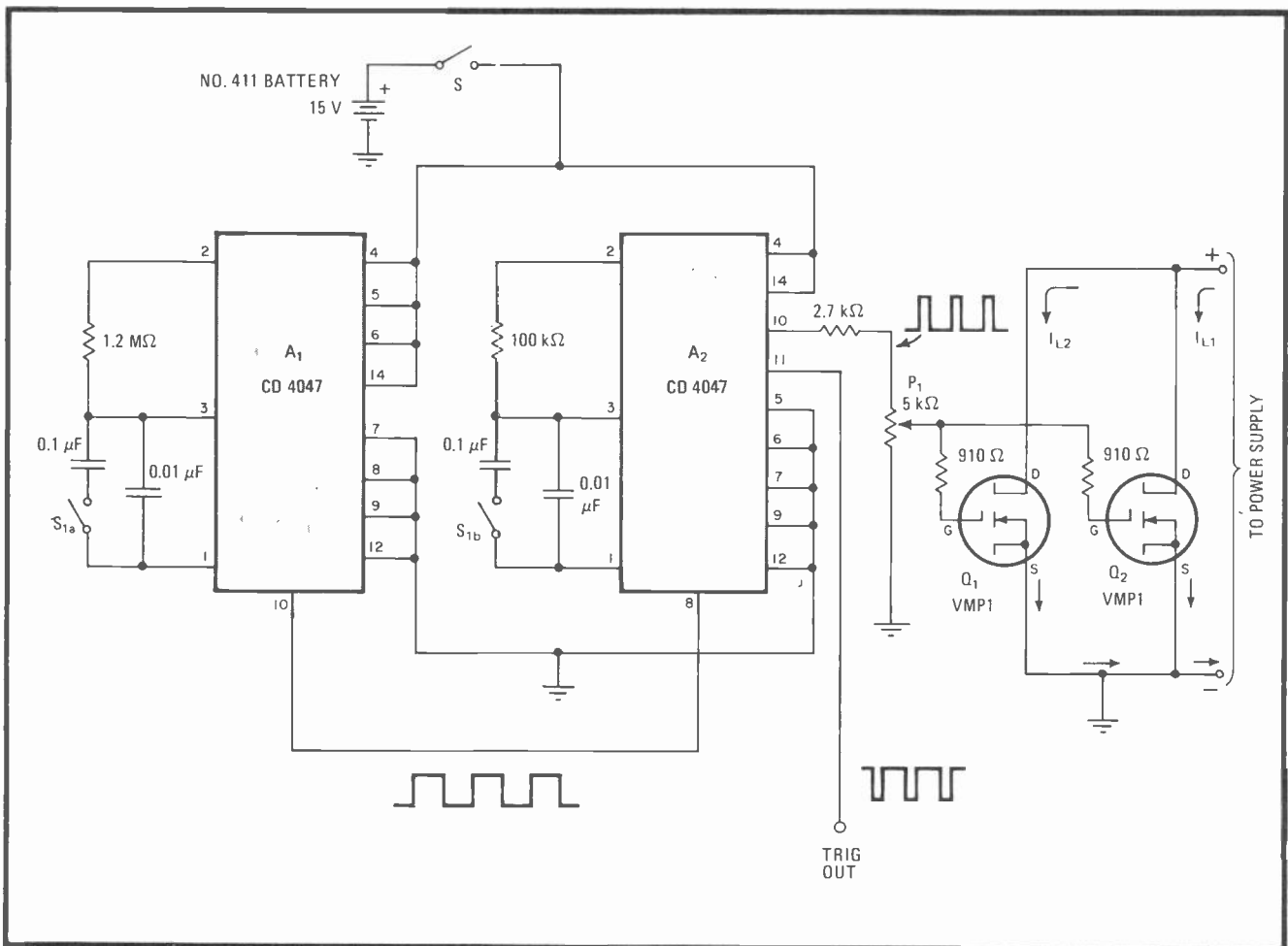
by William M. Polivka  
 Department of Engineering, California Institute of Technology, Pasadena

The transient response of a power supply is easily checked with the aid of this pulse loader, which periodically places a short circuit across the supply's output in order to simulate sudden load changes. Using complementary-MOS integrated circuits and V-groove MOS power transistors, the compact, self-contained unit runs on a battery, so that it presents no ground-loop problems to the supply under test.

As shown in the circuit for the pulsed load, astable

multivibrator A<sub>1</sub> and one-shot A<sub>2</sub> set respectively the frequency and the width of the pulses that switch on load transistors Q<sub>1</sub> and Q<sub>2</sub>. S<sub>1</sub> selects either of two combinations of frequency and width—in this case, 2 hertz at 25 milliseconds or 20 Hz at 2.5 ms. Note that a low duty cycle is required to reduce heat dissipation in Q<sub>1</sub> and Q<sub>2</sub>. A trigger signal for driving an oscilloscope or other instrument to observe the supply's response appears at pin 11 of A<sub>2</sub>.

Potentiometer P<sub>1</sub> sets the point at which Q<sub>1</sub> and Q<sub>2</sub> fire, so that the magnitude of the pulsed supply current passing through the load transistors can be selected from zero to the maximum capability of the V-MOS devices. Each field-effect transistor handles 2 amperes at 12 volts, values that derate to 400 milliamperes at 60 v. Moreover, an increase in supply loading may be attained simply by adding transistors in shunt at the output of the unit, as required. □



**Load dynamics.** Low-cost tester, with aid of scope, finds transient response of power supply by ordering periodic increase in supply current to simulate load changes. A<sub>1</sub> and A<sub>2</sub> set frequency and width of switching waveform. Q<sub>1</sub>–Q<sub>2</sub> sink current proportional to setting of P<sub>1</sub>.

# Pseudorandom generator has programmable sequence length

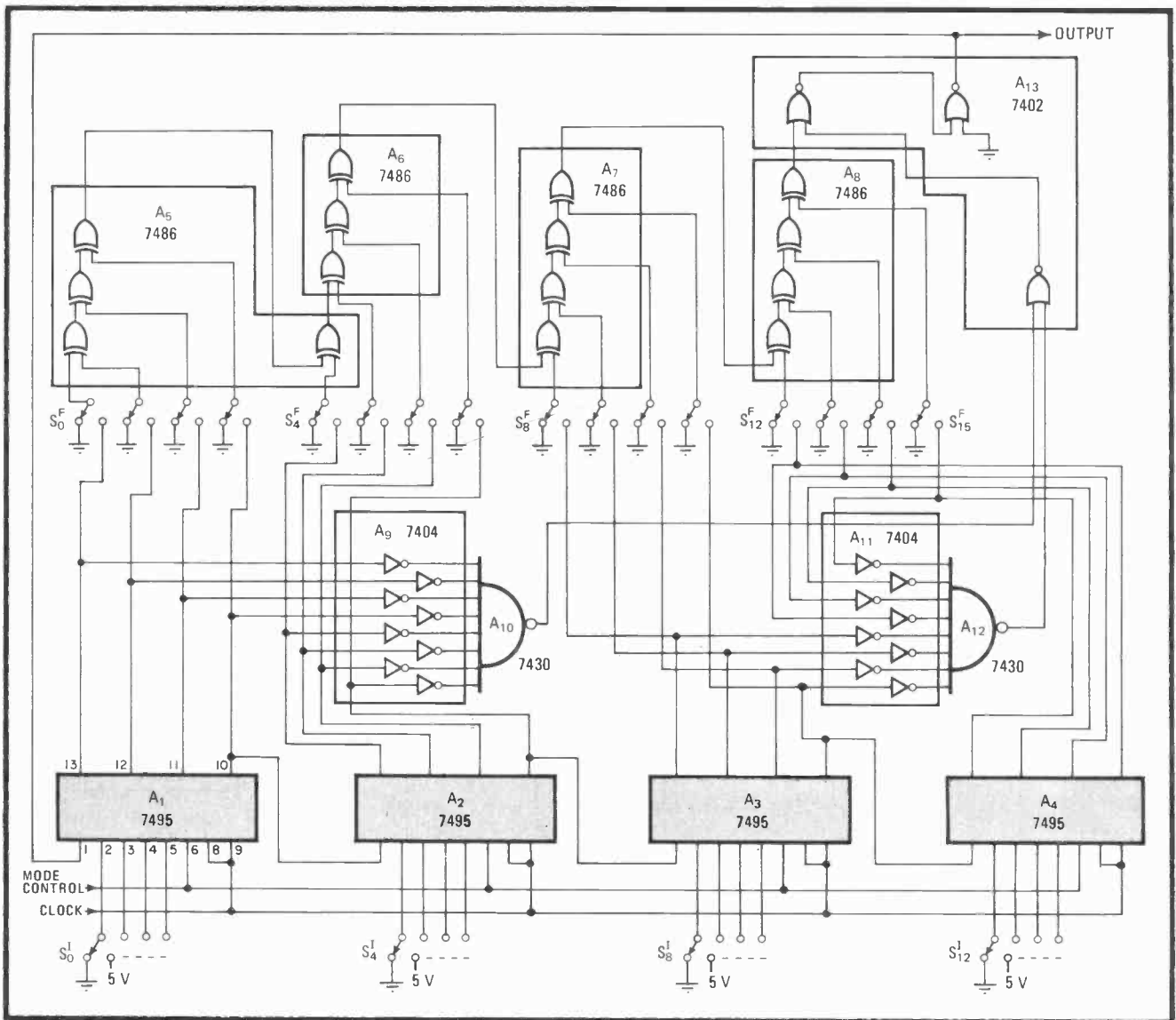
by Ajit Pal  
*Indian Statistical Institute, Calcutta, India*

Providing a pseudorandom binary sequence of order  $i$  in the range of 2 to 16, this generator will find many uses in fault-detection and speech-scrambling equipment. Any sequence having a maximum length of  $2^{16} - 1$  can be generated. If the sequence can be selected electronically, instead of mechanically by means of a manual-switching arrangement as shown, the unit will be extremely useful in automatic-test environments.

The pseudo-random sequence is produced with the aid of a 16-bit shift register and appropriate circuitry for

providing a feedback signal to the register's first stage.  $A_1-A_4$  are the 4-bit registers that comprise the 16-bit stage, wired to shift bits from left to right on every system clock.  $A_5-A_7$ , connected at the register's outputs, and  $A_8$  are exclusive-OR gates used to generate the feedback signal, which is determined by switches  $S_i^F$ . The switch positions are set in accordance with the primitive polynomial of the binary sequence to be generated. Note that the settings of the switches in the figure correspond to a sequence of length  $2^{15} - 1$ , or an equivalent primitive polynomial of  $x^{15} + x + 1$ .

$A_9-A_{13}$  detect the all-zero condition of  $A_1-A_4$  and ensure that the register will not be locked in that state on power-up or during normal operation. The mode control input otherwise allows  $A_1-A_4$  to be set at any point in the sequence as determined by the  $S_i^I$  switches. □



**Selection.** Switches  $S_i^F$  and  $A_5-A_8$  derive suitable feedback signal so that shift register  $A_1-A_4$  can generate a pseudorandom binary sequence of selectable length.  $A_9-A_{13}$  detect register's all-zero state and prevent register lock-up by generating logic 1 bit to  $A_1-A_4$  input during power-initialization period. Switches  $S_i^I$  initialize registers at any point in a sequence that may extend to  $2^{16} - 1$  bits.

# Reducing the dropout voltage of programmable regulators

by Carlo Venditti  
The Charles Stark Draper Laboratory Inc., Cambridge, Mass.

A programmable regulator's dropout voltage—the minimum allowable potential between its input ( $V_{in}$ ) and output ( $V_{out}$ )—can be improved by adding an external output stage and negative feedback. The resulting regulated output voltage ( $E_{out}$ ) not only approaches  $V_{in}$  more closely, but the current-drive capability is also better, thanks to the outboard power-transistor stage.

The design technique used to achieve this improved performance is described here for Fairchild's popular  $\mu A78MG$  regulator, which has a nominal dropout voltage of 3.0 volts. As shown in the figure, a change in  $V_{in}$  causes  $V_{out}$  to increase temporarily. The corresponding increase at  $E_{out}$  that is applied to the control input of the  $\mu A78$  forces  $V_{out}$  lower, toward the value it had initially. If the resistor network  $R_1$  to  $R_3$  is optimized,  $E_{out}$  can be brought to within 1.5 V of  $V_{in}$ .

Consider the case where the output voltage  $E_{out}$  is to be kept at 12.5 v  $\pm$  50 mV for a  $V_{in}$  ranging from 14 to 15.5 v. When  $V_{in}$  is at 14,  $V_{out}$  cannot be above 11, owing to the dropout voltage of the regulator. Thus with an output voltage of 12.5, the voltage at the base of  $Q_1$  is 13.1 (0.6 v higher).

Now  $R_1$  can be selected to pass a given value of

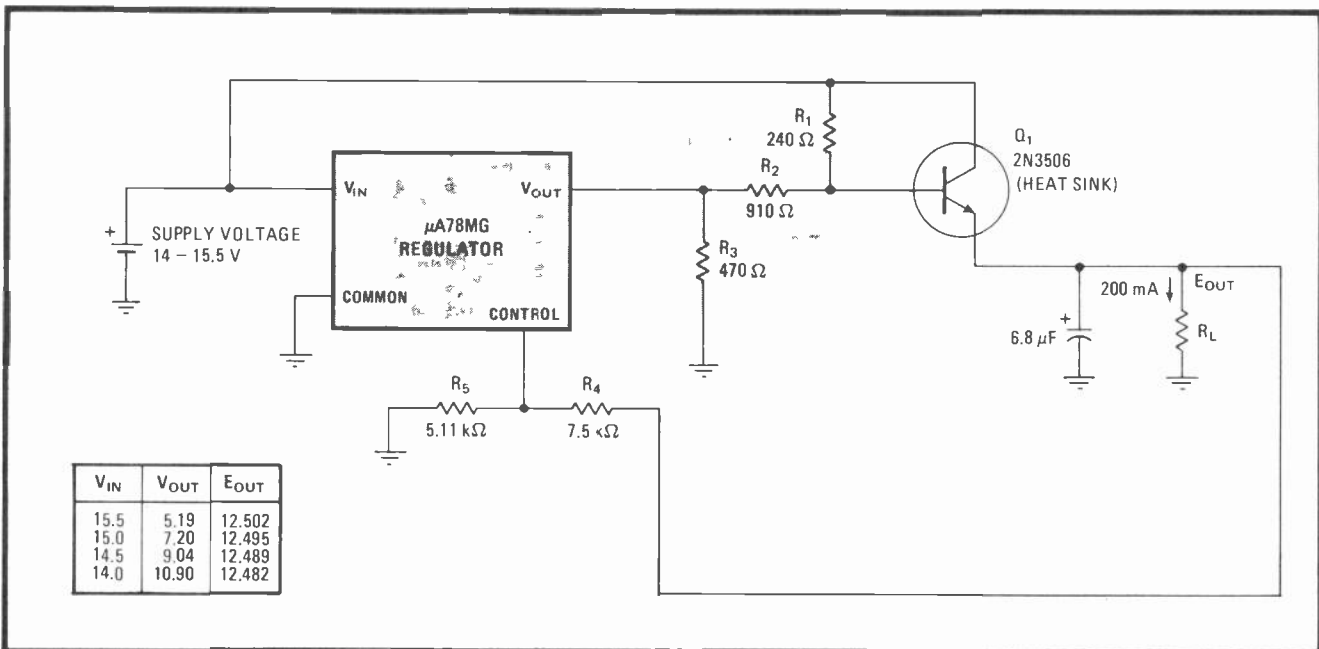
transistor base current,  $I_b$ , of say, 1.2 milliamperes, and a current through  $R_2$  of perhaps twice this value (2.4 mA), plus a small amount to account for variations in  $I_b$ . Thus  $R_1 = (14 - 13.1)v / 3.75 \text{ mA} = 240 \Omega$ , and  $R_2 = (13.1 - 11)v / 2.4 \text{ mA} = 910 \Omega$ .

The next condition to be addressed is the case where  $V_{in}$  assumes a value of 15.5 v, so that  $R_3$  may be determined. Because  $V_{out}$  ultimately decreases with an increase in  $V_{in}$ ,  $V_{out}$  should be made to move to its minimum value so that the maximum dynamic range of the circuit is realized. From the data sheet of the  $\mu A78$ ,  $V_{out(min)} = 5.0 \text{ v}$ . Note that changes in  $V_{out}$  are scaled by the  $R_2/R_1$  ratio, and these resistors ensure that a change of  $910/240 = 3.8 \text{ v}$  occurs for every 1-v increase in  $V_{in}$ .

Thus the current through  $R_2$  at this time will be  $(13.1 - 5.0)/910 = 8.8 \text{ mA}$ , and assuming the minimum (quiescent) current of the regulator is 2 mA, the current through  $R_3$  is  $(8.8 + 2.0) = 10.8 \text{ mA}$ . Therefore  $R_3 = 5/10.8 = 470 \Omega$ . The table summarizes the actual dynamic performance of the regulator. Note the apparent dropout voltage of the regulator has been reduced to  $14.0 - 12.482 \approx 1.5 \text{ v}$  when  $V_{in}$  is at its minimum.

The junction temperature of the on-chip power transistor is  $T_j = \theta_{JA}P_T + T_A$ , where  $\theta_{JA}$  is the junction to ambient thermal resistance (80  $\Omega$ , see data sheets) and  $T_A$  is the ambient temperature. Thus, assuming  $T_A = 25^\circ\text{C}$ ,  $T_j = 35^\circ\text{C}$ , well below the  $125^\circ\text{C}$  thermal shutdown temperature of the  $\mu A78$ .

A check on the chip's temperature will confirm that the regulator's thermal shutdown point has not been reached. The temperature reaches a maximum when  $V_{in} = 14.0$ . At this voltage, the regulator's output current is



**Closer.** Outboard power transistor stage, and resistor pad  $R_1$ – $R_3$  set  $E_{out}$  to within a few volts of  $V_{in}$ , so that  $(E_{out} - V_{in})$  is below  $\mu A78$ 's dropout value.  $Q_1$  also provides increased current capacity. Table summarizes dynamic range attained for example using technique discussed in text.

20.8 mA, and the output power is  $20.8 (14 - 11) = 62.5$  mW. The quiescent current is 4 mA (see data sheets), and the quiescent power drain becomes  $4(14 \text{ v}) = 56$  mW. As a consequence of these figures, the total output

becomes  $P_T = 118$  mW.



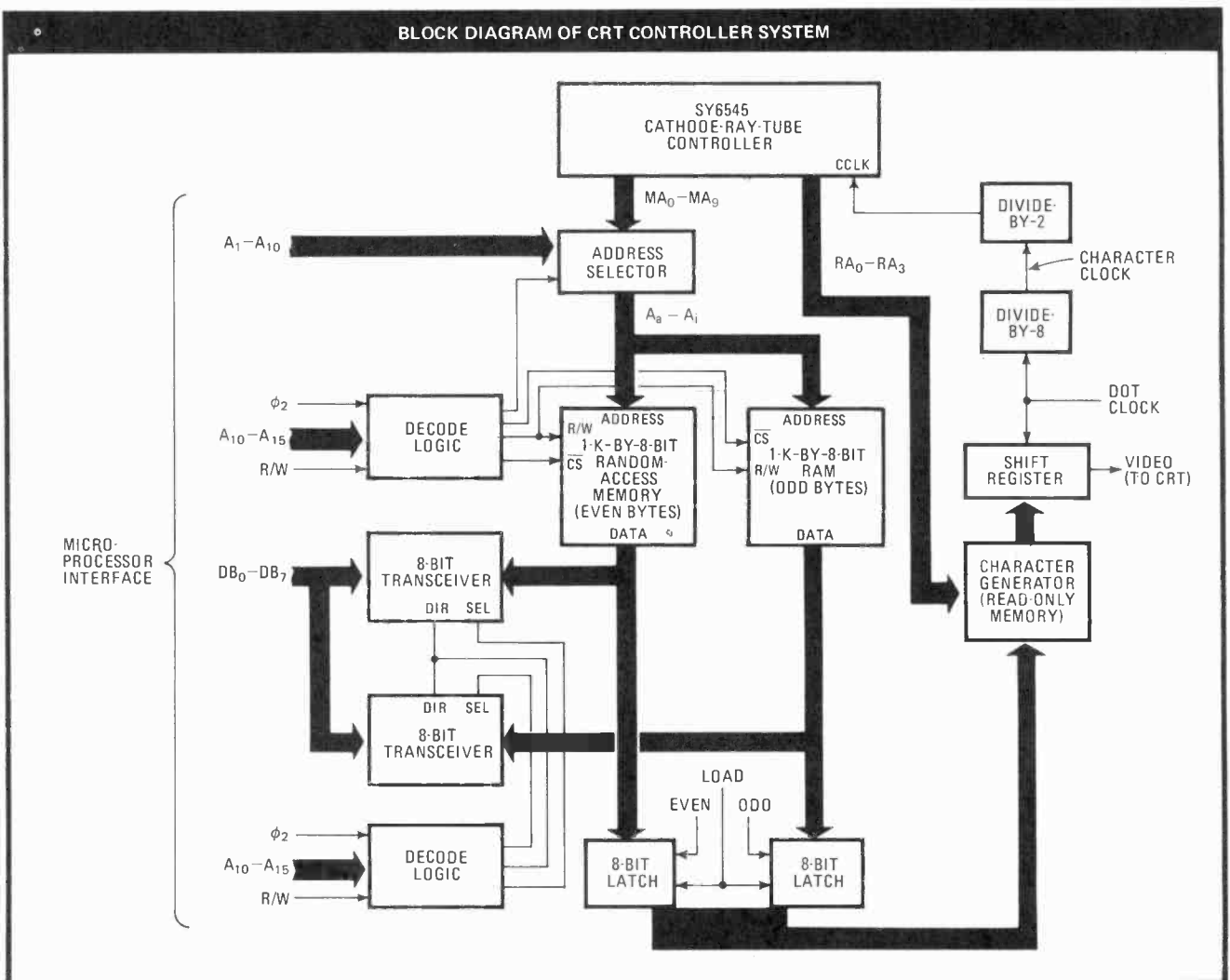
## Doubling the character rate handled by CRT controllers

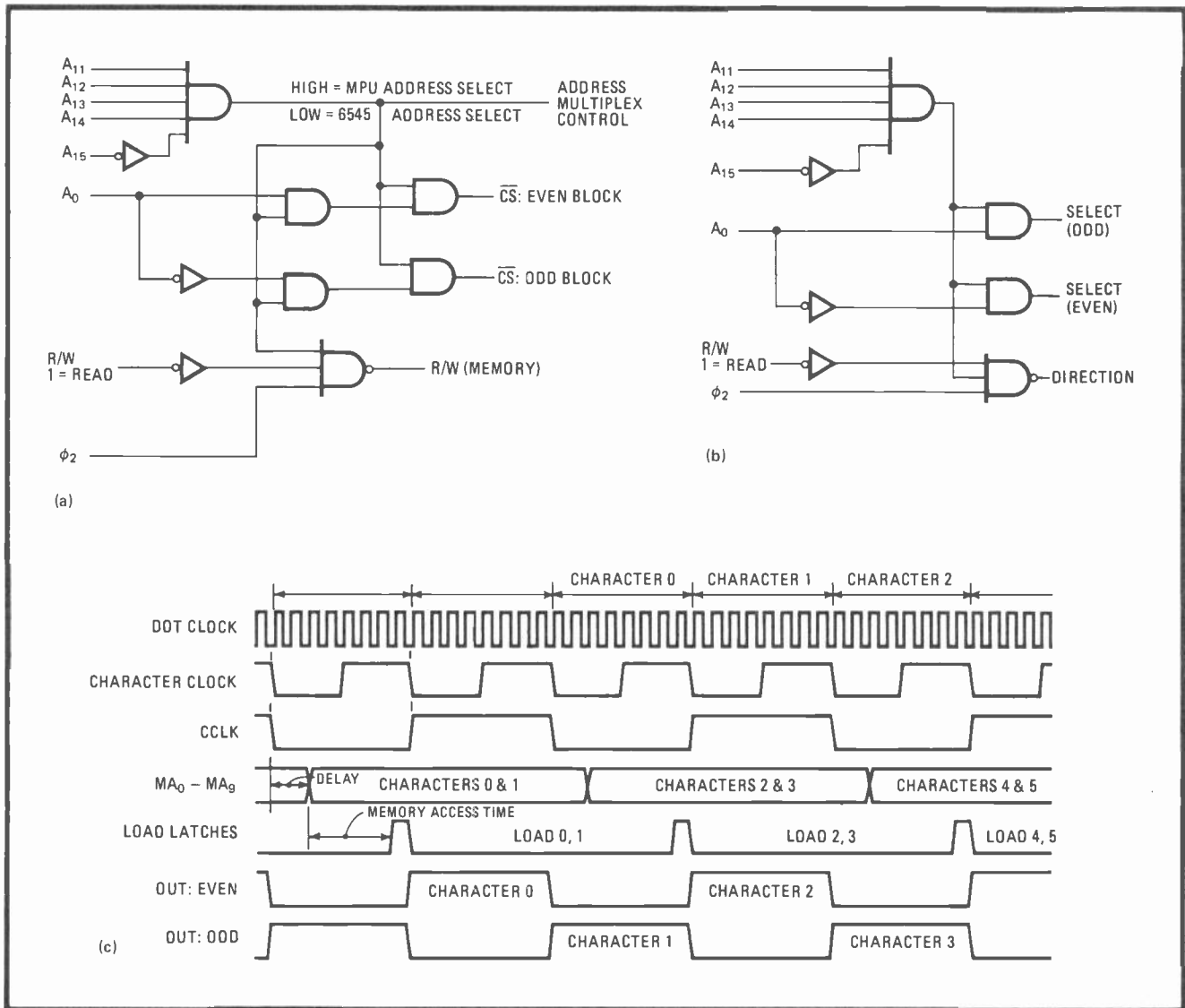
by Conrad J. Boisvert  
Synertek Inc., Santa Clara, Calif.

Controllers that transfer display information from a microprocessor to a cathode-ray tube can be made to operate at effective character rates in excess of the normal maximum value. Specifically, by accessing 2 bytes of data per fetch and implementing logic to apply the characters to the display one at a time, the effective character rate can be doubled. The technique is applied here to the Synertek SY6545 chip, although the principle can be extended to most of the popular controllers.

The system architecture necessary for doubling the effective character rate is shown in the block diagram. The memory scheme gives the microprocessor overriding priority in selecting the video-display memory. Other configurations could be implemented, but this is the simplest and focuses attention on the more significant aspects of the method. Also note that the video-display memory is assumed to be 8 bits wide (ASCII coding requires only 7 bits) and that 8 horizontal bits define one character.

A key circuit point is that the SY6545 address lines,  $MA_0$ - $MA_9$ , are routed through the address selector block to memory addresses  $A_a$ - $A_i$  of both the odd and even memory blocks. In this way, as the SY6545 steps through its states, the two memories are accessed simultaneously. Memory addresses  $A_1$ - $A_{10}$ , on the other hand, are routed through  $A_a$ - $A_i$ , with the memory address line,  $A_0$ , selecting either the even or odd memory, but not





**Hardware.** Logic for increasing character rate handled by CRT controllers uses readily available gates. Circuitry for memory control (a) and data transceivers (b) adapts system for two-character fetch and display. Timing diagram (c) details system operation.

both. Thus, a dual-port memory is configured, accessing the data memory as a 1-K-by-16-bit block, and the microprocessor as a 2-K-by-8-bit block.

The logic required to control the memory is shown in Fig. 2a. The chip-select lines  $\overline{CS}$  must always be low if the microprocessor is not addressing memory.  $A_{11}$ - $A_{15}$  correspond to the decoded memory-map location of the addressed memory, with  $A_0$  used to select either the odd or the even block. Under these conditions, the address selector (Fig. 1) is activated. The R/W signal may then be applied to the memories.

Similar logic for controlling the data-bus transceivers is shown in Fig. 2b. Here, the transceiver's odd or even select outputs are energized after inputs  $A_{11}$ - $A_{15}$  have settled. The transceivers are deactivated and the microprocessor data bus isolated from the video display if  $A_{11}$ - $A_{15}$  do not match the decode pattern.

The timing diagram clarifies the system operation (Fig. 2c). Note the character clock, which normally drives the SY6545's CCLK pin directly, is divided by 2 because two characters must be fetched per cycle.

The horizontal registers associated with the character total, the display, the sync position, and the sync width will be affected by the aforementioned modification, and steps must be taken to alter the way in which they are programmed. In any case, the value programmed must be half the value that is normally entered. For example, to achieve a display of 80 horizontal characters per line, the number 40 must be programmed into the horizontal display register.

Finally, external logic must be incorporated into the system to achieve a cursor output signal that will be active for each character handled. This function may be implemented with three NAND gates.

The SY6545's cursor output is first combined at one NAND gate with the even latch-select signal of Fig. 2b and the negated output of the PAO port signal of the SY6520 peripheral interface (not shown). PAO, the cursor signal, and the odd latch-select signal are joined at the input of the third (two-input) NAND, whose output represents the modified cursor signal. □

# Low-cost fiber-optic link handles 20-megabit/s data rates

by A. Podell and J. Sanfilippo  
*Loral Electronic Systems, Yonkers, N. Y.*

Providing an inexpensive link for the transmission and detection of digital signals over short distances, this fiber-optic system handles data rates in excess of 20 megabits per second. The system, which can be built for about \$90, including cable, processes all types of data—a continuous-wave clock waveform, a burst of N clock cycles, handshaking signals, or a non-return-to-zero (NRZ) stream.

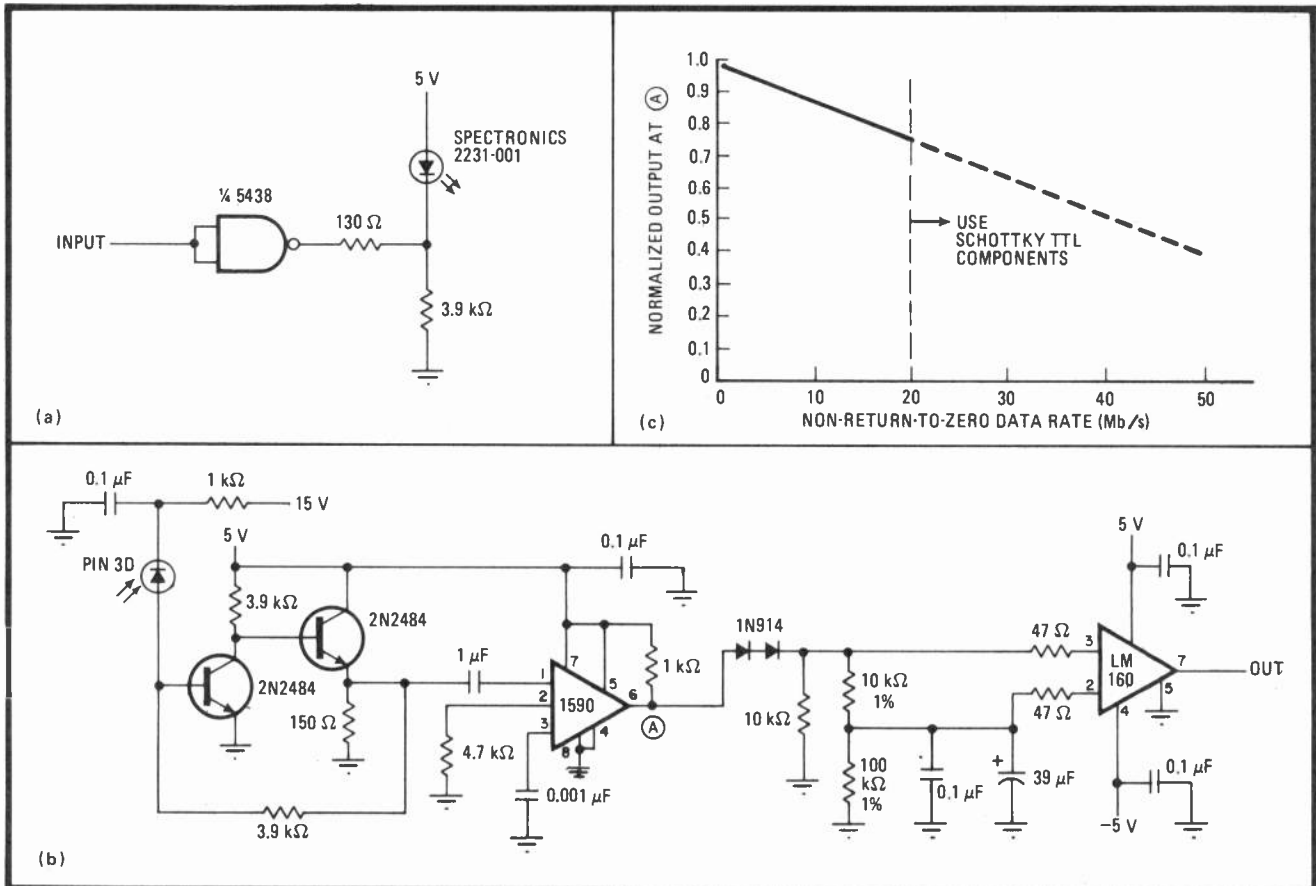
A TTL driver and a light-emitting diode serve well as the transmitter, shown in (a). The 5438 TTL driver is a two-input, open-collector NAND gate selected for its low power dissipation and 48-milliampere current-sinking capability. The LED is a gallium-arsenide device operating at 910 nanometers and provides 2 milliwatts of optical power at a forward current of 100 milliamperes.

The 130-ohm resistor sets the current through the LED at about 30 mA, and so the output power is about 0.6 mW in this circuit.

The receiver (b) is also simple and sensitive. The output from the p-i-n photodiode (labeled the PIN 3D device) is converted into a voltage by a two-transistor transimpedance amplifier. The 2N2484 transistors selected give low input capacitance, an adequate gain-bandwidth product, and the ability to detect small currents. Amplifier output is about 25 millivolts.

The MC1590 video amplifier that follows greatly boosts signal levels over a wide band (c). Two 1N914 diodes drop the output offset voltage of the single-ended amplifier, nominally at 4 volts, to within the input range of the LM160 comparator. The comparator's threshold is set by a simple voltage divider. The capacitors, across pin 2 and ground, combined with the 100-kilohm resistor, form a low-pass filter providing a threshold that varies with the comparator's supply voltage.

As for the electro-optical interface, the LED, which is contained in a TO-46 package, is easily mounted in an inexpensive window bushing made by AMP, model 530563-1. The PIN 3D photodiode can be mounted in



**Light bits.** Simple data transmitter (a) and a receiver (b) form the nucleus of a fiber-optic transmission system that is capable of handling all types of digital waveforms. Link operates over a wide band of frequencies (c). Cost of the 10-meter-long unit, including cable, is under \$90.

the same type of connector if desired. The need for delicate mounting adjustments is avoided here by using a fiber bundle of sufficient diameter, in this case 45 mils. Galite 2000 cable is satisfactory, and Valtec, Rank Industries, and others produce similar bundles.

The Galite cable has 210 fiber elements having an attenuation of 450 decibels per kilometer at 910 nm and a bandwidth-distance product of 15 megahertz/km. For a 10-meter-long link, therefore, the cable loss will be 4.5 dB and the bandwidth will be 1 gigahertz. With the measured loss of 1.5 dB in the LED-to-cable interface and a cable/detector interface loss of 3.9 dB, the total loss amounts to 10 dB. Thus, the 0.6-mW output of the LED is reduced to 0.06 mW at the receiver.

Transmitter layout is not critical in a one-way link. Duplex operation will require electrical isolation between transmitter and receiver components. There are several precautions to take in constructing the receiver. Notably, the lead from the anode of the detector diode to the transimpedance amp must be kept as short as possible. The output of the receiver should be isolated from all previous stages to prevent unwanted pickup. A ground plane is not a necessity, but is recommended for processing data rates greater than 10 megabits/s.

The link's signal-to-noise ratio is slightly less than 40 dB, implying a bit-error rate above  $10^{-8}$ . The system is operational over a temperature range of  $-40^{\circ}\text{C}$  to  $100^{\circ}\text{C}$ , and a supply variation of 4.5 v to 5.5 v. □

## Line-frequency converter transforms 50 Hz into 60 Hz

by Juan E. Piquinela  
Montevideo, Uruguay

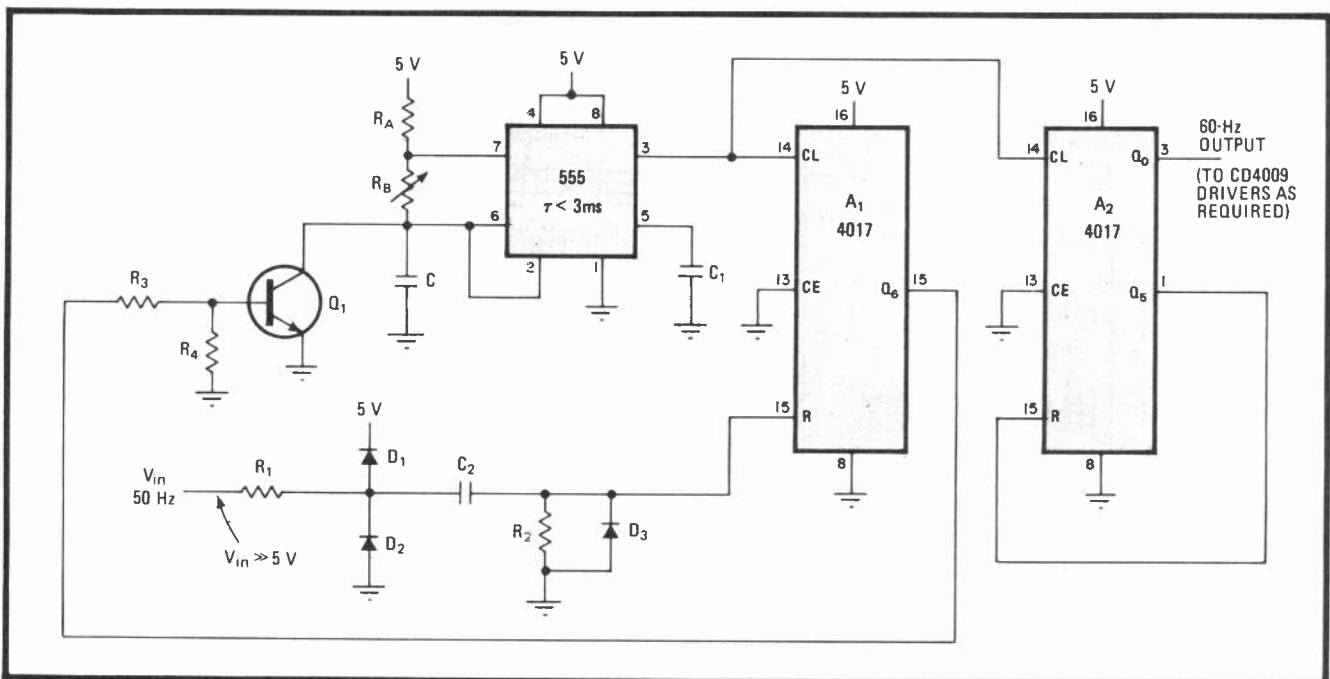
Low-power equipment driven from the 60-hertz power line can usually be expected also to work properly at 50 Hz—that is, except for electric clocks and other time-keeping devices, to which many a traveler outside North America will attest. For such devices, a circuit that provides a multiplication ratio of 6:5 for generating a 60-Hz output from a 50-Hz input is required. Such a low-cost, low-power circuit is shown here.

The 555 timer, operating as an astable multivibrator at 300 Hz, provides the 4017 counter,  $A_1$ , with six

count-pulses for every reset pulse from the 50-Hz line. The timer's period of oscillation—about 3 milliseconds—is not critical as long as six of its cycles are completed in less than 20 ms, the period of the 50-Hz line frequency.

On the sixth pulse,  $Q_6$  of  $A_1$  moves high and disables the timer through transistor  $Q_1$  by shorting capacitor  $C$ . Thus, independent of the period set for the 555, its average frequency is  $50 \times 6 = 300$  Hz. At the positive zero-crossing of the line voltage that occurs shortly after the sixth pulse,  $A_1$  is reset through  $R_1 - R_2$ ,  $C_2$ , and  $D_1 - D_2$ , and the process repeats.

Counter  $A_2$  provides a divide-by-five function at 300 Hz, thereby generating an output frequency of 60 Hz. C-MOS drivers or transistors can provide increased current capability as required. □



**On time.** Three-chip multiplier converts 50-Hz power-line frequency into 60 Hz for devices used in the U. S.  $A_1$  generates six pulses for every 50-Hz cycle, forcing 555 timer to generate average frequency of 300 Hz.  $A_2$  provides divide-by-five function on 555 waveform.

# Electronic security lock has nonvolatile latch memory

by Ray Oakley  
Plessey Semiconductors, Irvine, Calif.

Nonvolatile quad latches serve as the memory bank in this electronic security lock, which can be programmed with any one of more than 65,000 possible four-digit combinations. The number of combinations that can be selected for opening the lock can be greatly increased, simply by cascading the latches and their corresponding control circuitry.

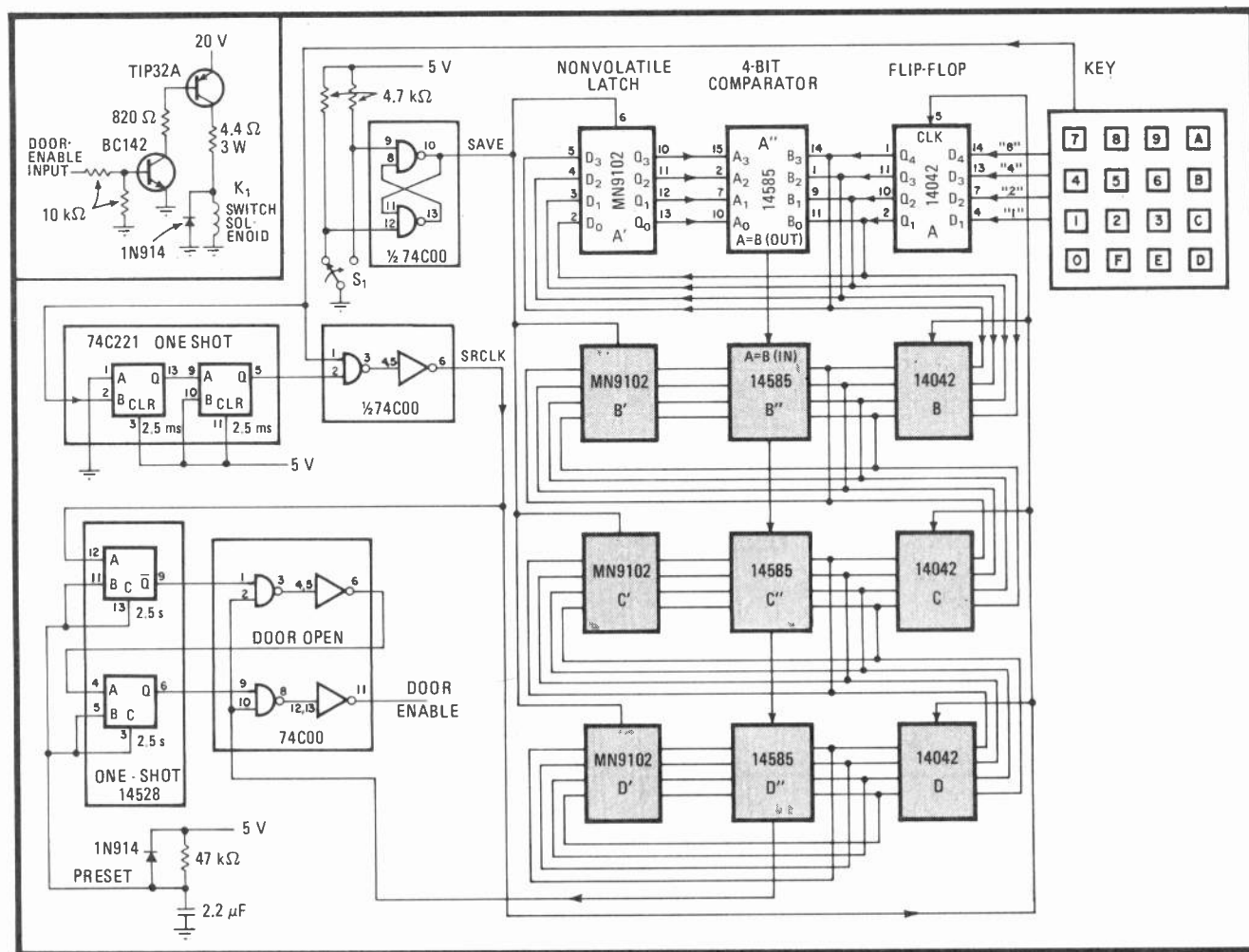
The desired four-digit combination is stored in the Plessey MN9102 latches by first entering the number via the keyboard, which provides a hexadecimal output. If the code were 3579, digit 3 would first be introduced to the D input of flip-flop A. At the same time, the signal KEY, which indicates contact closure, is generated. KEY produces clock signal SRCLK, generated by a monostable multivibrator, which prevents keyboard bounce and which clocks 3 into A.

Because the outputs of each flip-flop,  $n$ , are connected to the D inputs of the next flip-flop in the line,  $n + 1$ , the successive introduction of the remaining digits translates the digit 3 from A to flip-flop D, with the end result that 5 will be in flip-flop C, 7 in B, and 9 in A at the conclusion of the sequence. The outputs of A to D are also connected to latches A' to D', respectively, and so by activating switch  $S_1$ , momentarily in order to generate the SAVE signal, the digits can be stored in their corresponding latches.

Data can be retained in the latches for at least one year in the absence of applied power (+5, -12 volts). Typically, 10 million save operations can be made before device performance is affected.

In actual operation, the first digit keyed in is compared with the 9 stored in A', at comparator A''. Assuming the first digit keyed is a 3, there will be no output from the A = B port of the comparator. Neither will there be any output from B'' or C'' as the digits 5 and 7 are entered.

As the final digit, 9, is entered, however, digit 3 is placed in D, 5 moves to C, and 7 is stored in B. All comparators therefore indicate A = B, and a door enable signal is generated, thereby activating  $K_1$  after a user-selected delay provided by the 14528 one-shot. □



**Hardened.** Four-digit combination is kept in security lock's latch memory. Data will be retained in low-cost latches for at least one year in the absence of applied power. Matching input code entered via keyboard energizes relay  $K_1$  after user-specified delay.



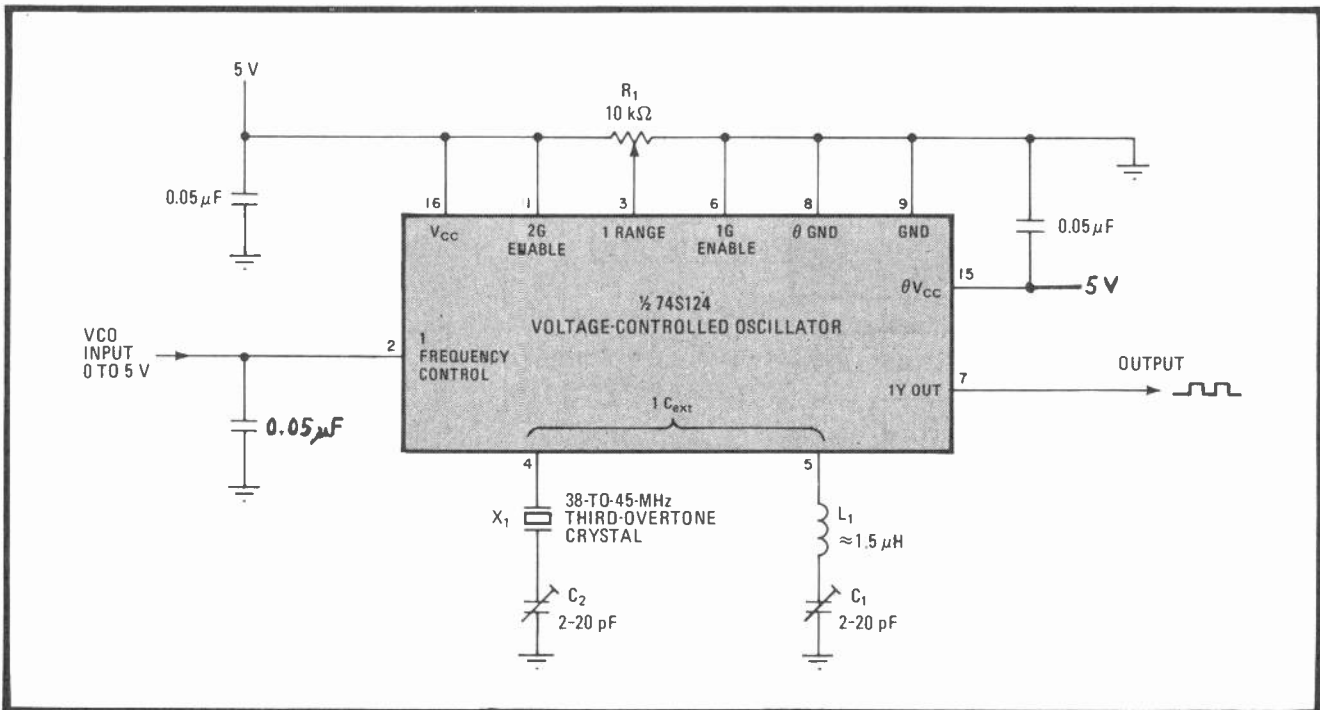
## LC network adapts PLL for crystal-overtone operation

by R. J. Athey  
National Research Council, Ottawa, Canada

Although Texas Instruments' popular 74S124 oscillator serves reliably in most instances as a crystal-controlled phase-locked loop, problems arise when overtone crystals are utilized for high-frequency (20 megahertz and above) operation. The difficulties may be overcome by adding an LC network in order to retain adequate system gain for oscillation at the required overtone and dampen oscillations at the fundamental frequency. This technique thereby forces the loop to lock onto the crystal's third-order output.

Although the range over which the PLL responds will be limited to about 1 kilohertz for a 0-to-5-v input signal, the method affords repeatable results and will enable use of the 74S124 beyond the normal limits imposed by fundamental-mode crystals. As shown in the figure,  $L_1$  and  $C_1$  are selected to be series-resonant at the desired overtone frequency. Assuming  $L_1$  is 1.5 microhenries, a  $C_1$  value of 2 to 20 picofarads will be adequate for tuning over the range of 38 to 45 MHz required in this particular application. The  $Q$  of both  $L_1$  and  $C_1$  should be reasonably high.

$C_1$ , along with  $R_1$ , serves as a gross frequency control. Unfortunately, the setting of  $R_1C_1$  will be rather critical. Although the range over which  $R_1$  is effective as a tuning element for a given  $C_1$  is narrow, a miniature carbon potentiometer will have sufficient resolution for making adjustments.  $C_2$  provides an offset for the desired third-overtone frequency. In general, the circuit will work satisfactorily for crystals working to 60 MHz. □



**Order of oscillation.** Addition of  $L_1C_1$  adapts TI's voltage-controlled oscillator for use as a high-frequency phase-locked loop utilizing an overtone crystal. LC network eliminates crystal's strong fundamental response, forces loop to lock onto slab's third-order output.

## Tone detector sharpens digital filter's response

by Steve Newman  
Los Angeles, Calif.

Using digital techniques to set the center frequency and the passband, this circuit will serve as a precision tone detector or as a control (transmission) gate for digital bandpass or band-blocking filters. The circuit elements can be easily cascaded to provide as great a degree of selectivity as required.

The general scheme is outlined in (a). Up counters  $A_1$  and  $A_2$  are preprogrammed to generate a carry signal

after  $N$  or  $M$  input pulses of  $f_{in}$ , respectively, where  $N$  is equal to or less than 16 and  $N$  is greater than  $M$ . The period of the reference signal  $f_{ref}$ , which is  $t_{ref}$ , determines the time each counter is enabled.

The output of the  $M$  counter clocks the presettable counter  $A_3$ , while the output of the  $N$  counter is connected to its clear input. Thus if  $M$  or more pulses occur during the time  $\frac{1}{2}t_{ref}$ , hereafter called  $t'_{ref}$ , the final counter generates carry pulses periodically (this circuit is intended to detect tones of fairly extended duration only). As a result, the output of the missing-pulse detector,  $A_4$ , can be forced high.

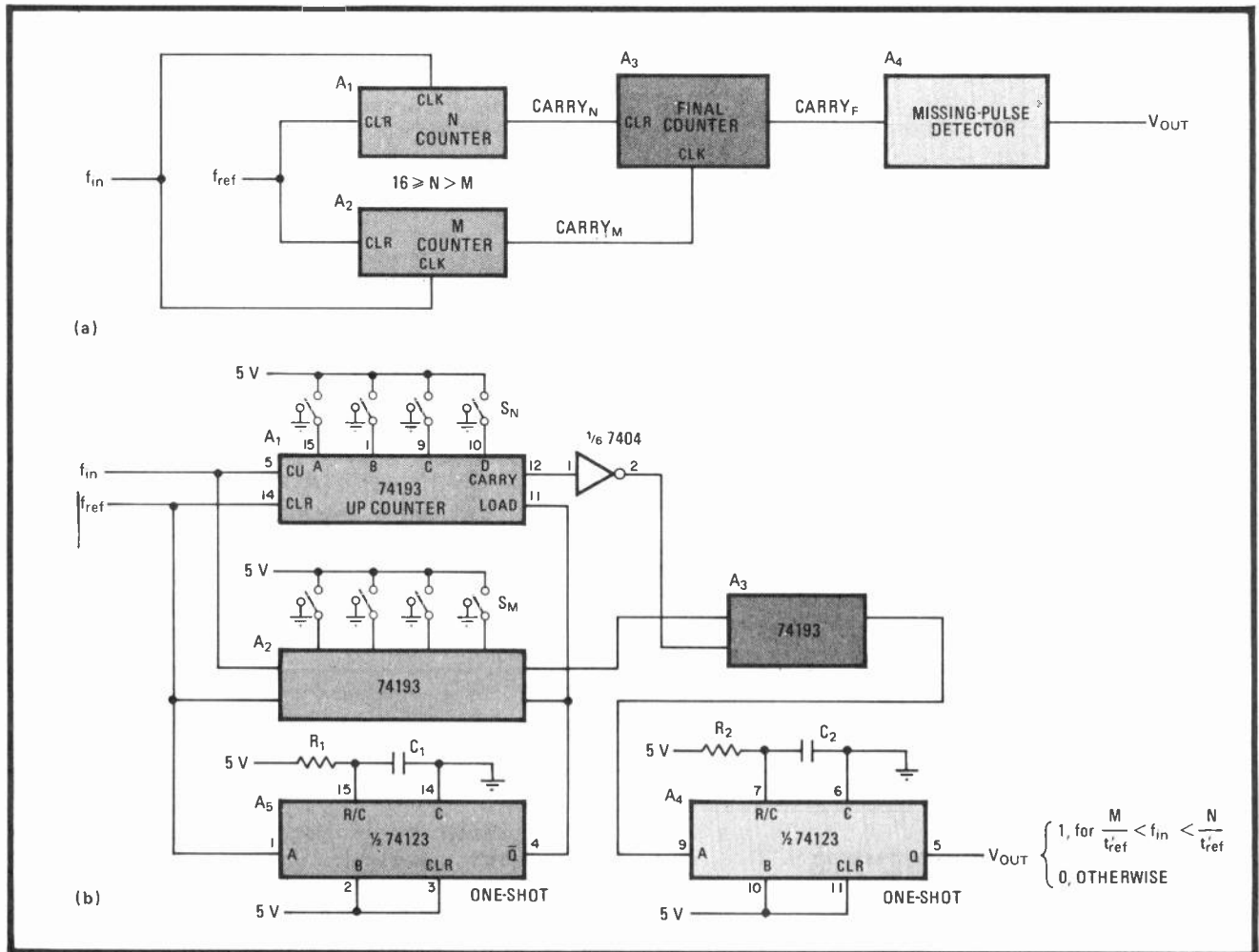
If, on the other hand, the incoming frequency is greater than  $N/t'_{ref}$ , presettable counter  $A_3$  is always reset before it can produce a carry pulse. Thus  $A_4$ , which requires a steady stream of pulses to keep it active, is forced low. If  $f_{in}$  is less than  $M/t'_{ref}$ ,  $A_3$  again cannot produce a carry pulse because there are no clock pulses from the  $M$  counter. Thus,  $V_{out}$  will be high only for the

case where  $M/t'_{ref} < f_{in} < N/t'_{ref}$ .

The actual circuit is shown in (b).  $A_1$  and  $A_2$  are enabled at the instant  $f_{ref}$  moves low.  $A_3$  and  $A_4$  assume the same functions described in (a). If the detection process must be sped up,  $A_3$  can be preset so that it generates a carry for every  $P$ th pulse from  $A_2$ , in the range 1 to 15. In general operation, however,  $A_3$  is not preset.

At the start of the measurement cycle,  $f_{ref}$  initiates the process whereby one shot  $A_5$  presets  $A_1$  and  $A_2$  to their switch-programmed values (switches  $S_N$  and  $S_M$  are active low). The reference frequency is selected in conjunction with  $S_M$  and  $S_N$  to provide almost any desired passband.

For example, if a frequency between 9.5 and 10.5 kilohertz ( $f_{in}$ ) must be detected,  $M$  can be arbitrarily selected to be 9 and  $N = 10$ . A  $t'_{ref} = 0.95$  millisecond is then required ( $f_{ref} = 526$  hertz at 50% duty cycle). Note the time constant  $R_1C_1$  must be much less than  $t_{ref}$ .



**Logical boundaries.** Tone detector sets limits of desired frequency range digitally. Using counting technique, circuit rejects tones whose frequencies are too high or low. Detector generates output only for  $2M/t_{ref} < f_{in} < 2N/t_{ref}$ , where  $f_{in}$  is input frequency,  $M$  and  $N$  are the  $M$ th and  $N$ th pulses that generate a carry from the  $M$  or  $N$  counters, respectively, and  $t_{ref} = 1/f_{ref}$ , where  $f_{ref}$  is the reference frequency.

$R_2 C_2$  must just exceed  $240/f_{in}$  to cover the case where  $M = 15$  and  $N = 16$ , whereupon as many as 240 input pulses are required to detect the tone. Under these conditions, however, the bandpass will be only 3% of the center frequency,  $f_o$ .

If greater selectivity is desired, a pair (or more) of 74193 up counters can be simply cascaded without

upsetting the basic operation of the M and N counter chains. With two counters in each chain, the range of M and N can be expanded to 256, whereupon a bandpass of only 0.2% of  $f_o$  can be selected. □

## D-a converter simplifies hyperbolic clock

by R. H. Riordan  
Cybec Electronics, Bentleigh, Australia

The hyperbolic clock circuit proposed by Baxter [*Electronics*, July 5, p. 132], which transforms a time function,  $t$ , into units of  $1/t$  in order to measure rate, can be made more compact by employing a one-chip digital-to-analog converter. Using the converter's monolithic ladder of 255 equivalent resistors in place of Baxter's discrete network for scaling provides greater resolution for a circuit of a given size and is easily modified for applications requiring a decimal output.

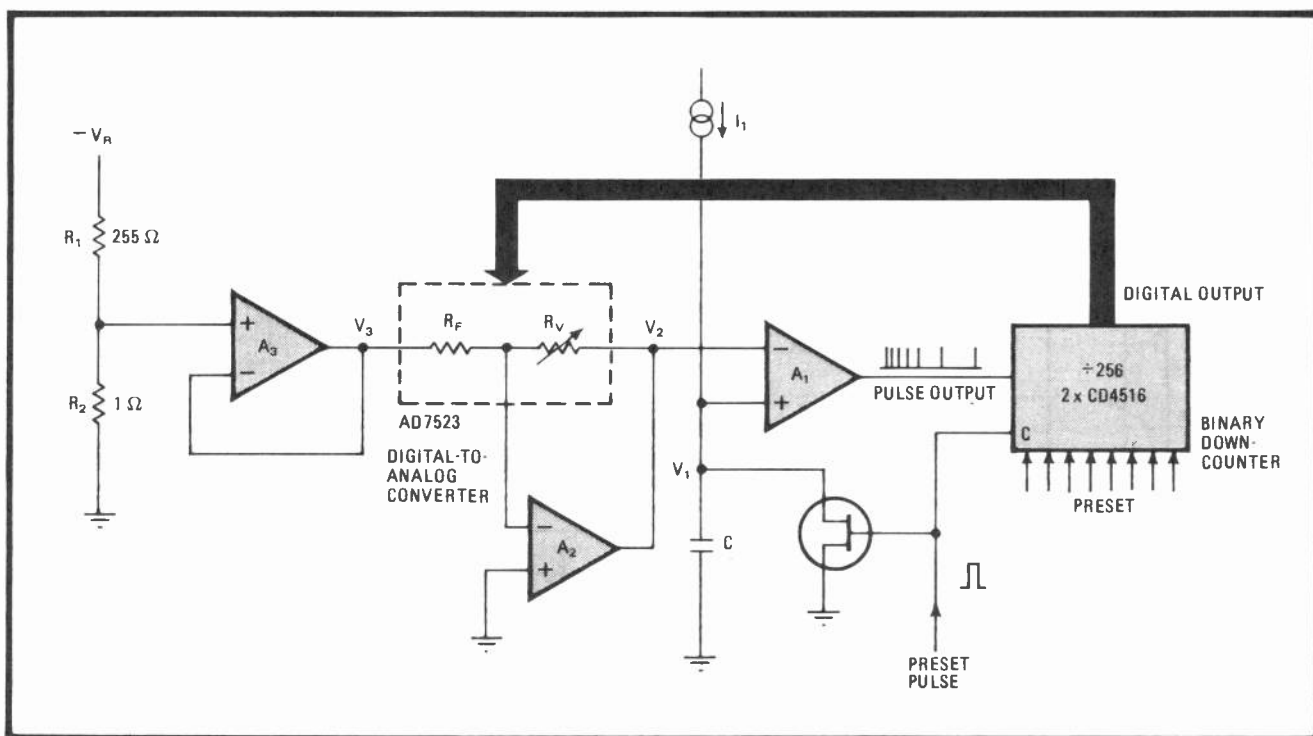
Initially, voltage  $V_1$  is set to zero and the 8-bit binary counter formed by cascading two C-MOS 4516 chips is preset to a count of 255. The converter is equivalent to a fixed resistor  $R_f$  and a variable resistor  $R_v$ , where  $R_v/R_f = 256/N$  and  $N$  is the output count of the 4516. The

converter is connected in the reverse of the normal configuration, so that  $V_2/V_3 = -R_v/R_f = -V_3(256/N)$ . But  $V_3 = -V_{ref}/256$ , so  $V_2 = V_{ref}/N$ .

At first,  $V_1 = 0$  and  $V_2 = V_{ref}/255$ . At  $t = 0^+$ , current generator  $I_1$  starts to charge capacitor  $C_1$ , and  $V_1$  begins to rise linearly with time. Whenever  $V_1$  climbs above  $V_2$ , comparator  $A_1$  generates a clock pulse, decrementing the counter and causing  $V_2$  to rise above  $V_1$  again. For any given count  $N$ , a clock pulse will be generated at a time  $t$  when  $V_1 = I_1 t / C = V_{ref}/N$ . Thus, until the counter reaches zero, the count at any instant will be proportional to the reciprocal of the elapsed time.

This circuit, as well as Baxter's, has a potential weakness in that if a single-step cycle does not result in  $V_2$  rising above  $V_1$ , a lock-up condition will occur. This danger is eliminated if a separate clock signal is provided for the counter, with  $A_1$  used only to enable the 4516s.

If decimal timing signals are required, it is a relatively simple matter to replace the d-a unit and the counter with their decimal-output equivalents. If a different step range is required, it can be selected accordingly by changing only  $R_1$  and  $R_2$ .  $R_1$  and  $R_2$  are also used to set the desired count range. □



**Turnabout.** Clock inverts time function,  $t$ , in order to measure rate. D-a converter's ladder network, driven by counter, generates stepping function that is compared to ramp voltage  $V_1$  at  $A_1$ .  $V_1$ 's linear increase and  $V_2$ 's monotonic rise are almost equal initially, but rates of rise diverge hyperbolically, so that counter is stepped at  $1/t$  intervals.  $R_1$  and  $R_2$  set step size;  $I_1$  sets scaling factor.

## Switching preamp improves a-d converter sensitivity

by Peter Bradshaw  
Intersil Inc., Cupertino, Calif.

The low-signal resolution of even the best analog-to-digital converters, including those equipped to eliminate input-offset disturbances, is limited by the noise generated at the inputs. But the resolution, and thus the true sensitivity, of a converter can be inexpensively improved by an order of magnitude if a switched, differential amplifier is employed at the input to precancel offset errors without affecting the normal conversion process.

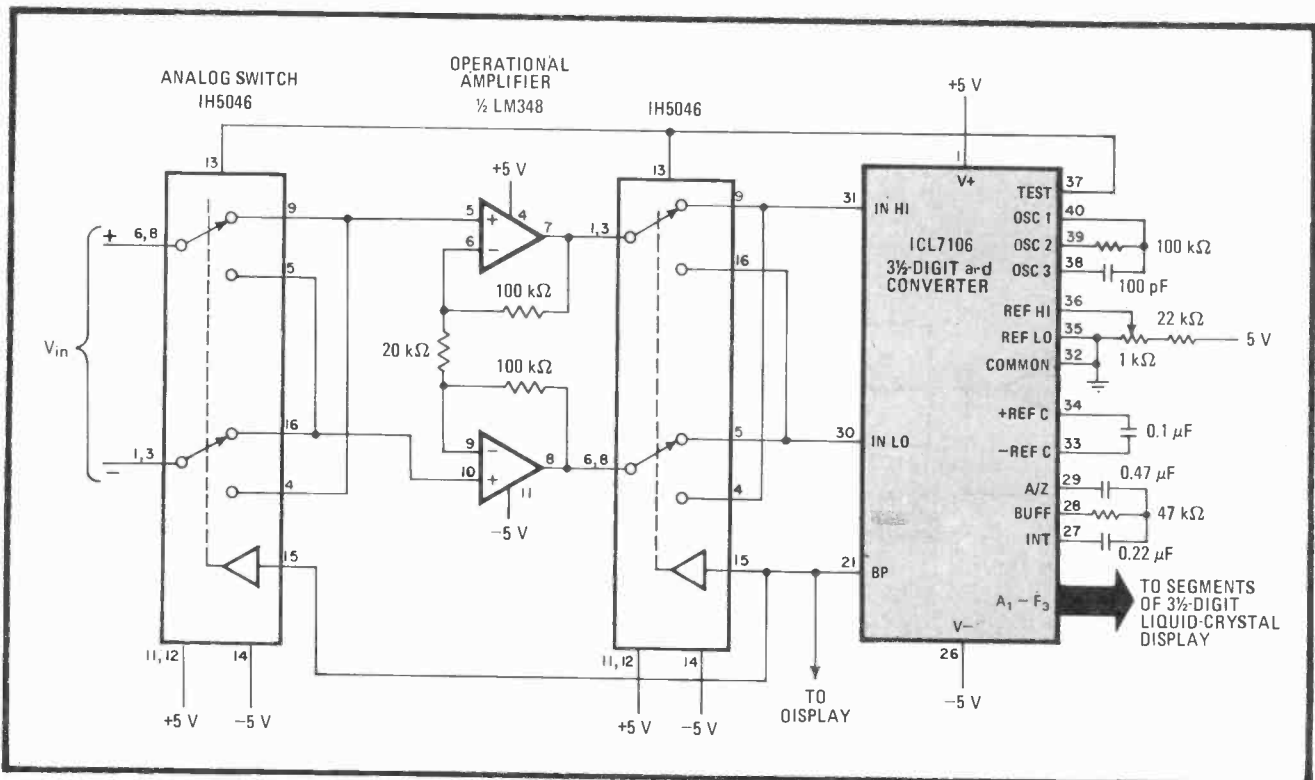
The technique is illustrated for Intersil's ICL7106 3½-digit autozero converter/display driver, which normally handles signals over the range of 100 millivolts to 2 volts. In such a converter, the small input noise voltage trapped on the autozero capacitor during a conversion sets the aforementioned lower signal-handling limit. The noise (which is caused by the equivalent noise resistance at the input, not a component of the signal) can be minimized to a great degree with preamplifiers having low offset voltage, but this can be a rather

expensive solution to the problem.

As shown, an alternative approach is to use the liquid-crystal-display backplane (BP) drive output of the ICL7106 to synchronously switch one half of the low-cost LM348 quad operational amplifier via analog switches so that, over a switching cycle, the input of the converter sees no instantaneous change in the magnitude or polarity of sample voltage  $V_{in}$ . Offset voltages, including that of the op amp, on the other hand, are virtually canceled because an equal but opposite noise component (average value is near zero) is applied to the IN HI (and IN LO) ports of the converter over a given interval. In this case, the switching (BP) signal is set at about 60 Hz, but this can be varied by suitable selection of the RC components at pins 38 and 39 of the ICL7106. In this configuration, excellent performance is obtained for input signals from 10-20 mv full scale.

Most dual (matched) op amps will be suitable for the switching task, but it is important that both the positive and negative slew rates of the device be reasonably close. Op amps having significant crossover distortion (such as the LM124/324) should not be used.

The CD4053 or the Intersil IH5046 will serve well as the analog switches. In the case of the 4053, 1½ devices will be required. Only one double-pole, double-throw switch is contained in each 5046, however, and so two of these devices would be required. □



**Precanceled.** Switching the signal-handling op amp at 60-hertz rate virtually eliminates input-offset errors of converter, thereby improving sensitivity. Converter's input sees no instantaneous change in  $V_{in}$  during switching cycle, and normal conversion process is not affected. But offset voltage at input is alternately fed to (+) and (-) ports; thus equivalent noise voltage over cycle is near zero.

# Ramp generator has separate slope and frequency controls

by Henrique Sarmento Malvar  
 Department of Electrical Engineering, University of Brasilia, Brazil

Isolating with four analog switches the frequency-determining portion of the circuit from that controlling the charging and discharging of its RC integrator, this ramp generator achieves independent selection of slope ratio and repetition rate. Such a unit is useful in a music synthesizer, where timbre must be changed without affecting a note's fundamental frequency.

Analog gates  $T_1$  and  $T_2$  are initially switched on, and therefore  $V_c$  is applied via operational amplifier  $A_1$  to the integrator built around  $A_2$  (see figure). Thus,  $-V_c$

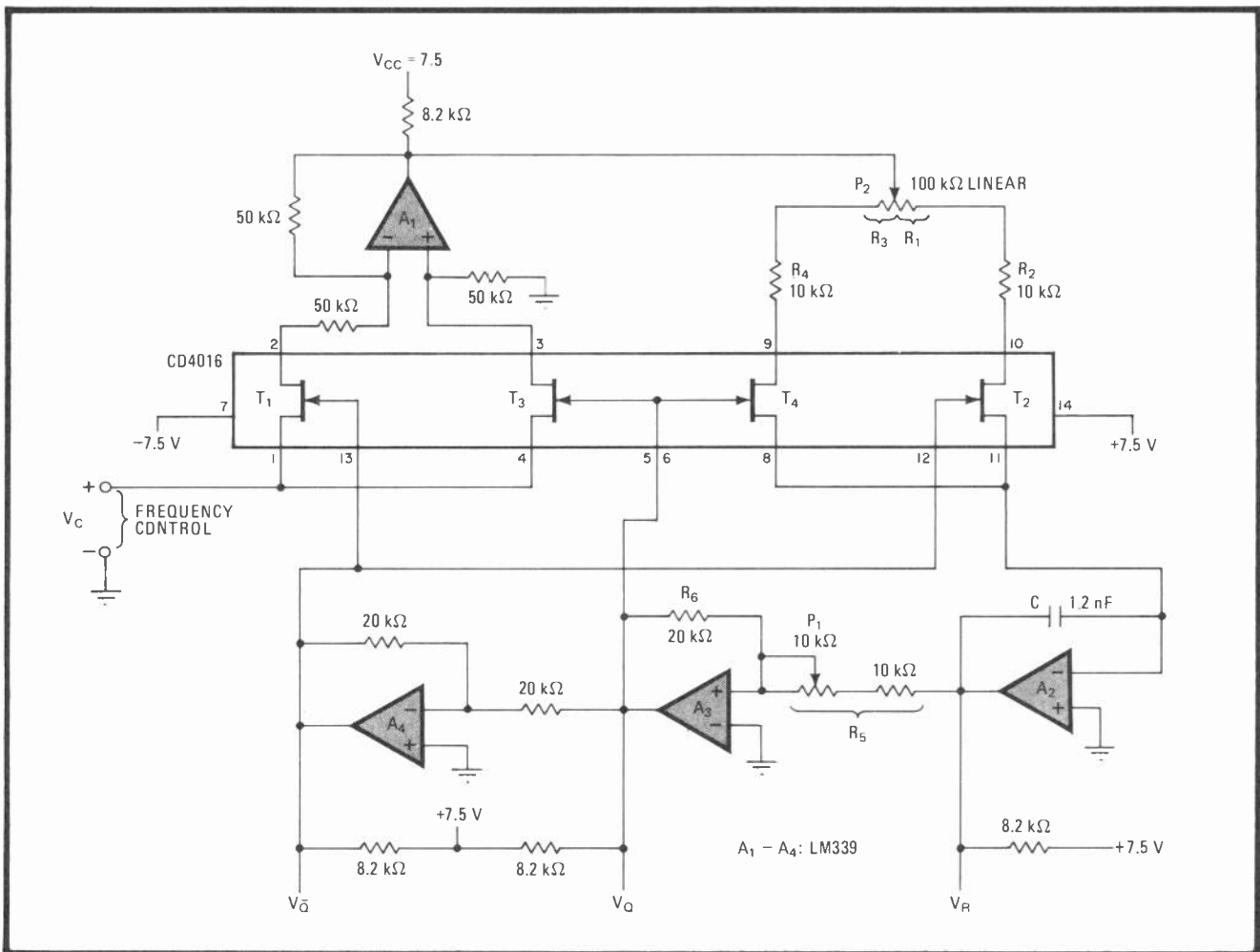
appears at the inverting input of  $A_2$ , and its positive-going output reaches voltage  $V_H$  in  $T_1 = 2V_H C (R_1 + R_2)/V_c$  seconds, where  $V_H = V_{cc}R_5/R_6$ .

At this time,  $A_3$  switches on and  $A_4$  goes off.  $T_1$  and  $T_2$  are thus disabled, and  $T_3$  and  $T_4$  are brought high so that  $+V_c$  is applied to the integrator. The output at  $A_2$  thus falls linearly toward  $-V_H$ , where time  $T_2 = 2V_H C (R_3 + R_4)/V_c$ .

The frequency of the ramp is given by:

$$f = 1/(T_1 + T_2) = R_6 V_c / [2CR_5 V_{cc} (R_1 + R_2 + R_3 + R_4)] = kV_c$$

where  $k$  is a constant (in the approximate range of 1 kHz/V) that can be adjusted with potentiometer  $P_1$ . Because  $R_1 + R_3$  is a constant, it is seen that an adjustment in potentiometer  $P_2$  will affect the slope ratio, but not the frequency. With the values shown, the slope ratio can be selected from 1/11 to 11. The slope ratio is given by  $T_1/T_2 = (R_1 + R_2)/(R_3 + R_4)$ . □



**Separation.** Transmission gates  $T_1$ – $T_4$  separate the portion of the ramp generator that determines the frequency from the circuitry that sets the charge and discharge times of its integrator, so that the up/down slope ratio and frequency can be independently selected. The inexpensive circuit, which costs less than \$10 and works in the audio range, is a useful timbre control in music synthesizers.

# One-chip power amplifier controls dc motor's speed

by Kuang-Lu Lee and Dennis Monticelli  
National Semiconductor Corp., Santa Clara, Calif.

Circuits for regulating the speed of small dc motors need not be expensive or complicated now that one-chip power operational amplifiers are available. In fact, using the power device (such as the LM13080) in a simple negative-feedback configuration provides better regulation than many speed controllers now on the market. In addition, common-mode rejection of power-supply transients is large.

As shown in (a), the circuit's reference voltage is established by  $D_2$  and  $R_3$  and filtered by  $R_5$  and  $C_1$ .  $D_1$  simply serves as a common-mode level shifter for the inputs of the op amp. Negative feedback around the op amp provides the controlled-voltage drive to the motor. Thus:

$$V_{\text{motor}} = (V_{D_2} + I_m R_3)(R_2/R_1) + V_{D_2}$$

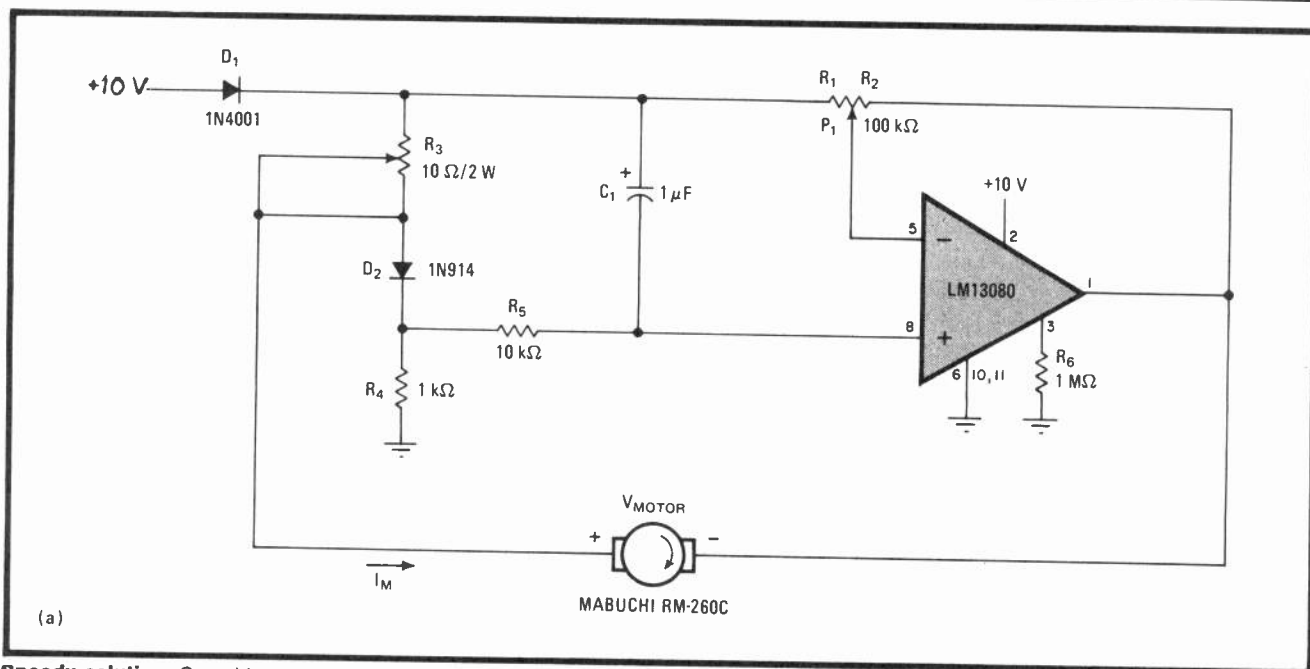
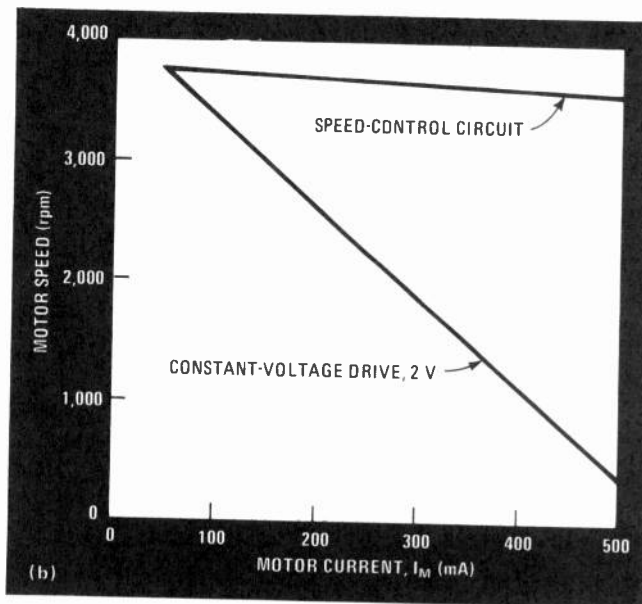
where  $V_{D_2}$  is the forward voltage drop of diode  $D_2$  and  $I_m$  is the current through the motor.

As the motor load increases,  $I_m$  increases, and this results in a corresponding increase in  $V_{\text{motor}}$ . To accommodate large changes in load,  $V_{\text{motor}}$  varies considerably. The amp therefore needs a 10-volt source voltage to provide sufficient swing, current, and power dissipation for most small motors. Powered by such a source, the LM13080 will handle up to 2 watts in free air and can deliver 0.5 ampere.

The optimum settings for potentiometers  $P_1$  and  $R_3$  are those that provide stable regulation. They are found

empirically with the actual motor to be used.  $P_1$  is first adjusted experimentally so that the motor will provide slightly fewer than the desired number of revolutions per minute.  $R_3$  is then increased until a minimal loss in speed is observed for a substantial increase in motor load. Note that excessive positive feedback via  $R_3$  will cause instability. Because the adjustments of  $P_1$  and  $R_3$  interact, it will be necessary to readjust both until the best settings are obtained.

The circuit's performance for a small motor is shown in (b). Note its superior performance with respect to a popular configuration that drives the motor from a constant-voltage source. □



**Speedy solution.** One-chip power op-amp circuit (a) makes simple, low-cost speed control for small dc motors. Circuit affords excellent common-mode rejection. Controller's rpm-vs-load performance (b) is superior to that of circuits utilizing a constant-voltage drive.

# Peak-reading millivoltmeter responds instantaneously

by William J. Mundi  
 Department of Psychology, Concordia University, Montreal, Quebec, Canada

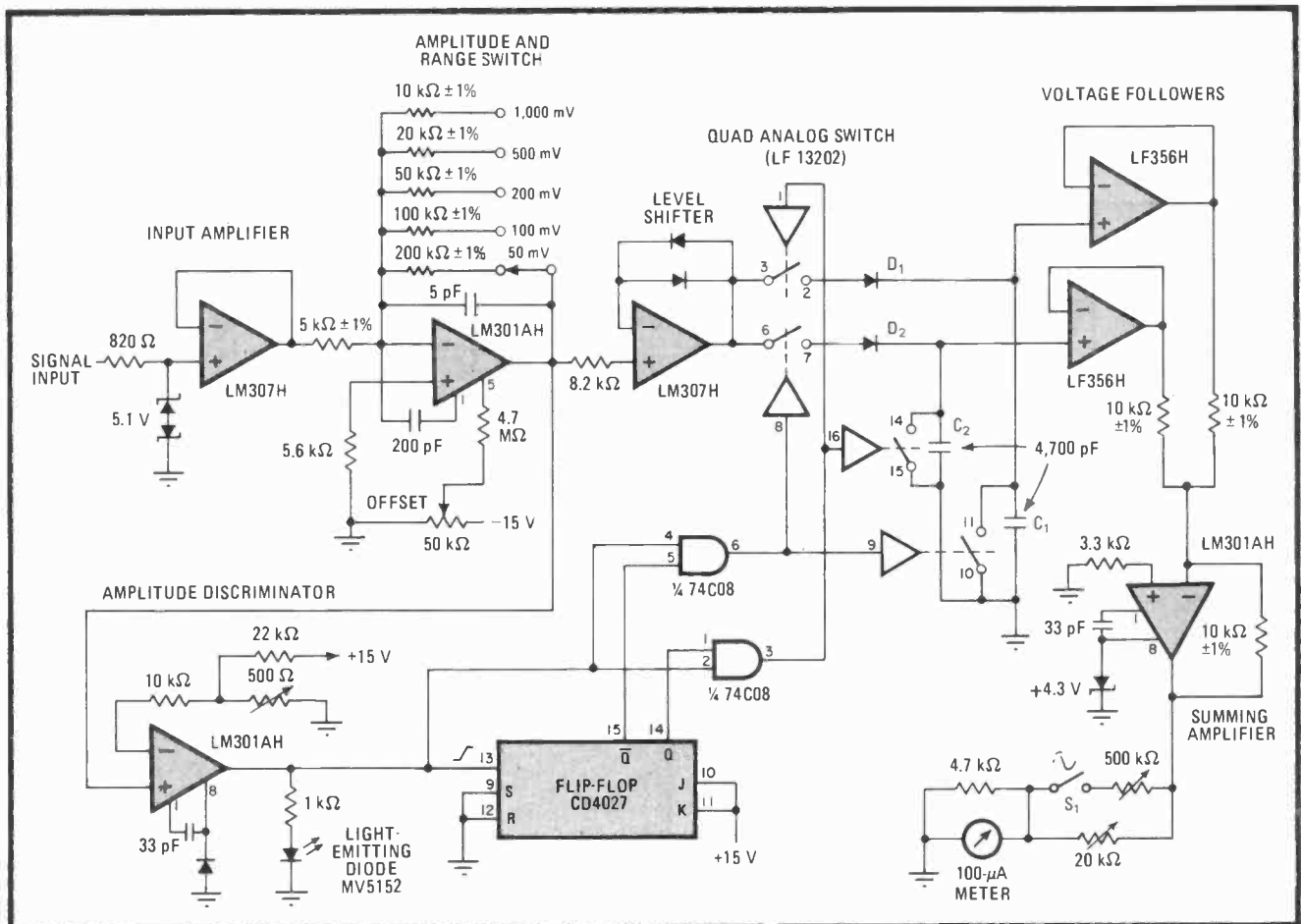
Requiring but a single pulse or cycle of a sine, square, or triangular wave in order to determine its peak value, this millivoltmeter-microammeter will serve as a respectable substitute for an oscilloscope, oscillographic recorder, or other instrument that must deliver an instantaneous response. Such a low-cost unit is extremely useful in biomedical applications, where the amplitude of certain electrophysiological variables of small magnitude has to be closely monitored.

The millivoltmeter processes either negative-going pulses or the negative portion of the incoming waveform. The signal voltage first passes through the LM307 input

amplifier and through the LM301 range amplifier (see figure). The level shifter that follows imparts a positive offset to the signal to compensate for the voltage drop of charging diodes  $D_1$  and  $D_2$ , which transfer the peak value of the wave to holding capacitors  $C_1$  and  $C_2$ . The voltages on  $C_1$  and  $C_2$  are then alternately applied to the input of the LM301 summing amplifier; any change in the amplitude of the input signal will thus be instantly reflected at the output.

Capacitor switching is achieved with a quad analog switch (LF13202), which in turn is driven by a toggled 4027 flip-flop that is triggered by the input signal and the LM301 amplitude discriminator. The 500-ohm potentiometer is used to set the input trigger voltage at any point near zero, a necessary condition for detecting small input voltages.

As  $C_1$  is charged,  $C_2$  is discharged, and vice versa. Thus the stored voltage on  $C_1$  or  $C_2$  is constantly and quickly updated without the need for a discharge cycle. Note that the zener diode at the input to the summing amplifier prevents it from overdriving the output meter.



**1. Quick update.** This meter requires only one negative pulse or half cycle of sine-, square-, or triangular-wave input to determine peak current or voltage amplitude. The applied signal charges capacitors  $C_1$  and  $C_2$  alternately, so that either can update immediately without the need for a separate discharge cycle. The meter's range is 0 to 1 V or 0 to 100  $\mu$ A. The output meter reflects instantaneous changes.

The output microammeter may be calibrated in millivolts through the use of its associated 20-kilohm and 500-kilohm potentiometers. Switch  $S_1$  must be closed in order to measure sinusoidal waveforms.

Although this meter has been used mostly for meas-

urement tasks below 100 hertz, it will work over a wide range of frequencies and thus is suitable for general-purpose audio-rate applications. As shown, the meter is useful for square waves to 8 kilohertz, sine waves to 10 kHz, and pulse widths down to 15 microseconds. □

## Talking meter voices dc voltage readings

by William S. Wagner

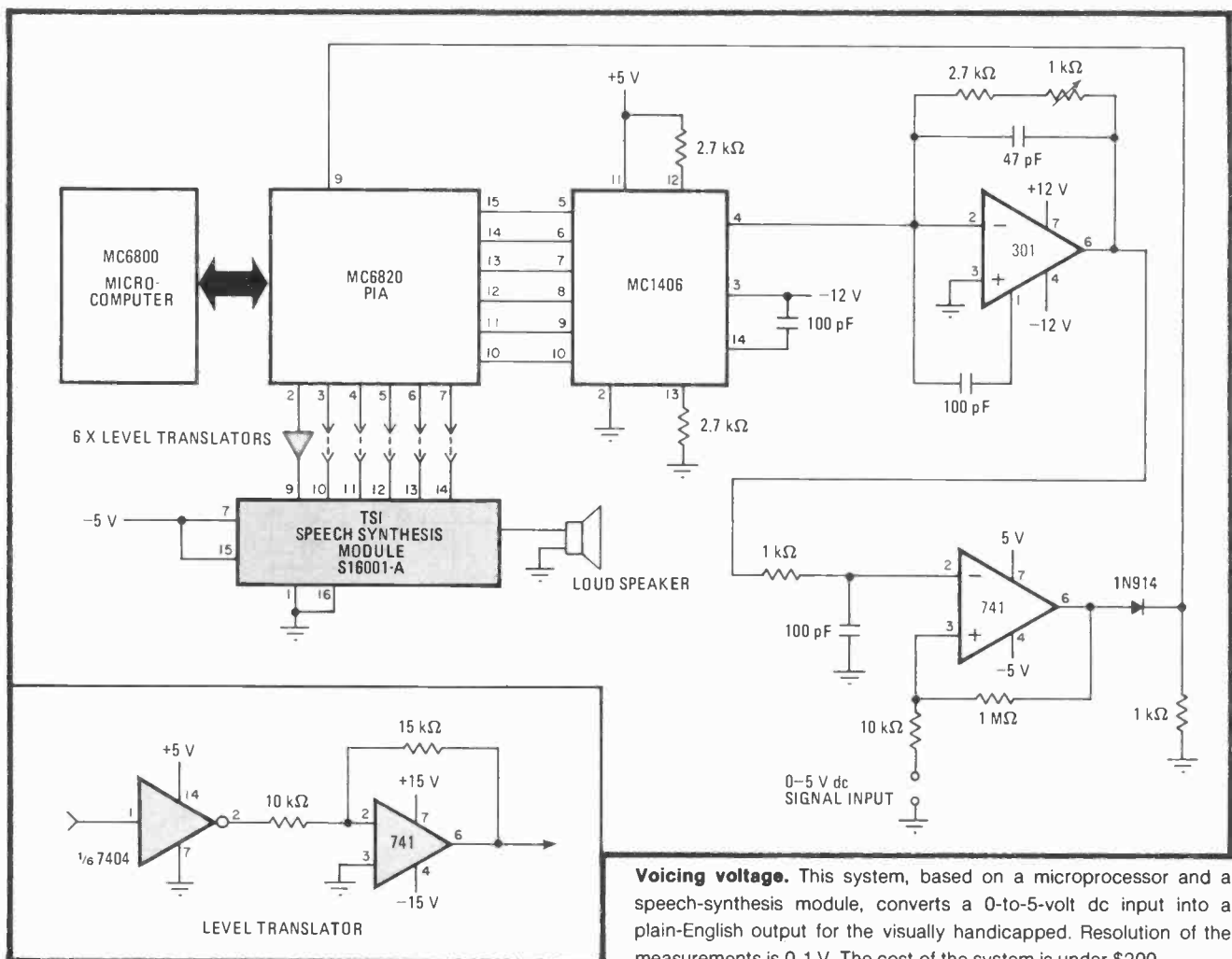
Northern Kentucky University, Highland Heights, Ky.

A relatively low-cost (\$150) speech-synthesis module, combined with an interface and a small program written for Motorola's 6800 microprocessor, will convert a dc input signal of 0 to 5 volts into a plain-English output with a resolution of 0.1 v. Thus the meter will be very useful to visually handicapped technicians.

The system is configured in much the same manner as the audible voltmeter previously described, which generates a set of short and long tones corresponding to the

voltage measured.<sup>1</sup> But in this instance, the S16001-A speech-synthesis module (from Telesensory Systems Inc., 3408 Hillview Ave., Palo Alto, Calif. 94304) serves as the output device. As a consequence, the software necessary to perform the voltage-to-audio conversion is much less, because it is handled by the synthesizer's internal circuitry.

As shown in the figure, the 0-to-5-v dc test voltage is compared with the output of the 6-bit 1406 digital-to-analog converter at the inputs of the 741 operational amplifier. If there is a voltage difference, the digital input to the 1406 is adjusted, under program control, until the voltage difference is minimized. The binary-coded-decimal word at the output of the 6820 peripheral interface adapter then represents the digital equivalent of the voltage measured. This word addresses the speech-synthesis module, which generates the corresponding voice response. Typical outputs will be heard as "three





## 68J0 TALKING-VOLTMETER PROGRAM

| Address | Mnemonic  | Address | Mnemonic  | Address | Mnemonic  |
|---------|-----------|---------|-----------|---------|-----------|
| 0000    | LDX 7F04  | 002B    | TAB       | 0059    | LDX FFFF  |
| 0003    | STX 8000  | 002C    | ORAB 20   | 005C    | DEX       |
| 0006    | LDX FF04  | 002E    | STAB 8000 | 005D    | BNE FD    |
| 0009    | STX 8002  | 0031    | LDX 0055  | 005F    | DECA      |
| 000C    | LDB FF    | 0034    | DEX       | 0060    | BNE F7    |
| 000E    | CLRA      | 0035    | BNE FD    | 0062    | PULA      |
| 000F    | STAB 8002 | 0037    | ANDB 0F   | 0063    | ANDA 0F   |
| 0012    | LDX 0055  | 0039    | STAB 8000 | 0065    | TAB       |
| 0015    | DEX       | 003C    | LDA A 02  | 0066    | ORAB 20   |
| 0016    | BNE FD    | 003E    | LDX FFFF  | 0068    | STAB 8000 |
| 0018    | TST 8000  | 0041    | DEX       | 006B    | LDX 0055  |
| 001B    | BPL 06    | 0042    | BNE FD    | 006E    | DEX       |
| 001D    | DECB      | 0044    | DECA      | 006F    | BNE FD    |
| 001E    | ADDA 01   | 0045    | BNE F7    | 0071    | ANDB 0F   |
| 0020    | DAA       | 0047    | LDAB 33   | 0073    | STAB 8000 |
| 0021    | BRA EC    | 0049    | STAB 8000 | 0076    | LDA A 04  |
| 0023    | LDS 00B0  | 004C    | LDX 0055  | 0078    | LDX FFFF  |
| 0026    | PSHA      | 004F    | DEX       | 007B    | DEX       |
| 0027    | LSRA      | 0050    | BNE FD    | 007C    | BNE FD    |
| 0028    | LSRA      | 0052    | ANDB 1F   | 007E    | DECA      |
| 0029    | LSRA      | 0054    | STAB 8000 | 007F    | BNE F7    |
| 002A    | LSRA      | 0057    | LDA A 02  | 0081    | JMP 000C  |

point seven," "one point oh," and "oh point nine."

The 66-instruction program is fairly simple. The first four steps initialize the system. The instructions contained between addresses 000C and 0021 make up the digital-voltmeter portion of the routine, where the aforementioned comparison and minimization of voltages at the inputs of the 741 op amp take place.

At minimization, the BCD word is stored in accumulator A at location 0024, which is the second location of the speech-synthesis section of the program. The analog equivalent of the most significant digit of voltage is then voiced at location 0039.

After a short delay to allow time for the word to be read, the word "point" is brought to the module's input register at 0047 and announced at location 0054. Following a second delay, the least significant digit of voltage is similarly presented to the output register at 0068 and transmitted at location 0073. The program then returns to the digital-voltmeter section of the routine. □

## References

1. William S. Wagner, "Digital voltmeter has audible output," *Electronics*, March 29, 1979, p. 120.

# Delay circuit replicates pulses of variable width

by John H. Davis  
Warm Springs, Ga.

Unfortunately, the simple and well-known circuit used to provide true pulse delay—whereupon the first of two one-shots connected in series sets the delay time desired and the second is set to generate a pulse having the same width—cannot be used if the input pulse width is variable. Fortunately, however, pulses of variable width can easily be handled by adding only a quad NOR gate and a few RC differentiators to a modified circuit, as shown here.

Differentiator  $R_1C_1$  provides a positive-going spike from the rising edge of the input pulse to be delayed, in

for the desired delay interval selected by potentiometer  $R_A$ . When the Q output returns to its high state, the RS flip-flop at the output, formed by two NOR gates, is set and the I port moves high.

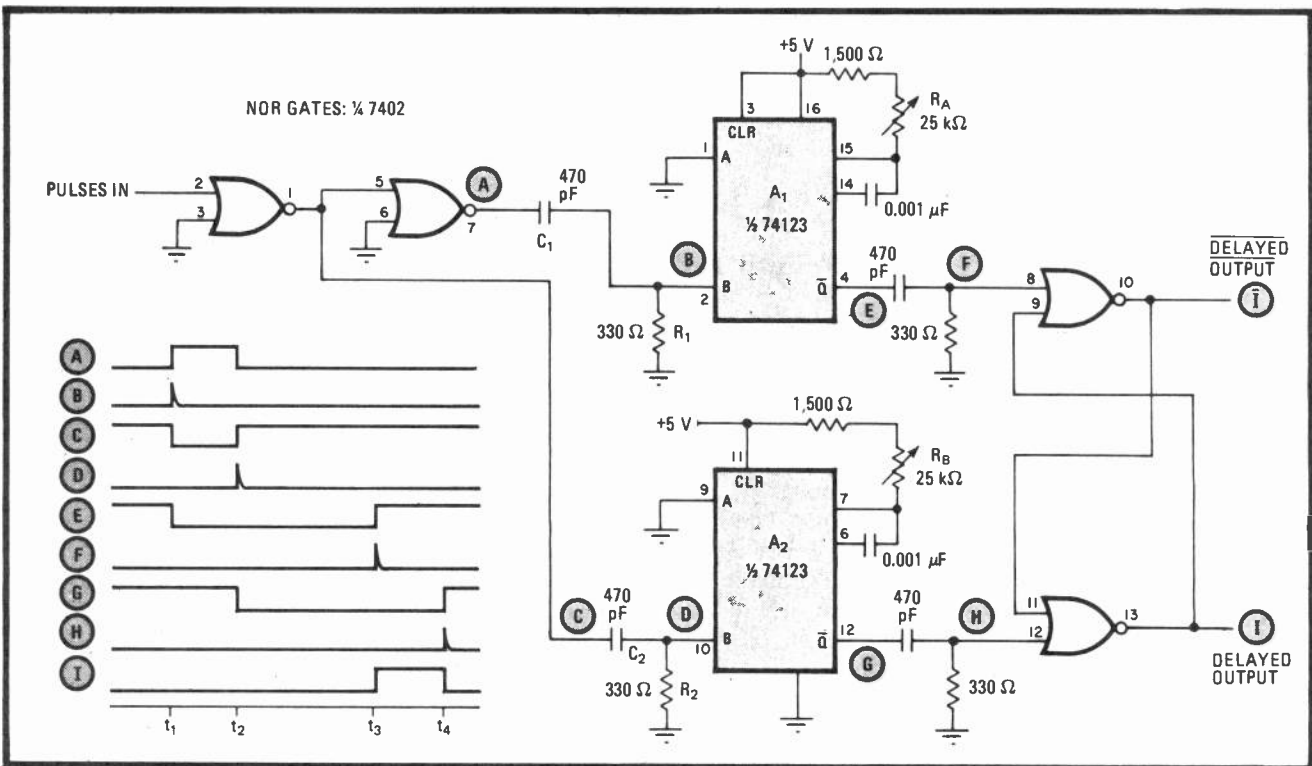
One-shot  $A_2$  is triggered by the falling edge of the input pulse through differentiator  $R_2C_2$ , and thus its  $\bar{Q}$  output goes low for a time (set by  $R_B$ ) equal to  $A_1$ 's delay interval. When  $A_2$ 's  $\bar{Q}$  output returns high, the NOR latch

returns to its low state. As long as  $\tau_{A1} = \tau_{A2}$ , the time during which I is high will always be equal to the width of the input pulse, assuming the delays are equal to or exceed the input pulse width. Pulses that are very much shorter than the set delay time will be reproduced less accurately.

This circuit provides delays over the range of 1 through 20 microseconds, but it is a simple matter to change timing components to achieve times into the millisecond region. Note that the maximum delay that may be set will be limited to the shortest repetition period in the pulse train and in practice should be set to a value less than this to allow for the one-shots to recover.

The circuit is equally suitable for implementation with positive or negative logic. Adjustment is simple. With positive logic,  $R_A$  should be set for the desired delay. A train of pulses of nominal width is then introduced at the input, and the I port is monitored with a scope while  $R_B$  is adjusted so that the pulse width at the output is equal to that at the input. The circuit will then automatically be calibrated for input pulses having any width. The calibration procedure is similar with negative logic, except that then it is easier to adjust  $R_B$  first.

Alternatively, both one-shots may be set for equal delay, but in practice this procedure will cause inaccuracies for very narrow input pulses. In any case, it will be advantageous if circuitry can be configured to program  $R_A$  and  $R_B$  simultaneously, so that the circuit has only one control. □



**Delayed duplication.** Parallel-connected one-shots and NOR gates provide set delay and maintain width of pulse, independent of its value. Low-cost unit will thus be useful for automatically synchronizing blanking pulses in TV systems and for similar applications.

# Frequency discriminator has ultra-sharp response

by S. J. Collocott, CSIRO Division of Applied Physics, National Measurement Laboratory, Sydney, Australia

Most rudimentary circuits for discriminating between two frequencies or two bands of frequencies sacrifice selectivity to simplicity. But this simple circuit, which uses just a frequency-to-voltage converter and a couple of general-purpose comparators, can differentiate between two frequencies separated by only a few hertz.

In this application, the circuit rejects all frequencies below 2.1 kilohertz, while passing others, although it is a simple matter to modify the discriminator to handle signals at any frequency. Input signals are introduced into the LM311 comparator ( $A_1$ ), which operates as a zero-crossing detector. Its output is then applied to one input of a dual NAND gate and  $A_2$ , the LM2917 frequency-to-voltage converter.

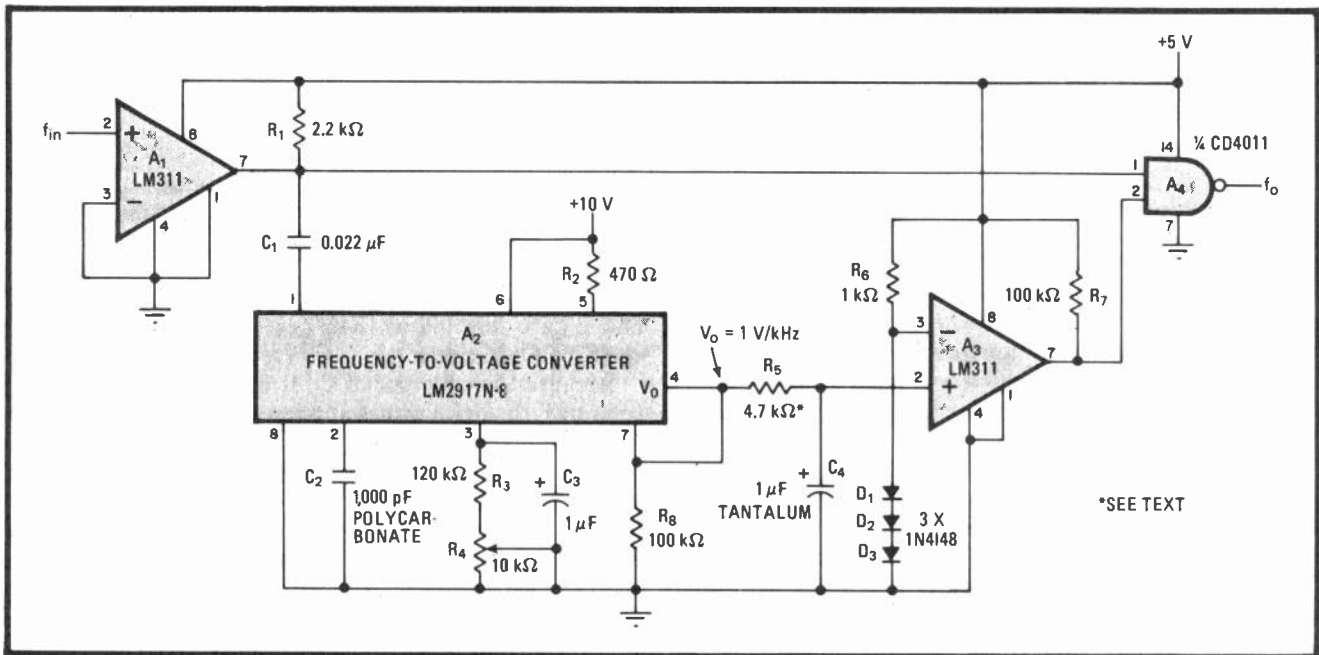
The converter, which drives the noninverting input of comparator  $A_3$ , generates an output of one volt for each

kilohertz applied at its input. Thus, when  $f_{in}$  is less than 2.1 kHz, the output of the converter is less than 2.1 volts, and  $A_3$  (whose noninverting input is biased at 2.1 v by diodes  $D_1$ - $D_3$ ) is low. Therefore, output gate  $A_4$  is disabled. If  $f_{in}$  moves above 2.1 kHz,  $A_3$  will go high and enable  $A_4$ , thereby permitting  $f_{in}$  to appear at the output.

The sharpness of the cutoff, which is determined by the transfer function of  $A_3$ , is approximately 1 Hz. The response time of the circuit is adjusted by  $C_3$  and  $R_5C_4$ . These components act to control the integration time at the output, ensuring that a steady dc voltage is attained after a nominal number of periods of  $f_{in}$ . If a fast response time is desired,  $R_5$  and  $C_4$  should be deleted.

The circuit is made to handle signals at any frequency by applying a variable control voltage at pin 3 of  $A_3$ , in lieu of the  $D_1$ - $D_3$  and  $R_6$  combination. And the discriminator can be used in other modes, to reject high frequencies, for example, or as a bandpass discriminator.

The discriminator that rejects high frequencies may be realized by simply reversing the inputs to  $A_3$ . For bandpass applications,  $A_3$  is replaced by a dual comparator, where the low- and high-cutoff frequencies are set by control voltages on the inverting and noninverting inputs of the comparators, respectively.  $A_4$  must then be replaced with a triple-input NAND gate. □

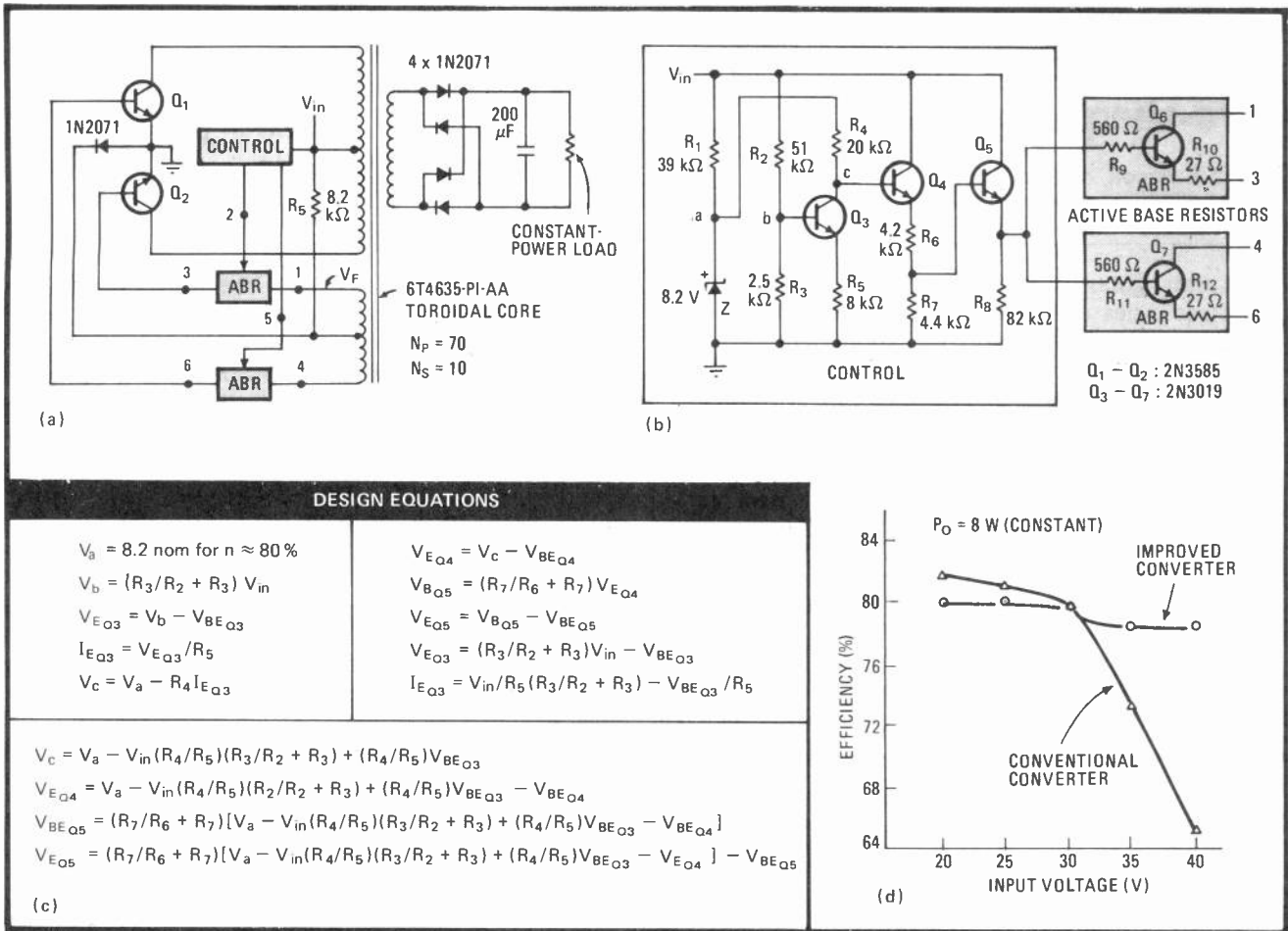


**Cycle cutoff.** Frequency-to-voltage converter and comparators combine simplicity and selectivity in this frequency discriminator. Transfer function of LM311 determines sharpness of cutoff, in this case being 1 hertz. Circuit can be made to handle signals at any frequency if variable voltage is introduced at pin 3 of  $A_3$ . Discriminator, configured in high-pass mode, can easily be modified for low-pass or bandpass duties.

# Dc-dc converter maintains high efficiency

by P. R. K. Chetty, Department of Electrical Engineering, California Institute of Technology, Pasadena

A simple control circuit enables this design to overcome the major drawback of the conventional dc-dc converter—its inability to maintain high efficiency over a wide range of input voltages. Varying the base drive to the converter's power-switching transistors as the inverse square of input voltage in order to achieve a near-constant ratio of output power to circuit losses, this unit attains efficiencies of 78% to 80% for  $20 < V_{in} < 40$ .



**Leveled.** High efficiency of conventional dc-dc converter (a) is maintained with control circuit (b) that generates base drive to switching transistors  $Q_1$ - $Q_2$  in inverse proportion to input voltage. Equations (c) aid design. Typical performance (d) is plotted.

In the ordinary converter (a), which would not include the control block shown and where a fixed resistor,  $R_b$ , would be substituted for the active-base-resistor block, an increase in  $V_{in}$  causes efficiency,  $n$ , to drop off as the inverse of the square of input voltage. As may be seen, this loss results because:

$$R_b = V_F/2I_b = [V_F n(V_{in} - V_{ce\text{sat}})hfe_{min}]/2P_o$$

and  $V_F = K V_{in}$ , where  $R_b$  is selected to drop half of the feedback voltage,  $V_F$ ,  $P_o$  is the desired output power,  $V_{ce(sat)}$  and  $hfe_{min}$  are the collector-to-emitter drop and current gain, respectively, of either power transistor, and  $k$  is a constant dependent on the turns ratio. Thus, combining the two equations above, it is realized that  $n$  is approximately equal to  $1/V_{in}^2$ , keeping other variables constant.

It can be further shown that if  $R_b$  is made to vary as approximately  $V_{in}^2$ , the efficiency will be a maximum at any given input voltage. Equivalently, efficiency will be maximum if the base drive to the switching transistors  $Q_1$ - $Q_2$  is made inversely proportional to  $V_{in}$ .

Although the circuit required to exactly satisfy Eq. 1 would be complex, a relatively simple configuration (b) will provide acceptable performance when it is added to the basic converter. Here, a three-transistor controller (component values given for  $P_o = 8 \text{ w}$ ) and two active-base-resistor networks drive  $Q_1$ - $Q_2$ .

As  $V_{in}$  increases, the voltage at point b increases.  $R_2$  and  $R_3$  are selected so that  $V_b$  is about 1 volt at  $V_{in\text{min}}$ , enabling  $Q_3$  to operate in active region.

Because the collector of  $Q_3$  is biased from a reference (point a), the drive signal applied to  $Q_4$  is a function only of the voltage applied to  $Q_3$ 's base. When the voltage at point B increases, the potential at point C decreases. Thus  $Q_4$ - $Q_5$ , biased in its nonlinear  $i_b$ - $e_c$  region, 'drives' switching transistors  $Q_1$ - $Q_2$  through  $Q_6$ - $Q_7$  with less base current. As a result, the resistance between points 1-3 (and 4-6) will vary approximately as  $V_{in}^2$ .

Only one operating variable must be determined empirically, the voltage at the base of  $Q_5$ ,  $V_{B_{Q5}}$ . Breaking the circuit at this point to connect a variable-voltage source, the user sets  $V_{in}$  to its minimum expected value. The variable-voltage source is then set to saturate  $Q_1$  and  $Q_2$  for a constant  $P_o$ , and its value ( $V_{b1}$ ) noted. The procedure is repeated to find  $V_{b2}$  for  $V_{in\text{max}}$ .

Now the design procedure may be initiated using the equations in (c) to determine  $R_6$  and  $R_7$ , given that  $V_{E_{Q5}}$  equals  $V_{b1}$  at  $V_{in\text{min}}$  and is equal to  $V_{b2}$  at  $V_{in\text{max}}$ . Experimental results for  $P_o = 8, 15 < V_{out} < 35$  and  $20 < V_{in} < 40$  are tabulated (d) versus the performance of a conventional converter. □

# Hall-probe adapter converts DMM into gaussmeter

by Henno Normet  
Diversified Electronics, Leesburg, Fla.

Using a constant-current dc source to maintain the specified accuracy of a Hall probe, this circuit adapts a 3½-digit multimeter for measuring magnetic flux density. The DMM can thus be made to measure densities of 20 kilogauss or more with a resolution of 10 gauss, and this accuracy is more than adequate for all but low-level leakage checks.

The current source built around the 723 voltage regulator will deliver upwards of a constant 50 to 210 milliamperes to the Hall probe (F. W. Bell BH-705 or Siemens FA22e, etc.), ensuring that the internal resistance of the probe, which changes with the field strength encountered, has little effect on the accuracy of the measurement. The linearity of the voltage-versus-flux response will be dependent on the probe's load resistor,  $R_1$ , whose value will be a function of the type of probe used (see individual data sheets).

Typical values will range from 3 to 10 ohms. Even with an optimum load, however, most probes will become nonlinear above 10 kilogauss, and at 15 kilo-

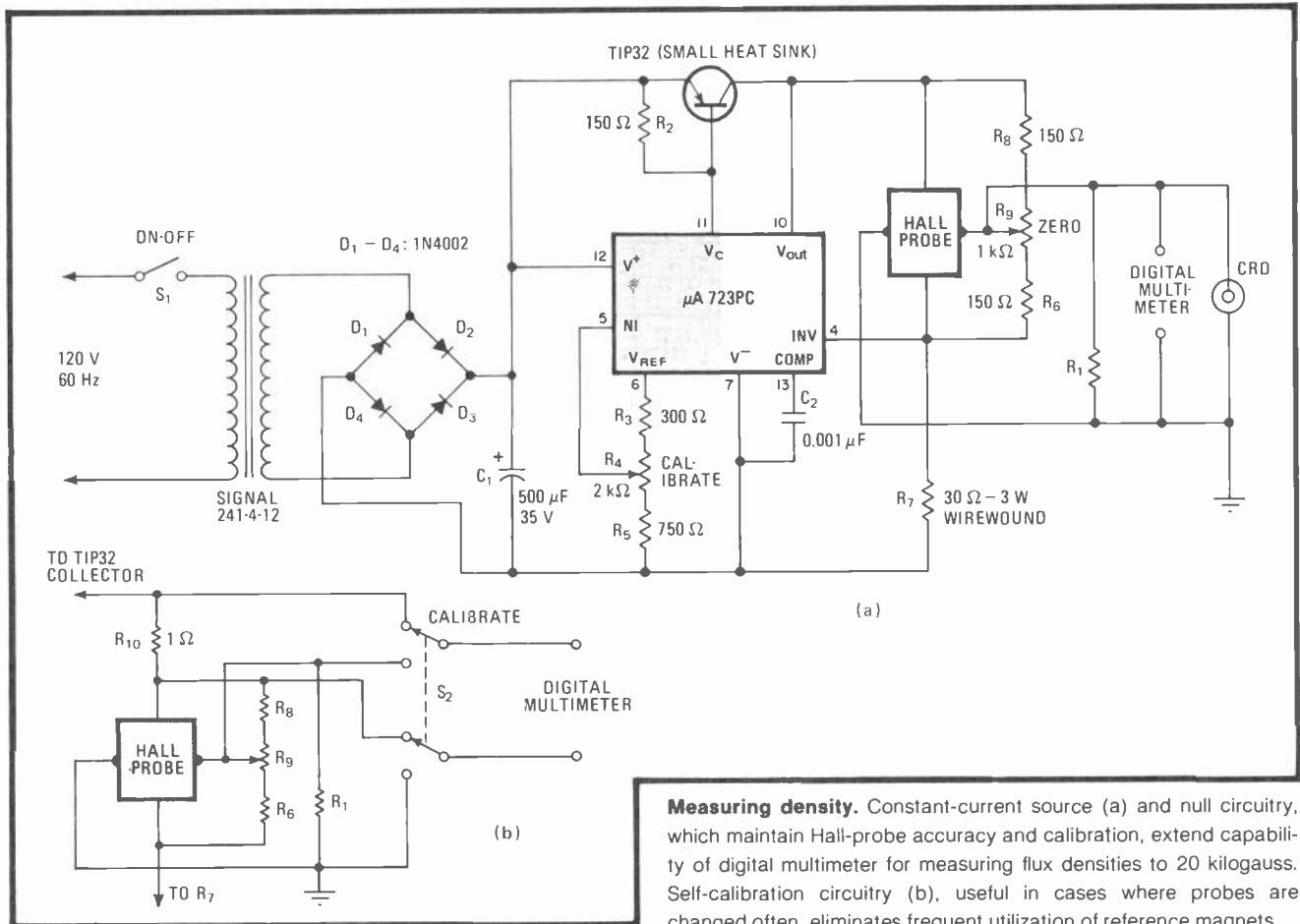
gauss the error is considerable. High-flux-density probes are available at increased cost.

To calibrate the adapter, the DMM is set to its 200-millivolt dc range. With the probe isolated from any magnetic field, potentiometer  $R_9$  is adjusted for a zero reading on the DMM. The probe is brought into the field of a calibrated reference magnet, and potentiometer  $R_4$  is adjusted so that the DMM displays a matching value. At these settings, the probe will deliver exactly 10 mv per kilogauss of flux density measured.

The adapter, in conjunction with an oscilloscope, will measure and display ac or pulsed fields; recalibration is not necessary. When used with a scope set for a vertical-channel gain of 10 mv per centimeter, the vertical axis calibration will be 1 kilogauss/cm.

A self-calibration feature that permits the unit to be calibrated without a reference magnet (after the initial adjustment) may be secured by adding a current shunt in the control-current circuit, plus a double-pole, double-throw switch, as shown in (b). This feature is useful when Hall probes are changed frequently.

Calibration is simple. Once the calibration constant for any given probe is determined (see the procedure above), it is only necessary to set switch  $S_2$  in the calibrate position and adjust  $R_4$  for an identical reading on the DMM when that probe is employed. □



**Measuring density.** Constant-current source (a) and null circuitry, which maintain Hall-probe accuracy and calibration, extend capability of digital multimeter for measuring flux densities to 20 kilogauss. Self-calibration circuitry (b), useful in cases where probes are changed often, eliminates frequent utilization of reference magnets.

# Autocorrecting driver rights pulse polarity

by Shlomo Talmor  
Hartman Systems, Huntington Station, N. Y.

This circuit provides positive-going output pulses for corresponding input signals of either polarity without the need for any manual intervention (that is, polarity switches). Utilizing a simple RC integrator, the unit automatically propagates positive-going signals having a duty cycle of less than 50% through to the output and inverts signals that have a duty cycle of greater than 50%, or are negative-going. The circuit is particularly useful in instrumentation and test-facility applications, where the polarity of the signal emanating from a port is often both positive- and negative-going at different stages of a complicated test sequence.

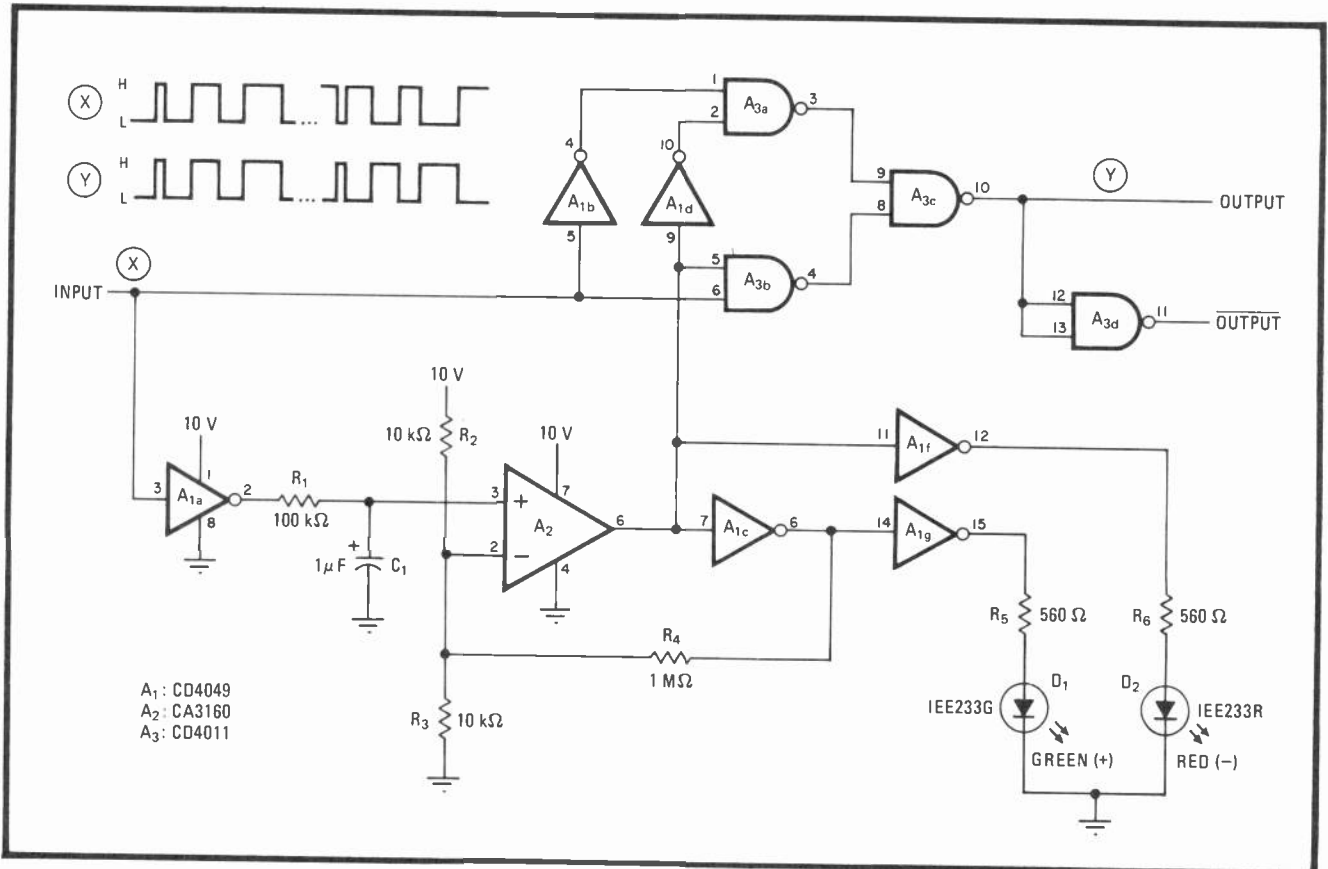
As shown in the figure, input pulses having a width and rate in the range of 1 microsecond to 1 millisecond are applied through inverter  $A_{1a}$  to integrator  $R_1C_1$ , thereby developing a dc voltage across the capacitor.

Thus, operational amplifier  $A_2$  goes high for positive-going input pulses having a duty cycle of less than 50%.  $A_{1b}$  and  $A_{1d}$ , along with NAND gates  $A_{3a}$  to  $A_{3c}$ , therefore propagate the input signal through to the output without an inversion.

If the duty cycle is greater than 50%, or if the incoming pulses are negative-going, the voltage developed on the integrating capacitor will be below 5 volts, which is the potential applied to the inverting input, and  $A_2$  goes low.  $A_{1b}$ ,  $A_{1d}$ , and  $A_{3a}$  to  $A_{3c}$  then act to invert any negative-going wave at the input to a positive one at the output and vice versa. In the case where the duty cycle is 50%, inverter  $A_{1c}$  provides the necessary hysteresis to  $A_2$  for proper switching.

Light-emitting diodes  $D_1$  and  $D_2$ , with  $A_{1f}$  and  $A_{1g}$ , provide visual indication of pulse polarity. Both the red and green diodes will light softly when the input signal has a duty cycle approximating 50%.

The range of the pulse width handled can be extended, at the expense of a lower rate, by increasing  $R_1$ . The response time of the circuit will of course be lowered. The supply voltage can vary from 5 to 15 volts, but if it is less than 7.5 v, a 15-kilohm resistor should be placed in series with pin 6 of  $A_2$  in order to properly drive the rest of the circuit. □



**Switch.** Three-chip driver accommodates both positive- and negative-going input signals, converting them both into positive-going output. Circuit propagates positive-going signals having a duty cycle less than 50% through to the output while inverting all other signals.

# Magnetic levitator suspends small objects

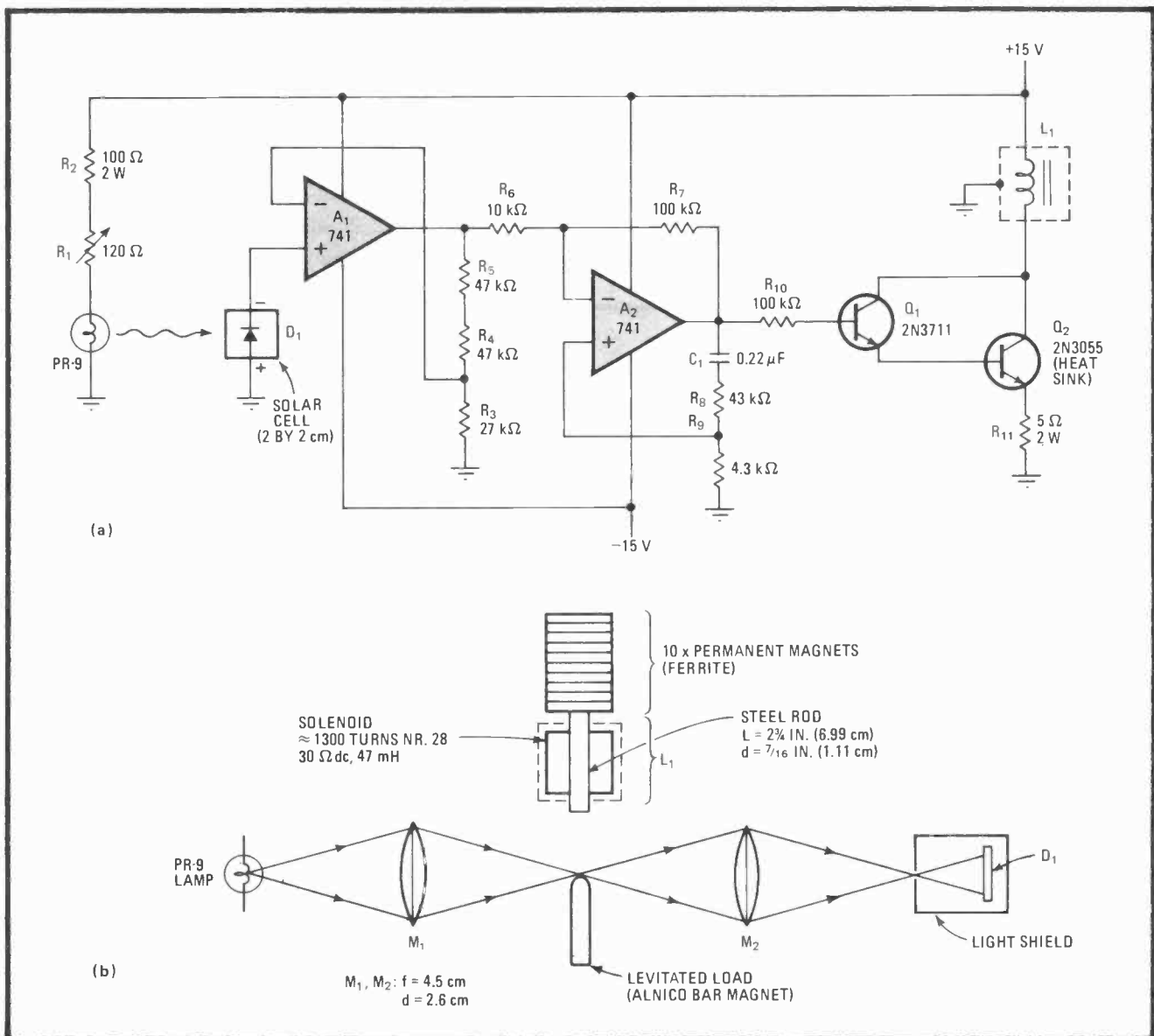
by Bob Leser  
Desert Technology, Las Cruces, N. M.

This circuit is a modern solution to the problem of securing frictionless bearings for small rotors and levitating small magnetic objects a few millimeters in space. Operational amplifiers replace the tubes used in earlier approaches, and an optical arrangement replaces the radio-frequency induction circuit originally used to position the object.

Potentiometer  $R_1$  (a) sets the current through the PR9 lamp and thus its brightness and the gain of the position-sensing circuit.  $R_1$  thus provides a fine adjustment of the

position of the magnetic object that is suspended beneath the levitation coil  $L_1$ . The optical position-sensing circuitry (b), which should be mounted horizontally under  $L_1$  if possible, includes two lenses to focus the beam via the levitated load to solar cell (photodetector)  $D_1$ . The light shield, with an aperture of approximately 3 millimeters, effectively eliminates background light. The suggested focal lengths and lens diameters are shown; as a check on the optics system, the beam should be aligned to yield a short-circuit current of 4 to 25 microamperes in  $D_1$ .

As for the basic circuitry,  $D_1$ 's output is amplified by about 5 by operational amplifier  $A_1$  and is then introduced to  $A_2$ , which is the all-important servo-loop stage.  $C_1$ ,  $R_8$ , and  $R_9$  provide positive feedback of the high-frequency components of the positioning signal. The stage thus generates the voltage derivative of the amp's output, preventing oscillations in the closed loop that would otherwise occur because of the lack of damping in



**Rising rotors.** Levitator circuit (a) suspends 1-in. steel spheres up to 2 1/2 millimeters off reference surface. Optical arrangement (b) sets object distance. Details of levitation coil construction are outlined. Permanent magnets set ultimate levitation range.

the position servo portion of the circuit. Any closed-loop oscillation will be manifest as vibration of the levitated object.

Output stage  $Q_1$  to  $Q_2$  is a discrete darlington pair that drives  $L_1$ . The coil itself has 1,300 turns around a steel rod 2.75 inches long and  $\frac{7}{16}$  in. in diameter. A stack of 10 small permanent magnets atop the coil provides a bias field extending the range of levitation beyond that which would be normally attained. The coil is surrounded by a grounded shield to reduce the amount of stray coupling

to the op amp inputs.

The most stable closed-loop condition is set by adjusting  $Q_2$ 's collector voltage to about 7.5 volts by altering the levitation distance between the sensing optics and  $L_1$ . Levitation distances in this circuit range from about 20 millimeters for a small Alnico bar magnet to  $2\frac{1}{2}$  mm for a steel ball with a diameter of 1 in.  $\square$

## C-MOS counter sets divider's modulus

by Arie Shavit  
Kiriati Tivon, Israel

The cost and power consumption of Albing's C-MOS variable-modulo divider<sup>1</sup> can be reduced even further with this circuit, which uses logic gates and four low-cost binary switches to replace one counter and the multiple-pole selector, respectively. Although the counter's modulus is set with the binary elements, thereby sacrificing the convenience of ordering up values in the familiar decimal form, the ease of interfacing the counter to

microprocessor-based control systems is immensely enhanced. Divider ratios of from 1 to 16 can be selected.

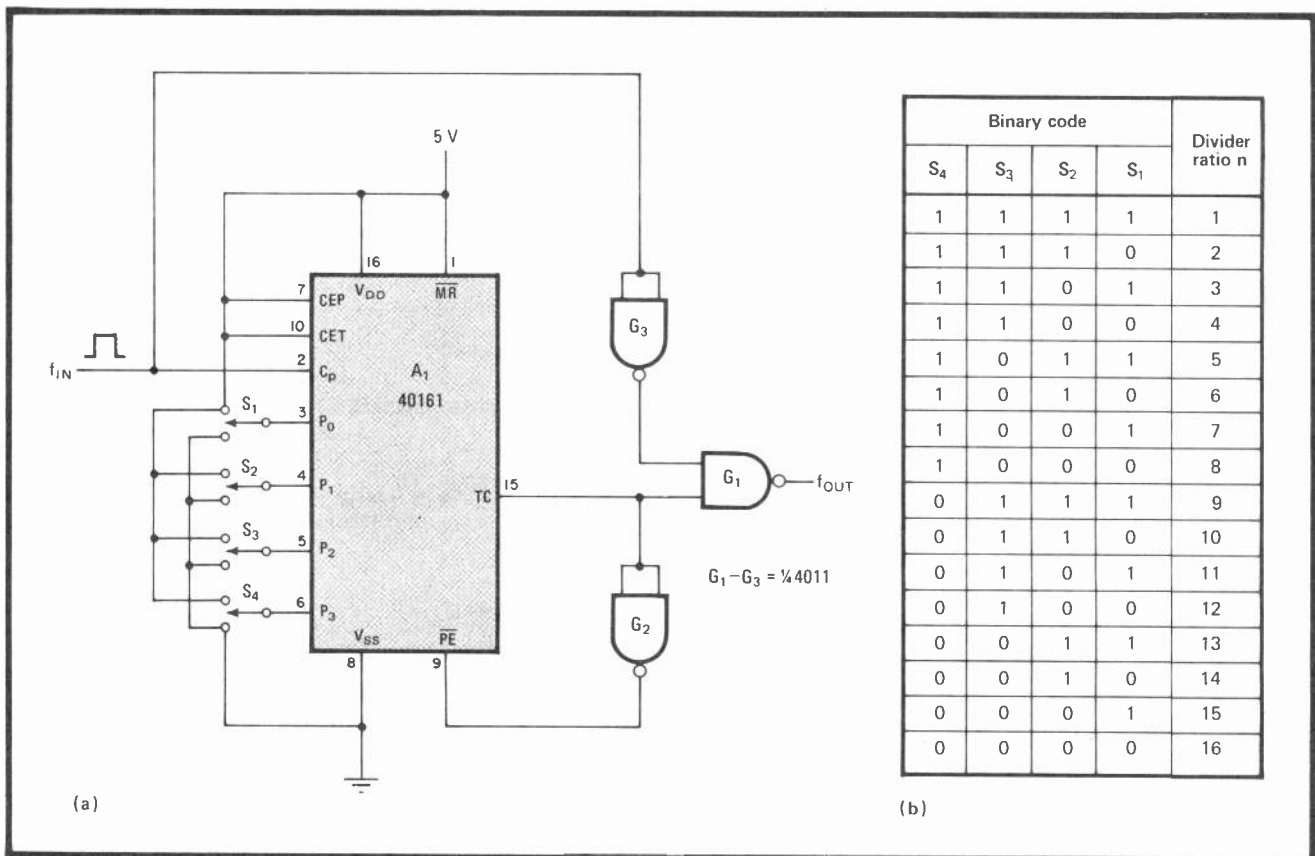
The 40161 synchronous binary counter,  $A_1$ , which has parallel-load capability, is stepped by input frequency  $f_{in}$ , as shown in (a). Switches  $S_1$ - $S_4$  set the binary representation of  $16-n$  at the parallel-load inputs  $P_0$ - $P_3$ , where  $n$  is the desired divider ratio, as shown in (b).

Output pin TC of  $A_1$  moves high after  $n$  cycles of  $f_{in}$ . Thus the output signal from gate  $G_1$  is a pulse of short duration having a frequency of  $f_{out} = f_{in}/n$ . TC is then inverted by gate  $G_2$  and used to reset the counter.

Gate  $G_3$  comes into play if a modulus of 1 is set. Under these conditions, TC remains high and  $f_{in}$  serves to gate itself to the output.  $\square$

### References

1. Bradley Albing, "C-MOS counter-decoder pair sets divider's modulus," Aug. 30, 1979, p. 140.



**Binary breakup.** Single counter and three gates simplify design of variable-modulo divider (a). Binary switches  $S_1$ - $S_4$  set counter to  $16-n$ , where  $n$  is desired divider ratio (b). Output of gate  $G_1$  is a pulse with a frequency equal to  $f_{out} = f_{in}/n$ , for  $1 \leq n \leq 16$ .



# Foldback limiter protects high-current regulators

by A. D. V. N. Kularatna  
Ratmalana, Sri Lanka

This circuit provides foldback protection for a series-regulated source that has to deliver high current. Because it requires no current-monitoring resistor, the circuit achieves wide dynamic response at good efficiency. It draws only 2% of maximum load current and its cost is reasonable.

Here, a low-current shunt-regulated module (a) provides the overload protection. This module is config-

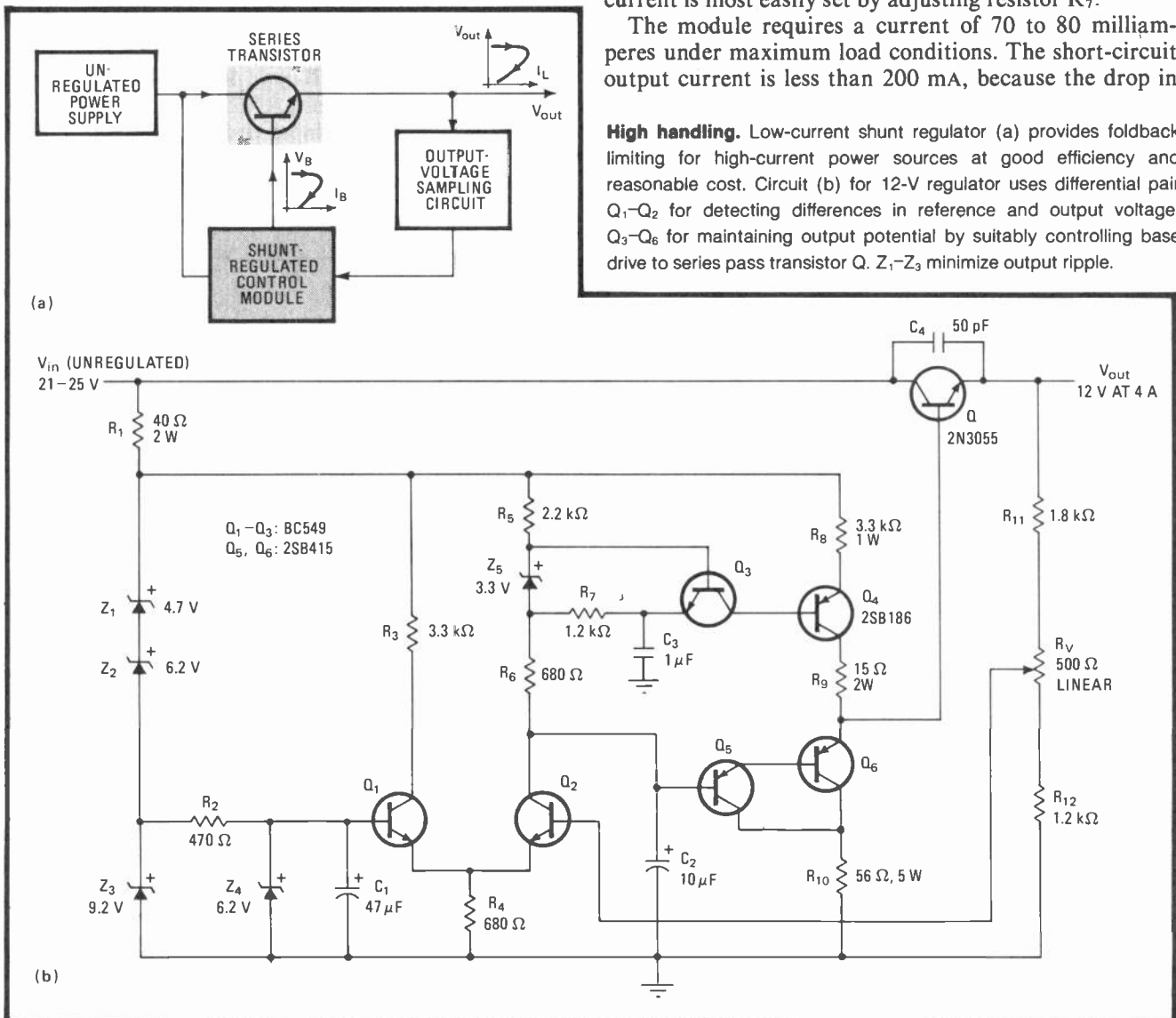
ured into the conventional regulator system to work as a switch, in which role it quickly turns off a series-pass transistor when the load current exceeds some predetermined value.

The circuit details are explained with the aid of the diagram (b) for a representative regulator designed to deliver 12 volts at 4 amperes. Transistors  $Q_1$  and  $Q_2$  form a differential amplifier, which compares a 6.2-v reference to a potential derived from the 12-v output through potentiometer  $R_V$ . Shunt elements  $Q_5$ - $Q_6$  act to maintain the potential at the base of  $Q$  constant for any load condition by taking up the difference between the set and the actual base drive.

It is necessary that the current source  $Q_3$ - $Q_4$  be set to  $I_L/h_{fe}$  for proper tracking, where  $I_L$  is the maximum load current and  $h_{fe}$  is the current gain of  $Q$ . The value of the constant current,  $I$ , is  $h_{fe}Q_4(V_{Z5} - V_{beQ3})/R_7$ , so that the current is most easily set by adjusting resistor  $R_7$ .

The module requires a current of 70 to 80 milliamperes under maximum load conditions. The short-circuit output current is less than 200 mA, because the drop in

**High handling.** Low-current shunt regulator (a) provides foldback limiting for high-current power sources at good efficiency and reasonable cost. Circuit (b) for 12-V regulator uses differential pair  $Q_1$ - $Q_2$  for detecting differences in reference and output voltage,  $Q_3$ - $Q_6$  for maintaining output potential by suitably controlling base drive to series pass transistor  $Q$ .  $Z_1$ - $Z_3$  minimize output ripple.



output voltage switches transistor  $Q_2$  off. The voltage across zener diode  $Z_5$  is then reduced to a very low value, and this action in turn lowers the voltage at  $Q_6$  and cuts down the base drive to  $Q$ .

Zener diodes  $Z_1$ - $Z_3$  were added to improve the ripple

characteristics of the supply. As configured, the source has an output ripple of 6 mV peak to peak.

The shunt regulator module can be easily configured for any output voltage mainly by selecting the appropriate zener-diode values. □

## Remote controller sets universal motor's speed

by Hari Herscovici  
Cordis Corp., Miami, Fla.

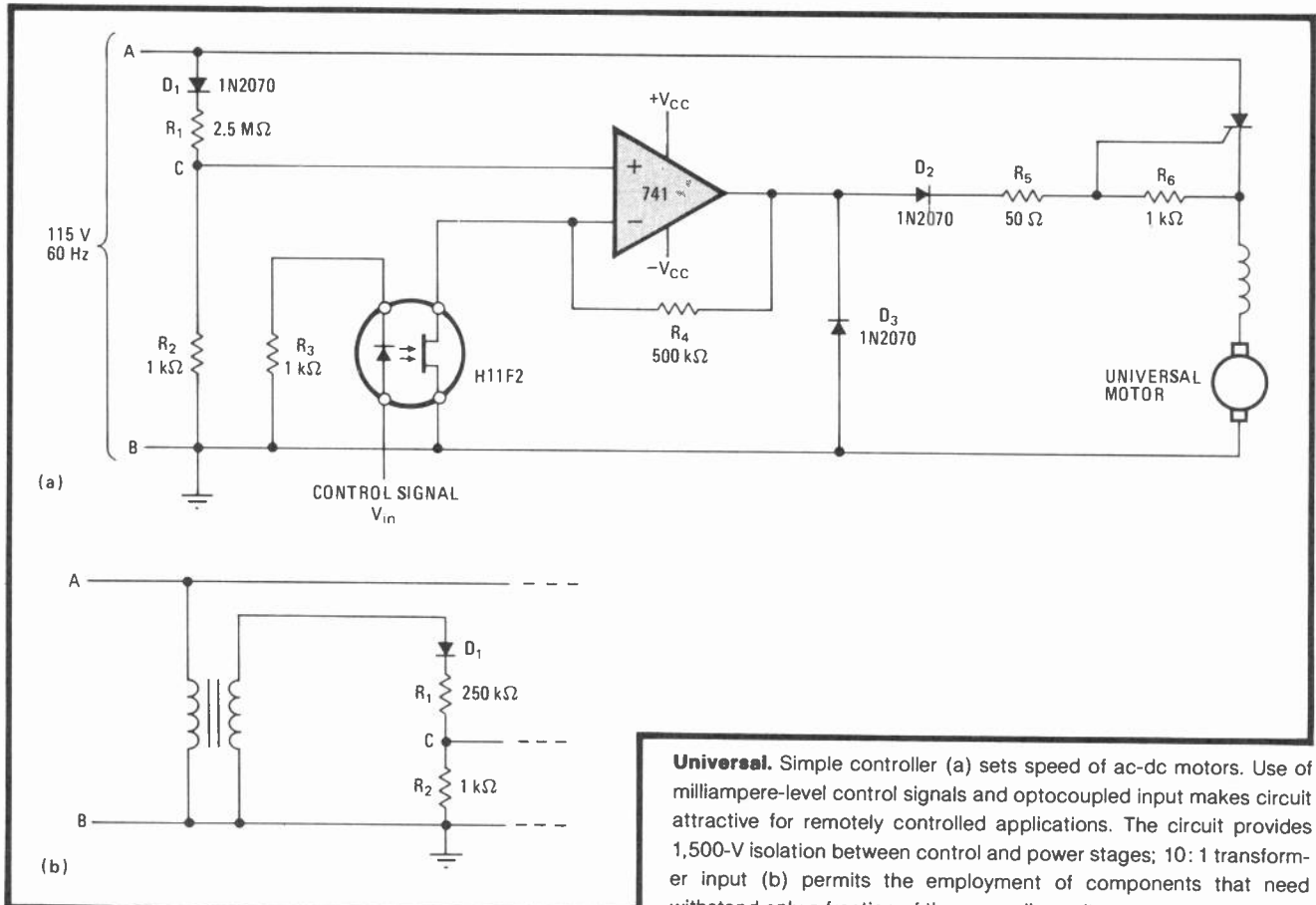
The speed of an ac-dc motor is easily set with this circuit. Millivolt-level input voltages drive its variable-speed control amplifier through an optocoupler that is isolated from the rest of the circuit to permit its use in remotely controlled applications.

Control signals in the range of 0 to 3 volts are applied to the optoisolator (GE H11F2) as shown (a). The resistance between the drain and source of the device's

field-effect transistor varies with input voltage  $V_{in}$ , and so the gain of the 741 operational amplifier, which amplifies the rectified 60-hertz power-line input, is controlled accordingly.

When the instantaneous output of the op amp is greater than the motor's counter electromotive-force voltage, diode  $D_2$  conducts and thus the silicon controlled rectifier is switched on. Power is thereby applied to the motor. The greater the difference between the op amp's output and the counter emf voltage at any instant, which indicates motor speed is lower than programmed, the earlier in the cycle the trigger pulse to the SCR occurs.

Diode  $D_1$  and resistors  $R_1$  and  $R_2$  have been selected so that the circuit will withstand a reverse voltage of 200 v. If a transformer-based input circuit (b) is substituted, however, it is only necessary for  $D_1$  to have a reverse-breakdown value of 20 v. □



**Universal.** Simple controller (a) sets speed of ac-dc motors. Use of milliampere-level control signals and optocoupled input makes circuit attractive for remotely controlled applications. The circuit provides 1,500-V isolation between control and power stages; 10:1 transformer input (b) permits the employment of components that need withstand only a fraction of the power-line voltage.

# High-voltage regulator is immune to burnout

by Michael Maida  
National Semiconductor Corp., Santa Clara, Calif.

The floating-mode operation of adjustable three-terminal regulators in the LM117 family make them ideal for high-voltage service. Because the regulator sees only the input-output differential—40 volts for the LM117—its voltage rating will not be exceeded for outputs in the hundreds of volts. But the device may break down if the output is shorted unless a circuit can be developed for withstanding the high voltage typically encountered and the output current is limited to a safe value in the event of a dead short.

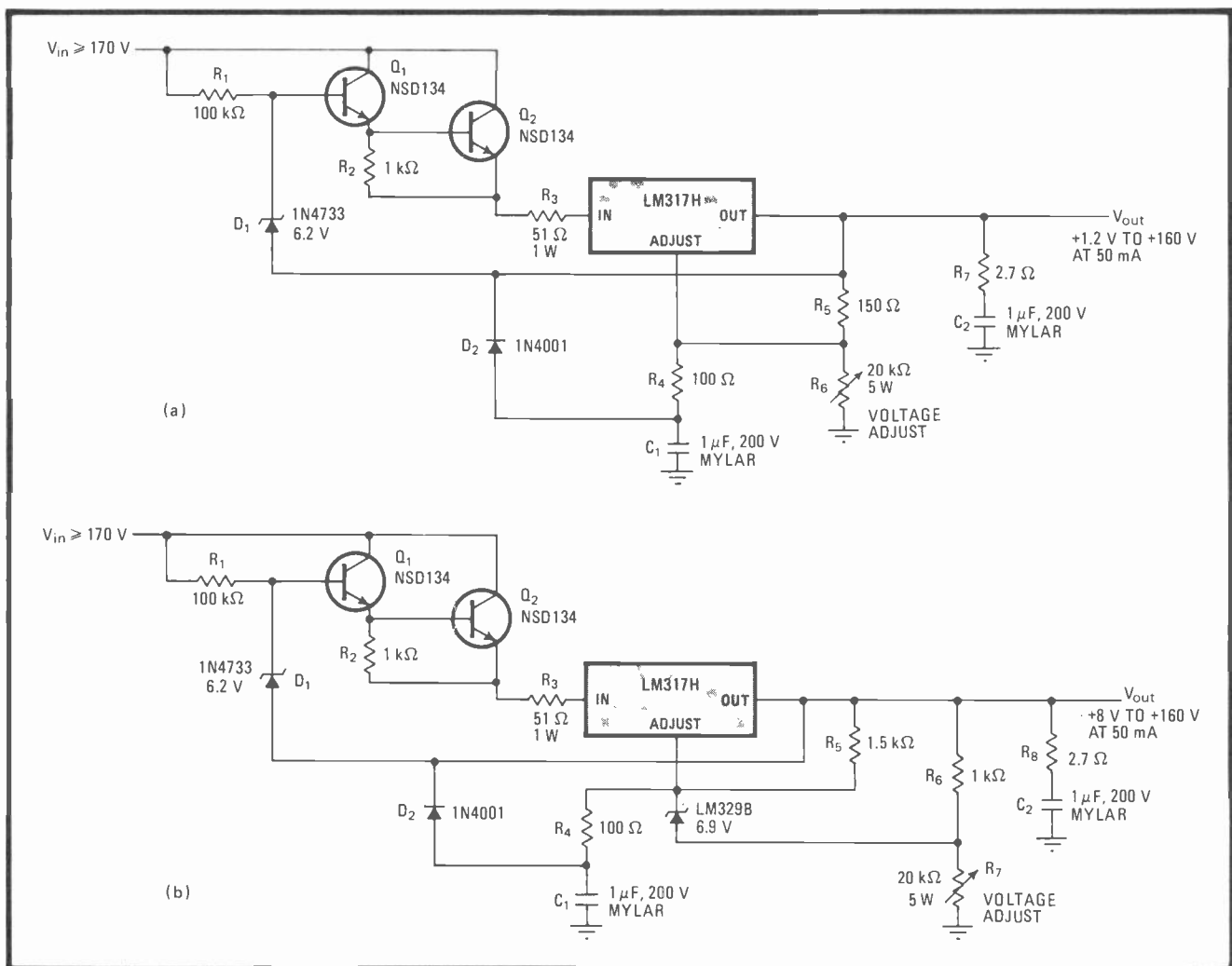
The circuit surrounding the regulator will serve to solve the problem. Zener diode  $D_1$  maintains a 5-v input output differential over the entire range of output voltages from 1.2 to 160 v. Because high-voltage transistors inherently have a relatively low  $\beta$ , a Darlington arrange-

ment is used to stand off the high input potentials.

The zener diode's impedance will be low, so that no bypass capacitor is required directly at the regulator's input. In fact, no capacitor should be used if the circuit is to survive a short at the output. Resistor  $R_3$  limits the short-circuit current to 100 milliamperes. The RC network at the output improves the circuit's transient response, as does bypassing the adjustment pin.  $R_4$  and  $D_2$  protect the adjustment input from breakdown, if there should be a short circuit at the output.

The approach shown in (b) will serve well in precision regulator applications. Here a LM329B 6.9-v zener reference has been stacked in series with the LM317's internal reference to improve temperature stability and regulation.

These techniques can be employed for higher output voltages and/or currents by either using better high-voltage transistors or cascaded or paralleled transistors. In any event, the output short-circuit current determined by  $R_2$  must be within  $Q_2$ 's safe area of operations so that secondary breakdown cannot occur. □



**Skirting shorts.** Three-terminal regulator (a), configured for high-voltage duties as a consequence of operating in the floating mode, is protected by appropriate circuitry against burnout due to shorts. LM329B zener (b) and minor changes improve stability and regulation.

# Bipolar current mirror scales, inverts signals

by Henry E. Santana  
Hewlett Packard Co., Loveland, Colo.

A pair of operational amplifiers and a few resistors build this precision current mirror. Though simple and low in cost, the circuit excels the usual designs because it not only offers true bipolar operation but also can scale and/or invert any ac or dc input signal.

Input currents are applied to op amp A<sub>1</sub>, which is biased by V<sub>ref</sub>. If I<sub>in</sub> is generated by a constant current source, V<sub>ref</sub> may be brought to zero. Otherwise, it should be set to some arbitrary value to maintain circuit bias.

A current-to-voltage converter at the input and a voltage-to-current converter at the output comprise the current mirror. As a consequence of the configuration, the voltage appearing at the output of A will thus be:

$$V_{A1} = V_{ref} + I_{in}R_1$$

for  $R_1 \gg R_2$  and  $R_L$ . The voltage applied to the output circuit is therefore:

$$V_2 - V_1 = I_{in}R_1$$

Writing the nodal equations for V<sub>L</sub>, V<sub>3</sub>, and V<sub>4</sub> yields these results:

$$I_L = -V_L(1/R_2 + 1/bR_2) + V_3(1/bR_2) + V_2(1/R_2)$$

$$V_3 = A_2(s)(V_L - V_4) = (GB/s)(V_L - V_4)$$

$$V_4 = V_1[a/(1+a)] + V_3[1/(1+a)]$$

where GB is A<sub>2</sub>'s gain-bandwidth product. Substituting V<sub>3</sub> and V<sub>4</sub> into the equation for I<sub>L</sub>, it is seen that I<sub>L</sub> = (R<sub>1</sub>/R<sub>2</sub>)I<sub>in</sub>, given that a = b and s ≪ GB/(1+b).

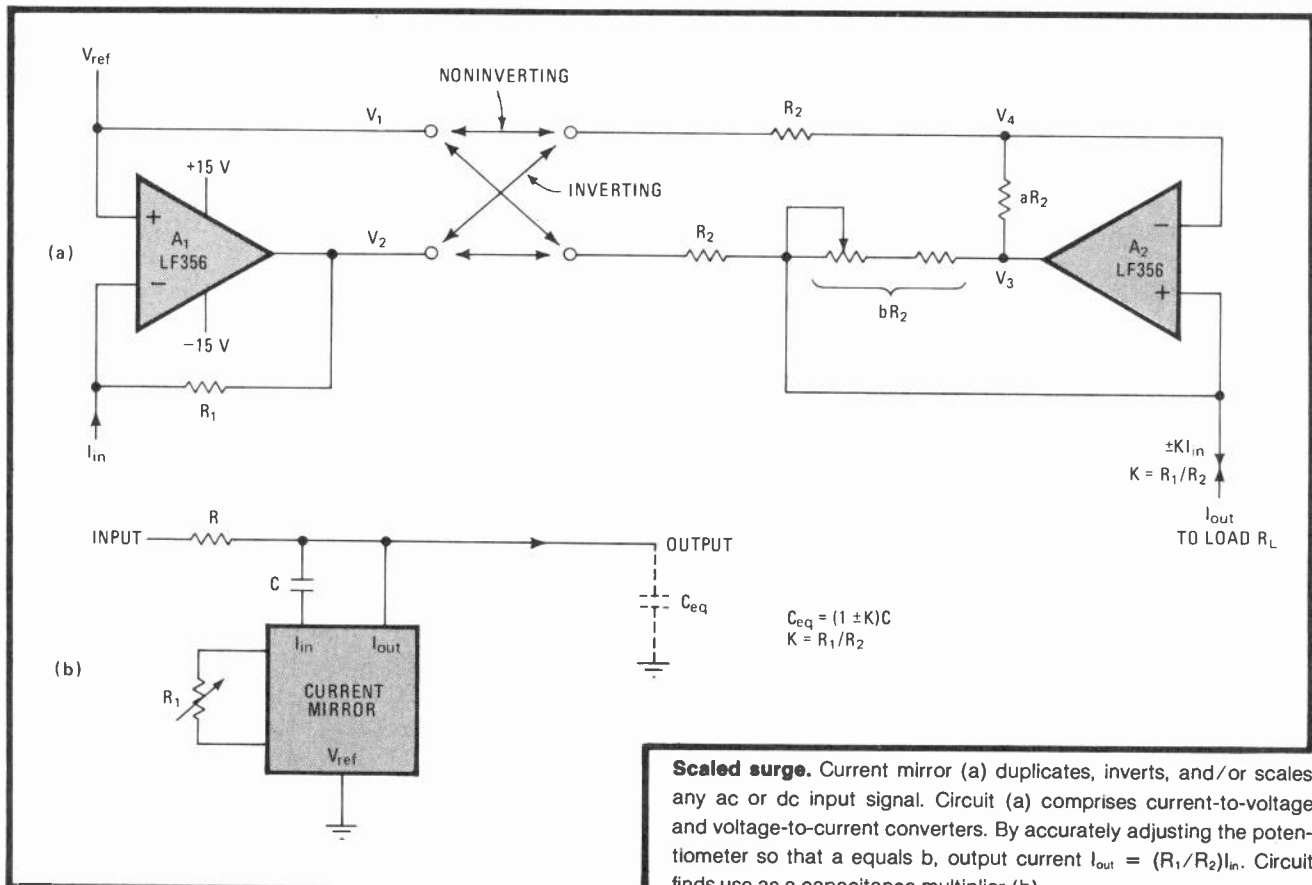
The output impedance can be set, within limits, by selection of aR<sub>2</sub> and bR<sub>2</sub>. The output impedance is:

$$Z_o(s) = \left[ \left( \frac{a}{1+a} \right) \left( s + \frac{GB}{1+b} \right) R_2 \right] +$$

$$\left[ s + \left( \frac{a-b}{1+a} \right) \left( \frac{GB}{1+b} \right) \right]$$

Since a must equal b for the circuit to work, this equation simplifies to Z<sub>o</sub>(s) = [1/(1+a)]{1 + [1/(1+a)]GB/s} R<sub>2</sub>, and no other assumptions about resistor ratios are made.

In addition to its use as a scaled current mirror, the circuit will find other not-so-obvious applications. Such an example is its use as a capacitance multiplier (b). □



**Scaled surge.** Current mirror (a) duplicates, inverts, and/or scales any ac or dc input signal. Circuit (a) comprises current-to-voltage and voltage-to-current converters. By accurately adjusting the potentiometer so that a equals b, output current I<sub>out</sub> = (R<sub>1</sub>/R<sub>2</sub>)I<sub>in</sub>. Circuit finds use as a capacitance multiplier (b).

# Digital phase shifter covers 0° to 360° range

by J. W. V. Storey  
Dept. of Physics, University of California, Berkeley

Offsetting the phase of a signal by digital means over the range of 0° to 89° in any quadrant, this low-power circuit is particularly useful in data-recovery systems that employ synchronous detectors. Unlike most RC phase shifters, the value set is independent of the input frequency.

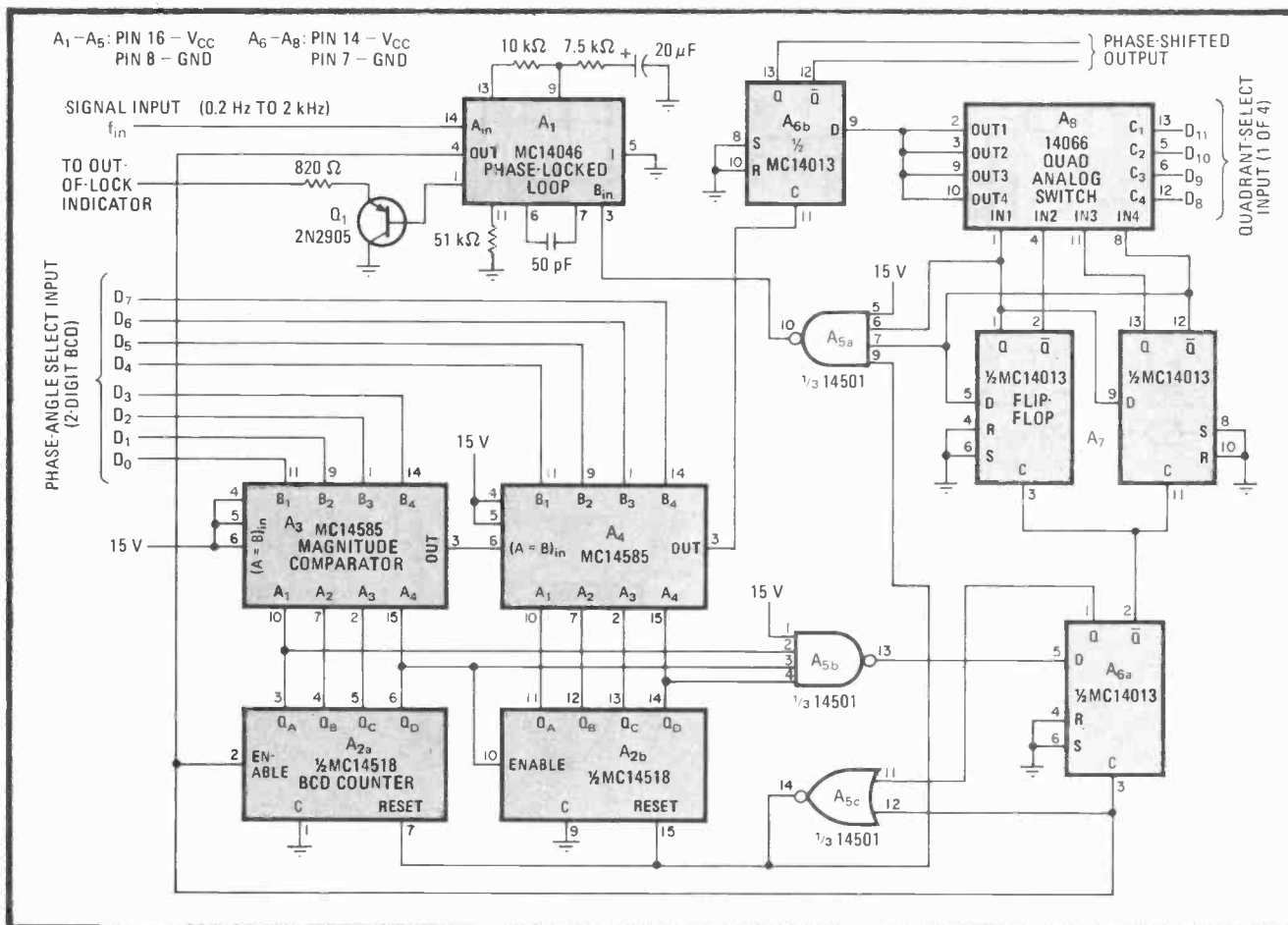
The input reference signal is first introduced to the 14046 phase-locked loop. Its output, which is set to generate a frequency 360 times that of  $f_{in}$ , is then applied to the 14518 binary-coded decimal counter, where it is divided by 10. A second, cascaded counter,  $A_2$ , divides  $A_{2a}$ 's output by 9, the 89th count of a 90-step cycle being detected by  $A_{5b}$ .  $A_2$  is then reset to zero on the 90th count by  $A_{6a}$  and  $A_{5c}$ .

The signal at the output of  $A_{6a}$  is thus at a frequency equal to  $4f_{in}$ . Flip-flop  $A_7$  performs a divide-by-four operation on this signal, at the same time generating four quadrature outputs. Meanwhile,  $A_{5a}$ , which gener-

ates one pulse per cycle of  $f_{in}$ , locks the PLL in phase with the zero count of  $A_2$ . Note that the operation of this divider chain is unaffected by the setting of the digital input lines.

The desired phase is selected by applying the appropriate digital signals  $D_0$ - $D_7$  in binary-coded decimal form. Thus, the output from  $A_3$  and  $A_4$  moves high when  $A_2$  counts to that number and clocks flip-flop  $A_{6b}$ . This action occurs four times per each cycle of  $f_{in}$ . The appropriate quadrant, available at  $A_7$ , is selected by digital inputs  $D_8$ - $D_{11}$ , the active quadrant corresponding to which one of the lines is high. Flip-flop  $A_{6b}$  thus produces a symmetrical square wave at  $f_{in}$  having a phase shift equal to the number of degrees specified plus 0°, 90°, 180°, or 270°. There is an additional phase shift of 0.5° at all settings because of the way the PLL is operated to achieve lock. The error can be eliminated by adding an inverter between the output of  $A_{5a}$  and the B input of  $A_1$ .

With the component values shown and a 15-volt supply, the circuit will operate over the range of 0.2 hertz to 2 kilohertz. Thumbwheel switches with 1-megohm pull-down resistors are used to set the phase-angle input lines. A four-position switch can be used to select the quadrant. With slight modification, the circuit will find application as a digitally controlled ignition timing system for internal-combustion engines. □



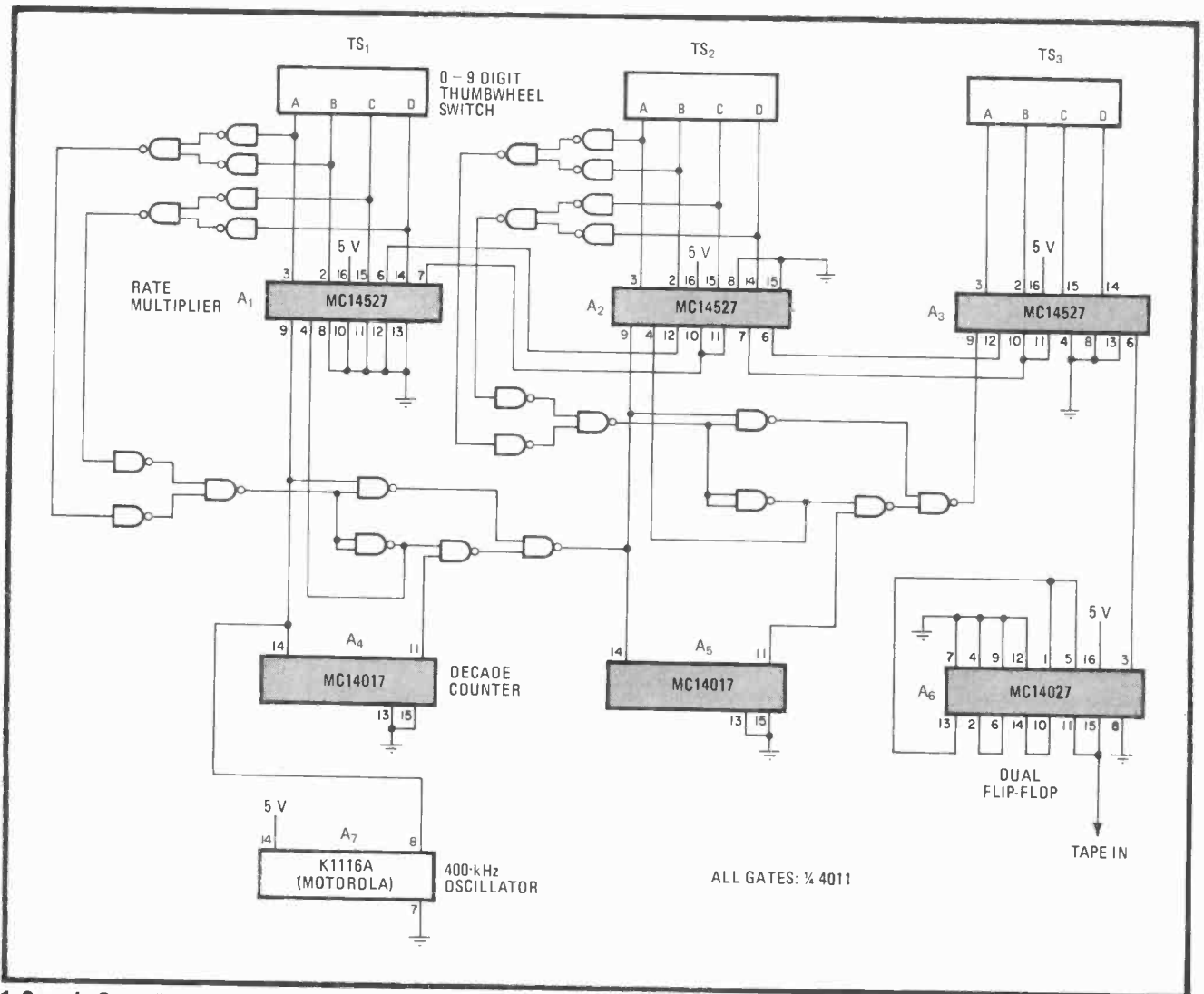
**Discrete degrees.** Circuit sets 0° to 360° phase shift of reference signal by digital means. Digital inputs  $D_0$ - $D_7$  determine displacement over 0° to 89° range,  $D_8$ - $D_{11}$  set quadrant. Output is thus 0° to 89° signal shifted by an additional 0°, 90°, 180°, or 270°.

# Frequency-marking controller indexes tape segments

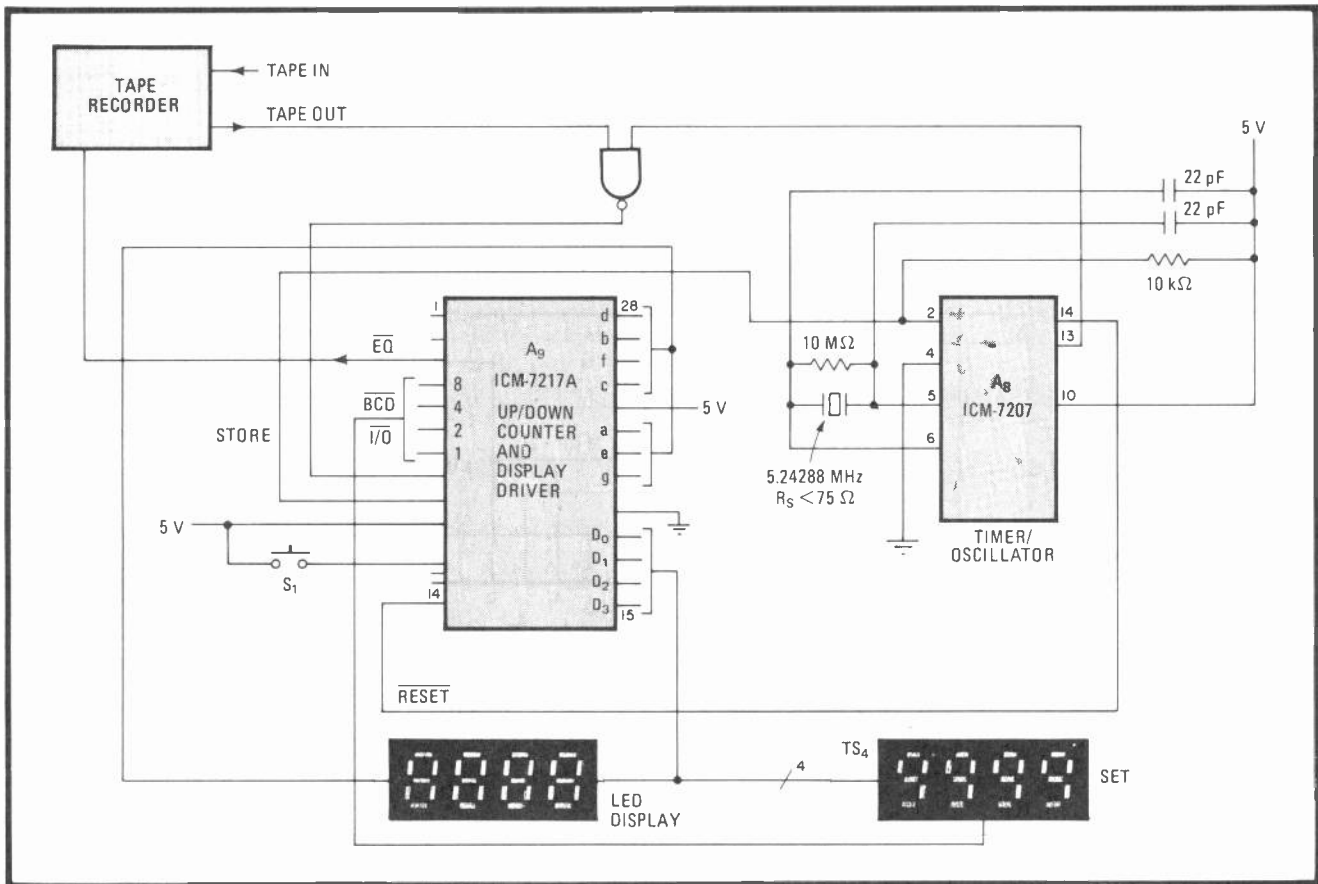
by Joe Lyle and Jerry Titsworth  
*Bendix Corp., Aircraft Brake and Strut Division, South Bend, Ind.*

Tape recorders with footage counters are virtually useless for providing accurate tape markers, mainly because of the slippage created by the electromechanical counter-capstan arrangement generally employed. This controller, which indexes the tape with a frequency-labeling technique during record and stops the recorder at any preselected point during playback, offers the user an easy way to label and isolate any desired segment.

The unit is divided into two subcircuits, for frequency synthesis and for control. In the synthesis portion, thumbwheel switches  $TS_1$ - $TS_3$  are used to set the desired frequency that is to be placed on tape. The 14527 rate multipliers  $A_1$ - $A_3$  and their associated gates multiply the output of the K1116A oscillator by 0.001 to 0.999, thereby delivering frequencies in the range of 400 hertz to 399 kilohertz, in 400-Hz steps, to the input of the divide-by-four flip-flop. Thus, frequencies from 100 Hz to 99.9 kHz (100-Hz steps) are presented to the tape recorder. Because of the audio response of the typical recorder and the limits of the readout circuit used, frequencies of up to 9,900 Hz can be placed on tape. Thus the user may introduce a report number or test number with a frequency burst of selectable duration that directly corresponds to that test (that is, a frequency of 400 Hz will mark the start of test number 400).



**1. Search.** Controller performs frequency labeling and searching functions to mark, isolate tape segments, respectively. Frequency synthesis portion injects tape markers over range of 100 Hz to 99.9 kHz, in 100-Hz steps.



**2. Retrieve.** Control portion compares number corresponding to frequency selected to that generated by tape on playback, halts recorder when both are equal. TS<sub>4</sub> sets the test number to be retrieved. LED display provides real-time readout of frequency measured.

The desired test is easily isolated on playback with the aid of the 7217A up-down counter/display driver, which is located in the control portion of the circuit. Thumb-wheel switch TS<sub>4</sub> is used to set the test number at which the recorder is to be halted.

Pressing switch S<sub>4</sub> loads the corresponding number into the device's on-board register. As the tape advances during playback, the 7217, which serves as a frequency

counter, compares the gated output of the recorder with the number that has been preset. The 7207A provides a 1-second gating time, after which it resets the 7217A's counter to zero. The LED display provides a real-time readout of the frequency measured.

Thus the equal (pin 3) output of the counter moves low if the tone matches the preset number. This signal is used (with appropriate logic) to halt the recorder. □

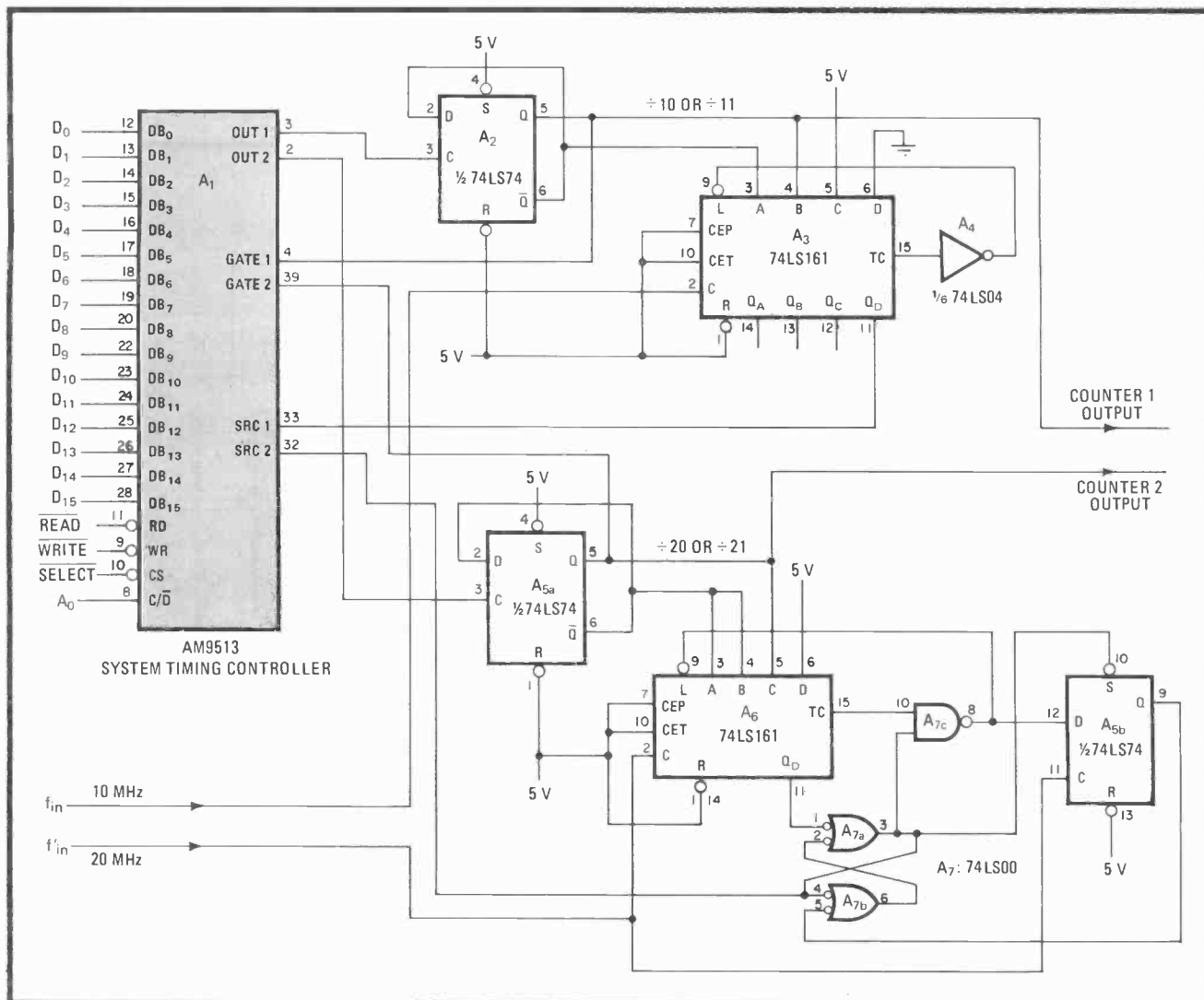
## High-frequency operation with the AM9513 controller

by Terence J. Andrews  
Vega Precision Laboratories, Vienna, Va.

The maximum source frequency of the Advanced Micro Devices' AM9513 system timing controller may be extended from 7 MHz to 20 MHz with this circuit. By

resolving timing intervals to 50 nanoseconds, the circuit significantly enhances the 9513's usefulness as a multiple programmable frequency divider. The improvement relies on the concept of swallow counting,<sup>1</sup> whereby the controller is made to operate synchronously with an external high-frequency clock. In particular, this circuit illustrates how the controller is configured to provide frequency division at 10 and 20 MHz as an example.

Here, the resolution obtained by either 10- or 20-MHz clocking can be selected as desired. A<sub>2</sub>-A<sub>4</sub> achieve operation at 10 MHz. Register 1 of the 9513 is first loaded via its 16-bit data bus with 01F5<sub>16</sub>, which instructs the



**Resolving divisors.** Swallow-counting improves resolution of AMD's 9513 system timing controller, thereby permitting pulse-train division at high frequency. Contents of the controller's load and hold registers set the divisor. Operation at 10 or 20 MHz can be chosen.

device to utilize incoming signals at pin 33 (SRC<sub>1</sub>) as its system clock and pin 4 (gate 1) to select either the device's hold or its load register for reloading each of the unit's five 16-bit counters upon receipt of a terminal count.<sup>2</sup> Counter 1 counts down in binary-coded-decimal fashion, with the contents of the load and hold registers determining the divisor.

In this application, only counters 1 and 2 of the device are used. Counter 1 begins to count down from a preset number on the rising edge of SRC<sub>1</sub>. SRC<sub>1</sub> in turn is driven by the 10-MHz clock through frequency divider A<sub>3</sub>. A<sub>3</sub> is programmed as a 10's complement counter and divides  $f_{in}$  by either 10 or 11.

However, counter 1 is loaded with the contents of the load register if Q of toggled flip-flop A<sub>2</sub> (and thus gate 1) is low; otherwise, the contents of the hold register are loaded into counter 1. Thus when counter 1, which holds the contents of the load register, steps down to zero, A<sub>2</sub> orders A<sub>3</sub> to divide by 10; when the counter steps down from a value preset by the hold register, division is by 11. Because in this feedback arrangement there is a change of state at OUT 1 each time the counter reaches 0, it is

seen that the contents of both the load and hold registers determine when A<sub>2</sub> is toggled and thereby determine the divisor. Although the numbers loaded into the hold and load registers of the timing controller are in the BCD form, the AM9513 can be programmed to count binary numbers as well.

To determine the divisor, N, multiply the contents of the hold register by 11 and the load register by 10 and add the results. Because the loading of 0001 into either register will cause improper operation, 0011 must be used instead. For example, if division by 301 is desired, the hold register should be loaded with 0011 (not 0001) and the load register with 0018 (not 0029). If 0000 is loaded into either register, a divisor of 10,000 will be the result. □

#### References

1. The TTL Applications Handbook, "Swallow Counters," Fairchild Camera and Instrument, August 1973.
2. AM9513 Applications Sheet, Advanced Micro Devices, 1979.



# Removing residual voltage in dc generator

by C. W. Bray  
*Memphis State University, Memphis, Tenn.*

The dc gain ( $E_g/E_f$ ) of a separately excited generator is an important parameter in its computer model or transfer function. However, direct measurement of this gain is often obscured by residual magnetism in the armature. The magnetism produces an unwanted dc voltage (several volts in a multikilowatt generator) that opposes the normal armature voltage induced by current in the field coil. With the circuitry shown, the output voltage due to residual magnetism can be reduced to a value less than 100 millivolts.

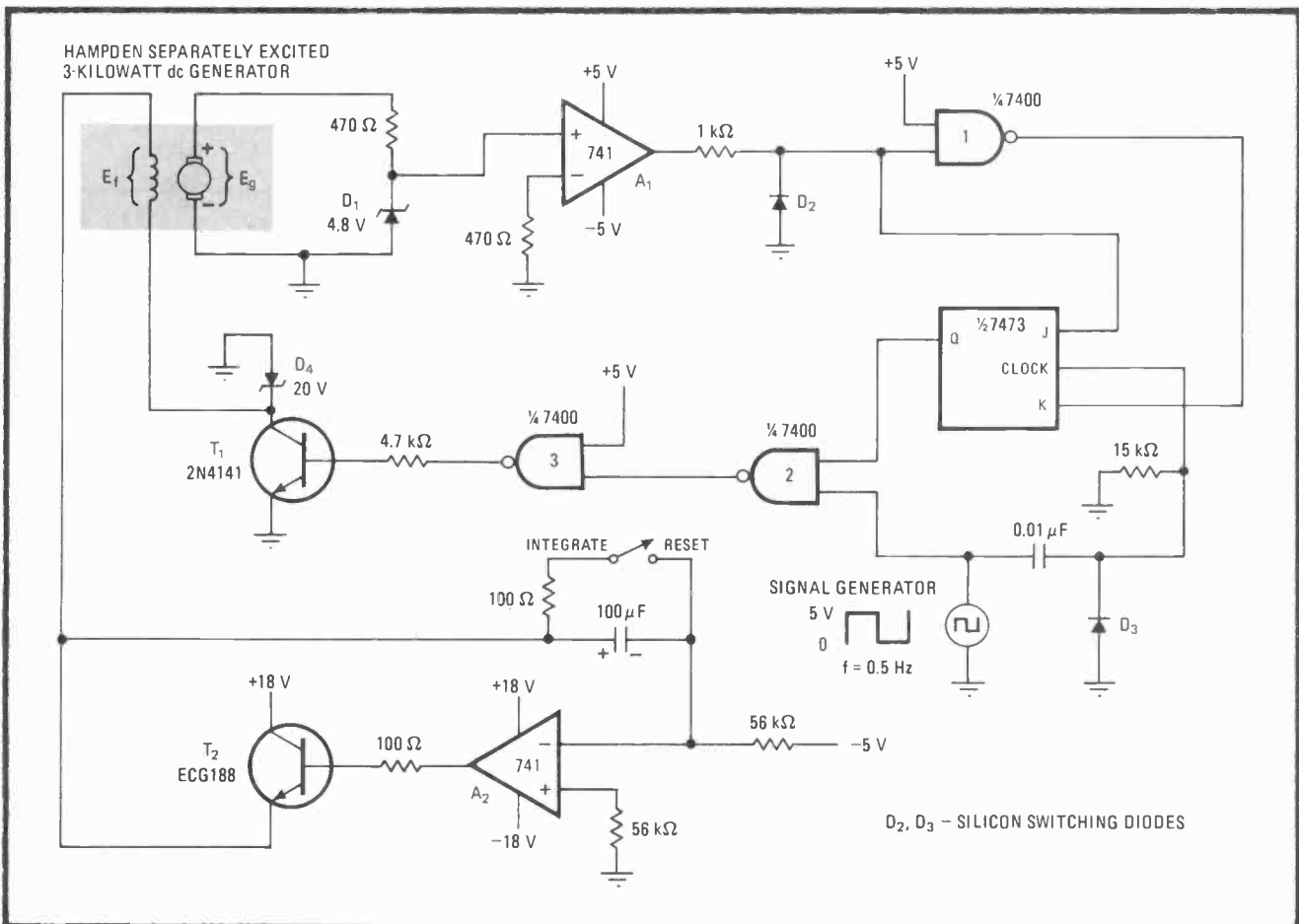
Assume the residual voltage to be canceled has a positive polarity. If the 5-volt square-wave source (shown in the lower right) is low, then gates 2 and 3 hold

transistor switch  $T_1$  off. The positive generator output is sensed by the comparator,  $A_1$ , which switches to its positive state. This output and its complement are used to set a J-K flip-flop.

When the square-wave voltage goes high, a positive pulse is applied to the clock input of the flip-flop. This drives the Q output of the flip-flop high, which, along with the positive square-wave voltage, turns  $T_1$  on, allowing current to pass through the field winding.

This current causes a voltage opposing the residual voltage to appear across the armature winding. The cycle repeats in synchronism with the square wave's period, until the output of the comparator goes negative (when the average residual voltage is close to zero or negative).

An increasing excitation voltage is provided by the integrator circuit  $A_2$ . The time constant selected for the integrator must be long enough so that each increment in field current will be small enough to prevent establishing residual voltage of the opposite polarity. Also, the frequency of the square wave should allow the field current to reach steady state during the time that the field is energized. □



**Residual removal.** Synchronously switched current through the field coil of a dc generator will create a voltage opposing the machine's unwanted residual output. Transistor,  $T_1$ , is switched on by a positive-going square wave to cancel the undesired voltage.

# Moving-dot indicator tracks bipolar signals

by Ted Davis  
Riverton, Ill.

Although bar- or dot-display chips are a simple means of indicating the instantaneous value of a signal, they respond only to unipolar levels, a definite drawback in processing audio-frequency signals with asymmetrical (bipolar) inputs. If reduced resolution is acceptable, one solution is to offset the audio voltage to the display chip. In this way it will be centered at half scale to allow for positive and negative signal excursions. Such a method is implemented in the scheme shown here.

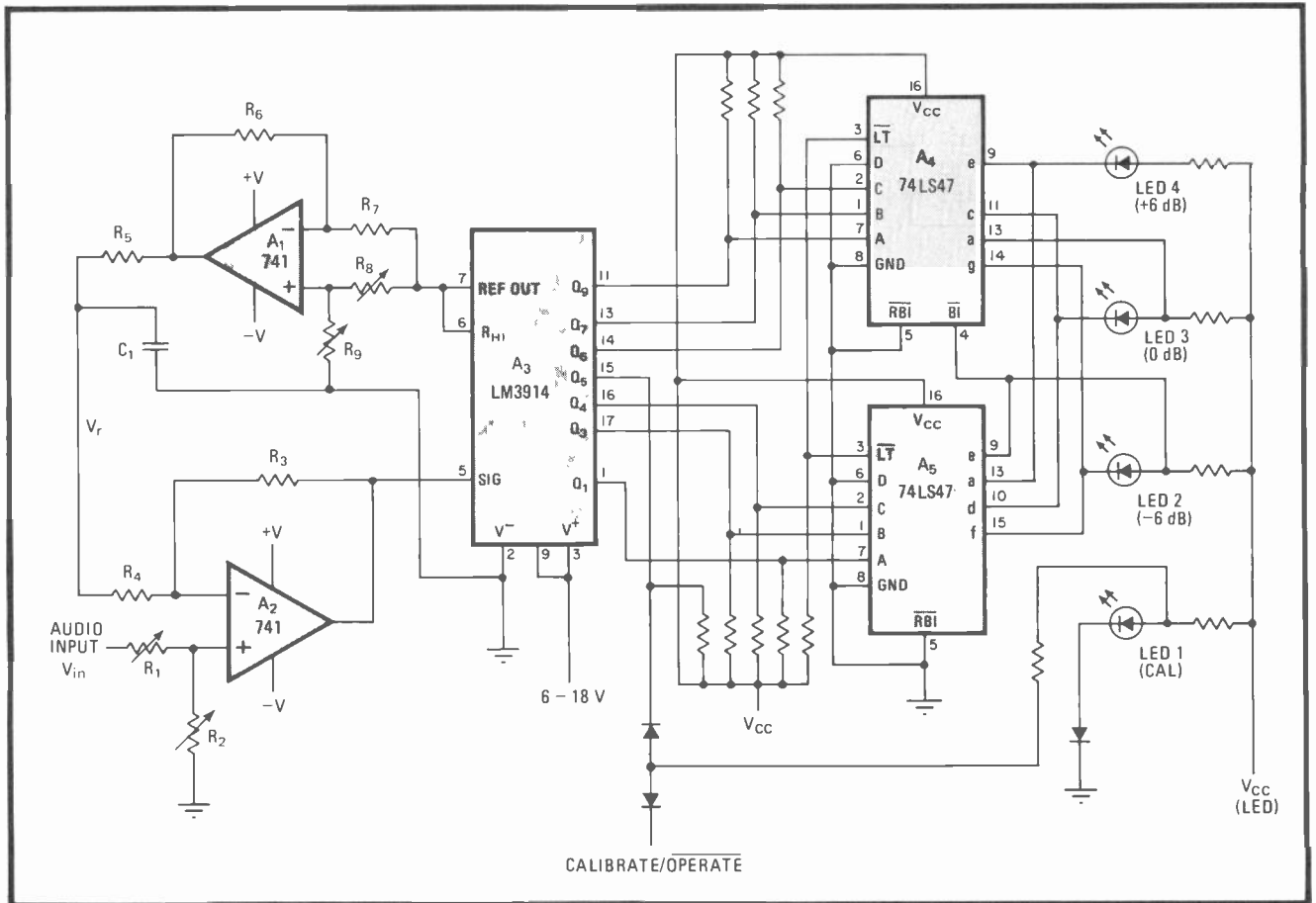
The circuit is configured to detect signal changes in 6-decibel steps, making it useful for audio-level monitoring. Other steps may be ordered by rewiring the output circuit appropriately. The unit may also be used as a bin-sorter or percent-change indicator for ac inputs or,

with removal of capacitor  $C_1$  and consolidation of resistors  $R_4$  and  $R_5$ , dc inputs.

Operational amplifier  $A_1$  applies a reference voltage to the inverting input of  $A_2$  so that it and the LM3914 bar/dot display may be offset by the desired amount. The value of the reference voltage, which is derived from the LM3914, is  $V_r = 1.25[-2R_9/(R_8 + R_9) + 1]$  assuming that  $R_6 = R_7$  and the reactance of  $C_1$  is negligible. The offset signal thus applied to the signal input (pin 5) of the LM3914 is  $V_r k$ , where  $k = R_3/R_4$ .

Assuming also that  $R_5 = R_3 - R_4$ , the offset voltage can be made to vary linearly from  $-1.25k$  to  $+1.25k$  and be centered at any value simply by adjusting  $R_8$  and  $R_9$ . To set the value at the mid-level digital output of the LM3914 dot or bar display, for example,  $R_8$  and/or  $R_9$  is varied so that  $Q_5$  trips and, through the 74LS47 BCD-to-seven-segment decoder/driver, dims light-emitting diode 1. The user should then back off on the setting until  $Q_5$  goes high again and then move the corresponding potentiometer halfway towards the position that would dim the LED once more.

Superimposed on the reference signal will be the component added by the audio signal, which at the



**Plus and minus.** Input of bar- or dot-display chip LM3914 is biased at user-set dc level so that it will respond to bipolar excursions of ac signals. Three LEDs serve as moving-dot indicator with a resolution of 6 dB. Truth table outlines circuit operation.

TRUTH TABLE: SIGNAL-LEVEL INDICATOR

| INPUT $V_{in}$ | $A_4$ |   |   |   |                  |                 |   |   | $A_5$ |   |   |   |   |   |                  |   | LED |   |   |           |           |                   |
|----------------|-------|---|---|---|------------------|-----------------|---|---|-------|---|---|---|---|---|------------------|---|-----|---|---|-----------|-----------|-------------------|
|                | D     | C | B | A | $\overline{RB1}$ | $\overline{BI}$ | a | c | e     | g | D | C | B | A | $\overline{RB1}$ | a | d   | e | f | 2         | 3         | 4                 |
| below 10%      | 0     | 1 | 1 | 1 | 1                | 1               | 0 | 0 | 1     | 1 | 0 | 1 | 1 | 1 | 0                | 0 | 1   | 1 | 1 |           |           | $\lambda$ (+6 dB) |
| 10% to 20%     | X     | X | X | X | X                | 0               | 1 | 1 | 1     | 1 | 0 | 1 | 1 | 0 | 0                | 1 | 0   | 0 | 0 |           | $\lambda$ | ( 0 dB)           |
| 20% to 40%     | 0     | 1 | 1 | 1 | 1                | 1               | 0 | 0 | 1     | 1 | 0 | 1 | 0 | 0 | 0                | 1 | 1   | 1 | 0 | $\lambda$ |           | (-6 dB)           |
| 40% to 60%     | 0     | 1 | 1 | 1 | 1                | 1               | 0 | 0 | 1     | 1 | 0 | 0 | 0 | 0 | 0                | 1 | 1   | 1 | 1 | ALL OFF   |           | (underrange)      |
| 60% to 70%     | 0     | 0 | 1 | 1 | 1                | 1               | 0 | 0 | 1     | 0 | 0 | 0 | 0 | 0 | 0                | 1 | 1   | 1 | 1 | $\lambda$ |           | (-6 dB)           |
| 70% to 90%     | 0     | 0 | 0 | 1 | 1                | 1               | 1 | 0 | 1     | 1 | 0 | 0 | 0 | 0 | 0                | 1 | 1   | 1 | 1 |           | $\lambda$ | ( 0 dB)           |
| above 90%      | 0     | 0 | 0 | 0 | 1                | 1               | 0 | 0 | 0     | 1 | 0 | 0 | 0 | 0 | 0                | 1 | 1   | 1 | 1 |           |           | $\lambda$ (+6 dB) |

X = don't care Input voltage  $V_{in}$  normalized to full scale at pin 5 of LM3914

output of  $A_2$  is equal to  $V_{in}R_2(k+1)/(R_1+R_2)$ . Thus positive and negative excursions of the ac signal will be detected by the LM3914. The scale factor is adjusted by applying the user-standard audio level to the input and adjusting  $R_1$  and/or  $R_2$  until the 0-dB LED just lights up.

The truth table outlines the overall operation of the circuit as a function of signal level. Note that the e segment of the low-order 6 shunts LED 2 in order to resolve a switching conflict between the 4 and 6 outputs. The 6 is also used to blank the high-order decoder when a negative-going 0-dB level is detected.

The values of the current-limiting and pull-up resistors depend on the logic family utilized; for TTL devices, 1-k $\Omega$  components will suffice throughout. Care must be taken

to ensure that the voltages developed at the e output satisfy the noise-margin requirements of the BI input of  $A_4$ ; that is, the total sink current at e must not raise the voltage above the maximum logic 0 level and the drop across LED 2 in series with the sink transistor must exceed the minimum logic 1 level.  $R_8+R_9$ , in parallel with  $R_7$ , set the sink current of the outputs of the LM3914.

The programmed current must be high enough to saturate the output transistors given the pull-up resistors used. The values of most of the other resistors are determined by the values of  $R_7$  through  $R_9$ . The value of  $C_1$  is determined by the value of  $R_4$  and the lowest frequency of  $V_{in}$ .  $\square$

## Low-level modulator sweeps generator over narrow range

by Ralph Tenny

George Goode & Associates, Dallas, Texas

A typical function generator's ability to sweep over a 1000:1 range of frequencies by means of an externally applied 0-to-10-volt modulating signal certainly enhances its usefulness. But sometimes narrow-range sweeps on the order of kilohertz are also needed, to check the response of a precision resonant circuit, for example. The problem is that, in most cases, the unit's front-panel controls cannot provide the required resolution. The one-chip circuit shown here, however, enables the setting of any dc voltage and provides for sweeping the control signal over a minimum of  $\pm 0.1\%$  of its value so that modulation of the preset center frequency will yield a proportionally small frequency variation.

Operational amplifier  $A_1$  serves as a 6-v source for biasing the inputs of  $A_2$ - $A_4$  at half the supply voltage, enabling the circuit to operate from a single supply (a).  $A_2$ , an integrator, and  $A_3$ , a voltage comparator operating with heavy feedback, generate the 100-hertz triangle wave needed to sweep the generator and the x input of

the oscilloscope used to display the response of the circuit under test.  $A_4$  is a simplified Howland Pump<sup>1</sup>, or bilateral current generator, which takes part of the sweep signal and uses it to modulate the preset dc voltage that drives the function generator.

When switch  $S_1$  is placed in the manual position and  $R_3$ 's arm is positioned at its extreme end (toward  $R_2$ ), the signal at the modulation output is dc, its amplitude determined by the setting of potentiometer  $R_2$ .  $R_2$  is thus used to set the center frequency of the function generator.

The dc value is modulated by placing  $S_1$  in the sweep position and adjusting  $R_3$  for the desired frequency sweep. Note that  $R_3$  approximates a summing junction for the preset dc level and a fraction of the sweep voltage in this application.

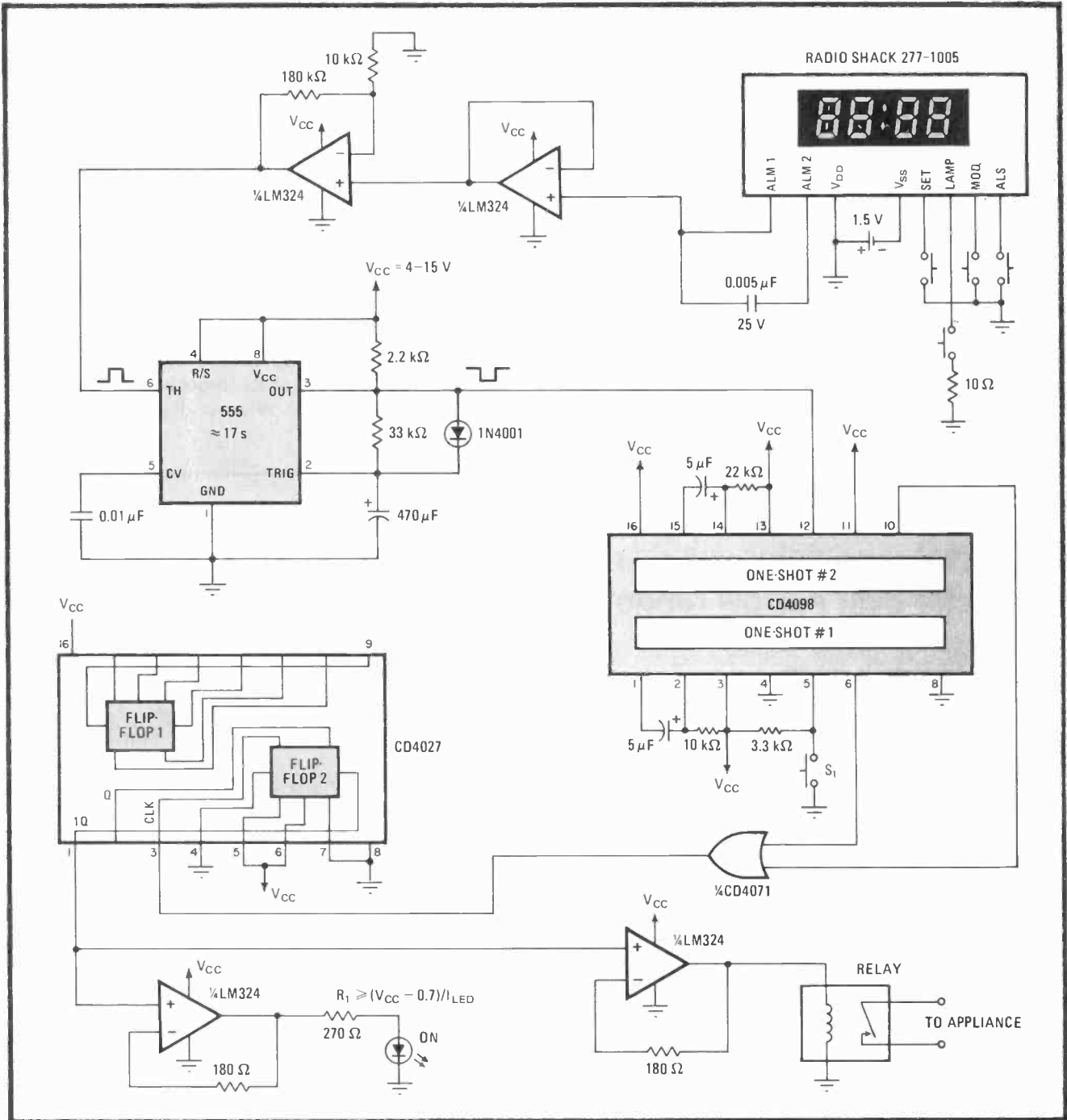
The setup in (b) illustrates a typical application for the circuit, whereupon it is necessary to characterize the response of a quartz crystal that has resonant and antiresonant frequencies less than 3 kHz apart. The frequency counter should be driven by the trigger output of the function generator to avoid interference with the crystal drive. The function generator's output is isolated from the crystal by a large resistor. A low-capacity oscilloscope probe should be used, and the effect of the probe's capacity on the measured crystal frequency taken into consideration. A manual control switch allows the operator to measure the resonant and antiresonant frequencies

by pressing the momentary-contact switch connected to the MOD input so that the hour digits flash. The SET switch is then pressed and held momentarily until the desired hour is displayed. The procedure is repeated for the minute display. A similar procedure sets the calendar day and date. Pressing the MOD and SET switch simultaneously starts the clock running.

To set the alarm time, the switch connected to the ALS port must be pressed twice within 3 seconds. The SET switch is then pressed and held until the desired alarm hour appears on the display. Again, ALS is pressed and SET is held for the setting of the minutes. Pressing ALS

once more will display the alarm time momentarily, then the display will return to actual time.

When the alarm time equals the actual time, ALM 1 and ALM 2 of the clock module generates a burst of 15 pulses, occurring at 1-s intervals for 15 s. This signal drives the 555 timer, which, configured as a non-retriggerable monostable, generates a 17-s pulse for setting the 4027 JK flip-flop through the dual 4098 one-shot. The flip-flop can then switch the relay on or off, depending on the quiescent state of one-shot 2 of the 4098. Depressing  $S_1$  changes the relay state from active-high to active-low, and vice versa. □



**On time.** Archer LCD alarm-clock module allows direct and precise setting of time to activate or shut off appliances. Pulsed alarm-signal output, not directly suitable for turning external devices on or off, passes through C-MOS interface so that relay is switched.

# Semiconductor thermometer is accurate over wide range

by Larry G. Smeins  
Hewlett-Packard Co., Loveland Instrument Division, Loveland, Colo.

Reducing the circuit complexity and simplifying the calibration of thermometers that use the base-emitter drop of a transistor to detect temperature changes, this circuit provides readings accurate to within  $\pm 2^\circ\text{C}$  over the range of  $-40^\circ\text{C}$  to  $+150^\circ\text{C}$ . Using the low-offset, low-drift characteristics of National's micropower LM-10 operational amplifier and Motorola's MTS-102 temperature sensor, the thermometer will compete with the more expensive platinum-resistance units.

The LM-10 is used to bias, scale, and zero the MTS-102 sensing transistor, thereby removing the need for a separate constant-current bias source for the sensor and an additional scaling and nulling circuit. Further, the well-defined characteristics of the MTS-102 permit single-point calibration of the thermometer.

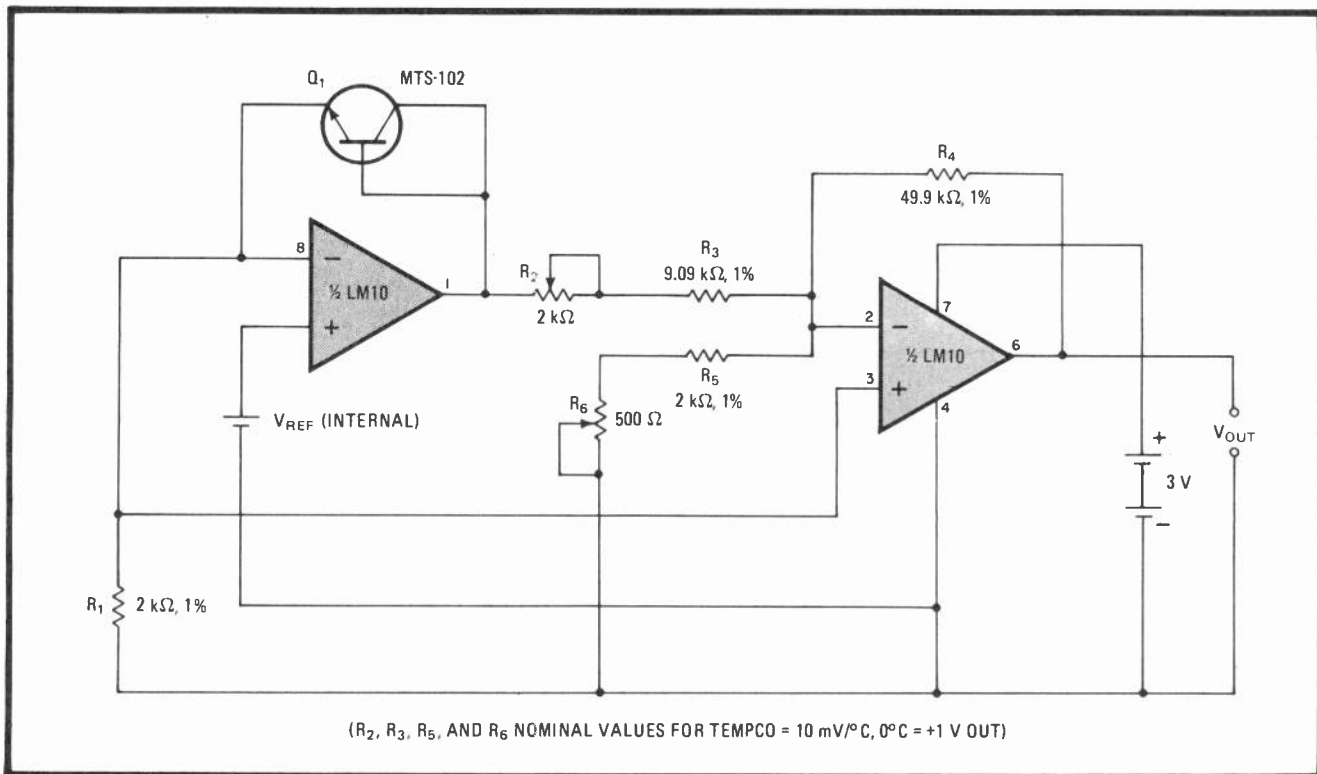
The MTS-102,  $Q_1$ , is placed in the feedback loop of the LM-10 reference amplifier. A constant-current bias is created by  $V_{\text{ref}}$  across resistor  $R_1$  giving  $I_{\text{bias}} = 0.2$

$\text{V}/2\text{k}\Omega = 100 \mu\text{A}$ . The voltage at the output of the reference amplifier will thus be  $V_{\text{ref}} + V_{\text{be}}$ . The second stage of the LM-10 is configured to provide a gain that is constant with respect to the temperature coefficient of the  $V_{\text{be}}$  drop and to subtract  $V_{\text{ref}}$  and  $V_{\text{be}}$  from the output at any desired reference temperature.

For a typical MTS-102, the  $V_{\text{be}}$  is 600 millivolts at  $25^\circ\text{C}$ , and its temperature coefficient is  $-2.25 \text{ mV}/^\circ\text{C}$ . The actual temperature coefficient for a particular device is thus  $\text{TC} = -2.25 + 0.0033(V_{\text{be}}' - 600) \text{ mV}/^\circ\text{C}$ , where  $V_{\text{be}}'$  is the measured base-emitter drop for the given sensor at  $25^\circ\text{C}$ . A corresponding offset voltage therefore appears at the output of  $A_1$ .

The gain-controlling elements of  $A_2$ , resistors  $R_2$ - $R_4$ , can be set so that the circuit's output-voltage-to-temperature slope will be correct for any sensor. The actual gain will be  $R_4/(R_2 + R_3)$ . Once the gain is set,  $R_5$  and  $R_6$  are adjusted to null the offset and yield the desired output voltage at any calibration temperature within the operating range of the circuit.

For very accurate calibration, a reference temperature source should be used to keep  $Q_1$  at  $25^\circ\text{C}$ . The  $V_{\text{be}}$  of  $Q_1$  can then be measured with a digital voltmeter and  $R_2$  and  $R_3$  set to null the offset.  $R_5$  and  $R_6$  are then set to yield an output voltage corresponding to the value that should be measured at  $25^\circ\text{C}$ . Using this technique, the calibration will be accurate to within  $\pm 1^\circ\text{C}$ .



**Hot number.** Micropower op amp and semiconductor made specifically for temperature-sensing applications reduce complexity and calibration procedure of thermometers that use  $V_{\text{be}}$  of transistors to detect temperature changes. Accuracy of device, no worse than  $\pm 2^\circ\text{C}$  over the range of  $-40^\circ\text{C}$  to  $+150^\circ\text{C}$ , and its simplicity enable it to compete with much more expensive units.

A simpler alternative is to set  $R_2$  and  $R_3$  to correspond with TC associated with the nominal  $V_{be}$  of the particular MTS-102 device used, zeroing the circuit at a reference temperature provided by an ice bath. Each MTS device is marked with their respective  $V_{be} \pm 2$  mV. This technique will provide calibration accuracy to  $\pm 2^\circ\text{C}$ . Either technique will provide accuracy to  $4^\circ\text{C}$  for all interchanged devices marked with the same  $V_{be}$ . But

interchangeability accuracy will vary to a greater degree with the MTS-103 and MTS-105 devices.

The circuit will also work with a conventional silicon transistor, such as a 2N3904, but for calibration purposes, its  $V_{be}$  should be measured between at least two points because it is not a specified parameter. The circuit is relatively insensitive to power supply voltage and it will operate satisfactorily over 2-to-40-v range. □

## Linear sense amplifier raises sensitivity of touch keyboard

by Jerry Dahl

IBM Corp., Research Triangle Park, Raleigh, N. C.

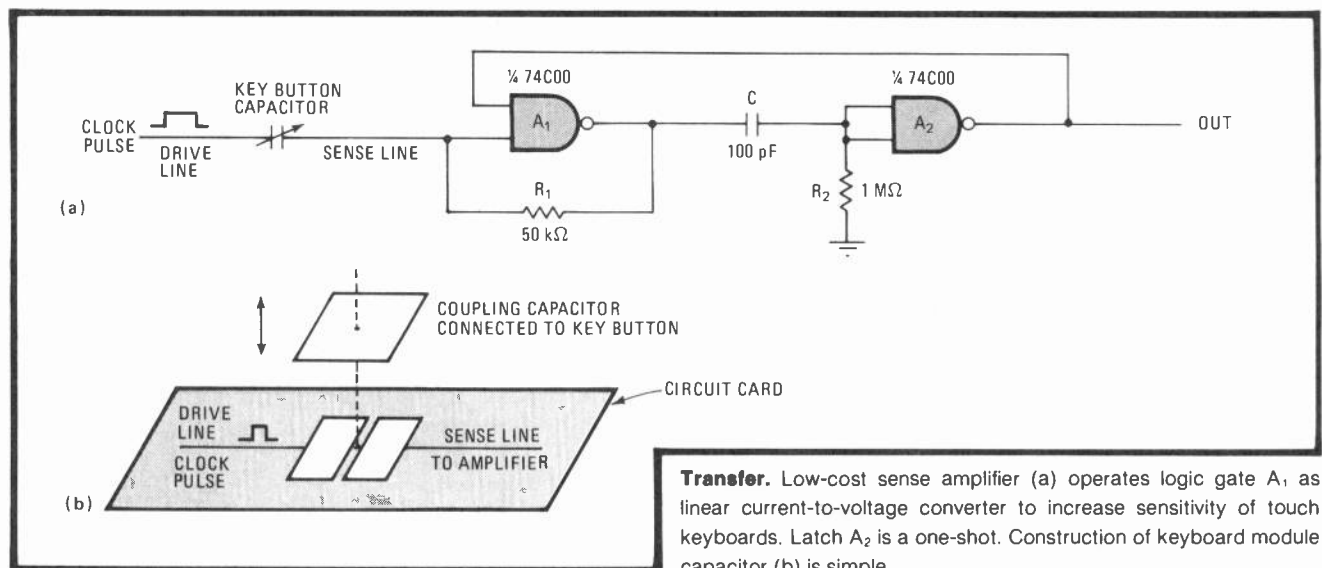
Keyboards relying on hand capacitance to simulate contact closure require a sense amplifier to detect the capacitive changes and thus determine when a key is depressed. Using one half of a complementary-MOS gate array, where one gate is operated in a linear mode to detect currents as low as 50 microamperes, this sense amplifier is not only simple and inexpensive but sensitive as well.

$A_1$  of the 74C00 quad NAND gate (a) serves as the amplifier, with  $A_2$  functioning as a latch.  $A_1$  is ac-coupled and operates as a self-biasing current-to-voltage

converter with a gain of 50 millivolts/ $\mu\text{A}$ . Its open-loop gain falls above 100 kilohertz, so the drive-line clock should have a frequency of about 10 kHz. For higher gain,  $A_1$  can be cascaded with other stages within the feedback loop  $R_1$ .

When signals having an amplitude of at least 50  $\mu\text{A}$  are coupled to the sense line via the coupling capacitor connected to the keybutton,  $A_1$  goes high and triggers  $A_2$  for about 70  $\mu\text{s}$ .  $A_2$  operates as a one-shot and thus it does not need to be reset.

The construction of the key module capacitor is shown in (b). The coupling capacitor is connected to the keybutton directly. The circuit-card pads are coated with a thin insulating epoxy covering that serves as the dielectric. When the keybutton is depressed, the clock pulse on the drive line will therefore be coupled to the sense line through the electric field of the capacitor. □



## Level shifter builds high-voltage op-amp block

by Leon C. Webb

Ball Corp., Aerospace Systems Division, Boulder, Colo.

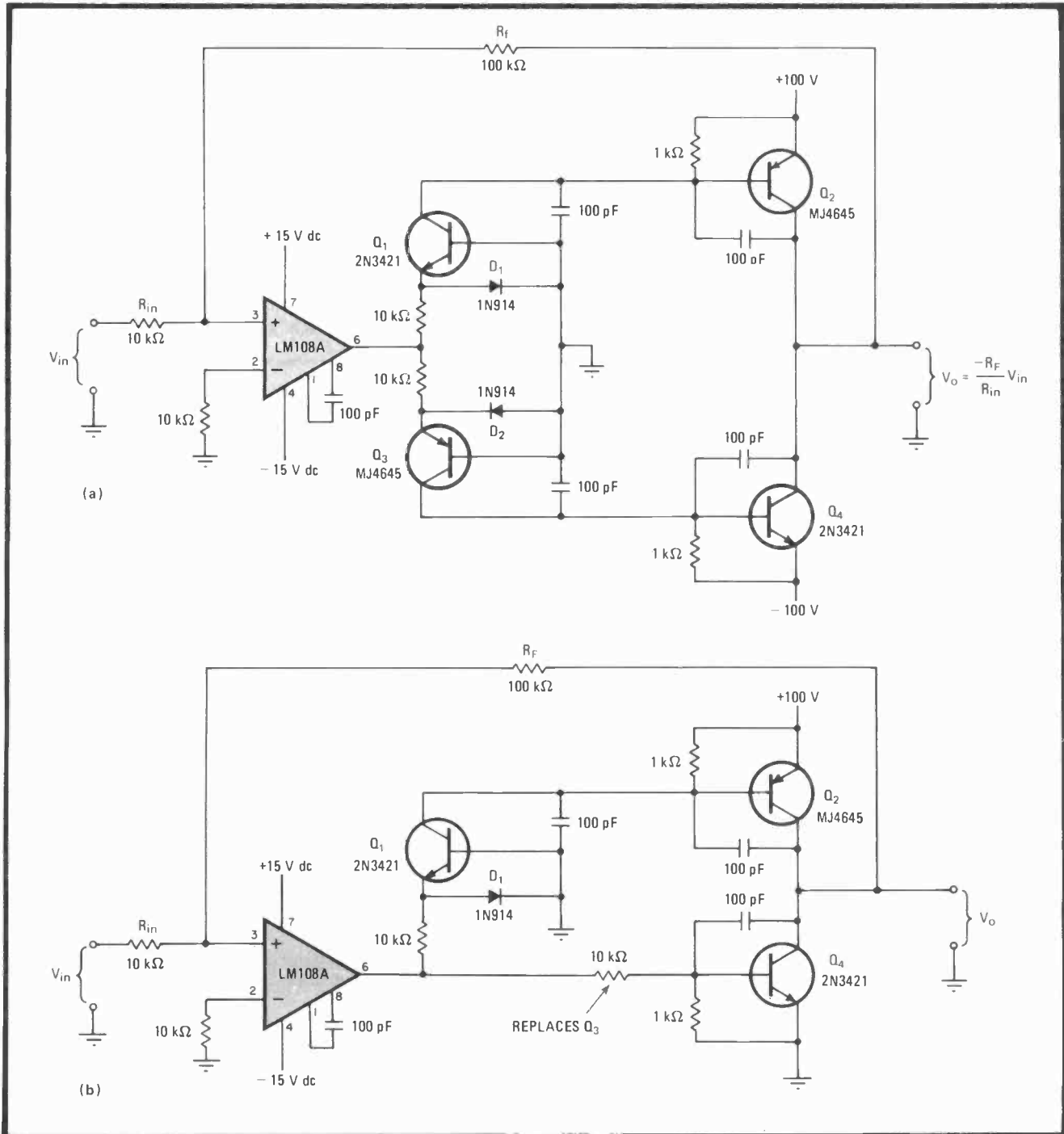
Placing a level-shifting network inside the major loop of an operational amplifier adapts it for high-voltage applications. The output swing of the circuit, which can be in the hundreds of volts, is limited only by the breakdown voltage of the active devices (in this case, transistors) used. At the same time, the op amp is isolated from high potentials, even in the absence of its  $\pm 15$ -volt supply voltages, by the attenuator formed by the amp's gain-

controlling resistor and the input resistance of the circuit and by the clamping action of the circuit's common-base stages.

The method can be applied to op amps that will generate either bipolar or unipolar voltage swings. As shown in (a) for the general voltage amplifier, which generates a bipolar swing, the op amp's output is transformed into an emitter current that flows through either transistor  $Q_1$  or  $Q_3$ , depending upon the polarity of the output voltage from the LM108A. As a result, a corresponding base current is applied to either transistor  $Q_2$  or

transistor  $Q_4$ , respectively, thereby turning it on to a greater or lesser degree. Thus,  $V_o$  assumes a value equal to a  $-10V_{in}$ , where the voltage multiplication holds true for  $-10\text{ v} < V_{in} < 10\text{ v}$ .

If only a unidirectional output is desired, the configuration shown in (b) will suffice. This circuit, which delivers only positive output voltages, has the same transfer function (that is,  $V_{out} = -10 V_{in}$ ) for  $-10\text{ v} < V_{in} < 0\text{ v}$ . If a negative-only voltage output is required, stage  $Q_1$  is replaced by a 10-k $\Omega$  resistor. The level-shifter's supply voltage must also be negative. □



**Translation.** Level-shifter adapts operational voltage amplifier (a) for high-voltage duty. Output swing of circuit is limited only by the shifter's supply voltage and the breakdown voltage of transistors used. For unidirectional output swings (b), simplified circuit will suffice.

# Converter in feedback loop improves voltage regulation

by David Abrams  
Winchester, Mass.

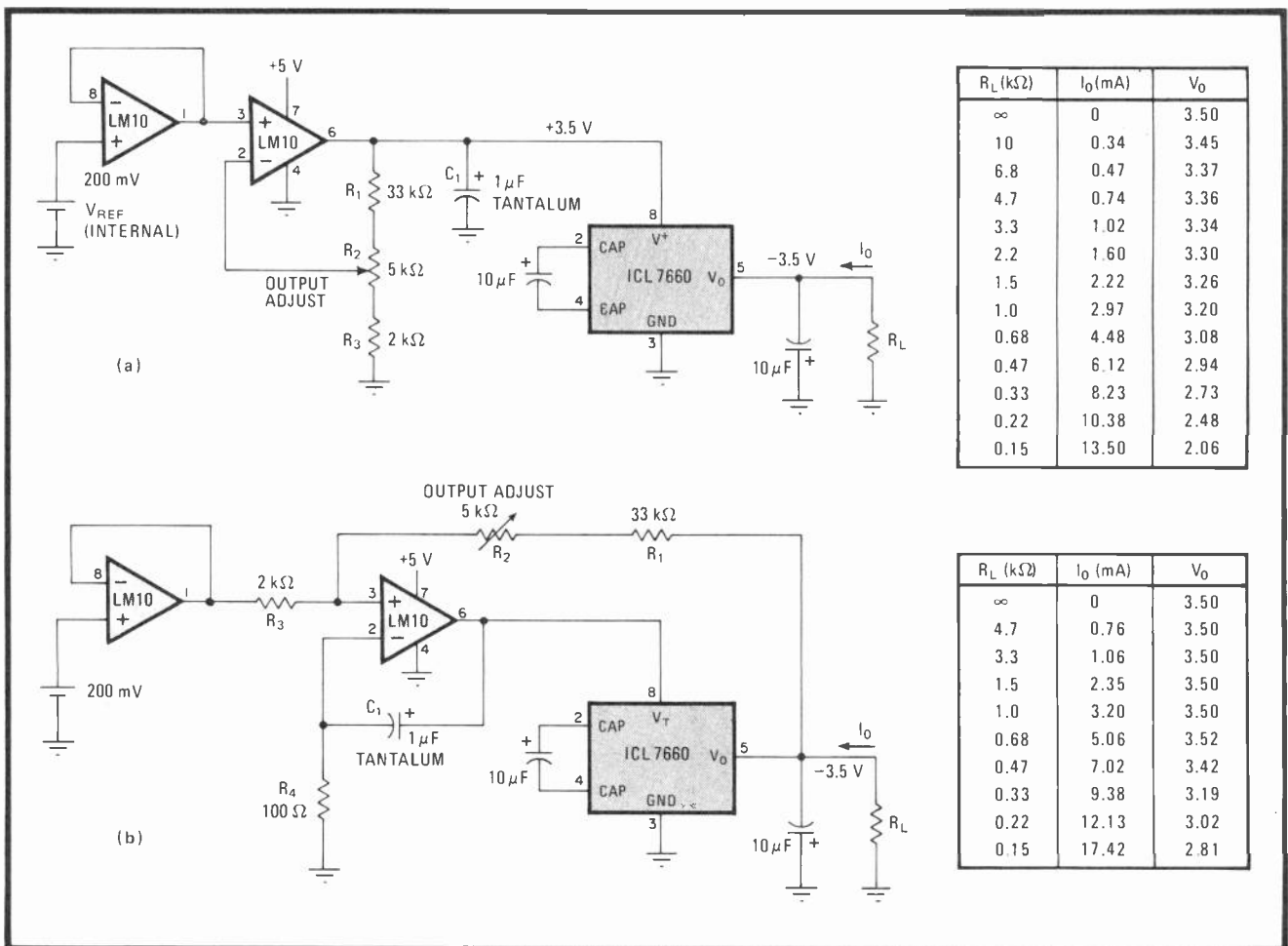
One of the most frustrating experiences a designer faces is to discover that his TTL or complementary-MOS circuit, which he intended for single-supply operation, actually requires a minus potential at some miniscule current for one or two of its integrated circuits. A new chip, Intersil's 7660 voltage converter, now enables the designer to obtain the minus voltage at low currents from a positive supply without the need for a transformer or other complicated inverter circuitry, and at low cost. In addition, placing the converter in a feedback loop that includes the chip's power—or driving—source permits a degree of voltage regulation that is not possible with the

conventional stand-alone driver configuration.

As shown in (a), the 7660 can supply  $-3.5$  volts to a single chip in a C-MOS or TTL system. The chip requires  $+3.5$  v, which is generated by the LM10 operational amplifier from the  $+5$ -v supply. Although some other low-voltage op amp and an external reference could be substituted, the LM10 will run off a single supply, has its own reference, and has an output stage that can swing within  $1/2$  v of the supply while delivering  $-20$  milliamperes to the 7660.

Though this circuit performs well at very low load currents, its output voltage drops rapidly as load currents increase (see table) because its output impedance is fairly high. At a no-load output voltage of  $-3.5$  v the converter exhibits an output resistance of about 100 ohms, but it will increase 50% for  $V_{out} = 2$  v. This value will render the 7660 useless in systems where more than a few milliamperes are required.

By adding a single resistor and configuring the circuit in (b), however, the converter can be made to perform much as an ideal voltage source for



**Regulatory loop.** Intersil's 7660 voltage inverter provides a negative output from a positive source without transformers (a), but voltage regulation is poor. Placing the 7660 in a feedback loop that includes the driving source (b) improves operation markedly.



loads of 1 kilohm or greater. The regulation for loads less than 1 k $\Omega$  will be much superior to that in (a), as seen in the table.

Here the circuit works as an inverting amplifier with a gain of  $-17.5$ , which is set by  $(R_1 + R_2)/R_3$ . The converter provides a gain of  $-1$ , requiring that the noninverting input of the op amp be used as the summing junction. Thus the circuit can still be run from a single supply because the LM10's input common-mode range includes the negative supply (ground, in this case).

$R_4$  and  $C_1$  provide local feedback around the op amp to stabilize the loop. Without these components, the delay between input and output voltage changes of the 7660 would cause the output of the LM10 to oscillate

between ground and  $+5$  v.

In operation, the feedback loop will force the op amp to try to hold the negative output voltage constant. Even at the higher currents, the output resistance is half of what it is in (a).

The circuit may also be used to supply negative voltages other than  $-3.5$  v. If higher voltages are desired, it is necessary to choose a supply voltage for the LM10 that will provide sufficient output from the op amp under the expected load conditions. In this case, the effective voltage gain of the 7660 drops from  $-0.99$  v to zero, and so the output voltage of the op amp must rise as the load current increases in order to compensate for the loss of gain.  $\square$

## PLL's lock indicator detects latching simply

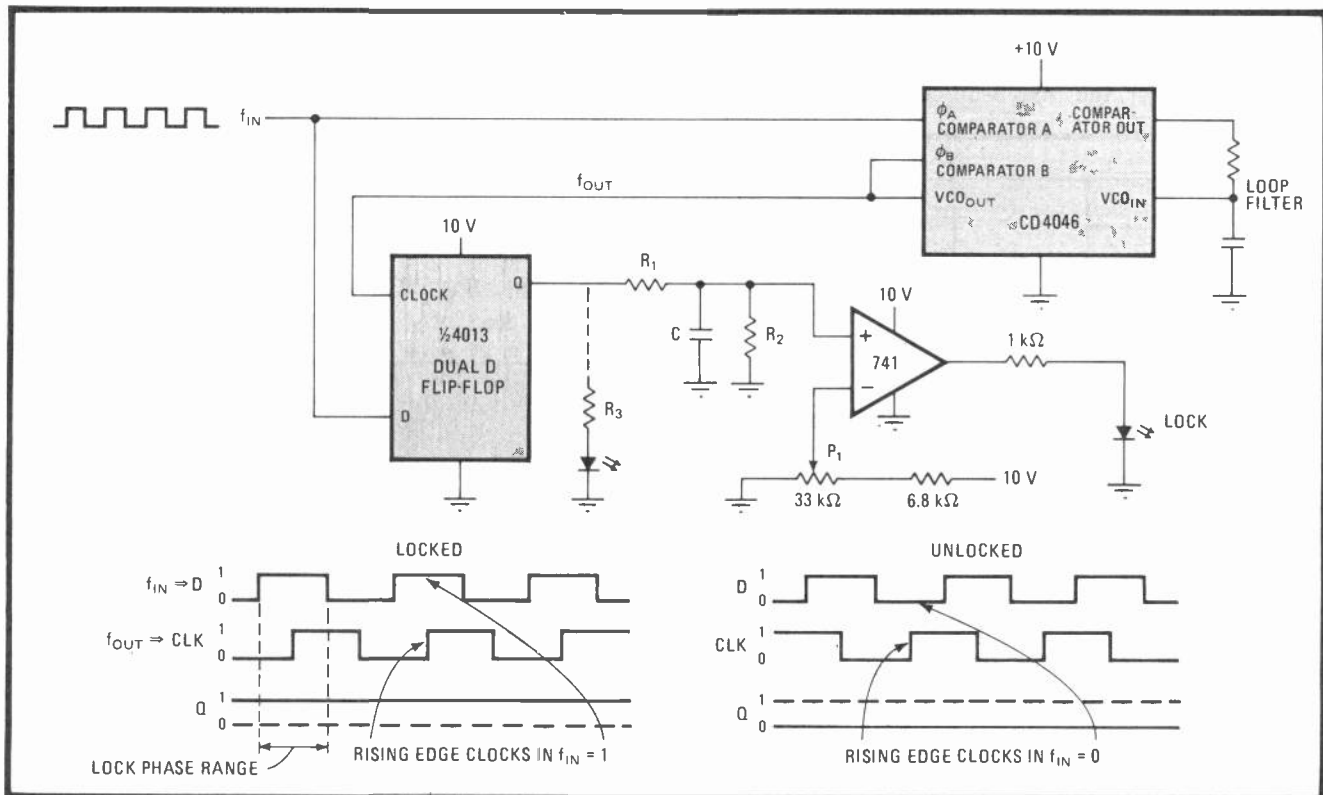
by Steve Kirby

Department of Electronics, University of York, England

Much less complex than some of the previously described lock indicators for phase-locked loops,<sup>1</sup> with no need to derive and utilize a multiple of the input frequency<sup>2</sup> for phase-comparison purposes, this circuit is easier to set up and use. It sacrifices nothing in the way of

accuracy and offers other advantages, such as the ability to lock onto harmonics of the input signal.

The locking technique is illustrated for the C-MOS CD4046 PLL, whose output leads the input by  $90^\circ$  when the lock state is achieved. The loop's capture ratio is such that lock can be maintained for a square-wave input signal no greater than  $+90^\circ$  and no less than  $-90^\circ$  out of phase with respect to  $f_{out}$ . The 4013 D flip-flop detects phase differences by clocking the state of  $f_{in}$  at  $f_{out}$ 's rising edge. Assuming the PLL and its associated loop filter are working properly, a steady  $Q = 1$  at the output of the flip-flop indicates the PLL is in or will shortly be in the lock state. The noninverting input of the 741 comparator will then rise to 10 volts through integrator



**Monitor.** Only two chips, flip-flop and comparator, are needed to detect lock condition in phase-locked loop. Rising edge of  $f_{out}$  clocks in logic 1s to D input of flip-flop under lock condition, causing  $A_1$  to go high and LED to light. Output of flip-flop is otherwise a random train of pulses, causing the voltage at the noninverting input of  $A_1$  to drop below  $P_1$ 's threshold, bringing  $A_1$  low and turning off the LED.

$R_1R_2C$ , and its resulting high-going output will light the light-emitting diode.

If the PLL no longer locks on frequency, the phase of  $f_{in}$  with respect to  $f_{out}$  will be random. The output of the flip-flop will thus be a train of variable-width pulses. The comparator input thus drops to approximately 5 v, and because potentiometer  $P_1$  sets the inverting input at approximately 7 v,  $A_1$  moves low, extinguishing the LED.

The lock detector will lock onto higher harmonics of  $f_{in}$ . With a 50/50 mark-to-space square-wave signal,

locking has been observed to the fifth harmonic.

If a less precise indication is tolerable, lock detection can be achieved with even fewer parts by placing an LED at the output of the flip-flop and eliminating the comparator circuitry. Resistor  $R_3$  should be selected to hold the LED dim for the out-of-lock condition. □

**References**

1. J. A. Connelly and G. E. Prescott, "Phase-locked loop includes lock indicator," *Electronics*, Sept. 5, 1974, p. 112.
2. R. P. Leck, "Logic gates and LED indicate phase lock," *Electronics*, May 29, 1975, p. 106.

## Three-chip logic analyzer maps four-input truth table

by C. F. Haridge  
University of Ottawa, Ontario, Canada

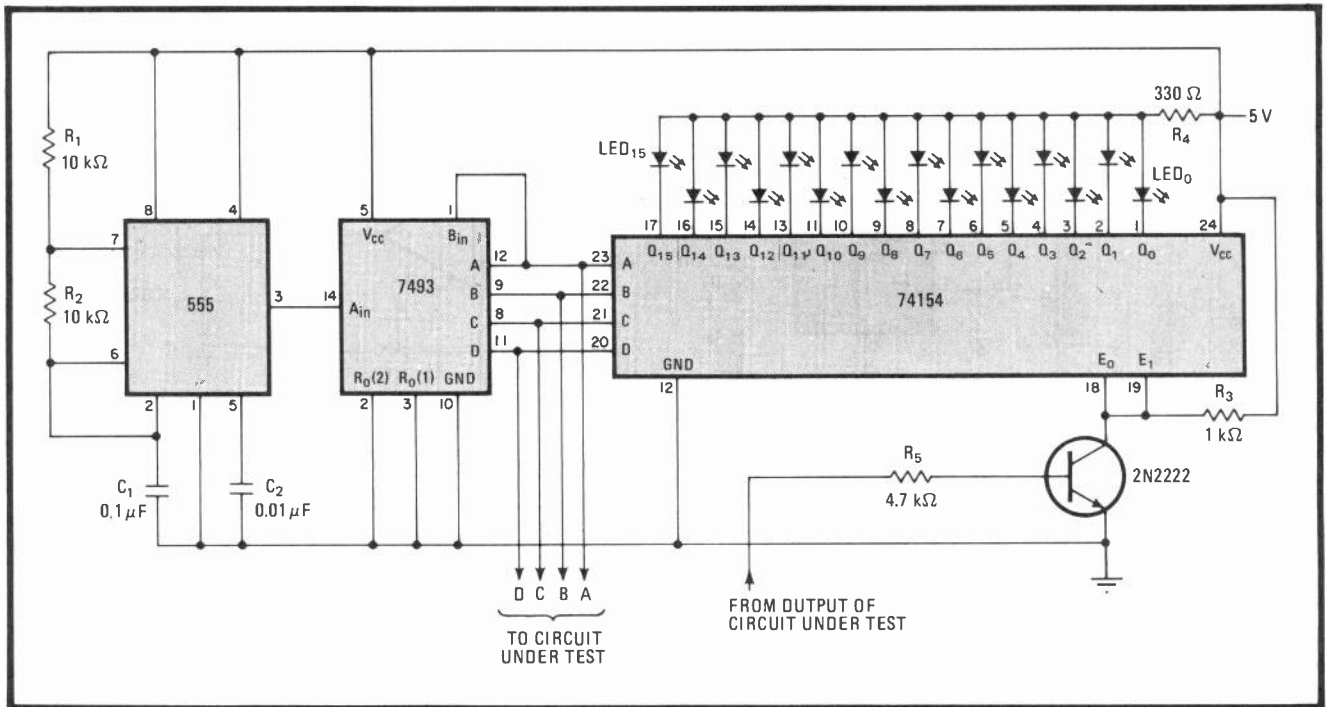
Providing an extremely simple and low-cost alternative to the use of an oscilloscope, this logic analyzer will determine the truth table of circuits with as many as four inputs. The state of the circuit for a single monitored output is displayed by a four-by-four array of light-emitting diodes arranged in a Karnaugh-map configuration. Resistor-, diode-, and transistor-transistor-logic circuits can be checked directly, and only one input/output buffer is required to check complementary-MOS designs.

The analyzer's three basic functions—timing, scanning, and display—are achieved with only three chips: the 555 oscillator, the 7493 4-bit counter, and the 74154

4-to-16-line decoder. The 555, running at a minimum frequency of 480 hertz to eliminate display flicker, clocks the 7493 through its 16 states continuously. As a result, a binary sequence of 0-15 periodically drives the four inputs of the circuit under test. These logic signals are also applied to the decoder chip. Consequently if the instantaneous output of the circuit point under test is high for any given set of input variables A-D, the LED corresponding to the 4-bit output number of the 7493 will light up.

The analyzer may be easily expanded to test circuits having more than four inputs by adding the appropriate number of counters, decoders, and LEDs. The clock frequency must also be increased to minimize flickering in the display.

A higher clock frequency will reduce the on-time of each LED, however. In order to compensate for this reduced brightness, resistor  $R_4$  must be made proportionally smaller. □



**Logic functions.** Low-cost logic analyzer, complete with light-emitting diodes arranged in Karnaugh-map configuration, monitor four-input circuit response. RTL, DTL and TTL circuits may be checked directly; only one I/O buffer is needed for C-MOS designs.

# PSK modulator resolves phase shifts to 22.5°

by Noel Boutin  
University of Sherbrooke, Quebec, Canada

Requiring little more hardware than the circuit proposed by Chawdhury and Das<sup>1</sup> and eliminating the software entirely, this phase-shift-keyed modulator offers an even more versatile and less expensive solution to sending binary data over long distances. One of its great advantages is that carrier phase shifts can be resolved to 16 bits—22.5°.

Only three low-cost chips and a means for generating four-input binary data are required, as shown. The carrier signal is first divided by 16 and applied to the CD4015 eight-stage shift register. Because the register is clocked by the carrier at a rate 16 times that of the signal to be shifted, a discrete eight-phase version of the carrier appears at the output of the register, each shifted by  $360/16 = 22.5^\circ$  from its neighboring stage. These signals are then introduced to the CD4051 multiplexer.

The first 3 bits of each of the modulating data inputs, A–D, address the CD4051 also. Thus any desired phase shift from 0° to 157.5° may be selected (see large table). The eight remaining values, from 180° to 337.5°, may be selected with the aid of the D input, which at the output of the last stage of the register inverts the phase of the signals that have already been generated.

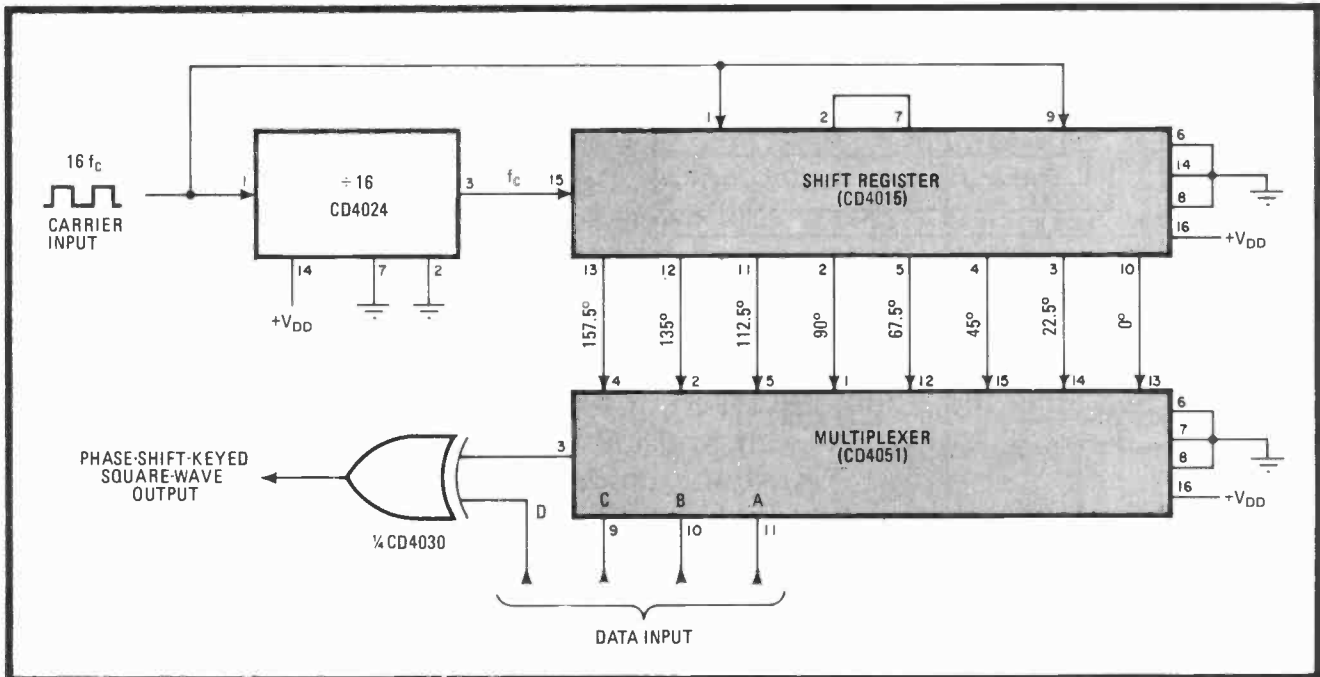
There may be instances where it is desirable to transmit fewer than 16 levels. The small table summarizes the A–D states required to achieve this.

**References**  
1. F. B. Chawdhury and J. Das, "8085 performs PSK modulation for data-line transmission," *Electronics*, Jan. 31, 1980, p. 108.

| DATA |   |   |   | φ      |
|------|---|---|---|--------|
| D    | C | B | A |        |
| 0    | 0 | 0 | 0 | 0°     |
| 0    | 0 | 0 | 1 | 22.5°  |
| 0    | 0 | 1 | 0 | 45°    |
| 0    | 0 | 1 | 1 | 67.5°  |
| 0    | 1 | 0 | 0 | 90°    |
| 0    | 1 | 0 | 1 | 112.5° |
| 0    | 1 | 1 | 0 | 135°   |
| 0    | 1 | 1 | 1 | 157.5° |
| 1    | 0 | 0 | 0 | 180°   |
| 1    | 0 | 0 | 1 | 202.5° |
| 1    | 0 | 1 | 0 | 225°   |
| 1    | 0 | 1 | 1 | 247.5° |
| 1    | 1 | 0 | 0 | 270°   |
| 1    | 1 | 0 | 1 | 292.5° |
| 1    | 1 | 1 | 0 | 315°   |
| 1    | 1 | 1 | 1 | 337.5° |

| NUMBER OF PHASE LEVELS | A    | B    | C    | D    |
|------------------------|------|------|------|------|
| 2 φ                    | 0    | 0    | 0    | DATA |
| 4 φ                    | 0    | 0    | DATA | DATA |
| 8 φ                    | 0    | DATA | DATA | DATA |
| 16 φ                   | DATA | DATA | DATA | DATA |

**Multiphase.** Three-chip circuit performs PSK modulation on square-wave input, resolving carrier shifts to 22.5°. First three bits of modulating data inputs select shifts from 0° to 157.5°, with D input required for higher values. Truth tables summarize operation.





# Time-shared analog bus multiplexes audio signals

by Colin Johnson  
Madison, Wisc.

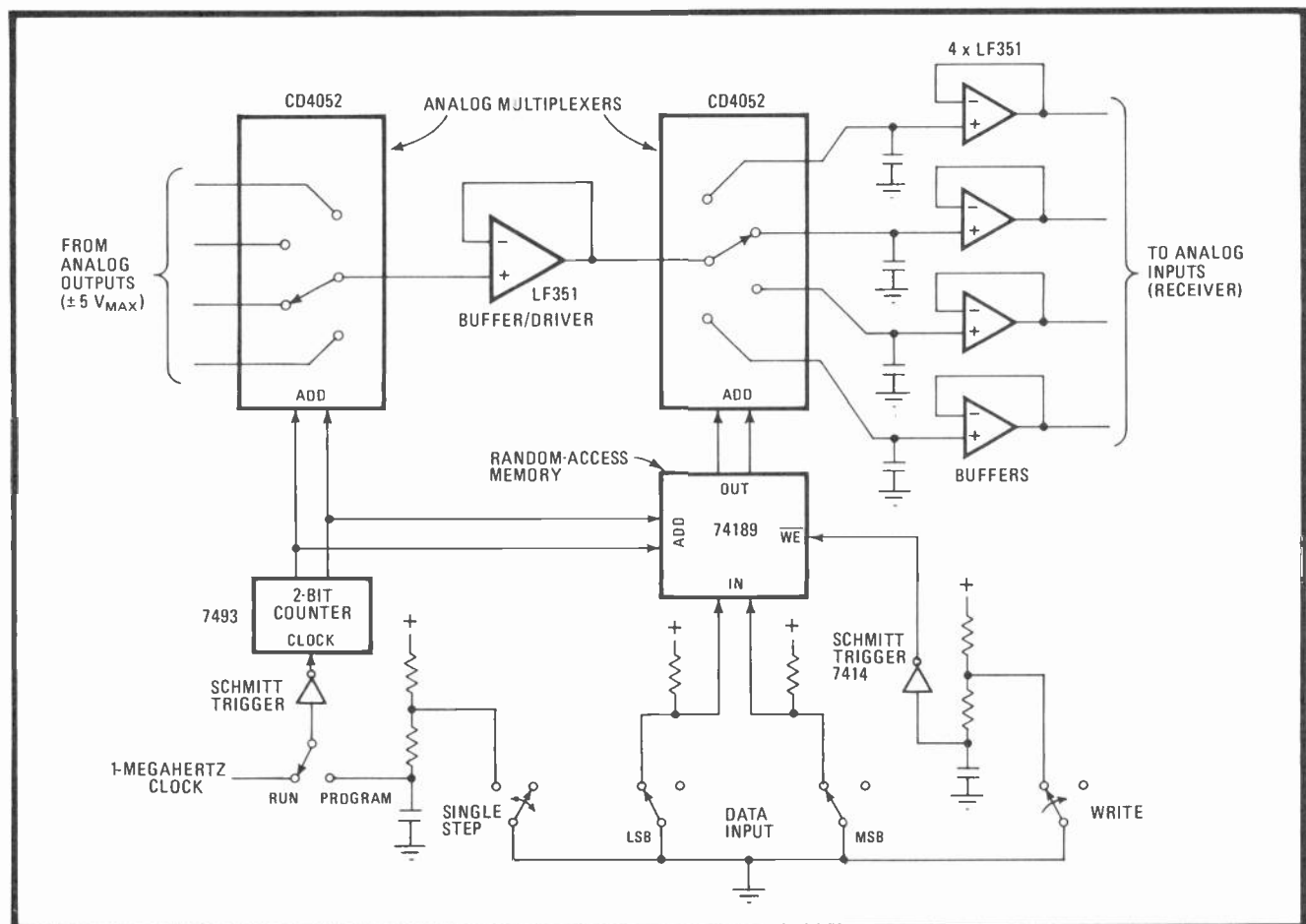
A multiplexed analog bus can be easily realized by means of complementary-MOS analog switches and rudimentary sample-and-hold circuits. Thus the advantages gained by the time-division multiplexing of digital signals—mainly the multichannel sharing of processing hardware—may be also secured for audio waveforms.

Each analog driver output is connected to the bus through an analog switch. Each analog receiver input is attached to the bus via a simple capacitor/operational-amplifier sample-and-hold stage. As each output is switched onto the bus, the corresponding inputs it is connected to are also engaged. During this aperture time, the hold capacitors are charged. The specific

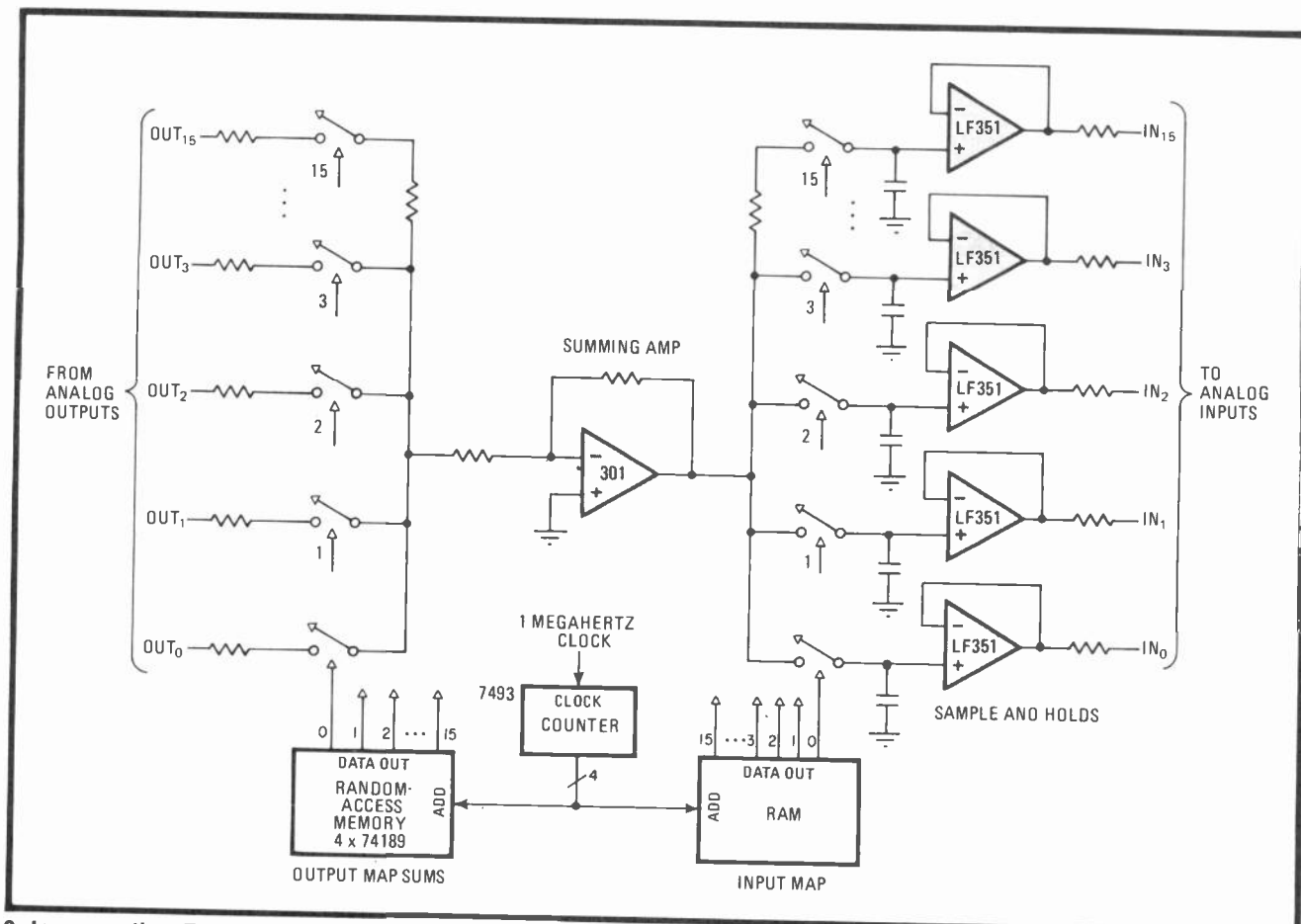
input/output map is stored in a random-access memory. If a computer is available, a memory-mapped scheme lets the user implement changes easily and affords convenient cataloging of any patch on a mass-storage device.

C-MOS analog multiplexers serve as the central switching element in the four-channel multiplexer shown in Fig. 1. These devices are bidirectional and have separate TTL-level address inputs, enabling the switching of analog input signals in the range of  $\pm 5$  v.

The bus technique is not confined to a four-input multiplexer, of course, and many other configurations can be constructed. Figure 2 shows a design using discrete analog switches and a summing amplifier that mixes 16 unique sums of outputs to any number of 16 inputs. Multiplexing is done at 62.5 kilohertz in this case (47 KHz if an additional 250-nanosecond settling time is permitted). This sampling frequency is sufficient to process audio signals below 20 KHz without significant distortion. When tape recording and other baseband equipment is used, a low-pass filter will be required to eliminate the switching noise that is generated. □



1. Four by four. Analog multiplexers combine four analog signals over a common bus. Counter, driven by 1-MHz clock, sequentially selects analog outputs and sends signals over bus to receiver. RAM containing input/output map delivers signals to required port.



**2. In summation.** Two RAMs and discrete analog switches enable multiplexer to deliver up to 16 sums of outputs to any number of 16 receiver inputs. Number of sums is proportional to length of RAM. Multiplexing is done at 62.5 kHz to ensure coverage of audio band.

## Implementing interrupts for bit-slice processors

by Vern Coleman  
Advanced Micro Devices Inc., Sunnyvale, Calif.

Interrupt detection and handling at the microprogram level can be easily implemented in the Am2900 bit-slice processor family thanks to versatile components like the Am2914 priority interrupt encoder and others. The interrupt scheme can generally be extended to other systems at the cost of additional circuitry.

As shown in the figure, the components required are the 2914, the 2910 microprogram sequencer, a 29775 programmable read-only memory, and two separate PROMs for mapping instructions from main memory and interrupt vectors from the 2914 into starting addresses for the 2910.

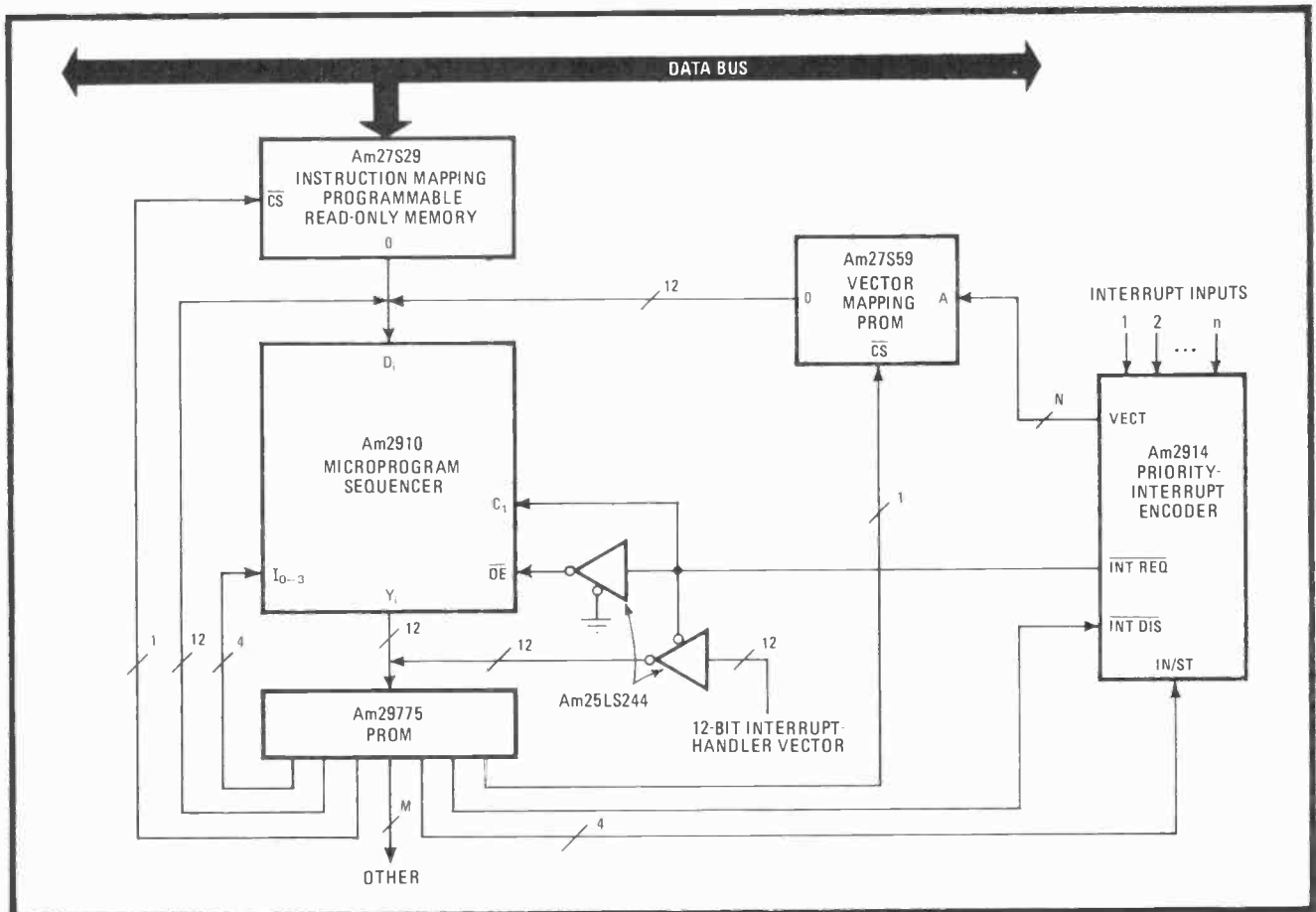
If an interrupt is detected by the 2914 as the 2910 executes an instruction, the interrupt-request output of the encoder moves low. This action turns off the carry input of the 2910, for all practical purposes causing the sequencer to halt for a microcycle. It also causes any

data that would normally appear at the  $Y_i$  outputs to be stored in the sequencer's program counter.

The interrupt request also forces the output of the sequencer into a high-impedance state. This allows an interrupt-handling vector to be applied at the  $Y_i$  outputs, thereby addressing the first instruction of the interrupt routine in the microprogram memory.

The 2914 is thus instructed to place an interrupt vector on its output port. The same word in microprogram memory also enables the output of the vector-mapping PROM to allow decoding of the interrupt vector. The result is then applied to the D inputs of the 2910 while it does a jump to the appropriate subroutine. Thus the first address of the interrupt routine is brought in, and the address to which the previously executed program is to return after the interrupt is serviced is stored away. If there is a point in the microprogram routing where no interrupts are to be allowed, a logic 0 can be applied to the interrupt disable input pin on the 2914.

The microcode for handling interrupts is shown in the table. The first entry commences with address I. This vector instructs the 2914 to execute a jump to subroutine if its condition code input is low. The encoder is then commanded to place its interrupt vector associated with the current interrupt request on its output port. At this time, it may be desirable to disable any further inter-



| Interrupt address | Am2910 instruction | Am2914                            |                   | Vector-mapping PROM | Data-mapping PROM |
|-------------------|--------------------|-----------------------------------|-------------------|---------------------|-------------------|
|                   |                    | Instruction                       | Interrupt disable |                     |                   |
| I                 | CJS                | Read vector                       | 0                 | 0                   | 0                 |
| I + 1             | —                  | Clear interrupt, last vector read | 0                 | 1                   | —                 |
| I + 2             | —                  | Enable interrupt request          | 1                 | 1                   | —                 |
| I + 3             | CRTN               | —                                 | 1                 | —                   | —                 |

**Stop.** Standard elements of the Am2900 family are easily configured to provide interrupt capability for bit-slice microprocessors. Architecture is applicable to stacked interrupt systems. Microcode for handling interrupts (see table) is fast and simple.

rupts, in which case the appropriate pin should be brought low, as explained above. A logic 0 is also placed on the vector-mapping PROM while a logic 1 is placed on the data-mapping PROM's output-enable lead and the pipeline output-enable of the 29775. Thus the vector-mapping PROM will be the sole source of any input to the D port of the 2910.

At address I+1, the interrupt associated with the previous vector read into the 2914 may be cleared, and the vector-mapping PROM disabled by bringing its output-enable lead high. At address I+2 and subsequent addresses, the 2914 may be commanded to accept any interrupt by use of the enable interrupt request. The vector-mapping PROM is first disabled with a logic 1

signal. At this time the interrupt-disable pin of the 2914 is deactivated. At the end of the interrupt routine, an exit is achieved via the conditional-return instruction of the 2910. A logic 0 should be simultaneously applied to the condition-code inputs of the sequencer.

There is nothing that precludes the use of this architecture in a stacked<sup>1</sup> interrupt system. The number of interrupts that can be stacked is limited by the depth of the 2910. It is only necessary to issue a simple command to return from the subroutine utilized to the main program, for each stacked interrupt. □

## Protected regulator has lowest dropout voltage

by Thomas Valone, A-T-O Inc., Scott Aviation Division, Lancaster, N. Y. and Kelvin Shih, General Motors Proving Ground, Milford, Mich.

Providing an output of 5 volts at 10 milliamperes for an input of only 5.012 v, this regulator is ideal for use in many micropower applications, such as regulating the output of lithium batteries that drive low-power detection and recording instruments in the field. The circuit is useful in high-current situations also, as it can deliver up to 1 ampere at 5 v for an input of only 6.0 v. Short-circuit protection in this instance is provided by a single V-groove MOS field-effect transistor.

Contributing to the low-dropout characteristic of the circuit is the 2N6726 output transistor, which has a large junction area that allows a lower emitter-to-collector drop than most other devices, including Darlington arrangements. Thus the input-to-output voltage differential, 12 millivolts, is 6% that of one of the best low-dropout regulators reported to date.<sup>1</sup>

The input-to-output differential is only 350 mV at a load current of 500 mA. The 2N6726 is physically a

small transistor but can dissipate 1 watt safely without a heat sink.

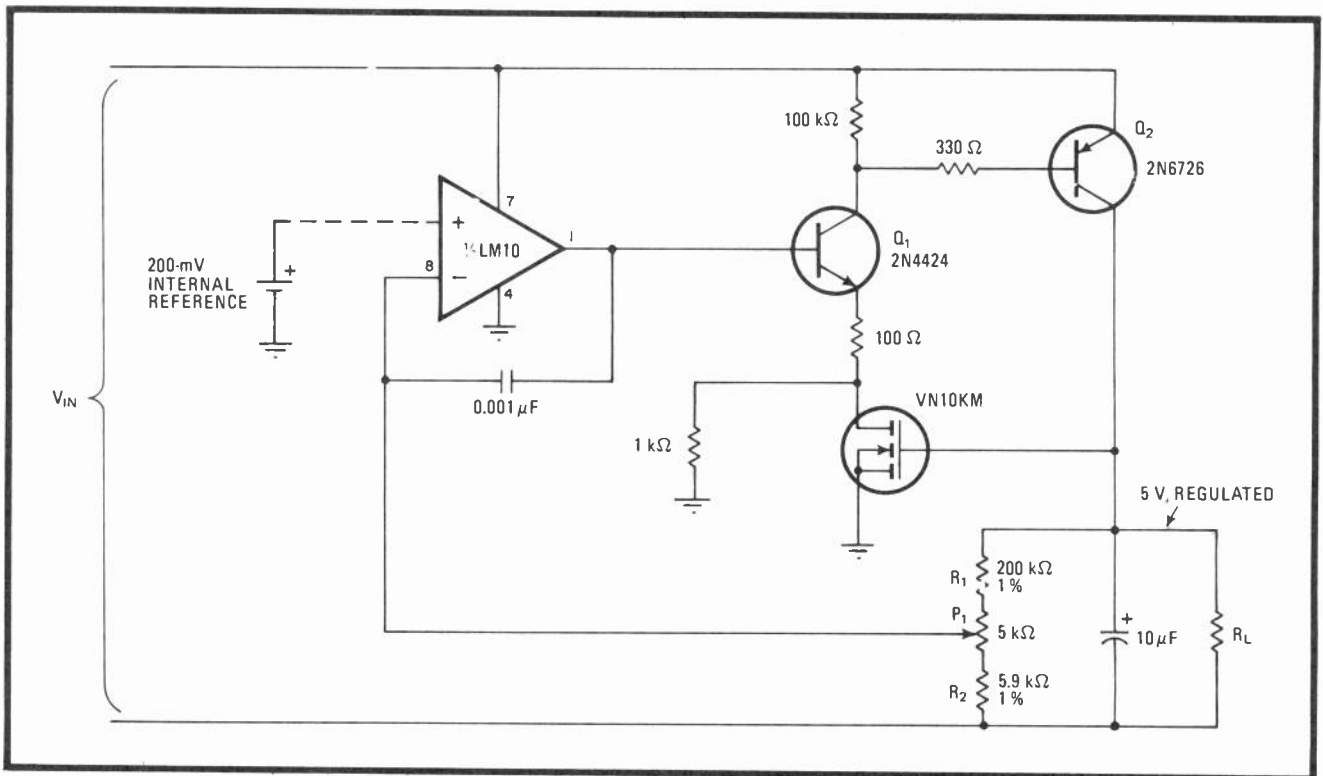
Short-circuit protection is provided by a Siliconix VN10KM, which presents a resistance of less than 10 ohms to the emitter circuit of the 2N4424 drive transistor under normal conditions. However, when the output is shorted to ground or excessive current is demanded, the drain-to-source resistance of the FET rises, safely shutting down the pass transistor. This characteristic can be used to advantage in adjustable current limiters, where the trip point is set by the input voltage. This method, incidentally, is more effective than any transistor foldback technique.

In operation, the LM10CH reference amplifier compares the voltage set by potentiometer P<sub>1</sub> to its internal 200-mV reference and through Q<sub>1</sub> acts to minimize voltage differences at the amplifier's input. With suitable selection of the component values in divider network R<sub>1</sub>-R<sub>2</sub>, the circuit will regulate over any voltage from 1 to 40 v. The operational-amplifier half of the LM10CH is available for other uses.

The load regulation is to within 0.3% for the range 0 to 100 mA and to within 1% for the range 100 mA to 1 A. The regulator's idle current is 320  $\mu$ A. □

### References

1. Kelvin Shih, "Micropower regulator has low dropout voltage," *Electronics*, April 12, 1979, p. 130.



**Dropout limit.** This low-power regulator, using output transistor operating in common-emitter configuration and having large junction area, can deliver 10 mA at 5 V for an input voltage only 12 mV higher and up to 1 A at 5 V for a 6-V input. Input-to-output voltage differential is only 650 mV at load currents of 750 mA. The V-MOS field-effect transistor provides short-circuit protection in such instances.



# Foldback limiter has minimal parts count

by Michael G. Lyngsie  
 MG-EL Consultants, Copenhagen, Denmark

Providing virtually the same function as the foldback limiter proposed by Kularatna,<sup>1</sup> but using a minimum of parts, this circuit delivers a well-regulated 24 volts at a maximum of 4 amperes. The circuit is extremely rugged and will meet all but the most demanding industrial requirements.

In operation, transistor  $Q_1$  operates as a differential amplifier to detect changes in output voltage and at the same time to keep track of the reference voltage,  $V_Z$ , which is constant as long as  $I_E R_6 < V_o - 6.8$ . The power-Darlington stage  $Q_2$ - $Q_3$  that follows serves as the series-pass transistor and its associated driver.

If there is a short circuit at the output or the load requires excessive current,  $I_E$  will also increase because  $Q_2$  and  $Q_3$  must be driven harder. This action causes  $Q_1$  to draw off a corresponding current that is normally delivered to the zener. Thus the zener voltage must fall, and foldback limiting is initiated. The quiescent current that will flow during foldback ( $V_o \approx 0$ ) is solely dependent on  $R_1$ , which re-initializes the supply upon removal of the overload condition.  $R_1$  can be made as large as desired, with the only limitation being that  $I_{R1}$  must be greater than the sum of the leakage current ( $I_{leak}$ ) through capacitor  $C_5$ , and  $I_{DC}$ .

Placing the series-pass transistor,  $Q_3$ , in the negative rail offers two distinct advantages. First, the device can be operated in the common-emitter configuration, enabling  $Q_3$  to provide voltage gain and current gain. This

enhances the dynamic range of the circuit. Secondly, most industrial equipment utilizes a negative ground, and so the power transistor can be directly mounted anywhere on the chassis for efficient cooling and the problem of electrical isolation can be eliminated. Furthermore, regulation is extremely fast because the only capacitors in the circuit are associated with the input filter ( $C_1$ ) and output bypass networks. Foldback action is not very fast, though, because of the large value of  $C_2$ . This capacitor can be made an order of magnitude smaller without sacrificing stability.

The output voltage will be held constant to 100 millivolts with this arrangement. Other voltages can be selected by altering the voltage-divider chain  $R_3$ - $R_4$ - $R_5$ . The maximum output current is approximately:

$$I_{max} = (V_o - 6.8)h_{fe Q2}h_{fe Q3}/R_6$$

neglecting  $I_B$  and the current flowing in  $R_2$ .

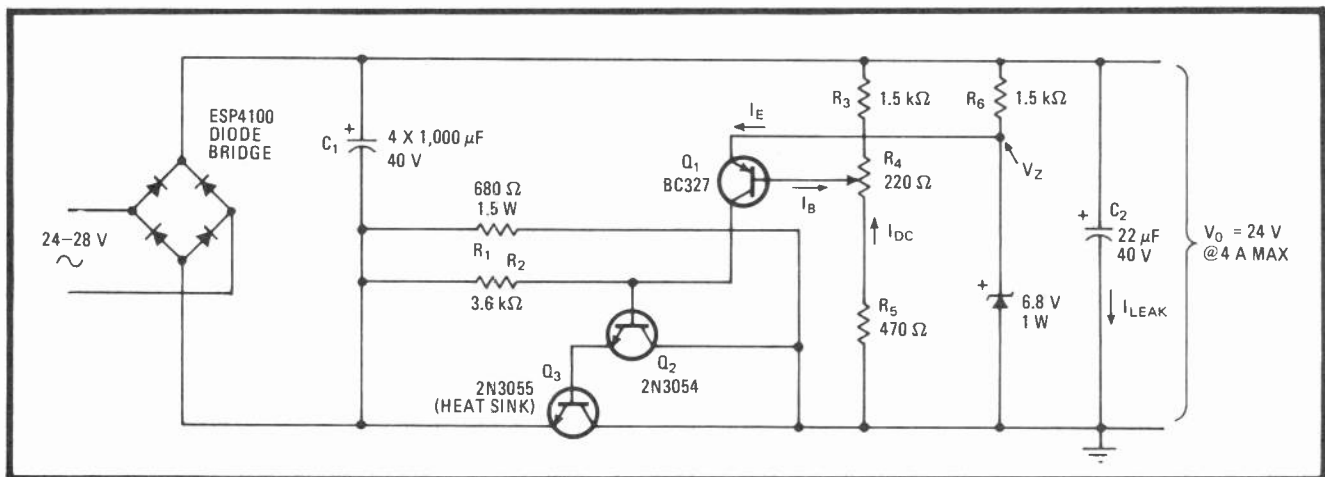
The circuit develops a slight positive temperature offset of 0.4 v after warmup, due to the positive temperature coefficient of the zener diode. If this offset proves to be annoying or unwanted, a forward-biased 1N4001 can be placed in series with the zener to eliminate the problem.

It is recommended that four 1,000- $\mu$ F capacitors be used for  $C_1$ , instead of a single 4,000- $\mu$ F device because of the high ripple currents (and heat generation) that will be encountered. Output ripple is only 20 mV peak to peak at 3.5 A. If desired, the ripple may be more than halved by the addition of another 1,000- $\mu$ F capacitor at the input. □

### References

1. A. D. V. N. Kularatna, "Foldback limiter protects high-current regulators," *Electronics*, Jan. 31, 1980, p. 98.

Designer's casebook is a regular feature in *Electronics*. We invite readers to submit original and unpublished circuit ideas and solutions to design problems. Explain briefly but thoroughly the circuit's operating principle and purpose. We'll pay \$50 for each item published.



**Rudimentary.** Simple but rugged and reliable foldback limiter delivers 24 V  $\pm$  100 mV at a maximum of 4 amperes. Output ripple is only 20 mV at 3.5 A and may be reduced further simply by placing additional capacitors at input. Placing series pass element,  $Q_3$ , in ground lead gives circuit good dynamic range and simplifies solution of classic mounting-vs-isolation problem in dealing with cooling of the power transistor.

# Low-cost autoranger scales DVM over four decades

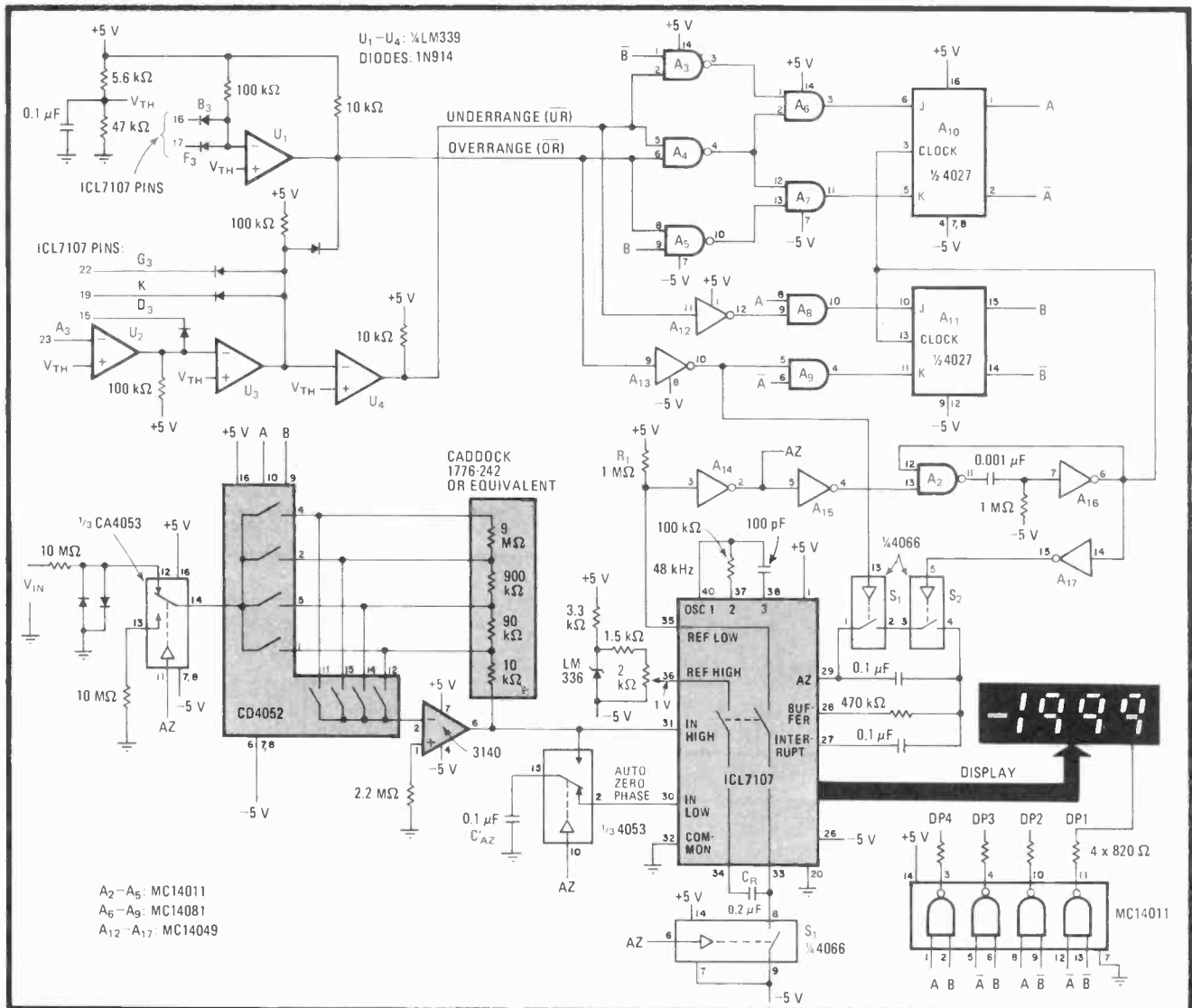
by L. Y. Hung  
Boston, Mass.

Autoranging capability can be added to a digital volt-meter with this circuit, which costs less than \$25. Built around a dual-slope integrating analog-to-digital converter to ensure greatest measurement accuracy, the unit scales a 3½-digit voltmeter over a range of four decades ( $\pm 1$  to  $\pm 1,000$  volts dc) without the need for complex feedback circuitry.

In operation (see figure), signals to the input are applied to the ICL7107 a-d converter through the range switch formed by the 4052 multiplexer and the attenuator that includes the CA3140 comparator and its accompanying decade resistor network. During each 333-

millisecond measurement cycle, the converter proceeds to eliminate the error caused by the comparator's offset (autozero phase), stores the input voltage (integrating phase), and displays the difference, in terms of a voltage, between the integration time and the time required to discharge a reference potential from capacitor  $C_R$  (display phase). The autorange circuit ( $A_3$ - $A_{13}$ ) that follows tracks both underrange and overrange conditions with the aid of a suitable detection circuit. It generates the appropriate signals for controlling the range switch and thus the gain of the attenuation network.

The autorange circuit determines underflow or overflow at the initial portion of the autozero phase. During this time, the voltage on pin 35 of the converter drops momentarily. The drop switches gate  $A_{14}$  and thereby closes switch  $S_1$ , an action that brings pin 35 to logic 0 and completes the charging cycle for  $C_R$ . The rising edge of the AZ signal that clocks the range switch is delayed about 1 millisecond by  $A_2$  and  $A_{16}$ , providing sufficient time to stabilize the display and to check for the under-range and overrange conditions.



**Searching.** DVM autorange circuit uses  $A_3$ - $A_{14}$  to detect underflow and overflow conditions by examining the output state of ICL7107 a-d converter, then sets gain of input attenuator network over four decades through 4052 range switch. Circuit cost is under \$25.

The range switch is an up-down counter. It will count down one state if an overrange signal is present and up one state if an underrange condition exists, over the binary range 00 to 11. The discharge path provided by switches  $S_2$ – $S_3$  reduces the residual charge on  $C_{AZ}$  during the de-integrating phase; otherwise continuous rocking between two adjacent scales may occur.

As for underrange and overrange detection, only one quad comparator need be connected to the ICL7107, as shown at the upper left. Both signals are derived from

the converter's seven-segment outputs. Underranging occurs if the displayed number is less than 200; for overrange, the number must be greater than 1,999.

A blank display on digit 3 indicates the overrange condition. A blank output on digit 4 and either a 1 or a 0 on digit 3 signifies underrange. In equation form:

$$\overline{UR} = \overline{OV} \cdot G_3 \cdot \overline{K} \cdot (\overline{A_3} + D_3)$$

where  $A_3$ ,  $D_3$ , and  $G_3$  are the display segments of digit 3 and  $K$  is the converter's thousands multiplier. □

## Improved burglar alarm discourages auto thieves

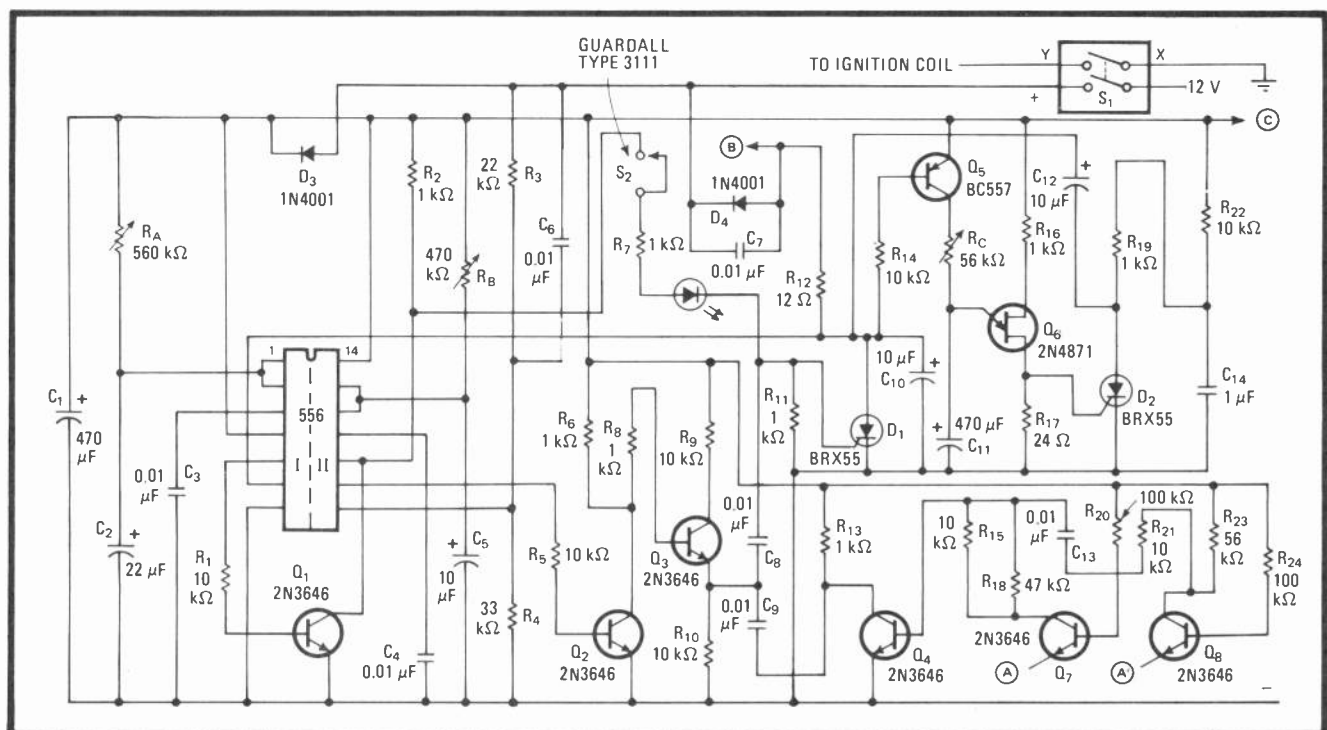
by Jose S. Correa de Quieros  
Engineering Faculty, University of Oporto, Portugal

Inexpensively detecting an increase in battery current—like that caused by the car's courtesy light—this automobile burglar alarm competes on a cost-vs-performance basis with any of the commercial all-electronic devices now available. The alarm also senses and responds to severe mechanical shocks of the kind caused by breaking glass. Standby current is only a few milliamperes.

Closing switch  $S_1$  arms the alarm through device I of the 556 dual timer after a time determined by  $R_A$  and  $C_2$ , enabling the driver to exit from the auto without triggering a false alarm. This switch also grounds the ignition coil so that it is impossible to start the engine.

Device II of the timer serves as the battery-discharge sensor. Voltage divider  $R_3$ – $R_4$  detects the small drop in the nominally set voltage at pin 8 (trigger input) of the 556 due to any current flow exceeding a few milliamperes.  $Q_2$  and  $Q_3$  then turn on (or  $D_1$  and  $Q_4$ , if lamps, radios, tape players, or other loads connected to point A or A' are disconnected by the thief), firing  $D_1$  and  $Q_5$  after a time determined by  $R_B$  and  $C_5$ . The horn relay at point B is then energized and timer  $Q_6$  initialized.  $R_B$  and  $C_5$  should be set to provide a delay of 5 seconds or so to enable the owner of the vehicle to enter and disarm the alarm. After a time set by  $R_C$  and  $C_{11}$  (maximum is 20 seconds),  $D_2$  fires, resetting  $D_1$  and the horn relay.

Capacitor  $C_1$  and diode  $D_3$  develop a dc average of the pulse train that is required to power the auto's clock via point C, effectively preventing the pulses from generating a false alarm. Severe mechanical shocks are detected by switch  $S_2$ , which is set with the aid of a screwdriver and a light-emitting diode that turns on when the switch elements make contact. When  $S_1$  closes in actual operation,  $D_1$  fires immediately to set off the alarm. □



**On guard.** Auto alarm detects small increases in battery current such as that caused by courtesy light activated by burglars, setting off horn relay after specified delay. Switch  $S_2$  senses mechanical shocks of the kind caused by breaking glass and sounds alarm immediately.

# LR oscillator indicates inductance directly

by John Jamieson  
 Technical Analysis Corp., Atlanta, Ga.

Inductance measurements accurate to within  $\pm 10\%$  may be made simply if the inductor is connected into the frequency-determining portion of this low-cost LR oscillator. Component values have been selected so that the oscillator's period, in seconds, equals 0.01 times the coil's inductance in henries, over the range from 0.5 millihenry to at least 10 H. Thus the inductance can be read directly from a period/frequency counter connected to the circuit's output.

$A_1$  of the TL084 operational amplifier serves as the integrator in the basic oscillator, with  $A_2$  a Schmitt trigger having trip points at one sixth and five sixths of the supply voltage and  $A_3$  a 1-to-20 voltage divider.  $A_4$  derives a voltage reference equal to half the supply voltage for driving  $A_1$ ,  $A_2$ , and  $A_3$ .

$A_3$  delivers a current into  $A_1$  of magnitude  $i_L = (1/L) \int V_L dt$ , where  $V_L$  is the initially negative output voltage of  $A_3$  and  $L$  is the inductance under consider-

ation. As a consequence, the output of  $A_1$  is a ramp of voltage  $V_o = RV_L t/L$ , where resistor  $R$  controls the gain of the stage, and  $t$  is time. Thus  $V_o$  rises linearly until  $A_2$ 's trigger point is reached, whereupon it switches and brings  $V_L$  high so that  $V_o$  begins to decrease linearly. The cycle is repeated when the Schmitt's lower threshold point is reached.

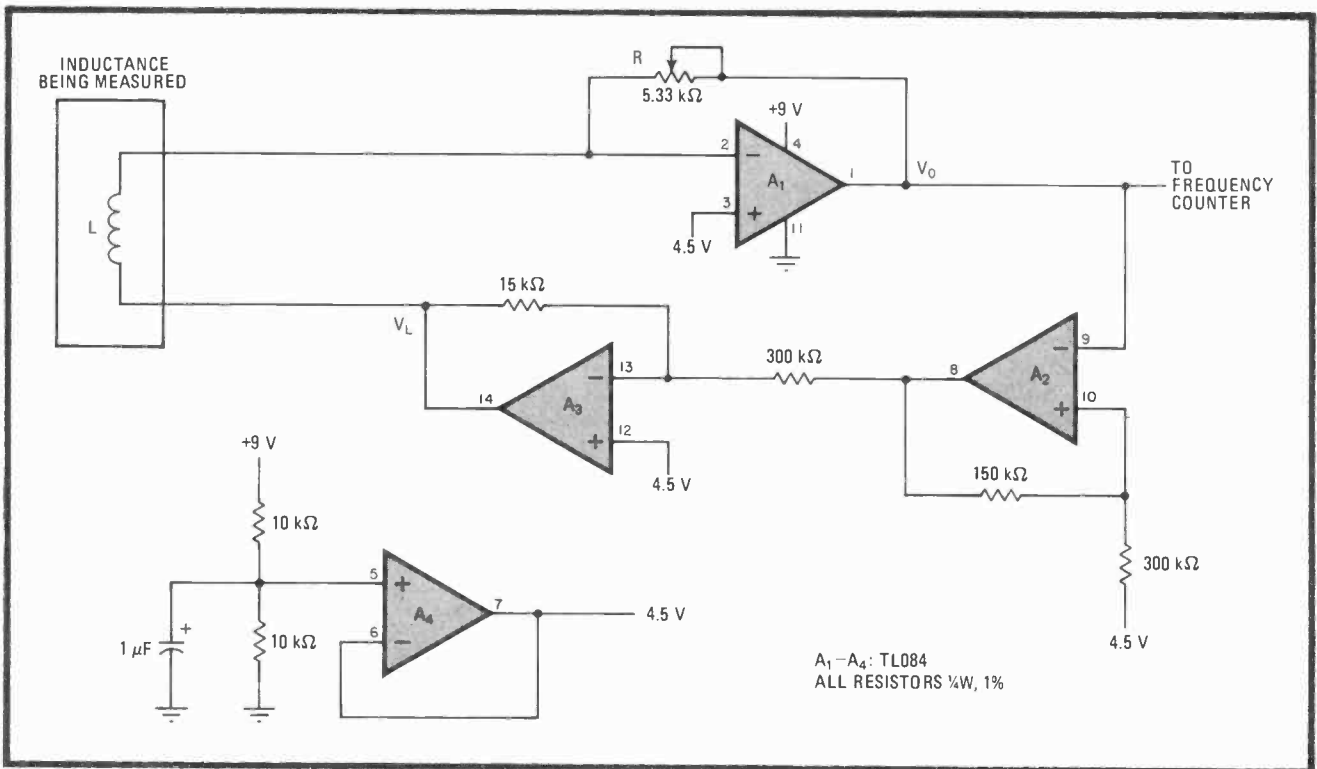
Selecting the period of oscillation to fall in the area of  $t = \tau/4$ , it is seen that  $V_o = (RV_L \tau)/(4L)$ , or  $L = (RV_L \tau)/(4V_o)$ . Because  $V_L \approx V_o/13$ , then  $L \approx R\tau/52$ . With  $R$  adjusted so that  $R/52 = 100$ ,  $L = 100\tau$ .

The preceding analysis assumes that the ohmic resistance of the inductor is small. For each ohm of resistance present below  $10 \Omega$ , there will be an approximate decrease of 0.1% in the accuracy of the measurement.

For inductors with considerable resistance, it will be noted that:

$$i_L = (1/L) \int V_L (1 - e^{-R_L t/L}) dt$$

where  $R_L$  is the resistance of the inductor, and so it can be shown that  $L = (-R_L \tau/4) \log_e(0.9975 R_L)$ . Thus to find the inductance, it is necessary to measure its resistance,  $R_L$ ; place the inductor in the circuit; and note the frequency of oscillation,  $\tau$ .  $L$  may then be calculated.  $\square$



**Self-measuring.** Inductance of low-resistance coils is measured to within  $\pm 10\%$  by noting frequency of LR oscillator of which the inductor is a part. Frequency counter may be used to indicate inductance directly, since period of oscillator, in seconds, is 1/100 of the inductance value in henries. Procedure is slightly modified for inductances having high impedance, most of which is ohmic for units having low hysteresis.

# One-chip multiplexer simplifies eight-trace scope

by Sam Curchack  
EDO Corp., Government Products Division, College Point, N. Y.

Displaying eight analog signals simultaneously with only a single-trace oscilloscope, this switching circuit can be built for even less (\$35) than the one proposed by Wright.<sup>1</sup> Circuitry is simplified, too, by the use of a one-chip, eight-channel differential multiplexer. And unlike most other arrangements, this unit is more versatile, having a chopped-mode and alternate-mode option and trace-positioning controls for each analog input.

In the chopped mode, which can be used at sweep speeds up to 50 microseconds/centimeter, all traces are referenced in time to input 1, which is the signal used to trigger the scope. Operational amplifiers (see inset) may be added for handling floating inputs. The 555 timer,

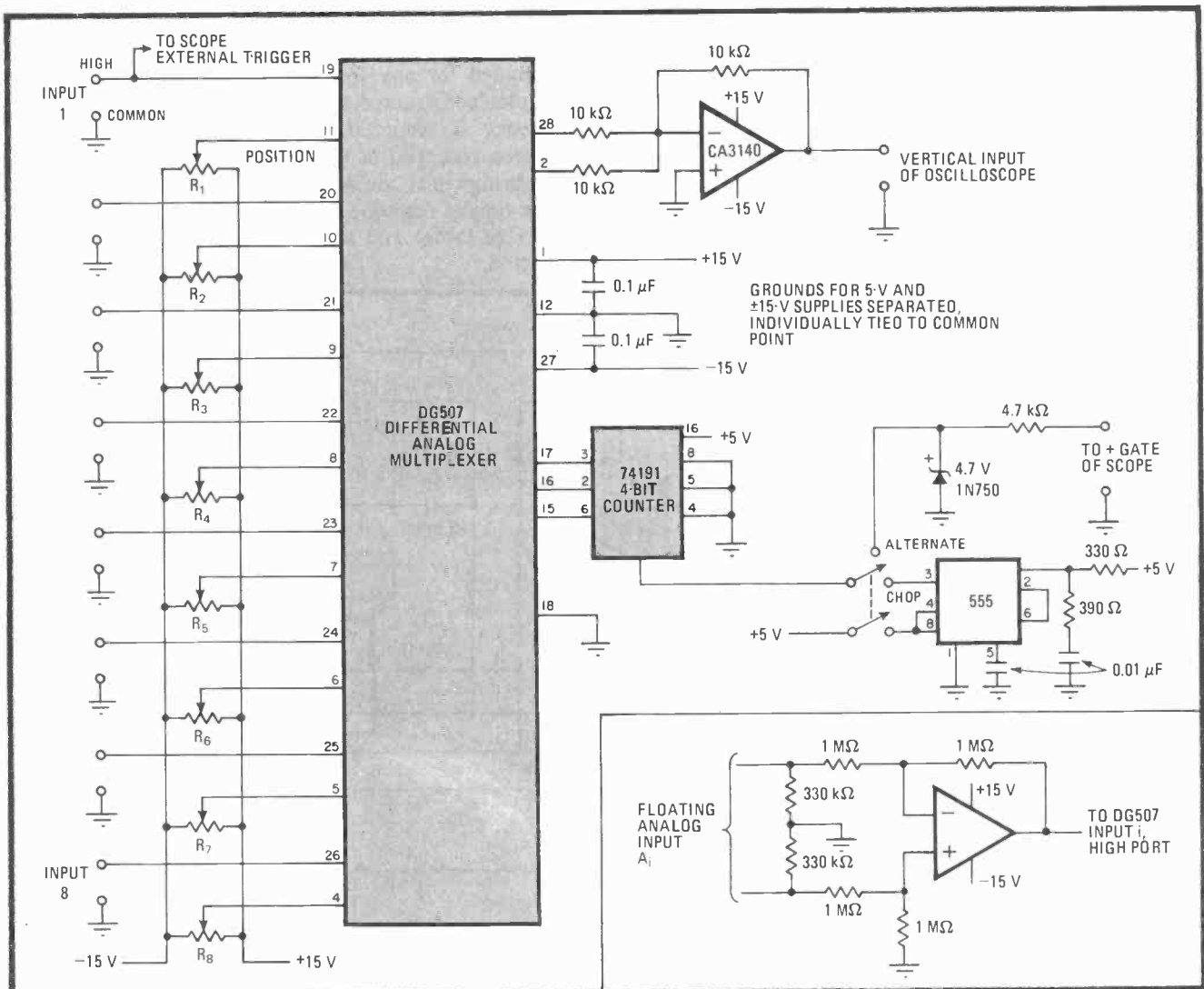
operating as an astable multivibrator, switches the 74191 4-bit counter at a 9- $\mu$ s rate, the sampling-bit time. This action in turn sequentially switches the DG507 multiplexer. As each input is selected, it is added to the dc output voltage of its positioning potentiometer ( $R_1$ - $R_8$ ).

At sweep speeds of 1 millisecond/cm and faster, the unit's alternate-mode option may be used. The 555 is deactivated and each analog input is switched in turn at any sweep speed selected by the user. The resulting display, devoid of most switching transients, is somewhat cleaner than can be achieved in the chopped mode. All other settings remain the same. A gating signal is required to synchronize the 4-bit counter, however. This signal is supplied by the scope's +GATE port.

More than 8 traces can be displayed on a dual-trace scope. With an additional 8-trace switching unit of the type previously described, 16 traces can be displayed. A large screen scope such as the Tektronix 7603 will be required for suitable resolution in this case. □

### References

1. George O. Wright, "Eight-trace scope display checks analog or digital signals," *Electronics*, Aug. 4, 1977, p. 108.



**Sweep switch.** Low-cost circuit displays eight analog signals on single-trace scope with aid of one-chip analog multiplexer. Alternate-mode (flicker-free above 200  $\mu$ s/cm) and chopped-mode options are available. Each trace may be individually positioned on screen.

# Test set characterizes FET's AGC response

by John Dunn  
Bertan Associates, Syosset, N. Y.

The relationship of a field-effect transistor's gate-to-source voltage ( $V_{gs}$ ) to its drain-to-source resistance ( $R_{ds}$ ), and consequently its suitability for use in automatic-gain-control circuits, can be found with the n-channel FET tester described here. Making the FET's  $R_{ds}$  a part of one leg of a Wien-bridge oscillator makes it possible for a technician to correlate the bridge's instantaneous output frequency with a bridge-generated voltage that corresponds to the applied  $V_{gs}$ . Because the frequency is related to  $R_{ds}$  by a simple equation,  $R_{ds}$  may be readily plotted against  $V_{gs}$ .

Operational amplifier  $A_1$  and zener diode  $D_1$  maintain a voltage of about 7.5 volts for the FET's source, with its uncommitted drain connected into the circuit such that under steady-state conditions the Wien bridge built around  $A_3$  is balanced at any given frequency for:

$$R_{ds}/(R_{fb} + R_{ds}) = (j\omega C_a C_b) / [j\omega R_a C_a (1 + j\omega R_b C_b) + (1 + j\omega R_b C_b) + j\omega C_a C_b]$$

Because  $\omega = 1/(R_a R_b C_a C_b)$ , the condition for balance simplifies to:

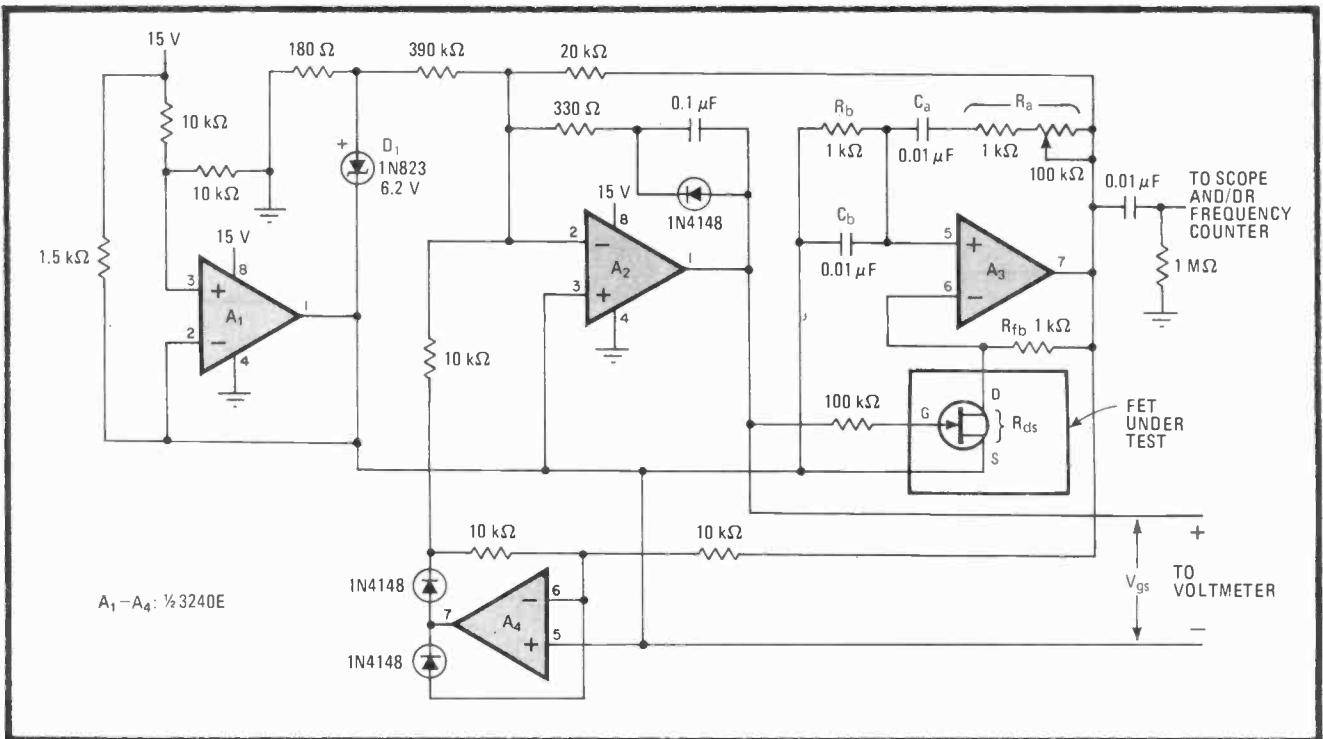
$$R_{ds} = R_{fb} / [(R_a/R_b) + (C_b/C_a)]$$

Noting that  $R_a = 1/(\omega^2 R_b C_a C_b) = 1/(4\pi^2 f^2 R_b C_a C_b)$ ,

| $V_{gs}$ | Frequency, Hz | $R_{ds}$ , $\Omega$ |
|----------|---------------|---------------------|
| 0        | 2149          | 17.9                |
| -0.5     | 2303          | 20.5                |
| -1.0     | 2465          | 23.4                |
| -1.5     | 2656          | 27.1                |
| -2.0     | 2893          | 32.0                |
| -2.5     | 3207          | 39.0                |
| -3.0     | 3683          | 50.8                |
| -3.2     | 3936          | 57.6                |
| -3.4     | 4314          | 68.4                |
| -3.6     | 4836          | 84.5                |
| -3.8     | 5604          | 110.3               |
| -3.9     | 6199          | 131.7               |
| -3.95    | 6560          | 145.2               |
| -4.0     | 6949          | 160.1               |

where  $f$  is the frequency of the oscillator, then  $R_{ds} = R_{fb} / [1/(4\pi^2 f^2 R_b C_a C_b) + (C_b/C_a)]$ . Thus  $R_{ds}$  may be determined for any frequency selected by  $R_a$ , and the AGC plot constructed if the corresponding  $V_{gs}$  for that frequency is recorded. Note that the required gate-to-source potential of 0 to  $-7.5$  v is derived from the Wien bridge itself via  $A_2$  and  $A_4$ .

The typical response of a Motorola MPF4391 is tabulated (see table) and may be used to check the tester's operation. □



**Charting gain.** Tester, with n-channel FET placed in leg of Wien-bridge oscillator, helps find relationship of FET's drain-to-source resistance ( $R_{ds}$ ) to its gate-to-source voltage ( $V_{gs}$ ), and thus its suitability for use in automatic-gain-control circuits. The common variable is frequency, which has an effect on  $R_{ds}$  via feedback voltage  $V_{gs}$ . The typical response of Motorola FET (table) aids in checking out the tester.

## Fm decoder improves SCA subcarrier detection

by Robert F. Woody  
Christiansburg, Va.

The 67.5-kilohertz subcarrier required for subsidiary communications authorization (SCA) service in the fm band can be recovered by a decoder that needs only two chips and one discrete amplifier. And it can be built for less than \$10. Besides using fewer parts than existing designs, this circuit provides higher output and offers greater versatility.

As an illustration of its advantages, the 4046 phase-locked loop in the decoder provides an output level approximately equal to the fm level at its input, thereby generating adequate drive to succeeding stages. In addition, the PLL's filter also serves as the deemphasis filter, thus eliminating the need for a separate network. Finally, upon loss of the subcarrier, the circuit generates a signal that can cue a recorded message to the audience receiving SCA service.

The decoder is attached to an fm receiver at its ratio-detector output, ahead of the deemphasis filter. For best performance, it is recommended that the signal be

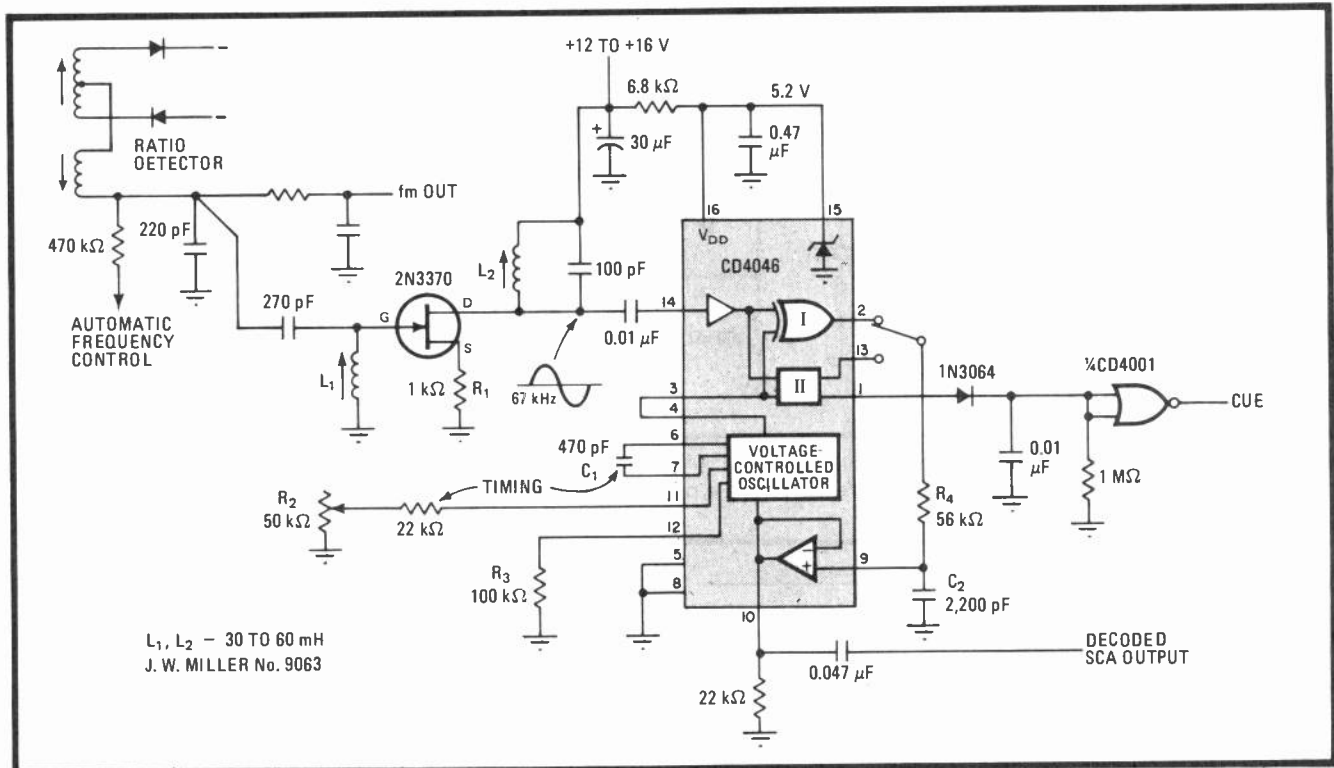
taken from a stereo receiver because its bandwidth, which is designed to be broad for the stereo carrier, provides good reception of the 67.5-kHz SCA signal.

The 2N3370 tuned field-effect-transistor amplifier separates the low-level subcarrier from the other program material, including the very strong stereo carrier. Resistor  $R_1$  yields maximum amplifier gain at 1 kilohm. This resistance can be increased to reduce the amplifier's gain for fm receivers that deliver high-level output signals. Values to 5 k $\Omega$  are within the amp's range.

The CD4046 PLL performs the decoding.  $C_1$  and  $R_2$  set the loop's center frequency.  $R_3$  sets the conversion gain (volts/radian) of the PLL's voltage-controlled oscillator. Increasing  $R_3$  makes the VCO less sensitive to input-voltage changes. Decreasing  $R_3$  reduces the SCA output level.

$C_2$  and  $R_4$  comprise the low-pass filter. As placed in the circuit, these elements also deemphasize the SCA signal at high frequencies, the amount of deemphasis being about 3 decibels at 1.3 kHz.

A string of pulses is emitted from pin 1 of the 4046 when the PLL is in lock. The pulses are rectified by the 1N3064 diode and filtered by the 0.01-microfarad capacitor. Thus a dc level is derived. Should the subcarrier disappear, however, the level will fall and the CD4001 NOR gate will go high. This signal can be used to cue the playing of recorded messages, such as typical commercial advertisements. □



**Simple service.** Improved fm decoder for detecting SCA subcarrier yields higher output, uses fewer parts, provides good selectivity and cue option. Requiring only two chips, and one tuned amplifier for separating the stereo from the SCA subcarrier, it costs less than \$10.

# Low-cost logarithmic amp works over one decade

by Christopher S. Tocci  
Becton-Dickinson Medical Systems, Westwood, Mass.

If extremely high precision is unnecessary and if the required dynamic range spans no more than one decade of input voltage, then this logarithmic amplifier will serve the application well. Use of a simple exponential generator, which is ultimately required to convert a voltage into its base-10 logarithmic equivalent, makes it possible to build the amp for a mere \$3 to \$4.

The overall system is shown in (a), with the schematic of the exponential generator shown in (b). Voltage divider  $R_1$ - $R_2$  applies 0.5 volt to RC combination  $R_3$  $C_1$  through op amp  $A_2$  on power-up in order to initialize the exponential growth process. As  $C_1$  charges, the output of  $A_2$  increases as shown in the curve until the Schmitt trigger,  $A_3$ , which has a switching threshold of 10 v, fires, turning on field-effect transistor  $Q_1$  and discharg-

ing  $C_1$  to about 1.0 v. The process then repeats, with switching occurring at a rate,  $\tau$ , determined by  $C_1$  and  $R_2$ . The op amp must have a minimum slew rate of:

$$\begin{aligned} dV_o(t)_{\max}/dt &= (1/\tau) e^{V_c/R_3 C_1} \\ &= (10 \log_e 10)/\tau = 23.03 f_s \end{aligned}$$

where  $f_s$  is the switching frequency. Thus at a switching frequency of 10 kilohertz ( $C_1 = 0.01 \mu\text{F}$ ,  $R_1 = 4.32 \text{ k}\Omega$ ) the slew rate must be at least 0.23 v/microsecond.

During each switching cycle, the exponential output is compared at  $A_1$  to the instantaneous input voltage,  $V_c$ , that is to be converted into its corresponding logarithm.  $A_1$ 's on time,  $D_v$ , is thus related to input voltage  $V_c$  by:

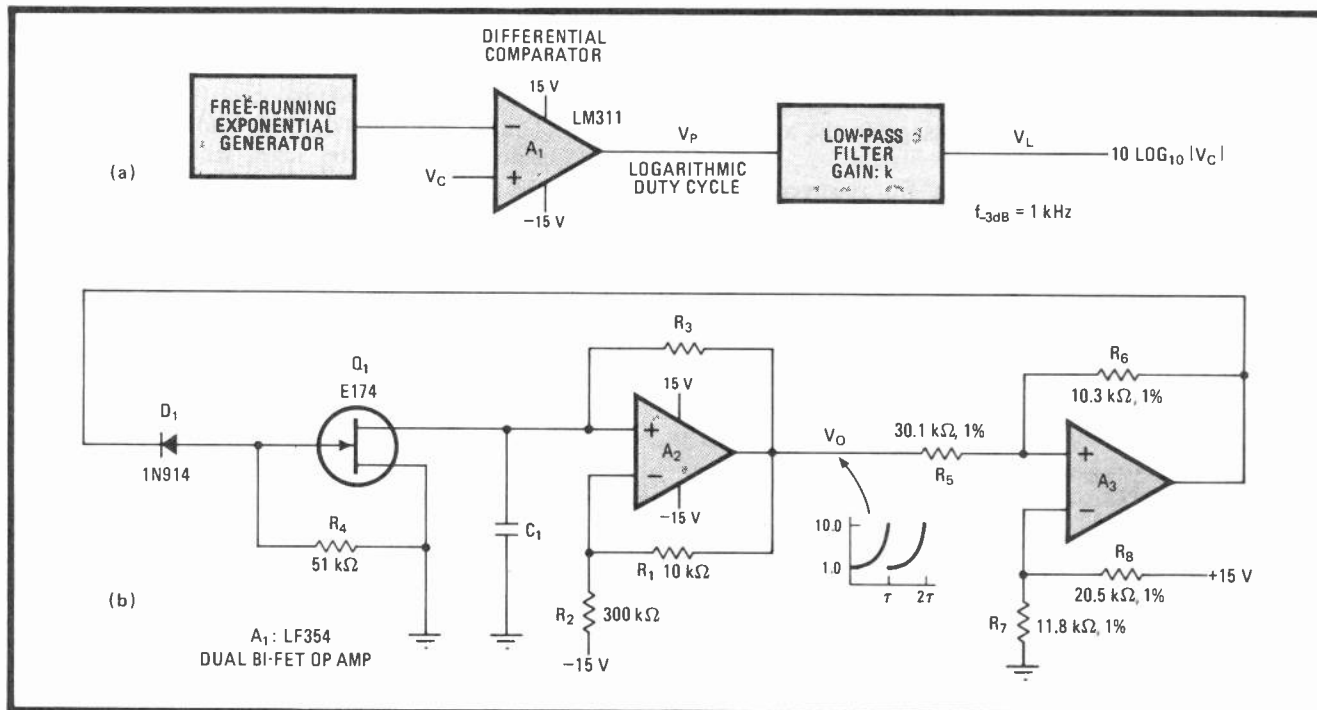
$$D_v = (t_{\text{on}}/\tau) 100 = \tau \log_e |V_c|/\tau = 0.434 \log_e |V_c|$$

where output voltage  $V_p$  corresponds directly to  $D_v$ , ignoring a scale factor.

The active low-pass filter of gain  $k$  that follows, which should be at least a third-order type for the best results, then finds the average value of  $V_p$  from:

$$V_L = \bar{V}_p = k(0.434) \log_e |V_c|$$

Choosing  $k$  such that  $k(0.434) = k(V_{p, \max}/\log_e 10) = 4.34$ , it is seen that  $V_L = 10 \log_{10} |V_c|$  for  $1 \leq V_c \leq 10$ .  $\square$



**Naturally.** Low-cost generator provides exponential waveform of sufficient accuracy in amplifier that takes logarithms over one decade of input voltage. Filter averages pulse-width-modulated equivalent of  $V_c$  produced by differential comparator,  $A_1$ , for  $V_L = 10 \log_{10} V_c$ .

# Hall sensors and flip-flop sustain pendulum's swing

by John Karasz  
Sperry Corp., Great Neck, N. Y.

This circuit offers a simple way to control and sustain oscillatory motion in a simple pendulum and in many other types of mechanical oscillators. Using Hall-effect sensors to detect the instantaneous position of the pendulum and to call for delivery of an energy burst through a flip-flop to keep it swinging, the circuit is a good alternative to the complicated electromechanical arrangements frequently employed. The cost of the entire circuit is also



relatively low, making it especially attractive.

When the small permanent alnico magnet that is part of the pendulum support rod comes into sufficiently close proximity to Hall sensor  $S_1$ , the sensor generates a negative-going pulse. This pulse sets the R-S flip-flop formed by two cross-coupled 74LS00 NAND gates,  $A_1$  and  $A_2$ . The Q output of the flip-flop, now at logic 1, energizes electromagnet  $L_1$ , thereby delivering energy to the pendulum via the field between the steel pendulum bob and  $L_1$ .

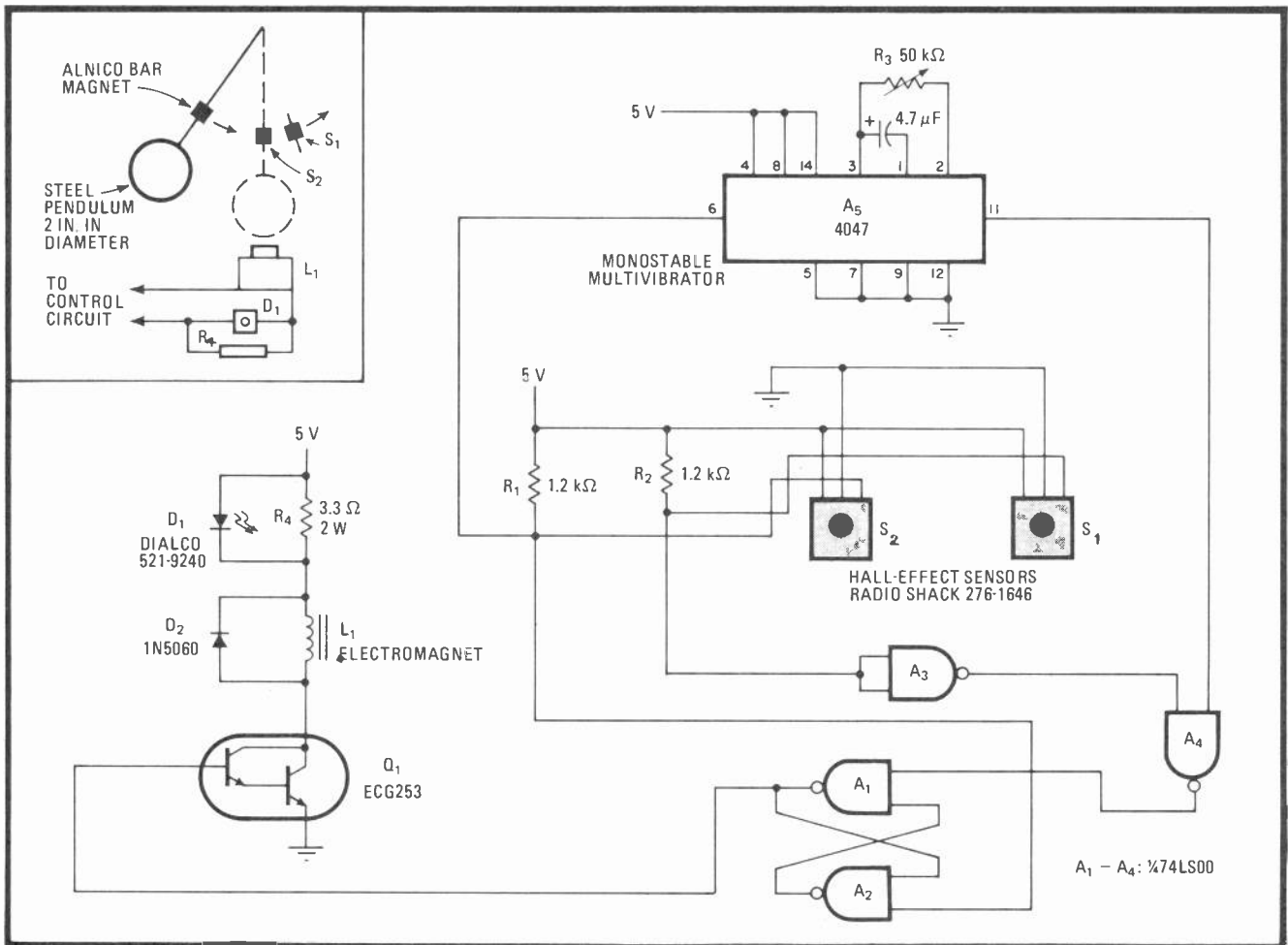
When the pendulum bob reaches the lowest point in its trajectory,  $L_1$  is deenergized by the negative-going pulse generated by sensor  $S_2$ , which clears the flip-flop. Simultaneously, one-shot  $A_5$  is triggered. Hence, as long as the Q output of  $A_5$  remains active low, the flip-flop cannot be retriggered because gate  $A_4$  cannot move to logic 0. This action prevents  $L_1$  from energizing and thus creating any drag effect on the pendulum. Also, it conserves power by limiting the time  $L_1$  is on.

In order to initialize the circuit at a relatively small pendulum swing, the period of the one-shot should be set for  $t = T/4$ , where  $T$  is the natural period of the pendulum. Because the oscillation frequency of a simple pendulum is  $\omega^2 = g/L$ , where  $\omega = 2\pi f$ ,  $g = 32.2$  feet per second squared, and  $L =$  the distance from the point

of support to center of mass of the pendulum bob, it may be seen that  $T = 2\pi(L/g)^{1/2}$ , and so  $t$  should be in the range of 0.32 to 0.36 s in a practical configuration, for  $T = 1.44$  s.

As for component considerations,  $L_1$  is constructed from 100 feet of AWG 24 enameled wire wound on a steel core  $1/16$  inch long and  $3/8$  in. in diameter. The alnico magnet is situated only about 0.45 in. above the top surface of the pendulum bob—in terms of metric units, approximately 12 millimeters away. The magnet is 3 mm wide, 3 mm high, and 8 mm long. The clearance between the magnet's pole face and the Hall-effect sensor's surface should be between  $1/32$  in. and  $1/16$  in. for best results. A small decoupling capacitor ( $0.033 \mu\text{F}$ , disk ceramic) is connected between the supply lead and ground of the 74LS00 chip to keep circuit transients caused by  $S_1$  or  $S_2$ 's firing from inadvertently setting the flip-flop to the wrong state.

Light-emitting diode  $D_1$  serves as a visual monitor, being lit when  $L_1$  is energized. When mounted at the base of the electromagnet, it facilitates a qualitative check on the performance of the system. □



**Keep swinging.** Hall-effect sensors detect instantaneous position of pendulum, direct flip-flops  $A_1$ - $A_4$  to generate energy pulse via field between  $L_1$  and pendulum bob in order to keep pendulum moving. One-shot  $A_5$  prevents flip-flop retriggering in any given cycle, thus stops pendulum drag, and conserves energy. Inset illustrates physical relation of bar magnet to pendulum and interface elements.

# Sampling filters simplify converter's offset measurement

by Dennis Knowlton, National Center for Atmospheric Research, Research Aviation Facility, Boulder, Colo.

A microprocessor-based data-acquisition system has difficulty in making corrections for input offset and gain drift when it uses active filters to remove the effects of aliasing, or system noise. In such circumstances, the filters' frequency response and settling time vary as a function of the sampling rate and the magnitude of the input signal. However, the difficulties encountered with these sampled-data systems may be overcome by means of a switched aliasing filter, so that the anomalies in filter response may be virtually neglected and the offset and gain drift may be readily determined under software control.

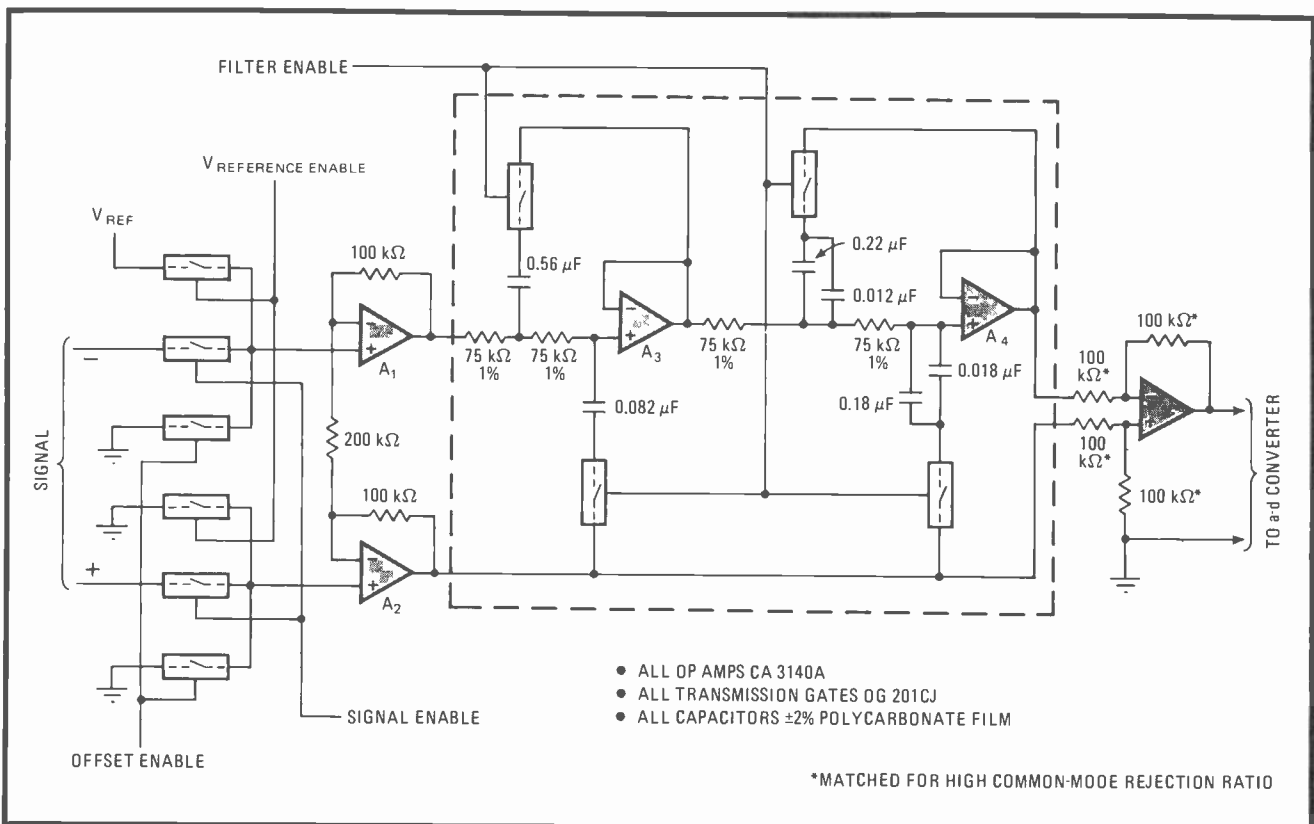
In the typical input stage leading to the system's a-d converter, the noninverting ports of op amps  $A_1$  and  $A_2$  are periodically switched to ground and to a reference voltage so that the circuit can be isolated from all external stimuli and its inherent offset and gain determined. This scheme eliminates potentiometers and the requirement for precision components. It also leaves the measuring task to the software routine, where time and temperature have no effect on system accuracy, and where the data can be corrected for actual gain and

offset by means of look-up tables.

Because of sampling, however, the filter's frequency-domain response becomes a factor and thus a significant amount of signal data can be lost during the filter's settling time. Switching the filter out at a very slow rate compared with the signal sampling rate, and doing so at a low duty cycle, eliminates the problem.

The key to the success of the circuit lies in the fact that in the standard active filter, the only energy-storage elements are capacitors. Switching these elements out of the circuit periodically transforms the filter into one that has a very high cutoff frequency; thus the filter is essentially out of the circuit and its op amps' offset and gain drift can be easily measured. When the capacitors, which store the instantaneous value of the driving signal, are switched back into the circuit, they perform their basic filtering function. Thus, assuming the use of fast op amps, a high-speed a-d converter, and low-leakage capacitors in the filter, the signal-path response of the filter is unchanged; yet, offset and gain drift can be determined.

Shown in the circuit example is a simple four-pole filter built around  $A_3$  and  $A_4$  whose components are selected to reject aliasing noise at 10 hertz. Signal-path sampling is done at 50 Hz and capacitor switching at 0.1 Hz for a duration of 12 microseconds. The input and output stages of the circuit all utilize standard differential amplifiers. □



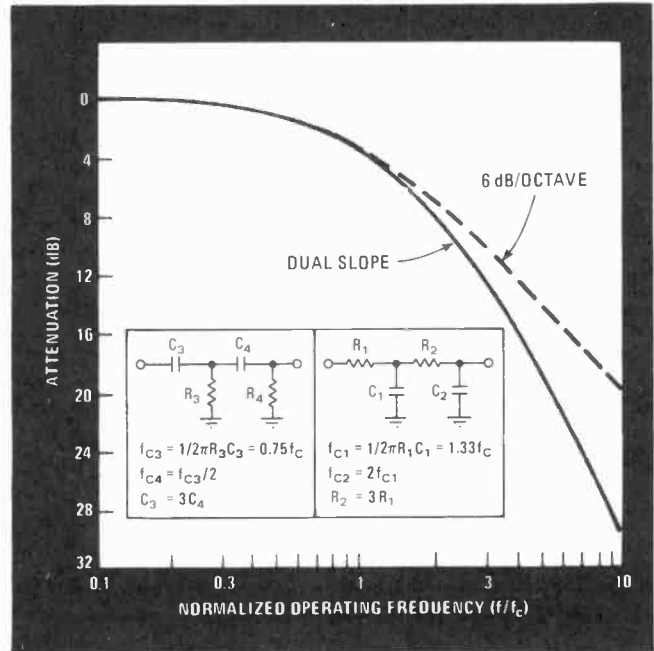
**Indeterminate.** Aliasing filter  $A_3$ - $A_4$  for data-acquisition system makes it impossible to ascertain input offset and gain drift unless it is itself of the sampling type. Filter's signal-path response will be unchanged, but stages' inherent imperfections can then be measured.

# Dual-slope filters optimize speaker's crossover response

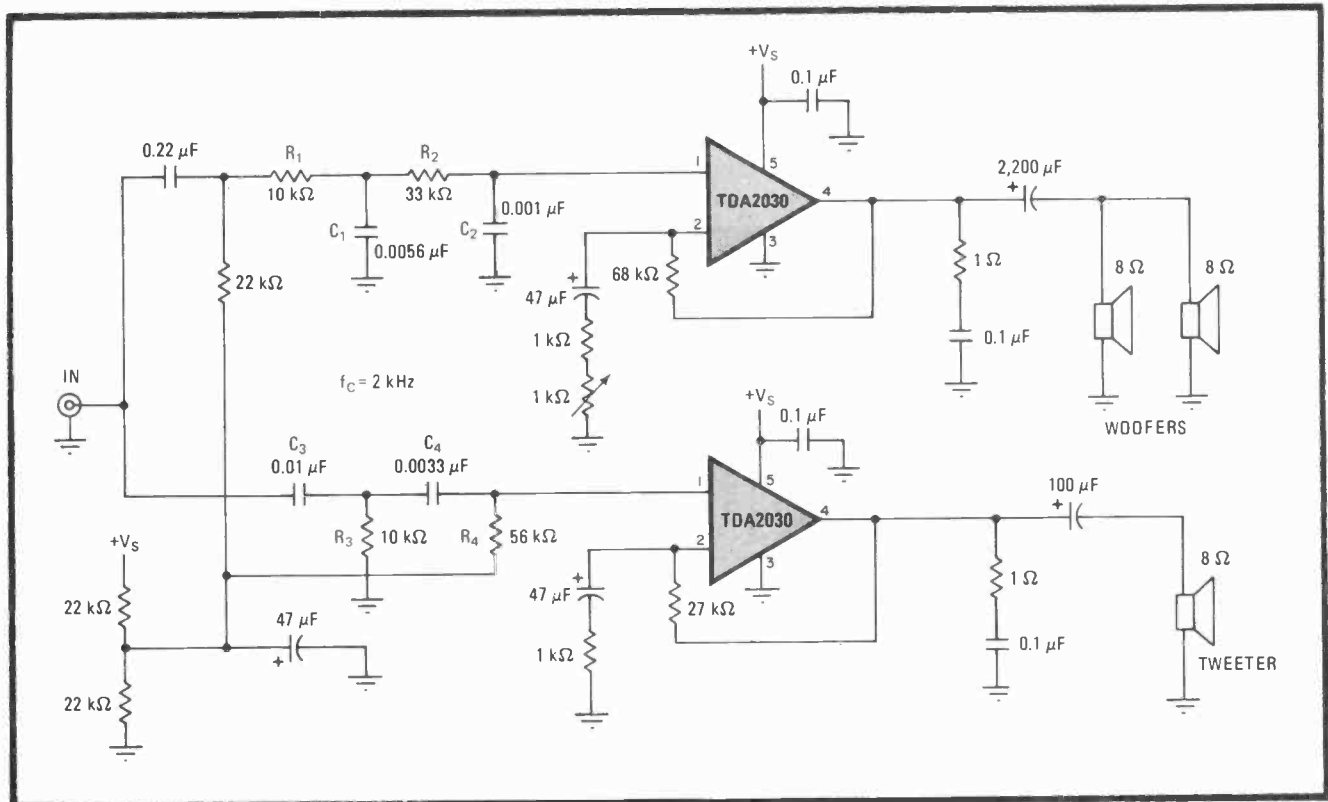
by P. Antoniazzi and A. Hennigan  
SGS-ATES Electronic Components, Milan, Italy

The crossover response, and thus the overall performance, of a two-way high-fidelity loudspeaker system can be significantly improved with these high- and low-pass networks. Staggering two cascaded RC filters in the woofer channel yields a slope of 6 dB/octave near the cutoff frequency,  $f_c$ , and a notably steeper 12 dB/octave beyond  $f_c$ . When combined with the complementary (inverted response) output of the tweeter section, optimum crossover characteristics are achieved at low cost and without audio-frequency discontinuities at  $f_c$ .

In general, many simple low-pass networks can provide a 6-dB/octave response at frequencies approaching  $f_c$  from the low side. When a single-pole filter is used, however, as is still done on occasion, the maximum roll-off beyond  $f_c$  can never be greater than 6 dB/octave. Unfortunately, the typical loudspeaker does not have a linear enough response to handle high-level signals (de-



**2. Response.** Dual-slope filter, using staggered RC networks, virtually eliminates drop-off in audio output at the cutoff frequency of hi-fi speakers, while providing a roll-off of greater than the usual 6 dB/octave. Equations for woofer and tweeter sections summarize design.



**1. Distortionless.** Staggered low-cost, low-pass filters in woofer channel achieve slope of 6 dB/octave approaching cutoff frequency  $f_c$  and 12 dB/octave above  $f_c$  without introducing quadrature phase shift and accompanying distortion produced by loudspeakers. When combined with complementary output of high-pass section, system achieves crossover characteristic devoid of audio discontinuities at  $f_c$ .

graded by only 6 dB/octave) at its high-frequency limits, and so distortion results.

With second-order filters (12 dB/octave), a loss of audio usually occurs at the crossover point. This phenomenon is caused by the  $+90^\circ$  phase shift of the low-pass network, which when combined with the  $-90^\circ$  output of the system's high-pass filter tends to cancel the audio output.

Using a third-order Butterworth filter solves both of the aforementioned problems, yielding a flat response from dc to near  $f_c$ , steep cutoff (18 dB/octave) above  $f_c$ , and a gradual phase change across the band of interest. But this method is expensive, requiring two or three op

amps and a large number of external components.

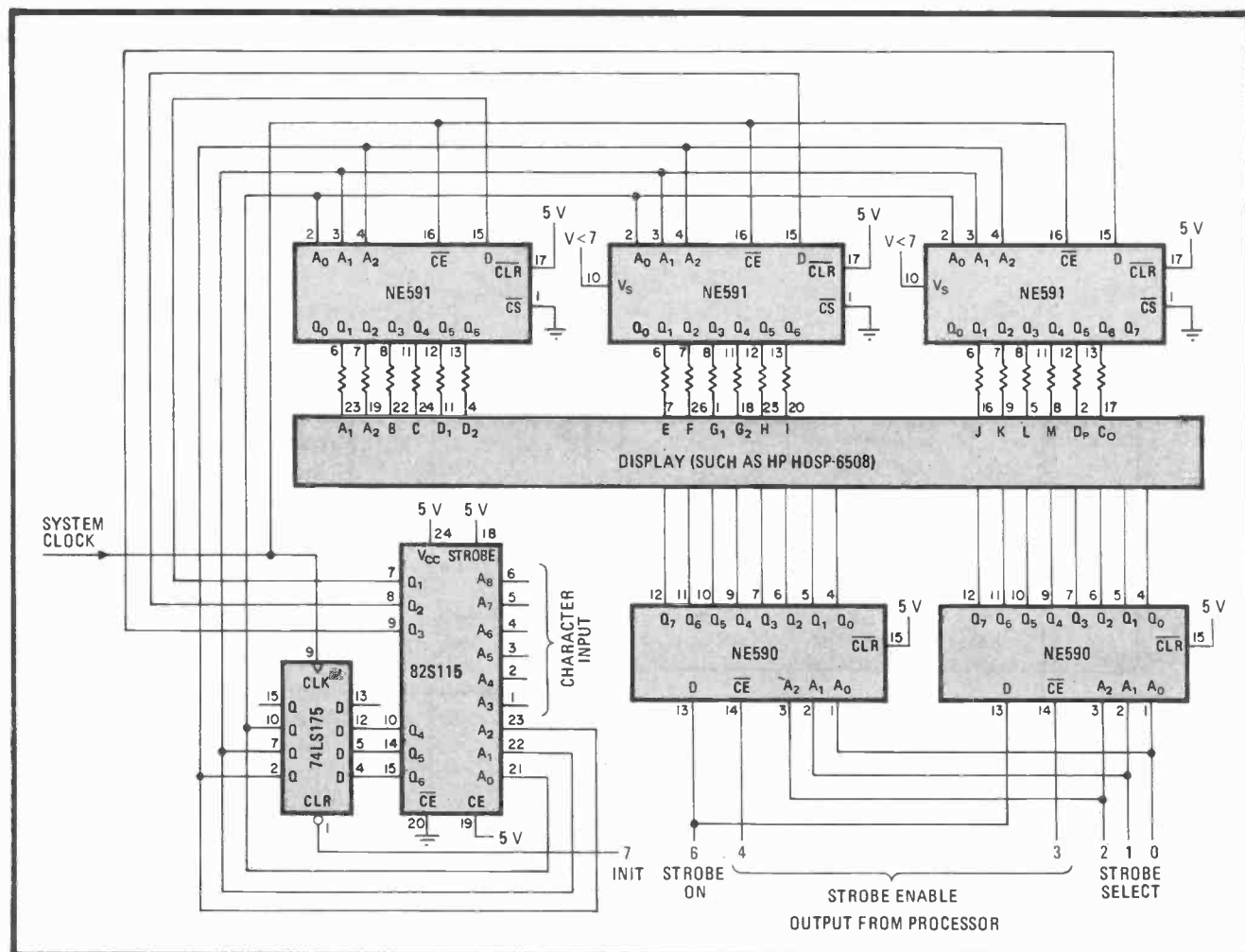
The dual-slope crossover network (Fig. 1) provides a viable answer to the problem. Staggering the responses such that the cutoff frequency of the first RC network is one half that of the second, attenuation at the crossover frequency will be 3 dB as in other systems, but the phase shift at  $f_c$  will be  $60^\circ$ ; thus the cancelation problem typical of second-order filters is avoided. This circuit is ideally suited to active loudspeaker systems.

The plotted response of the woofer section is shown in the curve, which is complete with the required design equations. Corresponding equations for the tweeter are also included. □

## Low-cost alphanumeric decoder drives British-flag display

by S. Cash Olsen  
Signetics Corp., Sunnyvale, Calif.

Converting 64-character ASCII into an 18-segment ("British-flag") display font, this microprocessor-controlled alphanumeric decoder is a low-priced (\$12) alternative to circuits costing up to five times as much. Most 18-segment displays (from Hewlett-Packard, Monsanto, and others) may be driven directly. And with the addition of high-breakdown output transistors to the driving circuitry, vacuum fluorescent panels and similar displays



**Charting characters.** Low-cost alphanumeric decoder converts ASCII symbols into 18-segment display representation. Segment information, stored as table in 82S115 PROM, is clocked out in 3-bit segments over six states for each character, placed in display via NE591 drivers at any location by NE590 strobe latches. PROM character-generation table outlines method utilized to create symbols.

READ ONLY MEMORY CHARACTER GENERATION

| Address          | Q <sub>6</sub> | Q <sub>5</sub> | Q <sub>4</sub> | Q <sub>3</sub> | Q <sub>2</sub> | Q <sub>1</sub> | Symbol |
|------------------|----------------|----------------|----------------|----------------|----------------|----------------|--------|
| 000 <sub>8</sub> | 0              | 0              | 1              | X              | X              | X              |        |
| 001              | 0              | 1              | 0              | 1              | 1              | 0              |        |
| 002              | 0              | 1              | 1              | 1              | 1              | 0              |        |
| 003              | 1              | 0              | 0              | 1              | 1              | 0              |        |
| 004              | 1              | 0              | 1              | 0              | 0              | 0              |        |
| 005              | 1              | 1              | 0              | 1              | 0              | 0              |        |
| 006              | 1              | 1              | 1              | 1              | 0              | 0              |        |
| 007              | 1              | 1              | 1              | X              | X              | X              |        |
| 010              | 0              | 0              | 1              | X              | X              | X              |        |
| 011              | 0              | 1              | 0              | 1              | 1              | 0              |        |
| 012              | 0              | 1              | 1              | 1              | 1              | 0              |        |
| 013              | 1              | 0              | 0              | 1              | 1              | 0              |        |
| 014              | 1              | 0              | 1              | 1              | 1              | 0              |        |
| 015              | 1              | 1              | 0              | 0              | 0              | 0              |        |
| 016              | 1              | 1              | 1              | 0              | 0              | 0              |        |
| 017              | 1              | 1              | 1              | X              | X              | X              |        |
| ⋮                | ⋮              | ⋮              | ⋮              | ⋮              | ⋮              | ⋮              |        |
| 770              | 0              | 0              | 1              | X              | X              | X              |        |
| 771              | 0              | 1              | 0              | 1              | 0              | 0              |        |
| 772              | 0              | 1              | 1              | 1              | 0              | 0              |        |
| 773              | 1              | 0              | 0              | 1              | 0              | 1              |        |
| 774              | 1              | 0              | 1              | 0              | 0              | 0              |        |
| 775              | 1              | 1              | 0              | 0              | 0              | 0              |        |
| 776              | 1              | 1              | 1              | 0              | 0              | 0              |        |
| 777              | 1              | 1              | 1              | X              | X              | X              |        |

requiring high voltage may be accommodated, also.

In general operation (see figure), the microprocessor coordinates character selection, strobe-timing, and overall control duties with the aid of the NE590 strobe drivers, the NE591 peripheral display drivers, and the 74LS175 quad latch. When suitably addressed, the 82S115 512-word-by-8-bit PROM, which stores all the ASCII characters, delivers a logic-state table corresponding to the character selected via the clocked 74LS175 and the NE591s.

The PROM functions both as a character-request look-up table and as a state machine, with the quad flip-flop holding the current machine state. Bit 7 of the processor initializes the state to zero at the beginning of a character-decode cycle.

Logic signals corresponding to the character desired are then applied to pins A<sub>3</sub>-A<sub>8</sub> of the PROM, and the device is clocked through seven states (see table) so that the desired segments are excited. The display is then strobed and the character thus placed in any desired location via command from pins 0 to 6 of the processor via the strobe latches, each latch of which is enabled separately. This process is repeated for up to 64 charac-

ters, the maximum that may be placed on the display at any given instant. Thereafter, as in all multiplexed displays, only one character is enabled at any time. All characters will appear to be displayed continuously, however, because of the high scanning rate.

As seen in the table, during each clocked state the PROM generates 3 bits of segment information. Six such states define the character produced. Thus only three display segments switch during each NE591 latching period, substantially reducing load transients and large load-current variations, which tend to cause difficulty in circuits of this kind. Only six of each NE591's eight outputs are used, to reduce power dissipation. Note that each device handles 6 of the total of 18 display segments for each character.

As the circuit is digital, neither layout nor component values are critical. The clock frequency, typically less than 5 MHz, should have a minimum pulse width (t<sub>w</sub>) of 100 ns, however, in order to ensure proper display and strobe latching. □

# Contact tester quantifies open-, short-circuit tendencies

by Steven Nirenburg and Wunnava V. Subbarao  
Florida International University, Miami, Fla.

Many present-day electronic systems, being modular in nature, rely heavily on connector blocks to hook the various functional units together. As such, it is becoming increasingly important to detect any momentary open-circuit or short-circuit tendencies of the system at the connector—especially in high-vibration environments—both in production-line testing and during actual operation. This tester detects both, while indicating if either condition persists beyond a given time preset by the user.

Consider the detection of an open-circuit tendency of contact  $S_1$ , as shown in the figure. For the purposes of discussion, the open-circuit condition is arbitrarily chosen to be one in which the resistance across  $S_1$  is greater than 10 ohms for a period equal to or greater than 100 microseconds.

On system reset, the 74192 counters and 7476 flip-flops are brought to logic 0. If  $S_1$  is closed, voltage  $V_1$  will be near zero and the outputs of comparators  $G_1$  and  $G_2$  will be high. Light-emitting diode  $D_0$  then glows, indicating the contact is closed.

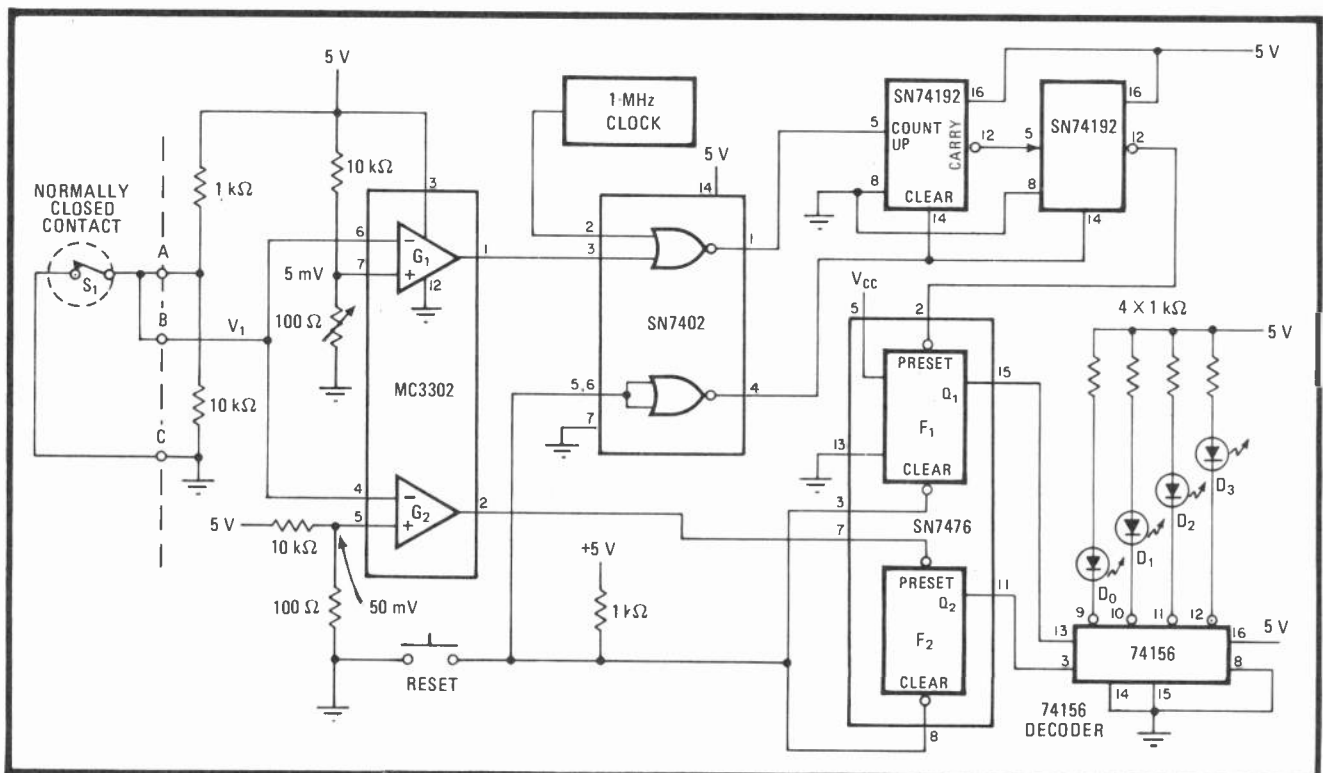
If  $S_1$  is momentarily opened or shows any contact deterioration,  $V_1$  rises slightly above ground potential, forcing  $G_1$  low and gating the output of the 1-megahertz clock through to the counters. Thus should the contact deterioration last for 100  $\mu$ s, 100 clock pulses will be counted and the resulting carry pulse generated from the second 74192 will set flip-flop  $F_1$ . And if the ohmic resistance across  $S_1$  goes above 10  $\Omega$ ,  $V_1$  will rise above 50 millivolts, forcing  $G_2$  low and flip-flop  $F_2$  high.

Thus  $D_1$  will glow if  $F_1$  is set and  $F_2$  is clear.  $D_2$  will glow if  $F_1$  is clear and  $F_2$  is set.  $D_3$  will light if both  $F_1$  and  $F_2$  are set, so that the predetermined open-circuit time and resistance of  $S_1$  may be readily recorded.

Short circuits are readily detected by connecting points A and B across the normally opened contact under test. When the contact is open,  $V_1$  is near zero and the system remains in the reset position, lighting up  $D_0$ . If shorted momentarily,  $S_1$  will cause either  $D_1$ ,  $D_2$  or  $D_3$  to light. For the values shown in the figure,  $D_1$  will glow if the short circuit exceeds 100  $\mu$ s or more;  $D_2$  indicates if  $S_1$ 's resistance is less than 1 M $\Omega$ ;  $D_3$  illuminates if both of the aforementioned conditions exist.

By changing the clock frequency or the counting limit, any time interval can be preset. Similarly, the impedance at which the circuit responds may be selected by adjusting the threshold voltage at  $G_2$ . □

Engineer's notebook is a regular feature in *Electronics*. We invite readers to submit original design shortcuts, calculation aids, measurement and test techniques, and other ideas for saving engineering time or cost. We'll pay \$50 for each item published.



**Connection.** Tester for block connectors, pc boards, and cable assemblies indicates if duration of open or short circuit in circuit pin or lead exceeds preset time and checks relative magnitude of resistance across switch or broken wire. Four LEDs indicate state of affairs.

## Reducing a PLL's phase jitter

by R. P. Leck  
Bell Laboratories, Crawford Hill, Holmdel, N. J.

The design of a phase-locked-loop frequency multiplier is sometimes constrained by its loop-damping and bandwidth requirements. In this case, harmonics related to the loop's input frequency are present at the output of the loop's phase detector, generating excessive sideband noise and thus excessive phase jitter. This occurs as a result of modulating the voltage-controlled oscillator with the filtered output of the phase detector. Adding an extra break, or corner, frequency to the PLL's filter response reduces this sideband noise, however, by reducing the modulation index at the loop's VCO.

A block diagram of a typical PLL frequency multiplier is shown in (a). Detector  $A_1$  compares the phases of the input signal,  $f_1$ , and a divided-down VCO signal,  $f_2$ , and generates a voltage proportional to the phase difference between the two. This signal, after passing through low-pass filter  $A_2$ , is applied to the VCO,  $A_3$ , to alter its output,  $f_{VCO}$ . As a result, the phase difference between  $f_2$  and  $f_1$  is minimized. The loop is in the locked state when  $f_1$  equals  $f_2$ .

The level of the sidebands that appear at the loop's output as a result of frequency-modulating the VCO with the filter's output are related to the modulation index of the harmonics; for a PLL multiplier, the index is given by:

$$\theta_o(s) = NK_o F(s) V_d / s$$

where  $N$  is the loop's divider constant,  $K_o$  is the voltage-to-frequency control function of  $A_3$  divided by  $N$ ,  $F(s)$  is the transfer function of the loop's low-pass filter, and  $V_d$  is  $A_1$ 's output voltage. Reducing the numerical value of  $F(s)$  reduces the modulation index,  $\theta_o(s)$ . The net effect is a reduction in the sideband noise at the loop's output.

The transfer function of the active loop filter typically used in PLL circuits (b) is:

$$F_2(s) = (s\tau_2 + 1) / s\tau_1$$

where  $\tau_1 = R_1 C$  and  $\tau_2 = R_2 C$ . Adding the capacitor  $C'$  across  $R_2$  as shown in (c) creates a second-order filter

whose transfer function is given by:

$$F_3(s) = (s\tau_2 + s\tau_3 + 1) / (s^2\tau_1\tau_3 + s\tau_1)$$

where  $\tau_3 = R_2 C'$ .

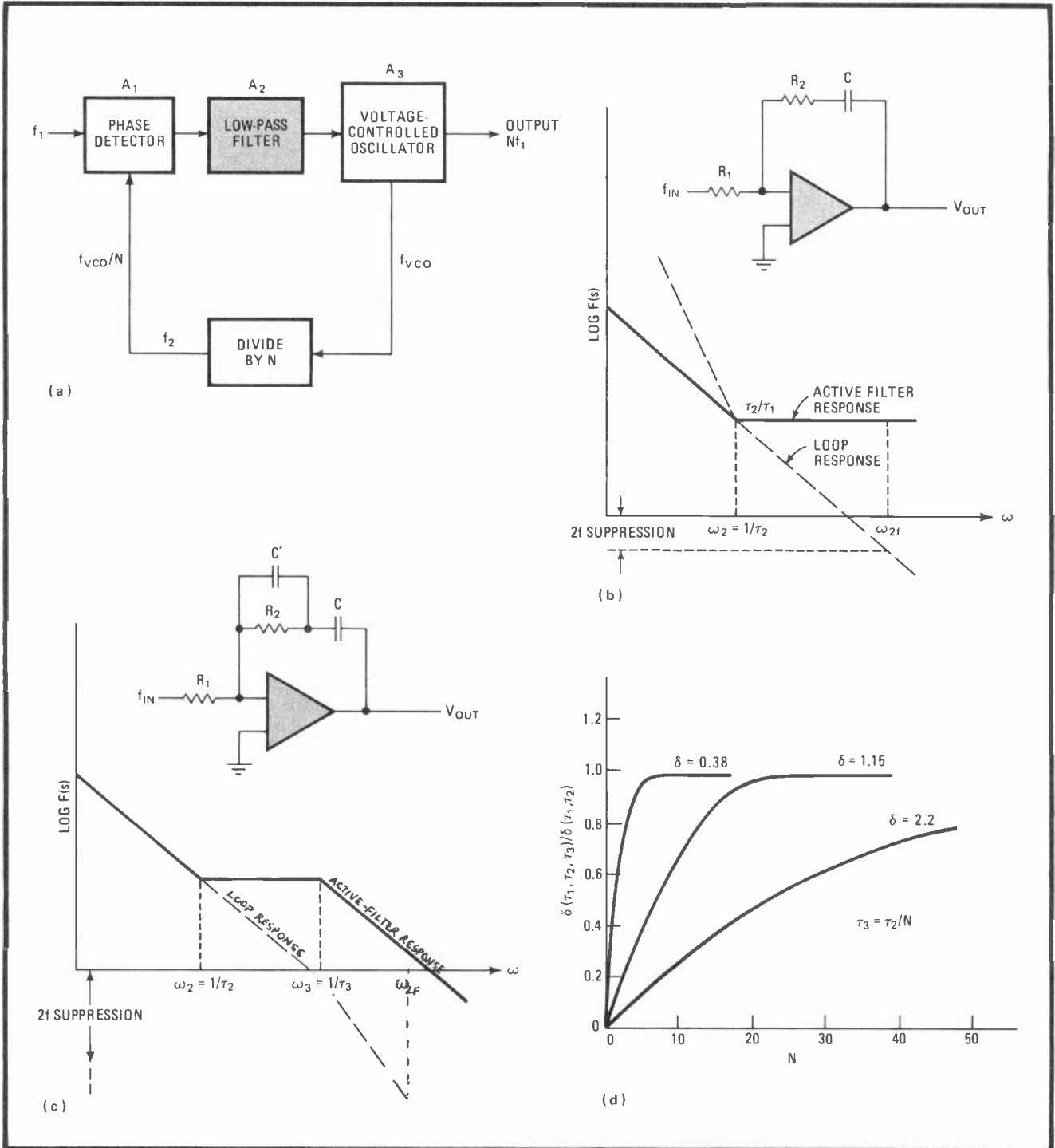
Note the corresponding curves of the filter's and PLL's open-loop response. If the harmonics in question are all above the added pole frequency,  $1/2\pi\tau_3$ , they will be attenuated because the magnitude of  $F_3(s)$  will be less than that of  $F_2(s)$ . At  $\omega_{2f}$  in (b), there is no additional suppression beyond whatever exists as a result of the low-pass filter and the integrating effects of the VCO. The attenuation of the unwanted harmonics is increased with the addition of  $C'$ .

It will be observed that adding  $C'$  creates a network with certain third-order characteristics that under some conditions can be unstable. However, as long as the loop gain of the originally unconditionally stable second-order loop is unchanged after  $C'$  is added and provided that the slope at which the loop's log-magnitude plot crosses the unity-gain axis does not exceed  $-40$  dB per decade, the new loop will behave more like the second-order one from which it derived. Both conditions are normally met in practice.

Placement of the additional breakpoint affects the loop's damping factor,  $\delta$ . As indicated in (d), the effects upon the damping factor start to become noticeable as  $\tau_3$  increases. From these curves, it is seen that a second-order loop with a damping of about a factor of 1 would have an approximately equivalent second-order damping of about 0.975 when  $\tau_3 = \tau_2/20$ .

As an example of how to use these curves as a design aid, consider a requirement for a PLL frequency multiplier with a damping factor of 1.2 and a bandwidth of 100 Hz. A standard second-order loop is designed to these specifications, but its output is found to contain excessive phase jitter (sideband noise). So a damping of 0.38, 1.15, or 2.2 is selected from (d) and the loop redesigned using the second-order equations customary in designing basic PLLs.

In this case, a damping factor of 2.2 is chosen.  $N$ , and hence  $C'$ , is determined by first calculating the ratio  $R = \delta(\tau_1, \tau_2, \tau_3) / \delta(\tau_1, \tau_2)$ . Given a required damping  $\delta(\tau_1, \tau_2, \tau_3)$  of 1.2 and a desired damping  $\delta(\tau_1, \tau_2)$  of 2.2,  $R = 0.55$ . From (d),  $N = 21.2$  for  $R = 0.55$ . Then  $\tau_3 = \tau_2 / N$  and  $C' = \tau_3 R_2$ . Placement of this value of  $C'$  across  $R_2$  in the loop's filter reduces the phase jitter to acceptable levels while maintaining the original damping and bandwidth requirements.  $\square$



**Breakpoint.** When operated as a frequency multiplier, phase-locked loop's phase detector (a) can generate harmonics that appear at circuit output. Conventional low-pass filter (b) cannot provide sufficient harmonic suppression. Incorporating capacitor  $C'$  (c) adds break frequency to filter response, enables increased rejection of harmonics, and reduces PLL's phase jitter. Effects of  $\tau_3$  on second-order damping are plotted (d) to aid in design example discussed in text.



# Digital voltmeter has audible output

by William S. Wagner  
Northern Kentucky University, Highland Heights, Ky.

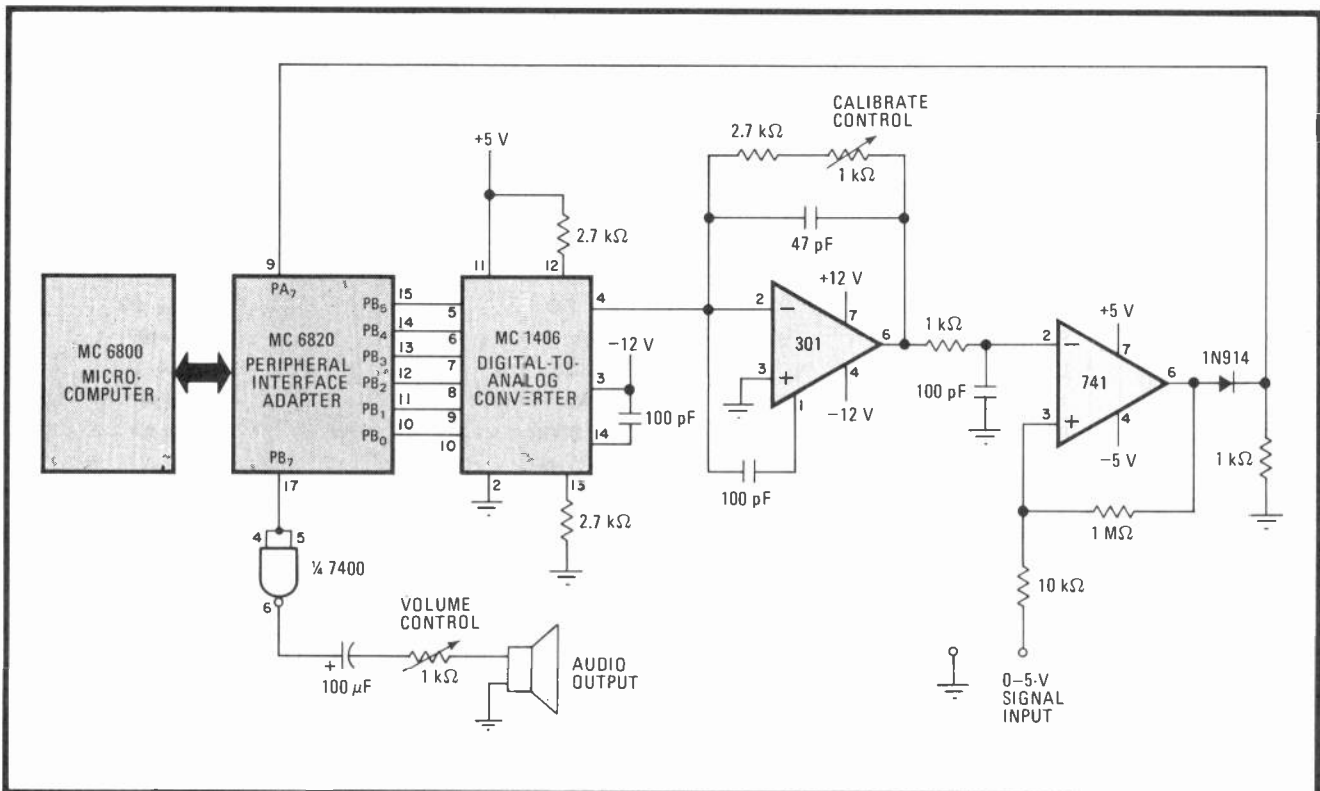
Using a program written for the 6800 microprocessor, and an appropriate interface, this system converts a 0-to-5-volt dc signal into an equivalent sequence of audio tones. Thus, the system will be particularly useful to visually handicapped technicians who troubleshoot logic circuits, as well as in applications where it is not practical to read the voltage from a standard voltmeter's display face.

The voltage to be measured is converted to a series of tones of short duration (dits) to represent quantities extending from 1 to 9. The quantity 0 is represented by a single tone (dah) of relatively long duration. A decimal point is represented by a pause. Thus, for example, 2.5 v yields an equivalent audio output of dit-dit, pause, dit-dit-dit-dit. An 0.3-v signal yields dah, pause, dit-dit-dit. And a 4.0-v signal generates dit-dit-dit-dit, pause, dah. The resolution of the measurement is about 0.1 v.

As implied in the figure, the 6-bit MC 1406 digital-to-analog converter is used in a feedback loop with the 741 operational amplifier for tone generation. The dc input signal is compared to the voltage at the inverting port of the 741. If there is a voltage difference, the digital input to the MC 1406 is adjusted, under program control, until the voltage difference is minimized. The binary word at the output of the MC 6820 peripheral-interface adapter then represents the dc voltage, and is converted to an audio output by the remainder of the program. The frequency and length of the individual tone, the time interval between digits, and the rate at which the dc input signal is sampled are all controlled by the software.

The program requires 250 bytes of memory. The first four instructions initialize the program. The instructions contained between addresses 000C and 00021 comprise the digital-voltmeter part of the routine. Steps 0012 through 0016 set a built-in delay in order to allow the analog portion of the interface sufficient time to update. The instructions commencing at 0018 cause the program to jump to the audio portion of the program (addresses 0023 through 00A0) when the aforementioned match of input and d-a voltages occurs.

In the analog part, the dc voltage is converted to a final 6-bit binary-coded word and stored in an accumulator. Each bit is checked to see whether it is a 0 or an



**Potential cure.** Microprocessor-based system transforms logic-range voltages into coded series of audio tones for technicians who are unable to observe standard voltmeters. The resolution of the measurements, limited by interface's d-a converter, is 0.1 volt.

6800 PROGRAM FOR AUDIO VOLTMETER

| Address | Mnemonic  | Address | Mnemonic | Address | Mnemonic  |
|---------|-----------|---------|----------|---------|-----------|
| 0000    | LDX 0004  | 005C    | BNE F7   | 010C    | BNE FD    |
| 0003    | STX 8000  | 005E    | PULA     | 010E    | DEX       |
| 0006    | LDX FF04  | 005F    | PSHA     | 010F    | BEQ 03    |
| 0009    | STX 8002  | 0060    | ANDA F0  | 0111    | COMB      |
| 000C    | LDB FF    | 0062    | BEQ 3F   | 0112    | BRA F0    |
| 000E    | CLRA      | 0064    | PULA     | 0114    | LDX 1FFF  |
| 000F    | STAB 8002 | 0065    | ASLA     | 0117    | DEX       |
| 0012    | LDX 0055  | 0066    | PSHA     | 0118    | BNE FD    |
| 0015    | DEX       | 0067    | BCS 11   | 011A    | PULA      |
| 0016    | BNE FD    | 0069    | PULA     | 011B    | DECA      |
| 0018    | TST 8000  | 006A    | ASLA     | 011C    | BNE E2    |
| 001B    | BPL 06    | 006B    | PSHA     | 011E    | RTS       |
| 001D    | DECB      | 006C    | BCS 13   | 0120    | LDX 03FF  |
| 001E    | ADDA 01   | 006E    | PULA     | 0123    | ORAB 7F   |
| 0020    | DAA       | 006F    | ASLA     | 0125    | STAB 8002 |
| 0021    | BRA EC    | 0070    | PSHA     | 0128    | LDAA 25   |
| 0023    | LDS 00B0  | 0071    | BCS 15   | 012A    | DECA      |
| 0026    | PSHA      | 0073    | PULA     | 012B    | BNE FD    |
| 0027    | ANDA 70   | 0074    | ASLA     | 012D    | DEX       |
| 0029    | BGT 03    | 0075    | PSHA     | 012E    | BEQ 03    |
| 002B    | JMP 0120  | 0076    | BCS 17   | 0130    | COMB      |
| 002E    | PULA      | 0078    | BRA 1A   | 0131    | BRA F0    |
| 002F    | ASLA      | 007A    | LDA 08   | 0133    | PULA      |
| 0030    | ASLA      | 007C    | JSR 0100 | 0134    | ASLA      |
| 0031    | PSHA      | 007F    | BRA E8   | 0135    | ASLA      |
| 0032    | BCS 0C    | 0081    | LDA 04   | 0136    | ASLA      |
| 0034    | PULA      | 0083    | JSR 0100 | 0137    | ASLA      |
| 0035    | ASLA      | 0086    | BRA E6   | 0138    | PSHA      |
| 0036    | PSHA      | 0088    | LDA 02   | 0139    | JMP 0053  |
| 0037    | BCS 0E    | 008A    | JSR 0100 | 0140    | LDX 03FF  |
| 0039    | PULA      | 008D    | BRA E4   | 0143    | ORAB 7F   |
| 003A    | ASLA      | 008F    | LDA 01   | 0145    | STAB 8002 |
| 003B    | PSHA      | 0091    | JSR 0100 | 0148    | LDAA 25   |
| 003C    | BCS 10    | 0094    | LDAA 02  | 014A    | DECA      |
| 003E    | BRA 13    | 0096    | LDX FFFF | 014B    | BNE FD    |
| 0040    | LDA 04    | 0099    | DEX      | 014D    | DEX       |
| 0042    | JSR 0100  | 009A    | BNE FD   | 014E    | BEQ 03    |
| 0045    | BRA ED    | 009C    | DECA     | 0150    | COMB      |
| 0047    | LDA 02    | 009D    | BNE F7   | 0151    | BRA F0    |
| 0049    | JSR 0100  | 009F    | PULA     | 0153    | PULA      |
| 004C    | BRA EB    | 00A0    | JMP 000C | 0154    | ASLA      |
| 004E    | LDA 01    | 00A3    | JMP 0140 | 0155    | ASLA      |
| 0050    | JSR 0100  | 0100    | PSHA     | 0156    | ASLA      |
| 0053    | LDAA 01   | 0101    | LDX 00FF | 0157    | ASLA      |
| 0055    | LDX FFFF  | 0104    | ORAB 7F  | 0158    | PSHA      |
| 0058    | DEX       | 0106    | STA 8002 | 0159    | JMP 0094  |
| 0059    | BNE FD    | 0109    | LDAA 25  |         |           |
| 005B    | DECA      | 010B    | DECA     |         |           |

integer from 1 to 9, so that it can be determined if short or long tones are to be produced by the dit and dah subroutines, respectively. The instructions commencing at 0053 sets a time interval between the processing of the first and second integers of the measured voltage, and

the instructions starting at 0094 set the time interval between readings, or samples.

The actual short-tone subroutine extends from addresses 0100 to 011E. The instructions specified from 0101 to 010F determines the length and frequency of the

short tones. Addresses 0114 through 0118 set the time interval between dits.

There are two subroutines for the generation of long tones. One is called (address 0120) when the first integer of the voltage measured is 0. The second is called (0140)

where the second integer is 0. Both contain instructions for setting the length and frequency of the long tone. □









